

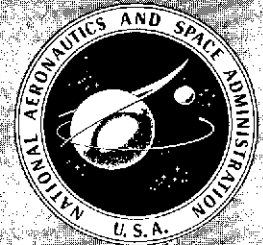
(NASA-SP-339) GAMMA-RAY ASTROPHYSICS  
(NASA) ~~425~~ p SOD HC \$2 90 CSCL C3B  
412

N78-14865  
THRU  
N78-14895  
Unclass  
25515

H1/29

# GAMMA-RAY ASTROPHYSICS

A symposium held at  
GODDARD SPACE FLIGHT CENTER  
Greenbelt, Maryland  
April 30—May 2, 1973



NATIONAL AERONAUTICS AND SPACE ADMINISTRATION

# GAMMA-RAY ASTROPHYSICS

A symposium held at NASA Goddard Space Flight Center  
April 30 to May 2, 1973, sponsored by the  
National Aeronautics and Space Administration and the  
American Physical Society

*Edited by*

Floyd W. Stecker and Jacob I. Trombka  
Goddard Space Flight Center

*Prepared by NASA Goddard Space Flight Center*



Scientific and Technical Information Office  
NATIONAL AERONAUTICS AND SPACE ADMINISTRATION  
Washington, D.C.

;

The requirement for the use of the International System of Units (SI) has been waived for this document under the authority of NPD 2220.4, paragraph 5.d.

---

For sale by the Superintendent of Documents,  
U. S. Government Printing Office, Washington, D. C. 20402

*Library of Congress Catalog Card No. 73-600345*

## FOREWORD

### Opening Remarks

by

**Dr. John F. Clark, Director**  
*Goddard Space Flight Center*

Significant advances have been made recently both in experimental and theoretical investigations in  $\gamma$ -ray astrophysics. It is thus most appropriate at this time to gather together to discuss the meaning of these results. This, then, is the first of what we hope will be many fruitful international symposia devoted exclusively to this subject.

Because of the controversial and still unsettled nature of some aspects of this young and exciting subject, it is fitting that we will devote fully one-half of our time to free and open discussion. We also will try to utilize the observational and theoretical data presented at this conference to help guide us in charting our future investigative efforts in  $\gamma$ -ray astrophysics. To this end, we will culminate the Symposium with a panel discussion on the future of this field.

The three days of the Symposium will be spent considering the observational data from about 0.3 MeV to a few hundred GeV and theoretical models of production mechanisms that may give rise to both galactic and extragalactic  $\gamma$ -rays. We also hope to measure a large interaction cross section between the theorists and experimentalists gathered here.

We feel that since Goddard Space Flight Center has been heavily involved in both the theoretical and experimental aspects of  $\gamma$ -ray astrophysics, it is fitting that such a symposium be held here. We thank the Division of Cosmic Physics of the American Physical Society for cosponsoring this meeting.

We further would like to thank the distinguished members of the international scientific community who have taken the time to come here and actively participate in this Symposium.

April 11, 1973

## PREFACE

The first international symposium and workshop devoted to gamma-ray astrophysics was held at Goddard Space Flight Center, Greenbelt, Maryland April 30 to May 2, 1973. The Symposium was cosponsored by NASA and the Division of Cosmic Physics of the American Physical Society. Significant advances have been made recently both in theoretical and experimental investigations in the field so that  $\gamma$ -ray astrophysics is coming into its own as a separate branch of astrophysics. This led Prof. Kenneth Greisen, of Cornell, who was one of the session chairmen, to make the remark that, this Symposium marks a "birthday of  $\gamma$ -ray astronomy."

Our philosophy in organizing the Symposium was to devote equal time to both theory and observation. To this end, the organizational work was shared by a theoretician and an experimentalist.

The Symposium was divided into morning sessions of invited papers which surveyed all aspects of present work on  $\gamma$ -ray astrophysics and related X-ray astrophysics, and afternoon workshop-discussion sessions where brief reports were contributed and discussions of controversial aspects of the field were held. The final afternoon session consisted of a review of the Symposium (contained here in the introduction) and a panel discussion on future directions for research in the field.

The formal program for the Symposium was as follows:

Monday, April 30, Morning

Chairman: Dr. George F. Pieper  
Goddard Space Flight Center

Dr. John F. Clark, Director,  
Goddard Space Flight Center  
Welcome

Lawrence E. Peterson, University of California at San Diego,  
and Jacob I. Trombka, Goddard Space Flight Center, on  
Low-Energy Gamma-Ray Observations (with emphasis on  
results from Apollo-15, -16, and -17 and discussion of  
induced activity in crystal detectors)

PRECEDING PAGE BLANK NOT FILMED

Floyd W. Stecker, Goddard Space Flight Center, on  
Mechanisms for Production of Diffuse Gamma-Ray  
Continuum Radiation

Donald D. Clayton, Rice University, on  
Prospects for Nuclear-Gamma-Ray-Line Astronomy

Monday, April 30, Afternoon

Chairman: Dr. James I. Vette  
Goddard Space Flight Center

David J. Forrest, University of New Hampshire, on  
Observations of Gamma-Ray Emission in Solar Flares

Reuven Ramaty, Goddard Space Flight Center, on  
Theory of Gamma-Ray Emission in Solar Flares

Vitaly L. Ginzburg, Academy of Sciences USSR, P.N.  
Lebedev Physical Institute, Moscow (remarks authorized  
by Prof. Ginzburg which were presented in his absence), on  
Gamma-Ray Astronomy and Cosmic-Ray Origin Theory

Workshop Session Discussion of:

1. Experimental techniques and errors involved in  
 $\gamma$ -ray measurements (spallation, and so forth)
2. Gamma-ray production mechanisms and theoretical  
production rates
3. Gamma-ray astronomy and cosmic-ray origin theory
4. Topics related to morning session

Tuesday, May 1, Morning

Chairman: Dr. Maurice M. Shapiro  
Naval Research Laboratory

William Kraushaar, University of Wisconsin, on  
Diffuse Soft X-Ray Observations

Donald Kniffen, Goddard Space Flight Center and  
Gerald Share, Naval Research Laboratory, on  
10-100 MeV Gamma-Ray Observations

Daniel Schwartz, American Science and Engineering, on  
Diffuse 1 keV - 1 MeV X-Ray Observations

Ramanath Cowsik, University of California at Berkeley, on  
Theory of the Diffuse X-Ray Background

Tuesday, May 1, Afternoon

Chairman: Dr. George W. Clark  
Massachusetts Institute of Technology

Workshop Session Discussion of:

1. Theory of  $\gamma$ -ray sources
2. Interpretation of SAS-2 results and related experimental results
3. Cosmological implications of  $\gamma$ -ray measurements
4. Solar and galactic  $\gamma$ -ray line emission

Wednesday, May 2, Morning

Chairman: Dr. Kenneth Greisen  
Cornell University

Roland Omnès, Laboratory of Theoretical and High-Energy Physics, Orsay, France, and Evry Schatzman and Jean-Loup Puget, Paris Observatory, France, on Baryon-Symmetric Cosmology and Gamma-Ray Observations

Gary Steigman, Yale University, on Antimatter in the Universe?

Wednesday, May 2, Morning

Giovanni G. Fazio, Harvard Observatory and Smithsonian Astrophysical Observatory, on Observations of Ultra-high Energy Gamma Rays

Arnold Wolfendale, University of Durham, England, on Theory of Ultra-high Energy Gamma Rays

Wednesday, May 2, Afternoon

Floyd W. Stecker  
Goddard Space Flight Center  
Concluding Remarks, Summary

**SPECIAL SESSION:** Panel Discussion on Future Directions in Gamma-Ray Astronomy

Jacob Trombka, Chairman, Goddard Space Flight Center  
Evry Schatzman, Paris Observatory  
Giovanni Fazio, Harvard and Smithsonian Astrophysical Observatories

Carl Fichtel, Goddard Space Flight Center  
 Albert Metzger, Jet Propulsion Laboratory  
 Kenneth Greisen, Cornell University  
 Glenn Frye, Case Institute  
 Floyd W. Stecker, Goddard Space Flight Center

Important new results on the diffuse  $\gamma$ -ray background as obtained by Apollo were presented by L. Peterson (University of California at San Diego) and J. Trombka (NASA/GSFC) and results obtained by SAS-2 were presented by D. Kniffen (NASA/GSFC), who also reported observations of the galactic plane. The results from SAS-2 confirm some important qualitative results first obtained by OSO-3 that the galaxy is an intense source of  $\gamma$ -radiation above 100 MeV and it stands out above the extragalactic background in this energy range. The spectrum is harder above 100 MeV than the  $\gamma$ -radiation seen at high galactic latitudes, which is presumably extragalactic. The SAS-2 results also indicate that the extragalactic (high-galactic latitude) background spectrum is quite steep above 40 MeV (roughly  $\propto E_{\gamma}^{-3}$ ).

Results from balloon observations by groups at the Max Planck Institute and the U. S. Naval Research Laboratory, reported by G. Share (NRL), are consistent with the Apollo and SAS-2 results, which present a continuous observational spectrum from 300 keV up to 135 MeV. These data suggest a bulge in the  $\gamma$ -ray spectrum above 1 MeV, in spite of background corrections which are of most importance below 4 MeV as discussed by J. Fishman and C. Dyer. This bulge has been interpreted as a new component of  $\gamma$ -radiation at energies above 1 MeV. This argument is even more important if the X-rays below 1 MeV are thermally produced and are falling off exponentially in energy above 100 keV as was suggested by D. Schwartz (American Science and Engineering) and R. Cowsik (University of California at Berkeley). Problems with the thermal interpretation were discussed by W. Kraushaar (University of Wisconsin).

The interpretation of the 1 MeV to 100 MeV bulge in the  $\gamma$ -ray spectra was discussed by F. Stecker (NASA/GSFC) who gave a review on  $\gamma$ -ray production mechanisms. He concluded that the excess is most likely caused by matter-antimatter annihilation. The Apollo and SAS-2 observational data present an excellent fit to the predicted annihilation spectrum up to 135 MeV. The matter-antimatter-symmetric cosmology was discussed by R. Omnès (Laboratory of Theoretical and High-Energy Physics, Orsay) and E. Schatzman and J. Puget (Paris Observatory, Meudon).

The exciting aspects of the matter-antimatter cosmology reported on by R. Omnès, E. Schatzman, J. Puget, and F. Stecker indicate that, in addition to implying baryon symmetry on a universal scale, it can explain such diverse phenomena as: the cosmic  $\gamma$ -ray background spectrum; the ratio of photons

to nucleons in the universe of  $\sim 10^9$ ; annihilation as the energy source for generation of large-scale turbulence leading to galaxy formation; and the consequent observed sizes, mean densities, and rotational velocities of galaxies. G. Steigman (Yale) discussed the observational restrictions on matter-antimatter cosmological models.

The galactic  $\gamma$ -ray flux in the 100-MeV range seen by SAS-2 and OSO-3 indicates an increase in the direction of the galactic center. The most likely implication is that there is a cosmic-ray gradient toward the galactic center, as was pointed out in remarks by A. Wolfendale (University of Durham) and in a communication by V. Ginzburg (Lebedev Institute, Moscow).

Measurements reported on the Crab Nebula and Pulsar by various groups were discussed by J. Share and talked about by K. Greisen, G. Fazio, and G. Frye. They indicate that the  $\gamma$ -ray spectrum from the Crab Nebula goes all the way up to the highest energies yet observed and that there are time variations at about  $10^{12}$  eV; this also tells us something about the magnetic field strength in the Crab Nebula. At ultra-high energies, A. Wolfendale (Durham) discussed the possibility of observing a flux of  $\gamma$ -radiation in the  $10^{19}$ - and  $10^{20}$ -eV energy range.

If cosmic rays in this energy range are universal and the cascading process which he discussed occurs, then we may very well be able to observe the resultant  $\gamma$ -rays. The situation is a little more pessimistic if there is an extragalactic magnetic field of average strength above  $10^{10}$  G, because synchrotron losses would then cut off the cascade process. So, by looking for these  $\gamma$ -rays in air showers, we may be able to learn something about ultra-high energy cosmic rays of metagalactic origin.

Wolfendale also discussed joint work with A. Strong and J. Wdowczyk on the possible electromagnetic cascading at lower energies in the early big bang universe to possibly explain the  $\gamma$ -ray background in the 1- to 100-MeV range or, alternatively, to use the  $\gamma$ -ray data to rule out cosmic-ray production at early epochs on the scale suggested by Hillas. This model requires a rather low intergalactic gas density at present of  $\sim 10^{-9}$  atoms/cm<sup>3</sup>.

There was much discussion of the 470-keV feature, which has been observed by R. Haymes' group (Rice) in the galactic center region. Three very interesting theoretical explanations of the 470-keV feature were presented. D. Clayton (Rice University), suggested that it may be caused by lithium. R. Ramaty (NASA) suggested that this feature could be attributed to red-shifted positron annihilation produced at the surface of neutron stars. M. Leventhal gave a very interesting interpretation that this feature may be due to positronium, and that the positronium spectrum has been altered by the finite energy resolution of the detector, so that the edge at 511 keV appears as a bump at  $\sim 470$  keV.

D. Clayton gave a review of astrophysical processes which should be important for the production of  $\gamma$ -ray line spectra. D. Forrest (New Hampshire) discussed the observations of  $\gamma$ -ray line emission in solar flares and R. Ramaty discussed the theoretical interpretation of these observations. In order to observe discrete line emission experimentally with  $\gamma$ -ray detectors, higher-energy resolutions are required. The use of solid-state detectors capable of such high-energy resolutions aboard satellites was considered by G. Nakano and W. Imhoff (Lockheed). Experimental results were also presented. A. Metzger (JPL) described the experimental detectors being planned for flight aboard HEAO utilizing solid-state techniques.

In planning the Symposium program, we purposely mixed the theoretical and observational papers in order to maximize the interactions between theoretical and observational workers in the field. However, for a more logical organization of the Symposium proceedings, we have divided this book into four sections, one on observations, one on theoretical papers, one on cosmological implications, and the last section consisting of an edited transcript of the panel discussion on the future of the field.

An examination of the transcripts of the discussion indicated that heavy editing was required in order to make sense out of some of the discussion. In addition, many of the speakers incorporated points made in the discussion into their final manuscripts. Thus, discussion material was eliminated which was deemed to be either incoherent or redundant after speakers were given a chance to revise any unclear material. The remaining discussion material is appended to pertinent chapters.

When this Symposium was organized, it was planned to cover all aspects of the field, so that the proceedings would be a comprehensive up-to-date reference. However, shortly after the Symposium was held, the exciting discovery of cosmic  $\gamma$ -ray bursts was reported by the Los Alamos group in the *Astrophysical Journal*. The editors therefore felt it important to attempt to include some discussion of this topic as a special addition to the proceedings. We have therefore added two special short papers on this subject prepared by people at Goddard Space Flight Center because of time limitations. These are an observational paper by Cline et al., on energy spectra of cosmic  $\gamma$ -ray bursts and a theoretical paper by Stecker and Frost on the stellar superflare origin hypothesis of these bursts. We realize that other and important work on this topic such as that by S. Colgate and the Los Alamos group should also be included in any well-rounded discussion, but, unfortunately this was not possible here because of our publication schedule.

F. W. Stecker  
J. I. Trombka  
Goddard Space Flight Center  
August 1973

## ACKNOWLEDGMENTS

We would like first of all to thank the many authors who have contributed solid, thoughtful manuscripts to these proceedings and who gave excellent presentations at the Symposium. We particularly appreciate the time and effort made by the authors to prepare this material under a severely short time schedule so that these proceedings would be available to the astrophysics community in a time comparable to that for publication of a journal article.

We would also like to thank Dr. Maurice M. Shapiro and Dr. Frank B. McDonald for coordinating this Symposium with the Division of Cosmic Physics of the American Physical Society. We would like to thank Dr. John F. Clark, Dr. George F. Pieper and Dr. James I. Vette, Dr. Theodore G. Northrop and Dr. Aaron Temkin for their support which enabled us to hold the Symposium at the Goddard Space Flight Center.

We also thank the attendees, many of whom came from great distances, for their contributions in making the Symposium a success.

Most special thanks go to Mrs. Sandra J. Walter, for her untiring work in handling almost all of the administrative details which are so numerous in an undertaking of this type, and to Barbara Welsh and Elizabeth R. Miller for help in preparation of these proceedings.

FWS

JIT

# CONTENTS

	<i>Page</i>
FOREWORD . . . . .	iii
PREFACE . . . . .	v
ACKNOWLEDGMENTS . . . . .	xi
SECTION 1—OBSERVATIONAL DATA . . . . .	1
Chapter I . . . . .	3
A. Diffuse Cosmic X-Rays Below 1 keV <i>William L. Kraushaar</i> . . . . .	3
Chapter II . . . . .	15
A. The X-Ray Emissivity of the Universe: 2 to 200 keV <i>Daniel Schwartz and Herbert Gursky</i> . . . . .	15
B. Atmospheric Corrections to Balloon X-Ray Observations <i>H. Horstman</i> . . . . .	37
Chapter III . . . . .	41
A. The Measurement and Interpretation of the Cosmic Gamma-Ray Spectrum Between 0.3 and 27 MeV as Obtained During the Apollo Mission <i>L. E. Peterson, J. I. Trombka, A. E. Metzger, J. R. Arnold,             J. I. Matteson, and R. C. Reedy</i> . . . . .	41
B. Induced Radioactivity Contributions to Diffuse Gamma-Ray Measurements <i>G. J. Fishman</i> . . . . .	61
C. Preliminary Results from the First Satellite of a High-Resolution Germanium Gamma-Ray Spectrometer: Description of Instrument, Some Activation Lines Encountered, and Studies of the Diffuse Spectra <i>G. H. Nakano, W. L. Imhof, J. B. Reagan, and             R. G. Johnson</i> . . . . .	71

	<i>Page</i>
D. Preliminary Results from the First Satellite of a High-Resolution Germanium Gamma-Ray Spectrometer: Backgrounds from Electron Bremsstrahlung and from Electron-Positron Annihilation <i>W. L. Imhof, G. H. Nakano, R. G. Johnson, and J. B. Reagan</i> . . . . .	77
E. Further Considerations of Spallation Effects <i>Clive Dyer</i> . . . . .	83
F. HEAO Gamma-Ray Astronomy Experiments <i>A. Metzger</i> . . . . .	97
Chapter IV . . . . .	103
A. Recent Observations of Cosmic Gamma-Rays from 10 MeV to 1 GeV <i>Gerald H. Share</i> . . . . .	103
B. Report on Gamma-Ray Astronomy Results Obtained in Europe Since the IAU Symposium No. 55 <i>K. Pinkau</i> . . . . .	133
C. Preliminary Results on SAS-2 Observations of > 30 MeV Gamma Radiation <i>D. A. Kniffen, C. E. Fichtel, and R. C. Hartman</i> . . . . .	139
Chapter V . . . . .	153
A. Observations of High-Energy Gamma Rays <i>G. G. Fazio</i> . . . . .	153
Chapter VI . . . . .	165
A. Observations of Gamma-Ray Emission in Solar Flares <i>D. J. Forrest, E. L. Chupp, A. N. Suri, and C. Reppin</i> . . . . .	165
Chapter VII . . . . .	175
A. Energy Spectra of Cosmic Gamma-Ray Bursts <i>T. L. Cline, U. D. Desai, R. W. Klebesadel, and I. B. Strong</i> . . . . .	175

	<i>Page</i>
SECTION 2—THEORY . . . . .	183
Chapter VIII . . . . .	185
A. The Astrophysics of the Diffuse Background of X-Rays and Gamma-Rays <i>Ramanath Cowsik</i> . . . . .	185
Chapter IX . . . . .	211
A. Mechanisms for Production of the Diffuse Gamma-Ray Continuum Radiation <i>F. W. Stecker</i> . . . . .	211
Chapter X . . . . .	249
A. Gamma-Ray Astronomy and Cosmic-Ray Origin Theory <i>V. L. Ginzburg</i> . . . . .	249
B. Galactic Gamma Rays: Models Involving Variable Cosmic-Ray Density <i>A. W. Strong, J. Wdowczyk, and A. W. Wolfendale</i> . . . . .	259
Chapter XI . . . . .	263
A. Prospects for Nuclear-Gamma-Ray Astronomy <i>Donald D. Clayton</i> . . . . .	263
B. Positronium Formation Red Shift of the 511-keV Annihilation Line <i>M. Leventhal</i> . . . . .	291
C. Nuclear Gamma-Rays from Solar Flares <i>R. Ramaty</i> . . . . .	297
Chapter XII . . . . .	315
A. Ultra-High Energy Gamma Rays <i>A. W. Strong, J. Wdowczyk, and A. W. Wolfendale</i> . . . . .	315
Chapter XIII . . . . .	329
A. A Comparison of the Recently Observed Soft Gamma-Ray Bursts with Solar Bursts and the Stellar Superflare Hypothesis <i>F. W. Stecker and K. J. Frost</i> . . . . .	329

	<i>Page</i>
SECTION 3—COSMOLOGY . . . . .	333
Chapter XIV . . . . .	335
A. Matter-Antimatter Cosmology	
<i>R. Omnès</i> . . . . .	335
B. The Deuterium Puzzle in the Symmetric Universe	
<i>B. Leroy, J. P. Nicolle, and E. Schatzman</i> . . . . .	351
C. Antimatter in the Universe?	
<i>Gary Steigman</i> . . . . .	361
Chapter XV . . . . .	367
A. Gamma-Ray Background Spectrum and Annihilation Rate in the Baryon-Symmetric Big-Bang Cosmology	
<i>J. L. Puget</i> . . . . .	367
B. Distortion of the Microwave Blackbody Background Radiation Implied by the Baryon-Symmetric Cosmology of Omnès and the Galaxy Formation Theory of Stecker and Puget	
<i>F. W. Stecker and J. L. Puget</i> . . . . .	381
SECTION 4—FUTURE DIRECTIONS IN GAMMA-RAY ASTRONOMY . . . . .	385
Chapter XVI	
A. A Panel Discussion on the Future Direction of Gamma-Ray Astronomy	
<i>Giovanni Fazio, Carl Fichtel, Glenn Frye, Kenneth       Greisen, Albert Metzger, Evry Schatzman, Floyd       Stecker, and Jacob Trombka</i> . . . . .	387
INDEX—LIST OF AUTHORS . . . . .	407

**SECTION 1**  
**OBSERVATIONAL DATA**

## A. DIFFUSE COSMIC X-RAYS BELOW 1 keV

William L. Kraushaar\*  
*University of Wisconsin*

### INTRODUCTION

The study of diffuse X-rays in the energy region below 1 keV has had a somewhat rocky past and has suffered from having attracted cosmological interest early in its young life. Much of the available data and interpretation can be found in recent review articles by Silk (1973, preprint), Felten (1972), Field (1972), and Kato (1972). In this short review I cannot discuss all the measurements or all the ideas that have been put forward. I will, therefore, restrict my discussion to a description of those features of the low-energy diffuse flux on which there is general observational agreement and to some interpretive matters that I believe have been overlooked or at least underemphasized. Also, most of the discussion will be restricted to the energy region below 280 eV, the Carbon-K edge.

### INTENSITY

The soft X-ray diffuse intensity is everywhere convincingly larger than would be expected from an extrapolation of the high energy isotropic, unabsorbed, and almost certainly, extragalactic power law spectrum. Data in support of this conclusion are shown in Figures I.A-1 and I.A-2, taken from papers by the Wisconsin (Bunner et al., 1971) and NRL (Davidsen et al., 1972) groups. The solid curves in both figures are the predicted proportional counter response given only the high-energy power law spectrum, with no interstellar absorption, as an input spectrum. The prominent bumps in these curves result from the X-ray transmission edges of the counter windows. The intensity ratio from pole to plane is about 3 to 1, and, while there can be some argument about a possible extragalactic contribution to the high latitude intensity, the plane intensity must be of relatively local origin because the column density for unit optical depth is only  $2.5 \times 10^{20}$  atoms/cm<sup>2</sup> or about 200 pc (with  $n = 0.4$  atoms/cm<sup>3</sup>) in these directions.

---

\*Speaker.

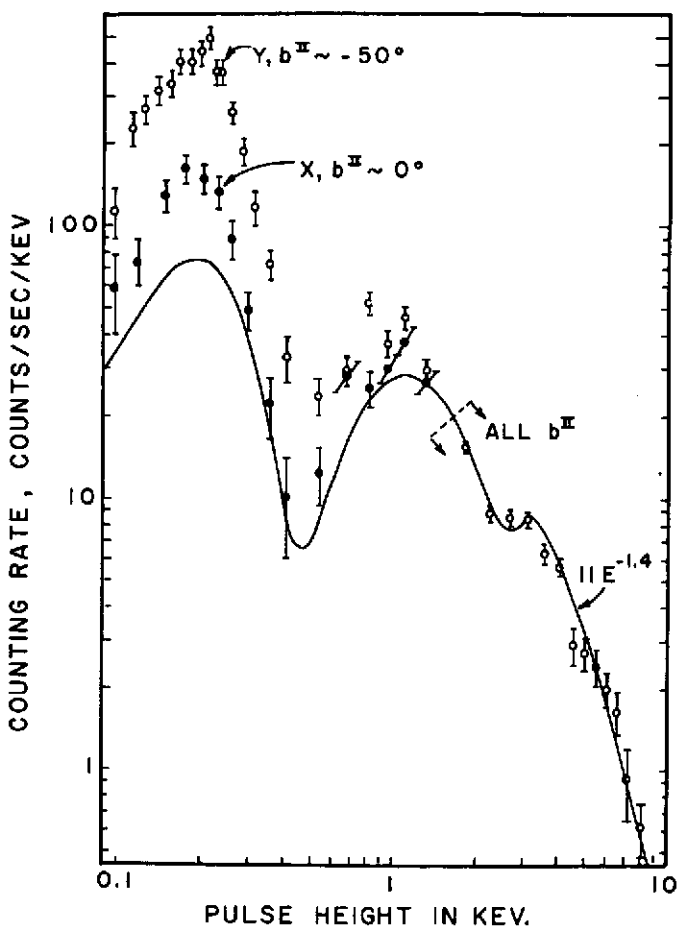


Figure I.A-1. Proportional counter pulse-height spectra near the galactic plane and at a high galactic latitude (Bunner et al., 1971).

### SPATIAL STRUCTURE

The soft X-ray intensity shows three broad classes of spatial structure.

First, there is the gross tendency for the intensity to be small in the galactic plane and enhanced by perhaps a factor of 3 at high northern galactic latitudes. This is shown in Figures I.A-3 and I.A-4, surveys of the NRL (Davidson et al., 1972) and Wisconsin (Bunner et al., 1972; Williamson, F. W., 1973; Sanders, W., 1973) groups. The polar enhancement is more obvious in the north than in the south, although there are some isolated line scans that make the case for apparent enhancement in the south more convincing (Bunner et al., 1969, 1971; Garmire and Riegler, 1972).

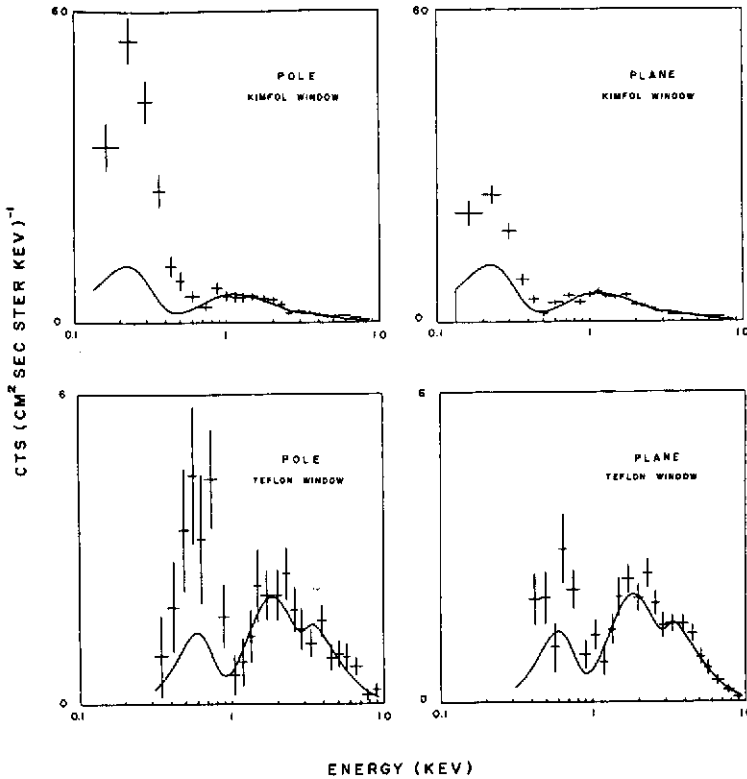


Figure 1.A-2. Pulse-height data taken with Kimfol and Teflon counter windows (Davidsen et al., 1972).

Secondly, the soft X-ray intensity is by no means just a simple function of galactic latitude nor is it correlated, except in the grossest sense, with the column density of interstellar hydrogen gas. There are large high intensity spatial features. None of these features except the North Polar Spur appear to correlate well with other astrophysical phenomena. Figure 1.A-5, taken from part of the Wisconsin survey (Bunner et al., 1972) shows soft X-ray counting rate versus time along the scan path plotted together with estimated expected transmission. The bands on the time axes coincide with the North Polar Radio Spur and approximately, it is seen, with regions of enhanced X-ray intensity. Notice that there is little if any detailed correlation of X-ray intensity with gas transmission. This, together with the observed large intensity in the galactic plane, is strong evidence that much of the soft X-ray emission originates within the bounds of the galaxy's interstellar gas.

Thirdly, there are at least three soft X-ray emitting regions of small angular extent: Puppis-A, Vela-X (Palmieri et al., 1971; Grader et al., 1970) and the Cygnus Loop (Seward et al., 1971). Three others have been reported but to

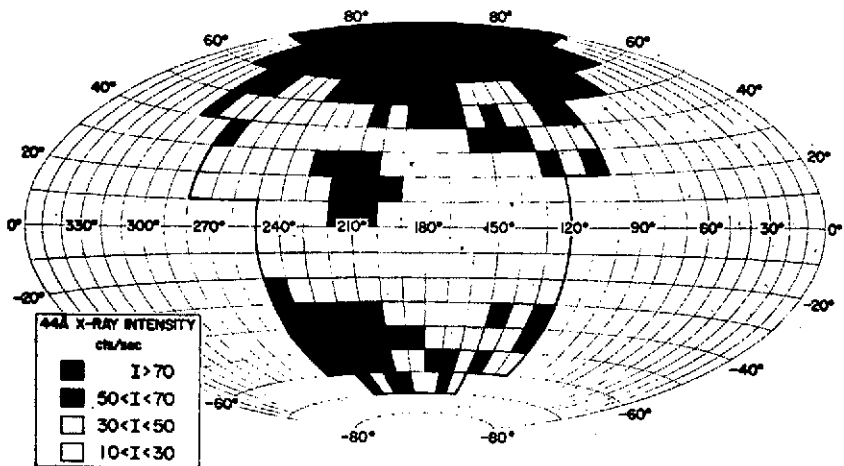


Figure 1.A-3. Spatial distribution of X-ray of  $E < 280$  eV. The coordinate system is centered at the galactic anti-center (Davidsen et al., 1972).

date have not been confirmed. The three confirmed sources are all supernova remnants, are at small galactic latitudes, and are of a class not numerous enough to account for the entire diffuse background. Of course, one or a few nearby remnants of large angular extent would confuse our whole picture. But galactic loop structures, aside from the North Polar Spur, do not appear to be strong soft X-ray emitters. Incidentally, the observation of soft X-ray emission from near the North Polar Spur has not been confirmed by others. Only one other observation near the Spur has been reported, but the sensitivity level is not clear (Hayakawa et al., 1972, preprint).

### NATURE OF THE LOCAL EMISSION

The nature of the local emission remains a mystery. Particularly puzzling is the relative constancy of the intensity in the galactic plane. Near  $l^{\text{II}} = 240^\circ$ ; for example, OAO-Lyman- $\alpha$  observations (Savage and Jenkins, 1972) show there are very small gas column densities out to several hundred parsecs. Similarly, the 21-cm emission profiles in this region show little or no low-velocity gas. Yet the soft X-ray intensity near  $l^{\text{II}} = 240^\circ$  appears featureless. If the emission in the plane were from a more-or-less uniformly-distributed population of stars, the soft X-ray intensity, one would think, would be large where the local absorbing gas density is small. Early type stars, it is true, are relatively rare in this region.

Also puzzling is the relation between the soft X-ray intensities measured in the  $E < 180$  eV (Boron-K edge filter) and  $E < 280$  eV (Carbon-K edge filter) regions (Bunner et al., 1973). X-rays of  $E < 180$  eV are more strongly attenuated by absorbing material. Thus in Figure 1.A-6 is shown the rates in the two types of

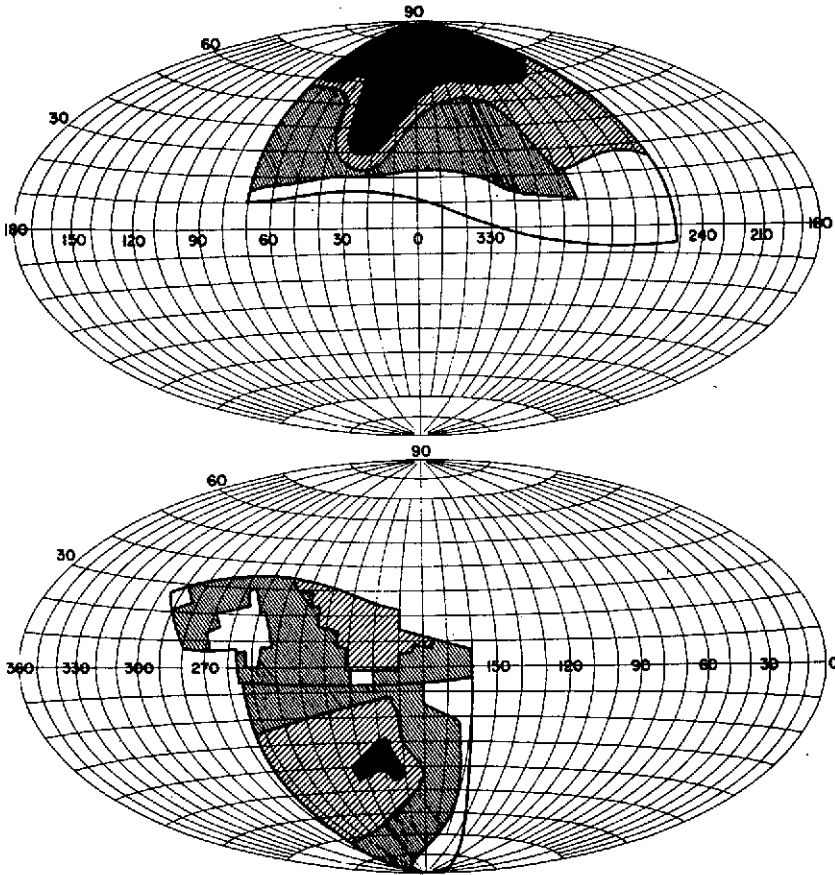


Figure 1.A-4. Spatial distribution of X-rays of  $E < 280$  eV. The upper coordinate system is centered at the galactic center, while the lower coordinate system is centered at the galactic anti-center (Bunner et al., 1972; Williamson, 1973 and Sanders, 1973).

detectors measured while the detectors were holding on a fixed high-latitude point as the rocket emerged from the Earth's atmosphere. As expected, the rates are not proportional to each other, but the Boron filter rate changes more rapidly than the Carbon-K filter rate. Yet when these two detectors scanned about the sky while free of atmospheric absorption, the two rates showed no systematic tendency that would suggest that intensity variations are due to simple variation in amount of absorbing material between source and detector. Apparently emission irregularities dominate spatial absorption features. Sometimes variations in the Carbon-K filter rates are accompanied by proportional variations in the Boron-K filter rates. This behavior is to be expected if diffuse X-ray emission and absorption are in equilibrium along the line of sight, or if the emission is so local that there is little (or at least constant) absorption in different directions.

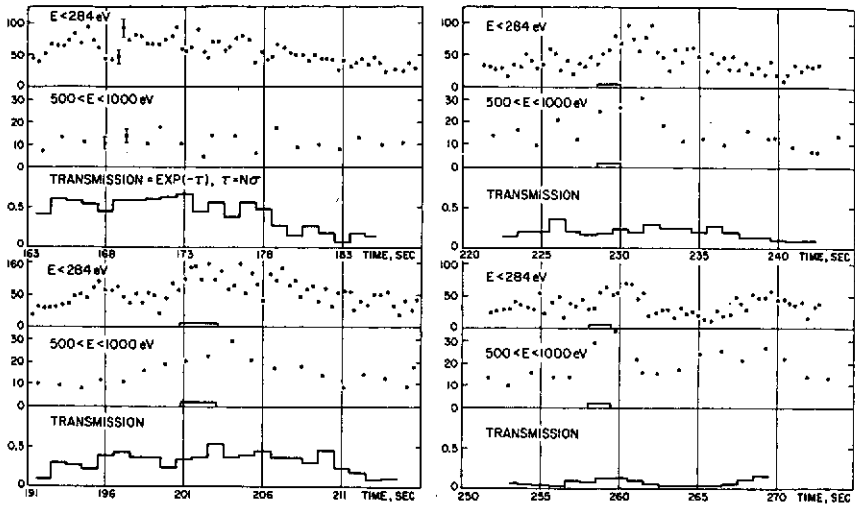


Figure 1.A-5. Counting rate of soft X-rays and X-ray transmission versus time along the scan path (data from Bunner et al., 1972).

Lack of confirmed discrete point sources of soft X-rays (Bunner et al., 1969) and the apparent granularity of the spatial structure of the diffuse flux (Gorenstein and Tucker, 1972) suggest that if the source is stars of a special type, their local space density must be large:  $\geq 10^2$  (pc) $^{-3}$  or more than 1 in 10 of all known stars.

In an early publication on this subject (Bunner et al., 1969), we suggested a population of stars with a scale height larger than that of the gas as a possible source of the soft diffuse X-rays. The model provides the enhanced intensity at high galactic latitudes, a source of the galactic plane emission, and requires no extragalactic component. At energies between 0.5 and 1 keV, however, the model predicts an enhanced intensity at intermediate galactic latitudes where absorption by the interstellar gas has not yet dominated the effect of increased path length through the emitting region. This enhanced intensity is not observed. The model has been discussed in more detail by several other authors (Gorenstein and Tucker, 1972; Garmire and Riegler, 1972; Davidsen et al., 1972; Kato, 1972; Hayakawa, 1972, preprint).

Emission by the interstellar gas itself would appear to provide a reasonable model for the origin of the diffuse X-rays in the galactic plane, because the absorption optical depth in the plane is large at whatever longitude. X-ray emission is a very inefficient process compared with ionization, however, and the resulting heating of the cool interstellar medium, if the X-rays are produced in the gas, cannot be accommodated even if a suitable charged-particle source is postulated ad hoc (Bunner et al., 1971). A multicomponent interstellar medium requires further

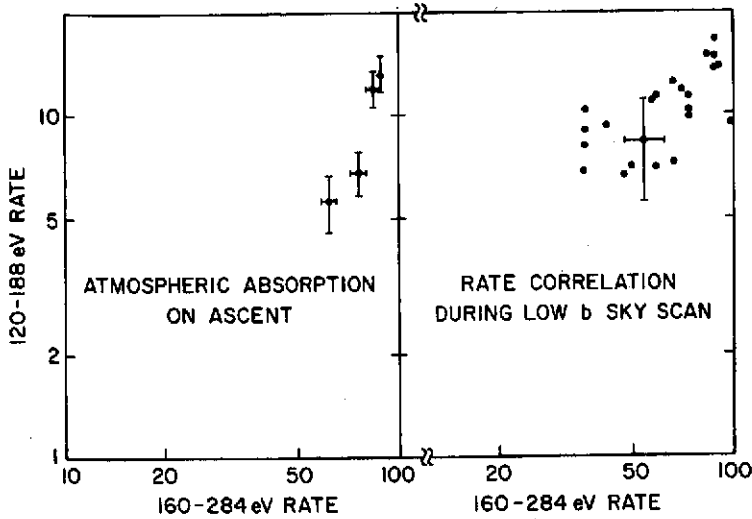


Figure 1.A-6. Counting rate of  $E < 180$  eV X-rays versus rate of  $E < 280$  eV X-rays (data from Bunner et al., 1973).

study as far as X-ray emitting possibilities are concerned. Emission by the interstellar gas or by objects with the same spatial distribution as the gas, results in an intensity proportional to  $(1 - e^{-\tau})$ , where  $\tau$  is the absorption optical depth. To match the observations, therefore, an extragalactic component is required and there results a net intensity proportional to  $A + B e^{-\tau}$ . This same form of the intensity dependence on  $\tau$  results from the assumption of extragalactic plus isotropic unabsorbed components, as discussed by Davidsen et al. (1972).

### EXTRAGALACTIC COMPONENT ?

Because of possible cosmological significance, there has been a persistent desire to have at least a large portion of the high latitude diffuse soft X-ray flux be interpreted as extragalactic in origin. The point is simply that the lack of red-shifted Lyman- $\alpha$  absorption in the spectra of quasars puts severe limits on the density of a possible intergalactic ionized gas. Hence, it is argued that if the universe is closed, the required mass must be in hot, ionized gas since the observed average density of mass in the form of galaxies is small by a factor of about 60. Extragalactic soft X-rays would provide a possible indicator of this hot gas. Or, turning the argument around, a demonstrated lack of extragalactic soft X-rays would put limits on the possible density and temperature of a postulated hot intergalactic medium (Field, 1972; Field and Henry, 1964).

The observed X-ray intensity enhancement toward the galactic poles, where the gas density is small and expected X-ray transmission is large, suggests but by no means demonstrates an extragalactic origin. In the first place, the sources could be mingled with or just outside the galactic gas. In the second place, the

correlation of intensity with expected gas transmission is poor. Of course, there are several possible causes for this poor correlation. The transmission is deduced from 21-cm hydrogen emission measurements, and helium, not hydrogen, is responsible for most of the soft X-ray absorption (Brown and Gould, 1970). There could be an unsuspected number of small unresolved cool clouds of gas, and these would confuse both the column density measurement and X-ray transmission estimates. These rationalizations would be comforting if we had prior knowledge of extragalactic soft X-rays and knew there to be no high-latitude galactic emission. But the reverse logic provides a decidedly weak case (if any) for a hot, intergalactic medium.

We hoped our search for absorption by the gas of the Small Magellanic Cloud (SMC) would clarify these matters. Before making the observation we decided among ourselves that the most unsatisfactory result possible would be an X-ray intensity that was constant as we scanned across the SMC for then, neither emission nor absorption by the SMC would be clearly demonstrated. That, of course, is exactly what happened (McCammon et al., 1971) as shown in Figure I.A-7.

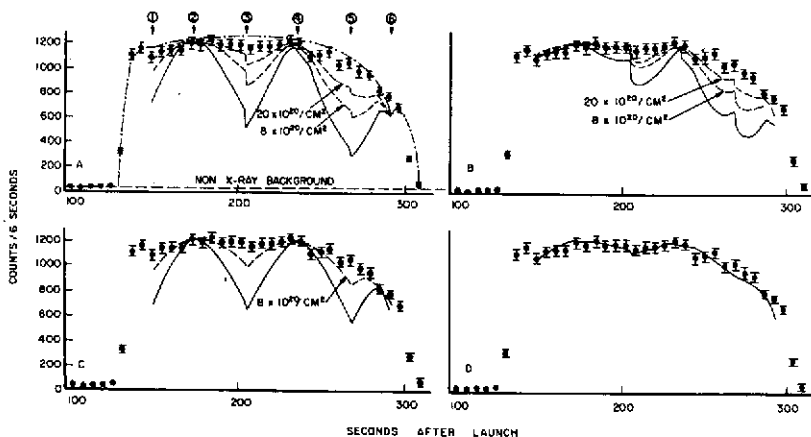


Figure I.A-7. X-ray counting rate of X-rays ( $E < 280$  eV) in directions near the Small Magellanic Cloud. Solid calculated curves assume in A: absorption by galactic and SMC gas; B: absorption by SMC gas only; C: absorption by galactic gas only; and D: extrapolated power law spectrum extragalactic; the rest: local origin, (McCammon et al., 1971).

Given this apparent lack of absorption by the SMC, we cannot exclude an extragalactic soft X-ray intensity ( $J_0$ ) that is just compensated by emission from the cloud itself. The consequences of this assumption, however, are rather interesting. Let  $S$  be the X-ray emission rate per nucleon of stellar matter in the SMC, and let  $n_s$  and  $n_g$  be the smoothed out and average nucleon density of stars and gas, respectively. If emission and absorption just compensate, then

$$J_o \sigma n_g = S n_s$$

where  $\sigma$  is the X-ray absorption cross section per hydrogen atom (Brown and Gould, 1970). The contribution to the extragalactic intensity from all galaxies out to a distance  $\sim c/2H$  is then

$$J_G \cong \frac{c}{2H} n_o S$$

where  $n_o$  is the average density of galactic matter. According to Noonan (1971),  $\rho_o$  for  $H = 50 \text{ km s}^{-1} \text{ Mpc}^{-1}$  is  $7.5 \times 10^{-32} \text{ g cm}^{-3}$  so  $n_o$  is  $\sim 4.2 \times 10^{-8} \text{ cm}^{-3}$ . We then have

$$\frac{J_G}{J_o} \cong \frac{c}{2H} n_o \sigma \left( \frac{n_g}{n_s} \right) \text{SMC}$$

In the SMC,  $n_g/n_s$  is about 0.5; therefore,  $J_G/J_o$  is about 0.8. In short, if we attempt to save the hot intergalactic medium by supposing that the lack of absorption by the SMC is really the result of self-emission, then the entire supposed extragalactic soft X-ray intensity, or at least a large portion would arise from the superposed emission from other galaxies. There is then little or no intensity left to be accounted for by the hot gas.

If instead we suppose the emission to be somehow proportional to the gas of the SMC and proportional to the gas in other galaxies too, with the same emissivity, the value of  $J_G/J_o$  is reduced by a factor of perhaps 10. This is because we estimate the ratio of gas mass to star mass in the SMC is about 10 times that of other galaxies.

Figure I.A-8 shows how the SMC measurement and measurements of the diffuse background radiation at higher X-ray energies restrict the temperature of a hot intergalactic gas. This is essentially Figure I.A-1 of Field and Henry (1964), but a Hubble constant  $H_o = 50 \text{ km} \cdot \text{s}^{-1} \text{ Mpc}^{-1}$  has been assumed rather than 100. The density assumed is sufficient to just close the universe ( $\Omega = 1$ ); the clumping factor ( $C = \langle n^2 \rangle / \langle n \rangle^2$ ) is taken as 1, the integration is carried out only to  $Z = 1$ , and the expansion is assumed to proceed with  $\gamma = 5/3$ .

As pointed out by Field (1972), the measured intensities in a real universe with a given  $T_o$  must exceed those plotted. Because the SMC measurement falls so near the "Big-Bang Envelope" line, it in fact (with  $H_o = 50$ ) excludes very little—only a band of temperatures near  $(2 \times 10^6) \text{ K}$ . On the other hand, and this is the point I wish to emphasize, the diffuse soft X-ray measurements cannot, taken alone, be said to provide positive evidence for a hot, dense, intergalactic medium.

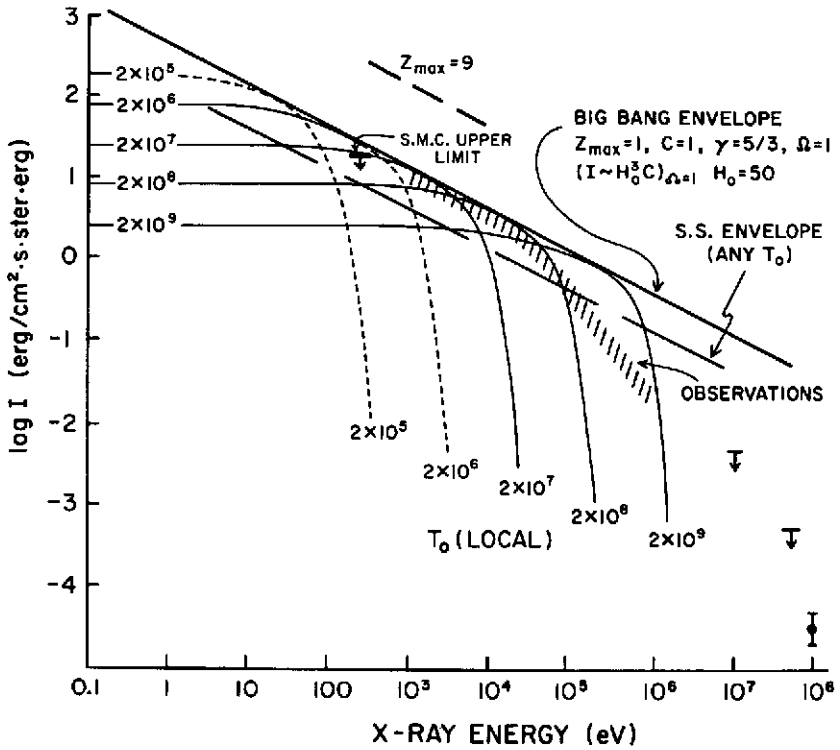


Figure 1.A-8. Predicted X-ray intensities from a hot intergalactic medium with density sufficient to close the universe (Field and Henry, 1964).

(Supported in part by NASA grant NGL 50-002-044)

## REFERENCES

- Brown, R., and R. Gould, 1970, *Phys. Rev. D.*, 1, p. 2252.
- Bunner, A., P. Coleman, W. Kraushaar, D. McCammon, T. Palmieri, A. Shilepsky, and M. Ulmer, 1969, *Nature*, 223, p. 1222.
- Bunner, A., P. Coleman, W. Kraushaar, D. McCammon, 1971, *Astrophys. J. Letters*, 167, p. 13.
- Bunner, A., P. Coleman, W. Kraushaar, and D. McCammon, 1972, *Astrophys. J. Letters*, 172, p. L67.
- Bunner, A., P. Coleman, W. Kraushaar, D. McCammon, and F. Williamson, 1973, *Astrophys. J.*, 179, p. 781.
- Davidson, A., S. Shulman, G. Fritz, R. Meekins, R. Henry, and H. Friedman, 1972, *Astrophys. J.*, 177, p. 629.

- Felten, J. E., 1973, *X-Ray and Gamma-Ray Astronomy, Proc. of IAU Symposium No. 55* (Madrid), H. Bradt and R. Giacconi, eds., D. Reidel, Dordrecht, Holland.
- Field, G. B., and R. C. Henry, 1964, *Astrophys. J.*, **140**, p. 1002.
- Field, G., 1972, *Annual Review of Astron. and Astrophys.*, **10**, p. 227.
- Garmire, G., and G. Riegler, 1972, *Astron. and Astrophys.*, **21**, p. 131.
- Gorenstein, P., and W. Tucker, 1972, *Astrophys. J.*, **176**, p. 333.
- Grader, R., R. Hill, and J. Stoering, 1970, *Astrophys. J. Letters*, **161**, p. L45.
- Hayakawa, S., T. Kato, T. Kohno, K. Nishimura, Y. Tanaka, and K. Yamashita, 1972, *Astrophys. and Space Sci.*, **17**.
- Kato, T., 1972, *Astrophys. and Space Sci.*, **16**, p. 478.
- McCammon, D., A. Bunner, P. Coleman, and W. Kraushaar, 1971, *Astrophys. J. Letters*, **168**, p. L33.
- Noonan, T. W., 1971, *Proc. Astron. Soc. Pacific*, **83**, p. 31.
- Palmieri, T., G. Burginyon, R. Grader, R. Hill, F. Seward, and J. Stoering, 1971, *Astrophys. J.*, **169**, p. 33.
- Sanders, W., 1973, unpublished Ph.D. Thesis, University of Wisconsin, Madison.
- Savage, B. D., and E. B. Jenkins, 1972, *Astrophys. J.*, **172**, p. 491.
- Seward, F., G. Burginyon, R. Grader, R. Hill, T. Palmieri, and J. Stoering, 1971, *Astrophys. J.*, **169**, p. 515.
- Williamson, F. W., 1973, unpublished Ph.D. Thesis, University of Wisconsin, Madison.

## A. THE X-RAY EMISSIVITY OF THE UNIVERSE: 2 TO 200 keV

Daniel Schwartz\* and Herbert Gursky  
*American Science and Engineering, Inc.*

### INTRODUCTION

This paper will discuss observational results on the diffuse X-ray background between 2 and about 200 keV. Appropriately to the sponsorship of this Symposium by the Laboratory for Theoretical Studies, we wish to present the results in a form suitable for theoretical discussion: namely, the volume emissivity function  $B(E)$  [ergs/s · Mpc<sup>3</sup> · keV emitted at energy  $E$ ]. The prescription for this is first to establish the spectral intensity  $I(E)$  [ergs/s · cm<sup>2</sup> · s · keV] measured at the earth, second to subtract the contribution due to known, discrete sources, and third to unfold the equation

$$I(E) = \frac{1}{d\Omega} \int \frac{B(E) dV}{4\pi D^2} \quad (\text{II.A-1})$$

which relates the measured intensity to the emissivity.

We may summarize the important characteristics of the diffuse X-ray background on which there is general agreement.

- A real, cosmic X-ray background exists, which may be truly diffuse or merely composed of discrete sources not yet resolvable. Nothing in this paper will depend on which of those two pictures one adopts.
- The diffuse X-rays are apparently isotropic over the sky, at least to an extent which precludes a galactic origin.
- All detailed theories have difficulty accounting for the production of the measured energy into the diffuse spectrum in the sense that they must hypothesize a rate of electron production, of heating, or of cosmological evolution which is not otherwise observed.

---

\*Speaker.

Strictly speaking, these three characteristics apply only to the energy range between 2 and 40 keV where the isotropy over the entire sky has been established by the X-ray experiments aboard the Uhuru and OSO-3 satellites.

### EXPERIMENTAL PROCEDURES

The measurement of the precise spectral flux density of an isotropic diffuse background is extremely difficult. The experimental problem is to determine, as a function of energy, what fraction of the instrumental output is due to internal background, where by the term "internal" we mean the output that the instrument would have if no diffuse X-rays within the nominal bandwidth entered the aperture. Internal background is also called "non-X-ray background," although in fact X-rays leaking from outside the aperture or higher energy X-rays which interact with only a partial energy loss may both contribute to internal background. Cosmic rays and geomagnetic particles are the primary ultimate sources of background.

Several basic techniques have been used for estimating internal background:

- The earth, assumed to emit no X-rays, has been used as a "shutter" and the entire instrument output obtained when the earth filled the field of view was assumed to be internal.
- A physical shutter that is opaque to X-rays has been flown. It either was moved into and out of place over the aperture or else used to cover one of several identical detectors.
- Different collimator solid angles have been flown, again either by motion of a shutter over one detector or fixed collimators over several identical detectors.

The satellite experiments have allowed an additional technique:

- Observation of the modulation of the internal background as a function of varying geomagnetic conditions, whereby it can be separated from the constant isotropic X-rays.

By and large, all the above techniques are adequate to give what might be considered first-order accuracy by astrophysical standards (that is, within 25 to 50 percent errors). However, the photon counting statistics formally imply a much higher precision; for a conservative example, a 200-s rocket flight might count diffuse X-rays at a rate of  $25 \text{ s}^{-1}$ , and accumulate 5000 counts between 2 and 10 keV. With statistical errors of only a few percent, the following inadequacies of internal background estimation (numbered to correspond to the techniques listed above) become apparent:

1. Below 10 keV the earth can sporadically emit X-rays due to auroral-type events. Above about 30 keV the atmospheric albedo becomes comparable to the diffuse X-ray background.

2. X-rays can be generated by interactions in a mechanical shutter and produce counts that would not be present when the aperture is open.
3. Data may be contaminated by diffuse geomagnetic electrons that appear identical to diffuse X-rays. For example, an electron of about 70 keV will on the average penetrate a 1-mil Be window with a few keV residual energy. However, because straggling is a dominant effect for subrelativistic electrons, a wide bandwidth (say 50 to 100 keV) of incident electrons might be able to contribute counts in the few keV range. These electrons are time variable, either trapped or precipitating, and can occasionally be found even on the L 1 magnetic shell (Schwartz, 1969). Electron fluxes far smaller than are significant for geomagnetic studies, of the order of  $0.01 \text{ (cm}^2 \cdot \text{s} \cdot \text{sr} \cdot \text{keV)}^{-1}$  at 70 keV, can contribute a few percent of the diffuse X-ray counting rate. The existence of electrons of about 10 keV as a severe, sporadic contaminant to one-fourth keV X-rays has been well known (Hill et al., 1970); however, the effect at higher energies in any given rocket flight has generally been ignored.
4. A truly constant internal background component, for example, radioactivity within the detector or vehicle, will not be modulated as a function of geomagnetic conditions.

The reality of effects 1 and 3 as significant considerations for observations between 7 and 40 keV was first shown by the OSO-3 experiment. Even when the internal background is measured perfectly accurately, it may simply change between the time it is estimated and the time when diffuse X-ray data is taken. Such changes may be due to motion of the vehicle in space, a change in orientation of the X-ray telescope axis relative to the earth's atmosphere or earth's magnetic field, a change in the configuration of matter around the detector, or temporal changes associated with geomagnetic activity. Table II.A-1 summarizes these background considerations, along with the principal method used and the most likely source of remaining systematic error.

To stress the difficulty of the absolute measurement of a diffuse spectral density, we may digress to a familiar example from the study of the universal microwave background. In radio astronomy an absolute flux is usually presented as the equivalent Rayleigh-Jeans blackbody temperature. Figure II.A-1 illustrates the derivation of the microwave temperature at 3.2 cm by Roll and Wilkinson (1966). Briefly, that experiment used a Dicke-type radiometer which measured the difference between an antenna horn pointed at the sky and a cold load maintained near liquid helium temperature. The top bar represents the measured cold load effective temperature. Each lower bar represents the result after applying the correction listed. The key feature here is that most of the corrections are of the same magnitude as the final result and therefore must be known to the same precision desired for the

Table II.A-1  
Internal Background

Method of Deduction	Used by	Contaminant	Might Affect
Earth occultation	PRL	Albedo	Leiden, PRL, Tata, Saclay
Opaque shutter	LLL, Bologna, ASE	Production in shutter	ASE, LLL
Variable solid angle	GSFC	Precipitating electrons	GSFC, Bologna, OSO-3, ASE, PRL
Modulation with vehicle motion	OSO-3, Leiden, PRL, Tata, Saclay	Radioactivity	OSO-3, LLL (satellite)

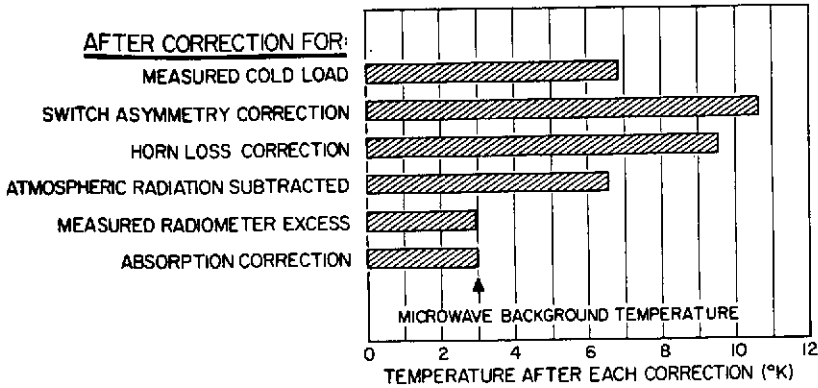


Figure 11.A-1. Derivation of the microwave temperature at 3.2 cm in the experiment of Roll and Wilkinson (1966). Several of the corrections have magnitude nearly equal to the final result of  $T = 3.0$  K. The random errors are an order of magnitude smaller than the estimated systematic effects.

microwave background. This experiment reported  $T = 3.0 \pm 0.5$  K, where the error represents an estimate of systematic effects. This 0.5 K error should be compared to a standard error of 0.06 K which the authors derived due to the random errors in each correction term. In general, only such random errors are reported for measurements of the X-ray background.

The generalizations discussed above, and the examination of the data presented below, has led us to adopt the following point of view: Most measurements of the flux density at various energies are reliable—they can be taken at face value with their quoted errors and compared with other results. However, direct measurements of a so-called “spectrum” by a single experiment are much less reliable or useful. The unreliability results because the uncertain systematic errors invariably are a different function of the energy than the diffuse X-rays. Thus, one or a few data points at one end of the energy range covered by a given experiment systematically distort the overall spectrum, even if many other spectral points are quite accurate. The usefulness of a spectral parameter is minimal for the following reasons: first, information is lost by reporting a few spectral parameters instead of many flux density measurements at various energies; second, the nonlinear least-squares fits which must be used (due to the complicated spectral response to the typical detectors) do not necessarily give unbiased estimates of the spectral parameters; third, the procedure starts by assuming a general form for the spectrum, such as power law or exponential shape; finally, it is not obvious how to combine spectral parameters from two different experiments spanning slightly different energy ranges—especially when each of those results has an estimated error that excludes the other. The spectral parameters which we will

present below should be interpreted first of all as merely giving a numerical representation of all the data, although one should certainly discuss the physical interpretation of any spectral representation.

### OBSERVATIONAL RESULTS

Figure II.A-2 presents a selection of published flux density points for the diffuse X-rays between 2 and 200 keV. The plot gives the energy flux in

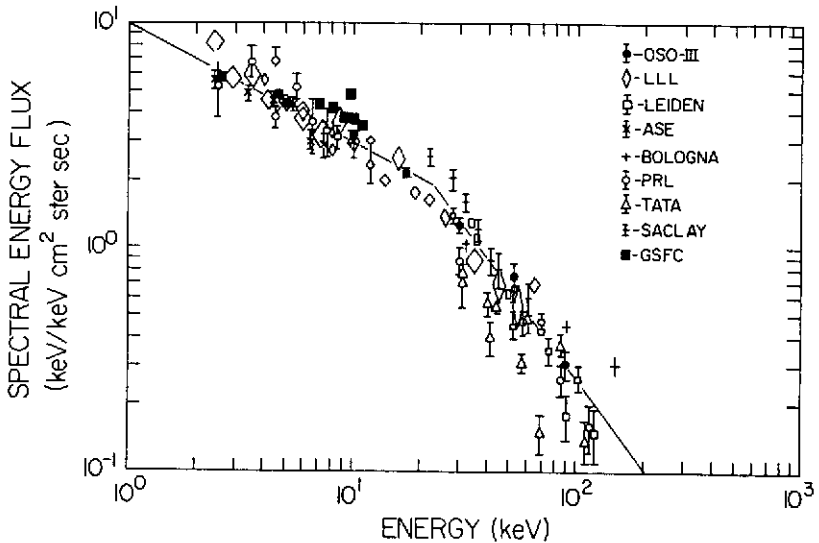


Figure II.A-2. A selection of published energy flux measurements of the diffuse X-ray background. Results presented only by giving spectral parameters, and points with greater than 30 percent error estimates are excluded. The data show a general consistency, with the high rate points around 10 keV and 150 keV possibly due to electron contamination. The slope increases with higher energy.

keV/keV·cm<sup>2</sup>·s·sr. Results reported only by giving spectral parameters are not included. Points with reported relative errors larger than 30 percent, and estimates of upper limits, are also excluded. In general, only the latest results of a given group are shown. Although the points with the smallest error bars tend to be hidden in such a plot, we can see that the bulk of the points do fall within a  $\pm 50$ -percent error band, and therefore we may expect the precision of the mean to be still higher. The balloon-borne measurements shown here (except for Manchanda et al., 1972) do not contain additional so-called "Compton scattering" corrections for reasons discussed below. The total data suggest a gradual steepening of the spectrum from a few keV up to 100 keV; detailed analysis of several of the experiments confirms this conclusion.

### Rocket-borne Observations

The key feature of rocket experiments is that they generally operate in the "cleanest" environment with regard to internal background. They are above the secondary cosmic radiation produced in the earth's atmosphere and below trapped particle populations. (Sporadic electron precipitation events may still affect any one observation.) The major drawback is that the observation lasts at most a few minutes. This usually does not allow, for example, a program that alternates measurements of diffuse and internal background to verify that the latter is constant.

Consider first the proportional counter observations shown in Figure II.A-2 (LLL: Palmieri et al., 1971; ASE: Gorenstein et al., 1969; GSFC: Boldt et al., 1969; PRL: Prakasarao et al., 1971). In this energy range, 2 to 10 keV, shielding and collimation is easily done with passive structural elements. The fields of view used range from 20 square degrees in the LLL experiment (shown as the eight largest diamonds between 2.4 and 8.7 keV) to 500 square degrees by GSFC. The PRL measurement was carried out at the geomagnetic equator; the GSFC and ASE flights from White Sands occurred at a magnetic shell of approximately  $L = 1.7$  to  $1.8$ . The PRL counters were filled with a xenon/methane mixture, the others with an argon/methane mixture. ASE and LLL determined internal background with a rocket door closed, PRL while looking at the earth, and GSFC by having a movable shutter that gave five different solid angles between 0.125 and 0.17 sr as well as a completely occulted position.

Agreement among the various experiments is rather good. This may be expected because proportional counters generally have several hundred  $\text{cm}^2$  areas and because the X-ray flux is constantly increasing to the lowest energies. The signal-to-background ratios obtained were between 3 and 10 to 1.

We have omitted two results which suggested spectral line features in the background around 5 and 7 keV (Ducros et al., 1970; Henry et al., 1971). Boldt et al. (1971), have reported an upper limit for such a feature at 7 keV of a factor of 10 below the NRL result. This applies to an observation at galactic latitudes from  $+40^\circ$  to the North Pole. It is probably fair to say that with the difficulties of establishing a continuum shape accurately, the existence of line fluxes remains to be proven in future experiments. We may comment that the unfolding of spectral data from a proportional counter response is by no means trivial. Such unfolding basically depends on calculation rather than calibration, since both the X-ray and particle spectra in space are very different than in the laboratory.

The proportional counter measurements may be compared with a satellite experiment of LLL (Cunningham et al., 1970; three small diamonds at 4.6, 8, and 12 keV). This involved a NaI crystal with a  $0.76\text{-cm}^2 \cdot \text{sr}$  telescope

factor aboard a polar orbiting satellite. A mechanical shutter periodically occulted the detector to allow background estimates. Only about 15 minutes of data (apart from solar and discrete source observations) was taken before a failure during the second day of operations.

The results of LLL (intermediate sized diamonds: Toor et al., 1970) and Bologna (Horstman-Moretti et al., 1971) were obtained with rocket-borne NaI counters. These detectors employed passive shielding lined with a plastic anticoincidence scintillator to define fields of view of about 900 square degrees. The Livermore data are noteworthy because this was the only experiment other than OSO-3 to span a range from below 10 keV to above 40 keV. The spectral results were reported as allowing a power law fit; however, the error bars above 30 keV are clearly large enough to be also consistent with a considerable change in slope.

The four data points of the Bologna group (a measurement of  $0.62 \pm 0.04$  at 52 keV is blacked out by other data points) are obtained with an ideal technique; one of four identical detector units is blocked so that internal background measurements are continually taken along with the diffuse X-ray data. Again, we suggest contamination by a sporadic electron population as the cause of the apparently high points at 90 and 150 keV. This is not an unlikely occurrence at the invariant magnetic latitude of  $38^\circ$  ( $L = 1.6$ ) of this observation. The 0.2-mm ( $54\text{-mg/cm}^2$ ) Al window would allow electrons of roughly 100 to 400 keV initial energy to enter the NaI volume with 50 to 200 keV residual energy, considering straggling. The OSO-3 upper limit of  $0.18\text{ keV}/(\text{keV}\cdot\text{cm}^2\cdot\text{s}\cdot\text{sr})$  at 150 keV, not shown in Figure II.A-2, cannot otherwise be reconciled with this data.

### Balloon-borne Observations

The dominant feature of the balloon-borne observations is that there exists a significant, diffuse flux of X-rays produced in the atmosphere. These must be separated from the diffuse cosmic X-rays by some indirect line of reasoning. Figure II.A-3 schematically illustrates the observational situation. The top solid curve is the counting rate that a vertically pointed telescope with a  $9^\circ$  to  $20^\circ$  cone-angle (as used in the four experiments plotted on the previous graph) might record as a function of atmospheric depth. The lower solid curve is that which a shuttered detector might record and is the internal background defined earlier. Only the Leiden-Nagoya group actually used such a shutter; the others effectively lumped internal background along with atmospheric.

At depths below 10 to  $20\text{ gm/cm}^2$ , the difference in the two curves is due entirely to the atmospheric X-rays. (We intend the figure to show that the atmospheric X-rays can have a different, although similar, dependence on depth compared to the internal background.) Both the internal and

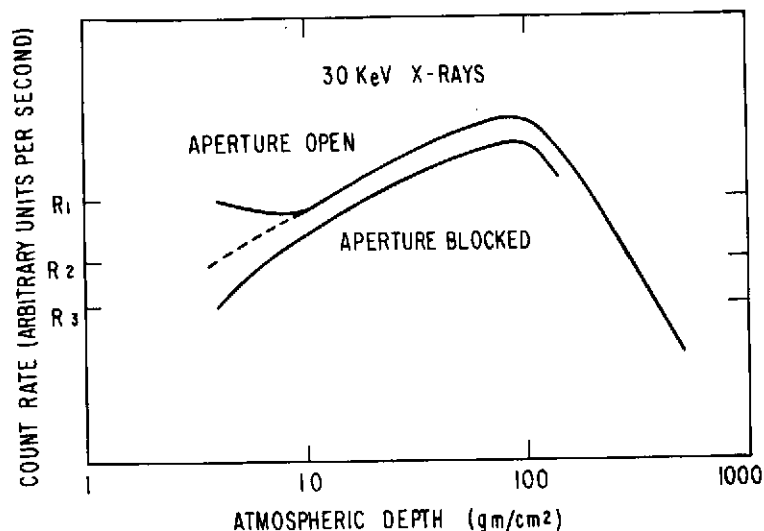


Figure 11.A-3. Representation of the counting rates of a vertically mounted, wide-aperture telescope. Diffuse X-rays cause the turn-up of the "aperture-open" curve. One must estimate the atmospheric contribution (dashed line) to deduce the diffuse intensity.

atmospheric background originate from the soft component of the energy degradation of the primary cosmic rays, and show the Pfozter transition maximum at about  $90 \text{ gm/cm}^2$ .

The turn-up of the rates at altitudes higher than about  $10 \text{ gm/cm}^2$  is interpreted as the observation of X-rays external to the atmosphere. X-rays of 30 keV have a mean free path of  $3.4 \text{ gm/cm}^2$  for photoelectric absorption compared to ceiling depths of 3 to  $7 \text{ gm/cm}^2$  attained in the various experiments. The dashed curve represents an extrapolation which each experimenter must make for the assumed behavior of the atmospheric X-rays. The difference ( $R_1 - R_2$ ) is then multiplied by the photoelectric attenuation at the given ceiling depth (which may be a factor of 2 to 8 correction) to derive the diffuse flux external to the atmosphere.

There has been some discussion (for example, Horstman and Horstman-Moretti, 1971) that additional corrections need be applied due to single and multiple scattering of diffuse X-rays by the atmosphere, which eventually enter the detector aperture. This discussion is important and valuable since such a physical process must certainly take place. However, it is not appropriate to apply such a correction to ( $R_1 - R_2$ ) for the following simple reason: Once the diffuse X-ray scatters in the atmosphere it loses its identity and is no different than an atmospheric X-ray that might be produced by

electron bremsstrahlung at the exact same location. But all the atmospheric X-rays have presumably been accounted for by the dashed line extrapolation. One may well ask whether the dashed line is an accurate extrapolation of the atmospheric background, but this is a very different and very important problem.

In principle, one could study the difference between  $R_1$  and  $R_2$  as a function of depth, and test whether it changes in the exact manner expected for photoelectric absorption of X-rays external to the atmosphere. In practice this is not decisive because the points below float altitude are only sampled for a relatively brief time during ascent or descent. As  $(R_1 - R_2)$  becomes smaller, the absolute error on this difference becomes larger, and it may be that the data allows anything between zero and infinite absorption.

Strictly speaking, we might say that the true atmospheric X-ray curve could vary considerably from the intuitively simple extrapolations used, and that there might in fact be no diffuse X-rays at all. Returning to Figure II.A-2, we can let the scatter of the data speak for itself in illustrating the intrinsic accuracy which has been obtained. The lowest and highest points, by the Tata Institute (Manchanda et al., 1972) and Saclay (Rothenflug et al., 1968) groups, used an exponential law extrapolation. The Leiden (Bleeker and Deerenberg, 1970) and Physical Research Laboratory (Rangan et al., 1969) groups used a power law extrapolation for the rates versus depth. Each pair of groups spanned magnetic shells at least from  $L = 1$  to  $L = 1.7$ .

The detectors used in these experiments were all NaI crystals with some combination of passive shield and plastic anticoincidence. These give relatively high susceptibility to internal background. As the groups at UCSD, UCB, and MIT have developed detectors with lower internal background by using  $4\pi$  active-anticoincidence techniques, they have systematically tended to reduce the solid angle and concentrate on discrete source observations.

We may suggest a prescription for obtaining a more objective determination of the atmospheric X-ray contribution at ceiling. This is based on the concept of a source function  $S(E, x)$  (X-rays of energy  $E$  produced  $(\text{cm}^3 \cdot \text{s})^{-1}$  at a depth  $x$ ). This technique has been used successfully by Peterson, Schwartz, and Ling (1973) to interpret counting rates of atmospheric  $\gamma$ -rays as a function of depth. Figure II.A-4 shows the basic geometry. The function  $S$  is strictly a convenient mathematical form, containing a few constants to be determined. With the detector in a fixed orientation at a depth  $h$ , the source function multiplied by the projected detector area  $A(\theta)$  and by the attenuation  $\exp(-\mu r)$  (where  $\mu$  is the total coefficient for any interaction) is integrated over all of space. The unknown constants in  $S$  should be determined while the detector is at large depths ( $h$ ) and/or while it is oriented downward. Then with the detector pointed upward at the float altitude,

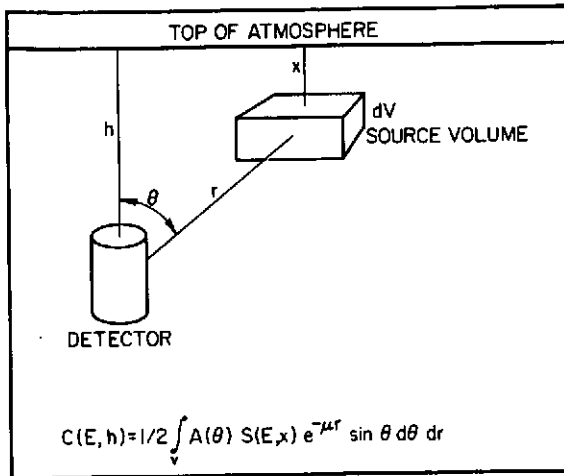


Figure II.A-4. Geometry for calculating the contribution of atmospheric X-rays to the counting rate  $C(E, h)$  of a detector at depth  $h$  (from Peterson et al., 1973). An empirical volume production rate function  $S(E, x)$  is constructed as a function of depth  $x$ . The integral over the volume of the atmosphere gives the contribution for a fixed detector orientation.

$C(E, h)$  would simply be calculated and subtracted from the total output. Physically, of course,  $S$  will contain a contribution from Compton-scattered diffuse X-rays; however, this need not ever be considered explicitly.

### OSO-3 Observations

Finally, we will discuss the data points obtained by the UCSD X-ray telescope aboard OSO-3. These points were relatively inconspicuous in Figure II.A-2 because of their small error bars; yet they are of significance as the only case in which a power law spectrum could not fit the data of one single experiment. Because of this significance, Schwartz and Peterson (preprint) have reconsidered the results with regard to some suggested corrections for spallation-induced radioactivity, fluorescence radiation from the shield, and energy dependence of the geometry factor, and we have confirmed the inconsistency of a power law with the OSO-3 data. The best fit of a power law gives  $\chi^2 = 20$  for 3 degrees of freedom.

Briefly, the OSO-3 experiment was a  $9.5 \text{ cm}^2$  NaI crystal, actively collimated by a CsI annulus to a  $23^\circ$  full-width half-maximum conical field of view. The satellite had a 550-km altitude,  $33^\circ$  inclination orbit so that magnetic shells from  $L = 1$  to  $L = 2$  were sampled, and the lower edge of the South

Atlantic trapped particle region was traversed during half of the 16 orbits per day. The data were telemetered in six logarithmically spaced channels between 8 and 210 keV. Certain integrated and solar-pointing rates were also telemetered.

The most serious contributor to the background was the existence of sporadic, charged particles. Selection criteria to minimize contamination were developed. These limited the upper threshold integral rate, required  $L \leq 1.2$ , and accepted data only when pointed within the local magnetic loss cone. This caused rejection of about 80 percent of the data.

The next most serious source of background was due to radioactivity, which built up when inside the trapped particle regions and which then decayed until the next traversal of the South Atlantic Anomaly. A 15-hour half-life decay curve gave a good fit to the monitor count rates in the interval 30 minutes to 12 hours after penetrating the particle belts. The activation coefficients derived from these monitor rates were used to correct the diffuse counting rates over the same time span. The diamonds and upper limit in Figure II.A-5 (taken from Schwartz and Peterson, preprint) show the effective spectrum at the NaI detector, due to radioactivity. Phenomenologically, this spectrum is interpreted as Compton scattered  $\gamma$ -rays from the  $Mg^{24}$  daughter produced by the reaction  $Al^{27} (n, \alpha) Na^{24}$  15 hour  $Mg^{24}$  taking place throughout the satellite. The solid line is a spallation spectrum measured by Dyer and Morfill (1971), and plotted with an arbitrary normalization. The horizontal bars integrate this spectrum over the OSO-3 energy channels and normalize it to be consistent with the 7.7- to 12.5-keV limit. Thus the spallation mechanism is probably not significant on this time scale.

This radioactivity correction could be made because it varied on a 15-hour time scale. However, radioactivity with a half-life of a week or longer would not decay significantly in one day and might in principle be a constant, unnoticed contaminant of the data. By subtracting the rates when looking at the earth from the sky rates on day 44 after launch, we show that at least 95 to 90 percent of the reported diffuse flux for the three channels from 7.7 to 38 keV cannot be contaminated by radioactivity. The points between 38 to 110 keV might require further downward correction, but this will only accentuate the inability of a single power law to fit the data.

Examination of the detailed rates versus time after launch in the 38- to 65-keV channel, compared with the predicted build-up curve using the proton dose by Dyer, Engel, and Quenby (1973) led us to conclude (Schwartz and Peterson, preprint) that at most one-third of that proton dose would be the appropriate normalization. We have increased the error bars of the upper channels so that such a radioactivity correction (if valid) would only reduce the quoted fluxes by 2 standard deviations.

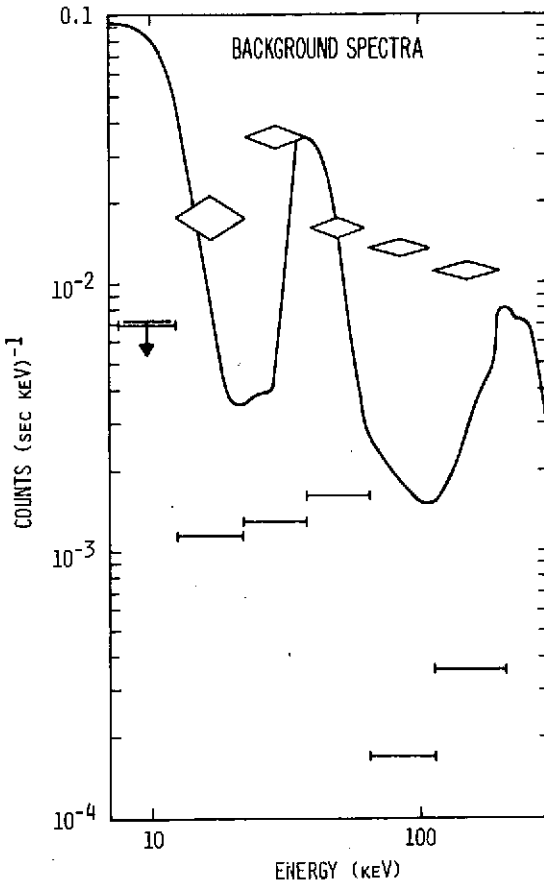


Figure II.A-5. Diamonds and upper limit: Effective spectrum of radioactivity background observed by the OSO-3 X-ray telescope immediately after emergence from the proton belts. Solid line: an effective spectrum due to spallation measured by Dyer and Morfill (1971) as the difference in CsI crystal output measured 86.5 minutes and 11.2 hours after irradiation. The normalization is arbitrary. Horizontal bars: The same spallation spectrum integrated over the OSO-3 energy channels and normalized for consistency with the measured limit at 10 keV (from Schwartz and Peterson, preprint).

The most significant correction necessary to the previous OSO-3 results has been the allowance for K-shell X-radiation escaping from inside the collimator, as suggested by Horstman (Dumas et al., 1973). Diffuse X-rays between 35 and a few hundred keV striking the inside of the CsI collimating annulus would not trigger the shield anticoincidence threshold. A certain fraction of the resultant K-escape X-rays will be emitted into the central detector, causing a spurious contribution to the 22- to 38-keV channel. The Monte Carlo program of J. Matteson, which has been used extensively at UCSD to predict background rates of X-ray and  $\gamma$ -ray detectors, was used to calculate an effective telescope factor (solid angle times area) for such fluorescent X-ray events as a function of the incident photon energy above 34 keV. The product of this telescope factor and the diffuse spectrum  $2200 E^{-3}$  previously estimated (Schwartz et al., 1970) was integrated from 34 to 210 keV. As a result, the point at 30 keV was reduced 17 percent.

### Summary

In Figure II.A-6 we attempt to summarize the most reliable data selected according to the following criterion; the experiment either was operated over a range of geomagnetic conditions or it incorporated some direct means for assessing effects of electron contamination. The Livermore rocket experiment (Palmieri et al., 1971) had a methane-filled anticoincidence proportional counter over the entrance to their argon detector. This experiment, of all the rocket and satellite observations, should be uniquely free of charged-particle contamination. The ASE experiment (Gorenstein et al., 1969) incorporated pulse-shape discrimination, which is sensitive to relativistic electrons which may deposit only a few keV total energy but spread out over a long path. That experiment also had one counter unit with a 1-mil Be window and three counter units with 3-mil Be windows. These windows would show very different transfer characteristics for the 70- to 100-keV geomagnetic electrons.

The three experiments of the Leiden-Nagoya group (Bleeker and Deerenberg, 1970) provide key evidence for the reality of a diffuse component above 40 keV. The experiments took place at  $20^\circ$ ,  $40^\circ$ , and  $50^\circ$  geomagnetic latitudes. The flux densities at the various latitudes are in reasonable agreement, while the inferred component of 20- to 40-keV atmospheric X-rays is a factor of 5 higher at the northern latitude.

The solid curve shows the function

$$I(E) \text{ (keV/keV cm}^2\text{-sr-s)} = \begin{cases} 10E^{-0.52} & \text{for } 1 \leq E \leq 23 \text{ keV} \\ 140E^{-1.37} & \text{for } E > 23 \text{ keV} \end{cases} \quad (\text{II.A-2})$$

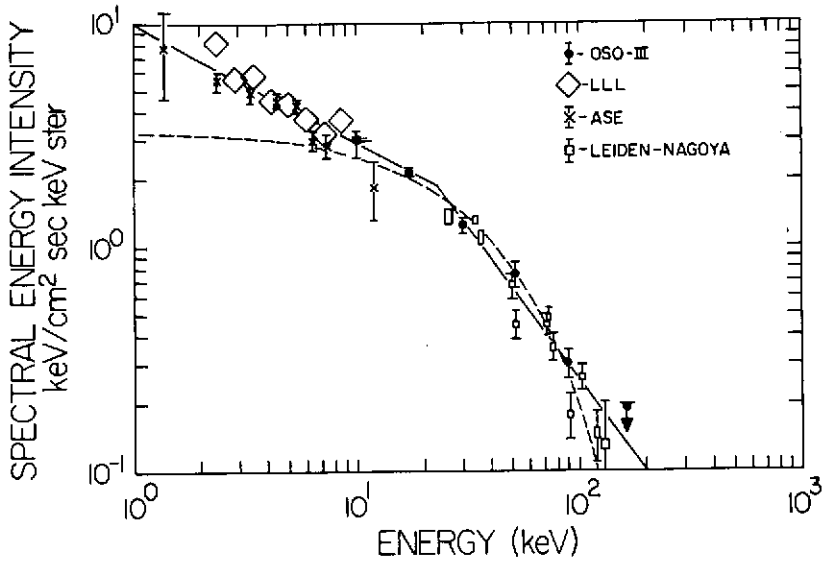


Figure 11.A-6. An attempt to select the most reliable experimental data between 2 and 200 keV. The observations either utilized some direct means for assessing effects of electron contamination or else operated over a range of geomagnetic conditions. The solid curve shows the power law  $10E^{-0.52}$  keV/(keV · s · cm<sup>2</sup>·sr) below 23 keV and  $140E^{-1.37}$  above 23 keV. The dashed line is the function  $3.3 \exp (-E/34.4)$ .

and the dashed curve is

$$I(E) = 3.3 \exp (-E/34.4) \tag{II.A-3}$$

(see Cowsik and Kobetich, 1972)

The sharp break in the power law representation does not have physical reality—this is merely a minimum parameter power law representation of the data. The key observational conclusion of such a representation is that the overall change in the slope is at least an exponent of 0.9. The errors in the power law indices are roughly  $\pm 0.1$  below 23 keV and  $\pm 0.15$  from 30 to 100 keV. The error in the effective kT of Equation (II.A-3) is somewhat larger, as we have arbitrarily tried to fit the data only in the 10- to 100-keV range.

In Figure II.A-7, we wish briefly to compare with the data from a few hundred eV to a few MeV. We have not attempted any completeness in the higher and lower energy data. The ASE point at 270 eV was obtained with a focusing collector and is an upper limit in the sense that Gorenstein and Tucker (1972) argue it might all result from galactic sources. The

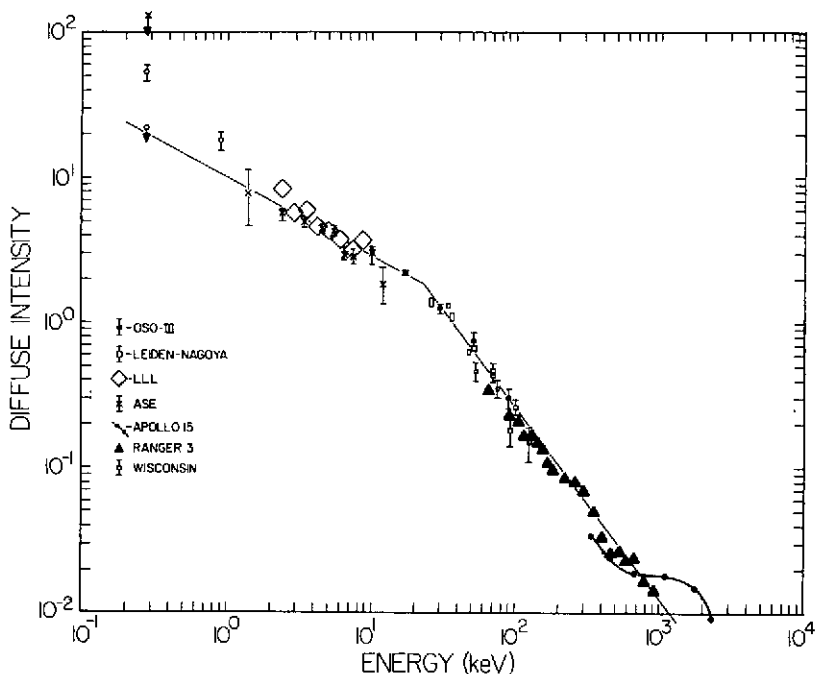


Figure II.A-7. The data and power-law fit of Figure II.A-6 is shown along with a sample of measurements at higher and lower energies. The Ranger-3 data are only an energy-loss spectrum, while for the Apollo results the true photon spectrum has been unfolded and a correction applied for spallation induced radioactivity.

Wisconsin upper limit is based on the absence of absorption by the Small Magellanic Cloud (McCammon et al., 1971, see also Chapter I.A). The Ranger-3 data (Metzger et al., 1964) represent only an energy-loss count rate spectrum, while the Apollo-15 data (Trombka et al., 1973) have been unfolded to a photon spectrum and corrected for spallation induced radioactivity (see Chapter III.A).

### THE EMISSIVITY FUNCTION

If we assume a constant emissivity  $B(E)$  per unit coordinate volume, through which we look a distance  $R_{\max}$ , then Equation (II.A-1) becomes simply

$$I(E) = \frac{1}{4\pi} B(E) R_{\max} \quad (\text{II.A-4})$$

Equation (II.A-4) holds to within a factor of 2 for the popular models of Friedmann cosmologies, providing there are no significant evolutionary effects and providing that we take  $R_{\max} = 1/2 (c/H_0)$ . We will adopt  $H_0 = 75 \text{ km/s} \cdot \text{Mpc}$ . Then from Equation (II.A-2), we have

$$B(E) = \begin{cases} 2.1 \times 10^{-26} E^{-0.52} \text{ keV}/(\text{cm}^3 \cdot \text{s} \cdot \text{keV}) & \text{for } E \leq 25 \text{ keV} \\ 2.9 \times 10^{-25} E^{-1.37} \text{ keV}/(\text{cm}^3 \cdot \text{s} \cdot \text{keV}) & \text{for } E \geq 25 \text{ keV}. \end{cases}$$

For the integrated emissivity between 2 and 7 keV,  $B = 2.2 \times 10^{39} \text{ ergs/s} \cdot \text{Mpc}^3$ . We stress that  $B$  is determined directly from the observations, and subject to the qualifications above, it will not change significantly. The red shift will preserve a power-law shape.

### CORRECTION FOR DISCRETE SOURCES

Characteristics of the classes of discrete extragalactic sources identified in the 2U catalog (Giacconi et al., 1972) are summarized in Table II.A-2. In Figure II.A-8 we illustrate how they modify the emissivity function. We must stress that the spectra and total emissivities are very poorly determined for the cases where we only have one object in the class: the Seyfert galaxy NGC 4151, the radio source Cen A, and the quasar 3C 273. We have normalized the total power of each source according to the quantity  $n_{0j}$  and represented its spectrum as the flat end of the range allowed by Uhuru in order to obtain the closest agreement to the background shape. The solid curve is the power-law representation presented earlier. The higher dashed curve represents the subtraction of the identified extragalactic sources. The bottom dashed curve represents a possible residual emissivity if we hypothesize that the unidentified high-latitude sources are a new class of extragalactic object that produces one-half the background observed from 2 to 7 keV.

### INTERPRETATION AS THERMAL BREMSSTRAHLUNG

Figure II.A-9 replots the data on a semilog scale. Correction for discrete sources allows the exponential fit to hold above 5 keV. The two solid curves (Field, 1972) are the temperature-independent lower limits to radiation from a hot intergalactic plasma of sufficient density to close the universe. In the big bang model, the gas is suddenly heated to a temperature  $T_0$  at an epoch  $z = 1$  and cools adiabatically with an index  $\gamma = 5/3$ . Field uses a Hubble constant  $H_0 = 50 \text{ km/s} \cdot \text{Mpc}$ . The predicted spectrum is approximately exponential with e-folding energy  $k T_0$  and would be tangent to the lower limit curve at  $E_0 = (0.57) k T_0$ . The observed radiation falls a factor of 2 below the minimum, and the discrepancy is worse if the

Table II.A-2

## Contribution of Discrete Sources to the X-Ray Background

Source	No. in 2U Catalog	Spectrum (kT, for 1-10 keV range)	Luminosity ( $\dot{J}$ ) ergs/sec	Density $n_k$ (Mpc) <sup>-3</sup>	Emissivity $B_k \frac{\text{ergs}}{\text{s} \cdot (\text{Mpc})^3}$	Fraction of Background f
Normal galaxies	3	5 keV	$2 \times 10^{39}$	0.03	$6 \times 10^{37}$	0.027
Giant radio galaxies	1	10 - 15	$3 \times 10^{41}$	$3 \times 10^{-5}$	$9 \times 10^{36}$	0.004
Seyfert galaxies	1	(1.5 - 6.5)	$10^{42}$	$3 \times 10^{-4}$	$3 \times 10^{38}$	0.14
Rich clusters	5	5 - 8	$3 \times 10^{44}$	$2.5 \times 10^{-7}$	$7.5 \times 10^{37}$	0.034
OSOs	1	(4 - 15)	$3 \times 10^{45}$	$10^{-8}$	$3 \times 10^{37}$	0.014
Subtotal	11				$4.8 \times 10^{38}$	0.22
Observed background		15 - 20			$2.2 \times 10^{39}$	1.0
Unidentified sources	22	4 - 6	$5 \times 10^{43}$	$10^{-5}$	$5 \times 10^{38}$	0.25 ?

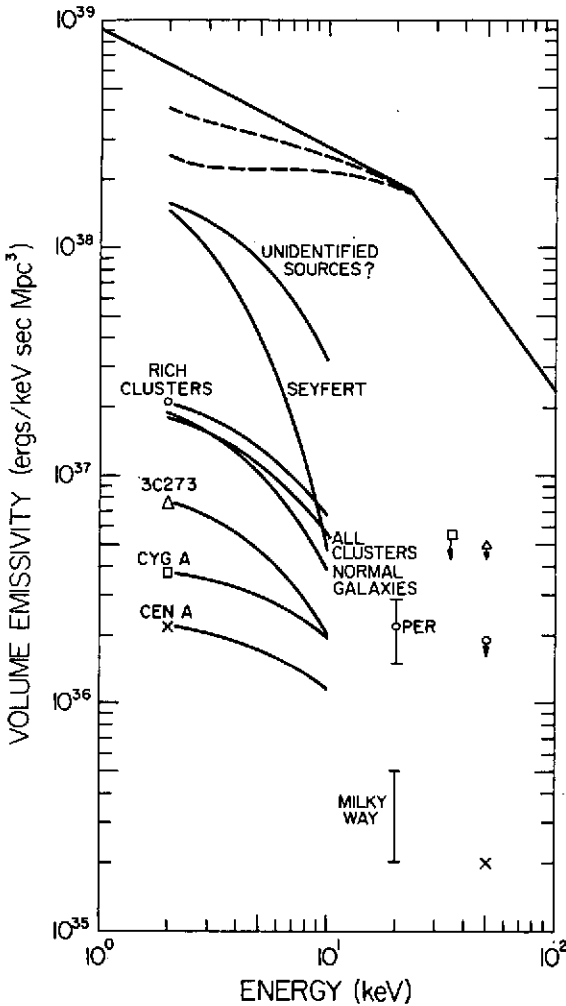


Figure II.A-8. Volume emissivity functions: Top line is emissivity derived from power-law representation of Figure II.A-6; five curves for identified extragalactic sources are derived from estimates of intrinsic luminosity and spectra based on the 2U catalog; upper dashed curve corrects diffuse emissivity for these sources; lower dashed curve is resulting diffuse emissivity if we postulate that unidentified high latitude sources (observed to have a spectrum with  $kT = 5$  keV) comprise 50% of the 2-7 keV diffuse background; points at 20 keV are from UCB and UCSD OSO-7 experiment.

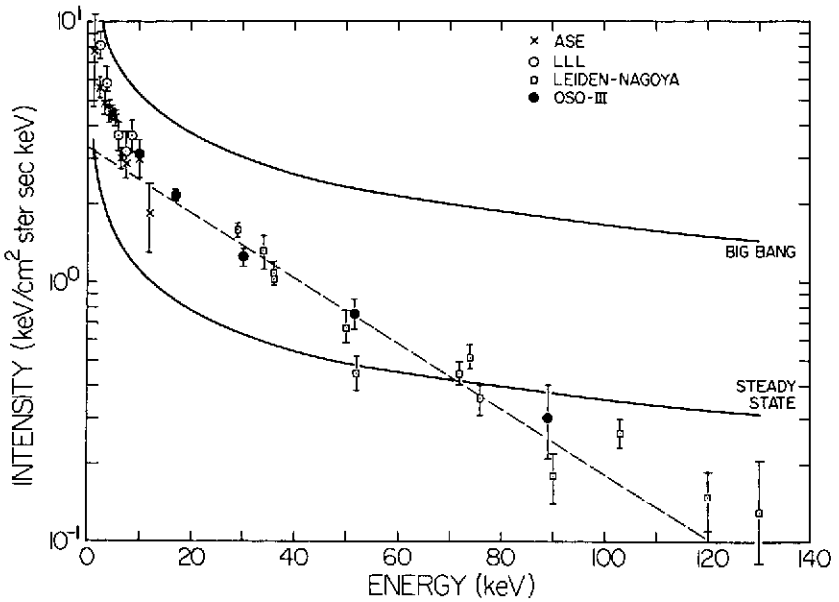


Figure 11.A-9. The data from Figure 11.A-6 are plotted on a semilog scale. The dashed line is the function  $3.3 \exp(-E/34.4)$ . The solid lines are "lower limits" to the emission from a hot intergalactic plasma of sufficient density to close the universe calculated by Field (1972) with a Hubble constant  $H_0 = 50 \text{ km/s} \cdot \text{Mpc}^3$ . The X-ray observations are at a factor of two discordant with the big bang model.

intergalactic medium is not smooth. The disagreement implies one or more of the following:

- The density of intergalactic plasma is  $2^{1/2}$  less than required for a closed universe, or  $n_0 = 2 \times 10^{-6} \text{ particle cm}^{-3}$ ;
- The Hubble constant is a factor  $2^{1/3}$  smaller, or  $H_0 = 40 \text{ km/s} \cdot \text{Mpc}$ ;
- The temperature  $T_0 \leq 3 \times 10^7 \text{ K}$ .

We hope we have not spent too much time discussing X-ray results at a  $\gamma$ -ray symposium. We have tried to make the point that the X-ray observations have a relatively high level of precision and that we can start using them to do some interesting physics. We look for many more exciting results and new ideas to come as study of the spectrum and of the isotropy is extended into the MeV region.

#### ACKNOWLEDGMENTS

We acknowledge conversations with L. Peterson, C. Dyer, B. Dennis, and H. Horstman regarding interpretation of the OSO-3 X-ray data. We thank E. Kellogg and S. Murray for discussion of the Uhuru results on extragalactic sources.

(This research was supported by NASA contract NAS 8-27973.)

#### REFERENCES

- Bleeker, J. A. M., and A. J. M. Deerenberg, 1970, *Astrophys. J.*, **159**, p. 215.
- Boldt, E. A., U. D. Desai, S. S. Holt, and P. J. Serlemitsos, 1969, *Nature*, **224**, p. 677.
- Boldt, E. A., U. D. Desai, S. S. Holt, and P. J. Serlemitsos, 1971, *Astrophys. J. Letters*, **167**, p. L1.
- Cowsik, R., and E. J. Kobetich, *Astrophys. J.*, **177**, p. 585.
- Cunningham, C., D. Groves, R. Price, R. Rodrigues, C. Swift, and H. Mark, 1970, *Astrophys. J.*, **160**, p. 1177.
- Ducros, G., R. Ducros, R. Rocchia, and A. Tarrus, 1970, *Astron. and Astrophys.*, **7**, p. 162.
- Dumas, A., H. Horstman, E. Horstman-Moretti, and D. Brini, 1973, *X-Ray and Gamma-Ray Astronomy, Proceedings of IAU Symposium No. 55*, (Madrid), H. Bradt and R. Giacconi, eds., D. Reidel, Dordrecht, Holland.
- Dyer, C. S., A. R. Engel, and J. J. Quenby, 1973, *X-Ray and Gamma-Ray Astronomy, Proceedings of IAU Symposium No. 55*, (Madrid), H. Bradt and R. Giacconi, eds., D. Reidel, Dordrecht, Holland.
- Dyer, C. S., and G. E. Morfill, 1971, *Astrophys. and Space. Sci.*, **14**, p. 243.
- Field, G., 1972, *Annual Review of Astronomy and Astrophysics*, **10**, Annual Reviews Inc., Palo Alto, p. 227-260.
- Giacconi, R., S. Murray, H. Gursky, E. Kellogg, E. Schreier, and H. Tananbaum, 1972, *Astrophys. J.*, **178**, p. 281.

- Gorenstein, P., E. M. Kellogg, and H. Gursky, 1969, *Astrophys. J.*, **156**, p. 315.
- Gorenstein, P., and W. Tucker, 1972, *Astrophys. J.*, **176**, p. 333.
- Henry, R. C., G. Fritz, J. C. Meekins, T. Chubb, and H. Friedman, 1971, *Astrophys. J. Letters*, **163**, p. L73.
- Hill, F. W., R. Grader, and F. D. Seward, 1970, *J. Geophys. Res.*, **75**, p. 7267.
- Horstman-Moretti, E., F. Fuligni, and D. Brini, 1971, *Il Nuovo Cimento*, **6 B**, p. 68.
- Horstman, H., and E. Horstman-Moretti, 1971, *Nature Phys. Sci.*, **229**, p. 148.
- Manchanda, R. K., S. Biswas, P. C. Agrawal, G. S. Gokhale, V. S. Iyengar, P. K. Kunte, and B. V. Sreekantan, 1972, *Astrophys. and Space Sci.*, **15**, p. 272.
- McCammon, D., A. N. Bunner, P. L. Coleman, and W. L. Kraushaar, 1971 *Astrophys. J. Letters*, **168**, p. L33.
- Metzger, A. E., E. C. Anderson, M. A. Van Dilla, and J. R. Arnold, 1964, *Nature*, **204**, p. 766.
- Palmieri, T. M., G. A. Burginyon, R. J. Grader, R. W. Hill, F. D. Seward, and J. P. Stoering, 1971, *Astrophys. J.*, **169**, p. 33.
- Peterson, L. E., D. A. Schwartz, and J. C. Ling, 1973, *J. Geophys. Res.*, in press.
- Prakasarao, A. S., D. P. Sharma, U. B. Jayanthi, and U. R. Rao, 1971, *Astrophys. and Space Sci.*, **10**, p. 150.
- Rangan, K. K., P. D. Bhavsar, and N. W. Nerurkar, 1969, *J. Geophys. Res.*, **74**, p. 5139.
- Roll, P. G., and D. T. Wilkinson, 1966, *Phys. Rev. Letters*, **16**, p. L405.
- Rothenflug, R., R. Rocchia, D. Boclet, and P. Durouchoux, 1968, *Space Res. VIII*, p. 423.
- Schwartz, D. A., 1969, unpublished Ph. D., Thesis, University of California at San Diego.
- Schwartz, D. A., H. S. Hudson, and L. E. Peterson, 1970, *Astrophys. J.*, **162**, p. 431.
- Toor, A., F. D. Seward, L. R. Cathey, and W. E. Kunkel, 1970, *Astrophys. J.*, **160**, p. 209.
- Trombka, J. I., A. E. Metzger, J. R. Arnold, J. L. Matteson, R. C. Reedy, and L. E. Peterson, 1973, *Astrophys. J.*, **181**, p. 737.

## B. ATMOSPHERIC CORRECTIONS TO BALLOON X-RAY OBSERVATIONS

H. Horstman\*

*University of Bologna*

The group at Bologna (Brini, Fuligni, and Horstman-Moretti) has some new results on the diffuse background between 30 and 200 keV from a second rocket flight. On this particular flight we used detectors with different geometric factors intending to apply the usual idea about these, that is, that the counting rate for one detector is the effective geometric factor of the detector times the diffuse flux with the instrumental background added on. Two different detector shapes were used, one long and one short, with the geometric factor of one being about twice the other. We would like to assume that the background is the same in both detectors and that the diffuse flux is isotropic. Then, we extrapolate the counting rate to zero geometric factor to find the instrumental background; it is really like fitting the difference between the counting rates of the two detectors. Because of this, the statistical errors of the results are larger on this flight than on our previous flight in which we used a screened detector to determine the background. The only difficulty with this method is that the background of the two detectors is not really the same.

Ground measurements of local diffuse X-rays indicate that the longer detector has the higher background. This longer detector has the smaller geometric factor, and so, when we try to do the extrapolation to zero geometric factor, we obtain an overestimate of the instrumental background. If the same effect occurs at altitude, the present results on the diffuse flux have to be considered as lower limits. A power-law fit gives  $47 E^{-2.1 \pm 0.25}$  photons  $(\text{cm}^2 \cdot \text{s} \cdot \text{sr} \cdot \text{keV})^{-1}$ . See Figure II.B-1.

We have recently corrected our old S-11 results for the lead-K X-ray of the collimator and also found a mistake in the geometric factor program which led us to decrease the derived fluxes by 13 percent. The corrected spectrum

---

\*Speaker.

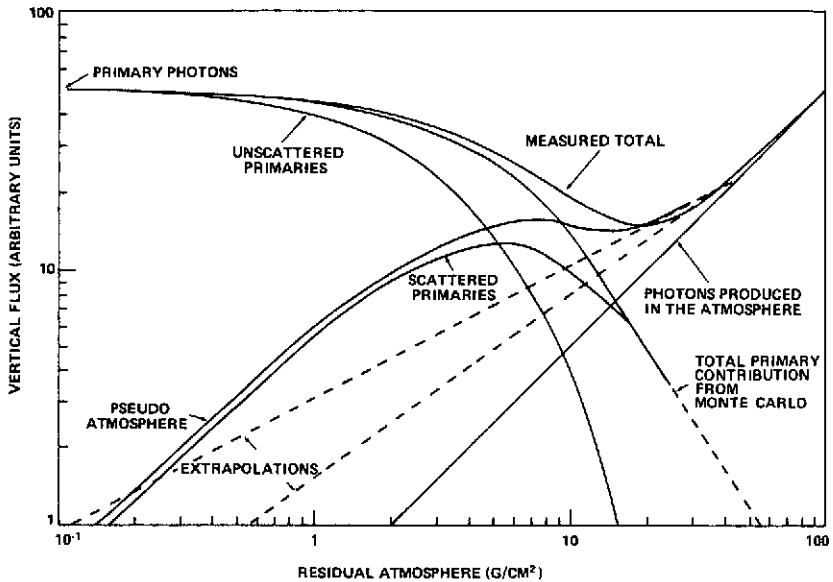


Figure II.B-1. Rough dependence on the depth for 40-keV photons assuming a power-law dependence of the atmospheric X-rays.

is  $36 E^{-2.0 \pm 0.1}$  photons  $(\text{cm}^2 \cdot \text{s} \cdot \text{sr} \cdot \text{keV})^{-1}$ . This lies somewhat above the new results by an amount which can be explained by the different methods used for the background determination.

Both of these results could be subject to the contamination by precipitating electrons mentioned by Schwartz (Chapter II.A) but the agreement between the two results is not bad. If there are electrons there, either they are constantly precipitating or they are a small fraction of the flux observed. I can, unfortunately, say little about possible contamination.

The present results lie slightly above and somewhat overlapping the Indian balloon results corrected for Compton scattering and lie more on top of Bleeker's uncorrected results. That brings up the other point that I wanted to talk about which is the question about Compton scattering that Schwartz brought up (see Chapter II.A). I could not let that remark go by because I feel it contains a misinterpretation of the transport of the primary X-rays in the atmosphere.

If I understand Dan (Schwartz) correctly, he was saying that these Compton corrections are "not appropriate" because once a photon is scattered it is just like an atmospheric X-ray. Because the only means to distinguish photons is by their depth dependence, this would mean that the primary scattered flux follows the same depth dependence as the atmospheric X-rays; therefore, when the extrapolation is performed, the scattered diffuse primary X-rays are also extrapolated out. It is, however, easy to see roughly what the depth dependence of the scattered primary-photon flux is, and where the peak intensity is reached. The results of our Monte Carlo calculations for the propagation of the diffuse primary X-rays in the atmosphere show that, for a given downward direction and energy, the intensity of unscattered plus scattered photons falls off exponentially to a good approximation with depth ( $\exp(-\mu_1 x)$ ). The unscattered photons also have an exponential dependence on the depth ( $\exp(-\mu_2 x)$ ). The calculation shows that  $\mu_1$  is much smaller than  $\mu_2$ . At zero  $\text{gm/cm}^2$ , the flux of scattered photons is zero; therefore the flux of scattered photons alone has a dependence on the depth of the form

$$\exp(-\mu_1 x) - \exp(-\mu_2 x)$$

At 50 to 60 keV, for example, this results in a maximum flux at about  $8 \text{ gm/cm}^2$ . The intensity of the atmospheric X-rays instead peaks around  $100 \text{ gm/cm}^2$ , so that the two behaviors versus depth are quite different.

It should be noted that the counting rates from residual atmospheres of  $15 \text{ gm/cm}^2$  and greater are used to derive the depth dependence of atmospheric X-rays. The peak of the scattered primary radiation lies above those depths and cannot be included in any simple extrapolation so the  $\mu_2$  coefficient cannot be used. A significant amount of primary scattered X-rays is still present at  $15 \text{ gm/cm}^2$ ; lower depths are really more appropriate for the fitting if the  $\mu_1$  coefficient is to be used. The exact form of the depth dependence of the atmospheric X-rays at small depths is, of course, debatable.

My main point here was that the scattered celestial X-rays create a bump at small depths which sits on top of the extrapolation of the atmospheric X-rays when the standard guesses for the depth dependence are used. (See Figure II.B-1.)

So all I am saying is that the scattered photons are in there with the ones that come there unscattered, and you cannot get rid of them by extrapolating in this way.

**DISCUSSION**

*Horstman:*

Have I interpreted correctly what you said this morning? (See Chapter II.A.)

*Schwartz:*

I disagree with exactly what you say, but yes, you are repeating what I said this morning. (See Chapter II.A.)

*Horstman:*

My point was that you were stating that you don't need to use the Compton corrections. All I am saying is that if you arrived at the correct flux at some altitude, if you have succeeded somehow in subtracting out the atmospheric contribution, the atmospheric X-rays, then what you have to do with the remainder is to correct for the multiple Compton scattering.

*Schwartz:*

That is what I disagree with. I say once an X-ray interacts in the atmosphere, it is an atmospheric X-ray.

*Horstman:*

How can you tell? It doesn't have a label on it.

*Schwartz:*

That is what I am saying. It does not have a label. Once it is Compton-scattered at a place in the atmosphere, it is exactly as if an electron had produced it there by bremsstrahlung.

*Horstman:*

From the calculation, it comes out that, if you look at the vertical flux of scattered plus unscattered photons, it goes roughly exponentially. The absorption curve varies with energy, but it is roughly exponential at any energy.

If you can succeed in separating the celestial from the atmospheric component, all you do is use that different absorption coefficient to try to find the celestial component on top of the atmosphere.

*Clark (Session Chairman):*

I think that we have pinpointed a problem. Perhaps we should try to resolve that at coffee.

**A. THE MEASUREMENT AND INTERPRETATION OF  
THE COSMIC GAMMA-RAY SPECTRUM BETWEEN  
0.3 AND 27 MeV AS OBTAINED DURING  
THE APOLLO MISSION**

L. E. Peterson\*

*University of California at San Diego*

J. I. Trombka\*

*Goddard Space Flight Center*

A. E. Metzger, *Jet Propulsion Laboratory*;

J. R. Arnold and J. I. Matteson, *University of California at San Diego*; and

R. C. Reedy, *Los Alamos Scientific Research Laboratory*

**INTRODUCTION**

During the transearth portion of the Apollo-15 and -16 missions, data on the spectrum of the total (diffuse and discrete sources) cosmic  $\gamma$ -ray background over the 0.3- to 27-MeV range were obtained (Trombka et al., 1973). An uncollimated 7.0 cm  $\times$  7.0 cm cylindrical NaI(Tl) scintillation counter located on a boom 7.5 m from the Apollo Service Module was used to perform the measurement. An analysis of the data obtained on Apollo-15 is presented here.

A major source of interference in determining the magnitude and shape of the cosmic  $\gamma$ -ray spectrum can be attributed to the cosmic-ray induced activation of the NaI(Tl) detector crystal. A NaI(Tl) crystal similar to that used during the Apollo-15 and -16 missions was flown aboard the Apollo-17 Command Module. This crystal was returned to earth and measurements of the induced activity were obtained. Preliminary analysis of the results are now available (Trombka et al., (in press)). Other sources of interference with respect to the determination of the diffuse  $\gamma$ -ray spectrum have also been considered. This interference or background was due to sources aboard the

---

\*Speakers.

spacecraft and cosmic-ray induced  $\gamma$ -ray emission from the spacecraft and material surrounding the detector. Attempts have been made to correct the measured spectrum for these background effects.

An upper limit measure of the  $\gamma$ -ray flux around 0.51 MeV was also obtained.

## INSTRUMENTATION

The Apollo-15 and -16  $\gamma$ -ray spectrometers (Alder and Trombka, 1970) consisted of a 7.0-cm-diam  $\times$  7.0-cm-long NaI(Tl) central detector viewed by a 7-cm (3 in.) photomultiplier. Except at the photomultiplier end, the crystal is surrounded by a 1-cm-thick plastic scintillator shield which detects charged particles. The plastic scintillator is viewed by a 4-cm (1.5 in.) photomultiplier and has a threshold of about 1.0 MeV for generating an anticoincidence event when interactions occur in the most optically unfavorable location. Central detector events with no shield anticoincidence are pulse-height analyzed into 511 channels and are transmitted at a maximum event rate of 369 counts/s. The shield rate, the coincidence rate, and the live time are transmitted every 0.328 s. The spectrometer and associated electronics are enclosed in a thermal shield and mounted on a boom which could be extended from one side of the Service Module by an astronaut. The components carried on the boom present  $\sim 5$  gm/cm<sup>2</sup> averaged over all directions. The astronaut could fully deploy the detector to 7.6 m from the spacecraft edge or position it at intermediate distances using stopwatch timing. Furthermore, he could step the high voltage supply or disable the anticoincidence.

## RESULTS

### Energy Loss Spectra

The data reported here were obtained during portions of the transearth coast of Apollo-15 from about 2200 hours August 4, to 1500 hours August 7, 1971, and represent approximately four hours of operation in the extended position. During this period the earth and moon solid angles were always less than  $10^{-2}$  sr and in the fully extended boom position, the spacecraft subtended  $\sim 0.28$  sr. Spectra were obtained with the detector at various boom positions, with the anticoincidence both on and off, and with the high voltage set to give several energy ranges up to 27 MeV. Although data were obtained over a 0.16- to 27-MeV range, the analysis reported here is based on energy losses  $> 0.3$  MeV. Calibration was obtained with a Hg<sup>203</sup> source and by means of known, easily identifiable spacecraft background  $\gamma$ -ray lines. Since long periods of time were used to obtain the data and the Command Service Module (CSM) rotated  $\sim 3$  rph in the ecliptic plane, counting rate anisotropies, if they exist, were averaged out.

Figure III.A-1 shows energy-loss spectra (for several important data modes) corrected for live time, channel width, and the isotropic detector geometry factor of  $57.5 \text{ cm}^2$ . Here counts have been summed over channels consistent with the detector-energy resolution which was 8.6 percent at 662 keV. With the exception of the strong line at 0.51 MeV, most of the  $\gamma$ -ray lines measured in board largely disappear with boom extension, leaving a continuum extending to 27 MeV, on which is superposed a number of weak lines. Since the intensity changed only by about a factor of five while the spacecraft solid angle changed a factor of 20, most of the count rate in the extended position is not of spacecraft origin. From a detailed analysis of the rates versus solid angle, we estimate  $\sim 6.6 \times 10^{-3} \text{ c}(\text{cm}^2 \cdot \text{s} \cdot \text{MeV})^{-1}$  at 2.4 MeV and  $\sim 1.9 \times 10^{-3} \text{ c}(\text{cm}^2 \cdot \text{s} \cdot \text{MeV})^{-1}$  at 5 MeV are due to the spacecraft. These are 0.1 and 0.2, respectively, of the spectrum with the boom extended.

The flat energy-loss spectrum of  $0.052 \text{ c}(\text{cm}^2 \cdot \text{s} \cdot \text{MeV})^{-1}$  above 5 MeV with the anticoincidence disabled in the extended position agrees with that value expected from the shield rate of 450 c/s, from which a cosmic-ray flux of  $3.50 \text{ (cm}^2 \cdot \text{s})^{-1}$  can be derived. The large ratio of cosmic-ray to photon energy losses near 27 MeV requires effective charged-particle rejection, which could not be measured before launch to the required accuracy. However, preliminary results from an identical experiment on the Apollo-16 in April 1972 confirm the Apollo-15 differential energy loss spectrum below 10 MeV to within approximately 12 percent. We interpret this as indicating that there were not systematic differences in the behavior of the instruments.

The energy loss spectrum with the anticoincidence enabled, and the boom in the extended position is compared in Figure III.A-2 with measurements obtained on other satellites during cislunar space flight. The NaI(Tl) Apollo-15 and -16 detectors were identical in size to the CsI(Tl) detector in Ranger-3 (Metzger et al., 1964) both of which differ only slightly from the NaI(Tl) crystal on the ERS-18 (Vette et al., 1970). The 8 kg mass on the end of the Apollo-15 boom is nearly the same as that system aboard the ERS-18, while the Ranger-3 detector carried only  $\sim 3$  kg. Clearly, the present data are in good agreement with previous measurements below  $\sim 2$  MeV, but are well below the 3.7- to 6.0-MeV point measured by the ERS-18, which is apparently erroneous.

### Equivalent Photon Spectra

The equivalent photon spectra, Figure III.A-3, have been obtained from the energy loss spectra in Figures III.A-1 and -2 by using a measured response "library" and a matrix inversion technique as described by Adler and Trombka (1970). The  $\gamma$ -ray lines are separated from the continuum by using

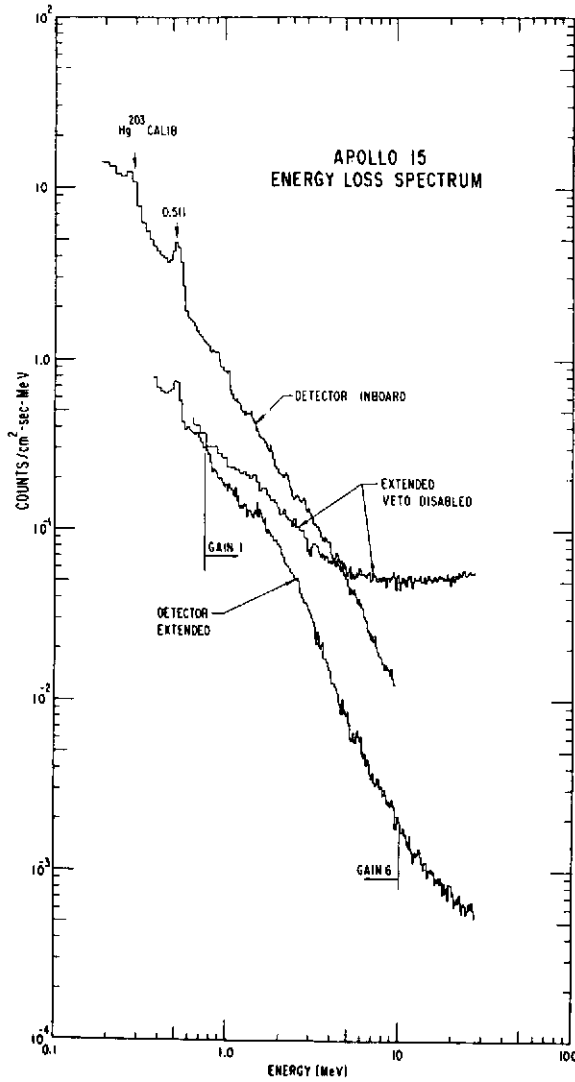


Figure III.A-1. Energy loss spectra in the 7.0-cm-diam by 7.0-cm-long NaI(Tl) scintillation counter measured on Apollo-15 during transearth coast. Since the rates decreased only a factor of about five when the detector was extended to 7.6 m, while the solid angle subtended by the spacecraft decreased a factor of 20, we interpret most of the rate in the extended position to be associated with cosmic  $\gamma$ -rays. The spectrum with the anticoincidence disabled agrees with that expected from cosmic-rays passing through the crystal edges.

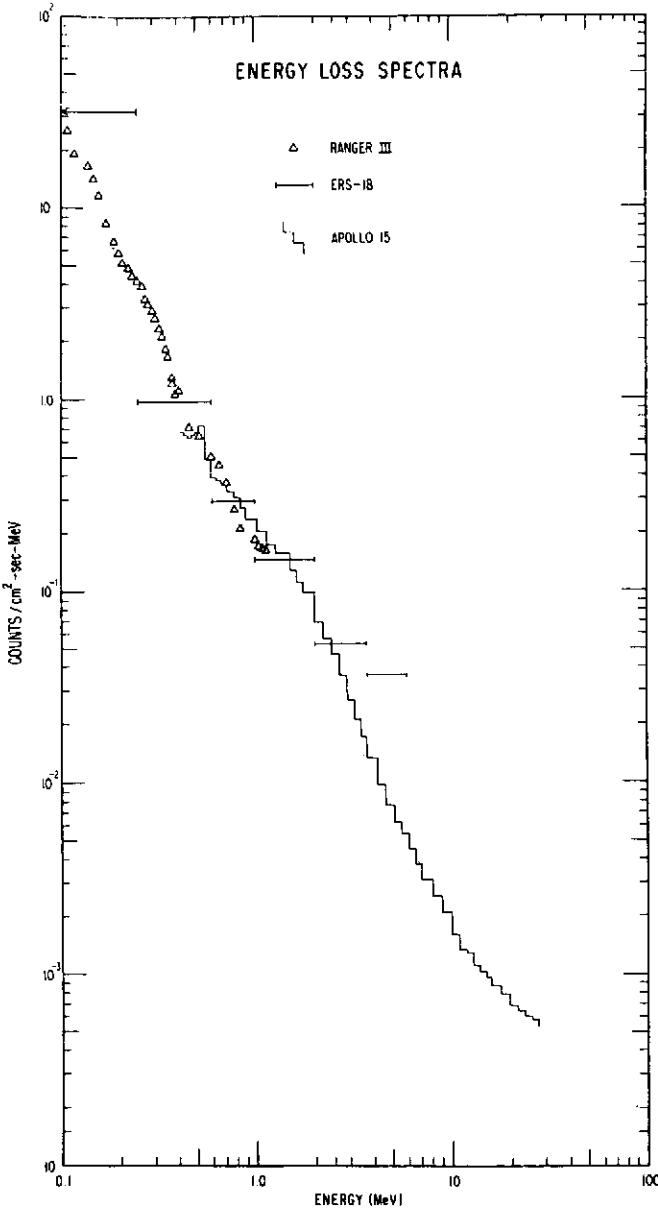


Figure III.A-2. Energy loss spectra are compared directly with other measurements obtained outside the magnetosphere. These data were obtained with counters that differ only slightly in geometry and materials.

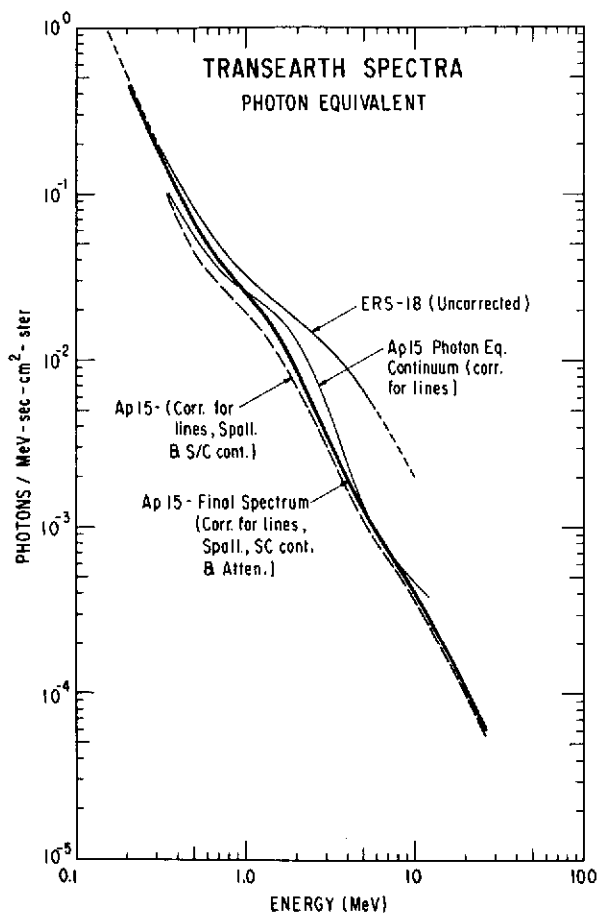


Figure III.A-3. Equivalent photon spectra derived from the Apollo-15 are shown at various stages of data correction. First, all components due to discrete  $\gamma$ -ray lines are removed, then the spacecraft continuum contribution and an estimate of energy losses due to spallation nuclei are subtracted. The final result contains a correction for absorption of local material, assuming all energy losses at this stage are due to an external isotropic  $\gamma$ -ray flux.

an iterative procedure, (Trombka et al., 1970; Reedy et al., 1973). Here the pulse-height spectrum is transformed to photon space where lines appear as discontinuities, which can be subtracted by requiring the remaining continuum to vary slowly with energy. This procedure results in the removal of 2.5 c/s over the 0.6- to 3.5-MeV range due to lines or about 17 percent of the energy loss spectrum and leaves a smooth equivalent photon continuum shown in Figure III.A-3.

The following are a few comments on the determination of the measured response library. The shape and detection efficiency of these library functions strongly depends on the angular distribution of the incident  $\gamma$ -ray flux. To illustrate this point, the detection probability (intrinsic efficiency) for a 7.0-cm  $\times$  7.0-cm cylindrical NaI(Tl) detector is given in Figure III.A-4 as a function of energy for two different cases: a parallel beam incident on the face of the crystal (the crystal axis is parallel to the beam) and an isotropic distribution of  $\gamma$ -rays. As can be seen, there is significant difference in the detection efficiencies over much of the energy region of interest. The shapes of the pulse-height spectra do not seem to change quite as radically as a function of the angular distribution of the incident flux. In order to transform from measurement or energy loss spectra to photon spectra, efforts were made to eliminate all background components in order to isolate the energy loss spectra characteristic of the diffuse component. The assumption was then made that this component was isotropic and the transformation was then performed using an isotropic-type response library. From a comparison of our experimental work (Trombka et al., 1971) with Monte Carlo calculations (Berger and Seltzer, 1972), we found that the response library function can be calculated theoretically for any energy and geometry needed in the analysis.

### Discrete Line Spectra

The discrete line spectrum in the measured cosmic-ray spectrum can be mainly attributed to natural radioactivity aboard the spacecraft (K-40 and Th), proton- and neutron-induced activation in the spacecraft and materials surrounding the detector, and activity induced in the detector itself. Using the technique considered in the section "Equivalent Photon Spectra," the continuous portion of the energy loss spectrum was determined, and the continuous spectrum was subtracted from the uncorrected energy spectrum. In this way, the energy loss spectrum characteristic of discrete lines is determined. The results are shown in Figure III.A-5. Identification of certain lines are also indicated. We believe that the following lines can be identified: (1) the 0.51-MeV line due to positron annihilation; (2) the 0.63- and 0.69-MeV lines due to proton-induced activation of the crystal producing  $^{124}\text{I}$  and  $^{126}\text{I}$ , the 1.47-MeV characteristics of  $^{40}\text{K}$ ; and (3) the

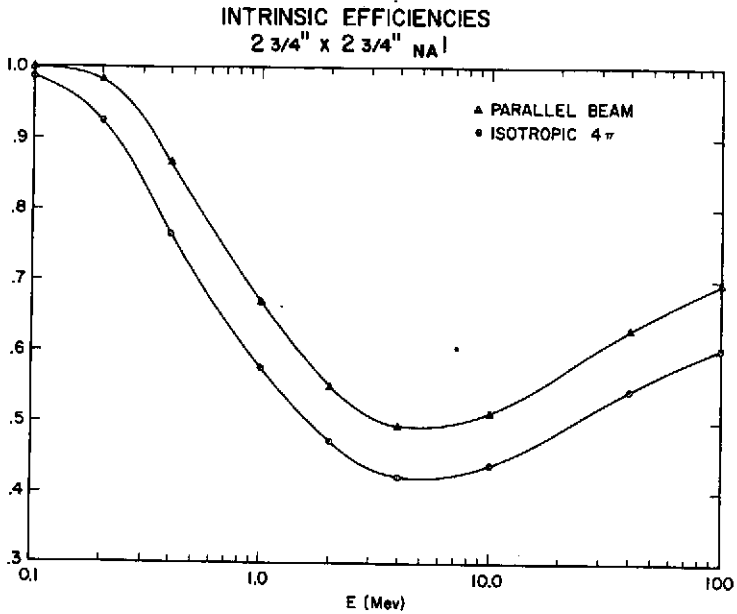


Figure III.A-4. Intrinsic efficiencies as a function of energy for a 7-cm by 7-cm NaI(Tl) detector. Both parallel beam and isotropic  $\gamma$ -ray fluxes are considered.

2.6-MeV line of thorium. Other lines due to thorium and  $(n, \gamma)$  and  $(n, n^1, \gamma)$  reactions on Mg, H, Al, O, and Na can also be presented.

#### Spallation Correction

Fishman (1972) has suggested that radioactive spallation nuclei produced by cosmic-ray interactions in the scintillation crystals might account for a large fraction of the counting rate measured in the 1- to 3-MeV region. Although a direct measurement of this effect in the cosmic-ray flux is difficult and has not been accomplished, calculations and laboratory measurements by Fishman (1972) and Dyer (private communication) have indicated the spectra shape and approximate magnitude of the energy loss spectrum. We have attempted to correct the spectra of Figure III.A-3 for this effect by subtracting from the equivalent energy loss spectrum a spallation model spectrum whose normal-

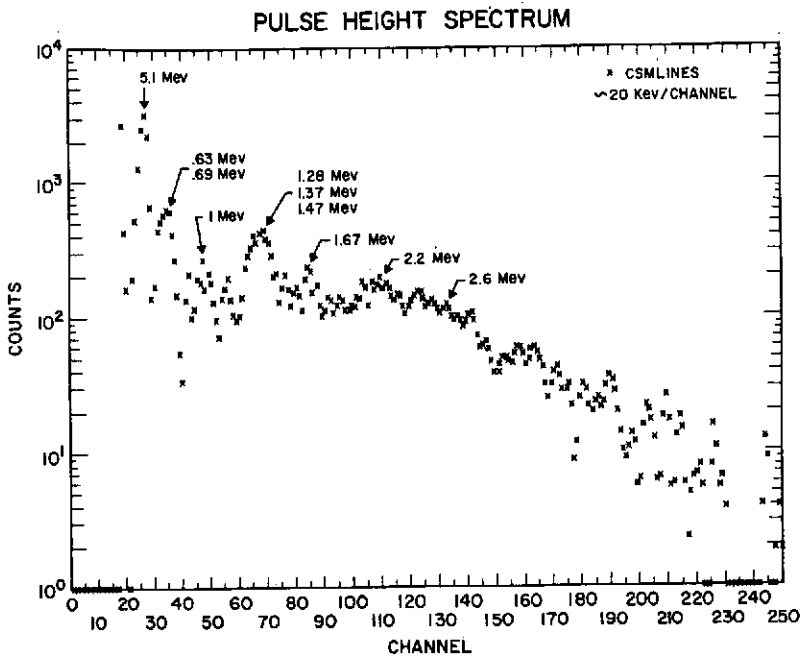


Figure III.A-5. Discrete-line energy loss spectrum from Apollo-15.

ization was a free parameter. Since spallation contributes mostly to the energy losses in the 0.6- to 3-MeV range, the normalization was determined, rather arbitrarily, by the criterion that the resultant photon spectrum be relatively smooth. This was found to occur when a spallation spectrum shape, based on the work of Fishman (1972), Dyer and Morfill (1971; private communication) but approximately half their calculated intensity, was subtracted out. As shown in Table III.A-1, this results in removal of about 16 percent of the energy loss spectrum in the 0.6- to 3.5-MeV range and a negligible amount at higher energies. Subtracting a much larger spallation component, such as the full Dyer and Morfill value, would give no energy loss spectrum in the 1- to 2-MeV range, while still requiring an external photon component above 3 MeV, which is not physically possible. Although there seems no doubt that a spallation energy loss contribution exists, its spectral shape and intensity are only approximately known.

The spallation components are always subtracted out in energy loss space. In an attempt to obtain experimental data on the extent of the proton-induced activity, a NaI(Tl) crystal was flown aboard Apollo-17. The crystal assembly was physically identical to that flown aboard Apollo-15 and

Table III.A-1  
Composition of Apollo-15 Energy-Loss Spectrum  
(transearth coast, deployed position)

Component	Energy Range	
	0.6-3.5 MeV	3.5-9.0 MeV
$\gamma$ -ray lines (percent) . . . . .	15.9	3.7
Spallation in NaI crystal (percent) . . . . .	15.8	0.5
Spacecraft continuum (percent) . . . . .	10.2	21.7
Cosmic upper limit (percent) . . . . .	58.1	74.1
Total (percent). . . . .	100.0	100.0

-16 (Adler and Trombka, 1970). The assembly aboard the Apollo-17 CSM did not include the photomultiplier, the proton anticoincidence mantle, and the thermal shield. The detector was a 7-cm  $\times$  7-cm right-cylindrical crystal. A glass plate was optically sealed to the crystal. MgO was used as the optical reflector inside the crystal assembly. This type of assembly permitted the crystal to be hermetically sealed and allowed for a simple procedure for optically coupling the crystal assembly to a photomultiplier tube after flight. The crystal and reflector were enclosed in a steel jacket. An identical second crystal assembly which was not flown was used as a control throughout the measurement program. After splashdown, the flight (that is, activated) crystal was returned to the recovery ship and optically mounted on a photomultiplier tube, and pulse-height spectra were obtained. The activated crystal was counted in a large, steel, low-level shield. The crystal counting started about one and one-half hours after the Command Module reentered the earth's atmosphere. Before splashdown the control (unactivated) crystal was optically sealed to a photomultiplier tube, and the background was determined in the steel shield. The same photomultiplier tube was used to count the activated and control crystal assemblies. After 30 hours of counting aboard the recovery ship, the detector was flown back to the Oak Ridge National Laboratory (ORNL) where measurements were continued. This permitted the observation of the decay of the longer-lived induced activities. Direct measurements of the induced activities were made again by optically sealing a photomultiplier tube to the activated crystal. Indirect measurements using both Ge(Li) detectors and a large scintillation  $4\pi$  detector in a low-level counting system at ORNL (Eldridge et al., 1973) were performed in order to determine the spectral distribution and intensity of the emitted radiations. The  $4\pi$  scintillation counter is divided into halves. Each half can be operated so as to require that there be coincidence events in both halves

before an event is analyzed and recorded (coincidence spectra) or the halves can be operated without the coincidence requirement, and events independent of their coincidence can be analyzed and recorded (singles spectra).

To date it has been possible to obtain qualitative identification of the following nuclear species:  $^{22}\text{Na}$  (2.6 yr),  $^{24}\text{Na}$  (15 hr),  $^{123}\text{I}$  (13 hr),  $^{124}\text{I}$  (4 days),  $^{126}\text{I}$  (13 days),  $^{128}\text{I}$  (25 min), and  $^{127}\text{Xe}$  (34 days). After suitable calibrations, quantitative concentrations of these radionuclides will be obtained. The present results indicate that the induced activity observed after recovery can be attributed mainly to species with half-lives of about half a day and longer. Decay products with shorter half-lives do not make a large contribution to the post-recovery integral count rate. This is not to imply that there are no short half-life components. In fact, the line at 0.44 MeV is characteristic of  $^{128}\text{I}$ . There are a few more regions with relatively short half-lives (in order of tens of minutes) that have not as yet been identified.

Figure III.A-6 shows the pulse-height spectrum obtained during the first hour and a half of counting after recovery. The spectrum has been corrected for background by subtracting the measurements obtained with the control crystal. Peak energies for the nuclides presently identified are indicated. The peak positions of  $^{123}\text{I}$ ,  $^{124}\text{I}$ ,  $^{126}\text{I}$ , and  $^{128}\text{I}$  are displaced 27 keV due to X-ray emission and absorption in the crystal after electron capture.

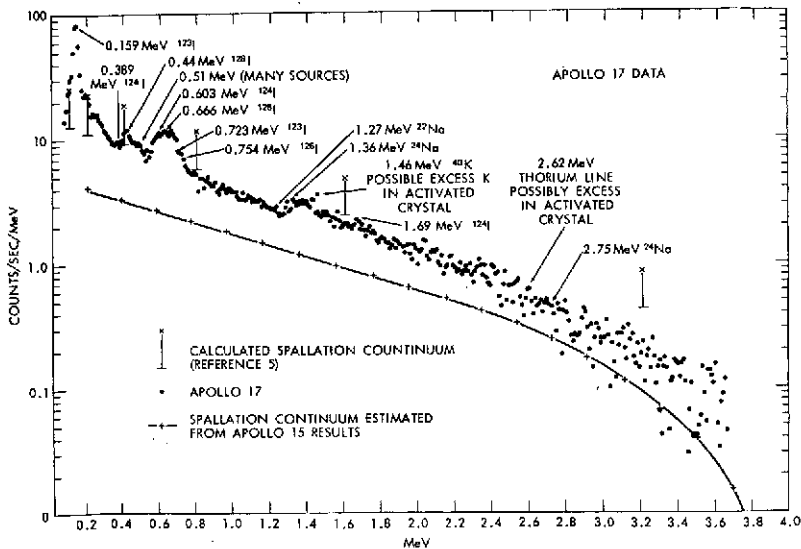


Figure III.A-6. Proton-induced activity in 7-cm by 7-cm NaI(Tl) crystal 1-1/2 hr after reentry. The background has been subtracted. Counting time was 1800 s. The spectrum measurement started 1-1/2 hr after reentry. The spectrum was obtained by direct internal counting of the activated crystal.

Measurements of the flight and control crystal carried out at the low-level counting laboratory at the Oak Ridge National Laboratory (ORNL) prior to flight indicated the K and Th content of the flight crystal to be slightly higher than that for the control crystal. Thus, one would expect some indication of these elements after background subtraction. The energy identification for  $^{124}\text{I}$ ,  $^{126}\text{I}$ , and  $^{24}\text{Na}$  have been verified by measurements made with the Ge(Li) detector and in the low-level counting system. Both energy and half-life information have been used to determine the presence of these nuclear species. The  $^{123}\text{I}$  and  $^{128}\text{I}$  were identified by use of the spectra obtained on board the carrier from both energy and half-life determinations.  $^{22}\text{Na}$  has been tentatively identified based on a preliminary analysis of the data obtained by the coincidence measurements in the low-level counting facility.  $^{127}\text{Xe}$  presence has been determined by the identification of energy lines at 0.172 MeV, 0.203 MeV, and 0.375 MeV using the Ge(Li) detector.

One factor requiring consideration was the difference in the environment during the Apollo-15 and -16 missions compared with Apollo-17 mission. First, the crystals aboard Apollo-15 and -16 were stowed in the Service Module and extended approximately 762 cm away from the vehicle for short periods of time, whereas the Apollo-17 crystal was stowed in the Command Module for the total flight time. Thus, there was a difference in the mass around the crystal which might cause a difference in the secondary proton and neutron flux in the region of the stowed crystals. Secondly, the exposure profile of the primary flux both in time and spectral distributions were different. The Apollo-17 crystal passed through the near-earth trapped proton flux twice before measurements, while the Apollo-15 and -16 detectors had passed through the trapped belts only once before measurement. The Apollo-15 measurement of diffuse  $\gamma$ -ray spectrum was made about 250 hr after lift-off, while the Apollo-17 measurements were made some 305 hr after lift-off. It has not as yet been determined how significant these differences are in terms of trying to infer the magnitude of the proton-induced activity in the Apollo-15 and -16 detectors from the Apollo-17 measurements.

The shape of the cosmic-ray-induced  $\gamma$ -ray pulse-height spectrum can be divided into two parts: the discrete-line spectrum and the continuous spectrum. The discrete-line pulse spectrum for activated nuclear species in the crystal is produced by monoenergetic  $\gamma$ -rays emitted after electron capture. The continuum for such nuclear species is produced by electrons, positrons, positron annihilation, and  $\gamma$ -rays (other than those emitted after electron capture) interacting in the crystal. If the material surrounding the crystal is radioactive (for example,  $^{24}\text{Na}$ , Th, or  $^{40}\text{K}$ ) then mono-

energetic  $\gamma$ -rays independent of the mode of decay can be seen in the crystal as a discrete-line pulse-height spectrum. In Figure III.A-6, the discrete lines are indicated and the continuous distribution can be seen underneath. The actual energy position should be moved  $\sim 27$  keV up in energy due to the summing of iodine-K X-ray line with the  $\gamma$ -ray line after K capture.

In the Apollo-15 transearth spectrum (Trombka et al., 1973), the  $^{124}\text{I}$  0.606-MeV and the  $^{126}\text{I}$  0.66-MeV lines can be identified. It has been calculated that the integrated count rate in this region above the continuum for Apollo-15 is half of that observed in the same region above the continuum for the Apollo-17 mission. This difference cannot be attributed to the difference in exposure time alone. Thus, the difference in local mass and the passage through the near-earth trapped radiation belts a second time may be the cause of this increase.

In Figure III.A-6 the magnitude of the continuum and associated error as predicted by Fishman (1973) is compared with the Apollo-17 measurement taken aboard the recovery ship. The magnitude of the continuum inferred from the Apollo-15 data (Trombka et al., 1973) is also shown. Its magnitude is consistent with the Apollo-17 results if it is considered that the discrete-line magnitude for  $^{124}\text{I}$  and  $^{126}\text{I}$  is down by a factor of two. This also assumes that the shorter half-lived nuclides and the prompt  $\gamma$ -ray emission is small compared to the longer half-lived emitters. Calculations (Dyer and Morfill, 1971) indicate that short half-lives may be quite important.

### Spacecraft Continuum

The following procedures were used to determine the magnitude of the spacecraft continuum.

Spectra were obtained with the detector positioned at 183 cm, 244 cm, 457 cm and 762 cm away from the spacecraft. An effective solid angle for each position was calculated for these positions. The discrete-line spallation backgrounds discussed in sections "Equivalent Photon Spectra" and "Discrete Line Spectra" were then subtracted from the energy loss spectrum at 183 cm and 762 cm. It was then assumed that the 183-cm spectrum characterized the energy loss spectrum of the continuous  $\gamma$ -rays spectrum emitted from the spacecraft. The intensity at 183 cm is reduced by the ratio of the effective solid angle at 762 cm to the effective solid angle at 183 cm. This then is a first estimate of the contribution of the spacecraft continuum at 762 cm. The spacecraft continuum contribution is then subtracted from the residual energy loss spectrum at 762 cm and a first estimate of the energy loss spectrum due to the diffuse component is

obtained. It is now assumed that the diffuse energy loss spectrum does not depend on the distances of the detector from the spacecraft (that is, the spacecraft occultation is ignored) and this first approximation is subtracted from the energy loss spectrum at 183 cm. A second approximation of the continuous energy-loss spectrum from the spacecraft at 183 cm is obtained. This new continuous energy-loss spectrum is corrected for change in solid angle to obtain its contribution at 762 cm (25 ft) and then subtracted from the original residual energy-loss spectrum at 762 cm (25 ft) in order to obtain a second approximation of the diffuse energy-loss spectrum. The procedure as described above is continued for another two iterations, and it was found that the shape of the diffuse energy-loss spectrum did not change significantly between the last two iterations. After the last iteration, the energy-loss spectrum was then converted to photon spectrum. The transformation was accomplished using library functions and efficiencies characteristics of isotropic flux distributions.

### Cosmic Photon Spectrum

The photon spectrum incident on the central detector, shown in Figure III.A-3 as a dashed line, has also been corrected for the various interferences discussed in the preceding sub-sections. The contribution of the various components over the 0.6 to 3.5 MeV and the 3.5 to 9.0 MeV ranges are summarized in Table III.A-1. Despite the many corrections, about 50 to 75 percent of the energy losses cannot be accounted for by presently understood local processes and therefore must originate externally. Obtaining the photon spectrum incident isotropically on the spectrometer requires a correction for local matter. Taking this to be equivalent to a uniform shell 5.0 gm/cm<sup>2</sup> thick of Al surrounding the NaI crystal, and correcting for absorption, but not scattering, results in the final photon spectrum shown in Figure III.A-3. We have assumed the photon continuum extends as  $E^{-2.0}$  above 27 MeV; however, the result is rather independent of this shape.

Systematic errors, which are difficult to estimate, completely dominate the statistical uncertainties in this analysis. Correcting for the spacecraft lines can be done to high precision. The effective solid angle for continuum production in the spacecraft may be less certain. No correction has been made for production in local material, which is believed to be small (Vette et al., 1970). We estimate the equivalent photon spectrum, before correction for spallation, to be accurate to about  $\pm 20$  percent. The spallation correction cannot be much larger than that indicated in Figure III.A-3. Correcting for absorption, but not scattering, results in an upper limit to the external flux.

These results can be compared to those of others who have presented spectra at various stages of correction. The Apollo-15 photon equivalent continuum is considerably below that determined from ERS-18, which had no corrections for  $\gamma$ -ray lines, effects of local material, or spallation and which apparently had an instrumental malfunction at higher energies. The final photon Apollo-15 spectrum is compared with balloon and low altitude satellite work (Golenetskii et al., 1971; Vedrenne et al., 1971; Damle et al., 1971) in Figure III.A-7. The result of the reference is considerably above the other work and is therefore not shown. Although the low-latitude observations should not require a significant correction for spallation, they do require an altitude-and latitude-dependent model to correct for cosmic-ray produced  $\gamma$ -rays and, in some cases, an additional large correction for counter efficiency.

The new results, in addition to being in reasonable agreement with the more recent work above 1 MeV, also agree with data near 100 keV (Pal, 1973) when extrapolated as an  $E^{-2}$  power law. Furthermore, the Apollo spectrum is consistent with new data on the diffuse component near 30 MeV (Mayer-Hasselwander et al., 1972; Share et al., 1973). Figure III.A-7 shows some of these results, as well as at 100 MeV obtained from the OSO-3 (Kraushaar et al., 1972, preprint).

Also shown in Figure III.A-7 is a single power law which has been suggested (Pal, 1973) as capable of representing the total cosmic  $\gamma$ -ray spectrum between approximately 0.02 and 1.0 MeV. It is clear that the derived Apollo-15 spectrum is well above this extrapolation, and even though we interpret our result as an upper limit, we do not believe that the remaining small corrections and uncertainties can reduce the final cosmic spectrum to the extrapolated value.

## DISCUSSION

Assuming that the  $\gamma$ -ray fluxes are of extragalactic origin (Stecker et al., 1971) a number of workers have attempted to account for the spectra shown in Figure III.A-7. Compton scattering of electrons leaking from radiogalaxies (Brecher and Morrison, 1969), red-shifted  $\gamma$ -rays from  $\pi^0$  decays produced by cosmic-ray collisions at an early epoch of the expanding universe (Stecker, 1971), nuclear  $\gamma$ -rays from supernovae in distant galaxies (Clayton and Silk, 1969), intergalactic electron bremsstrahlung (Arons et al., 1971; Stecker and Morgan, 1972; Stecker et al., 1971) and matter-antimatter annihilation (Stecker et al., 1971) have all been suggested. Vette et al. (1970), in attempting to account for the ERS-18 data, fitted a model in which a  $\pi^0$ -decay component produced at an epoch with a red shift  $\approx 70$  was super-imposed on a Compton scattering X-ray background. Based on the present data,

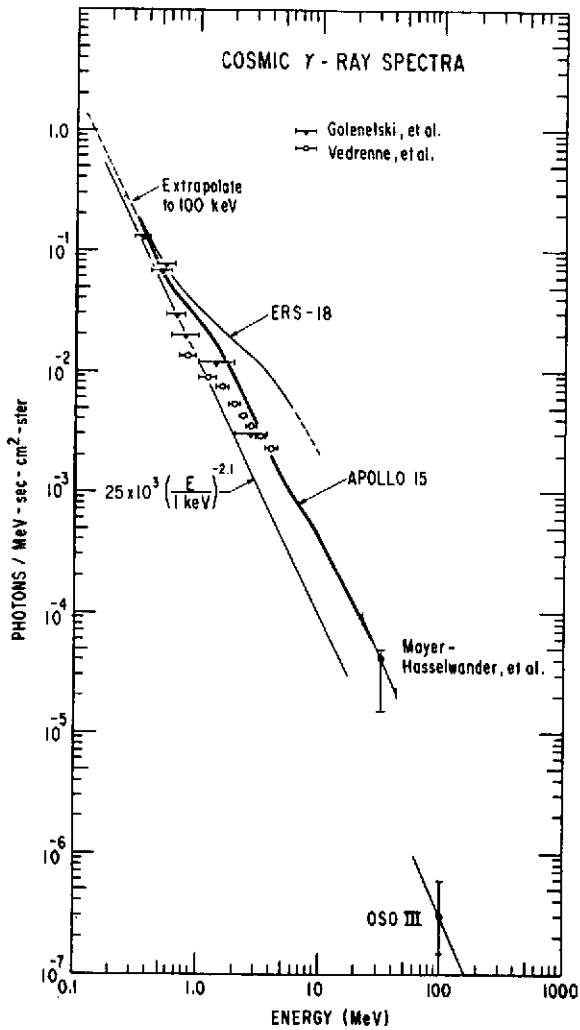


Figure III.A-7. The cosmic-photon spectrum derived from the Apollo-15 data agrees with previous results below 1 MeV but is well below that determined from the ERS-18 at higher energies. Limits derived from balloon and low-altitude satellite work, despite large corrections for efficiency and cosmic-ray produced  $\gamma$ -rays, are in agreement with the Apollo results.

the intensity of the flux required at very early epochs is reduced somewhat. The final spectrum of Apollo-15 does require an additional component above a simple power law. A discussion of the theoretical consequences of these results is given by Stecker elsewhere in these proceedings (see Chapter IX.A).

The analysis process used here subtracts out all discrete  $\gamma$ -ray lines and produces a smooth continuum, as presented in Figure III.A-3. Discrete  $\gamma$ -rays of cosmic origin, if they exist, would therefore be removed along with known spacecraft and spallation contributions. Only considerable further analysis can separate these components and place valid limits on possible cosmic components.

The  $\gamma$ -ray line near 0.51 MeV has an intensity after correction for spacecraft production and local absorption estimated to be  $3.0 \pm 1.5 \times 10^{-2}$  photons  $(\text{cm}^2 \cdot \text{s})^{-1}$ . The uncertainty is an estimate of the effect of systematic errors in the correction for weak  $\gamma$ -ray features near this energy and for detector efficiency and absorption. The 0.51 MeV  $\gamma$ -ray measured on Apollo-15 cannot originate in the spacecraft because this component decreases less rapidly with spacecraft solid angle than the continuum. The intensity of the line seems inconsistent with upper limits on the cosmic flux at 0.51 MeV of  $< 10^{-2}$  photons  $(\text{cm}^2 \cdot \text{s})^{-1}$  obtained from balloon measurements (Chupp et al., 1970) and on Ranger-3 (Metzger et al., 1964). Since Ranger-3, which also measured in interplanetary space, had considerably less matter locally to the detector, it may be possible to attribute the flux to annihilation of positrons produced by cosmic-rays or spallation  $\beta^+$ -decays in the local mass. It is also possible that low-energy positrons of either solar or cosmic origin with a flux of  $\sim 10^{-2}$   $(\text{cm}^2 \cdot \text{s})^{-1}$  could stop and annihilate in the inert matter surrounding the detector. Such a mechanism has been suggested by Stephens (private communication) and is in fact consistent with the interplanetary medium flux of  $2 \times 10^{-2}$  positrons  $(\text{cm}^2 \cdot \text{s})^{-1}$  at approximately 2 MeV reported in Cline and Hones (1970). Haymes (Johnson, Harnden, and Haymes, 1972) has reported a  $\gamma$ -ray line at  $\sim 470$  keV whose intensity is  $2 \times 10^{-3}$  photons  $(\text{cm}^2 \cdot \text{s})^{-1}$  originating from the galactic center. The  $\gamma$ -ray line measured on Apollo-15 is definitely at  $0.511 \pm 0.012$  MeV, and the  $2 \sigma$  upper limit to a  $\gamma$ -ray at 0.47 MeV is  $\sim 2 \times 10^{-3}$  photons  $(\text{cm}^2 \cdot \text{s})^{-1}$ , based on the analysis of 4 hr of data.

#### ACKNOWLEDGMENTS

The work described in this paper was carried out in part under NASA Contract No. NAS7-100 at the Jet Propulsion Laboratory, California Institute of Technology, in part under NASA Contract No. NAS9-10070 at the University of California, San Diego, and in part under USAEC Contract W-7405-Eng-36 at the Los Alamos Scientific Laboratory of the University of California.

## REFERENCES

- Adler, I., and J. I. Trombka, 1970, *Physics and Chemistry in Space*,  
3, J. G. Roederer and J. Zahringer, eds., Springer-Verlag, New York.
- Arons, J., R. McCray, and J. Silk, 1971, *Astrophys J.*, **170**, p. 431.
- Berger, M. J., and S. M. Seltzer, 1972, *Nuc. Inst. and Methods*, **104**, p. 317.
- Brecher, K., and P. Morrison, 1969, *Phys. Rev. Letters*, **23**, p. L802.
- Chupp, E. L., D. J. Forrest, A. A. Sarkady, and P. J. Lavakare, 1970,  
*Planetary and Space Science*, **18**, p. 939.
- Clayton, D. D., and J. Silk, 1969, *Astrophys J. Letters*, **158**, p. L43.
- Cline, T. L., and E. W. Hones, 1970, *ACTA Phys.*, **29**, Supp 1, p. 159.
- Damle, S. V., and R. R. Daniel, G. Joseph, and P. J. Lavakare, 1971,  
*Astrophys. and Space Sci.*, **14**, p. 473.
- Dyer, C. S., and G. E. Morfill, 1971, *Astrophys. and Space Sci.*, **14**, p. 243.
- Eldridge, J. S., G. D. O'Kelley, K. J. Northcutt, and E. Schonfeld, 1973,  
*Nuc. Inst. and Methods*, in press.
- Fishman, G. J., 1972, *Astrophys J.*, **171**, p. 163.
- Golenetskii, S. V., E. P. Mazets, V. N. Il'inskii, R. L. Aptekar, M. M. Bredov,  
Uy. A. Gur'yan, and V. N. Panov, 1971, *Astrophys J. Letters*, **9**, p. L69.
- Johnson, W. N., III, F. R. Harnden, Jr., and R. C. Haymes, 1972,  
*Astrophys J. Letters*, **172**, p. L1.
- Mayer-Hasselwander, H. A., E. Pfeffermann, K. Pinkau, H. Rothermel, and  
M. Sommer, 1972, *Astrophys J. Letters*, **175**, p. L23.
- Metzger, A. E., E. C. Anderson, M. A. Van Dilla, and J. R. Arnold, 1964,  
*Nature*, **204**, p. 766.
- Pal, Y., 1973, *X-Ray and Gamma-Ray Astronomy, Proceedings of IAU  
Symposium No. 55*, (Madrid), H. Bradt and R. Giacconi, eds., D. Reidel,  
Dordrecht, Holland.
- Reedy, R. C., J. R. Arnold, and J. I. Trombka, 1973, *J. Geophys. Res.*,  
in press.
- Share, G. H., R. L. Kinzer, and N. Seeman, 1973, *X-Ray and Gamma-Ray  
Astronomy, Proceedings of IAU Symposium No. 55*, (Madrid),  
H. Bradt and R. Giacconi, eds., D. Reidel, Dordrecht, Holland.
- Stecker, F. W., 1971, *Nature*, **229**, p. 105.

- Stecker, F. W., 1971, *Nature*, **229**, p. 105.
- Stecker, F. W., and D. L. Morgan, Jr., 1972, *Astrophys. J.*, **171**, p. 201.
- Stecker, F. W., D. L. Morgan, Jr., and J. Bredekamp, 1971, *Phys. Rev. Letters*, **27**, p. L1469.
- Stecker, F. W., J. I. Vette, and J. I. Trombka, 1971, *Nature*, **231**, p. 122.
- Trombka, J. I., E. Eller, G. A. Osswald, M. J. Berger, and S. M. Seltzer, 1971, *USAEC Report Conf. - T10402*, **III**, p. III-43.
- Trombka, J. I., A. E. Metzger, J. R. Arnold, J. L. Matteson, R. C. Reedy, and L. E. Peterson, 1973, *Astrophys. J.*, **181**, p. 737-746.
- Trombka, J. I., R. L. Schmadebeck, M. Bielefeld, G. D. O'Kelley, J. S. Eldredge, K. J. Northcutt, A. E. Metzger, E. Schonfeld, L. E. Peterson, J. R. Arnold, and R. C. Reedy, Apollo-17 Preliminary Science Report, in press.
- Trombka, J. I., F. Senftle, and R. Schmadebeck, 1970, *Nuc. Inst. and Methods*, **87**, p. 37.
- Vedrenne, G., F. Albernhe, I. Martin, and R. Talon, 1971, *Astron. and Astrophys.*, **15**, p. 50.
- Vette, J. I., D. Gruber, J. L. Matteson, and L. E. Peterson, 1970, *Astrophys. J. Letters*, **160**, p. L161.

## B. INDUCED RADIOACTIVITY CONTRIBUTIONS TO DIFFUSE GAMMA-RAY MEASUREMENTS

G. J. Fishman\*

*Teledyne Brown Engineering*

The importance of the effects of cosmic-ray-induced radioactivity on diffuse  $\gamma$ -ray measurements has recently become apparent (Dyer and Morfill, 1971; Golenetskii, 1971; Fishman, 1972a). In view of the new Apollo-15 results, it is believed that a review of the physical processes involved and the derivation of the corrections due to induced radioactivity would be in order for this Symposium.

Induced radioactivity by protons in  $\gamma$ -ray detectors was first observed on the OSO-1  $\gamma$ -ray detector (Peterson, 1965) and subsequently observed by other detectors placed in earth orbit. The increased background and dead-time due to activation reduced the sensitivity of these experiments but discrete source observations were still possible due to the directionality of the detectors. However, observations of the diffuse  $\gamma$ -ray background are difficult due to the isotropy of the source and the various sources of background radiation which are impossible to eliminate completely. Therefore, all extraneous sources of background must be known and accurately accounted for in order to derive the diffuse cosmic component.

The most reliable measurements of the diffuse component in the MeV energy range have been made by detectors aboard spacecraft placed well outside the trapped radiation and with small amounts of local matter. One component of the background is the decay of radioactive spallation products formed when primary cosmic rays interact with the scintillation detector crystal. The counts produced by these spallation products within the detector are unaccompanied by anticoincidence events and are otherwise indistinguishable from counts produced by external  $\gamma$ -rays. The counting rate induced in a NaI(Tl) crystal with a mass thickness of 25 gm/cm<sup>2</sup> is

$$F_c = 0.15 \times F_p \quad (\text{III.B-1})$$

---

\*Speaker.

where  $F_p \cong 3/\text{cm}^2 \cdot \text{s}$  is the nuclear active particle flux ( $E_p > 100 \text{ MeV}$ ). The above relation is derived from a statistical treatment of the decay characteristics of many spallation products and the total nuclear interaction cross section (Fishman, 1972a). The estimated uncertainty of Equation (III.B-1) is 30 percent.

The cross sections for the formation of individual spallation products are calculated from semi-empirical formulae first derived by Rudstam (1966) and recently modified and rendered more accurate by Silberberg and Tsao (1973). In a NaI(Tl) crystal, interactions with iodine will account for over 80 percent of the radioactive products. Table III.B-1 gives the cross section for producing radioactive spallation products from  $\text{I}^{127}$  at 200 MeV, 800 MeV, and 3000 MeV. These data were provided by the NRL group (Silberberg, Tsao, and Shapiro, private communication). Above 3000 MeV, there is no detectable change in cross sections with bombarding energy. Using these data, it is estimated that 70 percent of the total inelastic cross section of  $\text{I}^{127}$  (1260 mb) will result in the formation of radioactive products. This is indicated at the bottom of Table III.B-1 where the sum of the cross sections for the formation of radioactive spallation products is assumed to be 880 mb at each energy. Naturally, the higher bombarding energies tend to remove more nucleons from the target nucleus. This is illustrated in Figure III.B-1 where all products with formation cross sections greater than 10 mb from  $\text{I}^{127}$  are shown at various energies.

Although the total counting rate due to induced radioactivity is fairly well known from Equation (III.B-1), the spectrum that the counts will produce in a detector crystal is difficult to deduce for a variety of reasons. At the higher energies, representative of primary cosmic rays, several hundred products are formed and would need to be considered for an accurate calculation of the energy-loss spectrum. The decay branching ratios are not well known for many of these products, and the cross section for formation in many cases may be in error by as much as a factor of 2. Also, many of the nuclei have one or more long-lived isomeric states, and there is no means to determine in which state the spallation product will be formed. For these reasons, it is necessary to assume a spectral shape on the basis of other data. It is assumed that the decay spectrum would resemble the  $\gamma$ -ray spectrum from the decay of a large number of mixed fission products since the atomic number and the nuclear energy level spacings of these products are similar to that of the iodine spallation products. This spectrum has an exponential form:

$$\frac{dF}{dE} \propto \exp (E/E_e) \quad (\text{III.B-2})$$

Table III.B-1  
Major Radioactive Spallation Products from I<sup>127</sup>

Nucleons Removed			Element	Isotope	Half-Life	Isomeric Half-Lives	Cross Sections* (mb)		
Total	n	p					200 MeV	800 MeV	3000 MeV
1	1	0	I	126	13d		72	59	57
2	2	0	I	125	60d		83	41	36
2	1	1	Te	125	-	58d	49	24	21
3	3	0	I	124	4.2d		57	28	24
4	4	0	I	123	13h		41	20	18
4	3	1	Te	123	-	117d	49	24	21
5	5	0	I	122	3.5m		30	15	13
6	5	1	Te	121	17d	154d	46	24	21
6	6	0	I	121	2.1h		22	12	10
7	5	2	Sb	120	16m	5.8d	28	16	15
7	7	0	I	120	1.3h		15	8	8
8	7	1	Te	119	16h	4.7d	30	22	21
8	8	0	I	119	19m		24	20	10
Approximate remaining cross section for radioactive products						Sum	546	313	275
							334	567	605
						Total	880	880	880

\*Derived from the formulae of Silberberg and Tsao (1973).

where  $E_e$  is the e-folding energy. The value of  $E_e = 0.9$  MeV used in the previous paper (Fishman, 1972a) was taken from the data compiled by Goldstein (1959). A more recent measurement of the  $\gamma$ -ray spectrum from the spontaneous fission of  $U^{238}$  has been obtained (Sobel et al., 1973). Their work also shows the spectra well fitted by an exponential spectrum up to 20 MeV but with a higher e-folding energy, 1.41 MeV. A measurement of the spectral shape produced by long-lived NaI spallation products also yielded an exponential spectrum up to 3 MeV with an e-folding energy of 0.6 MeV (Fishman, 1972a, b). This spectrum

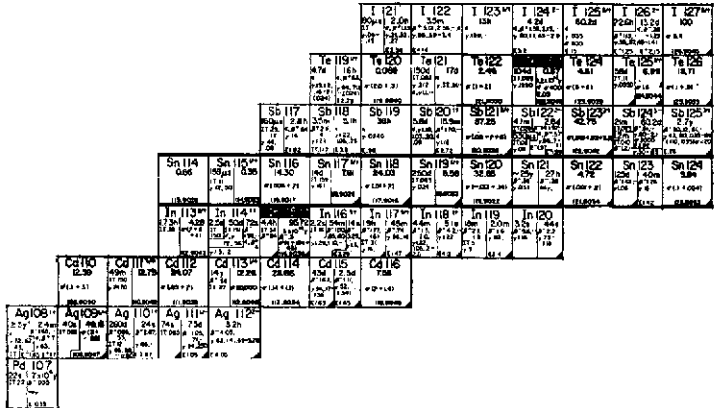
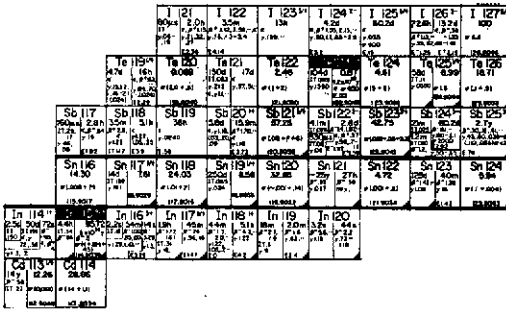


Figure III.B-1. Iodine spallation products produced at various proton bombarding energies. All products shown have a production cross section greater than 10 mb. Although more products are formed at higher energies, the total cross section remains nearly constant,  $\sim 1260$  mb. The segments shown are from the Chart of Nuclides (Goldman, 1966).

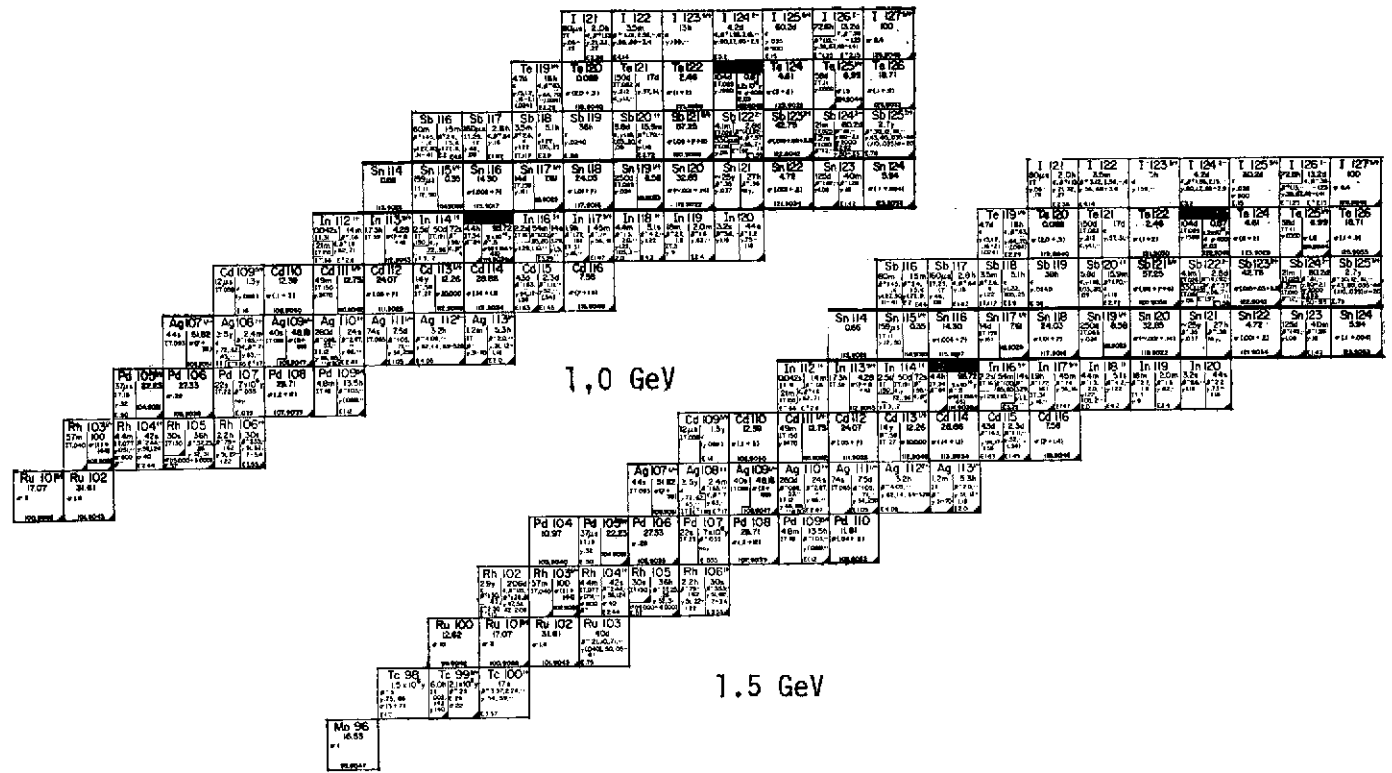


Figure III.B-1 (continued).

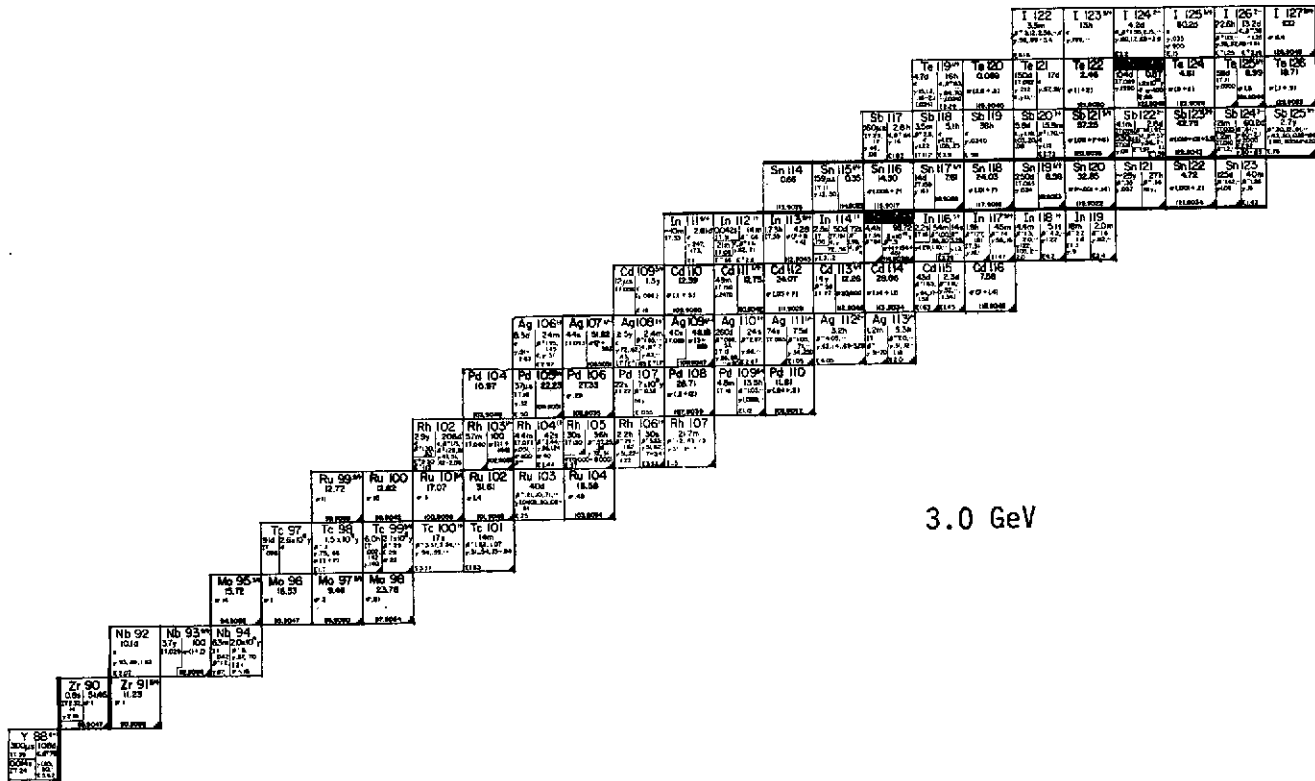


Figure III.B-1 (continued).

is thought to be softer than the actual spectrum of induced radioactivity occurring in diffuse  $\gamma$ -ray measurements because: (1) the measured spectrum did not include the contribution of very short-lived products which tend to have a harder spectrum, being further from stability (this trend is observed in the measured spectra) and (2) the bombarding proton energy was 600 MeV, considerably less than the average cosmic-ray energy producing activation. The three spectra mentioned above are compared in Figure III.B-2. The assumed exponential spectra were normalized to the total induced counting rate of Equation (III.B-1). The experimental data were corrected to include the short-lived products but otherwise normalized. The three spectra agree to within a factor of three up to a few MeV and diverge thereafter. The exponential drop-off at high energies is expected on theoretical grounds; spallation products with high excitation energies will decay by prompt  $\gamma$ -emission and particle emission rather than by delayed  $\beta$ -decay or internal decay. In addition to a continuous spectrum, the true spallation product spectrum is expected to have line features superimposed due mainly to electron capture decays of several iodine isotopes listed in Table III.B-1.

The two exponential spectra of Figure III.B-2 are directly compared with the Apollo-15, ERS-18, and Ranger-3 energy-loss spectra in Figure III.B-3. The important contribution of induced radioactivity in the 0.5-MeV to 5-MeV energy range is apparent. In fact, the hard exponential spectrum exceeds the measured energy loss from 2 MeV to 5 MeV, indicating that a softer spectrum is required. It can also be seen that induced radioactivity has little effect on the observed diffuse spectrum above 10 MeV from the Apollo-15 measurements.

In correcting the Apollo-15 results for spallation-produced counts, Trombka et al. (1973), required that the resulting spectrum be smooth and not dip at intermediate energies, since such a spectrum is physically improbable. On the basis of these assumptions, one-half of the calculated induced flux was subtracted. The factor-of-two discrepancy between the calculated induced spectrum and that which was corrected for is within the range of errors of the calculated induced radioactivity at the present. It is hoped that future accelerator measurements will more accurately determine the true spallation product spectrum so that direct and accurate corrections to the observed diffuse  $\gamma$ -ray flux can be made.

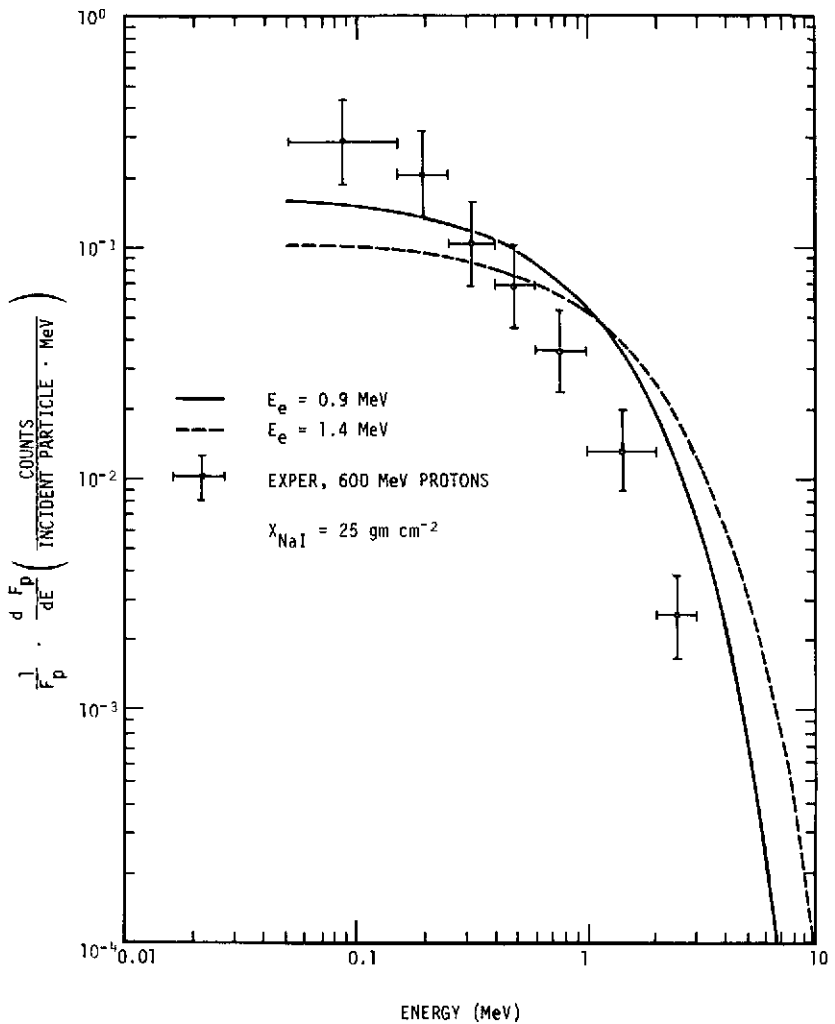


Figure III.B-2. Energy-loss spectrum of induced radioactivity. The data points are from direct measurements of 600 MeV proton-induced radioactivity in NaI(Tl), corrected for the expected contribution of unmeasured, short-lived products (Fishman, 1972b). Also shown are two exponential spectra described in the text, normalized to a total rate of 0.15 counts per incident high energy proton.

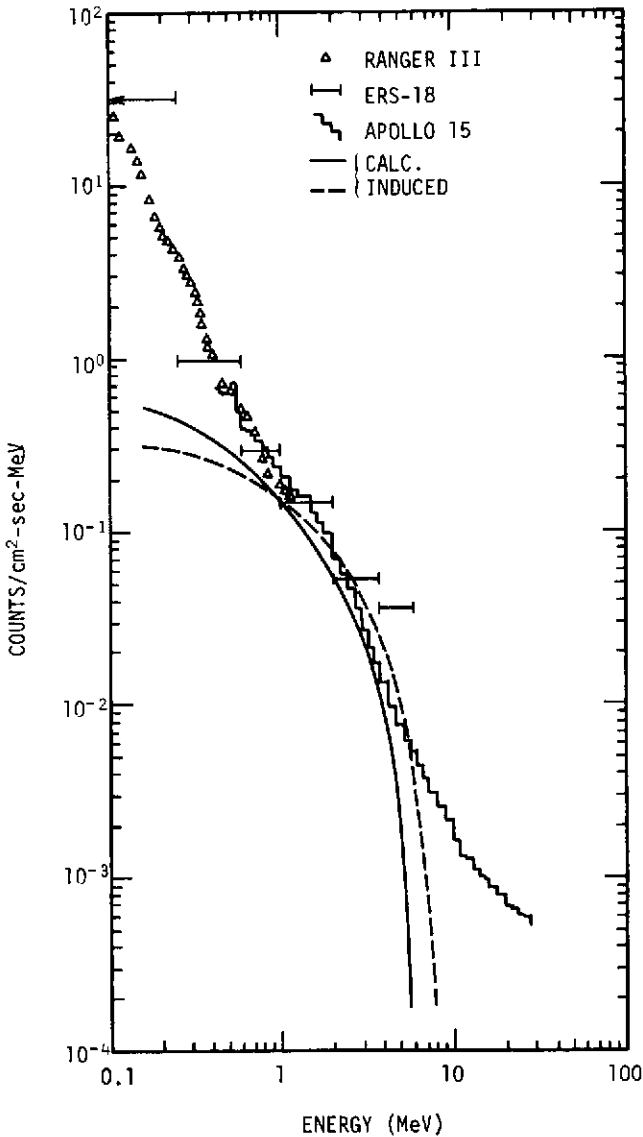


Figure III.B-3. Comparison of spectra measured in interplanetary space by three experiments (from Trombka et al., 1973) with the calculated exponential spectra from Figure III.B-2. A high-energy cosmic-ray flux of  $3 \text{ cm}^{-2} \cdot \text{s}^{-1}$  was assumed. In view of the Apollo-15 measurements, the softer spectrum (solid line) is more likely. The estimated error in the calculated induced spectrum is plus or minus a factor of two at any energy.

## REFERENCES

- Dyer, C. S., and G. E. Morfill, 1971, *Astrophys and Space Sci.*, **14**, p. 243.
- Fishman, G. J., 1972a, *Astrophys J.*, **171**, p. 163.
- Fishman, G. J., 1972b, Summary Report SE-SSL-1497, Teledyne Brown Engineering.
- Goldman, D. T., 1966, "Chart of the Nuclides," 9th Edition, General Electric Company.
- Goldstein, H., 1959, *Fundamental Aspects of Reactor Shielding*, Addison-Wesley Publishing Company, Reading.
- Golenetskii, S. V., 1971, *Astrophys J. Letters*, **9**, p. L69.
- Peterson, L. E., 1965, *Geophys. Res.*, **70**, p. 1792.
- Rudstam, G., 1966, *Zeits. fur Naturforschung*, **21a**, p. 1027.
- Silberberg, R., and C. H. Tsao, 1973, *Astrophys J.*, Supplement No. 220.
- Sobel, H. W., A. A. Hruschka, W. R. Kropp, J. Lathrop, F. Reines, M. F. Crouch, B. S. Meyer, and J. J. Sellschop, 1973, *Phys. Rev. C*, **7**, p. 1564.
- Trombka, J. I., A. E. Metzger, J. R. Arnold, J. L. Matteson, R. C. Reedy, and L. E. Peterson, 1973, *Astrophys J.*, **181**, p. 737.

**C. PRELIMINARY RESULTS FROM THE FIRST  
SATELLITE OF A HIGH-RESOLUTION GER-  
MANIUM GAMMA-RAY SPECTROMETER:  
DESCRIPTION OF INSTRUMENT, SOME  
ACTIVATION LINES ENCOUNTERED,  
AND STUDIES OF THE  
DIFFUSE SPECTRA**

G. H. Nakano\*, W. L. Imhof, J. B. Reagan, and R. G. Johnson  
*Palo Alto Research Laboratory*

Gamma radiation from terrestrial and extraterrestrial sources has been investigated with a high-resolution lithium-drifted germanium, Ge(Li), spectrometer-cryogen system flown on board a low-altitude, spin-stabilized, polar-orbiting satellite (1972-076B) launched on October 2, 1972. The application of large germanium spectrometers in  $\gamma$ -ray astronomy provides the high-energy resolution required to facilitate the detection of monoenergetic nuclear  $\gamma$ -rays and to search for sharp structural features in the diffuse background spectrum. Sources giving rise to these types of  $\gamma$ -radiation in terms of nucleosynthesis were reviewed by Clayton at this Symposium (Chapter XI.A) and  $\gamma$ -ray emission produced in solar flares also was discussed by Forrest (Chapter VI.A) and Ramaty (Chapter XI.C). Although lithium-drifted germanium detectors have been flown on a few occasions in high-altitude balloon experiments, (Jacobson, 1968; and Womack and Overbeck, 1970), this is the first time high-resolution detectors of this type have been flown on a satellite. In this paper we present a brief description of the instrument and discuss some very preliminary results obtained from earth orbit. In Chapter III.D we shall discuss some of the important backgrounds encountered in the satellite flight. These two papers represent a brief review of topics presented at the Annual Meeting of the American Geophysical Union (Nakano et al., 1973; Imhof et al., 1973).

The important features of the spectrometers are shown as a cross-sectional view in Figure III.C-1. In the flight system we employed solid cryogen coolers, which provide obvious design advantages in the zero-G environment.

---

\*Speaker.

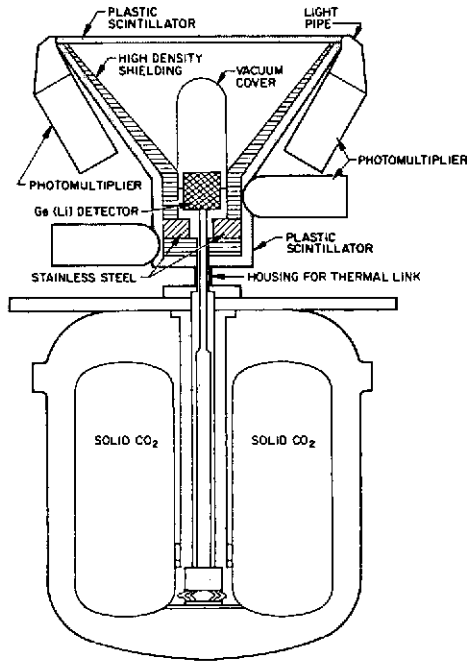


Figure III.C-1. A cross-sectional view of the important features of the Ge(Li) spectrometer. Each instrument weighed 83 kg (163 lb).

The 50 cm<sup>3</sup> Ge(Li) detector, with an active area of 15 cm<sup>2</sup>, is maintained at cryogenic temperatures by a copper thermal link which is coupled to the cooler consisting of sufficient CO<sub>2</sub>, about 15 kg (35 lb), to provide a one-year lifetime. The operating temperature of the detector (130 K) is somewhat higher than the liquid nitrogen temperature normally used in the laboratory (Nakano and Imhof, 1971). The instrument is collimated to  $\pm 45^\circ$  by a large tungsten shield weighing  $\sim 20$  kg ( $\sim 45$  lb) which provides a minimum of 30 gm/cm<sup>2</sup> shielding outside the viewcone. A plastic-scintillator anticoincidence system completely surrounds the shield except for a small access port for the thermal link and is viewed by four photomultiplier tubes. Gamma-ray pulses from the Ge(Li) detector corresponding to energy losses ranging from 40 keV to  $\sim 2.8$  MeV are analyzed by the 4096 pulse-height analyzer with an overall systems resolution of 3.5- to 4.0-keV full width at half-maximum (FWHM) (1.33-MeV Co<sup>60</sup>). The output digital addresses from the pulse-height analyzer are stored on an onboard tape recorder which affords data coverage on a worldwide basis. A maximum rate of 1625 addresses/s can be recorded, and the counting rates are sampled once every 32 milliseconds.

The geometry of the experiment is illustrated schematically in Figure III.D-1 of the following paper (Imhof et al., 1973). It is important to note that the satellite was launched into a noon-midnight, sun-synchronous orbit (inclination  $\sim 98.4^\circ$ ) with apogee and perigee of 761 km and 736 km, respectively. The vehicle has a spin period of 5 s and is magnetically torqued to maintain the spin vector perpendicular to the orbit plane so that in daylight (descending node) the sun is always viewed once per spin period. Two identical  $\gamma$ -ray spectrometers were mounted antiparallel to each other and offset  $\pm 15^\circ$  from the vehicle's equatorial plane. Unfortunately, one of the instruments failed at launch. The other instrument performed successfully for about 10 days and then suffered a serious degradation in gain and energy resolution; however, after a few weeks it made a rather remarkable recovery and subsequently operated at about 90 percent of its original gain with somewhat degraded resolution of about 10 keV as compared to the original 3.5 keV at the 59.6-keV line. The following discussion is confined to data obtained during the first 10 days of operation when the resolution was 3.5 to 4.0 keV over the entire spectrum.

A representative pulse-height spectrum is shown in the top section of Figure III.C-2 where the data, integrated over all spin angles, are summed from several low background passes at low and midlatitudes. In addition to the 59.6-keV  $\gamma$ -ray line from the  $\text{Am}^{241}$  in-flight calibration source, several discrete  $\gamma$ -ray peaks are observed in the data. Some of these lines have been identified and are associated with isomeric transitions induced in the germanium sensor itself (Womack and Overbeck, 1970) and with short-lived radioactivations produced in the tungsten shielding. In Table III.C-1, the more prominent lines present in the spectrum are tabulated with their probable production modes. The most prominent line, always present in the data, is the 511-keV electron-positron annihilation radiation, a significant portion of which apparently are produced on the satellite as indicated by the comparatively high count rate and by the lack of substantial intensity modulations with spin angle. The overall pulse-height spectrum is characterized by a rather hard continuum which is again a manifestation of locally produced high-energy background.

In spite of difficulties due to the high-continuum background and large statistical errors, the diffuse background  $\gamma$ -rays of cosmic origin can be detected, particularly in the lower energy portion of the observed pulse-height spectra. In a preliminary analysis the data from selected low background passes in the equatorial region were grouped into four spin quadrants. The bottom two spectra presented in Figure III.C-2 correspond to data taken when the look direction of the detector is in the upward quadrant and in the downward quadrant, respectively. It should be noted that below 200

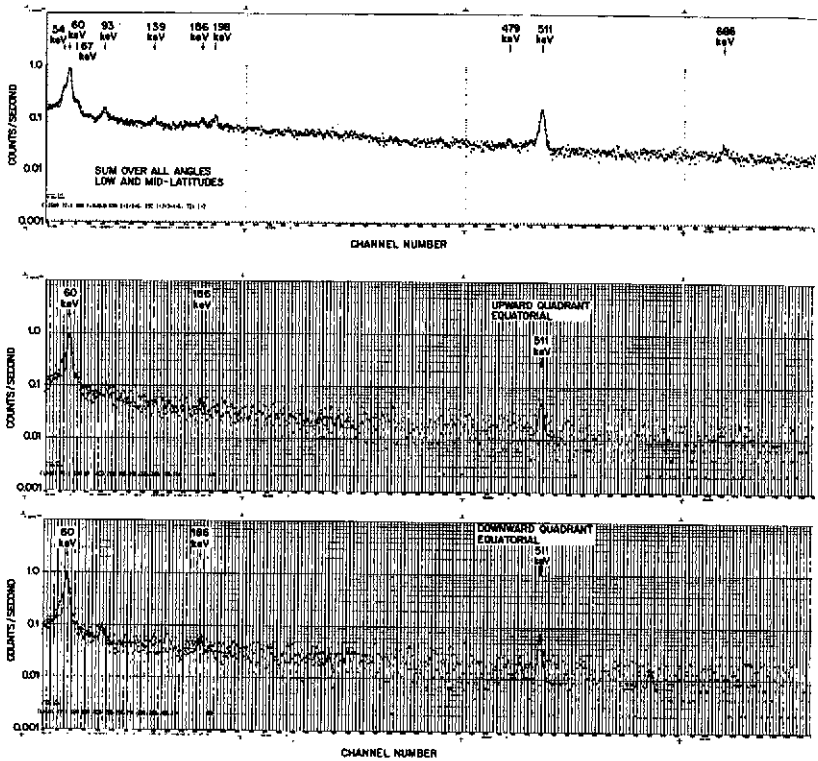


Figure III.C-2. A representative pulse-height spectrum where the data, integrated over all spin angles, are summed from several low- and midlatitude passes (top section). Pulse-height spectrum from related low-background passes in the equatorial region when the look direction of the detector is in the upward direction (middle section) and with downward direction (bottom section).

keV in the continuum portion of the spectrum between peaks, the counting rates appear to be greater in the upward viewing spectrum than in the downward spectrum. This feature is confirmed when counts in the corresponding channel intervals are summed to improve statistics and are directly compared. A detailed analysis of the data, taking proper account of the shielding and detection efficiencies, has just begun. At high energies it is more difficult to obtain definitive measurements of the diffuse background since the general backgrounds are relatively high.

Table III.C-1  
Gamma-Ray Peaks Observed (Preliminary)

$E_\gamma$	Source
54 keV	$\text{Ge}^{73\text{m}}$ from $\text{Ge}^{72}$ (n, $\gamma$ ) $\text{Ge}^{73\text{m}}$
59.6 keV	$\text{Am}^{241}$ in-flight calibration source
67 keV	$\text{Ge}^{73\text{m}}$ from $\text{Ge}^{72}$ (n, $\gamma$ ) $\text{Ge}^{73\text{m}}$
93 keV	
139 keV	$\text{Ge}^{75\text{m}}$ from $\text{Ge}^{74}$ (n, $\gamma$ ) $\text{Ge}^{75\text{m}}$
186 keV	
198 keV	$\text{Ge}^{71\text{m}}$ from $\text{Ge}^{70}$ (n, $\gamma$ ) $\text{Ge}^{71\text{m}}$
479 keV	$\text{Re}^{187}$ from $\text{W}^{186}$ (n, $\gamma$ ) $\text{W}^{187} \xrightarrow[\text{1d}]{\beta^-} \text{Re}^{187}$
511 keV	Positron/electron annihilation
686 keV	$\text{Re}^{187}$ from $\text{W}^{186}$ (n, $\gamma$ ) $\text{W}^{187} \xrightarrow[\text{1d}]{\beta^-} \text{Re}^{187}$

Our spectrometer design was not optimized to study discrete stellar sources, and its sensitivity to photons is quite limited above a few hundred keV. Nevertheless, by making detailed analyses of the angular distributions and spectral variations with geomagnetic latitude, we hold some prospects of investigating the diffuse background spectrum, of detecting  $\gamma$ -ray line emissions from solar flares and, perhaps, of searching for positron annihilation radiation coming from the direction of the galactic center.

(Supported by the Office of Naval Research, the Advanced Research Projects Agency, and the Lockheed Independent Research Program.)

## REFERENCES

- Imhof, W. L., G. H. Nakano, R. G. Johnson, and J. B. Reagan, 1973, *Trans. American Geophys. Union*, **54**, p. 435.
- Jacobson, A. S., 1968, Thesis, University of California at San Diego.
- Nakano, G. H., and W. L. Imhof, 1971, *IEEE Trans. Nucl. Sci.*, NS-18, p. 258.
- Nakano, G. H., W. L. Imhof, J. B. Reagan, and R. G. Johnson, 1973, *Trans. American Geophys. Union*, **54**, p. 435.
- Womack, E. A., and J. W. Overbeck, 1970, *J. Geophys. Res.*, **75**, p. 1811.

**D. PRELIMINARY RESULTS FROM THE FIRST  
SATELLITE OF A HIGH-RESOLUTION  
GERMANIUM GAMMA-RAY SPECTRO-  
METER: BACKGROUNDS FROM ELECTRON  
BREMSSTRAHLUNG AND FROM  
ELECTRON-POSITRON  
ANNIHILATION**

W. L. Imhof\*, G. H. Nakano, R. G. Johnson, and J. B. Reagan  
*Lockheed Palo Alto Research Laboratory*

In continuation of the previous talk we shall now consider in more detail some of the backgrounds encountered in the first satellite flight of a lithium-drifted germanium spectrometer. This is a brief summary of a recent presentation at the annual meeting of the American Geophysical Union (Nakano et al., 1973; Imhof et al., 1973). We have just seen that in the flight data several  $\gamma$ -ray lines are observed and that these have been attributed to isomeric states produced by cosmic rays interacting in the instrument. Fortunately, the intensities of these lines are rather low. By far the most prominent background line experienced is that at 511 keV. Smooth backgrounds attributable to electron bremsstrahlung are also commonly encountered in the satellite measurements. The bremsstrahlung backgrounds can be divided into two basic classes: (1) those arising from radiation belt electrons stopping in the vicinity of the spectrometer, and (2) bremsstrahlung produced by electrons precipitating into the earth's atmosphere. The latter phenomenon can be a significant source of background even when the satellite is thousands of kilometers away from the radiation belts. The geometry for observing two of these common sources of background, the 511-keV peak and the bremsstrahlung continuum, is illustrated schematically in Figure III.D-1. This drawing shows that 511-keV  $\gamma$ -rays are produced in the atmosphere by cosmic rays at all latitudes and that bremsstrahlung associated with electron precipitation can be observed from a satellite even at fairly low latitudes, although it is a more prevalent background at higher latitudes.

---

\*Speaker.

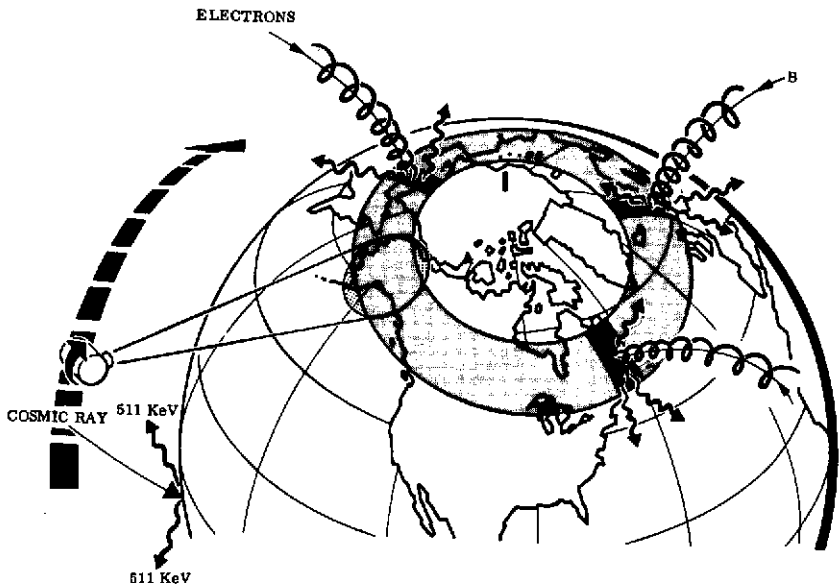


Figure III.D-1. Schematic illustration of the satellite geometry. The viewing cone of the spectrometer is shown for observing the bremsstrahlung associated with electron precipitation at high latitudes.

The aforementioned backgrounds are best illustrated by presenting some typical energy spectra measured during the satellite flight. The spectra shown in Figure III.D-2 were taken at a variety of geomagnetic latitudes and with the spectrometer in various look directions. In the top section is shown a typical spectrum associated with electrons precipitating into the atmosphere. When the  $\gamma$ -ray spectra are compared with the electron spectra that are measured with an electron detector on the same satellite (at a time when the satellite passes directly through the environment of the precipitating electrons), the shapes are consistent with the bremsstrahlung calculations of Berger and Seltzer (1972; 1973). At the time the bremsstrahlung spectrum in Figure III.D-2 was taken, the satellite was over the South Pole of the earth and no radiation belt particles were in the immediate vicinity. The bremsstrahlung spectrum produced by trapped electrons when the satellite is actually in the outer radiation belt is often harder in spectral shape than that associated with precipitating electrons. This is attributable to the fact that the energy spectrum of the trapped electrons is frequently harder than that of the precipitating electrons. However, even the hardest bremsstrahlung spectra observed do not present a serious background for observations above a few hundred keV. For example, when the satellite is in the heart of the outer radiation belt the 511-keV peak can usually be seen with little interference.

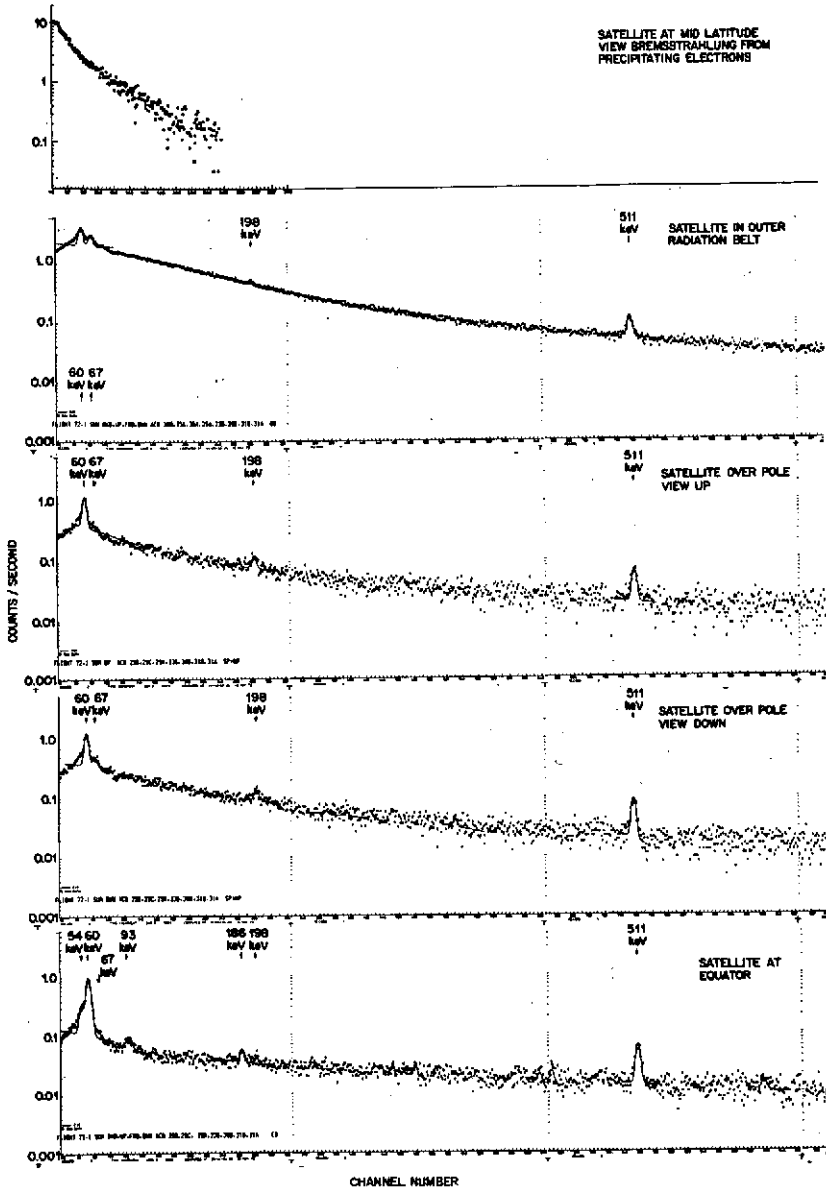


Figure III.D-2. Some selected energy spectra measured during the satellite flight. In the top section is shown a spectrum associated with electrons precipitating into the atmosphere. The bottom three sections contain spectra measured over the earth's polar cap regions and near the Equator.

The bottom three sections of Figure III.D-2 contain spectra measured over the earth's polar cap regions and spectra obtained near the Equator. Over the polar caps the 511-keV line intensity is significantly higher when the spectrometer is pointing downward. This increase in counting rate, when viewing in the downward direction, is attributed to electron/positron annihilation radiation produced in the atmosphere by cosmic-ray interactions. From a preliminary analysis of the data, the counting rates and latitude variations are found to be consistent with balloon observations of the 511-keV intensities. At low latitudes where the 511-keV production rate is weaker, the contribution from the atmosphere is less evident in the data. It should be noted that the continuum background is also weaker at low latitudes. We are presently studying the data to see if there is an increase in the 511-keV rate when the satellite is in the outer radiation belt, as a possible indication of the existence of trapped positrons. At this early stage of the data analysis only an upper limit has been found for the fluxes of trapped positrons. In any event, their possible contribution to the background is negligible.

For unfolding the background contributions it is a great advantage to have the spectrometer placed on a spinning satellite. This is clearly illustrated in Figure III.D-3 where the counting rate profiles of the  $\gamma$ -ray spectrometer and of an electron spectrometer on board the same satellite are shown. The top section represents data taken during a complete orbit of the satellite, including two polar cap crossings and four outer radiation zone crossings. Both the electron and  $\gamma$ -ray spectrometers respond significantly in the outer belt regions. In addition, on this orbit that occurred at a time of high geomagnetic activity, significant increases in the  $\gamma$ -ray counting rates were observed over the polar caps and Equator-ward of the belts. One of the regions where the  $\gamma$ -ray counting rates were enhanced is shown in the middle section of the figure on a more expanded time scale. Here one can clearly see the pronounced modulation in counting rate. Some individual spin profiles, summed over six spins to improve statistics, are shown in the bottom section of the figure. With a careful analysis of the data, the bremsstrahlung source distributions can be unfolded from the data (Imhof et al., 1973). Likewise, when analyzing the data for  $\gamma$ -rays originating from other sources, the bremsstrahlung contributions can often be eliminated with the selection of data at desirable positions and look directions.

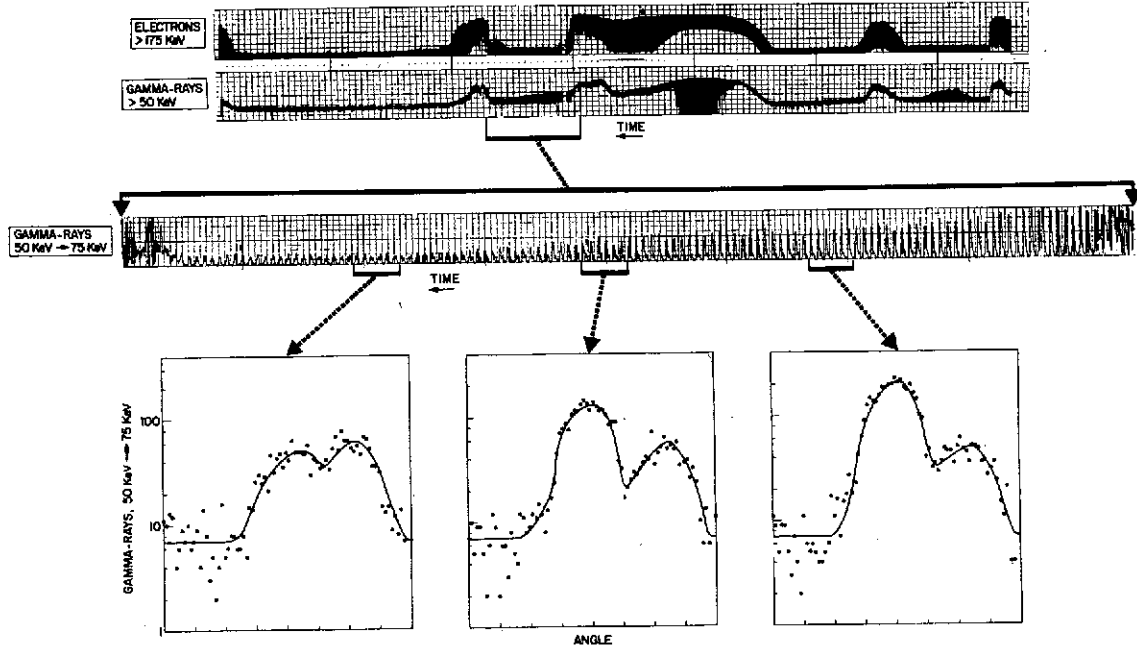


Figure III.D-3. Counting rate profiles of the  $\gamma$ -ray spectrometer and of an electron spectrometer during an orbit of the satellite. One region of the orbit is shown in the middle section on a more expanded time scale. In the bottom section are shown selected individual spin profiles over six spins.

The results presented here are taken from a very preliminary analysis of the data acquired in the first satellite flight of a high resolution Ge(Li)  $\gamma$ -ray spectrometer. This flight has demonstrated the practicability of flying such a system on a satellite and has provided much information on the backgrounds encountered. These data will represent an important basis for designing future  $\gamma$ -ray spectrometers for satellite usage.

(Supported by the Office of Naval Research, the Advanced Research Projects Agency, and the Lockheed Independent Research Program)

#### REFERENCES

- Berger, M. J., and S. M. Seltzer, 1972, *J. Atm. Terr. Phys.*, **34**, p. 85.
- Imhof, W. L., G. H. Nakano, R. G. Johnson, and J. B. Reagan, 1973, *Trans. American Geophys. Union*, **54**, p. 435.
- Nakano, G. H., W. L. Imhof, J. B. Reagan, and R. G. Johnson, 1973, *Trans. American Geophys. Union*, **54**, p. 435.

## E. FURTHER CONSIDERATIONS OF SPALLATION EFFECTS

Clive Dyer\*  
*Imperial College*

I just want to reinforce what Dr. J. Fishman has said by presenting a few results which we arrived at independently at Imperial College, London. We undertook an investigation to estimate the effects of South Atlantic Anomaly Traversals on the future UK-5 hard X-ray telescope that was primarily aimed towards discovering the effects of the activation of the central detector crystal by trapped protons.

We were able to see from the results that cosmic-ray effects would also be important, and these I'll mainly talk about here.

We based our estimates both on the Rudstam formula and, as J. Fishman has pointed out, also on an extensive number of irradiation experiments.

Figure III.E-1 summarizes the results of an accelerator experiment in which we irradiated the UK-5 central crystal which was 5 cm long and 3.4 cm diameter of CsI with 155-MeV protons.

Figure III.E-1 shows the energy-loss spectra that we obtained soon after irradiation.

As Dr. Fishman pointed out, it is important to measure these decays over a wide range of times. He mentioned down to 10 microseconds.

We measured the activation after one minute, which is the quickest we could get the crystal out of the beam and optically seal it on our photomultiplier tube; thus, we have in fact experimentally measured decays down to shorter half-lives than Fishman was able to, and perhaps we have to apply less of a unit to the estimated correction due to extrapolation back to these short half-lives.

---

\*Speaker.

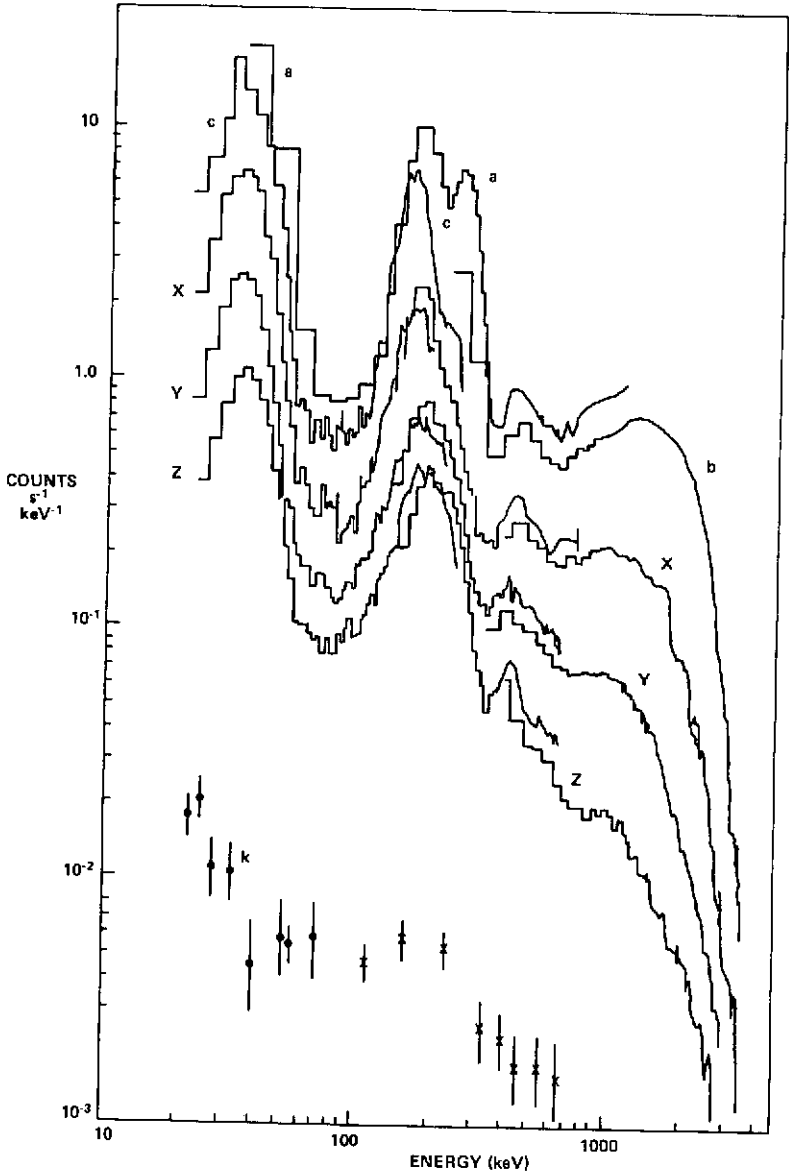


Figure III.E-1. Pulse-height spectra of the proton-induced activation of 3.4-by 5-cm CsI (UK-5 central detector) as a function of time after low-dose irradiation. Shortest period after irradiation is 1 min and the longest period of time is 2 hr.

These spectra all show the peak on the left, which is the K-capture peak at about 35 keV. A second major feature is found at around 170 to 200 keV, depending on the time after irradiation that the spectral measurement is made, and it is due to  $\gamma$ -emissions from a number of isotopes, which will be listed.

The time scale of the decays goes from 1 min on the highest curve in Figure III.E-1 down to 2 hr on the bottom curve. Also shown are features just above 400 keV and maybe just above 600 keV. You can see these features more clearly in Figure III.E-2.

The other major feature is the  $\beta^+$ -continuum of decays, which is the important feature when it comes to correcting the Apollo results, and this gives the shape shown around 1 MeV.

As you can see, the spallation continuum is quite hard to start with, but it decays away quickly because of the shortness of the half-lives of the  $\beta^+$ -decays. It drops at about 3 to 4 MeV very steeply.

Figure III.E-2 also shows the longer half-life decays. We obtained these by giving a higher dose to a second crystal. You really need to expose the crystals to two different dosages to cover the wide range of decays from a minute to several hundred days. These half-life decays run from Curve P at the top of Figure III.E-2 (taken 7 hr after irradiation when the rate was down) down to the very bottom curve which is going into the background about 200 days after irradiation.

You can see that the  $\beta^+$ -emitters have really decayed away quickly, and we are left with quite a number of important line features at 35 keV and around 200 keV, 400 keV, and 600 keV.

I will not go into the isotopes for those, because I can provide lists to interested individuals.

Figure III.E-3 shows the results of computations based on the Rudstam formula for the number of isotopes produced in such a crystal and due to different types of energetic particles. We used a typical inner-belt spectrum, we assumed monoenergetic 155-MeV protons to compare with the experiment, and we also assumed cosmic rays of 2 GeV in energy where the spallation cross-section becomes independent of energy.

The short-term decays are listed in Table III.E-1. You can see a number of  $\beta^+$ -emitters. There are none longer than 2 hr so that they decay very quickly. Table III.E-2 shows the longer half-life decays, mainly electron captures. One can see decays at around 200, 400, and 600 keV and at long half-lives of around 150 days, which can build up activity over a satellite history. One can observe the rates building up if the detector is flown for a sufficiently long time, of the order of several hundred days.

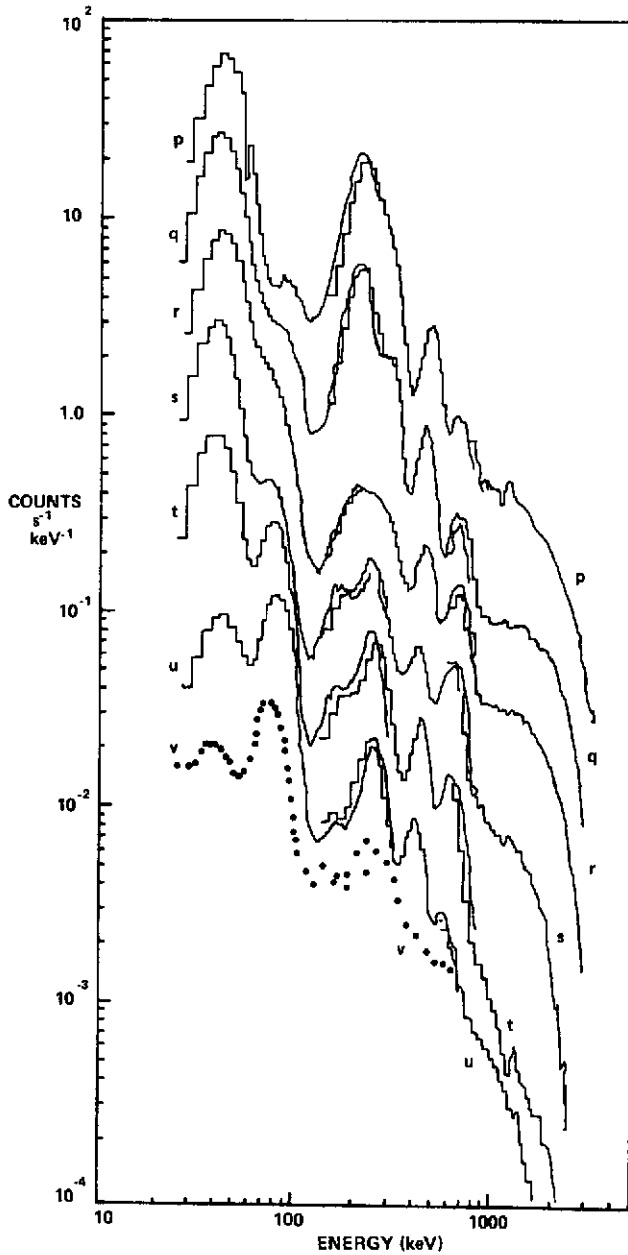


Figure III.E-2. Pulse-height spectra of the UK-5 detector as a function of time after high-dose irradiation. Shortest period after irradiation is 1 min; the longest period is several hundred days.

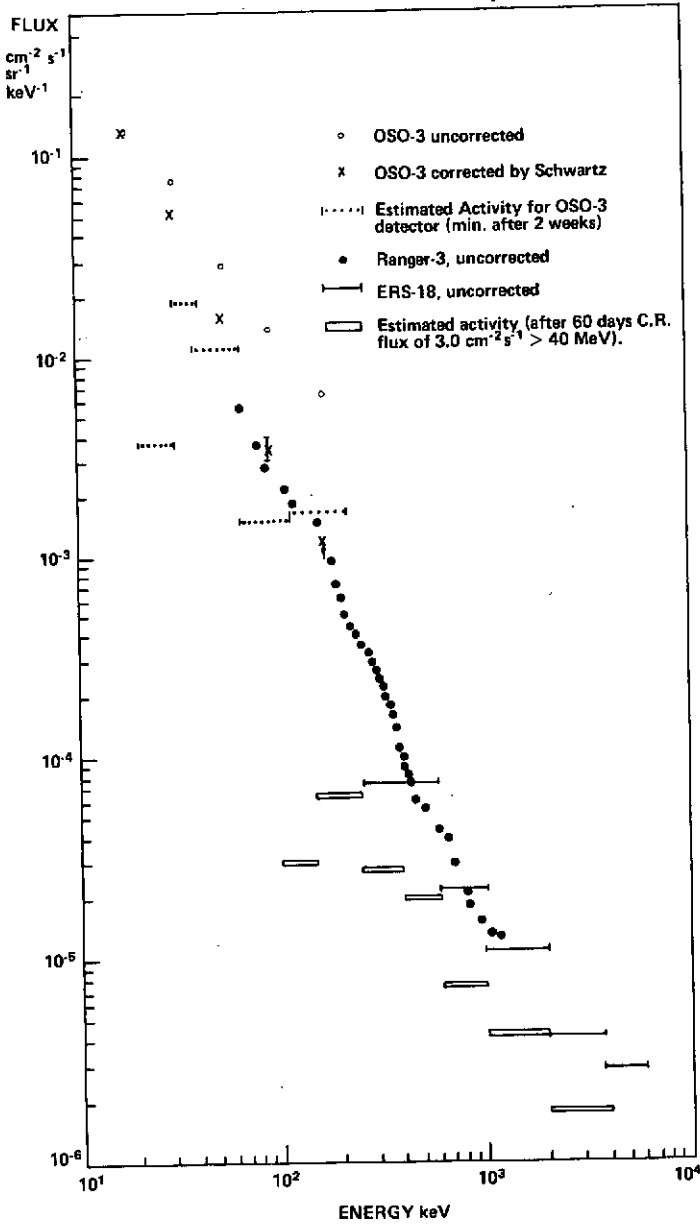


Figure III.E-3. Uncorrected measurements of the diffuse X-ray spectrum and estimated corrections for induced activity.

Table III.E-1  
Short-Term Decays

Isotope	Decay Mode and Energy (MeV)	Half-Life $\tau_{1/2}$ (mins)	Predicted Numbers Produced		
			(i) Inner Belt	(ii) 155MeV	(iii) Cosmic Rays
$^{55}\text{Cs}_{130}$	$\beta^+$ 1.97 $\beta^-$ 0.442	30	3199 —	3183 —	576 —
$^{55}\text{Cs}_{128}$	$\beta^+$ 3.0 (70%) 2.5 (30%) E.C. (25%) 0.460 (20%) 0.285 (20%)	3	8623 —	8448 —	3063 —
$^{55}\text{Cs}_{127}$	E.C. $\gamma$ 0.406	360	11959	11190	5743
$^{55}\text{Cs}_{126}$	$\beta^+$ 3.8 (82%) E.C. (8%) 0.426 (7%)	1.6	13947 —	12158 —	8834 —
$^{54}\text{Xe}_{125}$	$\gamma$ 0.187 0.056 0.243 E.C.	1080	4324 —	3431 —	3529 —
$^{54}\text{Xe}_{123}$	$\beta^+$ 1.7 0.148	120	6584 —	4068 —	8385 —
$^{53}\text{I}_{123}$	E.C. $\gamma$ 0.160	780	8340 12411	7929 12124	3322 3492
$^{53}\text{I}_{122}$	$\beta^+$ 3.0	4	11935 17598	10918 16695	6477 6806
$^{53}\text{I}_{121}$	$\beta^+$ 1.2 0.21	96	14395 21015	12345 18876	10367 10894
$^{52}\text{Te}_{127}$	$\beta^-$ 0.70	560	6000 9060	6000 9060	6000 9060
$^{51}\text{Sb}_{118}^m$	$\beta^+$ 3.1	3.5	1577 2229	967 1479	2305 2422
$^{51}\text{Sb}_{117}$	E.C. $\gamma$ 0.161	168	2609 3648	1376 2104	4641 4877
$^{51}\text{Sb}_{116}$	$\beta^+$ 2.4 1.3	15	3592 4969	1601 2449	7646 8035
$^{50}\text{Sn}_{111}$	E.C. (71%)	35	657 865	105 198	2847 2992

Table III.E-2  
Long-Term Decays

Isotope	Energies of $\gamma$ -rays (MeV) and Branching Ratio	Half-Life $\tau_{1/2}$ (days)	Predicted Numbers Produced		
			(i) Inner Belt	(ii) 155MeV	(iii) Cosmic Rays
$^{55}\text{Cs}_{132}$	E.C. 0.670	6.2	6000 —	6000 —	6000 —
$^{55}\text{Cs}_{131}$	E.C.	10	1716 —	1659 —	212 —
$^{55}\text{Cs}_{129}$	E.C. 0.380	1.3	5507 —	5508 —	1410 —
$^{55}\text{Cs}_{127}$	E.C. 0.406 (80%)	0.25	11959 —	11190 —	5743 —
$^{54}\text{Xe}_{131}^m$	0.163	12	70 —	67 —	9 —
$^{54}\text{Xe}_{129}^m$	0.196;0.040	8	367 —	367 —	94 —
$^{54}\text{Xe}_{127}$	E.C. 0.370 (40%) 0.203 (60%)	34	1505 —	1408 —	723 —
$^{54}\text{Xe}_{125}$	E.C. 0.187; 0.243	0.7	4324 —	3431 —	3529 —
$^{54}\text{Xe}_{123}$	0.148	0.08	6584 —	4068 —	8385 —
$^{53}\text{I}_{126}$	E.C. (55%) 0.386 (34%); 0.650 (33%)	13	6000 9060	6000 9060	6000 9060
$^{53}\text{I}_{126}$	E.C.	60	2899 4382	2750 4206	575 604
$^{53}\text{I}_{124}$	E.C. (70%) 0.605 (95%)	4	5159 7742	4964 7591	1469 1544
$^{53}\text{I}_{123}$	E.C. 0.160	0.5	8340 12411	7929 12124	3322 3491
$^{52}\text{Te}_{125}^m$	0.110; 0.035	58	136 206	129 197	27 28
$^{52}\text{Te}_{123}^m$	0.089; 0.159	104	685 1020	652 996	273 287
$^{52}\text{Te}_{121}^m$	0.082; 0.214	154	2564 3743	2199 3362	1846 1960
$^{52}\text{Te}_{121}$	0.570 (87%); 0.506 (13%)	17	14395 21015	12345 18876	10367 10894
$^{52}\text{Te}_{119}$	E.C.	4.5	6082 8693	4264 6520	7176 7541
$^{51}\text{Sb}_{122}$	0.566 (66%)	2.8	71 105	65 99	31 40
$^{51}\text{Sb}_{120}$	E.C. 0.089; 0.199	6	397 574	312 477	371 389
$^{51}\text{Sb}_{119}$	E.C.	1.66	834 1192	585 894	984 1034
$^{50}\text{Sn}_{117}^m$	0.159; 0.162	14	284 397	150 229	505 530

Notice that there are no  $\beta^+$ -decays in Table III.E-2. None of the  $\beta^+$  emitters which are produced have half-lives of the order of days. These isotopes have very short half-lives.

Experimental data of this sort enables you to plot decay rate against time after radiation. If you normalize these data to a typical cosmic-ray flux, taking  $3 \text{ particles/cm}^2 \cdot \text{s}$  as the intensity (because this is the magnitude of the flux quoted for the time of the ERS-18 measurement), plot all these decay curves, and find the area under them, you can estimate the activity built up after a certain time after radiation. Using this method, the activity build-up for up to 60 days after radiation was obtained. This is the ERS-18 time scale, and we thus came up with the correction shown in Figure III.E-3 for the measurement obtained during that flight.

The left end of Figure III.E-3 shows corrections that apply at the lower energy end of the spectrum and will not be discussed here. At the high-energy end, in the region of 1 MeV, I show the ERS-18 points in the usual manner, depicting a flattening and an apparently erroneous channel that goes from 4 to 6 MeV. And I show our estimates of the build-up activity correction due to the cosmic-ray flux. I believe this is the sort of correction which Jack Trombka has tried taking away, and I'm a little puzzled as to why it's a factor of 2 too high.

Dr. J. Fishman says these calculations are good to perhaps 20 percent, and I don't think they are off by a factor of 2, particularly in our case as we obtained measurements up to 3 a minute after irradiation. Here there is no arbitrary factor depending on the theoretical computations of the half-life distribution. We simply took the experimental data and found the area under the decay curves. As Dr. Fishman pointed out, what might be missing in this procedure is half-lives from  $10 \mu\text{s}$  to 1 min, which would raise these estimates even more and might produce a few decays in excess of 4 MeV. I don't know that these  $10\text{-}\mu\text{s}$  to 1-min half-lives would be too important, but they might extend a correction to above 4 MeV where the present estimate of the  $\beta^+$ -energy deposition falls over. Also, I believe that Apollo-15 gave the same energy-loss spectrum as the ERS-18 results, and my correction in the 1- to 2-MeV channel is around 50 percent—I'm not sure how you say that a 50 percent correction produces a hole in the spectrum if subtracted from the total spectrum. Perhaps that's a good note to end on and start the discussion.

## DISCUSSION

*Shapiro:*

Dr. Dyer and Dr. Fishman both use a reasonable cosmic-ray flux, but as was pointed out, the energy even in the case of 600-MeV protons is quite a bit

below the average cosmic-ray energy. In Dyer's case, it is roughly a factor of 20 below the average, and I'm wondering what influence this might have upon the estimated corrections?

*Dyer:*

Well, that is a matter of concern. I'd like to see flight detectors actually irradiated and that type of technique used to do the corrections. I think this is the only way of doing it. You need to measure three types of radiation: short half-life radiation, then radiation with a half-life of a minute to several hours, and finally radiation with a half-life of several hours to several days.

I wouldn't think it would lower the correction, having a more energetic beam striking. I think you still get a very large number of  $\beta^+$ -emitters produced, and I don't see how they are going to be a factor of 2 different from the 155- or 600-MeV radiation.

*Member of the Audience:*

The cross sections for the production of those products above about 600 MeV are reasonably constant, aren't they?

*Shapiro:*

Well, I'm more disturbed about the 155 MeV calculations.

*Member of the Audience:*

One-hundred and fifty-five is low. Above the 600 MeV or so, as Jerry Fishman said, the cross sections seem to be reasonably constant or at least they are slowly varying.

*Shapiro:*

How much difference would it make whether you use Rudstam's original formula or the improved Silverberg corrections?

*Member of the Audience:*

In that connection my guess is that the effects of the heavier nuclei would be more than proportional to their number, and I wonder if you have considered that?

*Dyer:*

That if you got a higher energy irradiated flux you produce larger nuclei?

*Vette:*

No,  $\alpha$ -particles in the cosmic rays.

*Dyer:*

No, I've not considered that. I wouldn't consider it so important, less than 1 percent.

*Vette:*

As I recall also, your (Dyer) calculations would indicate you would see a buildup running at least 60 days after launch, or something like that?

*Dyer:*

Yes, it would be confined to the lower energy end of the  $\gamma$ -ray spectrum in the 100- to 200-keV region where you could detect this sort of buildup. As I pointed out, these  $\beta^+$ -emitters decay with a half-life of less than 2 hr, and therefore, you don't see any buildup after 2 hr in the 1-MeV region. So maybe experimentally you can get a handle on the buildup by looking for the buildup in the 100-keV region after a few days and use that factor to give you a measure of the  $\beta^+$ -correction.

*Vette:*

As I recall from the ERS-18 results, there were no time changes after a couple of days. There were some changes which might have been due to activation, but there was really nothing after the first 2 or 3 days. There seemed to be some problems in correlating some of the calculations with some of the observations.

*Forrest:*

On the OSO-7 we also observed some of these induced  $\gamma$ -ray lines. I think all of the features are predicted, but some of the predicted features are not seen. This may indicate that some of the predictions are overestimated.

*Dyer:*

Are you talking about cesium iodide?

*Forrest:*

We have both on OSO-7: the sodium iodide detector and the cesium iodide shield.

*Trombka:*

What if we have, for instance, a microsecond dead time after each proton event, how would that change your predicted values? In other words, on Apollo-15 and -16, we're shut off because of the anticoincidence mantle for certain periods after a proton event.

*Dyer:*

For how long is it?

*Metzger:*

In most cases on Apollo, it was a period of about 12 or 13  $\mu$ s.

*Dyer:*

Well, as Jerry Fishman mentioned, this gives the lower threshold above which you are interested in measuring the half-lives. You want to measure the half-lives in excess of 10  $\mu$ s and find the error in the decay curve down to the lower limit. Our present data has been obtained for times down to 1 min. The mystery is what happens in the 10- $\mu$ s to 1-min region. There might be additional decays there.

*Pieper:*

Just as a matter of opinion, I don't think you're going to get much of anything that is going to deposit more than 10 MeV in the detector at a time later than a dozen microseconds, or something of that sort. Shorter times of less than 1  $\mu$ s are possible, particularly if you do have an anticoincidence shield. But there aren't that many highly excited states in the kinds of isotopes you're going to find that are nearer your target nucleus, even reasonably near on the periodic chart.

You have to get down to the carbons and oxygens and the low Z-materials that have high excited states, and you don't form very many spallation products.

*Dyer:*

Right.

*Fishman:*

Right. What I had in mind was  $\beta$ - $\gamma$  cascades where you step through perhaps three or four different nuclei in rapid succession within a microsecond or so. I admit this is very unlikely, but it doesn't take much between 10 and 20 MeV to subtract from the measured fluxes.

*Metzger:*

Unless that happens beyond the dead time of the instrument, the instrument does not know that it has happened.

*Share:*

Can we go into the high-energy region?

*Vette:*

Yes, I want to open up the general discussion on observations, experimental problems, techniques, and then we might come back to the problems discussed by Dyer and Fishman.

*Share:*

I just want to make one point. If the spallation effect could possibly be taken as the cause of the lower energy feature in the 1-MeV region, then there remains a problem of the higher-energy region, 10 to 20 MeV, that Apollo has seen. The question does arise as to what occurs at the open end of the system which does not have the anticoincident plastic around it. I was wondering whether you have considered the cosmic-electron flux that could pass through that open end.

I made some quick estimations the other day and I came up with a number of something like 25 percent of the events observed in the Apollo-15 experiment could be due to cosmic-ray electrons just going through that open end of the detector. This is basing the estimation on the spectra of Simnet and McDonald.

In your paper (Peterson and Trombka, Chapter III.A) you did not mention your anticoincidence efficiency, but you did mention that you had a threshold of 1 MeV for detecting particles going through the anticoincidence shield. Have you determined that your anticoincident efficiency is better than one part in 500 or one part in a thousand. Without such rejection efficiencies, you would obtain an apparent  $\gamma$ -ray intensity in the 20-MeV region.

*Peterson:*

I think the problem of rejection efficiency must be more like one part in 50 or one part in 100. You can determine that if you look at the energy-loss curve given in our paper.

*Trombka:*

Yes, with the anticoincidence on and off one gets a feel for the rejection efficiency. The rejection efficiency curves presented in our paper (Chapter III.A)

were obtained with the anticoincidence shield both on and off during flight. These results were compared with ground studies of the rejection efficiency for the system as a function of energy.

In terms of the matter of the secondary electrons, there are two effects. In the first place, there is a glass plate in front of the scintillation detector. I don't know how many of the electrons will be stopped, but it should be an effective shield. Again, the problem of the dead time of the instrument should be considered because it would be shut off most of the time when such a cosmic-ray effect would occur.

*Peterson:*

I haven't worked out the numbers, but there's a fair amount of material in back of the scintillation detector so the electrons first of all have to pass through about  $20 \text{ gm/cm}^2$ , which means we're talking about 50-MeV electrons penetrating, probably. I don't know what the integral flux of 50-MeV electrons is, but it has to be on the order of  $\sim 10/\text{cm}^2 \cdot \text{s}$ .

*Member of the Audience:*

I think I'm confused about the factors of 2 in the magnitude of the spallation effect discussed by Trombka. If the spallation cross sections don't change very much between several hundred MeV and a few GeV, then most of the cosmic rays are around several hundred MeV and modulation effects could easily, I would have thought, give a factor of 2 in the magnitude of spallation combination. Now, is that not true?

*Vette:*

I think all of these are normalized to the observed cosmic-ray flux at about 50 MeV or so.

*Member of the Audience:*

At what time?

*Vette:*

At the time of the measurement.

*Trombka:*

I think that the problem lies in the comparison of the results obtained on Apollo-15 as compared with Apollo-17. On Apollo-17, we looked at the longer lived induced spallation lines. What we saw during the transearth measurements on Apollo-15 were rather distinct lines in the 0.57- to 0.7-MeV

region, which we attributed to spallation products. These lines were observed in the measurement made on the Apollo-17 detector after recovery. The difference in the induced activity calculated using the intensity in 0.57 to 0.6 MeV on Apollo-17 with that which I observed on Apollo-15 was a factor of two or three. That is, Apollo-17 intensity was higher than that observed on Apollo-15.

I realize the environment around the crystal on both flights was somewhat different. The Apollo-17 crystal was stored in the Command Module while the Apollo-15 crystal was in the Service Module. There is a difference in exposure time also: the 250 hr on Apollo-15, which is when we measured the transearth spectrum, as compared to 300 hr on Apollo-17. Thus, you know there is not a factor of 2 in that time difference.

## F. HEAO GAMMA-RAY ASTRONOMY EXPERIMENTS

A. Metzger\*

*Jet Propulsion Laboratory*

I will report information which is perhaps not known to all the theorists, and particularly the foreign guests, at this Symposium, namely, two  $\gamma$ -ray experiments in the 0.1- to 10-MeV region that had been planned as part of the initial HEAO program.

The first experiment is the combined UCSD-MIT experiment, based on a design originally proposed by Larry Peterson and his collaborators at the University of California at San Diego (UCSD) and recently modified to include aspects of an experiment proposed by Walter Lewin of the Massachusetts Institute of Technology (MIT). It will be flown, hopefully, on the first satellite of the reconstituted HEAO program in 1976 or 1977.

This experiment has been designed to measure and map the cosmic  $\gamma$ -ray spectrum. A schematic of the instrument is shown in Figure III.F-1. It is a large scintillation detector system that can obtain data in a number of modes.

The center detector is a 12.7-cm (5-in.) diameter by 7.6-cm (3-in.) long sodium iodide crystal viewed by a single photomultiplier tube. Around the central detector is an annular shield of cesium iodide for anticoincidence rejection of both charged particles and  $\gamma$ -rays. The full-width at half maximum field of view of the central detector is  $40^\circ$ . A phoswich of cesium iodide is located between the sodium-iodide crystal and its photomultiplier tube to provide rejection from the rear. The purpose of this is to provide a directional system with maximum sensitivity for the diffuse spectrum based on efficient suppression of the  $\gamma$ -ray flux entering outside the field of view. The annular shield is divided into two halves, and the capability exists for them operate as a pair spectrometer in coincidence with the central detector.

---

\*Speaker.

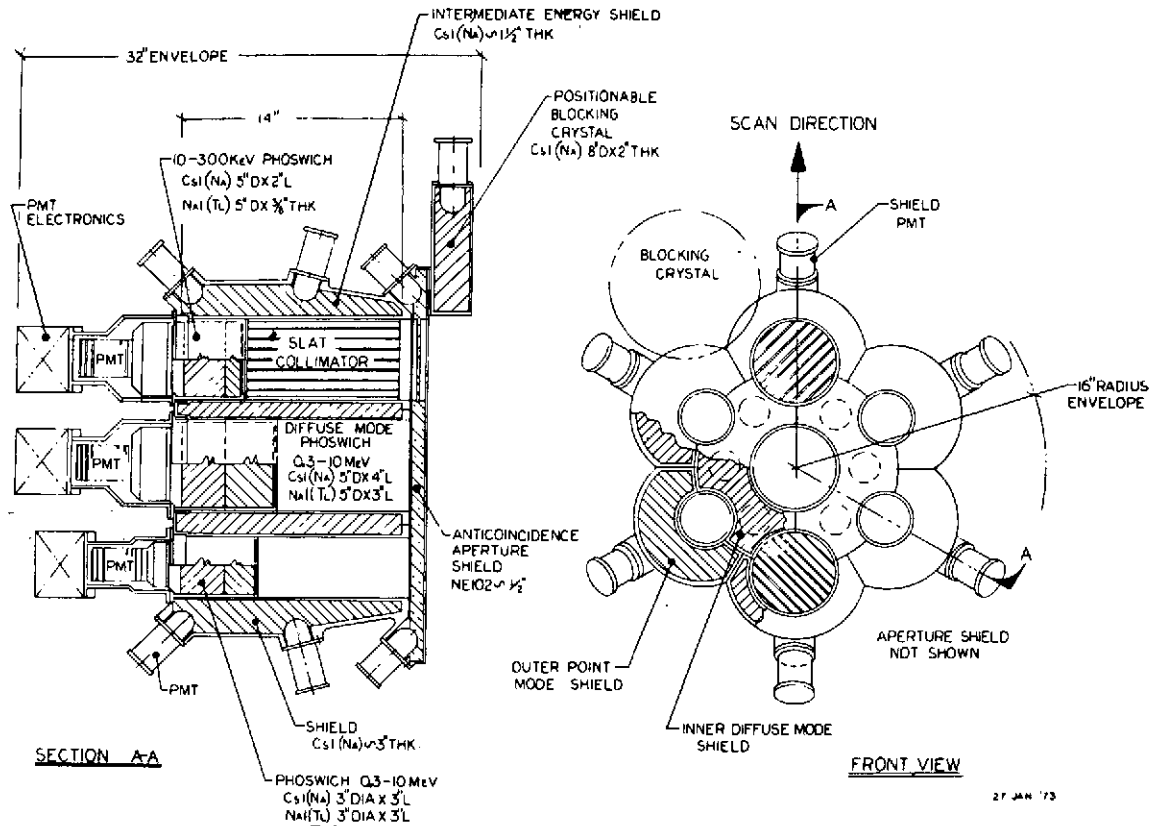


Figure III.F-1. UCSD MeV range  $\gamma$ -ray instrument extended 10- to 300-keV capability.

Around the inner system is a circular grouping of six detectors which are of two types. One type is shown with cross-hatching and is designed to be a low-energy detector system—there are two of these. Each one is a sodium iodide scintillator, 12.7 cm (5 in.) in diameter by 0.95 cm (0.375 in.) thick. They are designed to cover a range of roughly 30 to 300 keV and also have the phoswich configuration to provide rejection in the backward direction.

The field-of-view of each low-energy detector is  $1.5^\circ$  by  $20^\circ$  and that is achieved with a passive-slat collimator.

The four detectors of the other type positioned on the circle are designed to more accurately localize point sources than the central detector, so that the field-of-view of each of these is  $20^\circ$ . These sodium iodide crystals are 7.6 cm (3 in.) in diameter by 7.6 cm (3 in.) in length in order to cover the same energy range as the central detector. They also have the phoswich configuration. Outside the circle of six detectors is an external anticoincidence shield, which serves the circle of six as well as the central detector. So the anticoincidence shield is of varying thickness for the different detectors, with maximum effectiveness for the central detector.

There is sophisticated logic to allow this detector system to be commanded in any number of ways. For example, all of the scintillators around the central detector can be programmed to function in anticoincidence with the central detector. The reduction in background should be very significant in this case. It will be possible to position a blocking crystal above any of the seven primary detectors. In addition, the entrances to each of these detectors will be covered at all times by a thin sheet of plastic scintillator in order to remove electrons which might otherwise be mistaken for  $\gamma$ -rays.

The sensitivity of the system has been calculated as sufficient to detect a source one-thirtieth of the Crab's emission at 0.3 MeV, and one-third of the Crab's emission at 3 MeV.

The second experiment, one of the instruments accepted for the original HEAO-B mission, was a high-resolution  $\gamma$ -ray spectrometer that utilized solid-state detectors. This experiment was proposed by Bud Jacobson at the Jet Propulsion Laboratory (JPL). It has now been deferred, hopefully to the third launch of the revised program, although the payload of the spacecraft has not been set as yet. A schematic of this instrument is shown in Figure III.F-2.

This is an early version of the instrument. There have been a few changes, but the basic arrangement is the same. The system contains four Ge(Li) solid-state detectors. If the instrument can be kept at the present scale, each of the Ge(Li) detectors will have a volume of some  $60 \text{ cm}^3$  and a surface area of  $16 \text{ cm}^2$ . The

specified resolution is 2.5 keV close to 1 MeV, which means a resolution some 40 to 50 times better than one can expect to get from a sodium iodide detector.

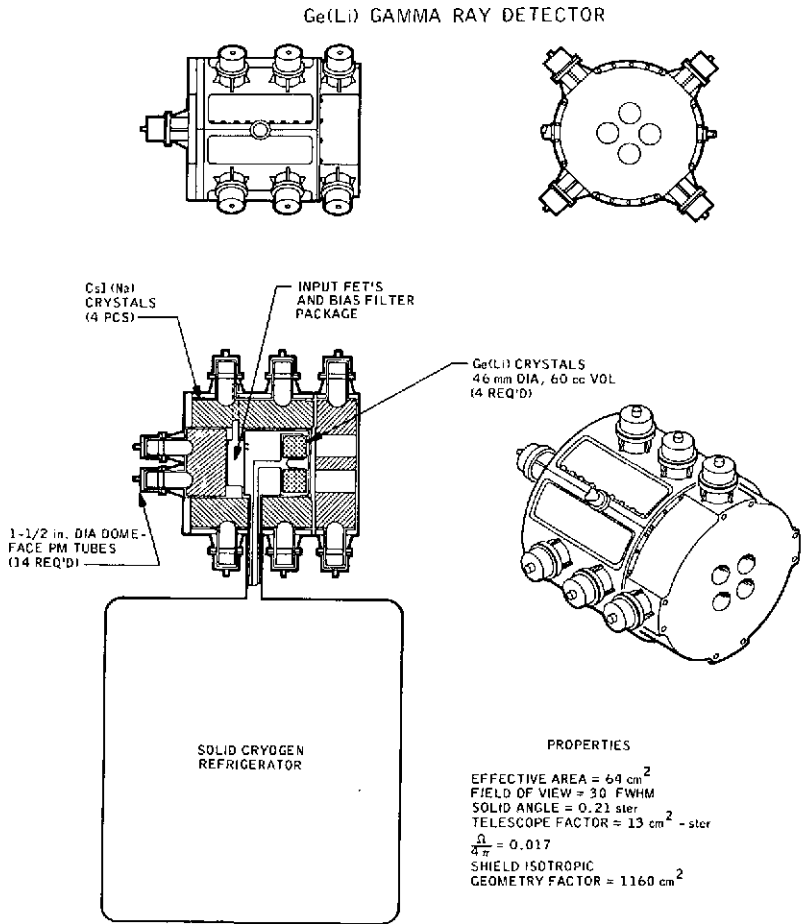


Figure III.F-2. HEAO Ge(Li) detector and refrigerator.

The solid-state detectors will be surrounded by a thick anticoincidence mantle of CsI(Na), which will be in two parts, covering the sides and rear, somewhat like a clam shell in configuration. Above the cluster of solid-state detectors will be a CsI(Na) collimator with holes drilled to permit access to the solid-state detectors. That is what defines the field-of-view which will be  $30^\circ$  full-width at half maximum, equivalent to a solid angle of 0.21 sr.

Cryogenic cooling is needed. The refrigerator presently planned is a two-stage sublimation unit using solid methane and ammonia. The arrangement of the heat-transfer system has been changed to exit from the rear instead of the side in order to improve thermal performance and simplify the mechanical design.

The electronics and command capability will be designed so that the system can function as a total absorption spectrometer, a sum-coincidence spectrometer, and a pair spectrometer.

The calculated line sensitivity at a  $3\sigma$  level as a function of energy is shown by the solid line in Figure III.F-3. These calculations have been carried considering the background contributions from the earth's albedo, the cosmic  $\gamma$ -ray spectrum, and an estimate of what the spacecraft is likely to produce. The sensitivities calculated are well below upper-limit predictions of line intensities for  $r$ -process  $\gamma$ -ray from the Crab Nebula.

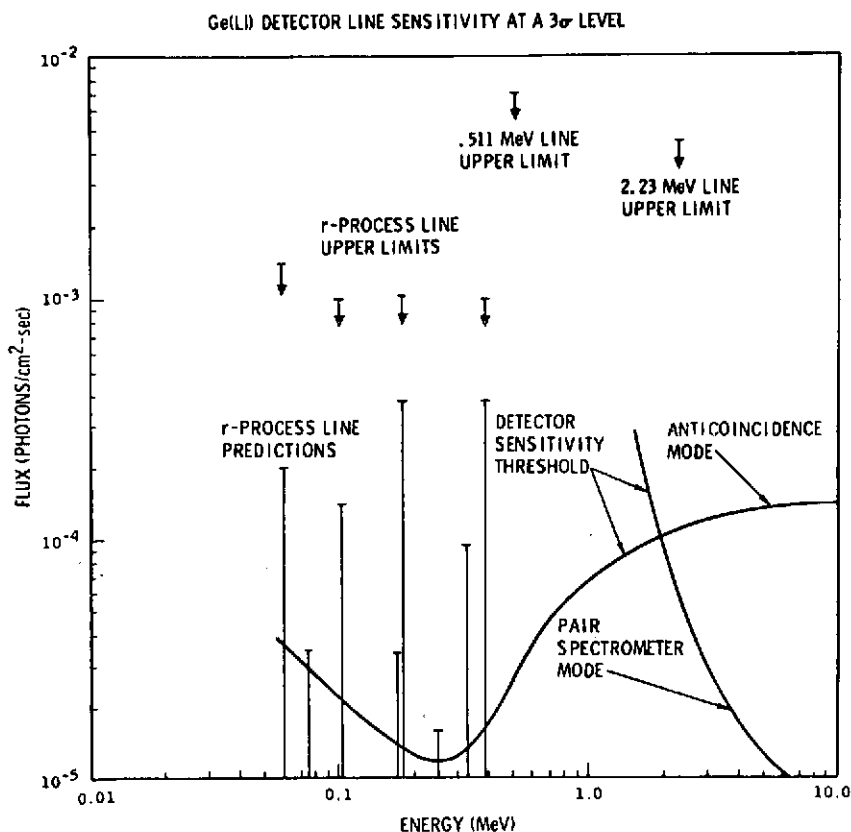


Figure III.F-3. Ge(Li) detector sensitivity to line spectra from a point source.

Figure III.F-4 shows the capability of the instrument in terms of predicted  $\gamma$ -ray line fluxes from supernova as calculated by Professor Clayton (see Chapter XI.A). The fluxes are based on a supernova occurring at a distance of 1 megaparsec, which means that a supernova of the estimated intensity could be detected at a distance of 9 megaparsecs or, alternatively, that at a distance of 1 megaparsec. Such a supernova could be seen for  $10^8$ s or for several years after its occurrence.

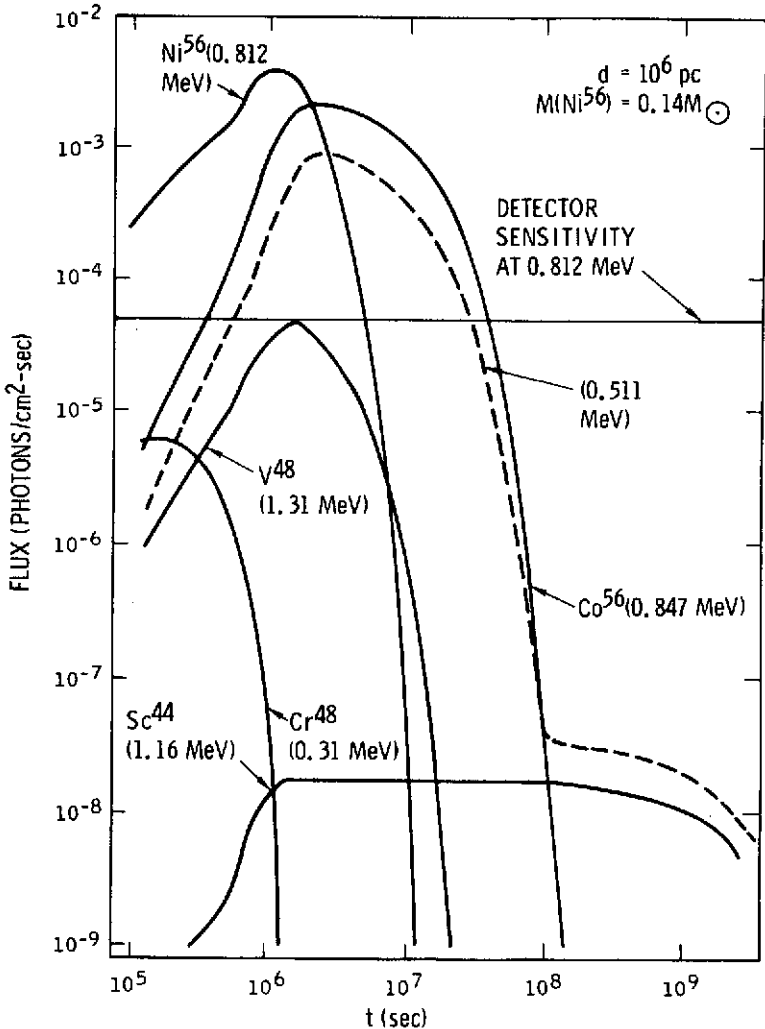


Figure III.F-4. Supernova  $\gamma$ -ray fluxes.

## A. RECENT OBSERVATIONS OF COSMIC GAMMA-RAYS FROM 10 MeV TO 1 GeV

Gerald H. Share\*

*Naval Research Laboratory*

### INTRODUCTION

Radio astronomy was born in the 1930's when Karl G. Jansky (1932; 1933) discovered a "steady hiss-type static of unknown origin" which he concluded "is fixed in space, that is, that the waves come from some source outside the solar system." The source was in the direction of the center of the galaxy. From further observations, Jansky demonstrated that radio emission is also observed, but with diminished intensity, when other regions of the Milky Way passed within the field of view of his antenna. Some 30 years later the newest branch of astronomy was born when a detector on board the OSO-3 satellite found that  $\gamma$ -ray photons  $10^{16}$  times more energetic than the radio waves were also emitted from the plane of the galaxy (Clark, Garmire, and Kraushaar, 1968). However, the similarity in the early histories of these two disciplines stops right there. Whereas Jansky discovered extraterrestrial radio emission while studying the arrival direction of thunderstorm static, the discovery of cosmic  $\gamma$ -rays came after more than a decade of intensive investigation by various laboratories.

In this paper, I shall discuss recent observations of cosmic  $\gamma$ -rays made subsequent to the discovery of energetic photons from the galactic plane. An extensive review of the field prior to 1971 has been compiled by Gal'per et al. (1972; also Fazio, 1973; and Pal, 1973). I shall treat three main areas under current investigation: (1)  $\gamma$ -ray emission from the plane of the galaxy, with emphasis on observations made in the vicinity of the galactic center; (2)  $\gamma$ -ray emission from the Crab Nebula and its pulsar; and (3) diffuse  $\gamma$ -radiation.

### GAMMA RADIATION FROM THE PLANE OF THE GALAXY

The OSO-3 telescope measured detectable intensities of  $\gamma$ -radiation emitted along the galactic equator at all galactic longitudes. These measurements are summarized in Figure IV.A-1, taken from a final report on the observations

---

\*Speaker.

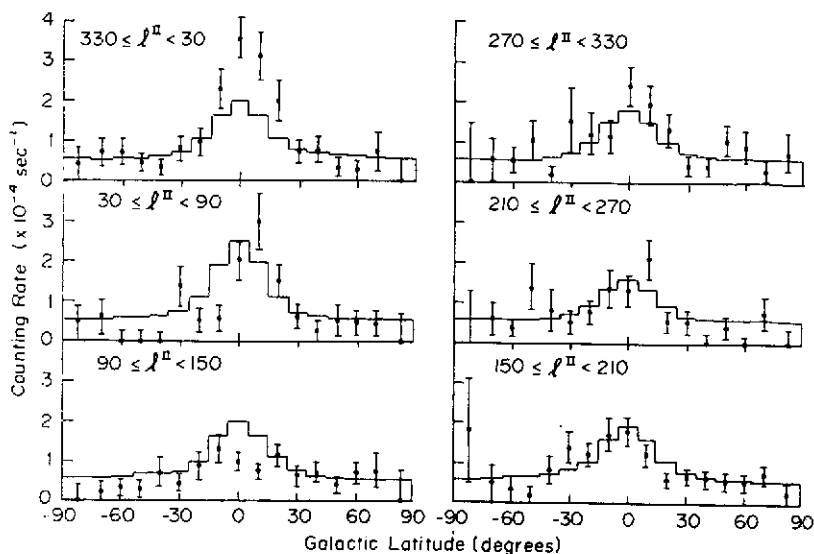


Figure IV.A-1. Variation of the counting rate of cosmic  $\gamma$ -rays observed from OSO-3 as a function of galactic latitude for successive  $60^\circ$  intervals of galactic longitude.

(Kraushaar et al., 1972). The variation in counting rate of the instrument is shown as a function of galactic latitude for six  $60^\circ$  intervals of galactic longitude. For comparison the authors have indicated by the histogram the expected rates, assuming that the radiation originated in collisions of cosmic-ray nuclei with interstellar gas. The galactic distribution of gas was obtained from 21-cm measurements of atomic hydrogen. The agreement between the expected intensity and their observations is good, with the exception of the region near the galactic center. In this region, they found that the measured intensity was significantly above the calculated value. Because the radiation appeared to be associated with diffuse emission from the plane, they expressed it in terms of an equivalent line intensity ( $\gamma/\text{cm}^2 \cdot \text{s} \cdot \text{rad}$ ) for an apparent width of  $\pm 15^\circ$  in latitude. For longitudes  $30^\circ < l^{\text{II}} < 330^\circ$ , they measured an average integral intensity of  $(3.4 \pm 1.0) \times 10^{-5} \gamma/\text{cm}^2 \cdot \text{s} \cdot \text{rad}$  for energies above 100 MeV; whereas in the vicinity of the galactic center, they found a broad maximum along the plane with an intensity of  $(1.1 \pm 0.3) \times 10^{-4} \gamma/\text{cm}^2 \cdot \text{s} \cdot \text{rad}$ .

As the angular resolution of the detector of OSO-3 was about  $\pm 15^\circ$ , the width of the apparent band of emission in directions away from the galactic center could have been almost entirely due to instrumental effects. However, the broad maximum in intensity, observed along the galactic equator in the direction of the center, could not be attributed entirely to instrumental effects.

Ögelmann (1969) suggested that the distribution of  $\gamma$ -ray emission from the plane could be accounted for by the distribution of known X-ray sources, assuming that they emitted photons with a hard spectrum,  $\propto E^{-2}$  in differential intensity. This suggestion could not be tested in greater detail by the OSO-3 detector because of its limited angular resolution.

Initial measurements at higher angular resolution were made predominantly in the Northern Hemisphere. Most of these instruments employed multiplate spark chambers as their prime detector, which permitted angular resolutions better than  $\pm 3^\circ$ . In some early reports, evidence was presented for emission of  $\gamma$ -rays from the plane of the galaxy in the vicinity of Cygnus (Valdez and Waddington, 1969; Frye and Wang, 1969; and Hutchinson et al., 1969). However, these measurements were of marginal statistical significance and, furthermore, indicated an intensity considerably above the revised intensity measured on OSO-3 (Kraushaar et al., 1972).

The higher intensities observed in the direction of the center of the galaxy prompted balloon expeditions to the Southern Hemisphere by various groups. Using a wire spark chamber with magnetic-core readout, the group at Goddard Space Flight Center investigated the galactic center region with an estimated angular resolution of  $\sim 2^\circ$  at 100 MeV. Their instrument was a prototype version of the SAS-B  $\gamma$ -ray telescope which was launched late in 1972. From a balloon flight conducted over Australia in 1969, Kniffen and Fichtel (1970; also Fichtel et al., 1972) confirmed the high  $\gamma$ -ray intensity in the vicinity of the galactic center ( $-25^\circ \leq \ell^{\text{II}} \leq +20^\circ$ ). Their results are summarized in Figure IV.A-2, where they have summed their data in  $2^\circ$  and  $6^\circ$  bands of latitude. On comparing the observed distribution with what they would have expected for atmospheric  $\gamma$ -rays, they found about a four standard-deviation excess within  $\pm 6^\circ$  of the galactic equator. The measured "line intensity"  $> 100$  MeV,  $(2.0 \pm 0.6) \times 10^{-4}$   $\gamma/\text{cm}^2 \cdot \text{s} \cdot \text{rad}$ , is in agreement with that obtained from OSO-3. Fichtel et al. (1972), also set an upper limit on the galactic flux emitted between 50 MeV and 100 MeV. This limit led them to conclude that at least 50 percent of the galactic flux comes from the decay of  $\pi^0$ -mesons produced in cosmic-ray collisions. They also searched for possible point sources in this vicinity and were unable to detect any at a sensitivity of about  $3 \times 10^{-5}$   $\gamma/\text{cm}^2 \cdot \text{s}$  above 50 MeV.

However, three other groups using balloon-borne instruments sensitive to photons  $> 100$  MeV have failed to detect diffuse emission from the galactic plane near the galactic center. The first group, a collaborative effort between Case Western Reserve University and the University of Melbourne, has reported results from a series of three balloon flights over Australia, during an investigation of  $\gamma$ -rays in the Southern Hemisphere (Frye et al., 1971a). Their investigation was performed with a multiplate spark chamber, and data were recorded on photographic film. They estimate their angular resolution to be  $\sim 2^\circ$  averaged over a typical spectrum for energies  $> 100$  MeV. The intensity

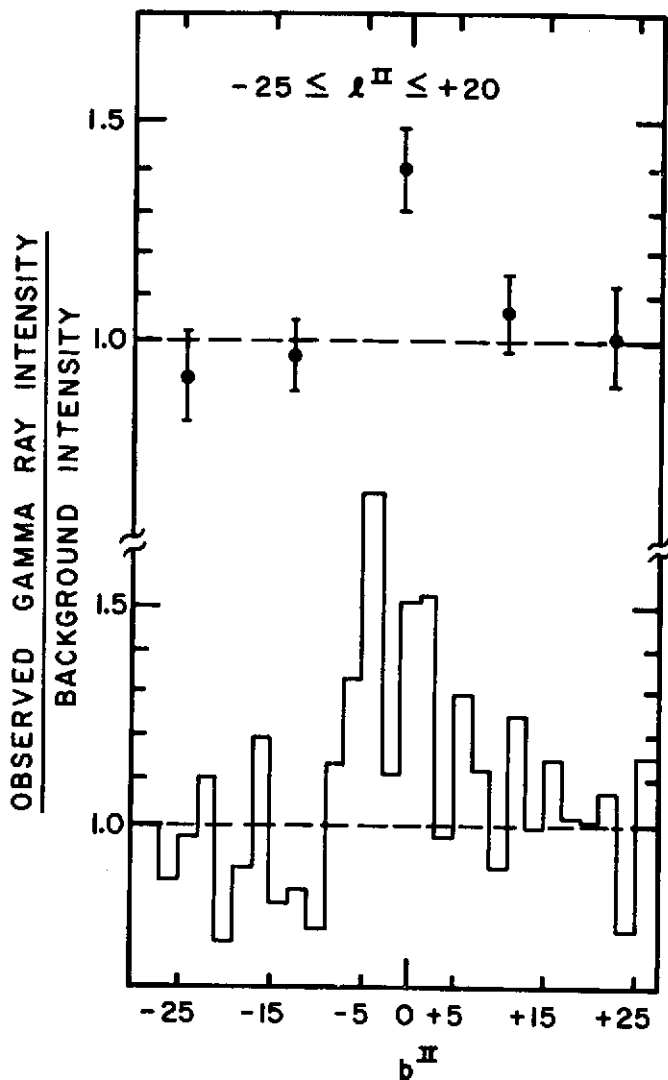


Figure IV.A-2. Ratio of observed line intensity of  $> 100$  MeV  $\gamma$ -rays to expected background intensity for  $-25^\circ \leq l^{\text{II}} \leq +20^\circ$ , plotted as a function of galactic latitude  $b^{\text{II}}$  (from Fichtel et al., 1972).

of  $\gamma$ -rays observed during these flights is shown plotted against the sine of galactic latitude in Figure IV.A-3, where the bin widths have been corrected for exposure and atmospheric contributions. Events specified as "R" refer to those exhibiting a straight single track emerging from one of the conversion layers

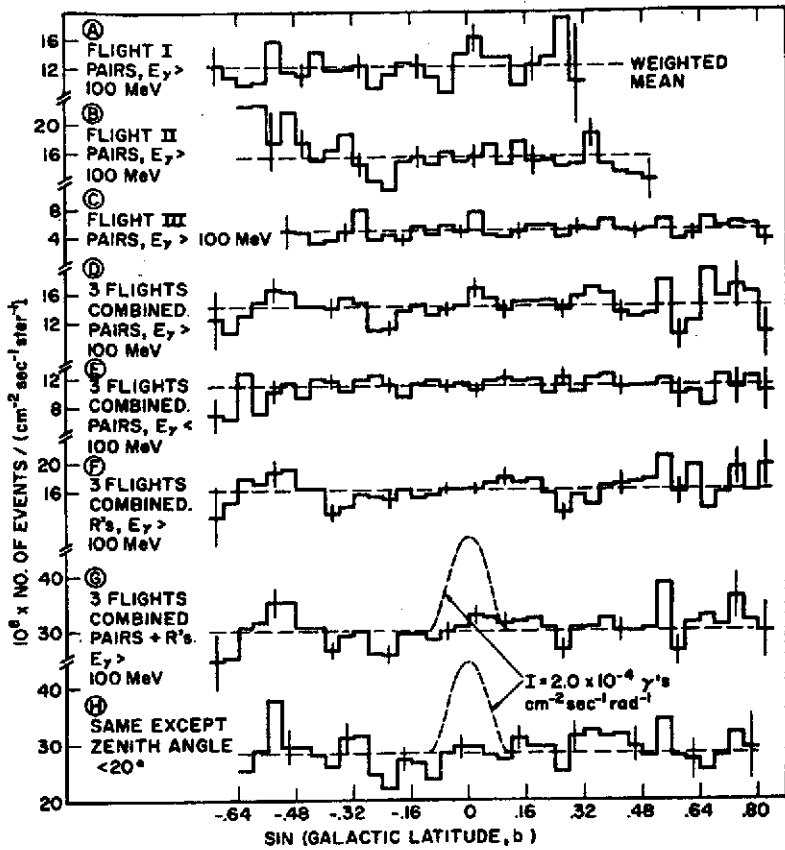


Figure IV.A-3. Variation in  $\gamma$ -ray intensity scanned across the galactic equator near the galactic center by Frye et al. (1971a). The dashed curves in parts G and H represent the intensity reported by Fichtel et al. (1972).

in the spark chamber. The summed data for the three flights are shown in parts G and H of the figure and are compared with the enhancement expected along the galactic equator, based on the intensity reported by Fichtel et al. (1972). With the sensitivity of these measurements, it is difficult to explain why the galactic emission was not detected.

Another observation, which has recently been published, was performed by the group at Minnesota (Dahlbacka et al., 1973). They used an instrument incorporating a nuclear emulsion stack as a converter for the  $\gamma$ -rays and a narrow-gap spark chamber to identify the proper events in the emulsion. With this technique an angular resolution better than  $1^\circ$  at energies  $> 100$  MeV can be achieved. The region of the galactic center was investigated during a balloon

flight over Australia in 1970. The number of events observed as a function of galactic latitude near the galactic center is shown in Figure IV.A-4. The upper plot was derived from measurements made on events located in the emulsion stack, whereas the lower plot was obtained from measurements of the spark chamber photographs ( $\sim 3^\circ$  resolution). The expected numbers of events are shown by the dashed curves, assuming that the events are atmospheric in origin. The distributions do not provide any evidence for emission from the galactic plane, although the upper limits set by the observations are not inconsistent with the intensities reported by Kraushaar et al., (1972) and Fichtel et al. (1972).

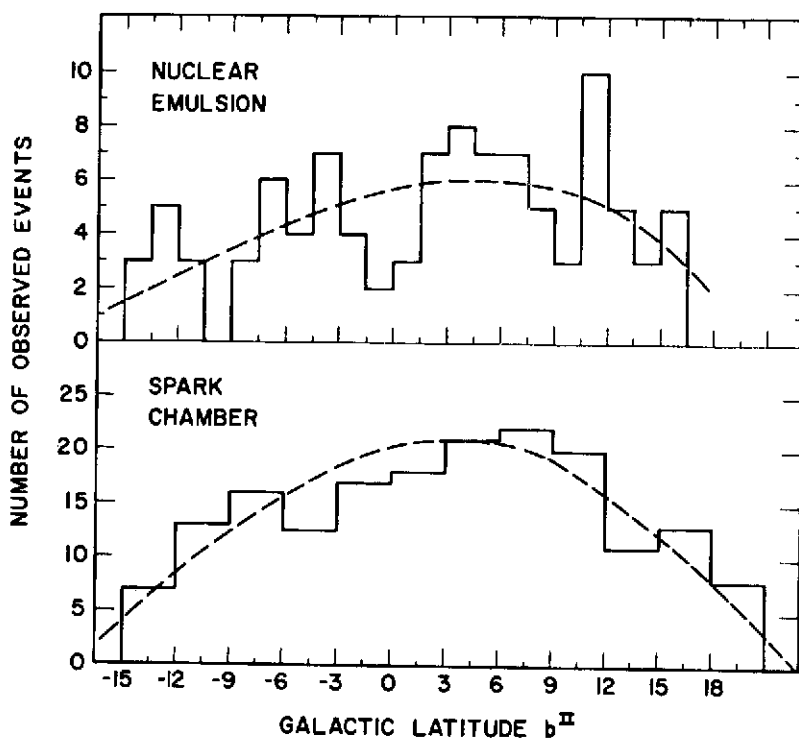


Figure IV.A-4. A histogram of the number of  $\gamma$ -ray events in strips parallel to galactic plane reported by Dahlbacka et al. (1973). The upper histogram is for events found in the emulsion and the lower one is for events observed in the spark chamber. The dashed curves represent the expected shape for no excess of emission from the galactic plane.

The third group, from the University of Southampton (Browning, Ramsden, and Wright, 1972), has reported evidence for point sources of  $\gamma$ -rays along the galactic plane near the center. They claim that these sources can account for the apparent diffuse intensity observed from the plane, and furthermore, that there is no residual diffuse intensity after the sources are subtracted. I shall return to these results later.

The above discussion indicates that there still appears to be some disagreement between the various experiments. Two recent measurements, made at energies significantly below those we have discussed, have helped to clarify the situation. Both were made over Argentina in the late fall of 1971 during the expedition "Galaxia '71." The first was performed by H. Helmken and J. Hoffman of the Smithsonian Astrophysical Observatory using a large area gas Cerenkov counter which employed a plastic scintillator as the converter for photons above 15 MeV. Although the instrument has good rejection properties for various backgrounds, it suffers from its relatively poor angular resolution,  $\sim 30^\circ$  full width at half maximum (FWHM). This requires that in searching for continuous emission from a possible  $\gamma$ -ray source, measurements must be made both on and off the source in order to determine the background level. From two balloon flights, Helmken and Hoffman (1973a) have reported that they detected a  $3.8 \sigma$  excess from the direction of the galactic center. Due to their detector's broad angular resolution, they were unable to determine whether the excess came from point sources near the center, or whether it could be attributed to emission from along the galactic plane.

The other experiment was performed by R. L. Kinzer, N. Seeman, and myself at the Cosmic-Ray Laboratory (Chief Scientist, M. M. Shapiro) at the Naval Research Laboratory (NRL). (A detailed description of this experiment will be published in *Astrophysical Journal* and can also be found in the Proceedings of the 13th International Cosmic Ray Conference.) Our experiment was similar in design to that flown by the Minnesota group; it incorporated a stack of nuclear emulsions with a wide-gap spark chamber in order to unambiguously identify the  $\gamma$ -ray interaction, as well as to provide an angular resolution of  $\sim 1.5^\circ$ . The difference between this instrument and the one flown by the Minnesota group resides in its energy range. Whereas the Minnesota detector had a threshold energy of about 100 MeV, our instrument had a low-energy threshold near 10 MeV and was relatively insensitive to photons  $\gtrsim 200$  MeV. The lower threshold was attained by design features which restricted the amount of material between the spark chamber and nuclear emulsion stack, reducing the scattering of the particles considerably and permitting low-energy electrons to be followed back into the emulsion.

The NRL experiment was flown to an atmospheric depth of  $2.5 \text{ g}\cdot\text{cm}^{-2}$  and was pointed in the direction of the galactic center. The distribution of  $\gamma$ -rays as a function of galactic latitude was obtained from a partial analysis of events located in the stack of emulsion and is shown in Figure IV.A-5. Plotted are

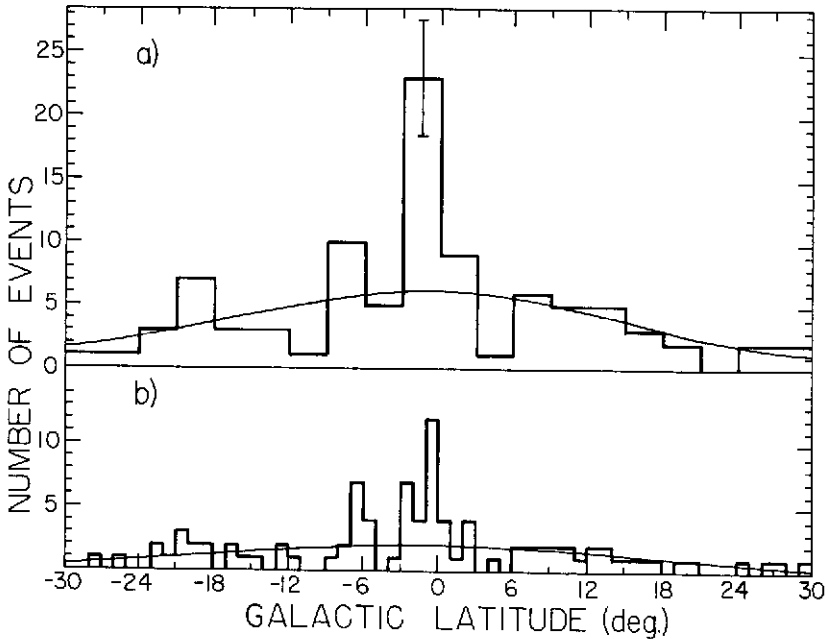


Figure IV.A-5. Distribution of observed  $\gamma$ -rays within (a)  $3^\circ$  and (b)  $1^\circ$  bands of galactic latitude for  $320^\circ < l^{\text{II}} < 40^\circ$  as reported by the NRL group. The curves are normalized to the observed events for  $|b^{\text{II}}| > 6^\circ$  and represent the distribution expected for  $\gamma$ -rays of atmospheric origin.

the number of  $\gamma$ -rays observed as a function of galactic latitude for  $3^\circ$ - and  $1^\circ$ -intervals. The curves superimposed on the histogram were normalized for  $|b^{\text{II}}| > 6^\circ$  and show the expected number of events, assuming the  $\gamma$ -rays were entirely of atmospheric origin. Evident is a significant excess of events within

$\pm 3^\circ$  of the galactic equator; 32 events were observed whereas only 13 were expected. The probability of randomly obtaining this excess of events is less than  $10^{-5}$ . The distribution of  $\gamma$ -radiation along the plane appears to be considerably narrower ( $\sim 3^\circ$  wide) than measured by either the OSO-3 or Goddard detectors.

From the measurements which I have discussed above, an integral spectrum for  $\gamma$ -rays emitted along the galactic equator in the vicinity of the galactic center can be constructed. This spectrum is shown in Figure IV.A-6. There is good agreement between the intensities measured by Kraushaar et al. (1972), and Fichtel et al. (1972), near 100 MeV. As mentioned earlier, the upper limit set by Minnesota is consistent with these measurements. Plotted at 15 MeV are the integral fluxes determined from the NRL observations for two assumed emission spectra,  $\pi^0$ -decay from cosmic-ray collisions with interstellar gas and a power-law representative of Compton collisions of high-energy electrons on starlight and microwave radiation. Due to its design, the NRL instrument is more sensitive to lower energy photons; therefore the estimated flux for a power-law spectrum is lower than that for the harder  $\pi^0$ -spectrum. Shown by the dashed lines are extrapolations of these measurements to higher energies. Within the uncertainties, our measurements and those at higher energies indicate that the  $\pi^0$ -mechanism can account for the observed emission; however, as shown by the dotted-dashed curve, a spectrum with equal contributions from both  $\pi^0$  and power-law production mechanisms provides a better fit to the observations. The flux measured by Helmken and Hoffman, if attributed entirely to emission from the plane, is higher than our observations and requires a much larger contribution from Compton collisions or bremsstrahlung.

The upper limit set by Frye et al. (1969), is in apparent contradiction with the other observations above 100 MeV, assuming that the emission comes from a narrow band along the galactic equator. This upper limit is consistent with our measurements at lower energies only for a fairly steep energy spectrum. However, preliminary spectral information obtained from our data appears inconsistent with such a steep spectrum.

#### SUGGESTED POINT SOURCES OF GAMMA RAYS IN THE VICINITY OF THE GALACTIC CENTER

Frye et al. (1969), reported the first evidence for emission from a point source in the vicinity of the galactic center. The source was designated Sgr  $\gamma$ -1 and was reported to have been observed on each of three balloon flights (Frye et al., 1971a). The combined statistical significance for all three observations was

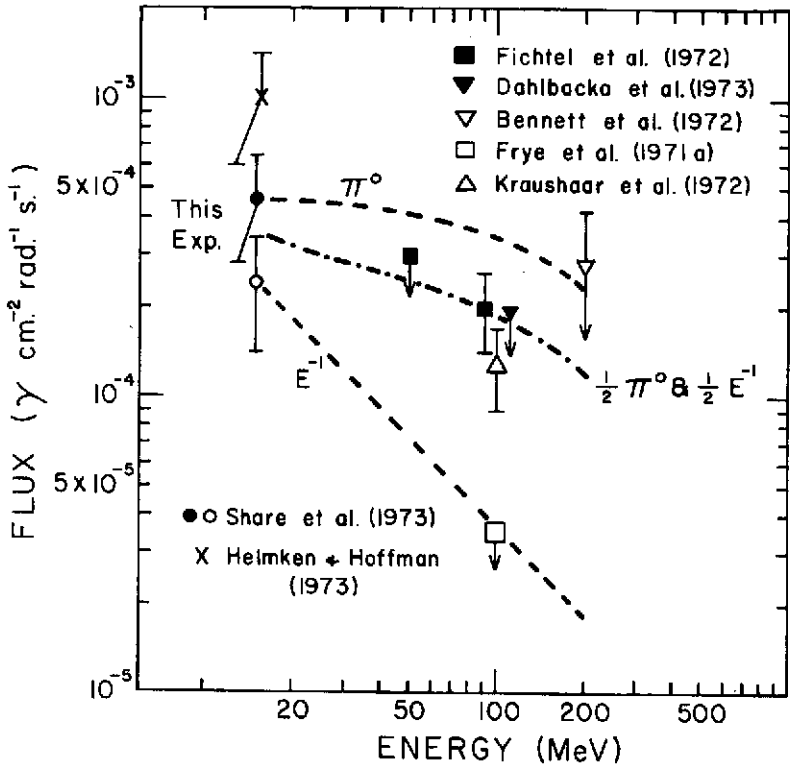


Figure IV.A-6. Measurements of the flux of  $\gamma$ -rays from the galactic plane near the center of the galaxy. The NRL measurements are given for three assumed spectra and are extrapolated to higher energies.

about four standard deviations. Subsequently, this group reported the observation of three additional sources, designated as  $\text{G}\gamma$  2+3,  $\text{G}\gamma$  341+1, and  $\text{Libra } \gamma$ -1. The first two had a combined significance of about  $4\sigma$  over background, after data from all three flights were summed. The third source was observed with a significance of  $6\sigma$  during one of their flights, but had not been observed by them during an earlier exposure. Table IV.A-1 summarizes the data on these possible sources. Other possible sources in the vicinity of the galactic center have been reported by the group in Southampton (Browning et al., 1972); however, their evidence is of marginal statistical significance. Data on these possible sources, as well as one mentioned by Dahlbacka et al. (1973), are also given in the table.

The region about the galactic center was investigated with the NRL telescope for emission of  $\gamma$ -rays with energies  $> 15$  MeV from point sources. A

Table IV.A-1  
Suspected Point Sources Near Galactic Center

Reported by	Identification	Galactic Coordinates		Flux > 100 MeV ( $\times 10^{+5} \gamma/\text{cm}^2 \cdot \text{s}$ )	NRL Results ( $\times 10^{+5} \gamma/\text{cm}^2 \cdot \text{s}$ )	
		$l^{\text{II}}$	$b^{\text{II}}$		> 10 MeV*	> 15 MeV**
Case-Melbourne (Frye et al.)	Sgr. $\gamma$ -1	$0^\circ$	$-18^\circ$	$1.5 \pm 0.5$	< 16	< 10
	G $\gamma$ 2+3 (GX 1+4?)	$2^\circ$	$+3^\circ$	$1.5 \pm 0.5$	< 22	< 6
	G $\gamma$ 341+1 (GX340-2?)	$341^\circ$	$+1^\circ$	$1.6 \pm 0.5$	< 36	< 12
	Libra $\gamma$ -1 (PKS 1514-24?)	$340^\circ$	$+30^\circ$	$2.4 \pm 0.6$ < 1.5	< 25	< 8
Southhampton (Browning et al.)	2U 1833-05?	$26.5^\circ$	$+1.5^\circ$	$2.9 \pm 0.8$	< 35	< 12
	2U 1813-14?	$17.5^\circ$	$+3.5^\circ$	$1.8 \pm 0.4$	< 43	< 8
	2U 1728-16?	$9.5^\circ$	$+6.5^\circ$	$2.1 \pm 0.6$	< 47	< 6
Minnesota (Dahlbacka et al.)	?	$352^\circ$	$+16^\circ$	2 - 5	< 32	< 8

\*Angular resolution  $\sim 10^\circ$

\*\*Angular resolution  $\sim 1\frac{1}{2}^\circ$

galactic map of the arrival directions of the observed  $\gamma$ -rays is shown in Figure IV.A-7. There is a concentration of events along the galactic equator between  $350^\circ$  and  $360^\circ$  in longitude, but limited statistics preclude the possibility of attributing, with certainty, this concentration to one or more point sources. However, if it were due to two equally intense point sources, their estimated fluxes above 15 MeV would each be  $\sim 6 \times 10^{-5} \gamma/\text{cm}^2 \cdot \text{s}$ . This same region is known, however, to contain an enhanced columnar density of atomic hydrogen (see for example, Garmire and Kraushaar, 1965) and therefore might be expected to exhibit an increased emission of  $\pi^0$ -decay  $\gamma$ -rays resulting from collisions with high-energy cosmic rays.

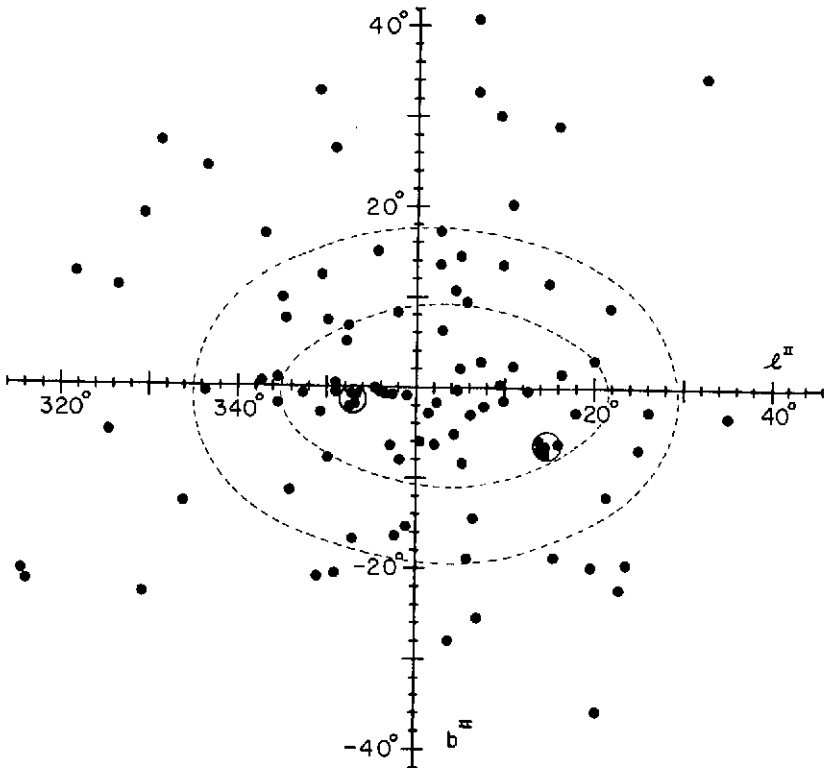


Figure IV.A-7. Galactic map of arrival directions of  $\gamma$ -rays reported by the NRL group. The RMS uncertainty in arrival direction is shown by the open circles. Regions within the dashed curves had relative exposures  $> 75$  percent and  $> 50$  percent.

None of the locations listed in Table IV.A-1 for possible  $\gamma$ -ray sources shows a significant concentration of events in Figure IV.A-7 (excluding Libra  $\gamma$ -1). A map of events obtained from a separate exposure to Libra  $\gamma$ -1 is shown in Figure IV.A-8. Again, there is no evidence for an excess in the direction of the suspected source. These exposures, therefore, failed to confirm the existence of any of the suspected sources. Upper limits (95 percent confidence level) placed on their intensities  $> 15$  MeV are given in the table. Limits placed on the fluxes above 10 MeV, also shown in Table IV.A-1, were derived from a broad resolution survey ( $\sim 10^\circ$ ) using only measurements from the NRL spark chamber. These limits indicate that if the sources are real, they must either be variable or their differential emission spectra must be significantly harder than a power-law in energy  $\propto E^{-2}$ .

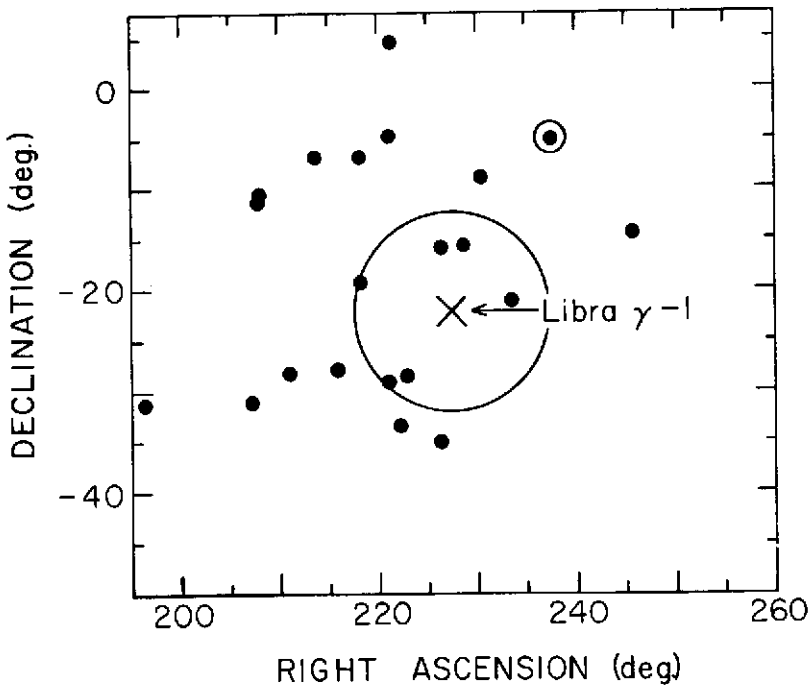


Figure IV.A-8. Map of arrival directions of  $\gamma$ -rays observed in a search by the NRL group for the variable source Libra  $\gamma$ -1.

O'Mongain (1973; see also Hearn, 1969) has recently studied the statistical methods employed in analyzing data for sources of  $\gamma$ -ray emission. He concludes that in many cases authors have underestimated the probability that the suspected sources could have been generated by statistical fluctuations.

### THE CRAB NEBULA AND ITS PULSAR

The Crab Nebula has been a target of  $\gamma$ -ray investigations for many years. However, prior to the discovery of the pulsar near the center of the Nebula, these investigations had failed to detect a significant signal from the Crab. Upper limits to the continuous emission above 100 MeV were placed at about  $2 \times 10^{-5} \gamma/\text{cm}^2 \cdot \text{s}$  (see for example, Frye and Wang, 1969).

The existence of the pulsar gave  $\gamma$ -ray astronomers an added dimension to investigate. Assuming that a large fraction of the energy emitted by the Crab was pulsed, then measurements performed at  $\sim 1$  ms resolution would benefit from the reduced background. In 1969, about one month after the observed "glitch" in the pulsar frequency, our group at NRL searched for emission of pulsed  $\gamma$ -rays above 10 MeV during a balloon flight over Texas (Kinzer et al., 1971a). The initial study was performed at about  $10^\circ$  resolution and provided evidence that pulsed  $\gamma$ -rays were emitted in phase with the optical peaks. Results from this study are shown in Figure IV.A-9, where the time of arrival of events originating  $< 10^\circ$  from the Crab are plotted in part (a) against the pulsar's optical phase; for comparison, the time of arrival of "background" events ( $> 10^\circ$  from the Crab) is shown in part (b). The evidence was of marginal statistical significance and prompted a more detailed study of the data at higher angular resolution using the stack of emulsions actively incorporated into the design of the telescope. The directions of  $\sim 50$  percent of the events occurring close to the times of arrival of both the primary and secondary optical peaks were determined to within about  $2^\circ$  from measurements in the emulsion; however, there was no significant concentration near the Crab (Kinzer et al., 1971b). This apparent disagreement with our earlier suggestion could be explained, however, as being due to the differing energy thresholds of the two samples of data. Indeed, a subsequent study of only low-energy events observed in the spark chamber confirmed the evidence for pulsation and furthermore, indicated that the pulsed emission at  $\gamma$ -ray energies may exhibit substructure with widths of  $\sim 0.5$  ms (Kinzer et al., 1973).

This suggestion of emission at the lower  $\gamma$ -ray energies prompted Albats et al. (1972), to alter their telescope in order to permit  $\gamma$ -rays with energies as low as 10 MeV to be detected. Their results from an exposure to the Crab are shown in Figure IV.A-10 for  $\gamma$ -rays with energies between about 10 and 30 MeV. Two samples of data are shown which have slightly different selection criteria. Both exhibit a striking excess within about 1 ms of the

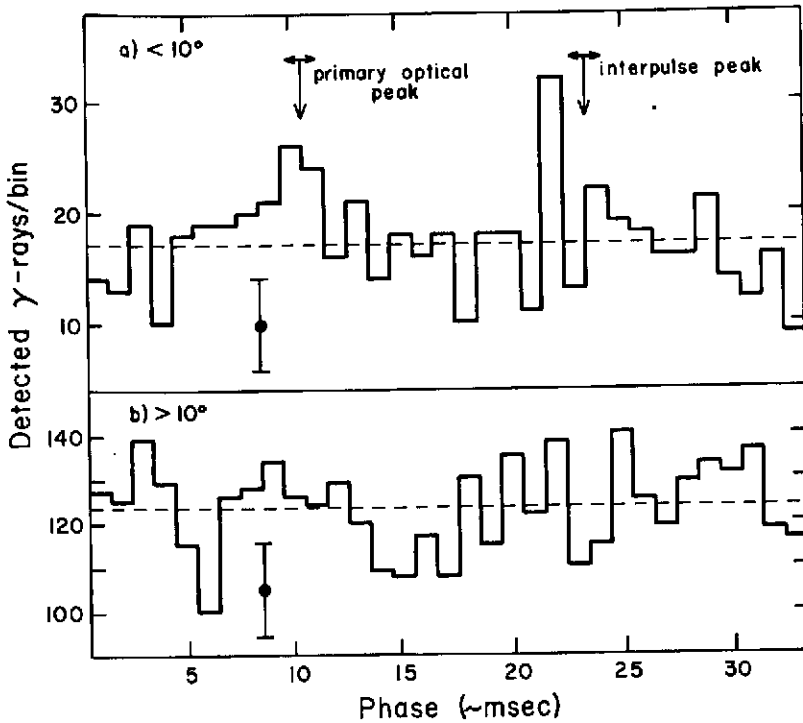


Figure IV.A-9. Number of  $\gamma$ -ray events  $\geq 10$  MeV observed by Kinzer et al. (1971), relative to the optical phase of NP0532. (a) Events pointing within  $10^\circ$  of the Crab; (b) events pointing outside  $10^\circ$  from the Crab. The dashed lines give the mean numbers ( $N$ ) of  $\gamma$ -rays/time-bin and the errors shown are  $\pm \sqrt{N}$ .

primary radio peak. Conspicuous by its absence, however, is any evidence of a pulse in the vicinity of the secondary radio peak. This is to be concentrated with measurements in the 100- to 400-keV region shown in Figure IV.A-11 and obtained by Kurfess (Kurfess and Share, 1973). In this lower-energy domain the secondary peak and interpulse region between the primary and secondary pulses contribute a substantial fraction of the X-rays emitted by the pulsar. The primary X-ray peak is found to occur within 0.5 ms of the primary optical peak. This suggests that the radiation emitted, from the radio band up to the high energy X-ray band, originates from a region no greater than about 150 km in extent; this distance is about 10 percent of the radius of the speed-of-light cylinder.

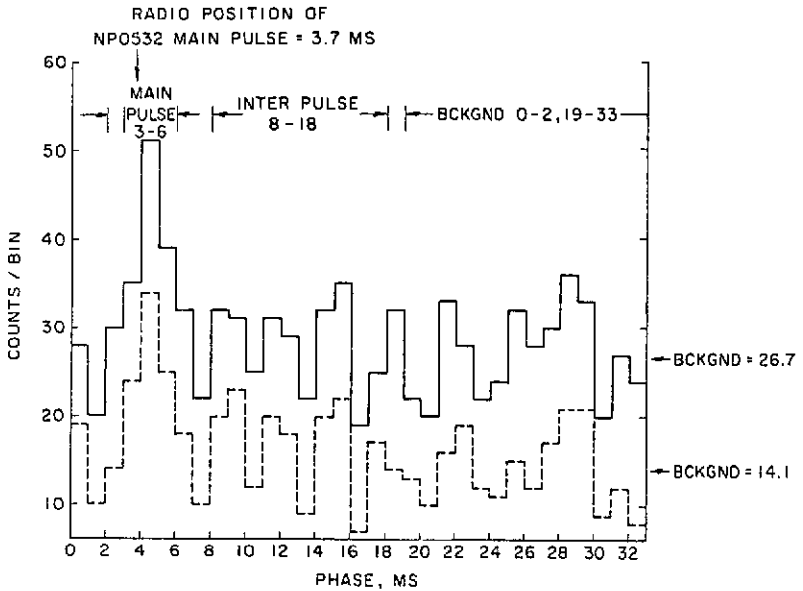


Figure IV.A-10. Number of  $\gamma$ -ray events 10 to 30 MeV observed by Albatz et al. (1972), within  $15^\circ$  of the Crab plotted relative to the radio phase of NP0532.

The close relationship in the phase of the primary peak appears to persist up to photon energies near 1 GeV and perhaps higher. Recent results from an experiment performed by the group at Cornell are shown in Figure IV.A-12 (McBreen et al., 1973). The measurements were made at energies above  $\sim 200$  MeV using a gas Cerenkov counter having a sensitive area of about  $45,000 \text{ cm}^2$ . In the energy range above 700 MeV, significant peaks were observed at both the location of the primary optical peak and secondary peak. In addition, the peak coincident with the primary optical pulse appeared to have an intrinsic width  $\sim 0.7$  ms. This is narrower than has been observed at optical and X-ray energies. Similar structure is also apparent in the lower energy range between 240 and 700 MeV, but is less significant statistically. The authors point out the possible existence of pulse structure in the interpulse region between the main and secondary peaks. Additional evidence for structure outside of the main peaks was reported by our group at NRL (Kinzer et al., 1973).

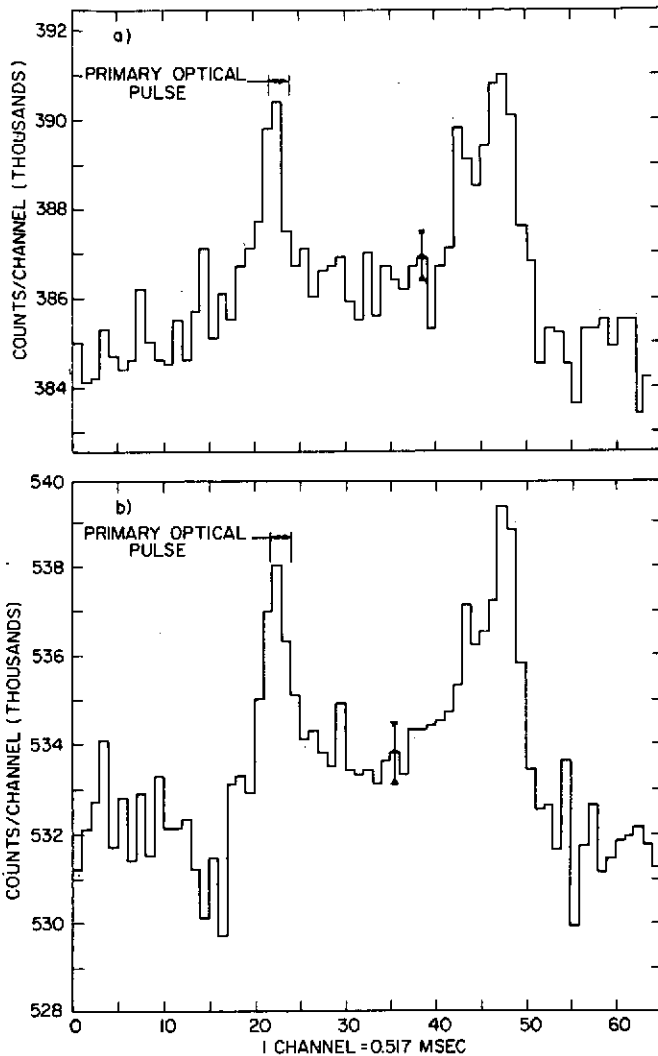


Figure IV.A-11. The X-ray "light curves" for photons from the Crab Pulsar between 100 and 400 keV observed by Kurfess (1971) during two balloon flights on (a) Oct. 10, 1970, and (b) Oct. 21, 1970.

Although questions remain concerning the shape of the pulsation and possible variability, evidence is mounting supporting the existence of  $\gamma$ -ray pulsations from the Crab. In order to illustrate the compelling nature of the evidence, I have summed in phase the 1-ms resolution data

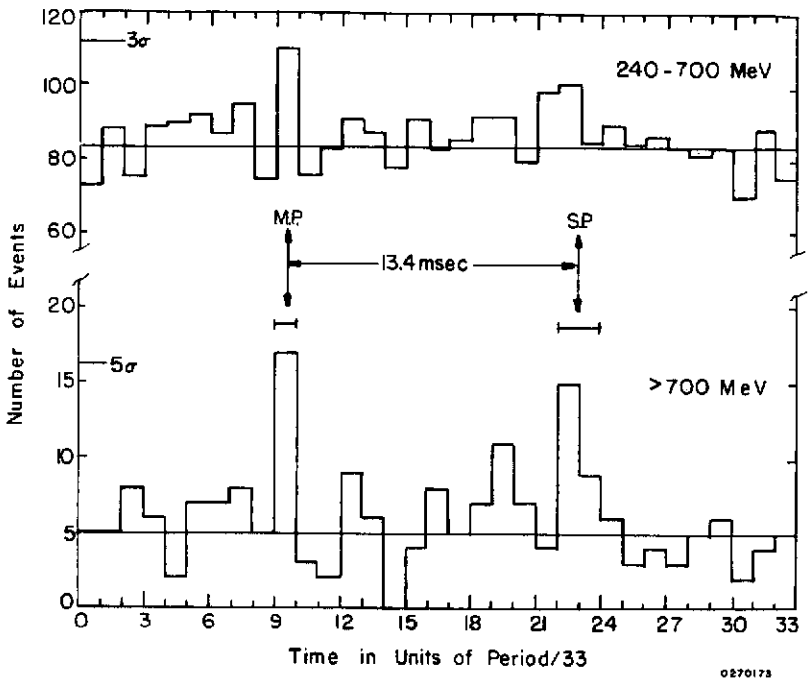


Figure IV.A-12. Phase histograms of two independent samples of  $\gamma$ -ray events observed with the Cornell  $4.5 \text{ m}^2$  Cerenkov telescope (McBreen et al., 1973). The events in the upper histogram originated within  $2^\circ$  of the Crab Nebula, while those in the lower histogram within  $1^\circ$  of the Crab. The arrival times of the optical main pulse and secondary pulse are shown. The indicated background levels were derived from the events recorded in the intervals 0 to 9 and 24 to 33 ms.

of NRL, Case-Melbourne, and Cornell. This summation is shown in Figure IV.A-13 where the data have been combined in 3-ms bins centered on the main optical peak. The ratio of the average number of events in 3-ms bins in the pulsed region to the average number in the background region is  $1.30 \pm 0.08$ . Furthermore, the bin centered on the main optical peak stands more than seven standard deviations above the background level.

Measurements of the intensity of pulsed  $\gamma$ -rays are summarized in Figure IV.A-14. The dashed line represents an extrapolation of a power-law fit to X-ray observations of the total emission from the Crab Nebula. The low-energy data, up to a few MeV, come from measurements with large area NaI crystals or plastic scintillators. At higher energies visual techniques using spark chambers were employed, with the exception of the recent measurements by Helmken and Hoffman (1973b) and McBreen et al. (1973), in

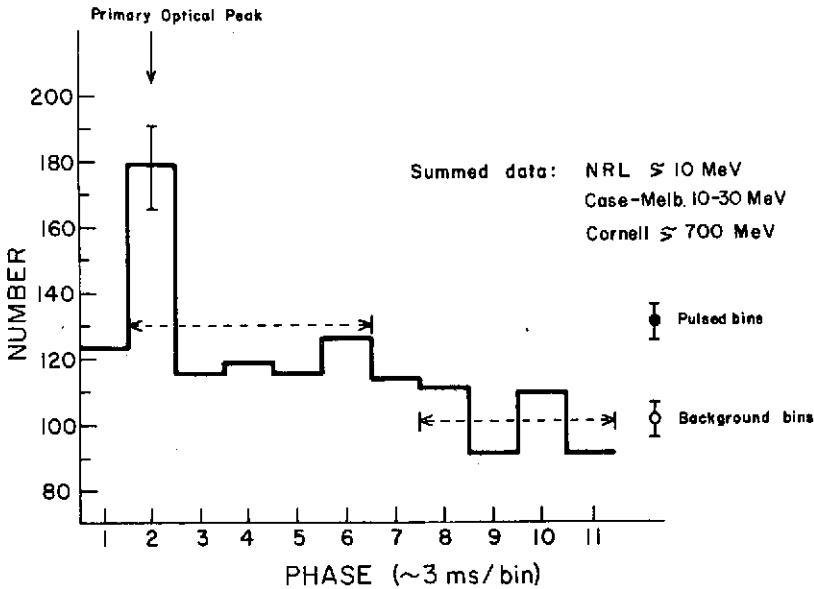


Figure IV.A-13. Summed phase histogram of  $\gamma$ -ray observations of the Crab Pulsar taken from Figures IV.A-9, 11, and 12. The original data were plotted at 1-ms resolution but are summed here in 3-ms bins in order to display the broad features of the observations.

which gas Cerenkov counters were used. In contrast to their measurement between 10 and 30 MeV, the higher energy measurement of Albats et al. (1972), does not show a significant pulse within 1 ms of the main radio peak; it does, however, show an excess in the broad pulsed region. Our upper limit plotted at 40 MeV comes from the emulsion analysis (Kinzer et al., 1971b). The upper limit above 100 MeV previously reported by the Saclay-Palermo-Milan collaboration (Leray et al., 1972) has been superseded by a recent measurement giving evidence for pulsed emission above 20 MeV (Parlier et al., 1973). It is apparent from the mixture of upper limits ( $2\sigma$ ) and claimed observations, that the sensitivity of the individual experiments require about an order of magnitude improvement in order to permit detailed studies of the Crab Pulsar.

Observations in the 100-MeV region by the Cornell group (McBreen et al., 1973) indicate that the total emission of the Crab Nebula is consistent with the power-law shown in Figure IV.A-14. This suggests that about half of the 0.1- to 1-GeV emission from the Crab Nebula comes directly from the pulsar. In the 10- to 100-MeV region only upper limits or marginal evidence for

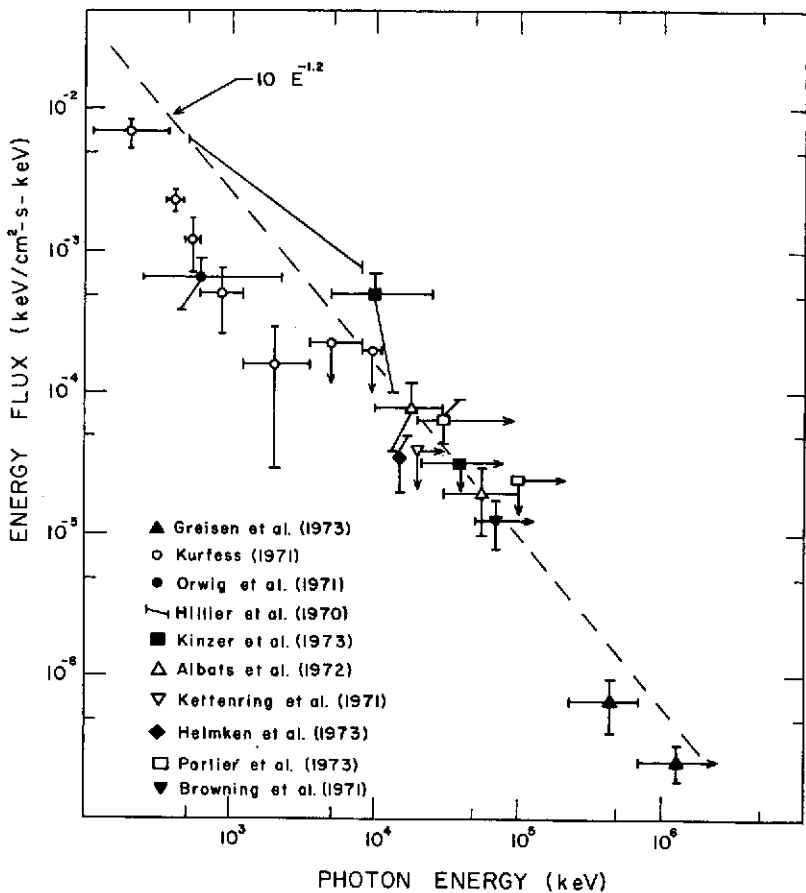


Figure 1V.A-14. Measurements of the time-averaged pulsed intensity of NP0532. The straight line represents an extrapolation of a power-law fit to the total emission spectrum of the Crab at X-ray energies.

continuous emission from the Crab Nebula have been obtained (Frye and Wang, 1969; Kinzer et al., 1971c; and Parlier et al., 1973). These limits are consistent with the power-law extrapolation and also suggest that the pulsed emission represents a large fraction of the total emission from the Crab Nebula.

#### DIFFUSE COSMIC GAMMA-RADIATION

One of the most difficult areas of experimental  $\gamma$ -ray astronomy is the investigation of the primary diffuse radiation. The non-visual detectors, such as NaI and CsI crystals, which are used at low energies, are susceptible to various backgrounds. These backgrounds can be caused by inefficiencies in anticoin-

idence counters, as well as by radioactive buildup from proton spallation and neutron interactions in the crystal and surrounding material (Pal, in press; Kasturirangan and Rao, 1972; Dyer and Morfill, 1971; and Fishman, 1972). At energies above 10 MeV, where both "non-visual" counter telescopes and "visual" spark-chamber telescopes have been employed, background contamination is still a problem. Inefficiencies in anticoincidence counters, which reject the intense fluxes of charged particles, can be a major problem in counter telescopes (Valentine et al., 1970). Although spark-chamber telescopes are capable of discriminating against this type of background, they may be susceptible to other more subtle forms, for example, local production of  $\gamma$ -radiation. In addition, detectors flown on balloons within the atmosphere, or on low orbiting satellites, must contend with the secondary atmospheric  $\gamma$ -radiation.

However, evidence continues to be compiled indicating the existence of a general diffuse glow of photons from the keV region up to energies of a few hundred MeV. A power law in energy is capable of fitting the general shape of the spectrum up to about 1 MeV, but there are suggestions of some departures from this spectrum. These departures include a possible steepening in the spectrum near 40 keV (Schwartz, Hudson, and Peterson, 1970) and a possible flattening above 1 MeV (Trombka et al., 1973).

In this section, I shall summarize the measurements made at energies above 10 MeV. Until recently, only upper limits to the intensity of the isotropic component of cosmic  $\gamma$ -rays had been reported (Clark, Garmire, and Kraushaar, 1968; Frye and Wang, 1969; Bratolyubova-Tsulukidze et al., 1970; Valentine, Kaplon, and Badhwar, 1970; Kinzer et al., 1971c). Further analysis of the data from OSO-3 has convinced Kraushaar et al. (1972), that the residual rate which their detector observed in directions away from the galactic plane was due to cosmic  $\gamma$ -radiation. The fact that this residual rate remained constant over a wide range of geomagnetic cutoff rigidities, and therefore charged particle intensities, was an important consideration in the conclusion of Kraushaar et al. (1972). Their detector also provided an indication that the spectrum of the radiation was softer than the spectrum from either the horizon of the earth or from the galactic plane, both believed to arise predominantly from  $\pi^0$ -decay  $\gamma$ -rays.

A recent measurement from within the atmosphere using a balloon-borne telescope has led to the suggestion by the group at the Max Planck Institut (Mayer-Hasselwander et al., 1972) that the intensity of diffuse  $\gamma$ -rays in the vicinity of 30 to 50 MeV is considerably above an extrapolation made between X-ray data and the 100-MeV observation of Kraushaar et al. (1972). The detector flown by the Max Planck group incorporated a multiplate spark chamber with magnetic core readout. During two balloon flights over Texas in 1971, their detector measured the intensity of  $\gamma$ -rays as a function of atmospheric depth. These measurements are plotted in Figure IV.A-15 and provide

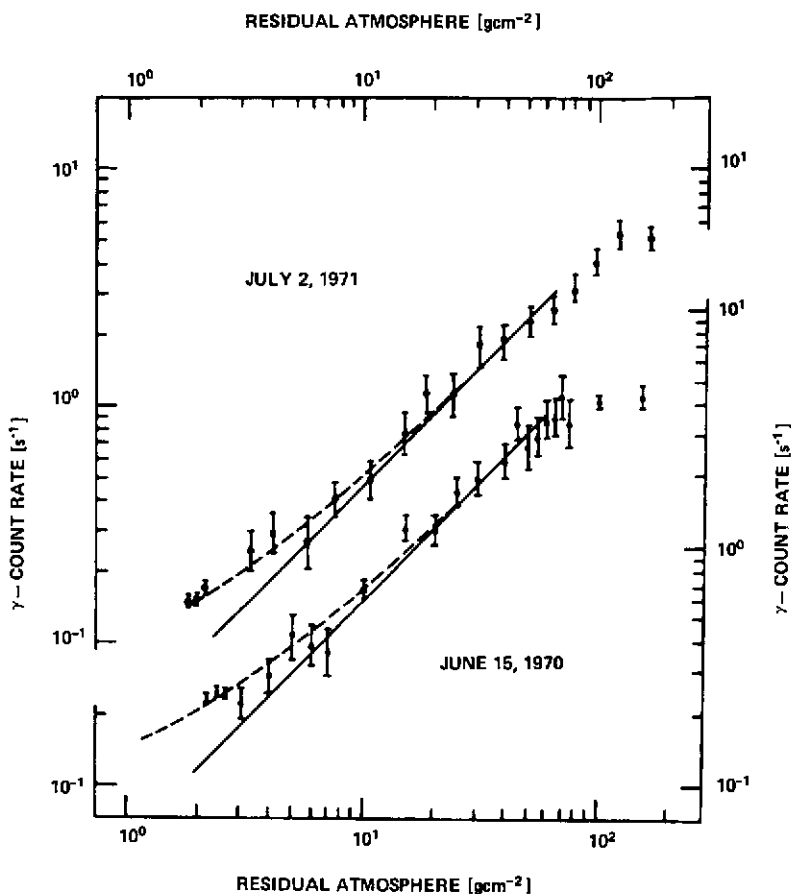


Figure IV.A-15. Counting rates of electron pairs as a function of residual atmosphere observed during two balloon flights conducted by the Max Planck Institut over Texas. The full lines are fits to the data deep in the atmosphere and represent the growth of secondary  $\gamma$ -rays. The dashed curves are fits to all the data obtained at depths  $\lesssim 50 \text{ g}\cdot\text{cm}^{-2}$ , assuming the presence of an extraterrestrial component of  $\gamma$ -rays.

evidence for a departure from the expected growth curve of atmospheric  $\gamma$ -rays. By extrapolating the measurements made between  $\sim 50 \text{ g}\cdot\text{cm}^{-2}$  and  $\sim 2 \text{ g}\cdot\text{cm}^{-2}$  to the top of the atmosphere, the authors found a residual rate over 10 standard deviations above zero. There were some differences in the absolute intensities measured during the two flights; in addition, a fairly large uncertainty of about  $0.5 \text{ g}\cdot\text{cm}^{-2}$  was present in the measurement of the atmospheric depth. However,

the authors did not feel that these uncertainties affected their conclusions concerning the existence of a cosmic diffuse component. They also presented evidence that the spectrum of this component was appreciably softer than the atmospheric spectrum. This conclusion was reached on the basis of measurements made on the distribution of the opening angles of pairs observed in the spark chamber. However, the observed increase in the average opening angle appears to occur abruptly at depths less than about  $3 \text{ g}\cdot\text{cm}^{-2}$  and is therefore suspicious.

During the NRL balloon flight over Argentina in 1971, an investigation was also made of the growth of atmospheric  $\gamma$ -rays as a function of depth in an attempt to establish the existence of the primary diffuse component. Advantage was taken of the increased cutoff rigidity (11.5 GV), which reduced the intensity of secondary radiation. The data are shown in Figure IV.A-16, where the counting rate of electron pairs is given in the left ordinate and the estimated intensity of vertically incident  $\gamma$ -rays is shown on the right. Data obtained over Texas ( $R \gtrsim 4.5 \text{ GV}$ ) are also displayed for comparison. A linear extrapolation of the data over Argentina gave evidence for a residual rate above the atmosphere which was about  $3.5 \sigma$  above zero (Share, Kinzer, and Seeman, 1972; and preprint 1972). An upper limit obtained from our Texas data (Kinzer et al., 1971c) is consistent with this residual rate.

Due to the difficulties in making measurements of this kind, we made a detailed investigation of various possible sources of background which might have simulated this residue. Among those investigated were local sources for producing the residual photons, such as the pressure vessel enclosing the system, and atmospheric  $\gamma$ -rays incident from the horizon. From our investigations we concluded that these sources were not likely to have contributed appreciably to the residue. There is however, another source of background that can account for the residual rate. In order to understand this background, we need to examine the NRL telescope.

A schematic drawing of the NRL telescope is shown in Figure IV.A-17. Downward  $\gamma$ -rays are detected after they convert in a stack of nuclear emulsion and produce either Compton electrons or electron pairs which trigger the proportional counter (P) and two scintillators (B) without the presence of an accompanying particle in any of the anticoincidence scintillators (A). The absorption-Cerenkov counter (C) restricts detected  $\gamma$ -rays to those below  $\sim 200 \text{ MeV}$ ; it also rejects about 50 percent of upward moving  $\gamma$ -rays converting in the Plexiglas block (C) and producing upward-moving low-energy electrons which can also trigger the telescope. These remaining upward-moving electrons are a likely source for the residual rate of  $\gamma$ -rays which we observed. However, as I mentioned above, only events appearing to be downward-moving electron-pairs were used in our growth curve. How then can these upward-moving electrons simulate downward-moving pairs? If the electrons are of low energy, they can be scattered

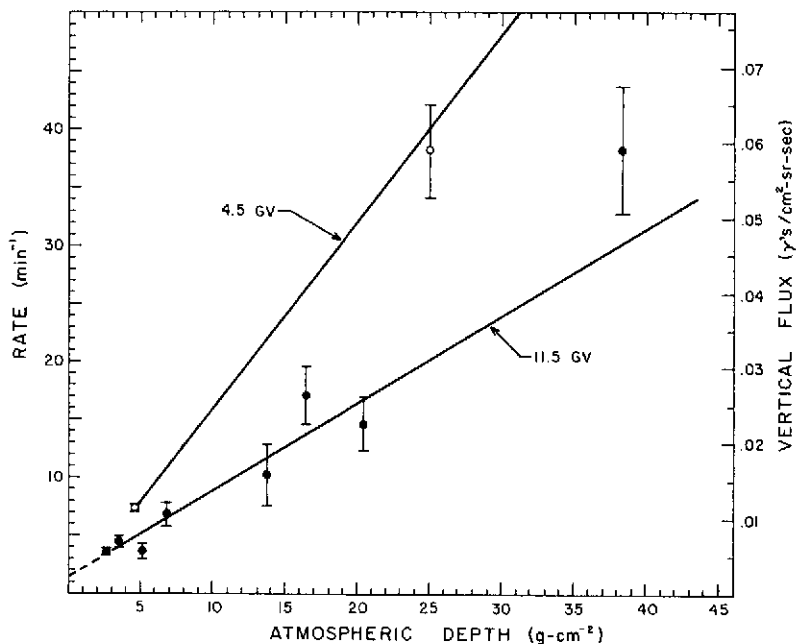


Figure IV.A-16. Vertical intensities of  $\gamma$ -rays  $10 < E < 200$  MeV at rigidities  $> 4.5$  GV and  $> 11.5$  GV as determined by the NRL group from the counting rates of "electron pairs" observed in its wide-gap spark chamber as a function of atmospheric depth. The lines are least-square fits and the errors shown are statistical. (Not shown is the rate  $100 \pm 13/\text{min}$  observed at  $55 \text{ g-cm}^{-2}$  for  $R > 4.5$  GV.)

appreciably in the emulsion and then emerge in the downward direction; the event would then appear to be a downward pair of low energy.

Another source for these low-energy electrons which can enter the detector's geometry is the splash albedo from the atmosphere. These electrons can pass through the space between the active walls of the spark chamber and the anti-coincidence cup surrounding the Plexiglas block. They will be detected and appear as downward pairs if they are scattered back out of the emulsion and have sufficient energy to reach the bottom coincidence counters (B).

We estimate that the combined rate from both of these types of events, which imitate downward electron-pairs, can contribute appreciably to our residual rate of pairs above the atmosphere. For this reason, we have concluded that our measurement must be interpreted only as an upper limit to the true diffuse  $\gamma$ -ray intensity.

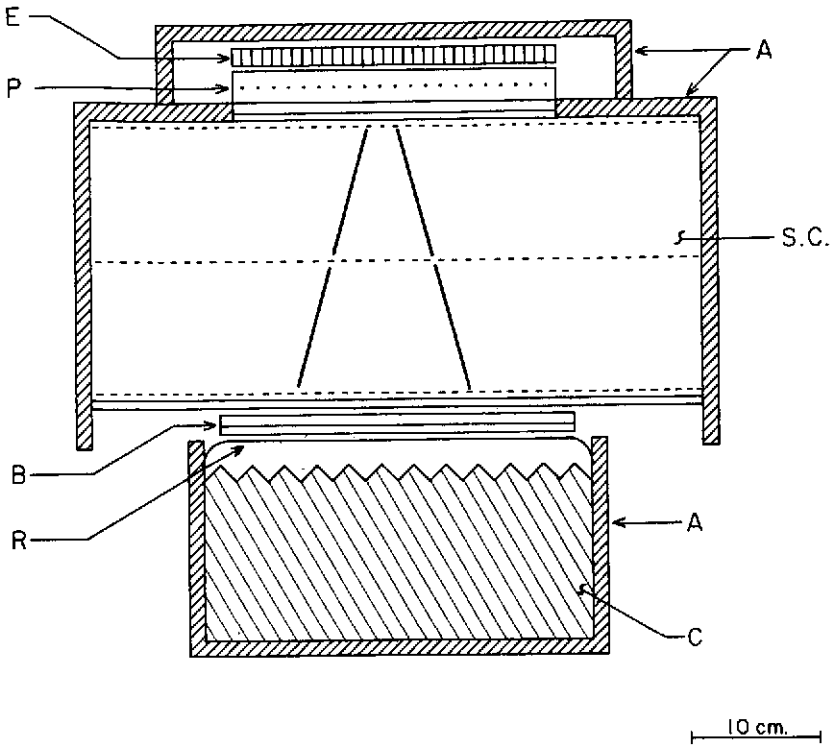


Figure IV.A-17. Drawing of the detector used by the NRL group showing an electron pair in the wide-gap spark chamber (S.C.). (A) plastic anticoincidence counters; (E) emulsion stack  $650 \text{ cm}^2 \times 1.25 \text{ cm}$ ; (P) multiwire proportional counter; (B) two plastic coincidence counters; (C) absorption Cerenkov counter of clear Plexiglas ( $15 \text{ g}\cdot\text{cm}^{-2}$ ). Cerenkov light from up-coming particles is reflected by (R) onto phototubes (not shown) imbedded in the block.

The measurements of diffuse  $\gamma$ -radiation above 1 MeV are summarized in Figure IV.A-18. The solid line represents an extrapolation of the fit of X-ray data to a power-law spectrum (Kasturirangan and Rao, 1972), while the dotted-dashed curves represent the uncertainty in this extrapolation. Measurements above 10 MeV are typically obtained over a wide range in energy; this range is shown by the dashed lines, and the points have been plotted at the median energy photon detected for an assumed  $E^{-2}$  spectrum. The data above 1 MeV from ERS-18 (Vette et al., 1970) were found to have been in error and have been superseded by measurements from Apollo-15 (Trombka et al., 1973; see also Trombka and Peterson, Chapter III.A). The measurements from Apollo-15 indicate that the energy spectrum of low-energy  $\gamma$ -rays flattens above about

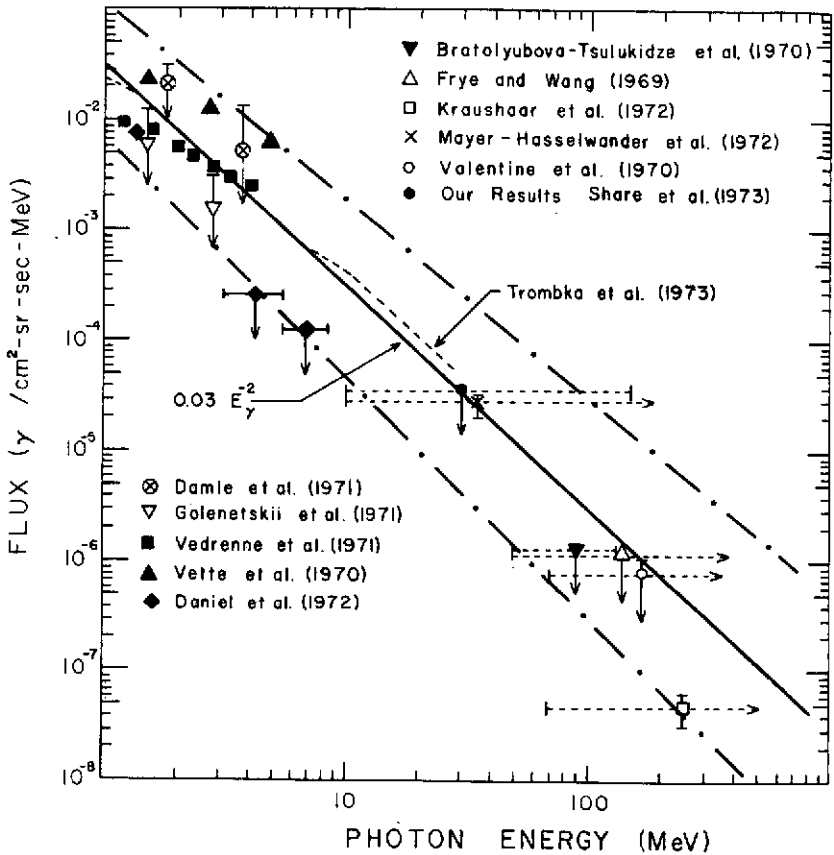


Figure IV.A-18. Measurements of diffuse cosmic  $\gamma$ -radiation. Energy ranges for observations  $> 10$  MeV are shown, and the fluxes are plotted at the median energy photon detected for an assumed  $E^{-2}$  spectrum.

500 keV; above 1 MeV their measured intensities are still higher than the upper limits reported by Golenetskii et al. (1971), and by Daniel, Joseph, and Lavakare (1972).

The intensity reported by Mayer-Hasselwander et al. (1972), at higher energies appears consistent with the data from Apollo-15. However, there may be a systematic error in the intensity given by Mayer-Hasselwander et al. (1972). They report that their measurement of the atmospheric  $\gamma$ -ray intensity is about 60 percent of the value calculated by Beuermann (1971); however, measurements by other groups indicate that the calculated flux may be too low (Fichtel, Kniffen, and Ögelmann, 1969; and Seeman, Share, and Kinzer, 1973). This

suggests that the primary diffuse intensity reported by Mayer-Hasselwander et al. (1972), might therefore be low by about a factor of two.

The upper limit determined by our measurement over Argentina, although consistent with the reported intensities, suggests that the flux of diffuse  $\gamma$ -rays near 30 MeV is lower than reported by either Trombka et al. (1973), or Mayer-Hasselwander et al. (1972). The fluxes reported by these authors are considerably above a power-law spectrum fit to both the X-ray observations and the 100 MeV measurements of Kraushaar et al. (1972). This had led to suggestions that an additional component may be needed to explain the results from 1 to 50 MeV. Theoretical models for generating this additional component have been recently summarized by Silk (preprint, 1973), Stecker (1973), and Strong et al. (1973). Further discussion can also be found in other sections of this volume:

### FUTURE OBSERVATIONS

Gamma-ray astronomy has finally emerged as an observational science. However, as is apparent from this summary of recent measurements, an improvement in sensitivity is required in order to permit more detailed investigations. The new generation of satellite detectors, ESRO's TD-1A and COS-B and NASA's SAS-2, represent the first step in providing the increased sensitivity. This is primarily due to the longer observation periods and lower  $\gamma$ -ray background intrinsic in satellite observations.

These detectors should be able to measure the energy spectrum of the diffuse radiation  $\gtrsim 30$  MeV and to begin to investigate its spatial isotropy. They should also have the sensitivity to verify the existence of the various possible point sources of  $\gamma$ -rays reported from balloon-borne observations and, furthermore, to study their energy spectra and to establish whether or not they are variable. There is also little doubt that these detectors will be able to investigate emission of diffuse  $\gamma$ -radiation from the galactic plane and to map its distribution at resolutions of  $\sim 3^\circ$ . These measurements of high-energy photons from the galactic disk, like the ones made 25 years earlier in the radio band, will substantially further our knowledge of the distribution of matter, magnetic field strengths, and cosmic-ray fluxes in the galaxy.

Continued work at balloon altitudes should be encouraged, especially in the light of the reduced funding for "expensive" satellite programs. These balloon-borne instruments should be designed with improved resolution in energy, angle, and timing in order to help compensate for the atmospheric background and to permit continued investigation of periodically pulsing objects such as the Crab Pulsar. Improved sensitivity for balloon-borne detectors should follow naturally from the development of high-altitude super-pressure balloons and from observations conducted at high geomagnetic cutoff rigidities.

## REFERENCES

- Albats, P., G. M. Frye, Jr., A. D. Zych, O. B. Mace, V. D. Hopper, and J. A. Thomas, 1972, *Nature*, **240**, p. 221.
- Bennett, K., P. Penengo, G. K. Rochester, T. R. Sanderson, and R. K. Sood, 1972, *Nature*, **238**, p. 31.
- Beuermann, K. P., 1971, *J. Geophys. Res.*, **76**, p. 4291.
- Bratolyubova-Tsulukidze, L. I., N. L. Grigorov, L. F. Kalinkin, A. S. Melioransky, E. A. Pryakhin, I. A. Savenko, and V. Ya. Yufarkin, 1970, *Acta Phys.*, **29**, Suppl. 1, p. 123.
- Browning, R., D. Ramsden, and P. J. Wright, 1971, *Nature Phys. Sci.*, **232**, p. 99.
- , 1972, *Nature*, **238**, p. 138.
- Clark, G. W., G. P. Garmire, and W. L. Kraushaar, 1968, *Astrophys. J. Letters*, **153**, p. L203.
- Dahlbacka, G. H., P. S. Freier, and C. J. Waddington, 1973, *Astrophys. J.*, **180**, p. 371.
- Damle, S. V., R. R. Daniel, G. Joseph, and P. J. Lavakare, 1971, *Astrophys. and Space Sci.*, **14**, p. 473.
- Daniel, R. R., G. Joseph, and P. J. Lavakare, 1972, *Astrophys. and Space Sci.*, **18**, p. 462.
- Dyer, C. S., and G. E. Morfill, 1971, *Astrophys. and Space Sci.*, **14**, p. 243.
- Fazio, G. G., 1973, *X-Ray and Gamma-Ray Astronomy, Proceedings of IAU Symposium No. 55* (Madrid), H. Bradt and R. Giacconi, eds., D. Reidel, Dordrecht, Holland.
- Fichtel, C. E., R. C. Hartman, D. A. Kniffen, and M. Sommer, 1972, *Astrophys. J.*, **171**, p. 31.
- Fichtel, C. E., D. A. Kniffen, and H. B. Ögelmann, 1969, *Astrophys. J.*, **158**, p. 193.
- Fishman, G. J., 1972, *Astrophys. J.*, **171**, p. 163.
- Frye, G. M., Jr., P. A. Albats, A. D. Zych, J. A. Staib, V. D. Hopper, W. R. Rawlinson, and J. A. Thomas, 1971a, *Nature*, **231**, p. 372.
- , 1971b, *Nature*, **233**, p. 466.
- Frye, G. M., Jr., J. A. Staib, A. D. Zych, V. D. Hopper, W. R. Rawlinson, and J. A. Thomas, 1969, *Nature*, **223**, p. 1320.
- Frye, G. M., Jr., and C. P. Wang, 1969, *Astrophys. J.*, **158**, p. 925.

- Gal'per, A. M., V. G. Kirillov-Ugryumov, B. I. Luchkov, and O. F. Prilutskii, 1972, *Soviet Phys. Uspekhi*, **14**, p. 630.
- Garmire, G., and W. L. Kraushaar, 1965, *Space Sci. Rev.*, **4**, p. 123.
- Golenetskii, S. V., E. P. Mazets, V. N. Ill'inskii, R. L. Aptekar', M. M. Bredov, Yu. A. Gur'yan, and V. N. Panov, 1971, *Astrophys. J. Letters*, **9**, p. L69.
- Hearn, D., 1969, *Nucl. Inst. and Meth.*, **70**, p. 200.
- Helmken, H. F., and J. A. Hoffman, 1973a, *Nature Phys. Sci.*, **243**, p. 6.
- \_\_\_\_\_, 1973b, *Proc. 13th Int. Conf. on Cosmic Rays*, Denver (in press).
- Hillier, R. R., W. R. Jackson, A. Murray, R. M. Redfern, and R. G. Sale, 1970, *Astrophys. J. Letters*, **162**, p. L177.
- Hutchinson, G. W., A. J. Pearce, D. Ramsden, and R. D. Wills, 1969, *Acta Phys.*, **29**, Supp. 1, p. 87.
- Jansky, K. G., 1932, *Proc. IRE*, **20**, p. 1920.
- \_\_\_\_\_, 1933, *Proc. IRE*, **21**, p. 1387.
- Kasturirangan, K., and U. R. Rao, 1972, *Astrophys. and Space Sci.*, **15**, p. 161.
- Kettenring, G., H. A. Mayer-Hasselwander, E. Pfeffermann, K. Pinkau, H. Rothermal, and M. Sommer, 1971, *Proc. 12th Int. Conf. Cosmic Rays*, Hobart, **1**, p. 57.
- Kinzer, R. L., R. C. Noggle, N. Seeman, and G. H. Share, 1971a, *Nature*, **229**, p. 187.
- Kinzer, R. L., N. Seeman, and G. H. Share, 1971b, *Proc. 12th Int. Conf. Cosmic Rays*, Hobart, **1**, p. 45.
- \_\_\_\_\_, 1971c, *Proc. 12th Int. Conf. Cosmic Rays*, Hobart, **1**, p. 51.
- Kinzer, R. L., G. H. Share, and N. Seeman, 1973, *Astrophys. J.*, **180**, p. 547.
- Kniffen, D. A., and C. E. Fichtel, 1970, *Astrophys. J.*, **161**, p. L157.
- Kraushaar, W. L., G. W. Clark, G. P. Garmire, R. Borken, P. Higbie, C. Leong, and T. Thorsos, 1972, *Astrophys. J.*, **177**, p. 341.
- Kurfess, J. D., 1971, *Astrophys. J. Letters*, **168**, p. L39.
- Kurfess, J. D., and G. H. Share, 1973, *Nature Phys. Sci.*, **244**, p. 39.
- Leray, J. P., J. Vasseur, J. Paul, B. Parlier, M. Forichon, B. Agrinier, G. Boella, L. Maraschi, A. Treves, L. Buccheri, A. Cuccia, and L. Scarsi, 1972, *Astron. and Astrophys.*, **16**, p. 443.

- Mayer-Hasselwander, H. A., E. Pfeffermann, K. Pinkau, H. Rothermel, and M. Sommer, 1972, *Astrophys. J. Letters*, **175**, p. L23.
- McBreen, B., S. E. Ball, Jr., M. Campbell, K. Greisen, and D. Koch, 1973, Preprint, to be published in *Astrophys. J.*
- Ögelmann, H., 1969, *Nature*, **221**, p. 753.
- O'Mongain, E., 1973, *Nature*, **241**, p. 376.
- Pal, Y., 1973, *X-Ray and Gamma-Ray Astronomy, Proceedings of IAU Symposium No. 55* (Madrid), H. Bradt and R. Giacconi, eds., D. Reidel, Dordrecht, Holland.
- Parlier, B., B. Agrinier, M. Forichon, J. P. Leray, G. Boella, L. Maraschi, R. Buccheri, N. R. Robba, and L. Scarsi, 1973, *Nature Phys. Sci.*, **242**, p. 117.
- Schwartz, D. A., H. S. Hudson, and L. E. Peterson, 1970, *Astrophys. J.*, **162**, p. 431.
- Seeman, N., G. H. Share, and R. L. Kinzer, 1973, *Proc. 13th Int. Conf. on Cosmic Rays*, Denver (in press).
- Share, G. H., R. L. Kinzer, and N. Seeman, 1972, *Bull. A.P.S.*, **17**, p. 524.
- , 1973, *Proc. 13th Int. Conf. on Cosmic Rays*, Denver (in press).
- Stecker, F. W., 1973, *Nature Phys. Sci.*, **241**, p. 74.
- Strong, A. W., A. W. Wolfendale, and J. Wdowczyk, 1973, *Nature*, **241**, p. 109.
- Trombka, J. I., A. E. Metzger, J. R. Arnold, J. L. Matteson, R. C. Reedy, and L. E. Peterson, 1973, *Astrophys. J.*, **181**, p. 737.
- Valdez, J. V., and C. J. Waddington, 1969, *Astrophys. J. Letters*, **156**, p. L85.
- Valentine, D., M. F. Kaplon, and G. Badhwar, 1970, *Acta Phys.*, **29**, Supp. 1, p. 101.
- Vedrenne, G., F. Albernhe, I. Martin, and R. Talon, 1971, *Astron. and Astrophys.*, **15**, p. 50.
- Vette, J. I., D. Gruber, J. L. Matteson, and L. E. Peterson, 1970, *Astrophys. J. Letters*, **160**, p. L161.

## B. REPORT ON GAMMA-RAY ASTRONOMY RESULTS OBTAINED IN EUROPE SINCE THE IAU SYMPOSIUM NO. 55

K. Pinkau\*  
*Max Planck Institut*

### INTRODUCTION

Since the IAU Symposium No. 55 in Madrid in 1972 (Pal, 1973; Fazio, 1973), little progress has been made in obtaining new results on celestial  $\gamma$ -rays in Europe.

The  $\gamma$ -ray experiment S-133 on board ESRO's TD-1 satellite worked through its first period of operational life from March 1972 to October 1972, when the satellite went into hibernation. The experiment was activated in February 1973 for a second all-sky scan. For this second scan, the trigger counter thresholds have been raised. It is hoped to thereby increase the  $\gamma$ -ray energy required to trigger the experiment, thus providing a kind of "two-color" all-sky scan in  $\gamma$ -rays in combination with the 1972 data.

Data analysis of this experiment has been very slow and tedious and is not as yet in such a state that first results could be presented. This is, in part, due to the fact that TD-1's tape recorders failed after the first two months of operational life, and the tapes of the very good real-time coverage provided by ESRO were slow in arriving. A more serious problem, however, was the severe background problem encountered. This requires that all spark chamber images be visually inspected, and this work has as yet not been finished.

In what follows, the results on measurements of the diffuse flux and on the Crab Pulsar NP 0532 are updated. The various reports on point sources discovered are, in the author's opinion, of a preliminary nature and require confirmation by independent measurement with good statistics.

### DIFFUSE FLUX

The present status of  $\gamma$ -ray measurements concerning the diffuse flux is well illustrated by Figure IV.B-1 (taken from Trombka et al., 1973), where the

---

\*Speaker.

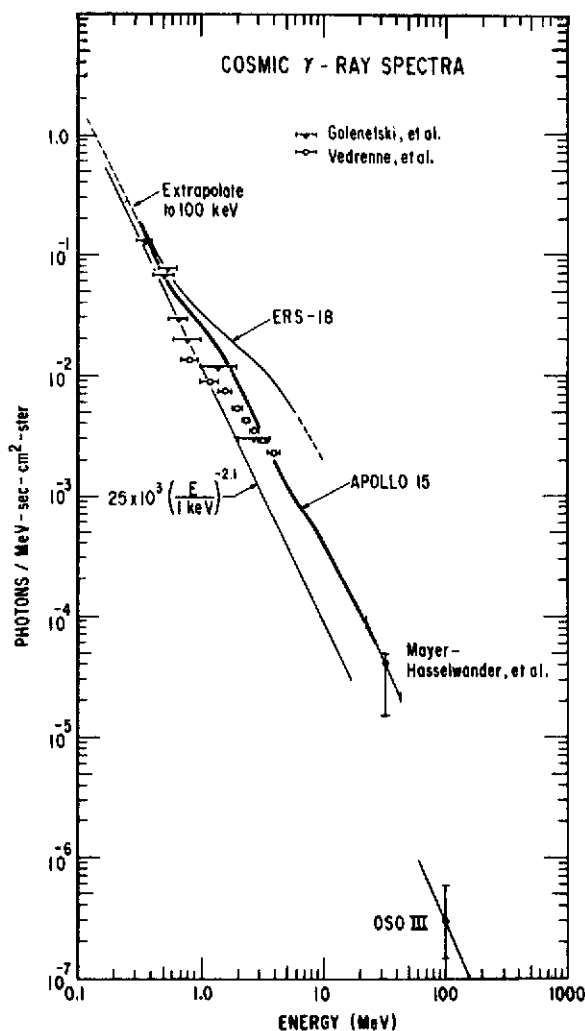


Figure IV.B-1. The cosmic photon spectrum derived from the Apollo-15 data agrees with previous results below 1 MeV but is well below that determined from the ERS-18 at higher energies. Limits derived from balloon and low altitude satellite work, despite large corrections for efficiency and cosmic-ray produced  $\gamma$ -rays, are in agreement with the Apollo results. (Trombka et al., 1973, also Chapter III.A)

results of Vedrenne et al. (1971), and Mayer-Hasselwander et al. (1972), are compared with the results of Golenetskii et al. (1971), OSO-3 (Kraushaar et al., 1972), and Apollo-15 (Trombka et al., 1973). (See Peterson and Trombka, Chapter III.A.)

Apart from OSO-3, the results seem to indicate that these authors find diffuse  $\gamma$ -ray fluxes in excess of the  $25 \times 10^3 (E/1 \text{ keV})^{-2.1}$  spectrum proposed by Pal (1973). It appears to be too early to speculate in detail about the physical significance of this still rather uncertain result. If all these findings are confirmed, the diffuse  $\gamma$ -ray spectrum would exhibit a shoulder below 100 MeV, as pointed out by Pal (1973). It is interesting to note that  $\gamma$ -ray production through the  $\pi^0$ -process at various red shifts in the past should integrate up to just such a shoulder. (See Stecker, Chapter IX.A.)

In this context, a remark concerning the analysis of  $\gamma$ -ray data appears justified. In the domain where pair production is dominant ( $\gtrsim 20 \text{ MeV}$ ),  $\gamma$ -ray astronomy experiments are triggered by the diverging beam of electron-positron pairs that are created close to the trigger-telescope. Multiple scattering causes these electrons to diverge, and the solid angle of such an instrument is not well defined.

Furthermore, if P is the probability that one of the two electrons triggers the instrument, the total triggering probability will be  $1 - (1-P)^2$ , thus causing a significant enhancement of the probability that a  $\gamma$ -ray incident at large zenith angles will actually trigger the counter because one of the electrons was scattered into the sensitive cone of the telescope.

These considerations show that the energy-angle response function ( $a(E, \theta)$ ) of a  $\gamma$ -ray counter telescope cannot be separated into one function of energy and another one dependent on angle only, as was assumed in the case of the OSO-3 data analysis (Kraushaar et al., 1972). Rather, the effective solid angle  $\Omega$  defined as

$$\Omega = \frac{\int 2\pi \sin \theta a(E, \theta) d\theta}{a(E, \theta = 0)}$$

will remain a function of energy, increasing with decreasing energy. This has the interesting consequence that the ratio of line flux factor to isotropic flux factor  $G_{\text{line}}/G_{\text{iso}}$  as defined by Kraushaar et al. (1972), will depend upon energy and thus on the assumptions on the line flux and isotropic flux energy spectra, respectively. This has to be borne in mind when comparing the results of OSO-3 of the galactic plane emission with that of high galactic latitudes.

### CRAB PULSAR NP 0532

In recent months, two results have been published that appear to establish the Crab Pulsar spectrum in the 10- to 100-MeV energy range. They are the measurements of Albats et al. (1972), and of Parlier et al. (1972). Figure IV.B-2

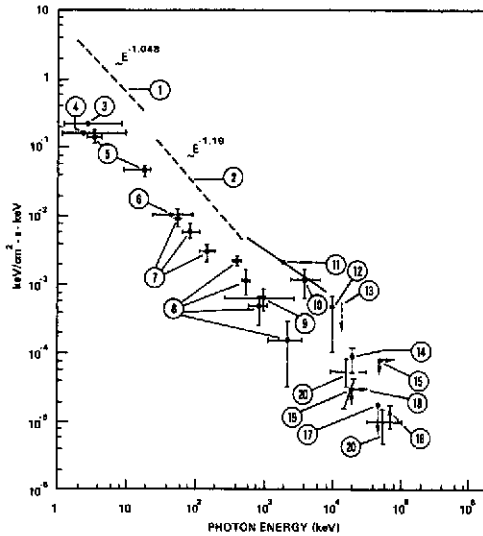


Figure IV.B-2. Crab Nebula spectrum (from Parlier et al., 1972).

shows the Crab Pulsar spectrum as presented in the paper of the Saclay-Milan-Palermo group (Parlier et al., 1972, see there for the references. Measurement point No. 20 is that of Albats et al., 1972).

These results are significant in two respects:

- First, the ratio of the continuous to pulsed flux from the Crab is about a factor of 6 at 0.1 MeV and this decreases to less than half that value at 20 MeV. Indeed, all the flux  $>20$  MeV could be pulsed.
- Secondly, while the interpulse appears to be dominant in the low energy  $\gamma$ -ray domain (Kurfess, 1971), both Albats et al. (1972), and Parlier et al. (1972), claim that the main pulse is dominant in their results. It would certainly be very interesting to study, with good statistics, the transition between these two different results in the 1- to 10-MeV region. (See also Chapters IV.A, IV.C and V.A.)

## CONCLUSION

Gamma-ray astronomy has been, and still is, a slowly developing branch of science. This is due to the very great experimental difficulties. Furthermore,  $\gamma$ -ray observations cannot be carried out from very simple, or small, spacecraft. It appears that the development of the field has also been slowed down by the comparatively large amount of time lost in the effort to obtain access to satellite space.

## REFERENCES

- Albats, P., G. M. Frye, A. D. Zych, O. B. Mace, V. D. Hopper, and J. A. Thomas, 1972, *Nature*, **240**.
- Fazio, G. G., 1973, *X-Ray and Gamma-Ray Astronomy, Proceedings of IAU Symposium No. 55*, (Madrid), H. Bradt and R. Giacconi, eds., D. Reidel, Dordrecht, Holland.
- Golenetskii, S. V., E. P. Mazets, V. N. Il'inskii, R. L. Aptekar, M. M. Bredov, Yu. A. Gur'yan, and V. N. Panov, 1971, *Astro. Letters*, **9**, p. 69.
- Kraushaar, W. L., G. W. Clark, G. P. Garmire, R. Borken, P. Higbie, C. Leong, and T. Thorsos, 1972, *Astrophys. J.*, **177**, p. 341.
- Kurfess, J. D., 1971, *Astrophys. J. Letters*, **168**, p. L39.
- Mayer-Hasselwander, H. A., E. Pfeffermann, K. Pinkau, H. Rothermel, and M. Sommer, 1972, *Astrophys. J. Letters*, **175**, p. L23.
- Pal, Y., 1973, *X-Ray and Gamma-Ray Astronomy, Proceedings of IAU Symposium No. 55*, (Madrid), H. Bradt and R. Giacconi, eds., D. Reidel Dordrecht, Holland.
- Parlier, B., B. Agrinier, M. Forichon, J. P. Leray, G. Boella, L. Marashi, R. Buccheri, R. Robba, and L. Scarsi, 1972, to be published in *Nature Phys. Sci.*
- Trombka, J. I., A. E. Metzger, J. R. Arnold, J. L. Matteson, R. C. Reedy, and L. E. Peterson, 1973, *Astrophys. J.*, **181**, p. 737.
- Vedrenne, G., F. Albernhe, I. Martin, and R. Talon, 1971, *Astron. and Astrophys.*, **15**, p. 50.

## C. PRELIMINARY RESULTS ON SAS-2 OBSERVATIONS OF $> 30$ MeV GAMMA RADIATION

D. A. Kniffen,\* C. E. Fichtel, and R. C. Hartman  
*Goddard Space Flight Center*

### INTRODUCTION

It was Morrison (1958) who first pointed out that the low interaction cross section of the high-energy  $\gamma$ -ray makes it a unique and valuable medium for obtaining information on many of the major energy transfers which take place in the universe. Furthermore, its chargeless state allows the information to be related to the regions in which the processes are occurring. In papers presented at this conference, Stecker, Ginzburg, and Clayton have pointed out that the spectra obtained from the observations of energetic  $\gamma$ -radiation may provide most important information concerning a number of astrophysical problems. These problems include the study of the distribution of high energy nuclei in the universe in space and time, the possible existence of antimatter on a universal scale, the origin of the  $> 50$  MeV galactic emission observed by Kraushaar et al. (1972), and other phenomena unique to large scale astrophysical bodies. In addition, the field of high-energy  $\gamma$ -ray astronomy provides an opportunity to extend our knowledge of the electromagnetic phenomena for diffuse and discrete source X-ray emission to high energies.

Within our own galaxy, high-energy  $\gamma$ -rays speak directly to the presence of energetic protons within discrete sources and in the galaxy as a whole through the broadly peaked but distinctive spectrum of  $\gamma$ -rays produced by the high-energy nucleons interacting with other nucleons. In this way, the cosmic-ray distribution throughout the galaxy may be studied as well as the high-energy particle gas surrounding individual objects from which cosmic rays have come. The picture that emerges will significantly aid in the understanding of the dynamics of our galaxy and the origin of energetic charged particle cosmic rays.

---

\*Speaker.

Beyond our galaxy  $\gamma$ -ray observations serve as an indicator of conditions existing in the cosmological past. In an expanding model of the universe, the density of matter was much greater in the past than it is observed to be in the present epoch. Two of the processes expected to be the most likely producers of  $\gamma$ -radiation on the universal scale are nuclear interactions of energetic cosmic radiation with the intergalactic gas and nucleon-antinucleon annihilation. Both processes produce a characteristic  $\pi^0$ -decay  $\gamma$ -ray spectrum in the rest frame, but the energy is degraded by the cosmological red shift caused by the expansion of the universe. Hence,  $\gamma$ -ray astronomy can address itself directly to the subject of cosmology.

Also expected to be important contributors to  $\gamma$ -ray production are the electromagnetic interactions important in X-ray astronomy, including the interactions of energetic electrons with matter (bremsstrahlung), with cosmic photon fields (Compton scattering), and with magnetic fields (magnetic bremsstrahlung).

Within discrete stellar objects, in addition to these mechanisms, there are other processes unique to the objects which may produce detectable levels of  $\gamma$ -radiation. Examples of such possibilities are the radioactive decay of the nucleosynthesis products as they are explosively ejected in supernovae (Clayton, 1973) and short intense burst of energetic photons emitted in the hydromagnetic shock wave following a stellar collapse (Colgate, 1968). The detection of  $\gamma$ -rays and the determination of their spectral characteristics during such events would provide most important clues to the validity of the theories which predict them.

The potential significance of  $\gamma$ -ray observations has led a large number of groups to develop a variety of detectors for the search of this rare photon in a very high background of energetic charged particle cosmic rays. The first unambiguous positive observations of extraterrestrial  $\gamma$ -rays above a few 10's of MeV was made by Kraushaar et al. (1972), with their OSO-3  $\gamma$ -ray detector, launched in 1968. This pioneering experiment measured a general diffuse flux and an enhanced emission from the galactic disk of  $\gamma$ -radiation above 50 MeV. Theoretical models for the origin of these observational fluxes have been difficult to obtain because of the limited angular and spectral resolution of the OSO-3 experiment. Share (Chapter IV.A) has reviewed other results obtained from a large number of detectors flown from balloons and satellites. Positive observations have been obtained for the diffuse flux, the galactic disk emission, and a large number of discrete sources, but conflicting evidence between experiments in some cases and marginal statistics in others has left a generally uncertain picture with the possible exceptions of pulsed  $\gamma$ -ray emission from the Crab Nebula Pulsar NP 0532 and the galactic plane emission.

In March of 1972, the first of the second generation of satellite  $\gamma$ -ray experiments was launched aboard the ESRO TD-1. The experiment consisted of a nine-deck vidicon spark chamber  $\gamma$ -ray telescope. On November 15, 1972, the SAS-2 was launched into orbit with a larger 32-deck magnetic core digitized spark chamber. These instruments should provide the sensitivity and angular and spectral resolution with the inherently low background of a satellite experiment needed to address many of the important questions in  $\gamma$ -ray astronomy.

In this paper we will give a description of the SAS-2 detector and present some of the preliminary results we have obtained.

## EXPERIMENT

Figure IV.C-1 is a schematic view of the SAS-2 telescope, a 32-deck spark chamber with a scintillator-Cerenkov counter charged-particle triggering telescope and a large plastic scintillator anticoincidence dome surrounding the entire experiment. Each spark chamber module is separated from the next by a 0.03 radiation length tungsten-pair production plate. The tungsten plates serve as scattering plates for the electrons following their formation, allowing the energy of each electron and hence of the incoming  $\gamma$ -ray, to be determined by analysis of the multiple scattering. This information is also used to obtain a weighted bisector of the pair for determining its arrival direction in spark chamber coordinates. A large number of thin plates are used so that the electron pair can be clearly identified and the arrival direction of the  $\gamma$ -ray can be accurately measured. The signature required for a trigger of the spark chambers is for a particle to pass undetected through the anticoincidence dome and to pass simultaneously (within about 500 ns) through the two elements of one of the four scintillator-Cerenkov charged particle telescopes. This coincidence triggers the application of high voltage across the spark chambers and initiates the readout system.

Figure IV.C-2 shows a photograph of a single wire grid module containing two planes of 200 wires each on opposite sides of the frame. The wires within a plane are parallel and orthogonal to the wires on the opposite plane. Each grid wire is threaded through a ferrite core contained on a shelf on the side of the frame. Two additional wires are threaded through each core to readout those set during an event. As a spark breaks down along the ion path remaining along the trajectory of a charged particle, the current flows along one or more affected wires in each plane of the grid, setting one or more cores. The readout of such set cores thus provides the coordinates of the charged-particle passage through that modular deck.

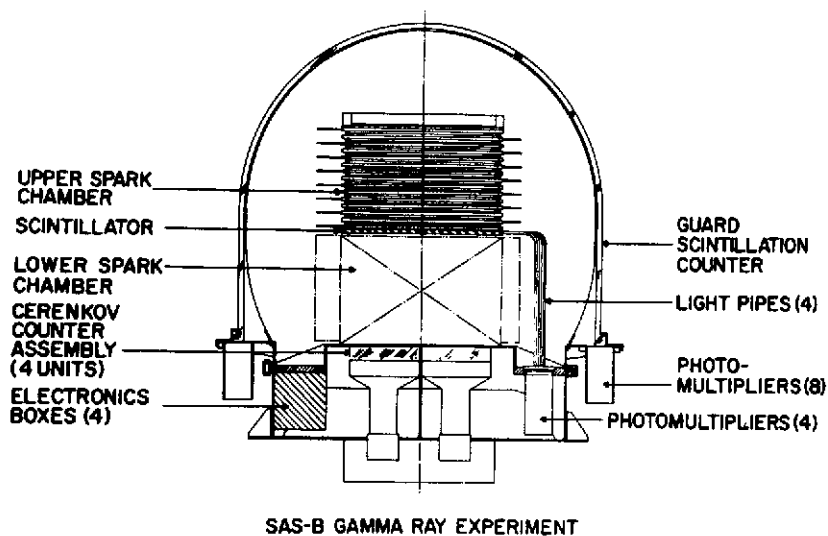


Figure IV.C-1. Schematic diagram of the SAS-2  $\gamma$ -ray spark-chamber telescope.

If the distribution of set cores is plotted separately for each of the two orthogonal planes, a picture is obtained such as that shown in Figure IV.C-3, which is a reproduction of a 16-mm microfilm frame of the two orthogonal views of a  $\gamma$ -ray pair production event. The scale for the vertical axis is compressed by a factor of three relative to the horizontal so incoming angles are exaggerated.

The flight unit was given a preflight calibration at a tagged photon facility established for this purpose at the 170-MeV electron synchrotron at the National Bureau of Standards in Gaithersburg, Maryland. The beam provides monoenergetic photons selectable over the 30- to 150-MeV energy interval. A very extensive calibration is currently underway using the essentially identical flight spare experiment unit. Until this calibration is complete, the results must be considered preliminary and flux and intensity values should be considered to be no better than about a factor of 1.5.

The characteristics of the telescope include an area of about  $540 \text{ cm}^2$ , a solid angle of about  $1/3 \text{ sr}$ , and an asymptotic high energy pair production efficiency of 29 percent. Timing accuracy of about 1 to 2 milliseconds allows a search for periodic emission. Arrival directions for 100-MeV  $\gamma$ -rays can be measured to about two degrees at 100 MeV. The energy threshold is about 30 MeV, although it is not sharp. Differential energy measurements can be made on 30- to 200-MeV  $\gamma$ -rays, and integral fluxes obtained for  $> 200$ -MeV  $\gamma$ -rays. A more detailed description of the experiment has been given by Derdeyn et al. (1972).

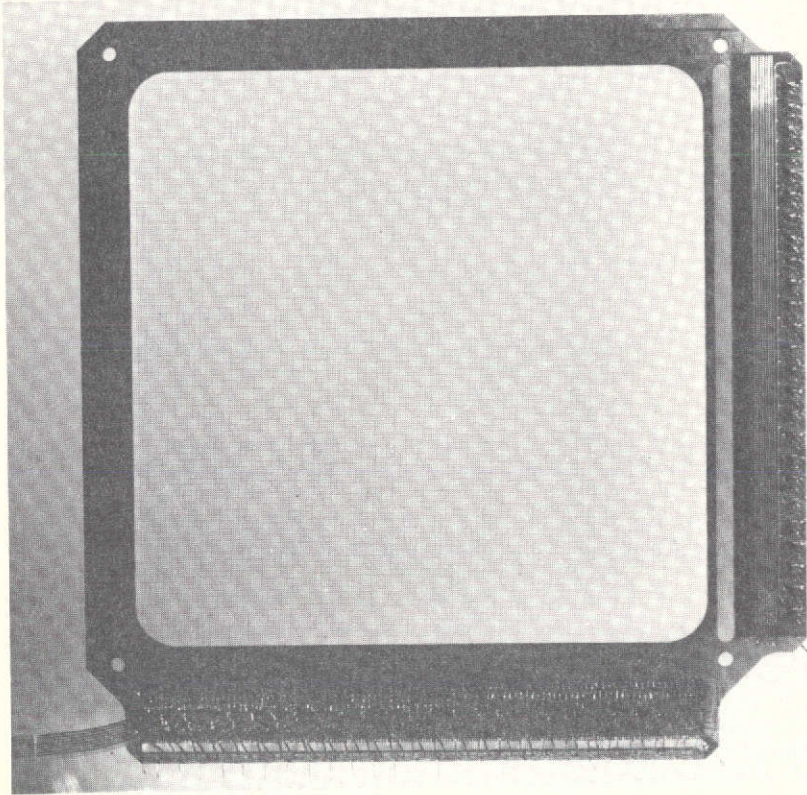


Figure IV.C-2. Photograph of a single wire grid spark-chamber module with two planes of 200 parallel wires. The direction of the wires in one plane is orthogonal to that in the opposite plane. Each wire is terminated through a ferrite core.

The experiment was launched as the sole experiment aboard the second of the Small Astronomy Satellites (SAS-2) on November 15, 1972. The orbital trajectory is essentially equatorial and approximately circular at a height ranging from 440 to 610 km above the earth's surface. Figure IV.C-4 gives an artist's concept of the telescope, surrounded by a gold colored thermal blanket, sitting atop the spacecraft control section. The satellite is spin stabilized with magnetic torquing of commandable electromagnets against the earth's magnetic field providing steering to any selectable point on the sky. Attitude is determined by a magnetometer-sun sensor combination and, to more precision, by a star sensor which is capable of determining the telescope pointing direction to about a quarter of a degree, thus allowing the directions of the  $\gamma$ -rays in spark chamber coordinates to be transformed into celestial and galactic coordinates.

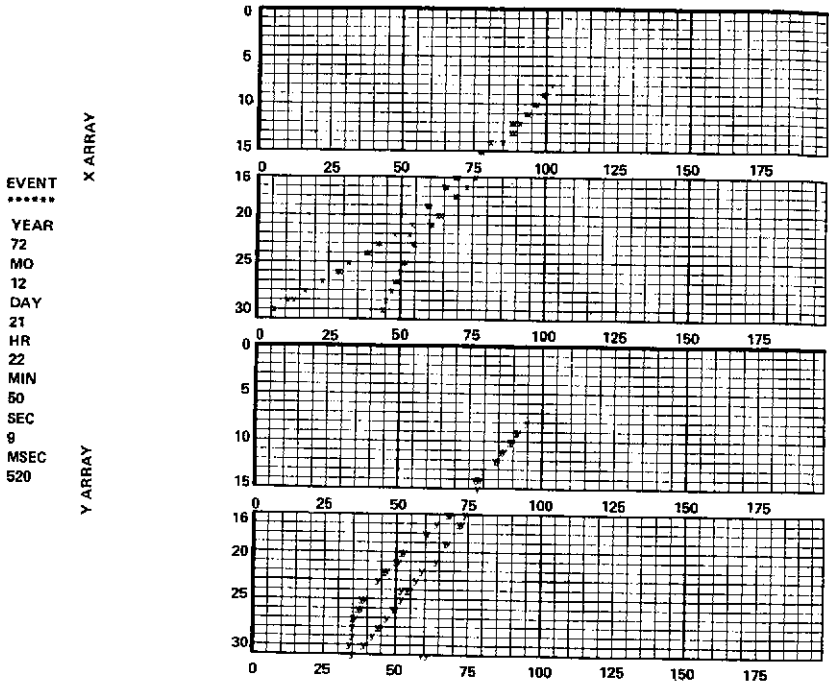


Figure IV.C-3. A microfilm plot of an event that presents two orthogonal views of the digitized trajectory of a pair of electrons produced by a  $\gamma$ -ray interacting with one of the tungsten plates between the 32 spark-chamber modules. The x's and y's denote cores set due to the passage of charged particles in the two orthogonal views. The vertical axis is compressed by nearly a factor of 3 relative to the horizontal, causing angles to be over-emphasized.

The viewing program has been chosen so as to examine each portion of the sky with about a one week exposure, with early emphasis on those regions of the sky expected to be most interesting in  $\gamma$ -rays. Figure IV.C-5 gives a view of the sky with the regions of the sky examined to date with the  $1/3$  sr field-of-view denoted by the cross-hatched area. Second-week exposures have already been obtained on the galactic center region as well as the anticenter, Crab Nebula region as denoted by the double cross-hatched area.

#### DATA ANALYSIS AND REDUCTION

SAS-2 data are recorded at a one-k bit/s rate on redundant onboard continuous-loop tape recorders. Once per orbit the recorded data

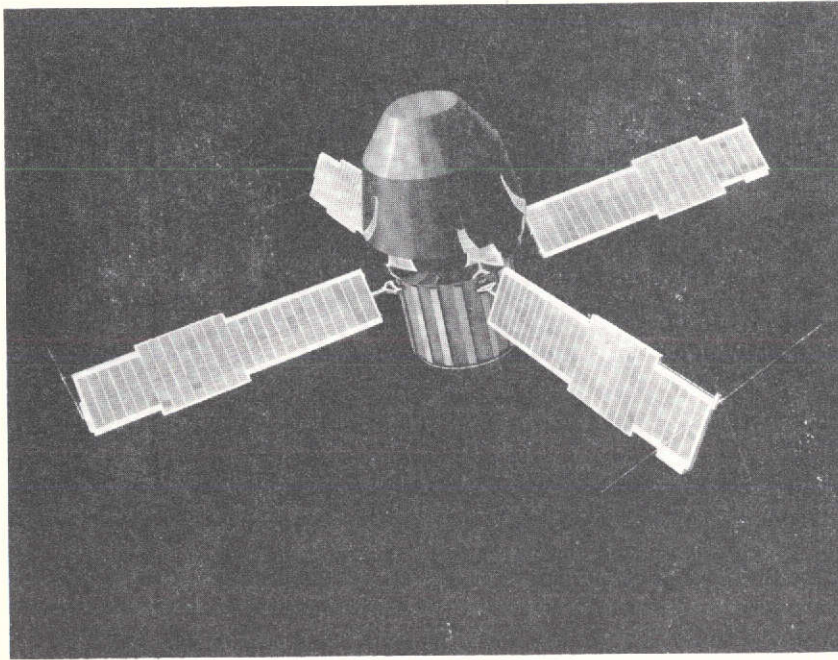


Figure IV.C-4. An artist's concept of the SAS-2 in orbit. The experiment surrounded by a thermal blanket sits atop the spin-stabilized spacecraft. Attitude is controlled by magnetic torquing.

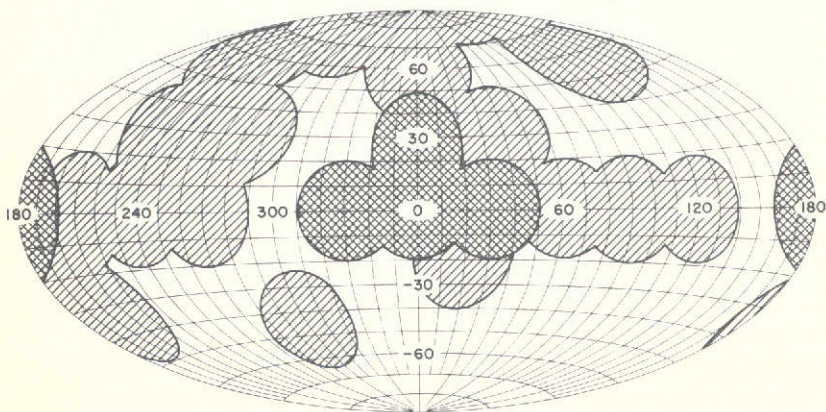


Figure IV.C-5. Regions of the sky in galactic coordinates viewed by SAS-2 through May 21, 1973. The cross-hatched regions are those viewed during the first 5 weeks after launch.

are transmitted at a 20 k bit/s rate to a tracking station located near Quito, Ecuador. Real-time data taken before and after the recorder playback is used to correlate the spacecraft clock with the station clock. This provides time in the data stream that is accurate to better than 2 ms in absolute time.

The data stream contains, in addition to spacecraft time, the spark-chamber event data, experiment and spacecraft control section housekeeping data (counter rates, voltages, currents, temperatures, pressures, and so forth), and aspect data from a digital solar aspect sensor, two fluxgate magnetometers, and an N-slit star sensor. Three orbits of data per day are transmitted via transmission links directly to the Goddard Space Flight Center (GSFC) to determine the aspect for the purposes of planning any necessary maneuvers. Maneuvers of the spin-stabilized spacecraft are accomplished by command of electromagnet torquing coils which provide fields that interact with the terrestrial field to provide maneuvering rates of up to about  $5.0^\circ$  a minute. Analog magnetic tapes of the remaining orbits are shipped to GSFC where time is correlated and the data placed in proper time sequence with any overlapping data eliminated. The magnetometer, sun sensors, and star sensors are used to determine the spark-chamber pointing direction to an accuracy of about  $0.25^\circ$ .

Analysis of the spark-chamber data is made by an automatic pattern recognition device designed to recognize the readout patterns produced as  $\gamma$ -rays interact in the tungsten plates to create electron-positron pairs (Figure IV.C-3). An alternate mode for analysis of the event data is made by interactive editing of the events with a graphics display unit. The results available at the present time have been obtained using the latter mode.

Events selected for editing have been carefully chosen to ensure that no ambiguities will be introduced into the measured fluxes by misidentification of spark chamber events. The selection is based on the following criteria: (1) only intervals that contain data taken when the spark chamber axis points away from the earth are chosen for analysis; (2) only  $\gamma$ -ray pair events are selected; (3) events that can masquerade as pair events as a result of interactions in the material of the side walls of the spark chamber are rejected for analysis; (4) events that set cores in the top grid are rejected to provide a veto for the rare events which form in the small amount of material between the coincidence counter and the spark chambers; and (5)  $\gamma$ -rays arriving at very large angles with respect to the detector axis are not included in the analysis. Edited events are automatically processed to obtain the energy and chamber arrival direction of each observed  $\gamma$ -ray according to procedures developed in the analysis of balloon data as described by Fichtel et al. (1972). The directional information is then combined with attitude and orbit data to provide the  $\gamma$ -ray arrival direction in celestial, galactic, geographic, and geomagnetic coordinates.

Events with zenith angles greater than  $90^\circ$  with respect to the outward radius vector of the satellite position are rejected from further consideration for the celestial analysis, safely avoiding the terrestrial horizon which lies at zenith angles greater than  $110.0^\circ$ .

The sensitivity of the telescope to each region of the sky is determined by an automatic analytic program that checks against all status conditions that affect sensitivity. In addition, the accumulation is made differentially in time in order to include instantaneous detector live time and to exclude those portions of the sky occulted by the earth.

## RESULTS

The results can be classified by three categories: diffuse, presumably extragalactic  $\gamma$ -rays coming from regions of the sky not associated with the galactic plane;  $\gamma$ -radiation from the galactic plane; and discrete sources of energetic  $\gamma$ -rays.

### Diffuse $\gamma$ -Radiation

For the regions of the celestial sphere, which we have examined thus far, there seems to be a weak, but finite component of high-energy  $\gamma$ -rays which exists for regions away from the galactic center. OSO-3, even with its much smaller sensitivity  $1.6 \text{ (cm}^2 \cdot \text{sr efficiency)}$  compared to about  $30 \text{ (cm}^2 \cdot \text{sr efficiency)}$  for SAS-2 above 100 MeV, also indicated a finite, apparently constant diffuse flux for regions of the sky which were far enough from the galactic plane that no portion of the relatively wide angle of the OSO-3 detector ( $\sim 35^\circ$ ) overlapped the galactic plane. From observations that SAS-2 has made, it now appears that in the region  $-20^\circ < \ell_{\text{II}} < +20^\circ$ , and  $b_{\text{II}} > 0^\circ$ , the flux reaches a constant level at least for  $b_{\text{II}} > +15^\circ$ . The data reported here come from the region of the sky centered at ( $\ell_{\text{II}} = 0$ ,  $b_{\text{II}} = +25^\circ$ ). The diffuse energy spectrum is presented in Figure IV.C-6. Notice that the spectrum is quite steep, steeper than other  $\gamma$ -ray spectra observed on SAS-2 or the earlier balloon work of the Goddard group (for example, Fichtel et al., 1972), including data on the galactic center region, the Crab, and the atmospheric secondary spectrum, upward or downward. The integral flux above 100 MeV is  $(3.9^{+1.1}_{-0.9}) \times 10^{-5} / (\text{cm}^2 \cdot \text{sr} \cdot \text{s})$  consistent with the OSO-3 result of  $(3.0 \pm 0.9) \times 10^{-5} / (\text{cm}^2 \cdot \text{sr} \cdot \text{s})$  averaged over all regions of the sky (Kraushaar et al., 1973). (Value corrected according to private communication with G. W. Clark, 1973.) The OSO-3 experiment did not measure the energy spectral shape.

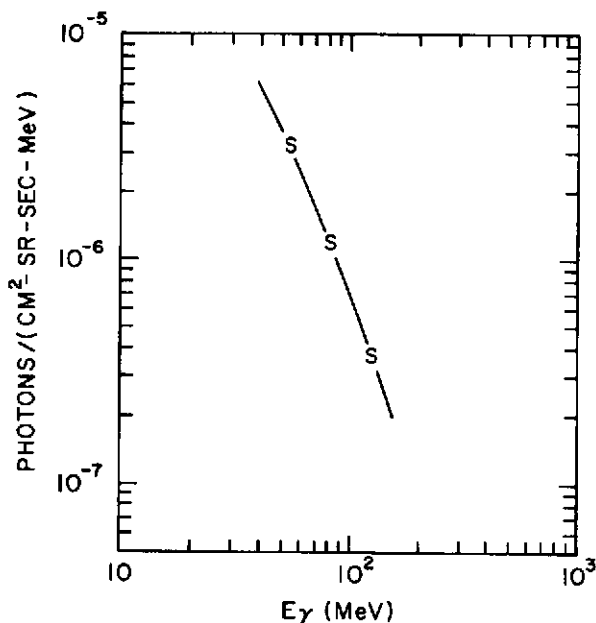


Figure IV.C-6. The diffuse  $\gamma$ -ray spectrum measured by SAS-2 for regions of the sky analyzed with  $|b_{\text{II}}| > 20^\circ$ . See text for a discussion of the specific region. For the present, a factor of uncertainty of 1.5 should be attached for each point.

### The Galactic Plane

SAS-2 has confirmed the high intensity of  $\gamma$ -rays coming from the galactic center region. The emission region extends along the galactic plane for at least  $60^\circ$  to  $70^\circ$  centered about the galactic center and is no wider than  $9^\circ$  full-width half-maximum for 100 MeV  $\gamma$ -rays and could be narrower, since there is still a final correction to be applied to the SAS-2 attitude data. The average intensity level for this region is about  $1.2 \times 10^{-4} / (\text{cm}^2 \cdot \text{rad} \cdot \text{s})$ , to which an uncertainty factor of 1.5 is attached until the SAS-2 calibration is complete. Whereas the average energy spectrum from this region is much harder than the diffuse radiation, the number of  $\gamma$ -rays between 30 and 60 MeV relative to the number above 100 MeV is inconsistent with a pure  $\pi^0$ -decay component. Apparently, there are other components with softer spectra. Because the SAS-2 aspect has not yet been determined with sufficient accuracy, at present the SAS-2 data would allow either a diffuse radiation or a sum of point sources for the soft component; however, there would have to be several (at least six)

point sources or there would have been a greater nonuniformity than was observed.

### Discrete Sources

High-quality attitude data are not yet available for a detailed study of discrete sources with SAS-2. However, a positive flux is detected for the Crab Nebula on the basis of an analysis of a sixth of the data available. A complete analysis of the data combined with accurate attitude data will allow a study of the energy spectrum of the Crab Nebula emission and the possible periodic pulsations from NP 0532.

No evidence is obtained for  $\gamma$ -ray emission from Sco X-1, with 95-percent confidence limits based on about a fourth of the data of  $1.7 \times 10^{-6}/(\text{cm}^2 \cdot \text{s})$  for  $\gamma$ -rays above 40 MeV and  $1.0 \times 10^{-6}/(\text{cm}^2 \cdot \text{s})$  above 100 MeV. A full analysis of a typical one-week exposure will allow 95-percent confidence limits of about  $2$  to  $3 \times 10^{-7}/(\text{cm}^2 \cdot \text{s})$  for sources for which no positive indication is obtained.

## DISCUSSION

### Diffuse Radiation

Figure IV.C-7 shows that the isotropic  $\gamma$ -radiation for  $|b_{\Pi}| > 20^\circ$  exhibits an enhancement relative to the single extension of the power-law spectrum valid in the X-ray region from 1 to 20 MeV and then a rapid decrease in intensity in the region from 40 to 200 MeV with an apparently reasonably smooth curve through the entire  $\gamma$ -ray region. Until more SAS-2 data from many regions of the sky have been analyzed with the full angular resolution, it is not possible to say that the radiation is truly uniform over the sky and uniform on a fine scale also. However, it seems a plausible hypothesis to assume that the regions examined thus far by SAS-2 are representative and to consider the possible origin of the radiation. There is, of course, the possibility that radiation is the sum of many, many weak sources of unknown origin. However, there are at least two other possibilities: one that the radiation comes from diffuse electrons interacting with matter, photons, or magnetic fields, and the other is that the  $\gamma$ -rays are of cosmological origin.

With regard to the diffuse electron possibility, bremsstrahlung seems unlikely because, at an energy where an increased slope would be expected, 1 to 10 MeV, due to an increasing rate of energy loss, the inverse is observed. For both synchrotron and Compton radiation, a power-law electron energy spectrum leads to a power-law photon spectrum, but with a different slope. The observed photon spectrum would imply a

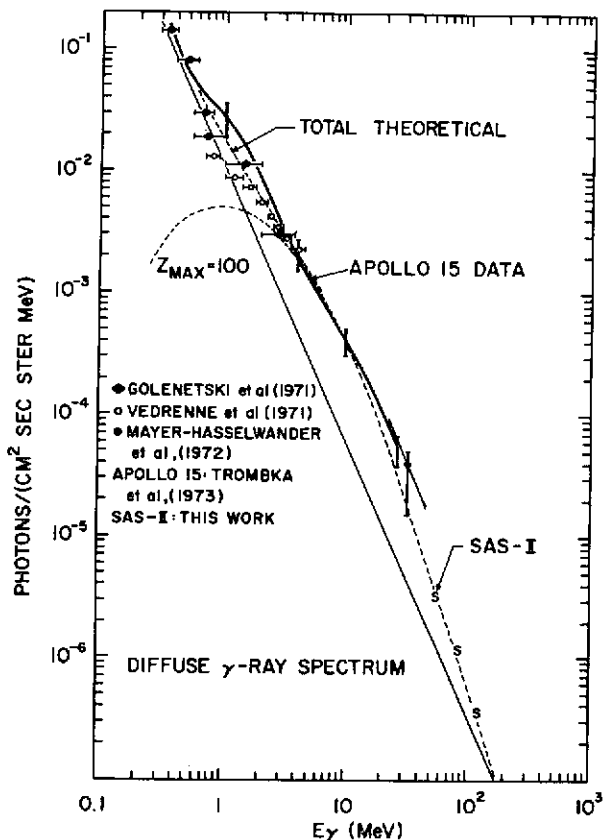


Figure IV.C-7. Diffuse radiation observed by several experiments. Also shown is the linear extrapolation of the X-ray data (solid line) and the spectrum predicted by Stecker et al. (1971), for  $\gamma$ -rays produced by the decay of neutral pions resulting from cosmic-ray interactions with interstellar matter in the cosmological past.

similarly shaped parent electron spectrum which would have features that are at least as sharp. There is no reason to expect such a spectral shape for diffuse electrons, although there is no experimental knowledge of the electron spectrum in the relevant energy range. Further, especially in the synchrotron case, the intensity seems too high to be consistent with reasonable estimates of the interstellar parameters.

Of the pure  $\gamma$ -ray cosmological hypotheses, there are two of which the authors are aware that seem to be possible candidates. They are the cosmic ray interstellar matter interaction model and particle-antiparticle annihilation in the baryon-symmetric big-bang model. In both theories, the resulting  $\gamma$ -ray spectrum, which is primarily due to  $\pi^0$ -decay, is red shifted substantially due to the expansion of the universe. These theories are discussed by Stecker et al. (1971), and Stecker in these proceedings (Chapter IX.A).

In an expanding model of the universe, the density of matter is much greater in the cosmological past than it is observed to be in the present. However, since the  $\gamma$ -radiation produced reaches us from large distances, the energy of the photons is degraded by the cosmological red shift caused by the expansion of the universe. One curve developed by Stecker (1969) involving red shifts up to about 100 is shown in Figure IV.C-7. The theoretical curve is seen to agree with experimental data reasonably well.

An alternative attempt to explain the  $\gamma$ -radiation through red-shifted  $\gamma$ -rays from  $\pi^0$ -decay arises from the big-bang theory of cosmology with the principle of baryon symmetry. Harrison (1967) was one of the first to propose a model of this type. Omnès (1969), following Gamow (1948), considers a big-bang model which is initially at a very high temperature and density, and then shows that, if the universe is baryon symmetric, a separation of matter from antimatter occurred at  $T > 30$  MeV. The initial phase separation of matter and antimatter leads ultimately to regions of pure matter and pure antimatter containing masses of the size of galaxy clusters. Stecker, Morgan, and Bredekamp (1971) have predicted the  $\gamma$ -ray spectrum which would be expected from annihilation at the boundaries of such clusters from the beginning of their existence. This spectrum is very similar to the one shown in Figure IV.C-7 in the energy range for which data exists, and is not included in the figure for that reason.

### Galactic Plane Radiation

Since the final-attitude data did not exist for SAS-2 at the time this article was written, discussion of the galactic center region must be limited to a summary of the broad features observed by SAS-2: (1) The enhancement of the galactic radiation in the region of the galactic center observed by OSO-3 is confirmed; (2) It is  $60^\circ$  to  $70^\circ$  in length along the plane and no more than  $9^\circ$  wide; (3) The energy spectrum is not a pure  $\pi^0$ -spectrum, but rather it also contains an enhanced flux below 70 MeV relative to that expected from a  $\pi^0$ -spectrum; and (4) The enhancement is not due just to a few point sources, although it could, of course, be due to a large number of point sources.

**Discrete Sources**

A discussion of the significance of discrete sources must await further data analysis; however, the sensitivity of SAS-2 should allow detailed study of a number of discrete sources and should allow us to place upper limits to the flux of objects with little or no emission that are almost two orders of magnitude lower than the existing upper limits.

**REFERENCES**

- Colgate, S. A., 1968, *Canadian J. Phys.*, **46**, p. S476.
- Derdeyn, S. M., C. H. Ehrmann, C. E. Fichtel, D. A. Kniffen, and R. W. Ross, 1972, *Nucl. Inst. and Meth.*, **98**, p. 557.
- Fichtel, C. E., R. C. Hartman, D. A. Kniffen, and M. Sommer, 1972, *Astrophys. J.*, **171**, p. 31.
- Gamow, G., 1948, *Phys. Rev.*, **74**, p. 505.
- Golenetskii, S. V., E. P. Mazets, V. N. Il'inskii, R. L. Aptekar', M. M. Bredov, Yu. A. Guryah, and V. N. Panov, 1971, *Astrophys. J. Letters*, **9**, p. L69.
- Harrison, E. R., 1967, *Phys. Rev. Letters*, **18**, p. L1011.
- Kraushaar, W. L., G. W. Clark, G. P. Garmire, R. Borke, P. Higbie, V. Leong, and T. Thorsos, 1973, *Astrophys. J.*, **177**, p. 341.
- Morrison, P., 1958, *Il Nuovo Cimento*, **7**, p. 858.
- Mayer-Hasselwander, H. A., E. Pfeiffermann, K. Pinkau, H. Rothermel, and M. Sommer, 1972, *Astrophys. J. Letters*, **175**, p. L23.
- Omnès, R., 1969, *Phys. Rev. Letters*, **23**, p. L38.
- Stecker, F. W., 1969, *Astrophys. J.*, **157**, p. 507.
- Stecker, F. W., D. L. Morgan, and J. Bredekamp, 1971, *Phys. Rev. Letters*, **27**, p. L1469.
- Trombka, J. I., A. E. Metzger, J. R. Arnold, J. L. Matteson, R. C. Reedy, and L. E. Peterson, 1973, *Astrophys. J.*, **181**, p. 737.
- Vedrenne, G., F. Albernehe, I. Martin, and R. Talon, 1971, *Astron. and Astrophys.*, **15**, p. 50.

## A. OBSERVATIONS OF HIGH-ENERGY GAMMA RAYS

G. G. Fazio\*

*Smithsonian Astrophysical Observatory and Harvard College Observatory*

### INTRODUCTION

At energies above  $10^{11}$  eV, the predicted fluxes of cosmic  $\gamma$ -rays from discrete sources are so small ( $< 1 \text{ m}^2 \text{ day}^{-1}$ ) that it becomes impractical to measure these fluxes with detectors in high-altitude balloons and satellites. However, this radiation can be observed, indirectly, with ground-based instruments. When high-energy  $\gamma$ -rays strike the earth's atmosphere, they generate a shower of particles that in turn emit a burst of Cerenkov light. In principle, a ground-based observer, using rather simple apparatus, can record the intensity and direction of either the particles or the Cerenkov light, or both, and hence determine the energy and arrival direction of the incident  $\gamma$ -ray photon. In the energy region between  $10^{11}$  and  $10^{13}$  eV, the shower particles are absorbed in the atmosphere; therefore, only the Cerenkov light technique can be used. It is this energy region in which most experiments are done and about which I will describe our recent results. Let me begin by first describing the instrumentation used in these experiments because it has bearing on the interpretation of the results.

### INSTRUMENTATION

In the absence of sufficiently strong sources of cosmic  $\gamma$ -rays, the design of experiments must be based on theoretical models of the properties of the Cerenkov light generated by air showers. These studies have been done by Zatsepin and Chudakov (1962), Zatsepin (1965), Long (1967), Rieke (1969), and Bosia, Maringelli, and Navarra (1972). In general, at  $10^{11}$  eV these light bursts of 3-ns duration have angular diameters of the order of  $0.5$  but, when viewed away from the shower axis, are elongated and displaced in angle toward the shower maximum. The number of Cerenkov photons per unit area at ground level is rather constant within 130 m of the shower core and falls rapidly beyond this radius. Therefore, a light detector with sufficient sensitivity

---

\*Speaker.

will be able to detect showers over an area of  $5 \times 10^4 \text{ m}^2$ . Thus, the principal advantages of this technique are the combination of a large sensitive area with good angular resolution.

There are also disadvantages. The basic one is that there is no equivalent of the anticoincidence counter to remove those showers generated by charged cosmic-ray particles; these are at least several hundred times more numerous. Another disadvantage is that the technique can be used only on clear, moonless nights.

To obtain the maximum possible light-collecting power and hence the minimum possible threshold energy, the Smithsonian Astrophysical Observatory (SAO) constructed a light reflector of 10-m aperture, mounted on an alt-azimuth antenna positioner. The reflector is located at the 2300-m level of Mount Hopkins, Arizona (Figure V.A-1). Based on theoretical calculations, the reflector, when used as a  $\gamma$ -ray detector pointed to the zenith, has a threshold energy of  $9 \times 10^{10}$  eV, an effective sensitive area of  $1.3 \times 10^4 \text{ m}^2$ , and an effective angular resolution of  $1^\circ$ . The maximum shower count rate at the zenith is about  $400 \text{ min}^{-1}$ . At angles away from the zenith, the threshold energy and the effective collecting area increase. There is no energy resolution in the integral counting mode other than this method of varying the threshold energy. Attempts are being made to achieve energy resolution by measuring the intensity of each Cerenkov light burst.

The primary cosmic radiation generates an isotropic background source of Cerenkov light bursts; hence, a  $\gamma$ -ray source can be distinguished by an increase in the number of showers detected in the direction of the suspected source. Two observational techniques have been used to detect this anisotropy: the drift-scan mode and the tracking mode. In the drift-scan mode, the reflector is aligned 20 to 30 min of right ascension ahead of the suspected source; the earth's rotation then sweeps the field-of-view of the detectors over the source. Many drift scans must be accumulated on each object, since the expected anisotropy is less than 1 percent. Although the drift-scan has advantages in terms of stability and ease of operation, it is most inefficient because less than 20 percent of the observing time is spent on the source. To increase the on-source observing time, the tracking mode was developed. In this mode, two phototubes are located at the focus of the reflector and separated by  $4.2^\circ$ . The reflector then tracks the source in such a manner that one phototube views the source while the other phototube views the background shower rate "off" source. Every 10 min, the fields-of-view are reversed. In this mode, approximately 90 percent of the time is spent observing the source.

The major limitation to the sensitivity of these experiments is the isotropic cosmic-ray background owing primarily to proton-initiated air showers (P-EAS). Several groups have sought to distinguish  $\gamma$ -ray-initiated showers (G-EAS) from

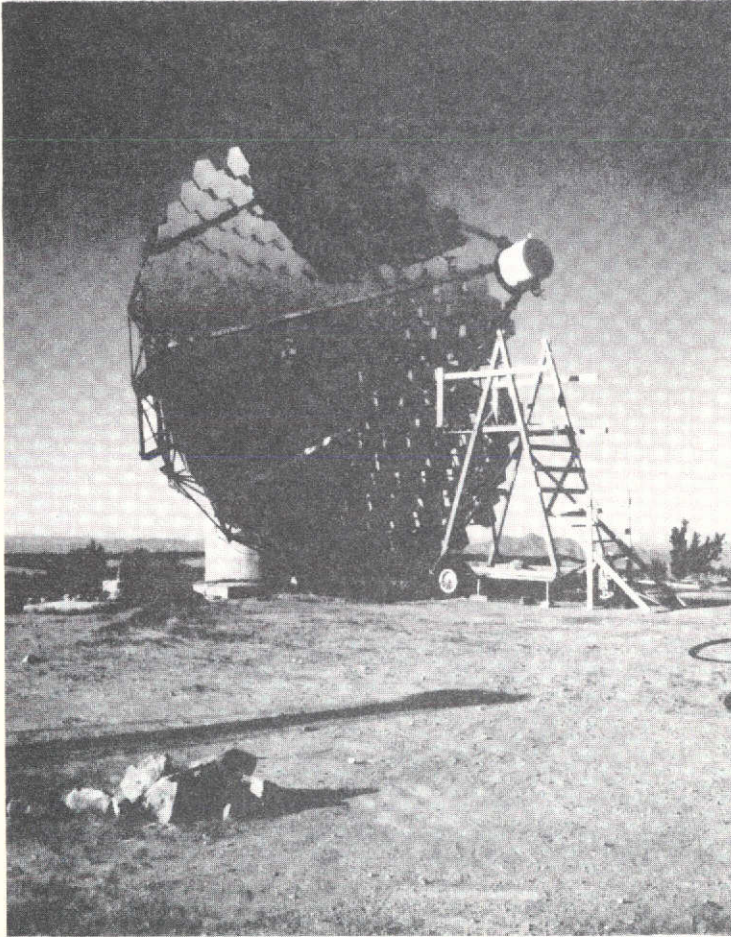


Figure V.A-1. The 10-m optical reflector located at the 2300-m level of Mount Hopkins, Arizona.

P-EAS by making use of subtle differences in the light distributions from the two types of showers (Tornabene and Cusimano, 1968; O'Mongain et al., 1968).

However, the most successful experiments in distinguishing the origin of the air shower have been performed by Grindlay (1971a; 1971b). He has presented evidence that he has been able to distinguish the Cerenkov light from the electrons at the maximum of the shower's electromagnetic cascade (height  $h_{\text{max}}$ ) from the Cerenkov light owing to the unscattered, penetrating shower "core" of predominantly pions, muons, and secondary electrons. These latter particles would be present only in P-EAS. The

technique uses two searchlight-mirror detectors operated in coincidence mode and separated by 70 m, with each mirror rotated inward from the source direction by an angle  $\theta$  so that each is pointed at the shower maximum (Figures V.A-2 and -3); for a  $\gamma$ -ray energy of  $10^{12}$  eV,  $h_{\max} = 6.2$  km and  $\theta = 0.35^\circ$ . A third mirror system is used to detect the penetrating shower core ( $h = 3.5$  km,  $\theta = 0.65^\circ$ ). Because the light from the lower component is relatively nearby, it is rich in the ultraviolet component and hence can be distinguished from light at the shower maximum. A G-EAS is registered only when light from shower maximum is not accompanied by light from the lower level.

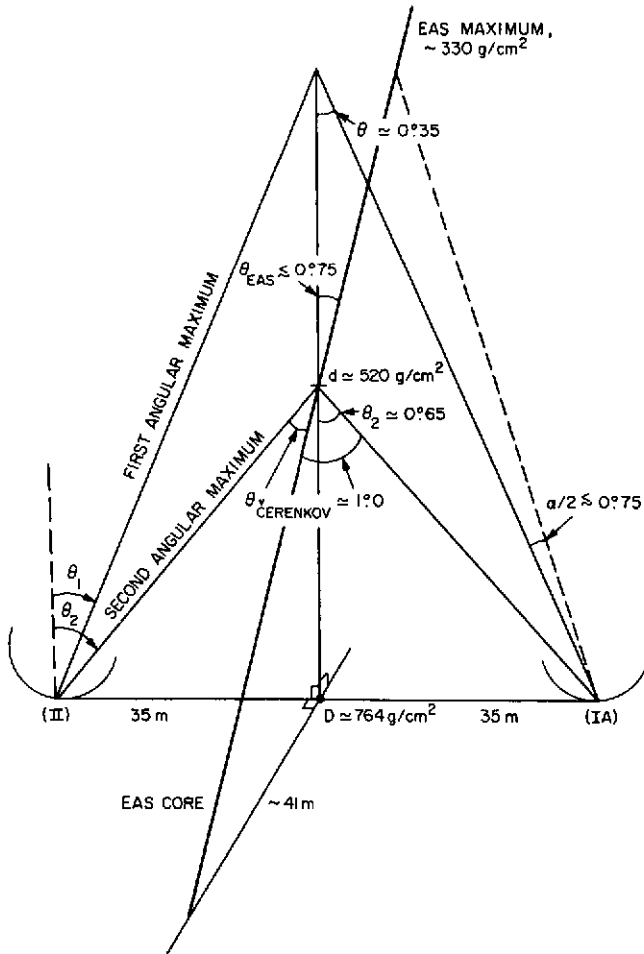


Figure V.A-2. Simplified geometry of the detection technique used by Grindlay to reject proton-initiated extensive air showers.

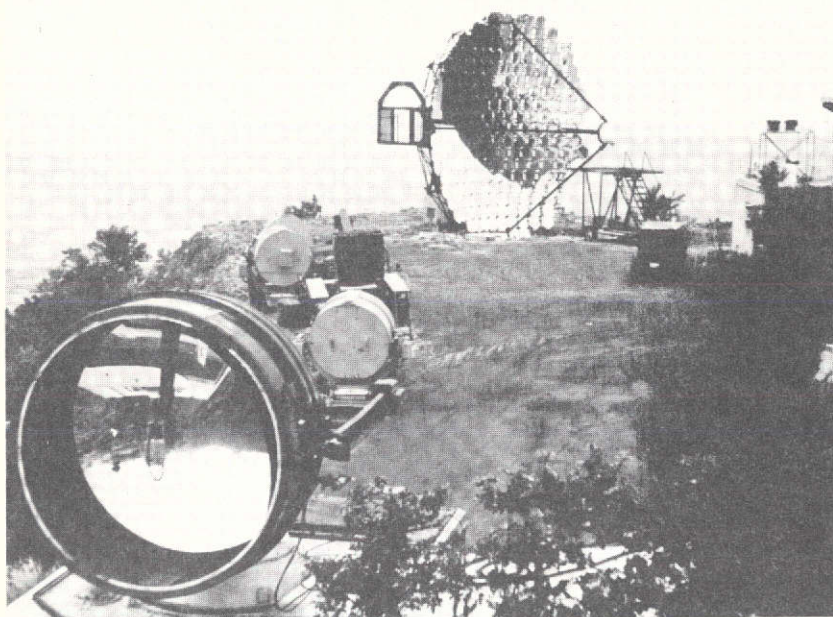


Figure V.A-3. Photograph of the series of 1.5-m searchlight mirrors used by Grindlay at Mount Hopkins, Arizona.

With this technique, Grindlay has been able to reach an average rejection ratio of 70 percent. For  $\gamma$ -ray energies  $\geq 5 \times 10^{11}$  eV, the combined effects of P-EAS rejection and increased angular resolution have made possible an order-of-magnitude increase in sensitivity over mirrors of the same size used in the normal modes. The drift-scan mode was used in these experiments, and the complicated pointing geometry permitted only 5 percent of the operating time on source. Recent experiments using the 10-m reflector and a 1.5-m searchlight mirror on an alt-azimuth antenna positioner permitted operation in the tracking mode and a considerable increase in operating time on source.

Grindlay, in cooperation with Prof. R. Hambury Brown's group at the University of Sydney, has converted the two 6.6-m reflectors of the stellar interferometer at Narrabri, Australia, for use as atmospheric Cerenkov light detectors (Figure V.A-4). P-EAS rejection was obtained with a second phototube located in an off-axis position on one of the reflectors, and the reflectors were operated in the tracking mode. Several discrete sources in the Southern Hemisphere were investigated for the first time in 1972.

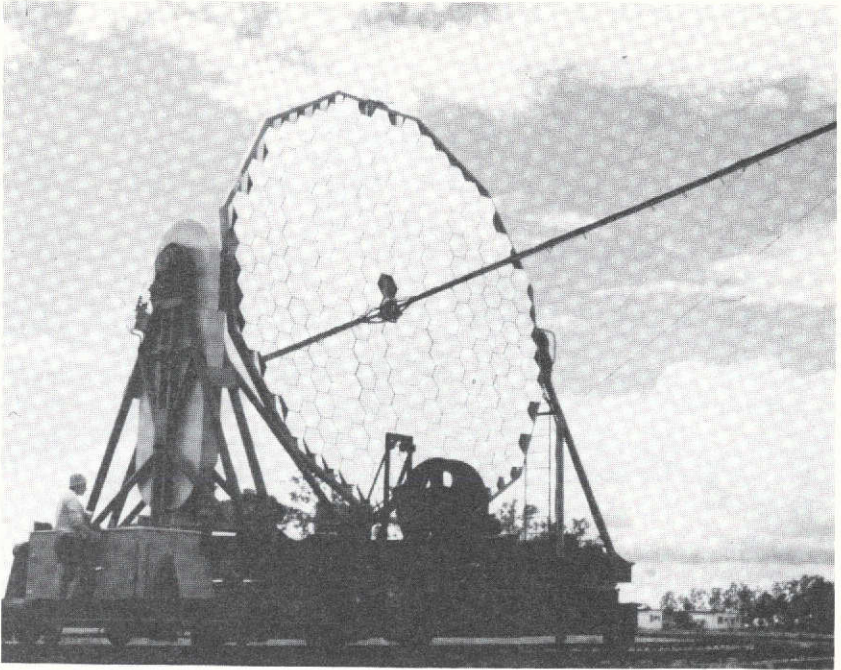


Figure V.A-4. One of the 22-foot reflectors at Narrabri, Australia.

#### OBSERVATIONS AND RESULTS

Since 1968, the 10-m reflector has been used to search for cosmic  $\gamma$ -rays from more than 27 discrete sources, including supernova remnants, pulsars, X-ray sources, magnetic variables, radio galaxies, and quasars. With the exception of the Crab Nebula, none of these sources was detected (Weekes et al., 1972). For  $\gamma$ -ray energies greater than  $2 \times 10^{11}$  eV, the upper limits to the flux were of the order of  $10^{-10}$  photon  $\text{cm}^{-2} \cdot \text{s}^{-1}$ . It takes approximately 10 hours of observation on source to reach these limits. An extrapolation of the X-ray spectrum of some of these sources would indicate a  $\gamma$ -ray flux in excess of this value. Simple Compton-synchrotron models for producing  $\gamma$ -rays in radio sources also predict fluxes above this value. Where enough information is known about these radio sources, the upper limits place important constraints on the source parameters, particularly the average magnetic field in the source.

Although other groups in the past have reported evidence for discrete  $\gamma$ -ray sources in this energy range (for example, Stepanian, Vladimirsky, and Fomin, 1972), we have investigated these same sources and have found no evidence of  $\gamma$ -ray emission.

During 1972, Grindlay's observations with the Narrabri reflectors in the Southern Hemisphere yielded preliminary evidence for  $\gamma$ -rays from several sources. No radiation above  $2 \times 10^{11}$  eV from the discrete source Sgr A at the galactic center nor from several of the 100-MeV  $\gamma$ -ray sources was reported by Frye et al. (1971). These results are very tentative and further observations have recently been made from April through June 1973.

The Crab Nebula is a very special case. Observations with the 10-m reflector over the years 1969 to 1972 indicate an average flux of  $\gamma$ -rays of  $4.4 \pm 1.4 \times 10^{-11}$  photon-cm $^{-2} \cdot$  s $^{-1}$  with energy above  $2.5 \times 10^{11}$  eV at the  $3.1 \sigma$  level (Fazio et al., 1972). This flux corresponds to an emission of  $6 \times 10^{33}$  ergs/s, which is significantly less than the X-ray emission of the Nebula. However, the  $\gamma$ -ray flux may vary with time, and the most significant flux ( $1.21 \pm 0.24 \times 10^{-10}$  photon-cm $^{-2} \cdot$  s $^{-1}$ ) may occur 60 to 120 days after a major spin-up of the Pulsar NP 0532. This increase was observed on three different occasions, and if only the flux in these intervals is used, the effect is at the  $5 \sigma$  level. The total  $\gamma$ -ray energy observed on each occasion was  $\sim 10^{41}$  ergs, an energy approximately equal to the energy of the pulsar spin-up.

The average  $\gamma$ -ray flux detected can be explained easily by a Compton-synchrotron model of the Crab Nebula, in which the  $\gamma$ -rays are produced by Compton scattering of relativistic electrons on their own synchrotron radiation (Gould, 1965; Rieke and Weekes, 1969; Grindlay and Hoffman, 1971). The primary unknown variable in this theory is the magnetic field in the Nebula; and, hence, a measurement of the  $\gamma$ -ray flux is a way of determining the average magnetic field. Figure VI.A-5 shows the current data along with the exact Compton-synchrotron model of Grindlay and Hoffman (1971). The data are best fitted with a value of  $\langle B_{\perp} \rangle = 2.5 \times 10^{-4}$  gauss in the uniform field model of the Nebula and by a value of  $B_{\perp\theta_0} = 10^{-3}$  gauss for a model based on a  $1/r$  field, where  $B_{\perp\theta_0}$  is the value of the field at the inner edge of the first wisp surrounding the pulsar.

The variability of the  $\gamma$ -ray flux is more difficult to explain. In a Compton-scattering process, the electrons have too long a lifetime. The synchrotron process requires electrons of the order of  $10^{17}$  eV in a field of  $10^{-3}$  gauss; these electrons have a lifetime of  $\sim 10^3$  s, and hence this process seems more feasible. The number of  $10^{17}$ -eV electrons required is small compared to the total number of electrons injected into the Nebula. The 60-day delay and the 60 to 120-day duration may be due either to a time delay in the electron-acceleration process, for example, in the wisps, or, assuming that the particles stream out from the pulsar, to the light-travel time in the geometry of the region where the synchrotron radiation is produced.

Because of this possible variation in the  $\gamma$ -ray flux from the Crab Nebula, it is important that the SAS-2 experiment monitor the 100-MeV flux from the Nebula for time variations. If, indeed, the 10-m reflector has detected a continuous flux of  $\gamma$ -rays at  $10^{11}$  eV from the Crab Nebula, it becomes particularly interesting to determine to what extent this flux is pulsed. Grindlay (1971c), using the proton-shower-rejection technique, first reported a pulsed flux of  $\gamma$ -rays from NP 0532 based on 42 drift scans in January 1971.

Ninety-nine additional scans were obtained during November and December 1971, which also showed evidence of a pulsed effect (Grindlay, 1972). Later, it was discovered that the November and December data were analyzed with the wrong period, owing to a computer-program error. Reanalysis of this data resulted in even more significant evidence of having detected a pulsed effect from NP 0532. The sum of all 141 drift scans exhibited a  $4.2 \sigma$  effect, but the primary and interpulse both appear to be 1.7 ms early with respect to the corresponding optical peaks. These data correspond to a pulsed flux above  $6 \times 10^{11}$  eV of  $8 \pm 6.5 \times 10^{-12}$  photon  $\text{cm}^{-2} \cdot \text{s}^{-1}$ .

Grindlay repeated the observations in 1973 by using the tracking mode to increase the observing time on the source. Preliminary analysis of the data again showed evidence of pulsed  $\gamma$ -rays, but the primary peak of the radiation may be delayed in phase from the optical pulse by 1.7 m (Grindlay et al., 1973). This repeated positive effect is most interesting, and it is still possible that Grindlay, using the proton-shower-rejection technique, has detected a pulsed  $\gamma$ -ray flux from NP 0532, but the present results do not give unambiguous proof.

Helmken et al. (1973), by using data on the Crab Nebula obtained with the 10-m reflector, have analyzed the arrival times of air showers for over 200 hours of these observations; the arrival times were recorded to a precision of 200  $\mu\text{s}$ . An analysis of the data by use of the optical pulsar period and phase revealed no statistical excess at the primary pulse of the interpulse. A typical upper limit to the flux at  $1.8 \times 10^{11}$  eV for a 1.3-ms bin width and  $E^{-1.1}$  spectrum was  $1.4 \times 10^{-11}$   $\text{eV} \cdot \text{cm}^{-2} \cdot \text{s}^{-1} \cdot \text{eV}^{-1}$ . Upper limits to the flux were also obtained at energies of  $3.0 \times 10^{11}$  eV and  $4.7 \times 10^{11}$  eV (Figure V.A-5).

The lower energy X- and  $\gamma$ -ray data are best fitted by a curve of the form  $1.0 E^{-1.1}$ . Extrapolated to the  $10^{11}$  eV energy region, the curve lies 2 orders of magnitude above the current upper limits. The extrapolated flux, if true, would be verified in less than 20 minutes of observations. Thus, an important result of this work is that the upper limits to the  $\gamma$ -ray flux indicate a major break in the pulsar spectrum between 1 and 100 GeV. When the

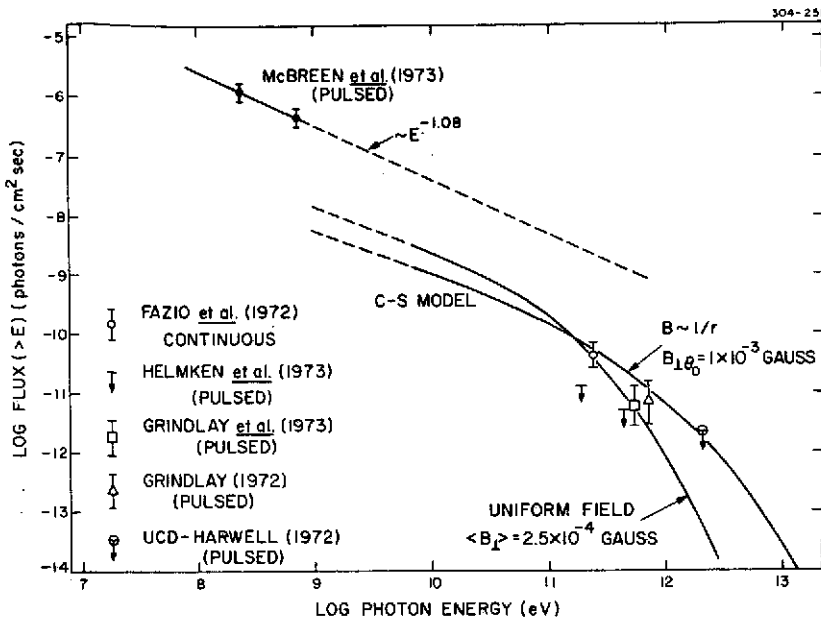


Figure V.A-5. Graph of recent results of the pulsed and continuous flux from the Crab Nebula. The solid lines represent the Compton-synchrotron model computed by Grindlay and Hoffman (1971) for a uniform magnetic-field model and for a field proportional to  $1/r$ .

previously reported positive continuous flux is taken with the present upper limits to the pulsed flux, it places an additional upper limit of 30 percent on the ratio of the pulsed-to-continuous component at  $10^{11}$  eV. This is a reversal of the trend at lower energies.

The University College, Dublin-Harwell group (N. Porter, private communication, 1972) also have evidence for a periodic flux of  $2 \times 10^{12}$  eV  $\gamma$ -rays from the pulsar, but, again, the primary pulse is not in phase with the optical pulse. If real, the effect would correspond to a flux of  $2 \times 10^{-12}$  photon-cm $^{-2}$  s $^{-1}$ .

## FUTURE EXPERIMENTS

It is particularly important to continue observations on the Crab Nebula for two reasons: (1) To determine if an increase in the continuous  $\gamma$ -ray flux is associated with the pulsar's spin-up; and (2) to determine if Grindlay's technique of rejection of proton-induced showers has detected a pulsed flux from NP 0532.

The next priority would go to observation of the sources seen in the 100-MeV to 1-GeV region with balloon-borne detectors, for example, the sources reported by Frye et al. (1971), and with the SAS-2 and TD-1 satellite detectors.

The sensitivity achieved in the current experiments has been the result of many hours of observation on a limited number of sources. It is still possible that there exist sources of detectable intensity that were not included in our survey or that were not observed in other regions of the spectrum. Therefore, Weekes et al. (1972), have proposed an all-sky survey of the Northern Hemisphere. Very few observations have been made in the Southern Hemisphere.

It is also possible that the  $\gamma$ -ray sources examined are time variable, which makes verification even more difficult. Delays between balloon-borne  $\gamma$ -ray detector flights are of the order of 6 months. One advantage of the atmospheric-Cerenkov light technique is that immediate observations can be made on a suspected source. In view of this, we ask groups that have discovered a possible source of cosmic  $\gamma$ -rays to communicate the information to us as soon as possible.

In all the above programs, an increase in detector sensitivity would be most helpful. In theory, the proton-shower-rejection technique used by Grindlay should significantly increase the sensitivity. Hence, it appears that the design of any future detectors should use this technique. One possibility is the construction of a second large reflector near the 10-m reflector at Mount Hopkins; another would be to lower the  $\gamma$ -ray threshold energy ( $E_t$ ) of the 10-m reflector. The current reflector mount could support a second 10-m reflector. Since  $E_t \propto A^{-1/2}$ , where  $A$  is the area of the reflector, doubling the area would reduce the threshold energy only by a factor of 0.7, but additional reductions could be made by increasing the frequency bandwidth and operating in the coincidence mode.

Continued studies of the structure of the Cerenkov light bursts produced in air showers are also necessary to maximize the efficiency of present detectors. For example, N. Porter has suggested that the geomagnetic field can have important effects on the angular distribution of Cerenkov light from extensive air showers.

#### ACKNOWLEDGMENTS

The results described in this paper, obtained with the 10-m reflector, have been produced through the efforts of many people. Trevor C. Weekes has been primarily responsible for the operation of the 10-m reflector with the assistance of Ed Horine. The pulsar data analysis was

done through the very patient efforts of Henry Helmken. George Rieke and Eon O'Mongain assisted in many of the observations and in the interpretation of the data. Jonathan Grindlay performed the Compton-synchrotron model calculations.

## REFERENCES

- Bosia, G., M. Maringelli, and G. Navarra, 1972, *Il Nuovo Cimento*, **9B**, p. 201.
- Fazio, G. G., H. F. Helmken, E. O'Mongain, and T. C. Weekes, 1972, *Astrophys. J. Letters*, **175**, p. L117.
- Frye, G. M., P. A. Albats, A. D. Zych, J. A. Staib, V. D. Hopper, W. R. Rawlinson, and J. A. Thomas, 1971, *12th Int. Conf. on Cosmic Rays*, Hobart, Tasmania, paper OG-24.
- Gould, R. J., 1965, *Phys. Rev. Letters*, **15**, p. 577.
- Grindlay, J. E., 1971a, *Il Nuovo Cimento*, **2B**, p. 119.
- , 1971b, *Smithsonian Astrophys. Obs. Spec. Rept.*, No. 334.
- , 1971c, *Nature Phys. Sci.*, **234**, p. 153.
- , 1972, *Astrophys. J. Letters*, **174**, p. L9.
- Grindlay, J. E., H. F. Helmken, T. C. Weekes, G. G. Fazio, and F. Boley 1973, Proc. 13th Int. Conf. on Cosmic Rays, Denver, in press.
- Grindlay, J. E., and J. A. Hoffman, 1971, *Astrophys. J. Letters*, **8**, p. L209.
- Helmken, H. F., G. G. Fazio, E. O'Mongain, and T. C. Weekes, 1973, *Astrophys. J.*, in press.
- Long, C. D., 1967, Ph. D. Thesis, National Univ. of Ireland.
- O'Mongain, E. P., N. A. Porter, J. White, D. J. Fegan, D. M. Jennings, and B. G. Lawless, 1968, *Nature*, **219**, p. 1348.
- Rieke, G. H., 1969, *Smithsonian Astrophys. Obs. Spec. Rept.* No. 301.
- Rieke, G. H., and T. C. Weekes, 1969, *Astrophys. J.*, **155**, p. 429.
- Stepanian, A. A., B. M. Vladimirovsky, and V. P. Fomin, 1972, *Nature Phys. Sci.*, **239**, p. 40.
- Tornabene, H. S., and F. J. Cusimano, 1968, *Canadian J. Phys.*, **46**, p. S81.

Weekes, T. C., G. G. Fazio, H. F. Helmken, E. O'Mongain, and G. H. Rieke, 1972, *Astrophys. J.*, **174**, p. 165.

Zatsepin, G. T., and Chudakov, 1962, *Soviet Phys.—JETP*, **15**, p. 1126.

Zatsepin, G. T., 1965, *Soviet Phys.—JETP*, **20**, 459.

## A. OBSERVATIONS OF GAMMA-RAY EMISSION IN SOLAR FLARES

D. J. Forrest\*, E. L. Chupp†, A. N. Suri, and C. Reppin‡  
*University of New Hampshire*

### INTRODUCTION

The primary purpose of this paper is to review the observations of solar flare-associated  $\gamma$ -rays. Some preliminary discussion of the features of the measurements will be given even though the full interpretation of the measurements is not complete, as far as understanding the physics of solar flares is concerned. The observations discussed here were first presented at the NASA Symposium on High Energy Phenomena on the Sun (Chupp et al., 1972), and a more detailed report has been published (Chupp et al., 1973).

The University of New Hampshire  $\gamma$ -ray detector, which is situated in the wheel section of the OSO-7 spacecraft, has been described in detail by Higbie et al., 1972. Briefly, it consists of a 7.6-cm by 7.6-cm NaI scintillator surrounded by and in anticoincidence with an active CsI shield. It is calibrated by a gated radioactive source (Forrest et al., 1972) twice each orbit and has an energy resolution of  $\approx 8$  percent FWHM at 662 keV. Two independent pulse-height spectra covering the energy range 0.3 to 9 MeV are simultaneously accumulated over an 180-s interval: one in the solar direction and one in the antisolar or background direction. An auxiliary 7.9-cm<sup>2</sup> NaI X-ray detector is also included in the instrument. It covers the energy range 7.5 to 120 keV in four energy bands, and a complete X-ray spectra is taken every 30 seconds.

---

\*Speaker.

†Alexander von Humboldt and Fulbright-Hayes Scholar on leave at the Max Planck Institute for Extraterrestrial Physics, Munich, Germany.

‡On leave from the Max Planck Institute for Extraterrestrial Physics, Munich, Germany.

### GAMMA-RAY OBSERVATIONS

Figure VI.A-1 shows the counting rate versus time in several energy bands covering the range 7.5 keV to 8 MeV observed during the 3B H $\alpha$  flare that began at  $\sim$ 0621 UT on August 4, 1972. Also shown is the radio burst at 19,000 MHz as reported in UAG-21 (Lincoln and Leighton, 1972). The rates in the energy interval 7.5 to 120 keV are from the X-ray detector, and the rate in the 0.35-to 8-MeV interval is from the central  $\gamma$ -ray detector. As can be seen, OSO-7 was eclipsed by the earth before the event was over, but according to the radio burst, most of the flash phase was observed. The time correspondence between the radio, X-ray, and  $\gamma$ -ray continuum is self-evident. Figure VI.A-2 shows some of the same rates on an expanded time scale. All of the rates were observed to increase above their preflare values at  $0621 \pm 1$  UT. Although the lower energy channels quickly reached their instrumental saturation level, the two higher energy channels did not. These channels indicated that the rates continually increased over a 200-s interval and then appeared to level off until the eclipse at 0632 UT. The pulse-height spectrum that was observed in the time interval 0623 to 0632 UT is shown in Figure VI.A-3. As can be seen, there is an increase in the energy continuum that extends above 3 MeV and two pronounced photopeaks at 0.5 and 2.2 MeV in the solar quadrant. The two peaks at 1.17 and 1.33 MeV are leakage peaks from the onboard Co<sup>60</sup> calibration source. The two peaks at 0.5 and 2.2 MeV have been interpreted as resulting from positron annihilation at 511 keV and neutron capture in hydrogen at 2.23 MeV. The time history of the counting rates in the two photopeaks are shown in Figure VI.A-4 where the 60- to 120-keV rate (X-ray Channel 4) is reproduced for comparison. Although the photopeak counting statistics in the individual 180-s scans are not sufficient to determine a detailed time history, it can be seen that the rates in the photopeaks follow the time history of the high-energy continuum quite closely.

The counting rate observed in association with the 3B H $\alpha$  flare that started at  $\sim$ 1517 UT on August 7, 1972, is shown in Figure VI.A-5. Also shown is the radio flux at 15,400 MHz (*Solar-Geophysical Data*, Report No. 342, February 1973). The OSO-7 spacecraft was in eclipse during the flash phase of the flare and no continuum X-rays with energies greater than 120 keV were observed after the spacecraft came out from eclipse at 1538 UT. However, evidence for line emission at 0.5 and 2.2 MeV was observed between 1538 and 1547 UT.

The time-averaged fluxes at these two energies observed on August 4 and 7 are given in Table VI.A-1. Also given are the fluxes observed at 4.4 and 6.1 MeV on August 4. These latter two lines have been interpreted as arising from C<sup>12\*</sup> and O<sup>16\*</sup>.

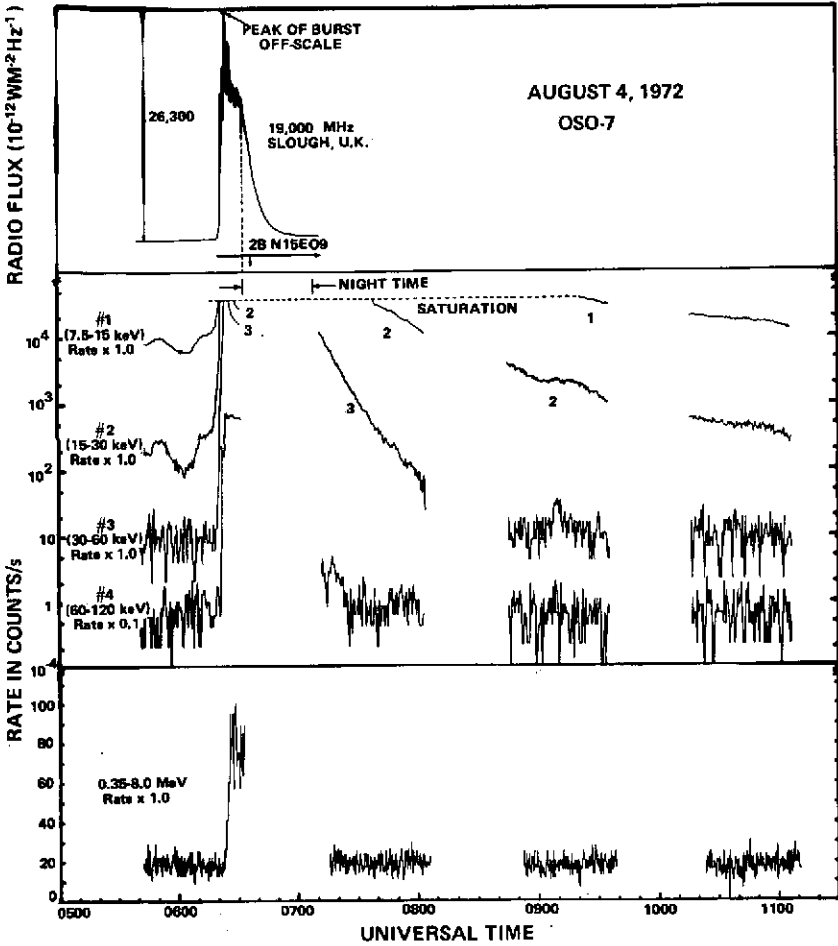


Figure VI.A-1. Counting rates and radio flux versus time for the flare on August 4, 1972.

**INTERPRETATION**

The  $\gamma$ -ray lines observed from the flare on August 4, namely, at 0.51, 2.23, 4.43, and 6.13 MeV (from positron annihilation, neutron capture on hydrogen, and excited states of  $C^{12}$  and  $O^{16}$ , respectively) have been predicted to be the most intense lines based on known cross sections, solar abundances, and assuming nuclear interaction of the energetic solar particles with the solar atmosphere (Lingenfelter and Ramaty, 1967). The ratio of the observed lines are those predicted to result from a spectrum of energetic solar particles

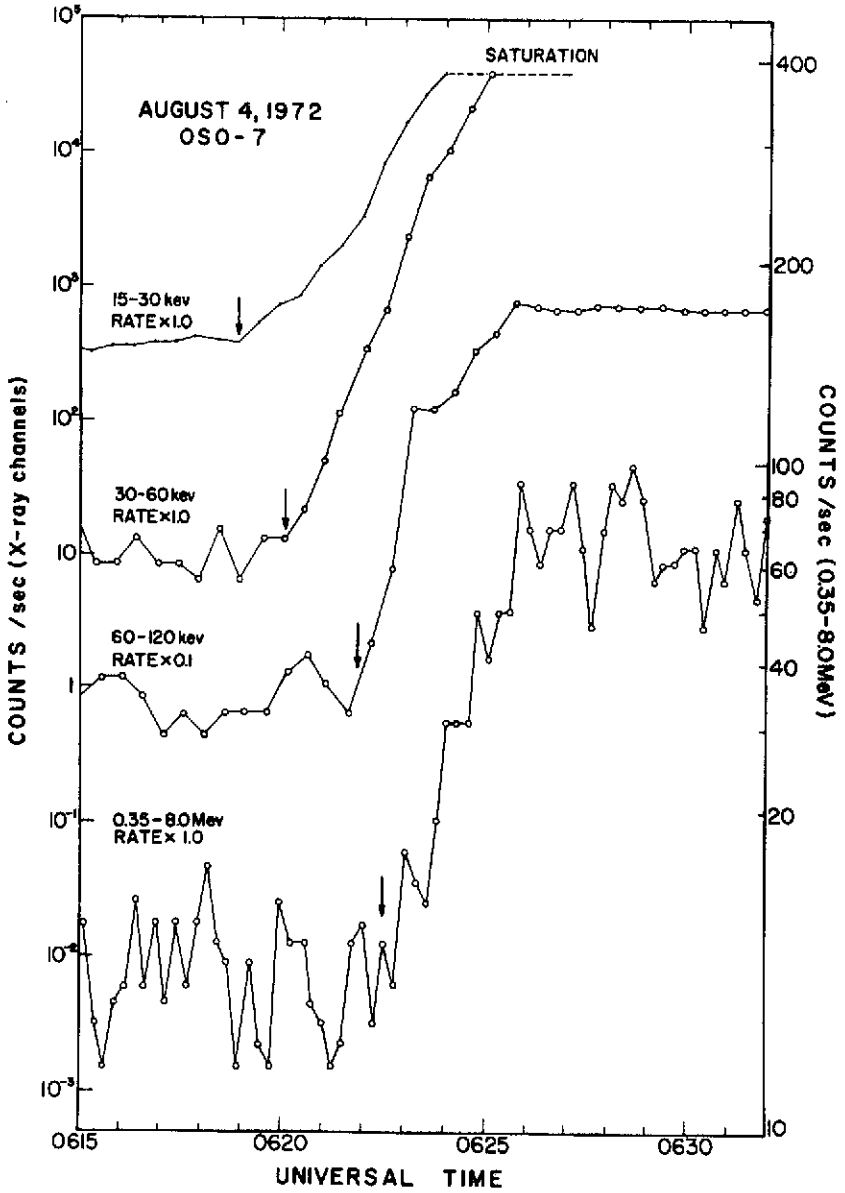


Figure VI.A-2. Counting rates on an expanded time scale for the flare on August 4, 1972.

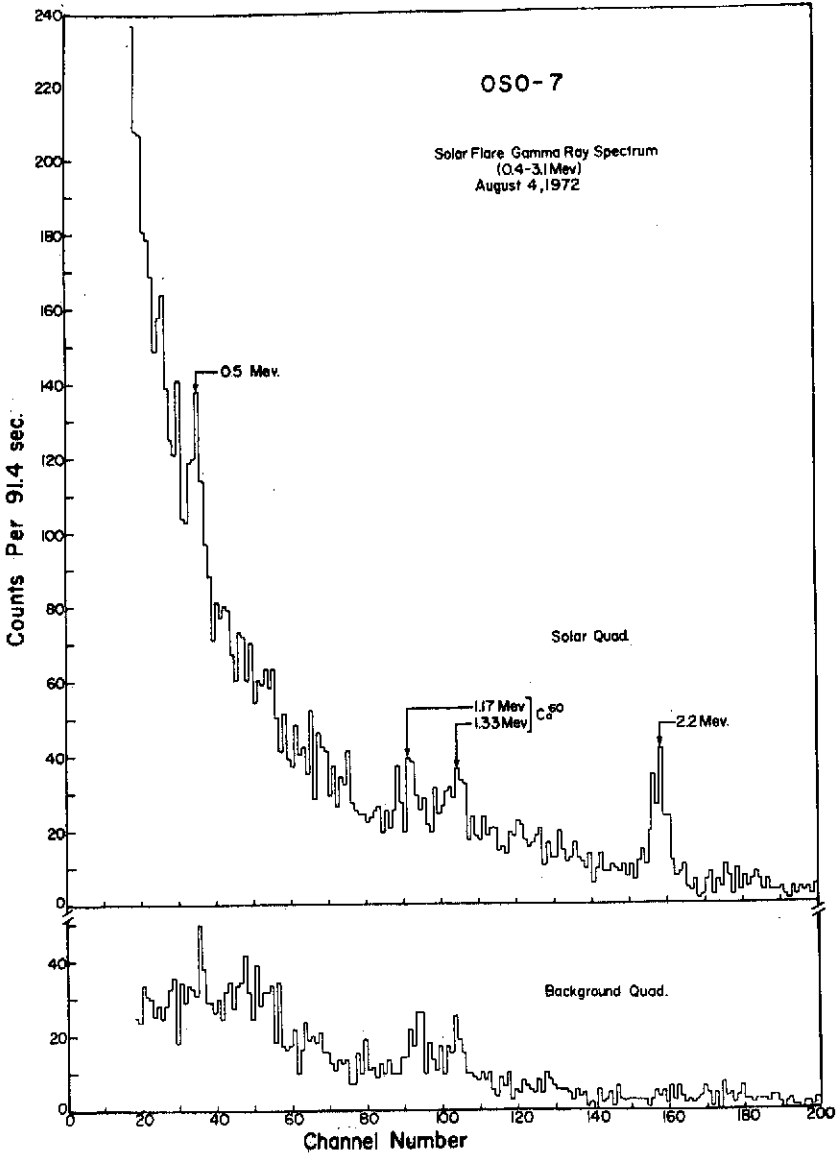


Figure VI.A-3. Pulse-height spectra recorded in the time interval 0623 - 0632 UT on August 4, 1972.

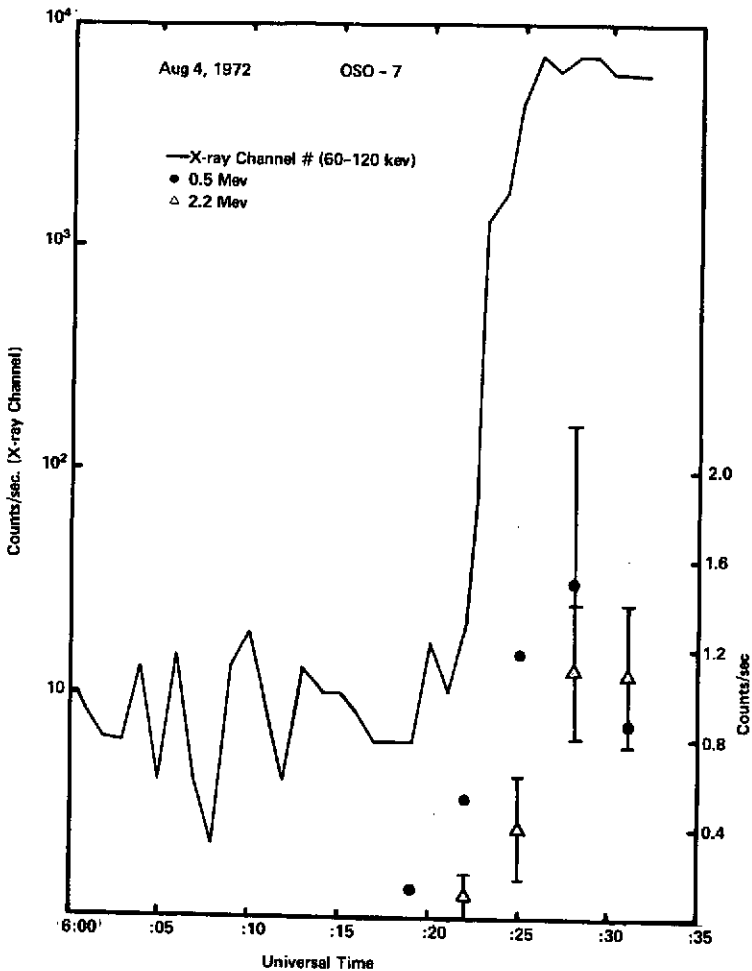


Figure VI.A-4. Time history of the photopeak counting rate on August 4, 1972.

of the form

$$N(>P) = N_0 \exp(-P/P_0)$$

where the characteristic rigidity  $P_0$  is in the range 60 to 80 MeV. The spectrum of energetic particles measured on satellite detectors near 1 AU between August 4 and 8 agree with this spectral shape (Ramaty and Lingenfelter, 1972). However, there is at least one reference to a ground level effect from this flare (Pomerantz and Duggal, 1973). If this is true, then at least a portion of the energetic solar particles must have had a much higher characteristic rigidity. The absolute intensity of the observed  $\gamma$ -ray line fluxes, however, is much lower

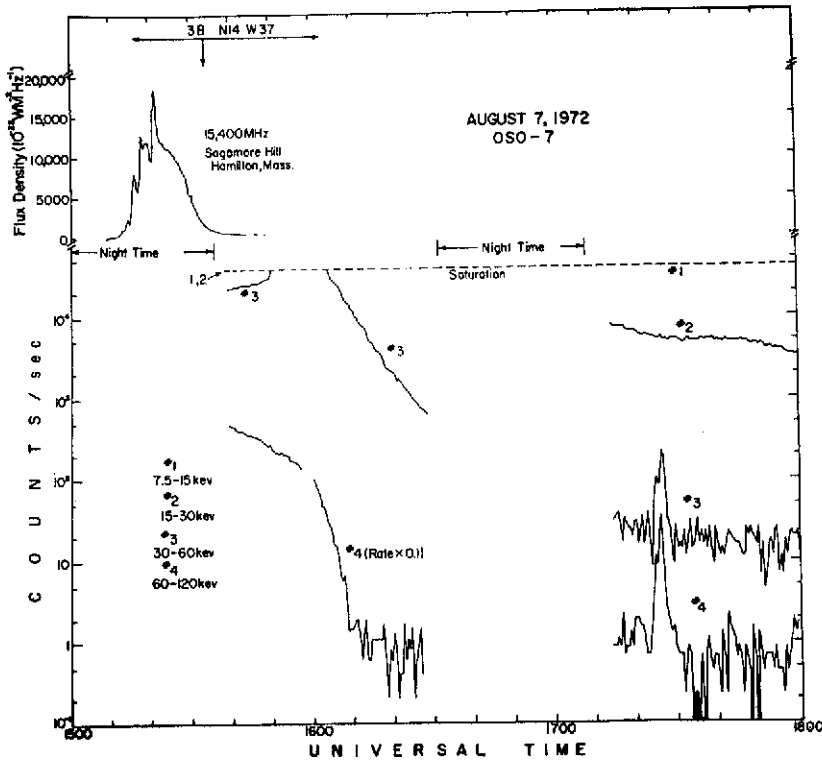


Figure VI.A-5. Counting rates and radio flux versus time for the flare on August 7, 1972.

(by a factor of  $10^2$  to  $10^3$ ) than was predicted from a flare of this magnitude. The intensity of the  $\gamma$ -rays is based mainly on the solar atmospheric density in the region where the particles interact and the number of energetic particles accelerated and released. In the past the only estimate of the total number of particles accelerated and released was based on measurements near 1 AU and model-dependent extrapolations back to the sun.

If the observed 200-s risetime of the very hard X-ray continuum is interpreted to be the time history of the rate of nuclear reactions producing the positrons and neutrons, then several other interesting results can be derived. First, unless the electrons and protons are accelerated and stored very high in the atmosphere and what we are seeing is the dumping of these particles into the denser lower atmosphere, then the time scale for converting some form of potential energy into the kinetic energy of relativistic particles is also 200 s. Second, a study of the risetime of the 2.2-MeV line flux indicates that the neutrons must have been captured in a region where the density

Table VI.A-1  
OSO-7 August 1972

Associated Flare and the Time of Observations	Designations and Solar Flux at 1 AU Photons $\text{cm}^{-2}\cdot\text{s}^{-1}$			
	0.5 MeV	2.2 MeV	4.4 MeV	6.1 MeV
3B ( $\text{H}\alpha$ ) Aug. 4, 1972 0624 - 0633 UT (Before $\text{H}\alpha$ Max)	$(7 \pm 1.5) \times 10^{-2}$	$(2.2 \pm 0.2) \times 10^{-1}$	$(3 \pm 1) \times 10^{-2}$	$(3 \pm 1) \times 10^{-2}$
3B ( $\text{H}\alpha$ ) Aug. 7, 1972 1538 - 1547 UT (After $\text{H}\alpha$ Max)	$(3.7 \pm 0.9) \times 10^{-2}$	$(4.8 \pm 1) \times 10^{-2}$	$< 2 \times 10^{-2}$	$< 2 \times 10^{-2}$

was  $\approx 2 \times 10^{17}$  protons/cm<sup>2</sup> (Reppin et al., 1973). That this region would be in the photosphere is expected since the neutrons, being uncharged, can easily escape from the region where they are produced to the higher density regions where they can be slowed down and captured. Also, the observed risetime of the 511-keV line cannot be more than 200 s. This fact, together with the known cross section for annihilation, implies that the density in the region where the positrons annihilate must be greater than  $2 \times 10^{11}$  electrons/cm<sup>3</sup>. A study of the line width of the 511-keV line observed on August 4 has led to an upper limit for the temperature in this same region of  $\approx 7 \times 10^6$  K (Dunphy et al., 1973). Because the positron is charged, it is reasonable to assume that the positrons are trapped in the region where they are produced, and that the above temperature is indeed an upper limit.

The observations of line emission on August 7, after the flash phase was over, were expected because of the  $\approx 200$ -s annihilation time for the positrons (some of the positrons are produced from radioactive isotopes with long half-lives) and the 100-s capture time for neutrons in the photosphere.

## CONCLUSION

The solar flare  $\gamma$ -ray observations reported here appear to be in general agreement with models and calculations proposed by Lingenfelter and Ramaty, 1967. Further study of these observations together with other observations of the same flare at other wavelengths and observations of particles should lead to a rather specific acceleration and interaction model for these flares. Of particular interest are the reported He<sup>3</sup> measurements (McDonald et al., 1973). He<sup>3</sup> in the intensities reported must have been produced in the same sort of nuclear reactions that produced the  $\gamma$ -rays.

(Supported by NASA Contract NAS 5-11054)

## REFERENCES

- Chupp, E. L., D. J. Forrest, and A. N. Suri, *Proceedings of Symposium on High-Energy Phenomena on the Sun*, Greenbelt, Maryland, September 28-30, 1972, R. Ramaty and R. G. Stone, eds., in press.
- Chupp, E. L., D. J. Forrest, P. R. Higbie, A. N. Suri, C. Tsai, and P. P. Dunphy, 1973, *Nature*, **241**, p. 33.
- Dunphy, P., E. L. Chupp, D. J. Forrest, and A. N. Suri, 1973, *Bull. American Phys. Soc.*, **18**, p. 695.
- Forrest, D. J., P. R. Higbie, L. E. Orwig, and E. L. Chupp, 1972, *Nucl. Inst. and Meth.*, **101**, p. 567.
- Higbie, P. R., E. L. Chupp, D. J. Forrest, and I. U. Gleske, 1972, *IEEE Trans. Nucl. Sci.* NS-19, No. 1, p. 606.

- Lincoln, J. Virginia, and Hope I. Leighton, 1972, World Data Center A, Report UAG-21; U. S. Department of Commerce, NOAA, Environmental Data Service, Ashville, North Carolina.
- Lingenfelter, R. E., and R. Ramaty, 1967, *High Energy Nuclear Reactions in Astrophysics*, B. S. P. Stern, ed., Benjamin, New York.
- McDonald, F. B., B. J. Teegarden, J. H. Trainor, W. R. Webber, and E. C. Roelof, 1973, *Bull. American Phys. Soc.*, 18, p. 697.
- Pomerantz, P., and S. P. Duggal, 1973, *Nature*, 241, p. 33.
- Ramaty, R., and R. E. Lingenfelter, *Proceedings of Symposium on High Energy Phenomena on the Sun*, Greenbelt, Maryland, September 28-30, 1972, R. Ramaty, ed., in press.
- Reppin, C., E. L. Chupp, D. J. Forrest, and A. N. Suri, 1973, *Proceedings 13th Int. Conf. on Cosmic Rays*, Denver, in press.

## A. ENERGY SPECTRA OF COSMIC GAMMA-RAY BURSTS<sup>\*,†</sup>

T. L. Cline and U. D. Desai  
*Goddard Space Flight Center*

R. W. Klebesadel and I. B. Strong  
*Los Alamos Scientific Laboratory*

### INTRODUCTION

The occurrence of intense, several-second duration bursts of 0.1- to 1.2-MeV cosmic  $\gamma$ -rays, recently found using multiple Vela satellites (Klebesadel et al., 1973), has been confirmed with measurements from the IMP-6 satellite. Observations regarding times of occurrence, photon flux, and temporal and spectral characteristics of the bursts are entirely consistent. In particular, since the IMP-6 instrument incorporates a hard X-ray detector with active particle rejection and full-time omnidirectional particle intensity monitoring, the results fully confirm and establish the hard X-ray or  $\gamma$ -ray nature of the incident flux.

Detailed differential energy spectra were obtained with the IMP-6 for six of the eight known events occurring during the March 1971 to September 1972 lifetime of the instrument. All of these are multiple-pulse events, with several seconds separation between distinct pulses of one or two seconds duration. The pulse spectra do not obey single-index power laws in energy, but can be simply represented by exponentials in photon flux throughout the 100- to 1200-keV region. The characteristic energies at maximum intensity appear to cluster near 150 keV, with indications that departures from this value can be interpreted as circumstantial, due to attenuation when the source is at great angles from the detector axis. These burst pulses appear to ride on a softer component that exhibits a longer decay-time constant, and has a characteristic exponent near 75 keV. There is no evidence for monoenergetic line structure in the several hundred-keV region, or for marked changes in the spectrum with time during a single pulse. Size spectra can be estimated

---

\*Post-Symposium observational paper, see Introduction.

†Published in *Astrophysical Journal Letters*, October 1, 1973.

to predict the frequencies of occurrence of smaller events for both a galactic model (for example, a new class of  $\gamma$ -ray flare star) and an extra-galactic model (for example, supernovae). In either case, the total emission is below the value currently obtained for the diffuse celestial X-ray background and is unlikely to account for any of its spectral features.

### INSTRUMENTATION

The IMP-6 satellite was launched on March 14, 1971, into an elliptic orbit with an initial apogee of over 200,000 km. Gamma-ray monitoring was provided on a nearly continuous basis, except for passes every 4.14 days through the magnetosphere, lasting several hours each. The detector was in operation from launch until May 2, 1971, and again for the period from June 9, 1971, to September 27, 1972. The instrument used consisted of a 6-cm (2.25-in.) diameter by 3-cm (1.5-in.) thick CsI(Tl) crystal, entirely surrounded by a thin plastic scintillator for particle rejection, viewed by a single PM tube. In addition to full-time monitoring of the rates of total intensity, particle intensity and  $\gamma$ -ray intensity, and energy spectra of incident  $\gamma$ -rays were measured by a 14-channel analyzer with simultaneous storage in all channels. The spectra were accumulated for one half of the time, for each  $\approx 6.3$ -s period from sun rise to sunset on the detector, determined by the optical aspect. This 50-percent duty cycle resulted in missing several of the very brief  $\gamma$ -ray bursts. The spectral accumulation times were fixed at  $\approx 5.1$  s so that the  $\approx 6.3$ -s lifetimes were asynchronously split into 2 or 3 intervals of shorter durations, making possible more than one spectral determination during some of the pulses. The gain of the system was cycled through four positions with changes at  $\approx 1$ -week intervals for purposes of in-flight calibration, so that some of the bursts happened to be observed with a 69- to 1150-keV dynamic range and some with a 53- to 880-keV range. The primary purpose of this  $\gamma$ -ray detector was used as a coincident annihilation spectrometer incorporated in a positron detector. The secondary objective was that of a solar-flare monitor, and it was in this mode of operation that these unexpected  $\gamma$ -ray bursts were observed.

### DATA OBSERVATION AND ANALYSIS

The times of occurrence of  $\gamma$ -ray bursts observed with multiple Vela satellite coincidences were used to identify coincident increases in the IMP-6  $\gamma$ -ray intensity. Six of the eight Vela events were observed well above the omnidirectional background, the others being missed because of the 50-percent detector duty cycle. It is possible that other events, of intensity too low to exceed the Vela threshold triggers, may also be observable with the IMP-6 instrument. Figure VII.A-1 shows the response of the IMP  $\gamma$ -ray detector to the event of June 30, 1971. During a several-second interval, the counts in

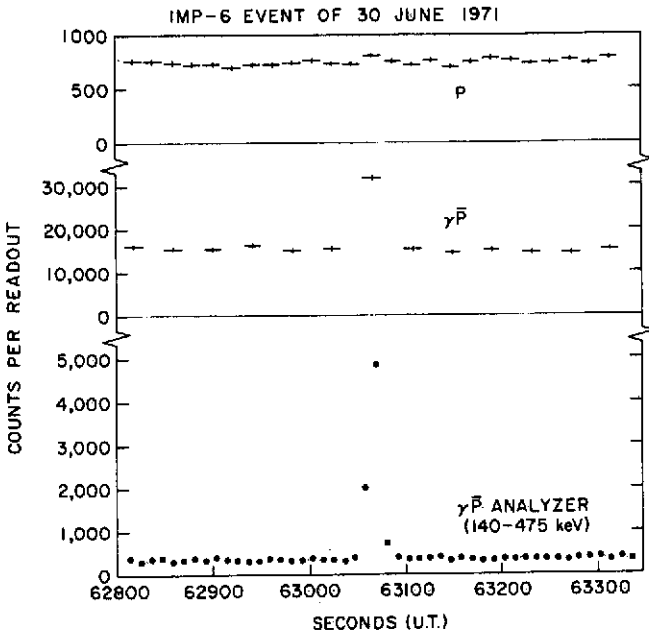


Figure VII.A-1. The response of the detector to a  $\gamma$ -ray burst, as indicated by the plastic anticoincidence (P), the CsI  $\gamma$ -ray detector ( $\gamma P$ ), and several channels added to give the 140- to 475-keV photon rate, where the  $\gamma$ -ray energy response is maximized. Each point samples two differential energy spectra.

the plastic scintillator (P) surrounding the  $\gamma$ -ray crystal increased by about 50, while the neutral counts in the crystal ( $\gamma P$ ) simultaneously increased by about 18,000. Pulses satisfying the  $\gamma$ -ray logic were fed to a multichannel analyzer, from which the outputs of three channels, added to provide the flux of 140- to 475-keV photons, indicated an increase during one  $\approx 5$ -s interval of nearly 5000 counts from a total omnidirectional and secondary background of about 400 counts. This illustrates the remarkable intensity of the bursts and shows that the response is entirely consistent with that of hard X-rays or  $\gamma$ -rays.

The times of occurrence and various properties of all Vela/IMP events observed during the IMP-6 experiment lifetime are listed in Table VII.A-1. The temporal structures of the observed bursts, known from the Vela results, were compared in order to determine over which intervals in the event structures the IMP spectra were obtained. Since the IMP-6 satellite was spinning,

Table VII.A-1.

Characteristics of  $\gamma$ -ray Burst Spectra  
 (Exponential fits in  $dn/dE$  provide  $I_0$  in units of  
 photons  $\text{cm}^{-2} \cdot \text{keV}^{-1}$ , and  $E_0$  in units of keV, both of which  
 have systematic uncertainties depending on relative look angle.)

Event	Burst	$I_0$	$E_0$	Look Angle
Mar. 15, 1971	2nd Max	1.9	156	Includes source ( $\alpha \approx 50^\circ$ , $\delta = -30 \pm 10^\circ$ )
Mar. 18, 1971	Decay of 1st	1.8	74	Spins through source
Jun. 30, 1971	1st Max	0.7	276	Source below satellite horizon
Jun. 30, 1971	2nd Max	5.5	142	Spins through source
Jun. 30, 1971	Decay of 2nd	0.7	110	Spins through source
Jan. 17, 1972	Decay of 1st	0.10	138	Source position undeter- mined
Jan. 17, 1972	2nd Max	0.35	184	Source position undeter- mined
Jan. 17, 1972	Decay	0.11	170	Source position undeter- mined
Mar. 28, 1971	1st Max	0.50	128	Source near or below horizon
Mar. 28, 1972	2nd Max	0.55	176	Source position undeter- mined
May 14, 1972	1st Max	0.8	166	Includes source ( $\alpha \approx 175^\circ$ , $\delta \approx +77^\circ$ )
May 14, 1972	2nd Max	0.8	152	Includes source

an analysis was also made for each burst to determine in which direction the detector was facing, relative to the source, at the moment each spectrum was obtained. Each of the six events was observed by the Velas to have at least two distinct pulses of up to a few seconds duration, separated by intervals of several seconds. The time resolution of the IMP  $\gamma$ -ray detector ( $\approx 2.5$  s)

permitted obtaining individual spectra for many maximum-intensity pulses and, for some cases, two separate spectra of a given several-second pulse. (Vela data show that a given maximum-intensity pulse can contain a variety of fast-time variations (Klebesadel et al., 1973); these are necessarily averaged over in the IMP spectra.) Figure VII.A-2a shows photon-number spectra,  $dn/dE$ , for several of the bursts, as sampled on a 6.3-s half-spin basis. It indicates that, in this energy region, relatively good fits to these raw data are obtained to exponentials of the form  $dn/dE = I_0 \exp(-E/E_0)$  photons  $\text{cm}^{-2} \text{keV}^{-1} \text{burst}^{-1}$ . The  $I_0$  and  $E_0$  values are listed in the table, along with the relative look direction accuracies. The directions of origin of the six events are known with widely varying accuracy; but, in the case of the June 30 event, it is known that the first spectrum was recorded when the source was below the satellite horizon of the detector. Thus, the harder (250-keV) spectrum may be accounted for by attenuation of the lower energy photons in the metal surface of the satellite. If that is also the case of the March 28, 1972, event, then all the pulses are consistent with 150-keV spectra. Two of the six events (March 15, 1971, and May 14, 1972) have unambiguously known source directions that are not far from the center of the field of view, and these are definitely 150-keV spectra. In addition, the March 18, 1971, event and a number of decays of the other events, not listed, are consistent with softer spectra, suggesting that a slower-time constant soft component is present in addition to the 150-keV peaks. Figure VII.A-2b (insert) shows the energy spectrum, or power spectrum averaged over the pulse burst duration,  $Edn/dE$ , of an event for which the source direction was known to be in the view direction. It is seen that the energy output is a maximum in this region. This may indicate that the photons released from the source objects are essentially  $\gamma$ -ray in nature, not composing X-ray distributions with spectral tails in the  $\gamma$ -ray region. If much softer X-rays are emitted in the primary burst, they most likely undergo relatively greater absorption near their region of origin.

## DISCUSSION

It is clear that the observed  $\gamma$ -ray bursts represent an entirely novel form of cosmic energy release. The durations of the individual pulses are typically 1 to a few seconds, and the separations between pulses in a given burst are up to 20-odd seconds. The temporal structure might therefore be compared to that of solar flares, but with time scales one to two orders of magnitude shorter, suggesting a conceivable source origin of  $\gamma$ -ray flare stars (see also

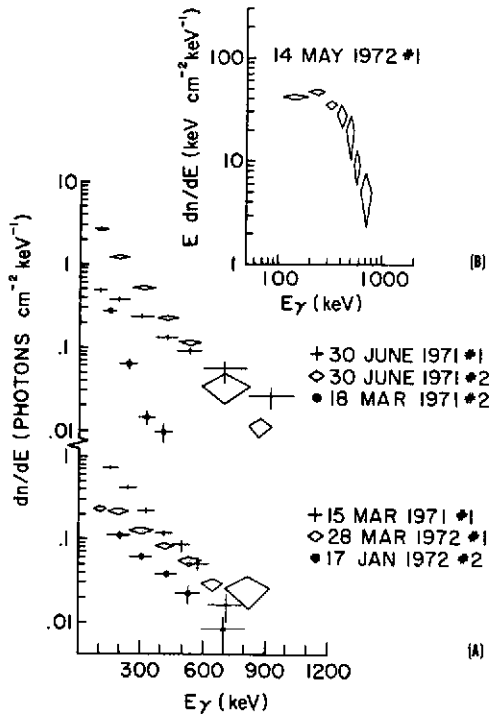


Figure VII.A-2. (a) Number spectra  $dn/dE$ , of several bursts, selected for the greatest variety of responses. The harder spectra are interpreted as due to attenuation of the incident beam by the satellite material in cases where the source was below the detector horizon. (b) The energy spectrum,  $E dn/dE$ , of a directly observed event is shown in the insert.

Stecker and Frost, Chapter XIII.A). The 150-keV energy spectra, including the one known case of the May 14, 1972, event which has a power law from 10 to 100 keV (Wheaton et al., preprint), contain too much emission in the X-ray region to fit  $\approx 150$  keV blackbody spectra. However, the spectra contain too little emission in the lower energies to be compared to the typical, steep X-ray spectra, having index of  $\approx -3$  or more, of most hard solar flares and many celestial X-ray sources. For those pulses which were observed with sufficient temporal resolution to obtain more than one spectrum per pulse, there is no evidence for changes in the characteristic energy during its extent (not illustrated). Further, there is no evidence for line structure in this energy region. It is possible, however, that great improvements

in energy and time resolution might show fine-scale spectral variability with a variety of monochromatic lines, which average out over 2-s summations.

An integral size spectrum can be constructed, assuming a power law with index  $-1.5$ , normalized to 6 or 8 events per 1.5 years with sizes greater than  $10^4 \text{ erg} \cdot \text{cm}^{-2}$  for the energy region above 100 keV. Since the 18 known events have source directions compatible with isotropy (Strong and Klebesadel, preprint) rather than with, for example, galactic plane clustering, the source objects must either have distances in the tens to hundreds of pc if galactic, or have distances of greater than several Mpc if extragalactic in nature. Thus, this size spectrum can be normalized for these two models in order to obtain predictions of the frequencies of occurrence of smaller events. In the case of extragalactic sources, for example,  $\gamma$ -ray rich and optically poor supernovae or other large collapsing objects, a summation of all emissions up to cosmological distances produces a total isotropic background intensity which is below the presently observed diffuse cosmic background in this energy interval. Thus, an extragalactic origin cannot be ruled out. Further, if all sources have spectra with  $\approx 150\text{-keV}$  exponentials, then the total cosmic spectrum will not extend into the several-MeV region with sufficient intensity to explain the bump in the diffuse cosmic background observed (Trombka et al., 1973) at those energies.

## REFERENCES

- Klebesadel, R. W., I. B. Strong, and R. A. Olson, 1973, *Astrophys. J. Letters*, **182**, p. L85.
- Trombka, J. I., A. E. Metzger, J. R. Arnold, J. L. Matteson, R. C. Reedy, and L. E. Peterson, 1973, *Astrophys. J.*, **181**, p. 737.

**SECTION 2**  
**THEORY**

**PRECEDING PAGE BLANK NOT FILMED**

## A. THE ASTROPHYSICS OF THE DIFFUSE BACKGROUND OF X-RAYS AND GAMMA RAYS

Ramanath Cowsik\*  
*University of California*

### INTRODUCTION

Studies in the field of X-ray and  $\gamma$ -ray astronomy have given rise to new insights into the structure and composition of our galaxy, the intergalactic space, and the universe itself. Since there have been many comprehensive reviews (Silk, 1970, and preprint; Felten, 1972) on the subject, we will describe here only our views on the origin of the diffuse X-ray and  $\gamma$ -ray background and some of the astrophysical implications of such a radiation background. In the same spirit, detailed references to all existing literature is not made, and one can refer to the comprehensive reviews for this purpose.

The range of energies that is of interest here extends from  $\sim 10^2$  eV to  $\sim 10^8$  eV, over six decades, and a variety of processes contribute to the generation of a diffuse background. In order to make statements about the distribution of the sources of the radiation background, we appeal primarily to the angular distributions of the radiations about us. Considerations based on plausibility of models of origin and on minimizing the energy requirements in the sources supplement the classification of the sources either as galactic or extragalactic. Our views on the origin of the various components are summarized in Table VIII.A-1.

Finally, in the section on the 100-MeV  $\gamma$ -ray flux, it is shown that the measured  $\gamma$ -ray fluxes at  $\sim 100$  MeV from the galactic disk place a rather stringent upper limit on the energy density of any background at submillimeter wavelengths.

---

\*Speaker.

Table VIII.A-1  
Origin of the Diffuse X-Ray and  $\gamma$ -Ray Background

Energy Range	Process	Source Region	Discussed In Section:
~250 eV - 2 keV	Thermal bremsstrahlung	Our galaxy and the external galaxies	Diffuse X-Ray
	Compton scattering of the 2.7 K photons	Intergalactic space	
~2 keV - 200 keV	Thermal bremsstrahlung	Intergalactic space	The 2 - 200 keV
~0.2 MeV - 10 MeV	Compton scattering of $\sim 10^4$ K photons	Cosmic ray sources in the galaxy	0.3 - 3 MeV $\gamma$ -rays
$\geq 100$ MeV	Compton scattering of starlight	Central regions of galaxy (extended source at the galactic center)	Gamma-rays in 100-MeV Range
	$\pi^0 \rightarrow 2\gamma$	Galactic disk (line source)	
	$\pi^0 \rightarrow 2\gamma ?$	Galactic halo? (isotropic background)	

### SOME IMPORTANT MECHANISMS FOR GENERATION OF X-RAYS AND $\gamma$ -RAYS

#### Thermal Bremsstrahlung

A high temperature plasma emits X-rays mainly through free-free transitions. Here the electrons that have a thermal energy distribution emit bremsstrahlung photons in the field of the ions. This process is weakly dependent on the exact

chemical composition of the plasma and the rate of X-ray emission by an optically thin plasma is given by (Hayakawa, 1969)

$$\begin{aligned}
 p_{\text{ff}}(E_x) &= \frac{1}{6\pi^3} \frac{e^2}{hc} \sigma_{\text{th}} n_e \left( \frac{mc^2}{kT} \right)^{1/2} \left[ \sum Z n_z g_{\text{ff}}(Z, T, E_x) \right] \\
 &\quad \times \frac{1}{E_x} \exp(-E_x/kT) \qquad \qquad \qquad \text{(VIII.A-1)} \\
 &= 0.81 \times 10^{-12} n_e^2 T^{-1/2} g_{\text{eff}} \times \frac{1}{E_x} \exp(-E_x/kT)
 \end{aligned}$$

For a plasma of solar composition the effective Gaunt factor ( $g_{\text{eff}}$ ) is approximately equal to unity. Equation (VIII.A-1) integrates easily to yield a cooling time

$$\tau \approx 1.96 \times 10^{11} T^{1/2} / n_e \text{ s} \qquad \qquad \qquad \text{(VIII.A-2)}$$

In galaxies, clouds of hot plasma can be created continuously, for example by supernova explosions. These will cool continuously emitting radiation. Then, at any time there will be an equilibrium distribution temperature of these clouds extending up to  $T_{\text{max}}$ , the maximum temperature of generation of these clouds. If all clouds are created at  $T_{\text{max}}$  and they cool mainly through the free-free process, then the integrated emission of all the clouds can be approximated by

$$p(E_x) \sim \frac{1}{E_x^2} \exp(-E_x/kT_{\text{max}}) \qquad \qquad \qquad \text{(VIII.A-3)}$$

Notice that this is steeper than the single temperature case by a factor  $\frac{1}{E_x}$ , indicating that there is less emission at high energies.

Besides free-free emission there would be free-bound and bound-bound transitions which will lead to sharp edges and lines in the emitted spectrum depending on the elemental abundances in the plasma.

**Decay of Neutral Pions**

Neutral pions are produced in the interaction of nuclear cosmic rays with ambient matter, and these pions decay almost instantaneously to two  $\gamma$ -rays. This subject has been studied extensively by Stecker (1971) and in Figure VIII.A-1 we show the spectrum of  $\gamma$ -rays generated through this process. It is very flat in the region of  $\sim 70$  MeV and has a spectral slope identical to the cosmic-ray beam at high energies.

### Compton Scattering of Thermal Photons

The importance of this process under astrophysical conditions has been made clear by the work of Morrison and his coworkers (see for example Brecher and Morrison, 1969). In this process a highly relativistic electron scatters a low-energy thermal photon into the X-ray energy region. Cowsik and Kobetich (1971; 1972) have made a detailed calculation of this process; this calculation is briefly outlined below.

Under most astrophysical conditions the spectral distribution of background low-energy photons can be taken to be the Planck function

$$K(\epsilon) = \frac{8\pi}{h^3 c^3} \frac{\epsilon^2}{\exp(\epsilon/kT) - 1} \quad (\text{VIII.A-4})$$

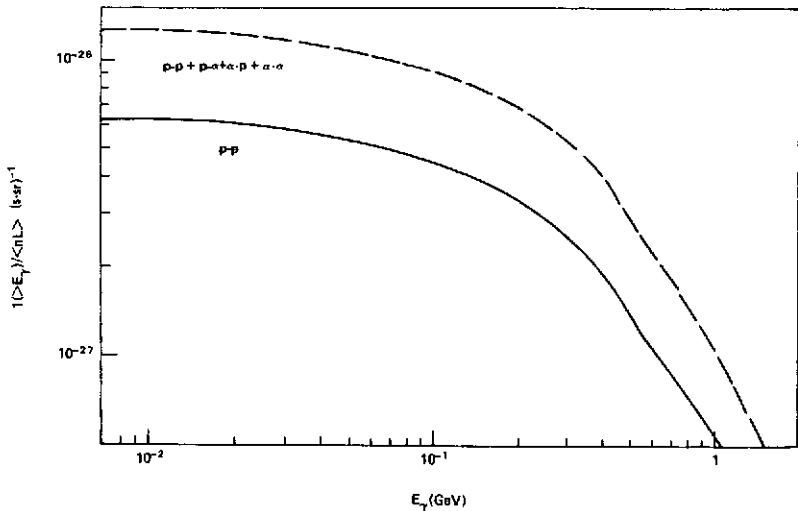


Figure VIII.A-1. The integral spectrum of  $\gamma$ -rays generated by cosmic-ray interactions with interstellar matter. Nuclei heavier than helium do not contribute significantly (Stecker, 1970).

The angular distribution of these photons is isotropic, that is

$$\frac{dn}{d \cos \theta} = \text{constant} \tag{VIII.A-5}$$

The exact expression for the differential Compton-scattering cross-section is quite involved. However, simplification occurs because the mean energy of the X-ray generated by this process is usually much smaller than the energy of the electron involved in the scattering. Accordingly, the differential scattering cross-section for the emission of an X-ray photon of energy  $E_x$  in a collision of an electron of energy  $\epsilon$  with a photon of energy  $\epsilon$  integrated over the angular distribution of the incoming and outgoing photons becomes (Hayakawa, 1969)

$$\begin{aligned} \sigma_c(E, \epsilon, E_x) = & \frac{\pi r_e^2}{4} \frac{(mc^2)^4}{E^3 \epsilon^2} \frac{E_x}{E} - \frac{(mc^2)^2}{E^3 \epsilon} \frac{E_x^2}{E} + \\ & \frac{4E_x}{E} \ln \frac{(mc^2)^2 E_x}{4E^2 \epsilon} + \frac{8E\epsilon}{(mc^2)^2} \end{aligned} \tag{VIII.A-6}$$

On making the substitutions

$$B = (mc^2)^2, D = \pi r_e^2/4 \text{ and } x = \frac{BE_x}{4E^2 \epsilon} \tag{VIII.A-7}$$

this reduces to (Blumenthal and Gould, 1970)

$$\sigma_c = \frac{8DB}{E^2 \epsilon} (1 + x - 2x^2 + 2x \ln x) \tag{VIII.A-8}$$

Consider now a delta-function spectrum of electrons,  $\delta(E-E_0)$ , generating X-rays by Compton scattering against a thermal photon field (Equation VIII.A-4).

This X-ray spectrum is shown in Figure VIII.A-2. In view of the fact that the universal thermal background of microwave photons is the most relevant to the discussion of the isotropic component of the X-ray background, the plot in Figure VIII.A-2 corresponds to  $T = 2.7$  K. The spectral shape for any other temperature is obtained by simply sliding the same curve by a factor  $T/2.7^\circ$  along the X-axis on a log-log graph.

The most important feature that is to be noticed in this figure is that the emission by electrons of single energy is over a very wide bandwidth, extending over a factor of 20 in X-ray energies, at half-maximum. Because of this large bandwidth, any kink or peak or other spectral feature in the electrons is smeared out over an extremely broad energy region of the X-ray spectrum. Apart from the broad bandwidth, the mean energy of the X-ray depends quadratically on the electron energy. This relationship further contributes to the smoothing of the X-ray spectrum relative to the electron spectrum.

The Compton scattering of 2.7 K photons in the intergalactic space by cosmic-ray electrons leaking from galaxies could lead to an important contribution to the X-ray background (Brecher and Morrison, 1969). In view of this, we

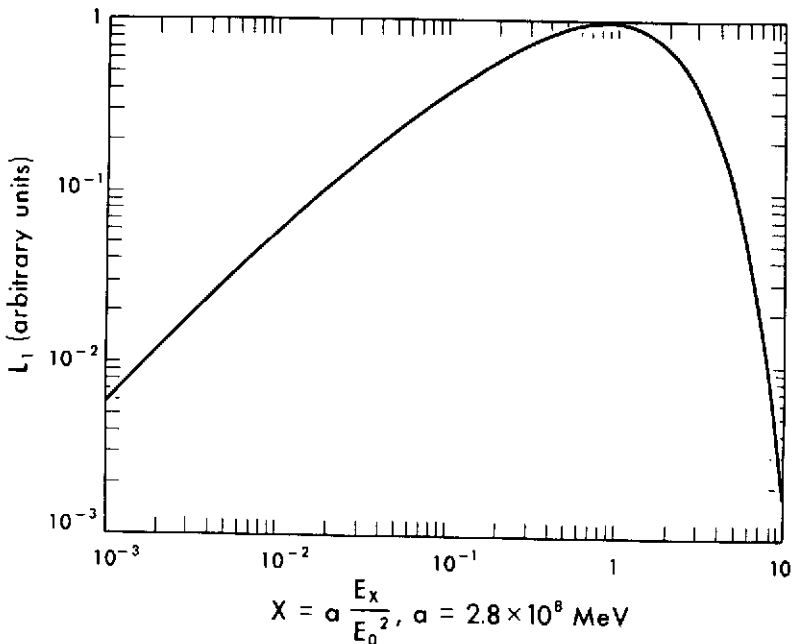


Figure VIII.A-2. The X-ray flux emitted in collisions of electrons of energy  $E_0$  with the 2.7 K photon field is plotted as a function of X-ray energy. Notice that the full width at half maximum is a factor of  $\sim 20$  wide; also, the mean X-ray energies related quadratically with the electron energy. These effects tend to yield an X-ray spectrum that is very much smoother than the electron spectrum. This fact was used to show that Compton scattering of the 2.7 K photons is not a significant source at  $\sim 30$  keV (Cowsik and Kobetich, 1972).

calculated the spectral shape of the electrons in the intergalactic space using the radio data of Lang and Terzian (1969). The expected X-ray spectrum is shown in Figure VIII.A-3 marked as  $L_{ig}$ . The normalization of this curve is arbitrary.

### DIFFUSE X-RAY FLUX BELOW A FEW keV

Since the early observations by Bowyer et al. (1968), there has been a substantial progress in our understanding of the diffuse flux at  $\sim 250$  eV. The observations and related theoretical considerations are reviewed comprehensively by Silk (preprint).

The comparison of the Compton X-ray flux from the intergalactic space ( $L_{ig}$  in Figure VIII.A-3) with the observed data indicates that this process may contribute significantly to the background below a few keV. However, since the normalization of this curve is somewhat arbitrary it is reasonable to expect that only a part of the observed flux indeed arises through this process. In view of the fact that our galaxy emits significantly in this bandwidth one may expect that the diffuse background is generated as a superposition of emission of all the galaxies in the universe. This suggestion was first made perhaps by Silk (1970) and has had much experimental confirmation due to the observation of several extragalactic sources using the Uhuru satellite (Gursky et al., preprint, Giacconi et al., preprint). We show in Table VIII.A-2 (taken from a preprint of Silk) the contribution of various types of extragalactic objects to the X-ray background at  $\sim 2$  keV.

Summing up the last column of the table shows that the sources contribute significantly at  $\sim 2$  keV. What is the spectrum of emission to be expected? If we try to fit a thermal bremsstrahlung spectrum to individual sources, the maximum temperature that is encountered in these extragalactic sources is  $\sim 2 \times 10^7$  K. Following our discussion concerning Equation (VIII.A-2) the cooling time of a plasma at this temperature is

$$\tau \approx \frac{1.96 \times 10^{11} (2 \times 10^7)^{1/2}}{n_e} \approx 10^{15} \text{ s} \approx 3 \times 10^7 \text{ yr}$$

taking  $n_e \approx 1$ . This cooling time is much smaller than  $1/H_0$  so that there would be a broad temperature distribution in the temperature of the plasma leading to a spectral shape as given by Equation (VIII.A-3). Viz

$$p(E_x) \sim \frac{1}{E_x^2} \exp(-E_x/kT_{\max})$$

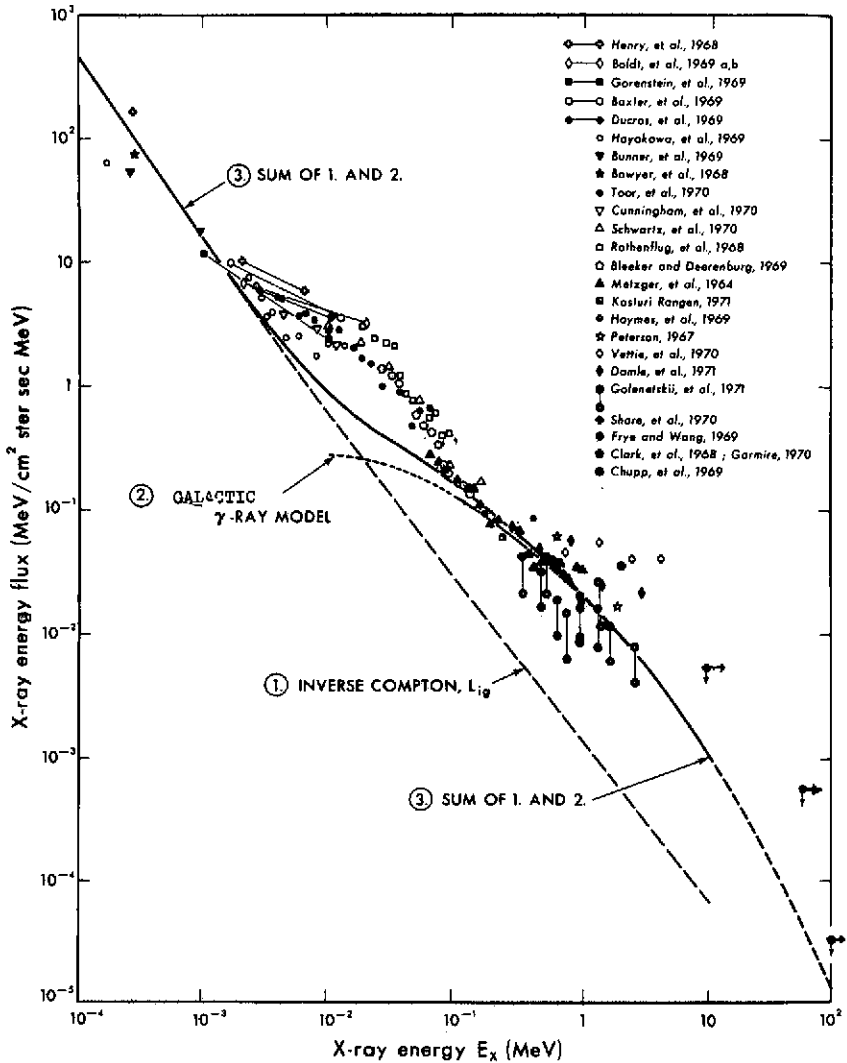


Figure VIII.A-3. The X-ray energy flux is plotted as a function of X-ray energy and compared with experimental data. Curve 1 is our calculation of the inverse Compton scattering; curve 2 is calculated using the galactic  $\gamma$ -ray model of Cowsik (1971); and curve 3 is the sum of the two contributions. The experimental data for X-ray energies  $E_x < 0.17$  MeV and  $E_x \geq 10$  MeV were taken from the review paper by Silk (1970) and for  $0.17$  MeV  $< E_x < 10$  MeV were taken from Damle et al. (1971), and Golenetskii et al. (1971). The enhanced emission at  $2$  keV  $< E_x < 200$  keV is attributed to a hot ( $3 \times 10^8$  K) intergalactic gas.

Table VIII.A-2  
 Contribution of Identified Extragalactic Sources to the  
 Isotropic X-Ray Background\*

Class	Source	$L_x(2-10 \text{ keV})_s^{\text{erg}}$	Local space density n ( $N=0.03 \text{ Mpc}^{-3}$ )	Flux $\frac{c}{4\pi H_0} \text{ nL}$ ( $\text{keV}/\text{cm}^2 \cdot \text{s}\cdot\text{sr}$ )
Small galaxies	LCM	$4 \times 10^{38}$		
	SMC Adopted mean	$1 \times 10^{38}$ $2 \times 10^{38}$	10 N	1.9
Normal galaxies	M31	$3 \times 10^{39}$		
	Our galaxy § Adopted mean	$5 \times 10^{39}$ $4 \times 10^{39}$	N	3.8
Radio galaxy	Cen A	$8 \times 10^{41}$	$10^{-3} \text{ N}$	0.74
Seyfert galaxy	NGC 4151	$2 \times 10^{41}$	$0.02 \text{ N}$	3.8
Abell I clusters† ‡	Centaurus	$4 \times 10^{43}$		
	Virgo Adopted mean	$1.5 \times 10^{43}$ $3 \times 10^{43}$	$2 \times 10^{-5} \text{ N}$	0.57
Abell II clusters†	Coma	$5 \times 10^{44}$		
	Perseus	$1 \times 10^{45}$		
	Abell 2256	$1 \times 10^{45}$		
	Adopted mean	$8 \times 10^{44}$	$5 \times 10^{-6} \text{ N}$	3.8
Quasar	3C273	$7 \times 10^{45}$	$3 \times 10^{-8} \text{ N}$	0.18

\*Data are taken from the Uhuru catalogue (Giacconi et al., 1972);  $H_0$  is set equal to  $50 \text{ km}\cdot\text{s}^{-1} \text{ Mpc}^{-1}$ .

†Only those sources identified with clusters and known to be extended are included.

‡The Centaurus and Virgo clusters are not in Abell's 1958 catalogue; however, they approximately correspond to Abell's richness class I.

§Estimated X-ray luminosity of our galaxy (Seward et al., 1972).

with  $T_{\text{max}} \approx 2 \times 10^7$  K. This spectral shape fits excellently the results below a few keV. Therefore, we conclude that free-free emission from the various extragalactic sources would contribute significantly to the X-ray background below few keV. However, the spectral shape is too steep to contribute significantly at higher energies.

### THE 2 TO 200 keV REGION AND POSSIBLE THERMAL BREMS-STRAHLUNG OF THE INTERGALACTIC GAS

Investigating the possible origin of the X-rays in this energy band we noticed (Cowsik, 1971) that thermal bremsstrahlung of a tenuous plasma at a temperature of  $3 \times 10^8$  K had the right spectral form to fit the observations. An emission measure,  $\int n_e^2 d\ell \approx 1.3 \times 10^{17}/\text{cm}^5$ , was required to give the observed intensities. Assuming no clumping (that is,  $n_e$  independent of  $\ell$ ) and taking

$$\int d\ell = \frac{2c}{3H_0} \approx 10^{28} \text{ cm}$$

one gets

$$n_e \approx 3 \times 10^{-6} \text{ cm}^{-3} \approx m_{\text{crit}} \approx \frac{3H_0}{8\pi G m_H}$$

for  $H_0 = 50$  km/s-Mpc. Therefore we suggested the possibility of a hot intergalactic plasma as a possible source of this background (Cowsik, 1971; Cowsik and Kobetich; 1972). The thermal bremsstrahlung fit to the experimental data after plausible subtractions of other emission mechanisms below 2 keV (see previous section) and above 200 keV (see following section) is shown in Figure VIII.A-4.

That a hot intergalactic medium could be the source in this region has been independently pointed out by Field (1972). Of course, the idea of a hot intergalactic medium is not new. It has been discussed in the context of continuous creation of matter in the form of neutrons in the steady-state cosmology by Gold and Hoyle (1959) and by Gould and Burbidge (1963). However, Petrosian and Ramaty (1972) have provided arguments based on excessive production of hard X-rays through the radiative decay of the neutron that continuous creation of matter as neutrons is forbidden by X-ray observations. The X-ray spectral observations in the region of 2 to 20 keV yield merely the temperature and emission measure of the radiating plasma. Therefore, the question arises as to whether the emission indeed comes from a hot intergalactic medium or from hot gas in various galaxies.

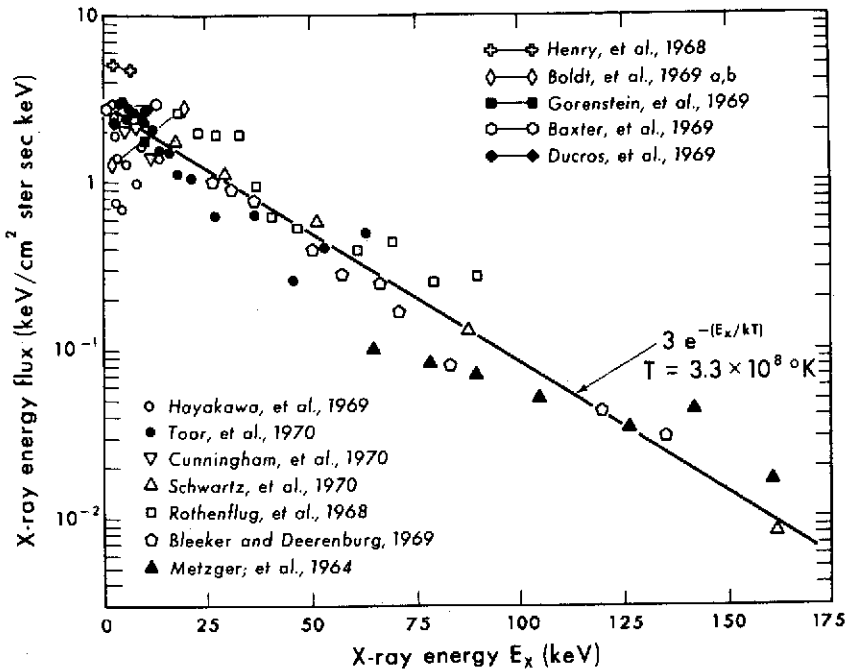


Figure VIII.A-4. The difference between the observed energy flux and the calculated flux (see Figure VIII.A-3) in the energy interval  $2 \text{ keV} < E_x < 200 \text{ keV}$  is plotted as a function of X-ray energy. The line represents the thermal bremsstrahlung emission for a hydrogen plasma at  $3.3 \times 10^8 \text{ K}$ . The line of sight integral  $\int N_e N_p dl$  for this emission is  $1.3 \times 10^{17} / \text{cm}^5$ . If one assumes no clumping and  $\int dl = 10^{28} \text{ cm}$ , one gets  $N_e \approx N_p \approx 3 \times 10^{-6} / \text{cm}^3$ . Such a density is adequate to close the universe if  $H_0 = 55 \text{ km/s-Mpc}$ .

We believe that there are indeed reasons that indicate that the hot intergalactic medium is the most plausible explanation of this emission. The high degree of isotropy as measured by Schwartz (1970) has been analyzed by Silk (preprint) to show that one needs at least  $10^7$  sources in the sky to yield the required degree of isotropy. This means that a reasonable fraction of the galaxies should contain hot plasma at  $3 \times 10^8 \text{ K}$ . In order that the spectrum of emission is not transformed by free-free cooling (Equations VIII.A-2, and -3)

$$\frac{1.96 \times 10^{11}}{n_e} (3 \times 10^8)^{1/2} > \frac{1}{H_0} = 3 \times 10^{17} \text{ s} \quad (\text{VIII.A-9})$$

which yields  $n_e 10^{-2}/\text{cm}^3$ . Even if one takes  $n_e \sim 10^{-2}$ , one finds that about 5 percent of all visible galactic matter should be at a temperature of  $3 \times 10^8 \text{ K}$  in order to generate an emission measure of  $1.3 \times 10^{17} \text{ cm}^{-5}$ . Firstly, most of the mass of the galaxies is concentrated in stars (temperature  $\sim 10^4 \text{ K}$ ), with gas contributing to less than 10 percent of the total mass. The galaxies would definitely be unable to contain gravitationally such a large amount of hot plasma.

There is a second argument in favor of a critical mass density existing in the form of a hot intergalactic plasma. This argument essentially invokes the intergalactic medium as a heat sink for the energy released during the synthesis of heavy elements in supernovae exploding in the galaxies. It has been pointed out that in our galaxy with a mass of  $\sim 10^{11}$  solar masses one needs  $\sim 10^9$  supernovae to generate the heavy elements. How much energy is released in this process? We may estimate that about one solar mass collapses to a neutron star in each event yielding an energy of  $G(1/2 M_\odot)/R$ . Thus the energy generated per unit mass of the galaxy

$$u = 10^9 \frac{G M_\odot^2}{R} \cdot \frac{1}{10^{11} M_\odot} = \frac{G M_\odot}{100R} \approx 2 \times 10^{18} \text{ erg/g}$$

using  $R \approx 10^6 \text{ cm}$ . This released energy is not seen as electromagnetic radiation in any frequency band, and this energy must therefore have gone into the kinetic energy of matter;  $5 \times 10^9 \text{ ergs/gm}$  corresponds to a temperature of  $\sim 10^{10} \text{ K}$ . This shows that we need to have approximately 100 times as much intergalactic matter as in the galaxies to absorb this energy so that the mean temperature of the universe may not be too high. With a hot intergalactic plasma of critical density (equal to  $\sim 50$  times the mass density contributed by the galaxies) one has a hot universe at  $\sim 3 \times 10^8 \text{ K}$ .

### 0.3 TO 3 MeV GAMMA RAYS

Stecker, Morgan, and Bredekamp (1971) have attempted to explain this flux of  $\gamma$ -rays as due to annihilation of matter and antimatter at  $z \approx 100$  in a baryon symmetric universe. However, neither the absolute intensity nor the isotropy of this radiation has been established. Therefore, we wish to investigate here the possibility that this radiation could be of local, galactic origin. In fact, there are indications in the cosmic-ray electron spectrum that such emission could be taking place from our galaxy. Before discussing this galactic source in detail we must emphasize that the burden of proof lies with experiments. Should they show that the radiation is indeed isotropic, one has to give away the galactic model, which is discussed below.

The cosmic-ray electron spectrum is well measured in the region of  $\sim 100 \text{ MeV}$  to  $\sim 100 \text{ GeV}$ ; it is shown in Figure VIII.A-5 after correcting for solar

modulation effects. The spectrum below a few GeV has a spectral index of  $\sim 1.6$ , but steepens to an index of  $\sim 2.6$  above a few GeV. This is not the true electron spectrum that is injected into the interstellar space by the cosmic-ray sources but is contaminated by interstellar secondaries generated by the nuclear component of cosmic rays. The positron flux gives a very good estimate as to the amount of this contamination. After subtracting the secondaries, the spectrum of electrons injected by the sources is shown in Figure VIII.A-6. Since the processes of cosmic-ray acceleration are electromagnetic in nature, one may safely assume that the spectrum of electrons accelerated by the sources is a simple power law with an index of 2.6 similar to that of the nuclear component. The difference in the energy between the accelerated spectrum and the injection spectrum must have been radiated away. If part of this radiation is due to Compton scattering against optical frequency photons then one obtains a  $\gamma$ -ray luminosity (Cowsik, 1971)

$$L(E_\gamma) = \frac{5}{(\beta-1)\sqrt{16}} \sqrt{\frac{3}{E_\gamma \epsilon}} \left\{ \left[ E_H^{p-1} + \left( \frac{m}{2} \sqrt{\frac{3E}{\epsilon}} \right)^{p-1} \right]^{-\frac{\beta-1}{p-1}} - \left[ E_\gamma^{p-1} + \left( \frac{m}{2} \sqrt{\frac{3E_\gamma}{\epsilon}} \right)^{p-1} \right]^{\frac{\beta-1}{p-1}} \right\} \quad \text{(VIII.A-10)}$$

$\beta$ ,  $S$ ,  $E_H$ ,  $E_T$  and  $p$  are constants derived from the electron spectrum and  $\epsilon \approx 3 \times 10^{-6}$  MeV is the assumed mean energy of the optical photon. The intensity as seen by a detector having isotropic response is shown in Figure VIII.A-7. One notices that the spectrum is insensitive to the parameter  $p$ . The general shape of the curve is essentially determined by  $\beta \approx 2.6$ , the spectral index of the cosmic-ray electrons at low and high energies, respectively. Despite this elegant fit to the data, one has to wait for measurements of angular distribution in this energy region before the galactic nature of the MeV  $\gamma$ -ray fluxes can be established.

**GAMMA RAYS IN THE 100-MeV RANGE**

The pioneering work of Clark, Garmire, and Kraushaar (1968) established the existence of a line source coincident with the galactic disk with an enhancement around the galactic center and a possible isotropic component. The measured intensity in the direction of the center is  $\sim 10^4 \gamma/\text{cm}^2 \cdot \text{s} \cdot \text{rad}$ , the line source elsewhere is about a third of this  $\sim 2$  to  $3 \times 10^5 \gamma/\text{cm}^2 \cdot \text{s} \cdot \text{rad}$ .

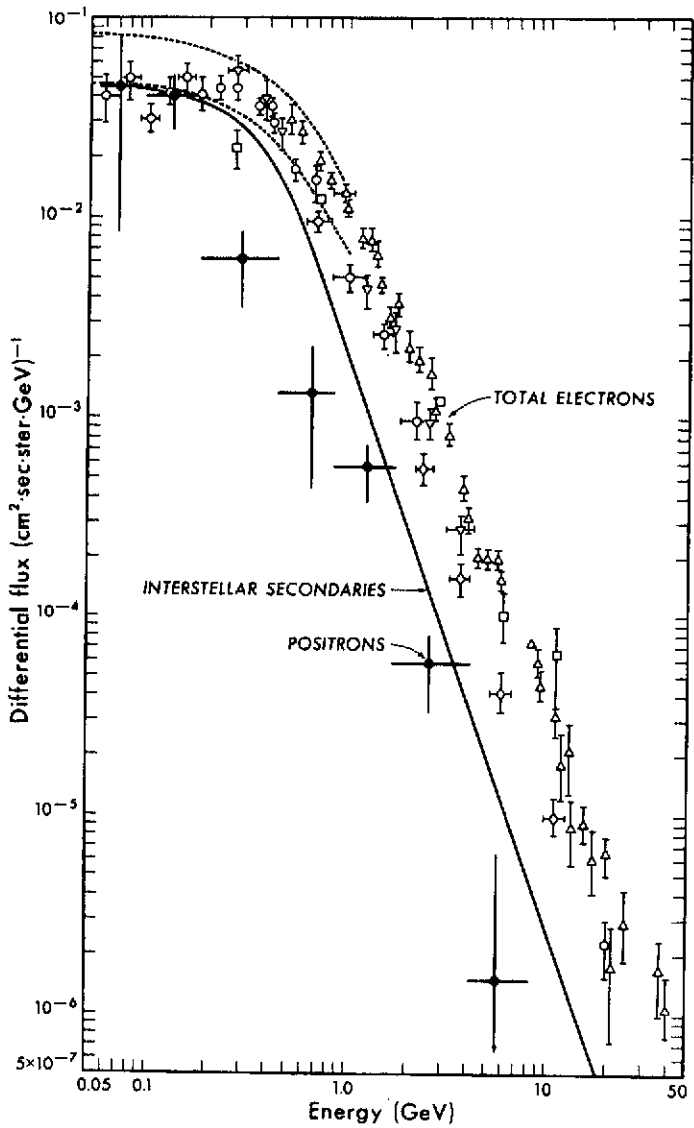


Figure VIII.A-5. Electronic component of cosmic rays in the interstellar space. The secondary electron flux generated by the nuclear component is normalized using positrons.

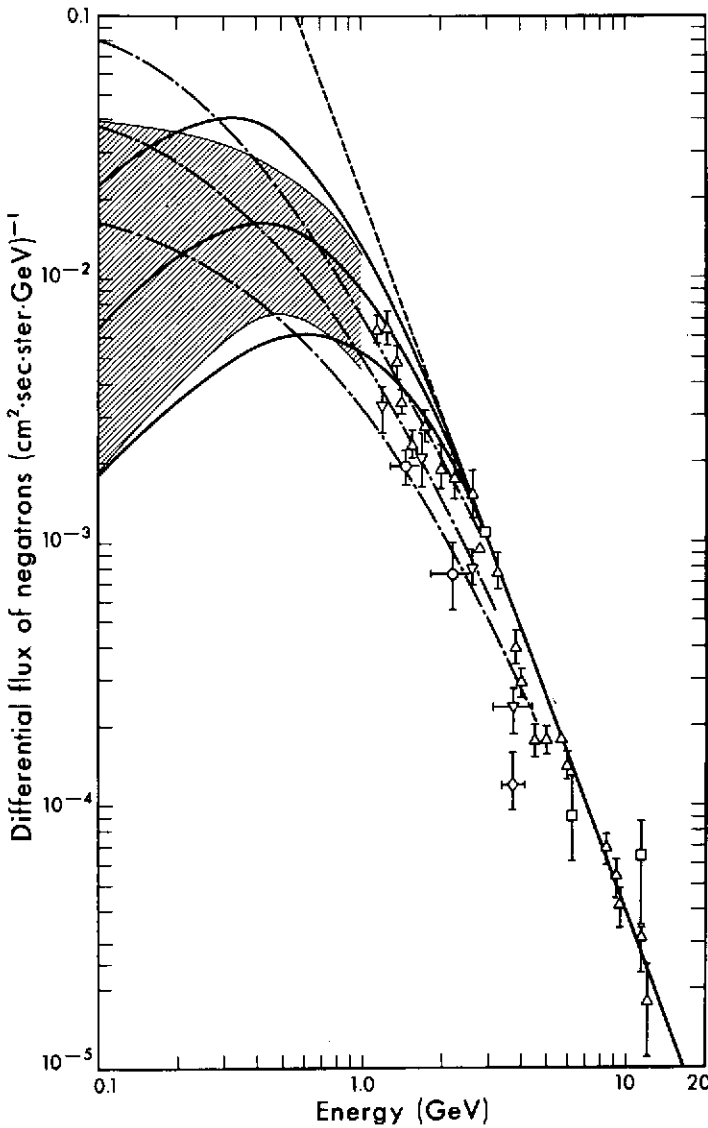


Figure VIII.A-6. The injection spectrum of primary cosmic-ray negatrons. Hatched area indicates uncertainties in the estimate. The predictions of the model are for  $p = 2$  (---) and  $p = 3$  (—);  $E_c = 0.5, 0.7, 1.0$  GeV starting from top. Since it is the difference between the accelerated power-law spectrum  $\sim E^{-2.6}$  and the injection spectrum that governs the  $\gamma$ -ray intensities the uncertainty in the  $\gamma$ -ray fluxes are within a factor of  $\sim 2$ .

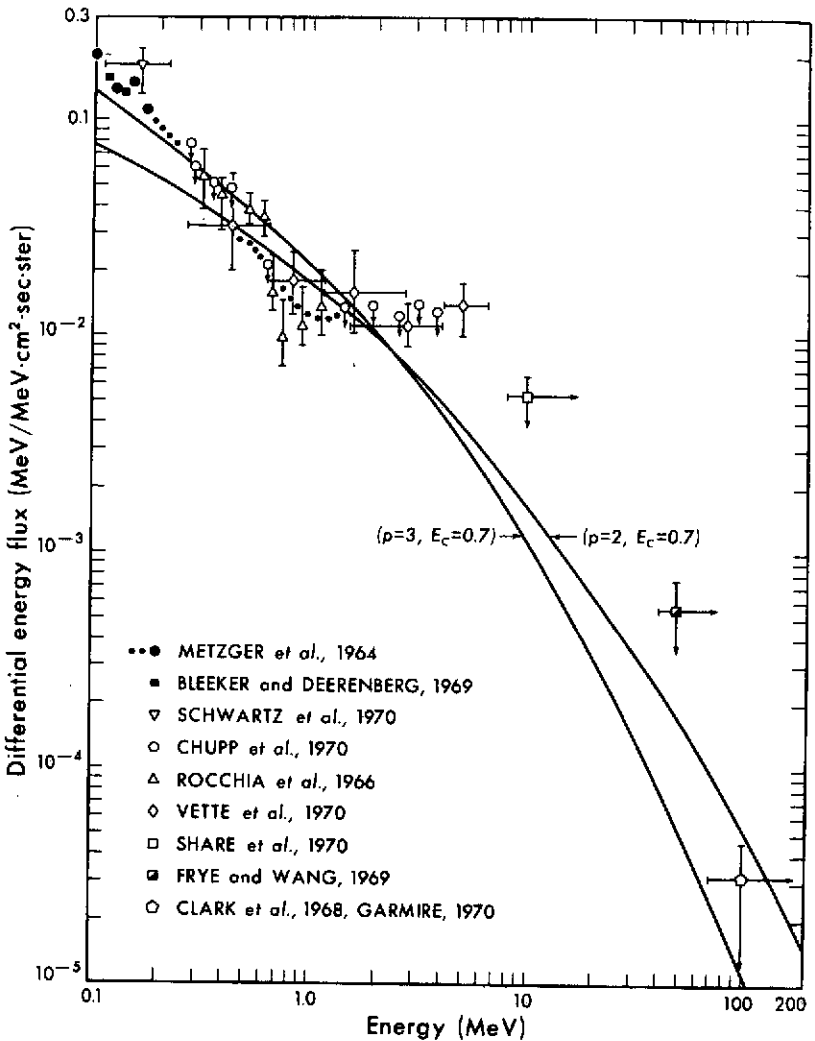


Figure VIII.A-7. A well defined background  $\gamma$ -ray flux (absolute normalization within X2) is predicted by model. For  $E_{\gamma} \ll 1$  MeV, there is a large flux of intergalactic origin. The model predicts correctly the primary gamma-ray slope and intensity that would generate the experimental response shown (Anand *et al.*, 1969; data from Silk, 1970).

The line source has been explained by Stecker (1969b) as due to production and subsequent decay of neutral pions by cosmic rays. If the same mechanism should yield the enhancement of the intensities near the center, one needs a substantially large enhancement of gas density near the central regions of the galaxy. There is no evidence, direct or indirect, for such an enhancement. On the other hand, there is evidence that the density of stars increases considerably towards the galactic center. The density distribution of stars as a function of galacto-centric distance  $\omega$ , is shown in Figure VIII.A-8 (Perek, 1962). The increase in mass distribution of stars towards the center is  $1/\omega^3$  and would be that of the distribution of starlight. With such

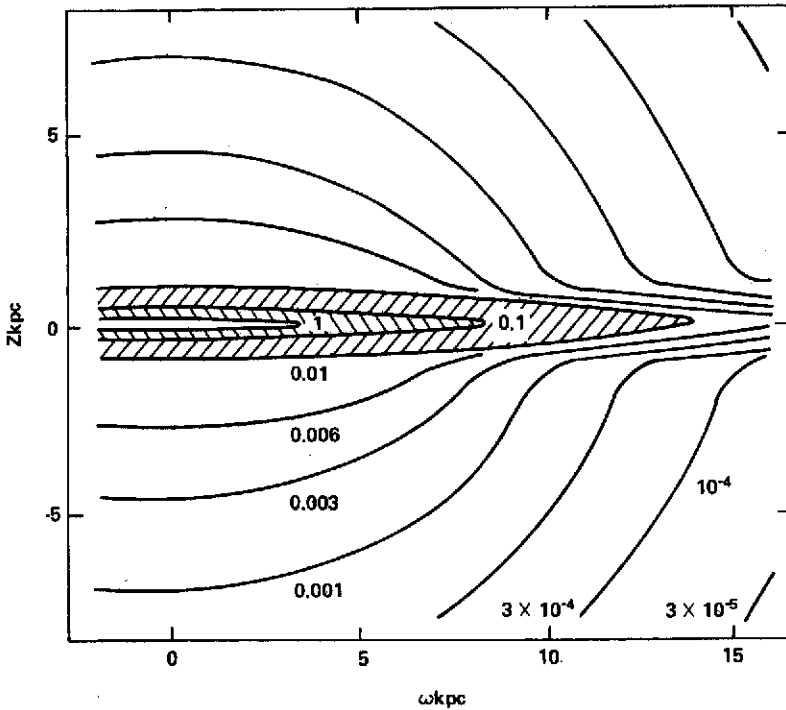


Figure VIII.A-8. The mass distribution in the galaxy in units of  $M_{\odot}/pc^3$  is shown as a function of cylindrical coordinates centered at the galactic center (taken from Perek, 1962).

enhanced starlight density, the Compton scattering of the cosmic-ray electrons of these photons would provide an intense  $\gamma$ -ray source. Preliminary

calculations of the angular distribution expected through this process is shown in Figure VIII.A-9 (Cowsik and Hutcheon, 1971). The actual calculations yielded only 70 percent of the intensity towards the galactic center as due to this process. If one adds the line source due to  $\pi^0 \rightarrow 2\gamma$  decay contributing  $\sim 30$  percent with a flat dependence on galactic longitude (Stecker, 1969b) then the emission from the galactic disk can be explained completely.

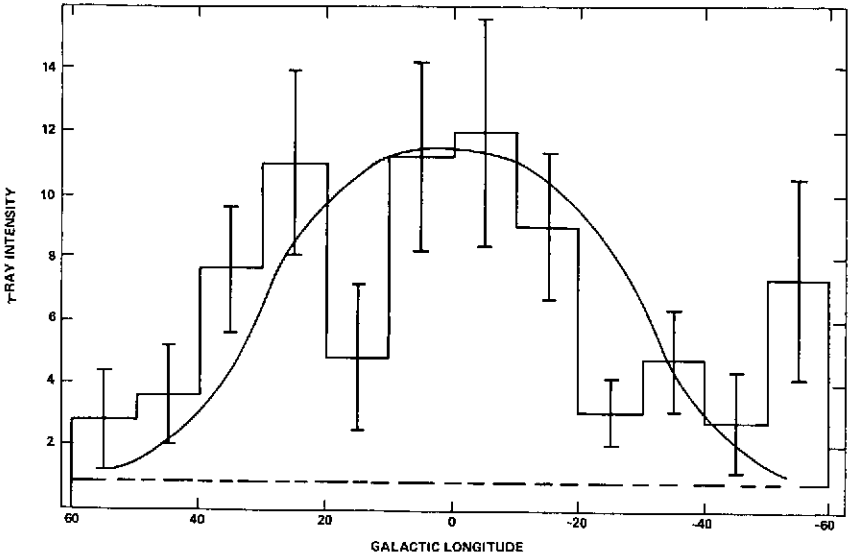


Figure VIII.A-9. The gamma-ray intensities that are calculated using starlight distribution implied by Figure VIII.A-8 are compared with results of Clark et al. (1968). The preliminary theoretical estimates are multiplied by  $\sim 1.4$  and then averaged over the aperture of the detector. It is seen that the Compton scattering of starlight contributes negligibly beyond  $\sim 60^\circ$  galactic longitude. Beyond this point the  $\pi^0 \rightarrow 2\gamma$  process discussed by Stecker (1969) dominates and should be added to the Compton fluxes to make a detailed fit to the observations.

What is the spectrum of  $\gamma$ -ray generated through the Compton scattering of starlight? The cosmic-ray electron spectrum has a spectral slope of  $\beta_1 \approx 1.6$  below  $\sim 3$  GeV and a slope of  $\beta_2 \approx 2.6$  above  $\sim 3$  GeV. The maximum and the mean energies of the scattered photons in the Compton process are given by

$$E_{\gamma\max} = 4 \left( \frac{E_e}{m} \right)^2 \epsilon$$

and

$$\langle E_\gamma \rangle = \frac{4}{3} \left( \frac{E_e}{m} \right)^2 \epsilon$$

(VIII.A-11)

The spectral slope of Compton  $\gamma$ -rays will be  $\alpha_1 = (\beta_1 - 1)1/2 = 0.3$  at low energies and  $\alpha_2 = (\beta_2 - 1)1/2 \approx 0.8$  at high energies. The typical  $\gamma$ -ray energy at the transition that takes place can be calculated by using Equation (VIII.A-11), with  $E_0 \approx 3$  GeV, and the mean energy of the starlight photon  $\sim 3$  eV (corresponding to a temperature of  $10^4$  K).

$$E_{\gamma\text{-transition}} \approx \frac{4 \left[ \frac{3 \times 10^9}{5 \times 10^5} \right]^2}{3} \times 3 \text{ eV} \\ \approx 150 \text{ MeV}$$

This means that below  $\sim 150$  MeV the spectral slope would be  $\sim 0.3$  and as such would be very difficult to distinguish from a  $\pi^0$  source. We now wish to emphasize the inevitability of the existence of a Compton source of  $\gamma$ -rays in the central regions of our galaxy. There is evidence both for the existence of high density of starlight near the galactic center (as discussed before) and for the relativistic electrons through their synchrotron emission; thus the Compton scattering must occur leading to significant  $\gamma$ -ray flux from the region of the galactic center. Detailed spectral shapes and sky maps due to this process will be presented at the Cosmic Ray Conference at Denver by Sullivan and Cowsik.

The isotropic component at  $\sim 100$  MeV has an intensity of  $\sim 10^{-5} \gamma/\text{cm}^2 \cdot \text{s} \cdot \text{sr}$ . At this moment it is hard to pinpoint a precise source for this radiation. We wish to add that the existence of an extended halo to our galaxy may contribute significantly to this flux, and also that a truly extragalactic component in this energy region cannot be excluded.

### THE 100 MeV $\gamma$ -RAY FLUX AND A LIMIT ON THE ENERGY DENSITY IN THE SUBMILLIMETER BACKGROUND

As pointed out in the previous section, the line source of  $\gamma$ -rays away from the galactic center can be completely explained as due to the decay of  $\pi^0$ 's produced by nuclear cosmic rays (Stecker, 1969b). This means that any other source of  $\gamma$ -rays must be very weak indeed. One such could be provided by the existence of intense submillimeter radiation which would then be scattered to  $\gamma$ -ray energies by cosmic-ray electrons. Thus, one may use the  $\gamma$ -ray fluxes to put stringent limits on the microwave background. This is done in Table VIII.A-3 taken from Cowsik (1972). From this table it is clear that the energy density in any radiation background over and above the universal thermal background at 2.7 K should be less than  $0.6 \text{ eV}/\text{cm}^3$ . In Figure VIII.A-10 this limit is shown in comparison with observations at microwavelengths.

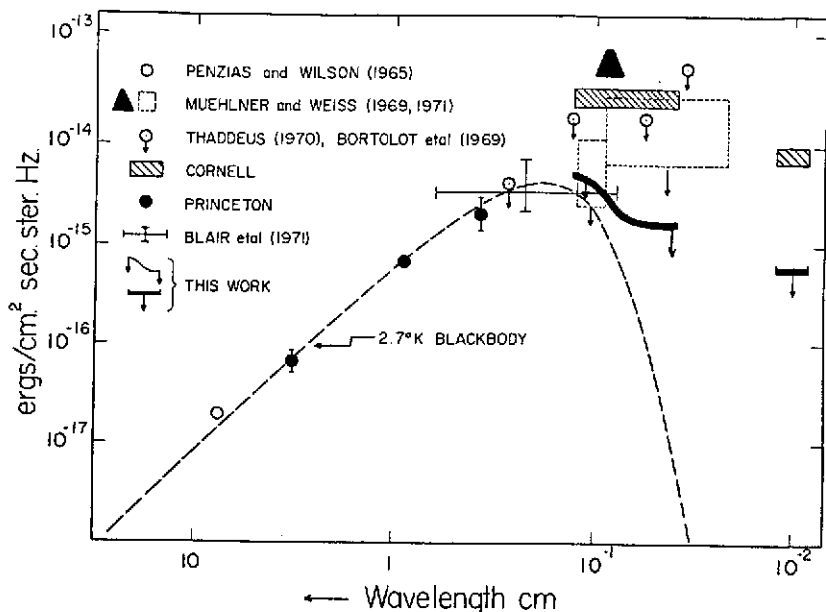


Figure VIII.A-10. Measured background radiation fluxes are compared with that expected from a blackbody at 2.7 K. The  $\gamma$ -ray fluxes measured by Kraushaar et al. (1972), put a stringent limit on the intensities allowable at submillimeter wavelengths. In plotting our upper limit of  $\sim 0.6 \text{ eV/cm}^3$  we have assumed that the background radiation has a bandwidth equal to that of the detector of the Cornell instrument.

### SUMMARY

Thus it appears that one has a reasonable explanation for a good part of the diffuse X-ray and  $\gamma$ -ray background that is observed over six decades in energy. Thermal sources seem to dominate up to an energy of  $\sim 200 \text{ keV}$ . Angular distribution measurements are essential in choosing between galactic and universal models for the intensities in the MeV region. The source of 100 MeV  $\gamma$ -rays from the disk and galactic center seem to be well understood as due to the decay of neutral pions and Compton scattering of starlight, respectively. These observations put a stringent limit on the energy density in any possible radiation background at submillimeter wavelengths.

I cannot close this review more effectively than by making a call for all experimentalists in the field to measure the angular distribution of photons in the MeV range, which is of very great astrophysical and cosmological importance, for it relates either to the cosmic-ray sources in our galaxy or to annihilation of antimatter in baryon symmetric cosmologies.

Table VIII.A.3  
Gamma-Ray Fluxes at  $E\gamma > 100$  MeV: Theory and Experiment\*

Source	Region of Sky Scanned	
	$60^\circ < l < 30^\circ, b = 0^\circ$ (disk)	$b = \pi/2$ (halo)
Experiment	Flux $(\text{cm}^2 \text{s rad})^{-1}$ $(3.4 \pm 0.6) \times 10^{-5}$	Flux $(\text{cm}^2 \text{s sr})^{-1}$ $(3 \pm 0.4) \times 10^{-5}$
$p + H \rightarrow \pi^0 \rightarrow 2\gamma$	$> 2.6 \times 10^{-5}$	$3.7 \times 10^{-6}$
$e + t (2.7^\circ) \rightarrow e + \gamma$	$> 1.1 \times 10^{-5}$	$1.1 \times 10^{-5}$
Residual	$< 0.9 \times 10^{-5}$	$2.3 \times 10^{-5}$
$e + e$ (sub-mm) $\rightarrow e + \gamma$	$4.5 n_{\text{ph}} \times 10^{-8}$	$4.4 n_{\text{ph}} \times 10^{-8}$
Maximum number density of sub-mm quanta	$n_{\text{ph}} < 200 \text{ cm}^{-3}$	$n_{\text{ph}} < 500 \text{ cm}^{-3}$
Corresponding energy density	$\rho$ (sub-mm) = $N_{\text{ph}}$ $< 0.25 \text{ eV}$	$\rho < 0.6 \text{ eV/cm}^3$

\*The radio disk is assumed to extend up to  $\sim 1$  kpc above the galactic plane in making the theoretical estimates. Because of the Gaussian response of the detector with angles, the expected counting rates increase more slowly than that proportional to the assumed thickness of the disk. Note that the estimates from the halo direction are uncertain and are to be given much lower weight.

**ACKNOWLEDGMENTS**

I want to thank Professor P. Buford Price and the members of his group for their active interest in this work.

(Supported in part by NASA grant NGR 05-003-376.)

**REFERENCES**

Anand, K. C., G. Joseph, and P. J. Lavakore, 1969, *Proc. Indian Acad. Sci.*, **71**, p. 225.  
 Blumenthal, G. R., and R. J. Gould, 1970, *Rev. Mod. Phys.*, **42**, p. 237.  
 Bowyer, C. S., G. B. Field, and J. Mack, 1968, *Nature*, **223**.  
 Brecher, K., and P. Morrison, 1969, *Phys. Rev. Letters*, **23**, p. 802.  
 Clark, G. W., G. P. Garmire, and W. L. Kraushaar, 1968, *Astrophys. J. Letters*, **153**, p. L203.  
 Cowsik, R., 1971, *Proc. 12th Int. Conf. on Cosmic Rays*, **1**, p. 334.

- \_\_\_\_\_, 1972, *Nature Phys. Sci.*, **239**, p. 41.
- Cowsik, R., and I. D. Hutcheon, 1971, *Ibid*, **1**, p. 102.
- Cowsik, R., and E. J. Kobetich, 1971, *Ibid*, **1**, p. 38.
- \_\_\_\_\_, 1972, *Astrophys. J.*, **177**, p. 585.
- Damle, S. V., R. R. Daniel, G. Joseph, and P. J. Lavakaro, 1971, *Proc. 12th Int. Conf. Cosmic Rays*, **1**, p. 84.
- Felten, J. E., 1972, *X-Ray and Gamma Ray Astronomy, Proc. of IAU Symposium No. 55* (Madrid), H. Bradt and R. Giacconi, eds., D. Reidel, Dordrecht, Holland.
- Field, G. B., 1972, *Ann. Rev. Astron. and Astrophys.*, **10**, p. 227.
- Gold, T., and F. Hoyle, 1959, *Paris Symp. on Radio Astronomy, IAU Symposium No. 9*, Bracewell, ed., p. 583.
- Gould, R. J., and G. R. Burbidge, 1963, *Astrophys. J.*, **138**, p. 969.
- Hayakawa, S., 1969, *Cosmic Ray Physics*, John Wiley and Sons, New York, p. 609.
- Kraushaar, W. L., G. W. Clark, G. P. Garmire, R. Borken, P. Higbie, G. Leong, and T. Thorsos, 1972, *Astrophys. J.*, **177**, p. 341.
- Lang, R. R., and Y. Terzian, 1969, *Astrophys. J. Letters*, **3**, p. L29.
- Perek, L., 1962, *Adv. in Astron. and Astrophys.*, **1**, p. 165.
- Petrosian, V., and R. Ramaty, 1972, *Astrophys. J. Letters*, **173**, p. L83
- Schwartz, D. A., 1970, *Astrophys. J.*, **162**, p. 439.
- Seward, F. D., G. A. Burginyon, R. J. Grader, T. Palmieri, and J. Stoering, 1971, *Astrophys. J.*, **169**, p. 515.
- Silk, J., 1970, *Space Sci. Rev.*, **11**, p. 671.
- Stecker, F. W., 1969a, *Astrophys. J.*, **157**, p. 507.
- \_\_\_\_\_, 1969b, *Nature*, **224**, p. 870.
- \_\_\_\_\_, 1971, *Cosmic Gamma Rays*, Mono Book Corp., Baltimore.
- Stecker, F. W., D. L. Morgan, and J. Bredekamp, 1971, *Phys. Rev. Letters*, **27**, p. L1469.

**DISCUSSION**

*Member of the audience:*

What is the evidence for the lifetime being  $10^{14}$ s for the electrons as distinct from nuclei?

*Member of the audience:*

You may say that Daniel's measurement indicating a steepening of the spectrum at 100 GeV may be taken as evidence, or you may say that electrons at 200 GeV propagate with the nuclei and you get a lifetime similar to that. I'm sure you are quite an expert in the field, and you know the answer.

*Member of the audience:*

There's a possibility but no proof positive at all.

*Member of the audience:*

We cannot prove anything, we can only give plausible statements.

*Member of the audience:*

Would you take issue with him? (Laughter)

*Member of the audience:*

Give or take an order of magnitude.

*Stecker:*

I'm not quite sure how you can calculate such a detailed  $\gamma$ -ray spectrum (Figure VII.A-7) when you took such crude numbers.

*Cowsik:*

I just calculated this using 1-eV photons and the spectrum that I get is what I have shown in Figure VIII.A-7. It's not detailed in the sense that it may have fluctuations or errors in it which may be a factor of two or something like that. From today's discussion, I conclude that we do not know the  $\gamma$ -ray flux to that kind of an accuracy.

*Stecker:*

You say there are enough 1-eV photons and cosmic-ray electrons to account for the total flux, and that it would be anisotropic?

*Cowsik:*

Yes. In MeV/MeV units, this would turn out to be  $3 \times 10^{-2}$ , or something like that.

*Stecker:*

These are Compton interactions you are talking about?

*Cowsik:*

Yes.

*Stecker:*

Because there are many calculations going back to those of Morrison?

*Cowsik:*

There is an essential difference. I'm not taking all the electrons in the galaxy and putting them inside a typical radiation density that exists in the galactic disk and asking what would be the spectrum that comes up. I'm doing something different (see text).

Something may be happening in the sources in which the originally accelerated power law is reduced. This can happen, let us say, if we can take an energy dependent leakage lifetime from the source region that can easily kill the lower-energy electrons more efficiently than the high-energy electrons. In fact, recent cosmic-ray data have evidence that indicates that even the nuclei in cosmic rays may have been stored in the sources.

*Member of the audience:*

I think it goes the other way.

*Cowsik:*

One has to discuss that. I don't want to discuss it in detail, but certainly the model that I'm using is allowing the electrons to be killed by this factor.

*Vette:*

What you are talking about here for the  $\gamma$ -ray production, is it in the galaxy?

*Cowsik:*

What I'm talking about here is in the sources.

*Member of the audience:*

The source is assumed to be inside of the galaxy?

*Cowsik:*

Yes.

*Vette:*

But you wouldn't expect this to be isotropic?

*Cowsik:*

Yes, this won't be isotropic. This will show enhancement in the galactic disk, but I do not know how much. The experimenters will have to comment on what kind of limits one can place on the anisotropy of MeV radiation. (See paper of Kniffen et al., Chapter IV.)

*Stecker:*

You're talking about essentially a large anisotropy because all the  $\gamma$ -rays are coming from sources in the galactic plane, and I'm wondering if any of the observational people here might mention their angular resolution and what their upper limit is on their anisotropy.

*Metzger:*

The slide I showed from Apollo-16 shows a clear demonstration of anisotropy and the background of the energy range up to about half a MeV. We don't have the statistics yet to look beyond that with the Apollo-16 data. We have looked with Apollo-15 data and we see anisotropy in a couple of cases corresponding to two of the five or six fixed position measurements which are made for the X-ray spectrometer during transearth coast, but we have not yet to our satisfaction pinpointed the source of that anisotropy.

*Stecker:*

What's the number on the anisotropy?

*Metzger:*

At the most, 5 percent above the mean.

*Stecker:*

And you show just where the Crab Nebula and the galactic center were? What would be your guess of the average anisotropy if you subtracted it?

*Metzger:*

I'd say less than 10 percent.

*Vette:*

Steve White, do you have any comments on the anisotropy from any of your measurements?

*White:*

Well, unfortunately, we had only one flight and we dedicated only a small amount of time to making the  $\gamma$ -rays in that one flight. We were looking primarily in the direction of the antigalactic center during that time although we had a little time devoted to looking outside, so we can't say anything.

*Steigman:*

Didn't you fellows see a marked anisotropy in the galactic plane?

*Vette:*

Oh, yes, at 100 MeV.

*Member of the audience:*

That's at high energy.

*Vette:*

You're not talking about 100 MeV, you're talking about 1 MeV.

*Cowsik:*

One- to 10-MeV range.

*Vette:*

There really hasn't been a good definitive measurement in the directional aspect of it. That's why I think some of the detectors we heard about today, particularly the Compton telescopes, do offer some possibility of making measurements there we haven't made today.

(See also related discussions by Kniffen et al., Chapter IV, and Stecker, Chapter IX.)

## A. MECHANISMS FOR PRODUCTION OF THE DIFFUSE GAMMA-RAY CONTINUUM RADIATION

F. W. Stecker\*  
Goddard Space Flight Center

### BASIC MECHANISMS

The basic mechanisms expected to be important in the production of cosmic  $\gamma$ -radiation were suggested by Morrison in a classic paper in *Nuovo Cimento* in 1958. They are Compton interactions with low-energy photons, bremsstrahlung interactions, cosmic-ray induced  $\pi^0$  production, and matter-antimatter annihilation. Of these four mechanisms, the first two involve cosmic-ray electrons and are electromagnetic processes, whereas the last two involve nucleons, mainly protons, and are strong interaction processes. Above 511 keV the  $\gamma$ -radiation from matter-antimatter annihilation arises mainly from the decay of  $\pi^0$ -mesons produced in the annihilation process, so that the kinematics involved in the last two processes is similar. Because this paper will be concerned mainly with diffuse continuum radiation rather than line radiation or radiation from point sources, the discussion here will be restricted mainly to the above four processes. (For a treatment of the theory of the production of cosmic-line radiation, see Clayton, Chapter XI.A.)

### COMPTON INTERACTIONS

The most astrophysically significant role which Compton interactions are expected to play in cosmic  $\gamma$ -ray production involves the interactions of relativistic cosmic-ray electrons with low-energy photons of the universal 2.7-K microwave blackbody radiation field. The microwave photons have an average energy near  $10^{-3}$  eV and a number density of  $\sim 400/\text{cm}^3$ , considered to be uniformly distributed throughout the universe. Compton interactions with cosmic-ray electrons can then produce  $\gamma$ -rays with typical energies of

$$\langle E_\gamma \rangle \cong 10^{-3} \gamma^2 \text{ eV} \quad (\text{IX.A-1})$$

---

\*Speaker.

where  $\gamma = (E_e/m_e c^2)$  is the Lorentz factor of the cosmic-ray electron. Thus a 50-GeV electron with a Lorentz factor of  $\sim 10^5$  will typically produce  $\gamma$ -rays of energy  $\sim 10$  MeV through Compton interactions with 2.7-K photons. We can define the "spectrum" of  $\gamma$ -rays from a single Compton interaction as the normalized probability distribution of  $\gamma$ -rays of energy  $E_\gamma$  expected to be produced by an electron of energy  $E_e$ . Such a spectrum turns out to be flat and rather broad around the average energy  $\langle E_\gamma \rangle$  (Heitler, 1954; Jones, 1965). Because  $\langle E_\gamma \rangle \propto \gamma^2$ , the spectrum of  $\gamma$ -rays produced by a power-law cosmic-ray electron spectrum of the form  $K_e E_e^{-\Gamma_e}$  will also have a power-law form  $K_\gamma E_\gamma^{-\Gamma_\gamma}$ , but with  $\Gamma_\gamma = (\Gamma_e + 1)/2$ . In fact, for interactions with a blackbody spectrum of low-energy photons at temperature (T), the Compton-generated  $\gamma$ -ray spectrum is given in photons/(cm<sup>2</sup>·s·sr·GeV) by

$$I(E_\gamma) \cong 6.22 \times 10^{-21} L [10^{-2.962\Gamma_e} f(\Gamma_e)] K_e T^{(\Gamma_e + 5)/2} E_\gamma^{-(\Gamma_e + 1)/2} \quad (\text{IX.A-2})$$

where L is the path length (cm) over which production occurs and  $E_e$  is in GeV with the factor  $f(\Gamma_e) \sim 1$  given by Ginzburg and Syrovatskii (1964). For example, if  $\Gamma_e \sim 2.6$ , then  $\Gamma_\gamma \sim 1.8$  for galactic cosmic-ray electrons. Because the 2.7-K blackbody radiation is believed to be universal, Compton interactions have been invoked to explain the cosmic X-ray background spectrum where the observed  $\Gamma_\gamma \sim 2$  and to set limits on the metagalactic cosmic-ray electron intensity  $w_{Mg,e}$  to show that it must be much less than the galactic value, that is,  $w_{Mg,e} \ll w_{G,e}$  (Felten, 1965; Gould, 1965; Fazio, Stecker, and Wright, 1966; Felten and Morrison, 1966; Cowsik, Chapter VIII.A; Ginzburg, Chapter X.A).

### ELECTRON BREMSSTRAHLUNG

Bremsstrahlung interactions are expected to take place between cosmic-ray electrons and interstellar and intergalactic gas and may be significant in producing low-energy  $\gamma$ -rays and X-rays both in the galaxy and in intergalactic space (Cowsik, Chapter VIII.A). The probability distribution spectrum for  $\gamma$ -rays from bremsstrahlung of a cosmic-ray electron of energy  $E_e$  is quite flat and may be approximated by

$$f(E_\gamma | E_e) \cong \begin{cases} E_e^{-1} & \text{for } 0 \leq E_\gamma \leq E_e \\ 0 & \text{otherwise} \end{cases} \quad (\text{IX.A-3})$$

so that the  $\gamma$ -ray production spectrum is given by

$$I_b(E_\gamma) = X^{-1} \int_0^L dr \langle \rho(\vec{r}) \rangle \frac{I_e(>E_\gamma)}{E_\gamma} \quad (\text{IX.A-4})$$

where  $\rho$  is the matter-density of the gas in  $\text{g/cm}^3$  and  $X$  is the average radiation length for interstellar matter and is  $\sim 65 \text{ g/cm}^2$ . We may also write Equation (IX.A-4) in terms of the atomic density ( $n$ , in  $\text{cm}^{-3}$ ) and the path along the line of sight ( $L$  in  $\text{cm}$ ) so that

$$I_b(E_\gamma) = 3.4 \times 10^{-26} nL \frac{I_e(>E_\gamma)}{E_\gamma} \quad (\text{IX.A-5})$$

It follows from Equation (IX.A-5) that for bremsstrahlung from cosmic-ray electrons following a power-law spectrum  $K_e E_e^{-\Gamma_e}$ ,  $\Gamma_\gamma = \Gamma_e$  (for relativistic electrons) so that, in general, the  $\gamma$ -ray spectrum from bremsstrahlung is steeper than that from Compton interactions.

### NEUTRAL PION DECAY

We next discuss the  $\gamma$ -radiation from the decay of  $\pi^0$ -mesons produced by cosmic-ray interactions between high-energy nucleons and gas nuclei in interstellar and intergalactic space. This process has received the most attention because it now appears that  $\pi^0$ -decay  $\gamma$ -rays from cosmic-ray interactions may account for almost all of the  $\gamma$ -radiation above 100 MeV observed in our galaxy (Fichtel et al., 1972; Clark et al., 1968; Stecker, 1969a; Stecher and Stecker, 1970; Cavallo and Gould, 1971; Ginzburg, Chapter X.A), because it has long been recognized as an important process for cosmic  $\gamma$ -ray production (Morrison, 1958; Pollack and Fazio, 1963; Ginzburg and Syrovatskii, 1964), because it has the most difficult spectrum to calculate theoretically (Hayakawa et al., 1964; Dilworth et al., 1968; Stecker, 1970; Cavallo and Gould, 1971; Levy and Goldsmith, 1972) and because various theoretical calculations are somewhat contradictory. I do not intend to break the tradition, in fact, I hope to help resolve here some of the contradictions that have arisen among the theoretical calculations.

Figure IX.A-1 shows the type of  $\gamma$ -ray spectra obtained from the decay of  $\pi^0$ -mesons with various simple energy spectra  $f(E_\pi)$ . Typically the spectrum is flat near  $m_\pi c^2/2 \sim 70 \text{ MeV}$ , and symmetric about this value on a logarithmic energy plot. These characteristics can easily be shown from the kinematics of  $\pi^0$ -decay (Stecker, 1971a) and they will not be repeated here. Figure IX.A-2 shows how a typical  $\pi^0$ -decay  $\gamma$ -ray spectrum can be built up from an arbitrary

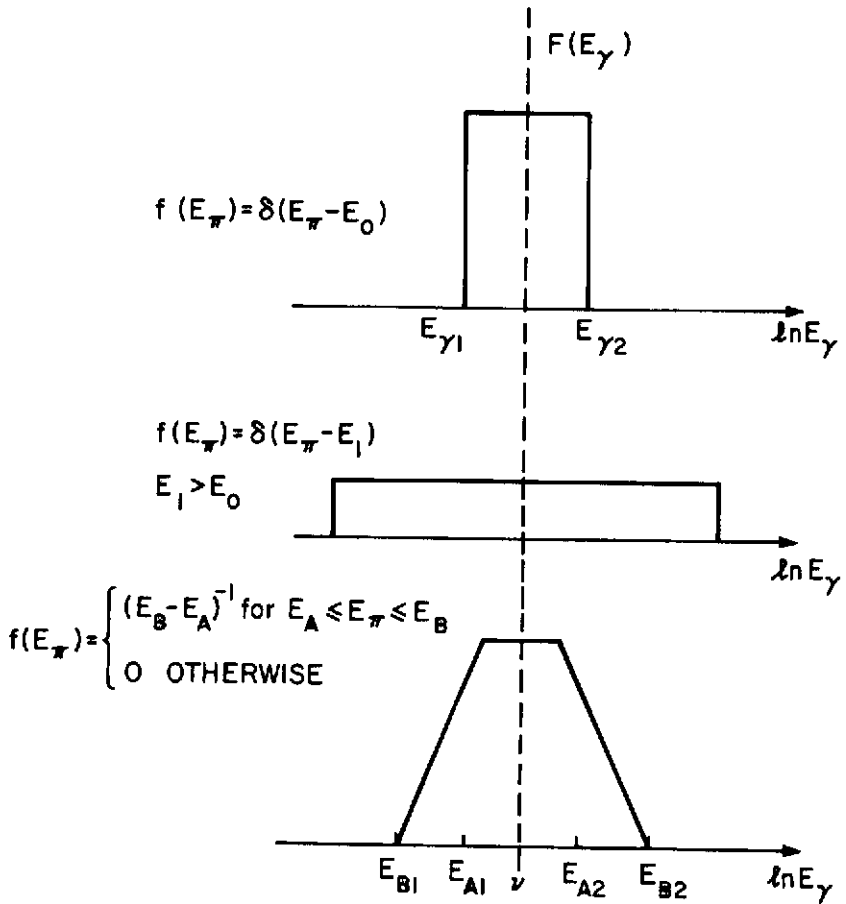


Figure IX.A-1. Gamma-ray spectra from the decay of neutral pions for various simple pion energy distributions ( $\nu \equiv m_\pi c^2/2$ ).

pion-energy spectrum, and that the spectrum always has a maximum at  $\sim 70$  MeV. Figure IX.A-3 shows the differential  $\gamma$ -ray spectrum obtained by Stecker (1970), illustrating the various expected characteristics. Figure IX.A-4 shows a comparison of the integral spectra obtained by Stecker (1970) and Cavallo and Gould (1971) normalized to compare the shapes obtained. The wiggles in the spectrum represent artifacts of the assumed pion-production models and should not be taken too seriously. The shapes of the two spectra are in good agreement and probably represent an accurate approximation to reality within the uncertainty indicated by the wiggles.

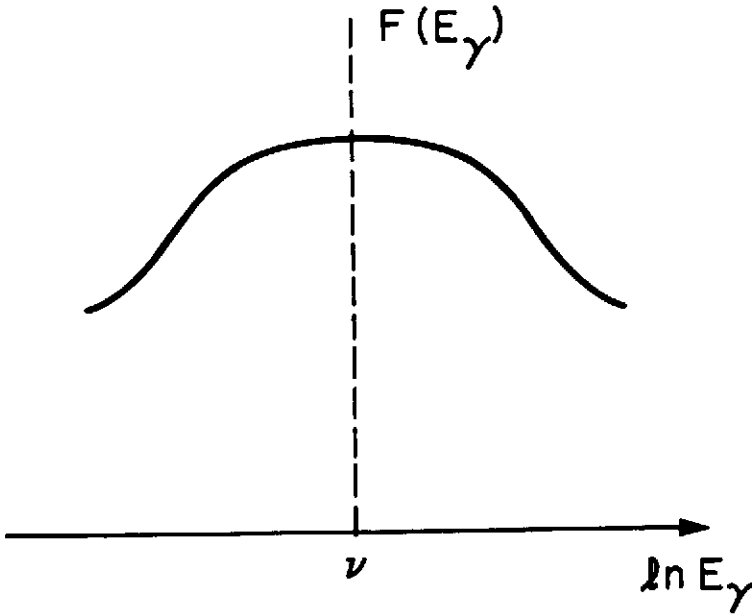


Figure IX.A-2. Idealized superposition of  $\gamma$ -ray spectra from the decay of pions having various energy distributions ( $\nu \equiv m_\pi c^2/2$ ).

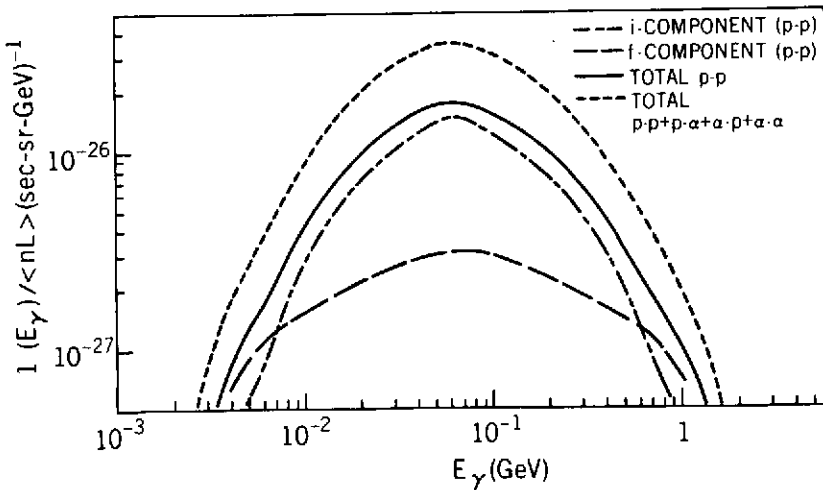


Figure IX.A-3. The calculated differential production spectrum of  $\gamma$ -rays produced in cosmic-ray interactions in the galaxy based on the "isobar (i)-plus-fireball (f)" model of Stecker (1970).

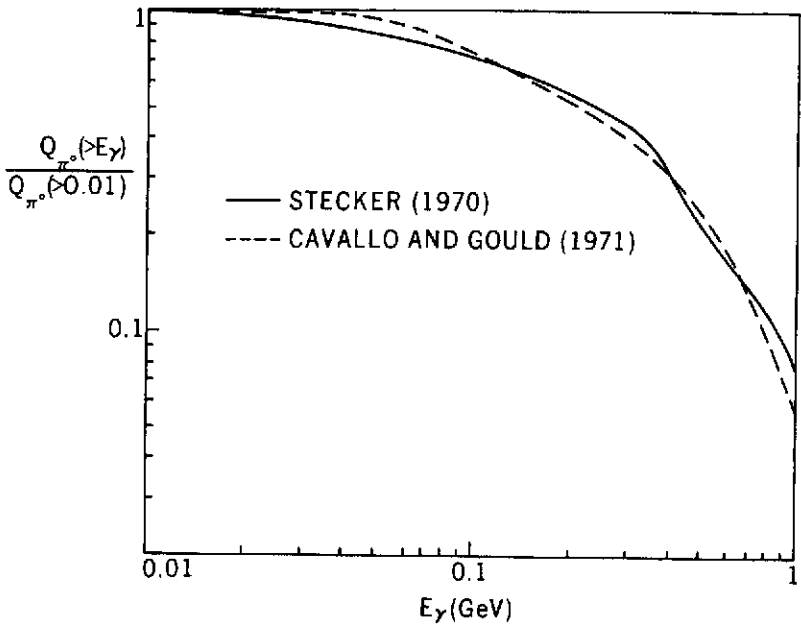


Figure IX.A-4. A comparison of the shapes of the integral galactic pion-decay energy spectra calculated by Stecker (1970) and Cavallo and Gould (1971). The total production rate is normalized to unity.

The largest discrepancy between the various calculations is in the total  $\gamma$ -ray production rates calculated by various workers. These rates are compared in Table IX.A-1.

Pollack and Fazio (1963) and Dilworth et al. (1968) obtained total  $\gamma$ -ray production rates per hydrogen atom which would be equivalent to roughly  $1.1 \times 10^{-25} \text{ s}^{-1}$  and  $1.0 \times 10^{-25} \text{ s}^{-1}$  respectively, for energies above 100 MeV. This corresponds to the quantity

$$Q_{\gamma, \pi^0} (> 100 \text{ MeV}) \equiv 4 \pi I_{\gamma} (> 100 \text{ MeV}) / \langle nL \rangle \quad (\text{IX.A-6})$$

Pollack and Fazio used the observed cosmic-ray spectrum at the earth for their calculations. Stecker (1970) used a demodulated cosmic-ray spectrum to estimate the galactic cosmic-ray spectrum and, for this reason, obtained a slightly higher value of  $1.3 \times 10^{-25} \text{ s}^{-1}$  for  $Q$  (see following discussion). From the OSO-3 satellite observations, Kraushaar et al. (1972) obtained an upper limit for  $Q$  of  $1.6 \times 10^{-25} \text{ s}^{-1}$ ; recently Stecker (1973) obtained a theoretical upper limit of  $\sim 1.5 \times 10^{-25} \text{ s}^{-1}$ , assuming a maximum solar demodulation effect to obtain a maximum galactic cosmic-ray spectrum as deduced by

Table IX.A-1

Gamma-Ray Production Rate from the Decay of  $\pi^0$ -Mesons  
Produced in Interstellar pp, p $\alpha$ ,  $\alpha$ p Cosmic-Ray Interactions

Reference	Energy Range	Rate/H Atom ( $\times 10^{25}$ ) s <sup>-1</sup>
Pollack and Fazio (1963)	> 0 MeV	1.2
Dilworth et al. (1968)	> 50 MeV	1.1
Stecker (1970)	> 100 MeV	1.3 $\pm$ 0.2
Cavallo and Gould (1971)	> 100 MeV	1.8 $\pm$ 0.54
Levy and Goldsmith (1972)	> 100 MeV	3.2
Kraushaar et al. (1972)*	> 100 MeV	< 1.6
Stecker (1973)	> 100 MeV	< (1.51 $\pm$ 0.23)

\*Inferred from observations.

Comstock et al. (1972). Thus, all of the above values for  $Q_{\gamma, \pi^0}$  are basically consistent. The value obtained by Cavallo and Gould (1971) appears to be somewhat high compared with the others, but a value of  $\sim 1.3 \times 10^{-25} \text{ s}^{-1}$  falls within their 30-percent error bracket. It is the author's opinion that a value of  $1.3 \times 10^{-25} \text{ s}^{-1}$  is close to a "best value" for  $Q_{\gamma, \pi^0}$ . The value of Levy and Goldsmith (1972) is a factor of  $\sim 2.5$  higher and requires some discussion.

Figure IX.A-5 shows an up-to-date summary of the accelerator data on total cross section ( $\sigma$ ) times multiplicity ( $\zeta$ ) for neutral pion production in p-p interactions for energies up to  $\sim 1500 \text{ GeV}$  shown as a function of kinetic energy ( $T$ ) (Stecker, 1973). These data are well approximated by the broken power law

$$\sigma_{\pi^0}(T) \zeta_{\pi^0}(T) \cong \begin{cases} 10^{-25} T^{7.64} \text{ cm}^2 & 0.4 \leq T \leq 0.7 \text{ GeV} \\ 8.4 \times 10^{-27} T^{0.53} \text{ cm}^2 & T \geq 0.7 \text{ GeV} \end{cases} \quad (\text{IX.A-7})$$

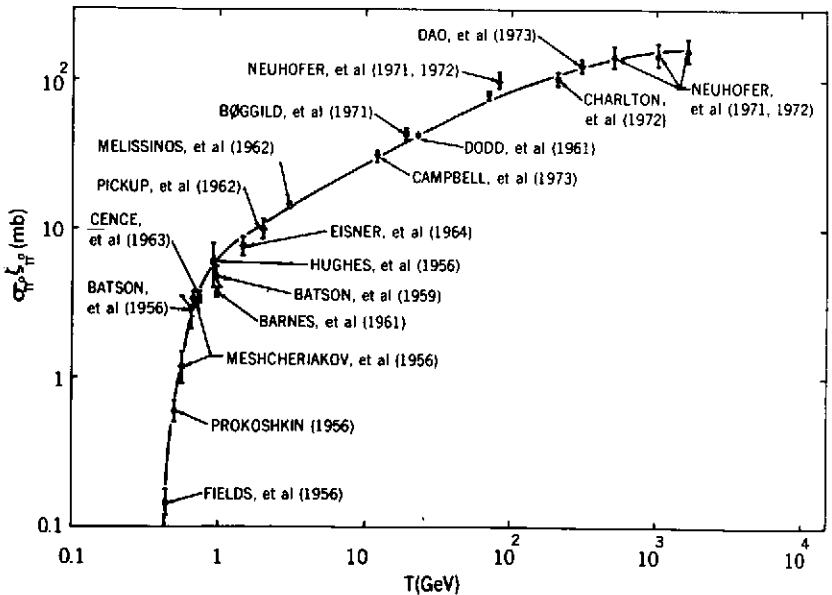


Figure IX.A-5. Cross section times multiplicity for neutral pion production in p-p interactions as a function of incident kinetic energy (from Stecker, 1973).

as the reader can verify from the figure. Taking the cosmic-ray spectrum  $I(T) = 0.15 T^{-2.2} \text{ cm}^{-2} \text{ s}^{-1} \text{ sr}^{-1} \text{ GeV}^{-1}$  used by Levy and Goldsmith (1972), the total  $\gamma$ -ray production rate from p-p interactions is given by

$$\begin{aligned}
 q_{\gamma H} &= 8\pi \int dT I(T) \sigma_{\pi^0}(T) \xi_{\pi^0}(T) \\
 &= 3.77 \times 10^{-25} \int_{0.4}^{0.7} T^{5.44} dT + 3.17 \times 10^{-26} \int_{0.7}^{\infty} T^{-1.67} dT \quad (\text{IX.A-8}) \\
 &= 0.66 \times 10^{-25} \text{ s}^{-1}
 \end{aligned}$$

Adding in the contribution from p- $\alpha$ ,  $\alpha$ -p, and  $\alpha$ - $\alpha$  interactions in the galaxy brings the total production rate per hydrogen atom up to  $\sim 10^{-25} \text{ s}^{-1}$ . There is, of course, some uncertainty in the assumption of the true demodulated galactic cosmic-ray spectrum as distinguished from that observed at the earth. However, using the upper limit to the demodulated cosmic-ray spectrum given by Comstock et al. (1972), an upper limit of  $(1.51 \pm 0.23) \times 10^{-25} \text{ s}^{-1}$  on the  $\gamma$ -ray production rate is obtained, with the error bracket reflecting the experimental error in the accelerator data on  $\sigma_{\xi}$ . The above value is consistent with the value of  $1.6 \times 10^{-25} \text{ s}^{-1}$  given by Kraushaar et al. (1972), which also represents an upper limit since it does not take account of the additional contribution from cool H and H<sub>2</sub> which may be adding to the observed flux.

Why then is there such a large discrepancy between the results presented here and those obtained by Levy and Goldsmith? The answer appears to lie in the difference between assumptions on the total cross section for  $\pi^0$ -production as a function of energy and the multiplicity ( $\xi$ ) assumed. While we have chosen to rely on measurements from accelerator experiments, Levy and Goldsmith adopt a theoretical multiplicity law based on the scaling hypothesis which may hold above 100 GeV. This logarithmic multiplicity law has some empirical support in the cosmic-ray measurements above 70 GeV cited by Levy and Goldsmith, but is contradicted in other cosmic-ray measurements so that the situation at high energies is not as yet clear (Sreekantan, 1972). The logarithmic multiplicity law, based on the scaling prediction, depends on arguments that hold asymptotically in the high-energy limit and that do not appear to be valid below 50 GeV. However, they may begin to be valid within the 50 to 300 GeV energy range, as evidenced by data obtained at the accelerator facilities at Serpukhov and Batavia (Slattery, 1972).

Figure IX.A-6 shows a solid-line fit to the data given in Figure IX.A-5 in comparison with the dashed line that shows the product  $\sigma_{\pi^0} \xi_{\pi^0}$ , based on the assumptions of Levy and Goldsmith for proton kinetic energies greater

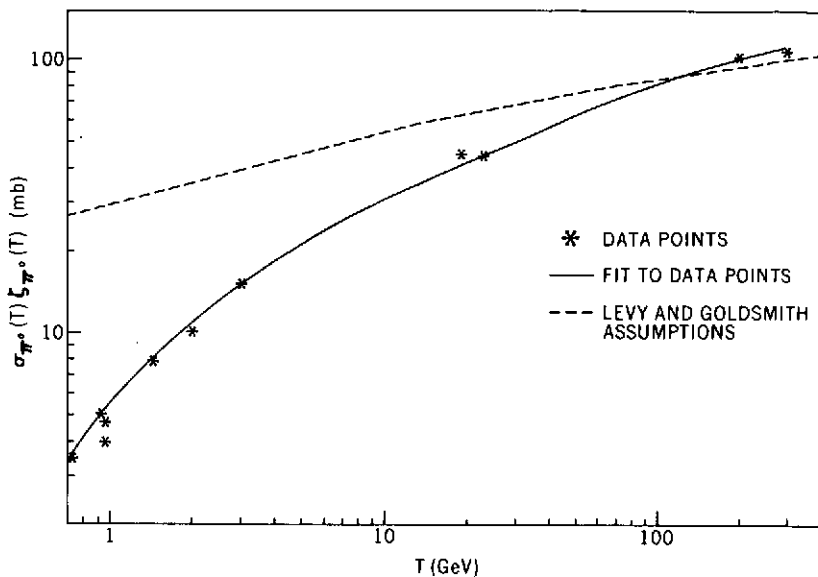


Figure IX.A-6. Comparison of accelerator data from Figure IX.A-5 with the assumptions made by Levy and Goldsmith (1972).

than 1 GeV. The Levy-Goldsmith assumptions show a reasonable fit to the data above 100 GeV where the scaling prediction may hold. However, below 100 GeV the dashed curve is, in all cases, above the data points. Figure IX.A-7 shows the  $\pi^0$ -production function for pp interactions given by the product  $\sigma_{\pi^0} \zeta_{\pi^0} I_p$ , based on the data given in Figure IX.A-5. This figure shows clearly that almost all of the  $\pi^0$ -mesons produced in cosmic-ray pp interactions involve cosmic-ray energies between 1 and 10 GeV. Figure IX.A-8 shows the integral  $\gamma$ -ray production function that is proportional to the integral of the curve shown in Figure IX.A-3, and is defined such that  $Q_{\gamma}^{(pp)} (< \infty)$  corresponds to the total  $\gamma$ -ray production rate/hydrogen atom/s from pp interactions alone (the number  $q_{\gamma H}$ ) given in the previous approximate calculation. It can be seen from Figure IX.A-8 that only 10 percent of the  $\gamma$ -ray production occurs in interactions involving protons below 1 GeV and perhaps another 10 percent occurs in interactions above 30 GeV. This means that (1) because cosmic-ray modulation effects are only important below 1 GeV, the uncertainty in the true cosmic-ray spectrum due to modulation effects produces only a small uncertainty in the total calculated  $\gamma$ -ray production rate, and (2) the uncertainty in the exact form of the pion-multiplicity law  $\zeta_{\pi}(T)$  above 30 GeV produces little uncertainty in the total  $\gamma$ -ray production rate. Indeed, 90 percent of the  $\gamma$ -rays are produced in interactions below 30 GeV where the form of the multiplicity law used by

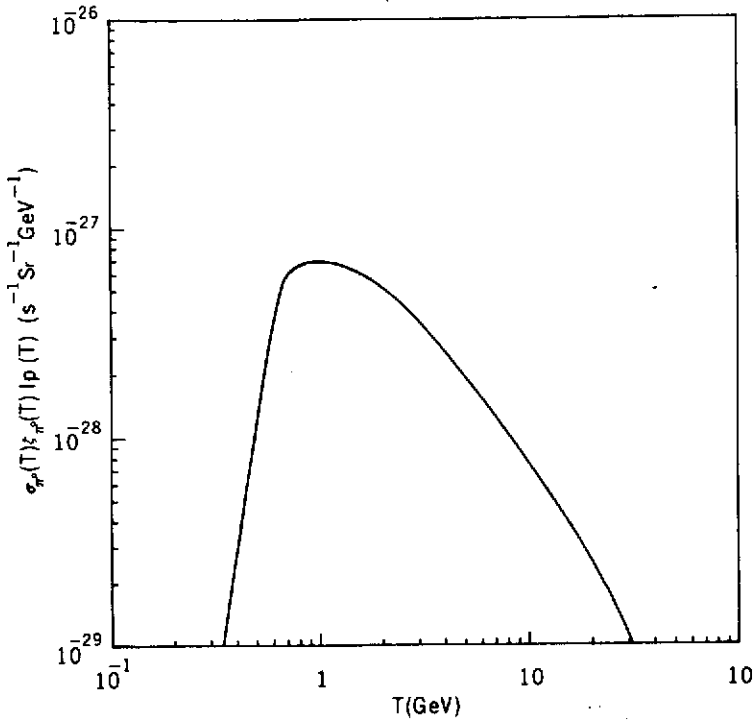


Figure IX.A-7. Differential neutral pion production function from p-p interactions.

Levy and Goldsmith does not hold. Figure IX.A-8 also shows that the median proton energy for  $\pi^0$ -production is  $\sim 3$  GeV. If we compare the values of  $\sigma_{\pi^0} f_{\pi^0}$  used by Levy and Goldsmith with those used here (Figure IX.A-6) at the median  $\pi^0$ -production energy of 3.3 GeV, we obtain a ratio of 2.5 which just corresponds to the ratio between the values for the total  $\gamma$ -ray production rate given by Levy and Goldsmith (1972) and the author (Stecker, 1970). Thus, the discrepancy between the two values is accounted for. The conclusion is that the Levy-Goldsmith value appears to be too high because it is based on an asymptotic multiplicity law that does not hold in the energy range where at least 90 percent of the  $\gamma$ -rays are produced.

### HIGHER ENERGY DECAY PRODUCTS

Mesons and hyperons are also produced in strong inelastic nucleon-nucleon interactions at somewhat higher energies and their important decay modes

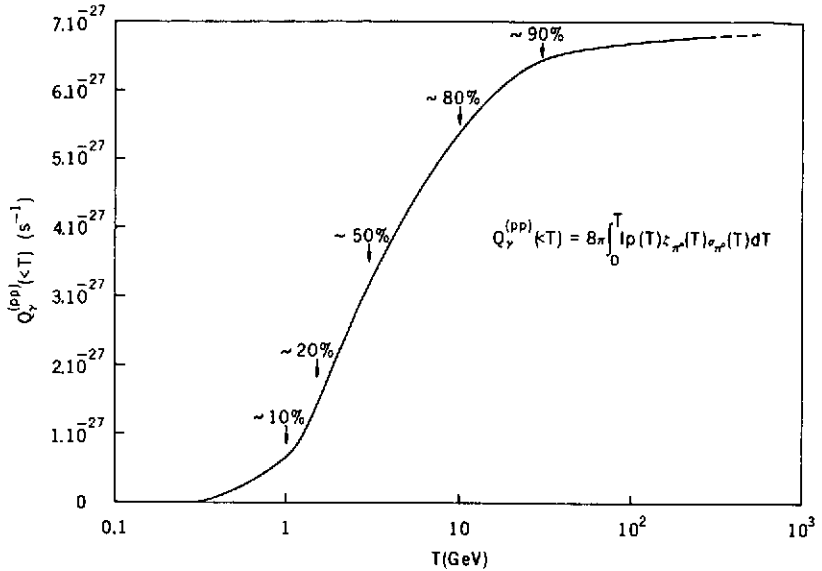


Figure IX.A-8. Integral  $\gamma$ -ray production function from the decay of neutral pions produced in p-p interactions.

leading to  $\gamma$ -ray production are summarized in Table IX.A-2. In addition, nucleon resonances can be formed which lead to decay chains involving  $\pi^0$ -mesons in particular. These processes have been discussed in detail by Stecker (1971a), with particular regard to the  $\gamma$ -ray spectra produced. In particular, it is found from accelerator measurements that hyperons and baryon resonances formed in p-p interactions tend to carry off a roughly constant fraction ( $\sim 60$  percent) of the energy of the incident proton; from this it can be shown that the resulting  $\gamma$ -ray spectra from the decay of these excited baryon states maintain the same power-law form as the incident cosmic-rays at higher energies: if  $I_{\text{cr}} = K_{\text{cr}} E_{\text{cr}}^{-\Gamma_{\text{cr}}}$ , then  $I_{\gamma, N^*, Y} \sim K_{\gamma} E_{\gamma}^{-\Gamma_{\text{cr}}}$ . In particular, if  $\pi^0$ -mesons are produced by a process leading to a multiplicity law  $\xi \propto E_{\text{cr}}^a$ , and given an average energy  $\propto E_{\text{cr}}^b$  where  $b = 1 - a$ , the resulting  $\gamma$ -ray spectrum has the form (at high energies)

$$I_{\pi}(E_{\gamma}) = K_0 E_{\gamma}^{-\Gamma_0} \quad (\text{IX.A-9})$$

where

$$\Gamma_0 = \frac{(\Gamma_{\text{cr}} + b) - (a + 1)}{b} \quad (\text{IX.A-10})$$

Table IX.A-2  
Gamma-Ray Multiplicity and Branching Ratios from  
Hyperon and Meson Decays

Decay Mode	Branching Ratio (R)	Multiplicity ( $\xi_\gamma$ )	$R\xi_\gamma$
$\pi^0 \rightarrow 2\gamma$	1.00	2	2.00
$\Sigma^0 \rightarrow \Lambda + \gamma$	1.00	1	1.00
$K^\pm \rightarrow \pi^\pm + \pi^0$	0.215	2	0.430
$K_1^0 \rightarrow 2\pi^0$	$\frac{1}{2}(0.311)$	4	0.622
$K_2^0 \rightarrow 3\pi^0$	$\frac{1}{2}(0.265)$	6	0.795
$K_2^0 \rightarrow \pi^+ + \pi^- + \pi^0$	$\frac{1}{2}(0.114)$	2	0.114
$\Lambda \rightarrow n + \pi^0$	0.331	2	0.662
$\Sigma^+ \rightarrow p + \pi^0$	0.510	2	1.02

and

$$K_o = \frac{2nLK_\rho \sigma_0 \chi_0^{[\Gamma_{cr} - (a+1)]/b}}{(\Gamma_{cr} + b) - (a+1)} \quad (\text{IX.A-11})$$

For the decay of  $\Sigma^0$ -hyperons, the spectrum is given by

$$I_{\Sigma^0}(E_\gamma) = K_{\Sigma^0} E_\gamma^{-\Gamma_{cr}} \quad (\text{IX.A-12})$$

with

$$K_{\Sigma^0} = \frac{K_{cr}}{2\Gamma_{cr}} nL\sigma_{\Sigma^0} \left( \chi_{\Sigma^0} \frac{M_{\Sigma^-}^2 - M_{\Lambda}^2}{M_{\Sigma}^2} \right)^{(\Gamma_{cr} - 1)} \quad (\text{IX.A-13})$$

(M denoting the mass of the particle subscripted) and for nucleon resonances (isobars)

$$I_i(E_\gamma) = K_i E_\gamma^{-\Gamma_{cr}} \quad (\text{IX.A-14})$$

with

$$K_i = \frac{2K_{cr} R_i nL}{\Gamma_{cr}^2} (2\chi_i)^{(\Gamma_{cr} - 1)} \xi_i E_\gamma^{-\Gamma_{cr}} \quad (\text{IX.A-15})$$

where  $\xi_i$  is typically  $10^{-1} - 10^{-2}$  (Stecker, 1971a). The relevant data for hyperons and isobars are given in Tables IX.A-3 to IX.A-5. Table IX.A-6 shows the relevant data for the fireball models of pion production (Stecker, 1971a) and the resultant differential  $\gamma$ -ray spectra at high energies are shown in Figures IX.A-9 and IX.A-10. The scaling hypothesis predicts a logarithmic increase in pion multiplicity with energy, but the resultant form of the  $\gamma$ -ray spectrum at high energies should be close to the result given in Figure IX.A-10.

### NUCLEON-ANTINUCLEON ANNIHILATION

Gamma-rays from the decay of  $\pi^0$ -mesons produced in nucleon-antinucleon annihilations have spectral characteristics typical of pion-decay  $\gamma$ -rays: a maximum at  $m_\pi c^2/2 \sim 70$  MeV and a nearly flat spectrum in the vicinity of

Table IX.A-3  
Hyperon Cross-Section Data

Proton Momentum (GeV/c)	Lambda Cross Section (mb)	Neutral Sigma Cross Section (mb)	Positive Sigma Cross Section (mb)
4.7	0.051	0.049	0.083
6	0.259	0.077	
10	0.472	0.196	0.239
23.1	Lambda + Neutral Sigma Cross Section = 0.77		
24.5	Lambda + Neutral Sigma Cross Section = 1.13		

Table IX.A-4  
Isobar Cross-Section Data

Incident Momentum (GeV/c)	Cross Section (mb)				
	$\Delta$ (1.237)	N (1.410)	N (1.518)	N (1.688)	$\Delta$ (2.190)
2.85	3.8	-	-	-	-
4.55	1.5	0.63	0.68	0.7	-
6	0.376	-	-	-	-
6.06	0.6	0.65	0.45	0.5	-
7.88	0.41	0.45	0.31	0.46	-
10	0.184	0.544	0.196	0.562	-
15	0.142	0.602	0.160	0.638	-
20	-	0.660	0.170	0.560	0.128
30	-	0.744	0.166	0.576	0.108

Table IX.A-5

Production and Decay Parameters for  
 $\Lambda$ ,  $\Sigma^+$ ,  $\Sigma^0$ ,  $N(1.410)$ , and  $N(1.688)$

Particle	Decay Scheme	Mass (GeV)	Production Threshold Energy (GeV) in P-P Collision	Branching Ratio for $\gamma$ -Producing Modes	Assumed Production Cross Section at High Energies (mb)	Decay Time (s)
$N(1.688)$	$N^+(1.688) \rightarrow N + \pi^0$	1.688	1.80	0.33†	0.6	$\sim 10^{-23}$
$N(1.410)$	$N^+(1.410) \rightarrow N + \pi^0$	1.410	1.24	0.33†	0.6	$< 10^{-23}$
$\Sigma^+$	$\Sigma^+ \rightarrow p + \pi^0$	1.189	1.90	0.510	0.8	$\sim 10^{-10}$
$\Sigma^0$	$\Sigma^0 \rightarrow \Lambda + \gamma$	1.192	1.90	1.00	0.4	$< 10^{-14}$
$\Lambda$	$\Lambda \rightarrow n + \pi^0$	1.115	1.70	0.331	0.4	$\sim 10^{-10}$

† For simplicity, it is assumed that all decays occur via the i-process. More precisely, ~10 to 15 percent of the decays occur via the production of two pions.

Table IX.A-6  
Parameters for Determining Gamma-Ray Spectra  
from Various Pionization Models

Model	Valid Energy Range	a	b	g/b		
				$\Gamma = 2.5$	$\Gamma = 2.7$	$\Gamma = 3.2$
Fermi Model	All $E_p$	0.25	0.75	2.67	2.93	3.6
One-fireball model	$E_p < 150 \text{ GeV}$	0.5	0.5	3.0	3.4	Not Applicable
Two-fireball model	$E_p > 10^3 \text{ GeV}$	0.25	0.75	Not Applicable	2.93	3.6
Landau model	All $E_p$	-	-	Gamma-ray spectrum Proportional to $E_\gamma^{-3.2}$		

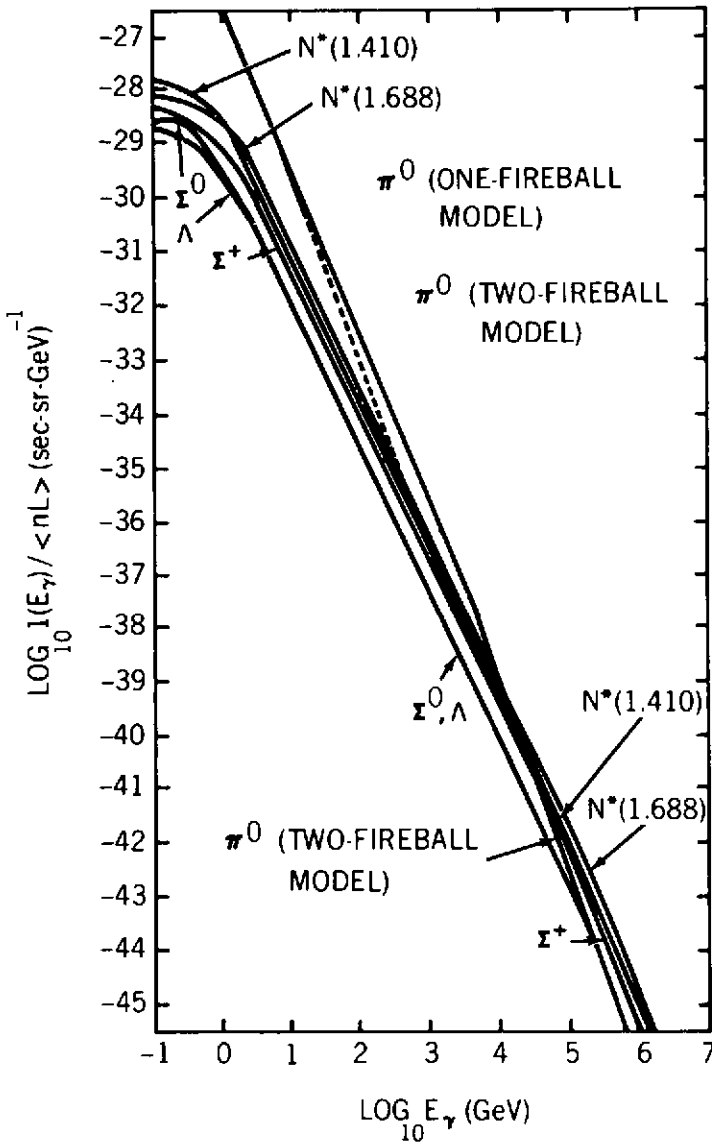


Figure IX.A-9. Calculated  $\gamma$ -ray spectra from various secondary particles produced in galactic cosmic-ray interactions (Stecker, 1971).

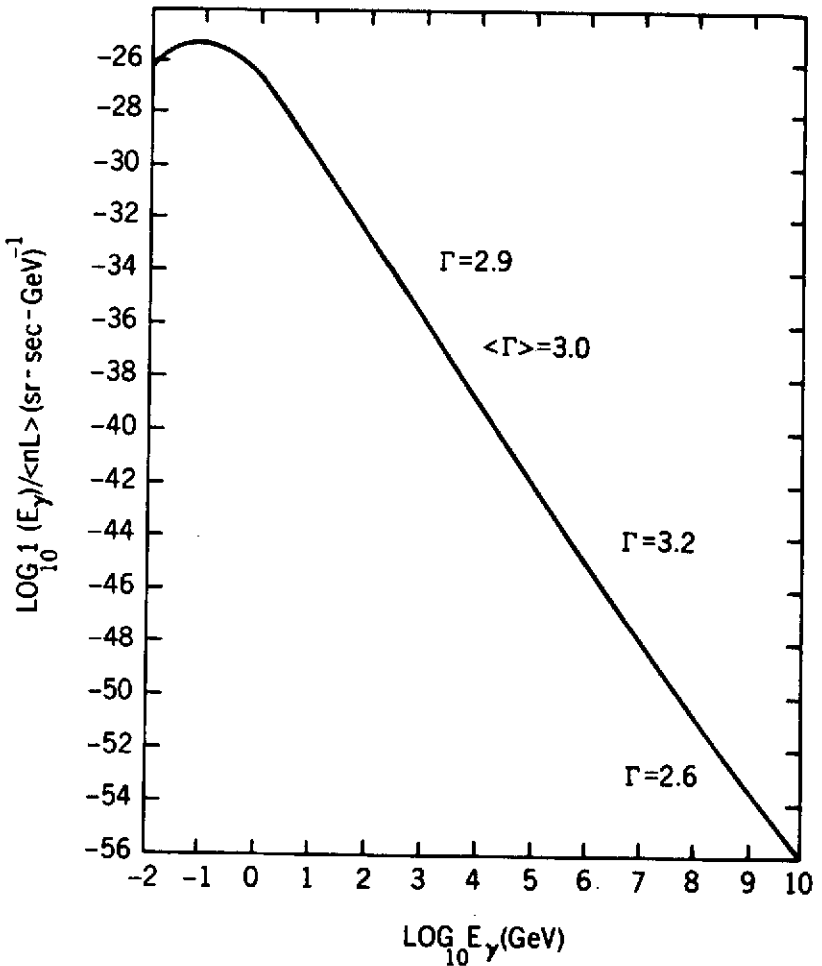
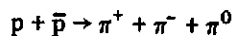


Figure IX.A-10. Total calculated galactic  $\gamma$ -ray production spectrum from cosmic-ray interactions (Stecker, 1971).

the maximum which is symmetric on a  $\log E_\gamma$  plot about the point  $m_\pi c^2/2$ . However, if the annihilations are assumed to occur near rest in the laboratory system (that is, in the universe) the spectrum is bounded between a maximum  $\gamma$ -ray energy of  $\sim 919$  MeV and a minimum energy of about 5 MeV. This is because the maximum energy given to a  $\pi^0$ -meson occurs in the three particle annihilation



(IX.A-16)

and is 923 MeV. (Two-particle annihilations involving  $\pi^0$ -mesons being forbidden by selection rules involving conservation of G-parity (Stecker, 1971a).)

Frye and Smith (1966), using accelerator data, and independently Stecker (1967, 1971a), using a theoretical pion-production model in p-p annihilation, have calculated the resultant  $\gamma$ -ray spectrum from p-p annihilation at rest. There is excellent agreement between the two calculations, and the resultant spectrum, on a logarithmic energy plot, is shown in Figure IX.A-11.

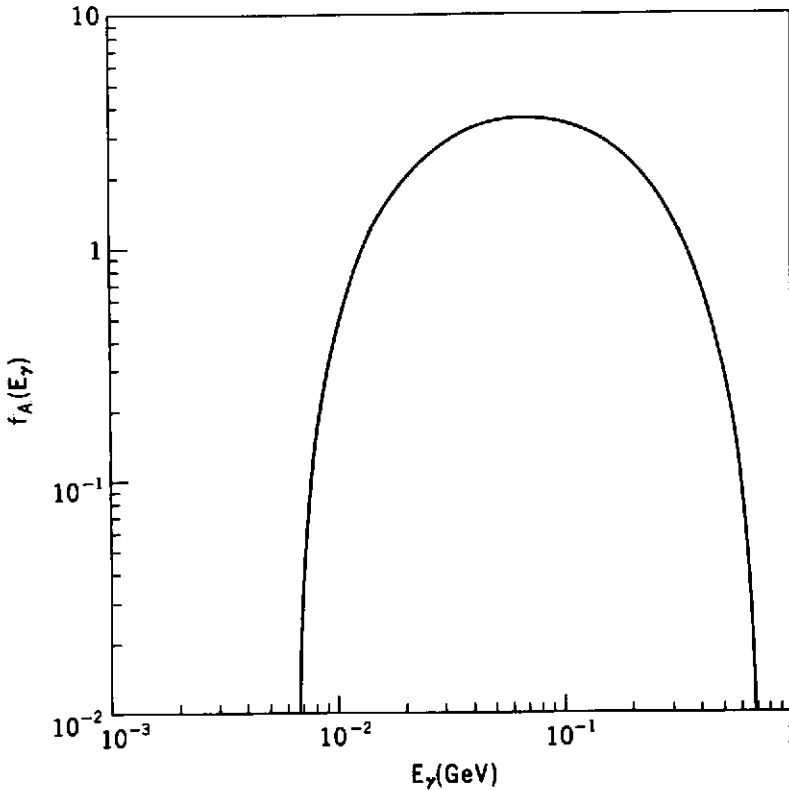


Figure IX.A-11. Normalized local differential  $\gamma$ -ray spectrum from p-p annihilation at rest.

### THE COSMOLOGICAL GAMMA-RAY BACKGROUND

We now turn to a discussion of the isotropic  $\gamma$ -ray background spectrum which is expected to be of cosmological origin. Figure IX.A-12 shows schematically the results of recent observations of this background spectrum by

Trombka et al. (1973), Mayer-Hasselwander et al. (1972), Share et al. (1973), and Kraushaar et al. (1972) (see also Chapters III.A, and IV.A, B, C).

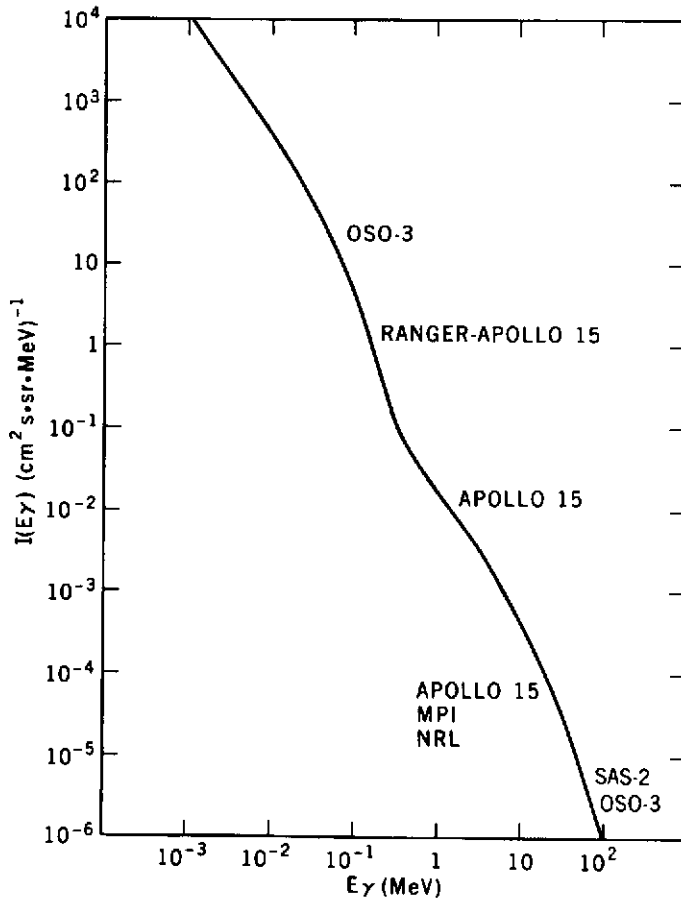


Figure IX.A-12. Recent observational results on the cosmic  $\gamma$ -ray background spectrum.

Results from the OSO-3 detector in the 10- to 100-keV energy range have shown that the background radiation in this range is isotropic to better than five percent over angular scales of 10 degrees (Schwartz, 1970). In the energy range between 0.2 and 4 MeV, Damle et al. (1972) have found evidence for the isotropy of the diffuse background flux. Above 50 MeV, the results from SAS-2 and OSO-3 (Share and Kniffen et al., Chapters IV.A and B) indicate that there is a relatively hard component of  $\gamma$ -radiation of galactic origin, and a true diffuse extragalactic background component observed at

high galactic latitudes that is soft ( $\sim E^{-3}$ ) and that connects smoothly with the Apollo data below 30 MeV (Figures IX.A-12, IX.A-13 and IX.A-14). The evidence would thus seem compelling that the spectrum represented in Figure IX.A-12 is of extragalactic origin and is therefore not consistent with the galactic-origin hypothesis suggested by Cowsik in Chapter VIII.A.

Because of the cosmological aspects relating to studies of the diffuse isotropic  $\gamma$ -ray background, it is necessary to discuss the physics of  $\gamma$ -ray production in past epochs; such radiation may be reaching us today from distances of the order of  $\sim 15$  billion light years. According to big-bang cosmology, the universe was in a smaller, denser state in the distant past and has been continually expanding. This general expansion has caused all electromagnetic radiation to be Doppler shifted to the red (that is, to longer wavelengths which implies lower energies). The red shift is usually designated by  $z \equiv \Delta\lambda/\lambda$ .

This red shift implies that a spectrum of  $\gamma$ -rays, for example, from  $\pi^0$ -decay (either from annihilation or cosmic-ray interactions), that has a maximum at  $\sim 70$  MeV locally, would have that maximum shifted to a lower energy if such radiation were produced at an epoch corresponding to a significant red shift. To find the total spectrum expected to be observed, we must integrate over all red shifts where  $\gamma$ -rays were being produced and weigh the integration with various factors of the quantity  $(1+z)$  (for a complete discussion, see Stecker, 1971a, Chapters 9 to 14). Also, for  $z \gtrsim 100$ , Compton interactions between  $\gamma$ -rays and intergalactic gas may result in energy loss for the  $\gamma$ -rays so that, in general, an integrodifferential transport equation involving  $E_\gamma$  and  $z$  must be solved in order to obtain the expected total  $\gamma$ -ray spectrum resulting from high red shift processes such as matter-antimatter annihilation (Stecker et al., 1971). Absorption processes such as pair-production mechanisms involving intergalactic gas and 2.7 K blackbody photons eliminate  $\gamma$ -rays with large red shifts from various parts of the observed spectrum. Gamma rays arising from any pion-decay process at cosmological distances contribute significantly to the isotropic background only above 1 MeV, because  $\gamma$ -rays at lower energies have been red-shifted by a factor of  $\gtrsim 70$ . Such a red shift corresponds to an epoch when the universe was opaque to  $\gamma$ -rays and absorption effects were important. The basic equation to be solved, the cosmological photon transport (CPT) equation, is of the form

$$\frac{\partial \mathcal{J}}{\partial t} + \frac{\partial}{\partial E} [-E H(z) \mathcal{J}] = \mathcal{Q}(E, z) - \kappa(z)_{AB} + \int_E^{\infty(E)} dE' \kappa(z)_{SC}(E|E') \mathcal{J}(E') \tag{IX.A-17}$$

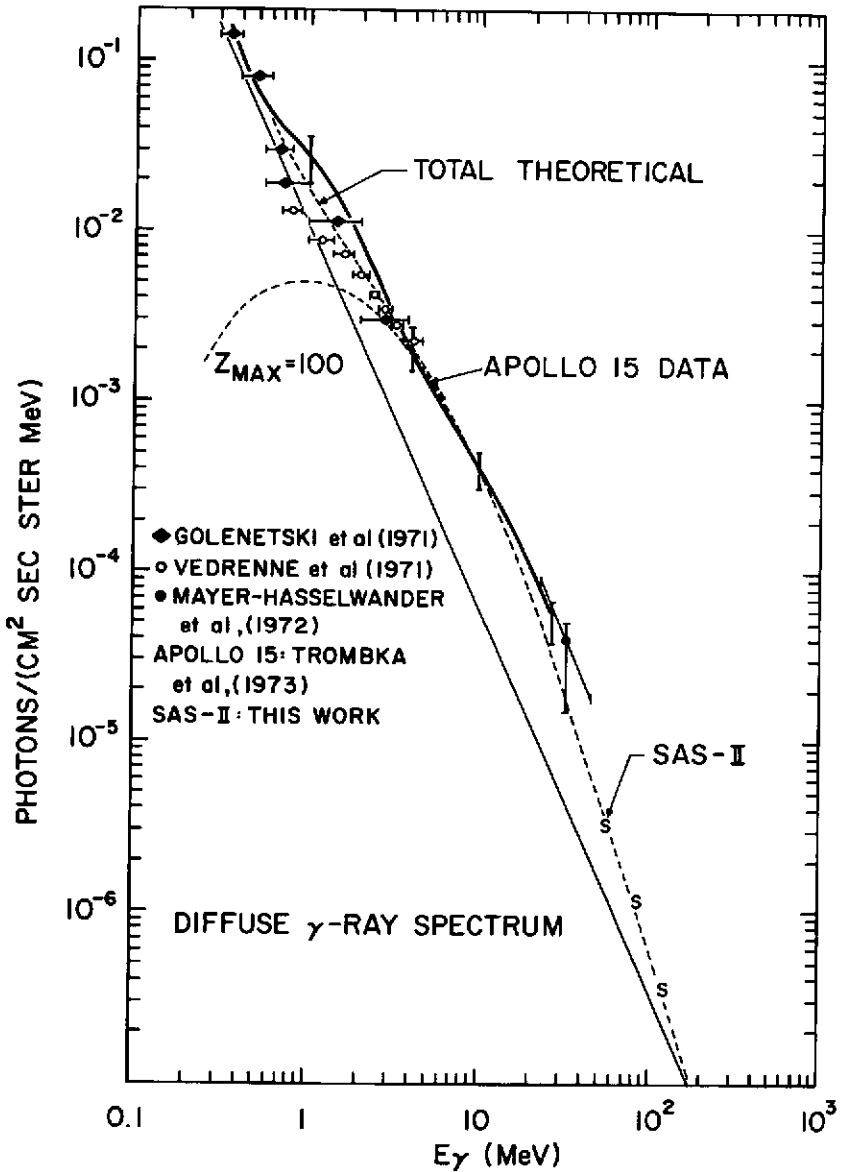


Figure IX.A-13. Comparison of the observed background with a two-component model involving the production and decay of neutral pions produced in intergalactic cosmic-ray interactions at red shifts up to 100. (See also Kniffen et al., Chapter IV.C.).

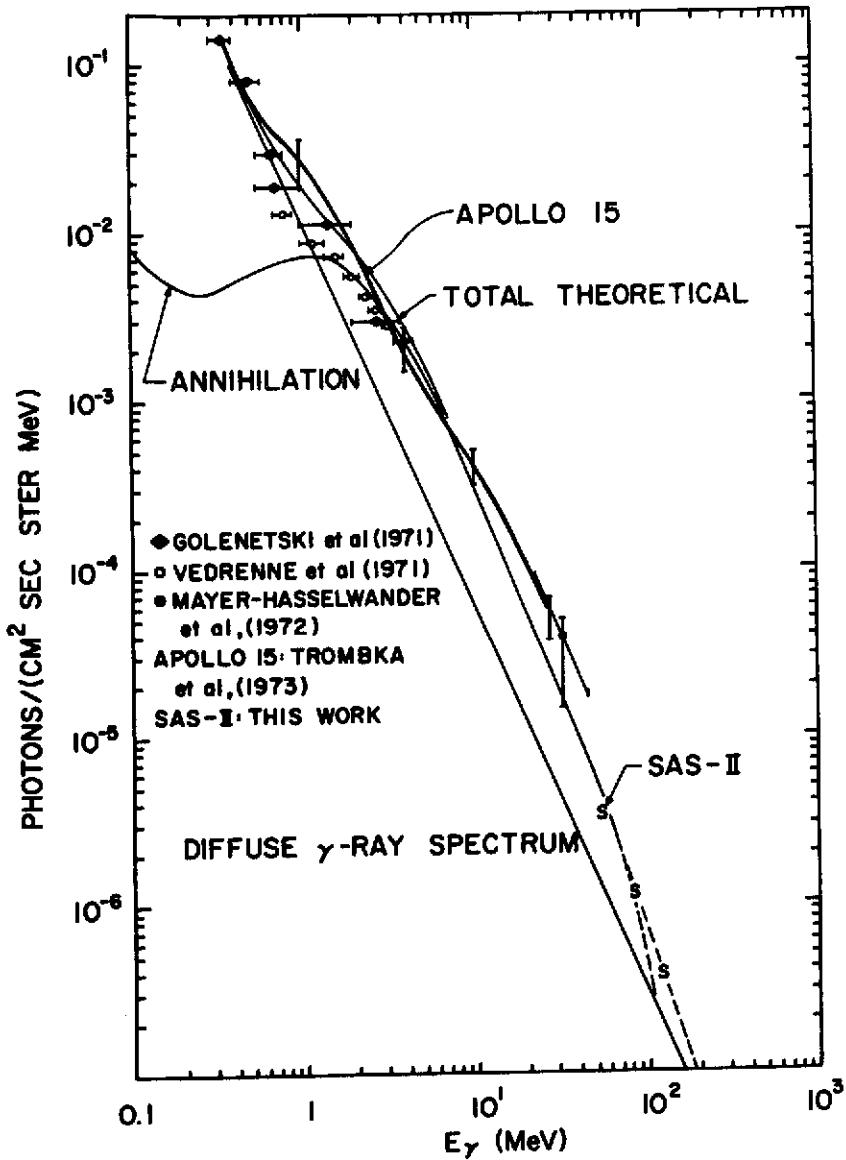


Figure IX.A-14. Comparison of the observed background spectrum with a two-component model involving the matter-antimatter hypothesis as discussed in the text.

where  $E$  is the photon energy, and  $\kappa_{AB}$  and  $\kappa_{SC}$  are the photon absorption and scattering rates (which are a function of  $z$  because the intergalactic gas density is assumed to scale as  $(1+z)^3$  because of the expansion of the universe). The script quantities for the  $\gamma$ -ray intensity and production rate

$$\mathcal{I}(E, z) \equiv (1+z)^3 I(E, z)$$

and

$$(IX.A-18)$$

$$\mathcal{Q}(E, z) \equiv (1+z)^3 Q(E, z)$$

are quantities comoving with the expansion, defined so that their red-shift-density dependence cancels out.  $\mathcal{E}(E)$  is an upper limit on the scattering integral defined by the Compton process and  $H(z)$  is the Hubble parameter which, in terms of the Hubble constant  $H_0$ , is given by the relation

$$H(z) = H_0 (1+z) [1 + \Omega]^{1/2} \quad (IX.A-19)$$

where  $\Omega$  is the ratio of the mean-gas density in the universe to the density needed to close the universe gravitationally. The term

$$\frac{\partial \mathcal{I}}{\partial t} = - (1+z) H(z) \frac{\partial \mathcal{I}}{\partial z} \quad (IX.A-20)$$

and the second term in Equation (IX.A-17) expresses the energy loss of the  $\gamma$ -rays because of the expansion red shift.

### COSMOLOGICAL SPECTRUM FROM MATTER-ANTIMATTER ANNIHILATION

Equation (IX.A-17) can be solved for cosmological models involving the annihilation of nucleons and antinucleons in a baryon-symmetric universe (Stecker et al., 1971; Stecker and Puget, 1972; Puget, 1972; Chapter XV.A).

Between  $\sim 5$  and  $\sim 50$  MeV, Equation (IX.A-17) reduces to a power-law form  $I(E) \propto E^{-\Gamma_{ANN}}$  (Figures IX.A-15 and IX.A-16) with the value for  $\Gamma_{ANN}$  estimated by Stecker and Puget (1972) to be  $\sim 2.5 < \Gamma_{ANN} < \sim 3.5$ .

### ABSORPTION EFFECTS—THE GAMMA-RAY WINDOW

In the vicinity of  $\sim 1$  MeV and below, absorption effects due to Compton scattering become important and cause the spectrum to bend over as shown in Figures IX.A-15 and IX.A-16. Figure IX.A-17 shows the critical red shift for absorption of  $\gamma$ -radiation as a function of observed energy. At lower energies, absorption is due to Compton interactions with intergalactic matter;

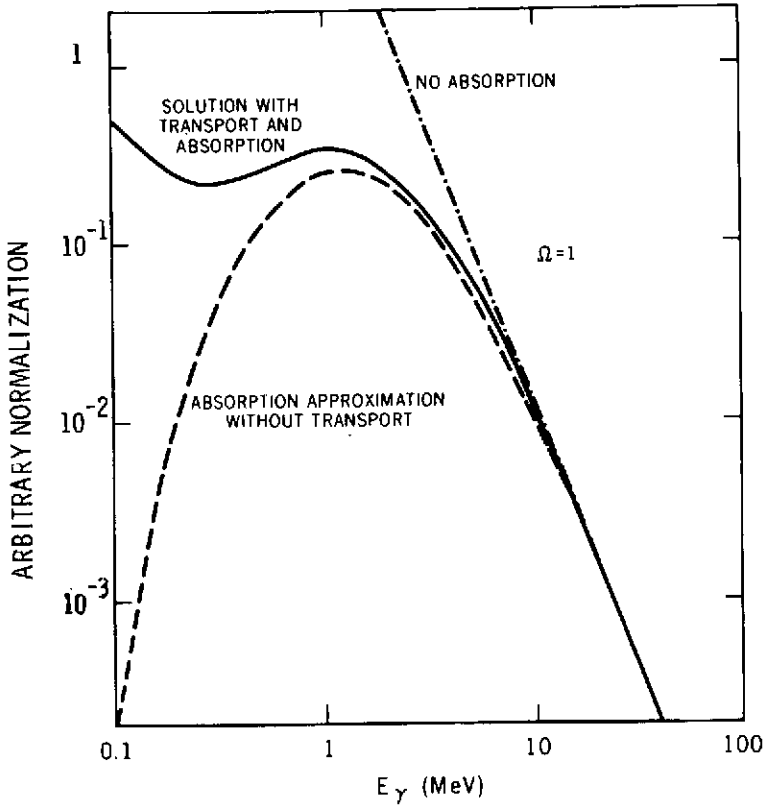


Figure IX.A-15. The cosmological  $\gamma$ -ray spectrum from matter-antimatter annihilation calculated by solving the CPT equation numerically for  $\Omega = 1$ . The solid line represents the complete solution. The other curves represent the effect of neglecting the absorption and scattering (transport) terms in Equation (IX.A-17).

in the intermediate range absorption is due to pair-production interactions with intergalactic matter (Arons and McCray, 1969; Rees, 1969). At the higher energies absorption is due to pair-production interactions with blackbody photons (Fazio and Stecker, 1970). There is a natural "window" between  $\sim 1$  MeV and  $\sim 10$  GeV which is optimal for studying cosmological  $\gamma$ -rays. Absorption effects come in below 1 MeV and above 10 GeV.

#### COSMOLOGICAL SPECTRUM FROM COSMIC-RAY PION DECAY

Figure IX.A-13 shows a two-component model normalized for a best fit to the observations involving the production of intergalactic  $\gamma$ -rays from cosmic-

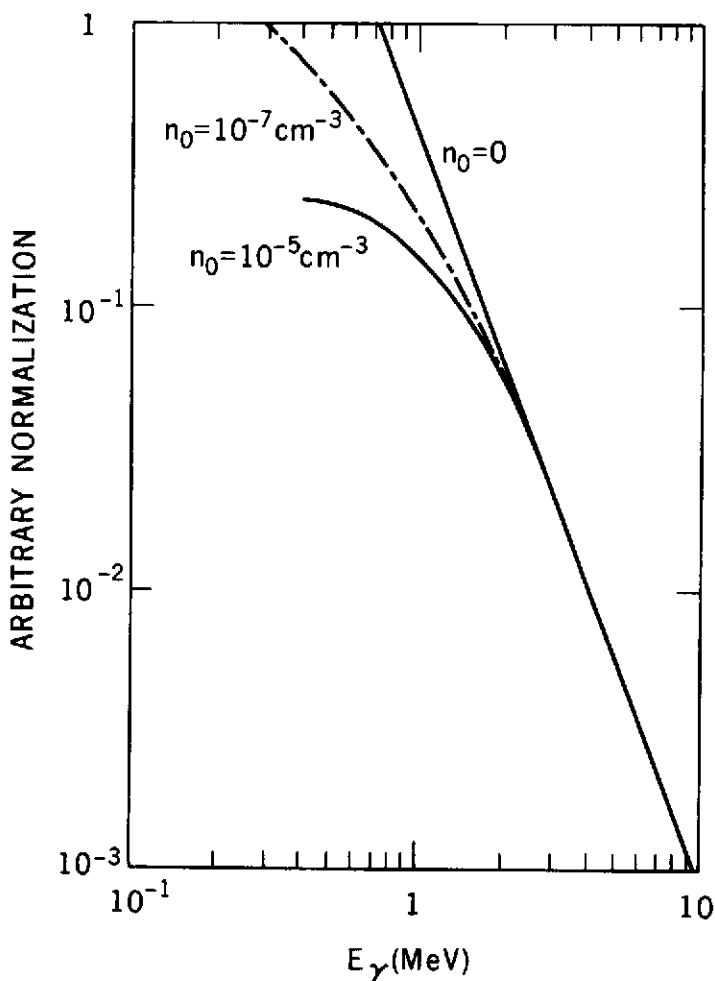


Figure IX.A-16. The effect of absorption of  $\gamma$ -rays at high red shifts by the protogalactic gas.

ray interactions with intergalactic gas producing  $\pi^0$ -mesons out to a maximum red shift of 100 (Stecker, 1969b, c, 1971b). The cosmic rays may be produced in protogalactic sources (protars). Three problems arise with this explanation: (1) even with a relatively steep assumed cosmic-ray spectrum ( $\sim E^{-2.7}$ ) the bulge in the theoretical spectrum may be too large to fit the observations, although this discrepancy may not be too serious considering observational uncertainties; (2) large amounts of energy are needed in cosmic-rays at high

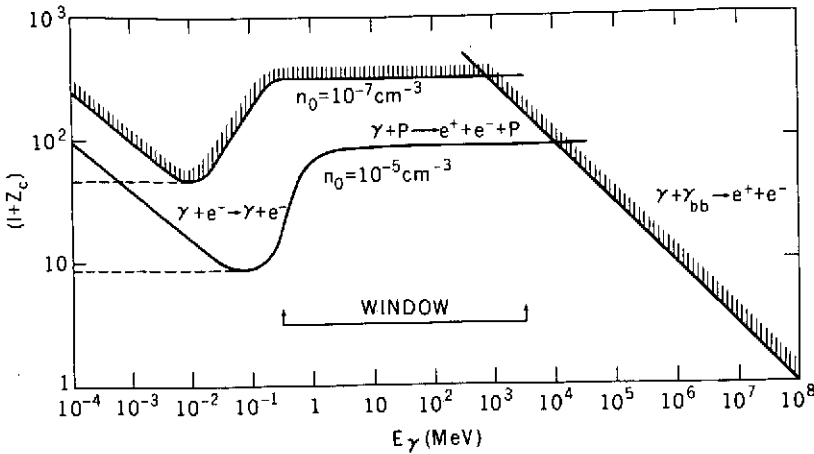


Figure IX.A-17. The critical red shift for absorption of  $\gamma$ -radiation as a function of observed  $\gamma$ -ray energy.

red shifts;\* and (3) the maximum red shift for cosmic-ray production ( $Z_{MAX}$ ) is a free parameter chosen to fit the observations. The matter-antimatter annihilation hypothesis does not suffer from the above mentioned problems. The parameter  $Z_{MAX}$  does not enter into the theory; annihilations occur at all red shifts and the 1-MeV flattening is an absorption effect as discussed earlier. The transport Equation (IX.A-17) was solved to determine the exact form of the spectrum. Energy considerations do not present a problem. Another advantage of the theory is that it arises as a natural effect in a cosmology such as that suggested by Omnès (Omnès, Schatzman, and Puget, Chapters XIV.A, B, and XV.A).

\*In a recent private discussion between the author and P. Morrison, it became apparent that the energy problems may not be too great with this (protar) hypothesis if, indeed, spinars existed at such red shifts of about 70 to 100 (Stecker, 1971b). If it is considered that each spinar produces approximately  $10^{62}$  ergs over a time scale of  $10^7$  to  $10^8$  years (Morrison, 1969), a time comparable to the Hubble time at these red shifts, then at most 20 percent of the presently observed galaxies are needed to have arisen from this early spinar state in order to provide the cosmic-ray energy needed to account for the diffuse  $\gamma$ -radiation above 1 MeV. At a red shift of about 70, the free-fall time for forming spinars from gas clouds is comparable to the Hubble time. This may provide a natural upper limit to the red shift ( $z_{MAX}$ ), for primordial cosmic-ray production in the spinar model. (It should, however, be noted that such spinars may arise in other ways (Stecker, 1971b) and that they may now be a class of moribund objects unrelated to galaxies as we see them now.)

### COSMOLOGICAL ANNIHILATION SPECTRUM COMPARED WITH OBSERVATIONS

Figure IX.A-14 shows a detailed comparison of the annihilation-hypothesis spectrum with present observations assuming  $\Gamma_{\text{ANN}} \cong 2.5$  (see discussion of Stecker and Puget, 1972). The two-component model shown presents an excellent fit to the observational data.

### COSMOLOGICAL COMPTON MODEL

Several other models of isotropic  $\gamma$ -ray production have been put forward recently. One suggestion is that the whole spectrum in the  $10^{-3}$ - to  $10^2$ -MeV range is due to Compton interactions of intergalactic electrons with the universal blackbody radiation (Felten, 1965; Gould, 1965; Hoyle, 1965; Fazio, Stecker, and Wright, 1966; Felten and Morrison, 1966). In its most recent version, Brecher and Morrison (1969) have attempted to explain the observed spectral features, namely, the steepening in the spectrum at  $\sim 40$  keV and flattening above 1 MeV, using the Compton hypothesis. The Brecher-Morrison spectrum is shown in Figure IX.A-18, superimposed on the data-curve of Figure IX.A-12. The fit is reasonable except at the extreme high- and low-energy ends of the energy range. However, Cowsik and Kobetich (1972) have recently recalculated the Brecher-Morrison spectrum using a true blackbody target spectrum and a more realistic energy distribution for Compton-scattered photons (rather than the  $\delta$ -function approximations used by Brecher and Morrison). The result is a smearing out of the spectral features of the Brecher-Morrison model into a smooth power-law spectrum. Other problems with the Brecher-Morrison model stem from the fact that in order to get a large enough flux generated, electrons are required to leak out of normal galaxies in a time much shorter than the  $\sim 10^7$  y deduced for protons on the basis of cosmic-ray isotropy measurements.

### COSMOLOGICAL BREMSSTRAHLUNG MODEL

Another hypothesis that attempts to account for the whole photon spectrum is the electron-bremsstrahlung hypothesis. Figure IX.A-19, which compares the spectrum generated by this process with the observations, shows an excellent fit with the theoretical spectrum based on calculations by Arons, McCray, and Silk (1971) below 1 MeV, and Stecker and Morgan (1972) above 1 MeV. The break at  $\sim 3.5$  MeV is due to energy loss by cosmic-ray electrons interacting with the 2.7 K blackbody radiation. Unfortunately, we again have severe energetic problems with this process, bremsstrahlung being an inherently inefficient  $\gamma$ -ray generating mechanism. Another problem lies in getting galaxies to leak low-energy nonrelativistic electrons at a fast enough rate. Assuming this could be done, an electron spectrum would be distorted by heating the intergalactic medium to  $10^9$  K. The problems with this mechanism

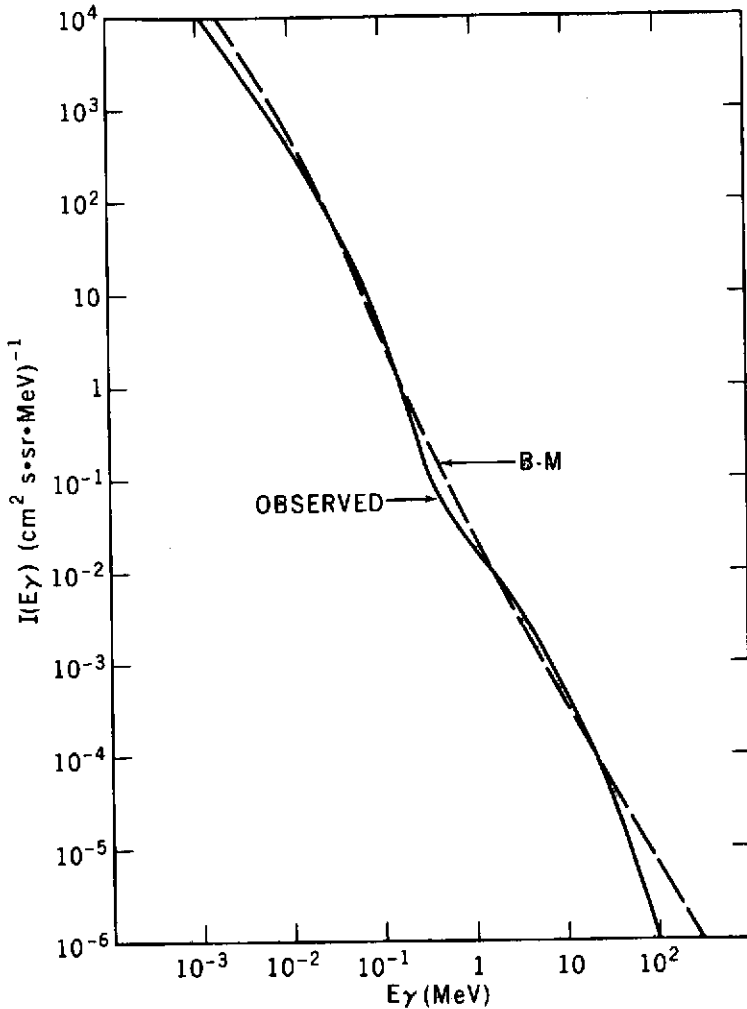


Figure IX.A-18. Comparison of the observed background spectrum with the Brecher-Morrison model.

have been discussed by Setti and Rees (1970), Prilutskii and Rozental (1971), and Cowsik and Pal (1971). (See also Cowsik, Chapter VIII.A.)

### RELATIVISTIC THERMAL SOURCES

One additional mechanism for producing a second component of  $\gamma$ -radiation was suggested by Sunyaev (1970), namely, thermal bremsstrahlung from relativistic electrons in a 20-MeV plasma in such objects as the nuclei of

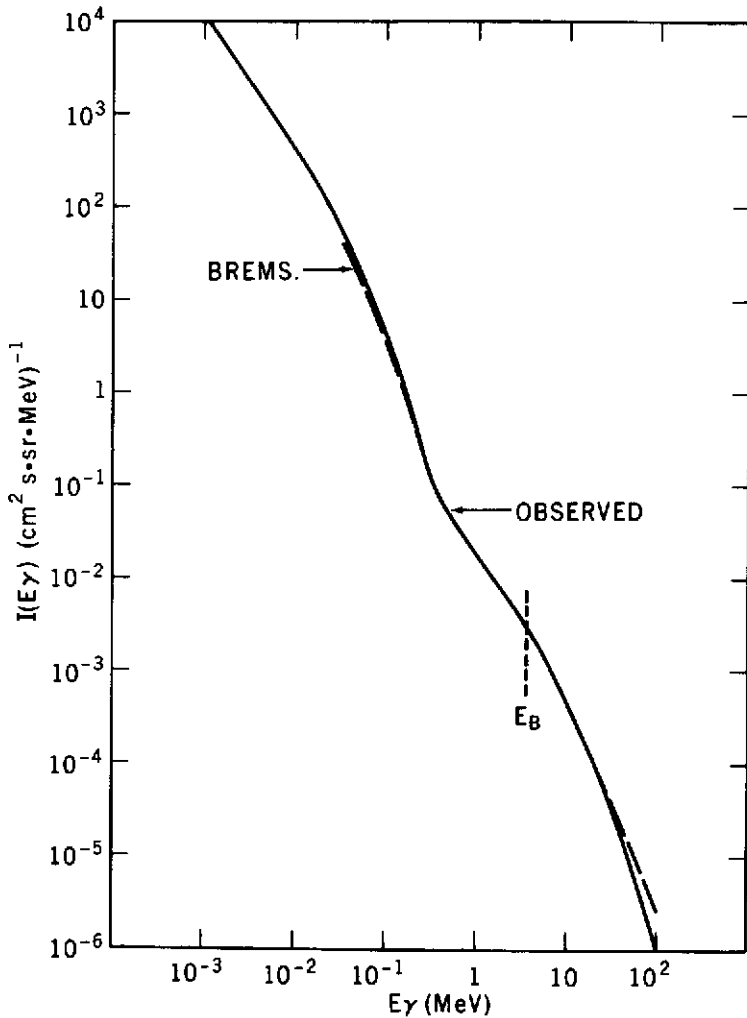


Figure IX.A-19. Comparison of the observed background spectrum with the electron bremsstrahlung model as discussed by Arons et al. (1971) and Stecker and Morgan (1972) with a spectral break at  $E_B = 3.5$  MeV as discussed by Stecker and Morgan.

Seyfert galaxies. This, of course, immediately presents the problem of having enough Seyfert galaxies to account for the observed flux. However, a much more serious problem with the fundamental physics of the mechanism has been pointed out by Prilutskii et al. (1971). They notice that in order to contain the hot relativistic plasma, a magnetic field is required of a strength

such that

$$\frac{H^2}{8\pi} \geq n_e kT \tag{IX.A-21}$$

In that case, the ratio (R) of the electron energy loss rate from synchrotron radiation to that from bremsstrahlung is of the order of

$$R \approx \frac{\sigma_T c (H^2/8\pi) (kT_e/m_e c^2)^2}{\alpha \sigma_T c n_e kT_e} \geq \alpha^{-1} (kT_e/m_e c^2)^2 \gg 1 \tag{IX.A-22}$$

for a relativistic plasma where  $kT_e > m_e c^2$  and  $\alpha^{-1} \approx 137$  ( $\sigma_T$  is the Thomson cross section). In fact, for a plasma of temperature  $T_{\text{MeV}}$  given in MeV,

$$R \approx 500 T_{\text{MeV}}^2 \tag{IX.A-23}$$

Thus, in an optically thin plasma, the synchrotron loss rate is the dominant loss term in the energy-equilibrium equation determining the equilibrium electron spectrum. This will ensure that the electrons have a nonthermal spectrum and produce nonthermal radiation. In addition, the 20-MeV cutoff in the electron spectrum suggested by Sunyaev (1970) will not exist. The details of the argument are further described by Prilutskii et al. (1971).

**SUMMARY—INTERPRETATION OF PRESENT OBSERVATIONS**

It is the opinion of the author, based on the previous discussion, that the most promising theoretical interpretation of the unexpected increase in the observed background flux of  $\gamma$ -radiation above 1 MeV, at present, is that this radiation has arisen from the annihilation of nucleons and antinucleons, primarily at high red shifts, on the boundaries between regions of matter and antimatter (Stecker et al., 1971; Stecker and Puget, 1972; Omnès, Schatzman, Puget, Chapters XIV.A and B and XV.A). This conclusion is, of course, conditional upon future observations and theoretical investigations.

The arguments presented in the paper of Steigman (Chapter XIV.C) put restrictions on baryon-symmetric cosmologies, but nonetheless are not in conflict with the particular cosmological model discussed here and in the papers of Omnès, Schatzman, and Puget (Chapters XIV.A, B, and XV.A).

Tables IX.A-7 and IX.A-8 summarize some of the significant aspects and spectral attributes of the various mechanisms important for the production of the diffuse cosmic  $\gamma$ -radiation. The last column in Table IX.A-7 lists the cosmic domains where the various mechanisms probably play an important

Table IX.A-7

Mechanism	Particle Primarily Involved	Interaction Type	Probable Importance
Compton interactions	Cosmic-ray electrons and low energy photons	Electromagnetic	Extragalactic interactions with 2.7 K blackbody photons
Bremsstrahlung interactions	Cosmic-ray electrons and cosmic gas	Electromagnetic	Extragalactic, possibly galactic below 10 MeV
Neutral pion production (inelastic cosmic-ray interactions)	Cosmic-ray protons and cosmic gas	Strong	Galactic, possibly extragalactic
Neutral pion production in matter-antimatter annihilation	Protons and antiprotons	Strong	Extragalactic, cosmological

Table IX.A-8

Mechanism	Gamma-Ray Spectrum Characteristics		
	Single Interaction	Galactic Spectrum	Cosmological Spectrum
Compton interactions	Flat at typical cosmic-ray energies Peaked toward high photon energy at ultrahigh energies. (Klein-Nishina Theory)	Power-law roughly $I(E_\gamma) \sim E_\gamma^{-2}$ Relation between exponents $\Gamma_c = (\Gamma_e + 1)/2$	Power-law roughly $I(E_\gamma) \sim E_\gamma^{-2}$ Relation between exponents $\Gamma_c = (\Gamma_e + 1)/2$
Bremsstrahlung interactions	Flat at relativistic energies. Peaked toward low photon energy at non-relativistic energies.	Power-law roughly $I \sim E_\gamma^{-3}$ $\Gamma_b = \Gamma_e^\gamma$ (relativistic) $\Gamma_b = (\Gamma_e + 1)$ , non-rel.	Power-law with possible changes of exponent at $\sim 0.04$ , $\sim 1$ , and $\sim 3.5$ MeV.
Neutral pion production (inelastic cosmic-ray interactions)	Flat and symmetric around $m_\pi c^2/2$ on a $\log E_\gamma$ graph (for decay of a single pion)	Maximum at $m_\pi c^2/2$ . Nearly flat near maximum and symmetric on a $\log E_\gamma$ graph. Power-law roughly $I \sim E_\gamma^{-3}$ above a few hundred MeV.	Maximum is red-shifted to some energy between $\sim 1$ and $\sim 70$ MeV. (Note: $m_\pi c^2/2 \cong 70$ MeV). Power-law at higher energies.
Neutral pion production in matter-antimatter annihilation	Flat and symmetric around $m_\pi c^2/2$ on a $\log E_\gamma$ graph (for decay of a single pion)	Expect nonexistent	Spectrum power-law between $\sim 5$ and $\sim 50$ MeV, turns over below 5 MeV and falls off more sharply above 50 MeV.

role. The results from OSO-3 and SAS-2, as summarized in these proceedings in the papers of Share and Kniffen et al. (Chapters IV.A and C), indicate that in the energy range above 50 MeV, there is a distinct hard component of galactic origin and a much softer, high galactic latitude component of extragalactic origin. The galactic component appears to be predominantly (that is, greater than 50 percent) of  $\pi^0$ -decay origin and therefore is small relative to the steep extragalactic component much below 50 MeV. The extragalactic component fits onto the Apollo data (see Peterson and Trombka, Chapter III.A) below 30 MeV, so that all indications are that the flux below 30 MeV is overwhelmingly extragalactic. Because the galactic flux is much harder above 100 MeV than the extragalactic flux, the galaxy stands out well above the extragalactic background at these energies. However, below 30 MeV, the galaxy becomes relatively dim and blends into the background as only a small perturbation. These conclusions are contrary to the galactic origin hypothesis for 0.2- to 10-MeV  $\gamma$ -radiation discussed by Cowsik in Chapter VIII.A, but at present appear to be more consistent with recent satellite observations as presented at this conference.

If the galactic disk component of  $\gamma$ -radiation is primarily of  $\pi^0$ -decay origin, I will stand by my previous arguments (Stecker, 1969a; Stecher and Stecker, 1970; Stecker, 1971a, Chapter 8) that the OSO-3 measurements of Kraushaar et al. (1972) and those obtained by SAS-2 (Kniffen et al., Chapter IV.C) indicate that there may be a substantial amount of molecular hydrogen in the galaxy. This is implied by my recent calculations of the  $\gamma$ -ray production rate (Stecker, 1973) which confirm my earlier calculations of  $1.3 \pm 0.2 \times 10^{-25} \text{ s}^{-1}$  (Table IX.A-1), but are now on a much more solid basis. Forthcoming results from the SAS-2 and Copernicus satellites should settle the question in the near future.

In the galactic center region, the flux should be somewhat softer than in the disk as a whole because of a significant component from Compton interactions (Stecher and Stecker, 1970; Stecker, 1971a, Chapter 8). Preliminary observational results suggest that this is the case (Share, and Kniffen et al., Chapters IV. A and C). Again, here we await the final results from SAS-2.

The note of anticipation is appropriate here because it seems that at the time of this first international  $\gamma$ -ray astrophysics Symposium, we are on the threshold of a new era of observational  $\gamma$ -ray astronomy.

## REFERENCES

- Arons, J., and R. McCray, 1969, *Astrophys. J. Letters*, **158**, p. L91.  
Arons, J., R. McCray, and J. Silk, 1971, *Astrophys. J.*, **170**, p. 431.  
Brecher, K., and P. Morrison, 1969, *Phys. Rev. Letters*, **23**, p. 802.

- Cavallo, G., and R. J. Gould, 1971, *Il Nuovo Cimento*, 2 B, p. 77.
- Clark, G. W., G. P. Garmire, and W. L. Kraushaar, 1968, *Astrophys. J. Letters*, 153, p. L203.
- Comstock, G. M., K. C. Hsieh, and J. A. Simpson, 1972, *Astrophys. J.*, 173, p. 691.
- Cowsik, R., and E. J. Kobetich, 1972, *Astrophys. J.*, 177, p. 585.
- Cowsik, R., and Y. Pal, 1971, *Cosmic Ray Astrophys.*, Tata Institute Press, Bombay.
- Damle, S.V., R.R. Daniel, G. Joseph, and P.J. Lavakare, 1972, *Nature*, 235, p. 319.
- Dilworth, C., L. Maraschi, and G. C. Perola, 1968, *Il Nuovo Cimento*, 56 B, p. 334.
- Fazio, G. G., and F. W. Stecker, 1970, *Nature*, 226, p. 135.
- Fazio, G. G., F. W. Stecker, and J. P. Wright, 1966, *Astrophys. J.*, 144, p. 611.
- Felten, J. E., 1965, *Phys. Rev. Letters*, 15, p. L1003
- Felten, J. E., and P. Morrison, 1966, *Astrophys. J.*, 146, p. 686.
- Fichtel, C. E., R. C. Hartman, D. A. Kniffen, and M. Sommer, 1972, *Astrophys. J.*, 171, p. 31.
- Frye, G. M., and L. H. Smith, 1966, *Phys. Rev. Letters*, 17, p. L733.
- Ginzburg, V. L., and S. I. Syrovatskii, 1964, *Origin of Cosmic Rays*, New York, Macmillan.
- Gould, R. J., 1965, *Phys. Rev. Letters*, 12, p. L511.
- Hayakawa, S., H. Okuda, Y. Tanaka, and Y. Yamamoto, 1964, *Prog. Theo. Phys. (Japan) Suppl.* 30, p. 153.
- Heitler, W., 1954, *Quantum Theory of Radiation*, Oxford Press, London.
- Hoyle, F., 1965, *Phys. Rev. Letters*, 15, p. L131.
- Jones, F. C., 1965, *Phys. Rev.*, 137, p. B1306.
- Kraushaar, W. L., G. W. Clark, G. P. Garmire, R. Borken, P. Higbie, C. Leong, and T. Thorsos, 1972, *Astrophys. J.*, 177, p. 341.
- Levy, D. J., and D. W. Goldsmith, 1972, *Astrophys. J.*, 177, p. 643.
- Mayer-Hasselwander, H. A., E. Pfefferman, K. Pinkau, H. Rothermel, and M. Sommer, 1972, *Astrophys. J. Letters*, 175, p. L23.
- Morrison, P., 1958, *Il Nuovo Cimento*, 7, p. 858.

- Morrison, P., 1969, *Astrophys. J. Letters*, **157**, p. L75.
- Pollack, J. B., and G. G. Fazio, 1963, *Phys. Rev.*, **131**, p. 2684.
- Prilutskii, O. F., Y. P. Ochelkov, I. L. Rozental, and I. B. Shukalov, 1971, *Izvestia Akademii Nauk SSSR*, **35**, p. 2453.
- Prilutskii, O. F., and I. L. Rozental, 1971, *Aston. Zh.*, **48**, p. 489.
- Rees, M. J., 1969, *Astrophys. J. Letters*, **4**, pp. L61 and L113.
- Schwartz, D., 1970, *Astrophys. J.*, **162**, p. 439.
- Setti, G., and M. J. Rees, 1970, *Non Solar X- and  $\gamma$ -Ray Astronomy, I A U Symp. No. 37*, (Rome), L. Gratton, ed. D. Reidel, Dordrecht, Holland, p. 352.
- Share, G. H., R. L. Kinzer, and N. Seeman, 1973, *X-Ray and Gamma-Ray Astronomy, Proc. of IAU Symp. No. 55*, (Madrid), H. Bradt and R. Giacconi, eds. D. Reidel, Dordrecht, Holland.
- Slattery, P. 1972, *Phys. Rev. Letters*, **29**, p. L1624
- Sreekentan, B. V., 1972, *Space Sci. Rev.*, **14**, p. 103.
- Stecker, T. P., and F. W. Stecker, 1970, *Nature*, **226**, p. 1234.
- Stecker, F. W., 1967, *Smithsonian Astrophys. Obs. Spec. Report.*, **261**.
- , 1969a, *Nature*, **222**, p. 865.
- , 1969b, *Astrophys. J.*, **157**, p. 507.
- , 1969c, *Nature*, **224**, p. 870.
- , 1970, *Astrophys. and Space Sci.*, **6**, p. 377.
- , 1971a, *Cosmic Gamma Rays*, NASA SP-249, (Washington, D.C., U.S. Gov't. Print. Off.).
- , 1971b, *Nature*, **229**, p. 105.
- , 1973, *Astrophys. J.*, **185**, p. 499.
- Stecker, F. W., and D. L. Morgan, 1972, *Astrophys. J.*, **171**, p. 201.
- Stecker, F. W., D. L. Morgan, and J. Bredekamp, 1971, *Phys. Rev. Letters*, **27**, p. L1469.
- Stecker, F. W., and J. L. Puget, 1972, *Astrophys. J.*, **178**, p. 57.
- Sunyaev, R. A., 1970, *Pis'ma Zh. Eksp. Teor. Fiz.* **12**, p. 381.
- Trombka, J. I., A. E. Metzger, J. R. Arnold, J. L. Matteson, R. C. Reedy, and L. E. Peterson, 1973, *Astrophys. J.*, **181**, p. 737.

## A. GAMMA-RAY ASTRONOMY AND COSMIC-RAY ORIGIN THEORY

V. L. Ginzburg\*

*P. N. Lebedev Physical Institute*

The science of  $\gamma$ -ray astronomy will yield entirely new information that cannot be obtained by optical, radio, or X-ray astronomy and which will be important for the entire study of high-energy astrophysics, including the astrophysics of cosmic rays and the problem of their origin. Indeed, only  $\gamma$ -ray astronomy allows us to study the nuclear component of cosmic rays far from the earth. (We will refer to the nuclear component here as "cosmic rays" and the electron-positron component as "relativistic electrons.")

Before the present  $\gamma$ -ray observations, we had only indirect knowledge about the cosmic rays far from the earth; this knowledge was obtained mainly by radio observations. The radioastronomical data, as is well known, enable us to obtain the form of the relativistic electron spectrum, but the spectrum itself and the corresponding energy density of the electrons ( $w_e$ ) can be deduced only by making an additional assumption about the strength of the magnetic field ( $H$ ) in the radiating region. To estimate the energy density of the cosmic rays ( $w_{cr}$ ), we have also to assume a relation between  $w_{cr}$  and  $w_e$ . In fact, it is usually assumed that they are proportional, that is,

$$W_{cr} = \kappa_r W_e = \kappa_H^{-1} (H^2/8\pi)V \quad (\text{X.A-1})$$

Here  $w_{cr} = w_{cr} V$ ,  $W_e = w_e V$ , and  $(H^2/8\pi)V$  are respectively the energy of the cosmic rays, the relativistic electrons, and the magnetic field in the source of volume  $V$ ,  $\kappa_r = (w_{cr}/w_e)$  and  $\kappa_H = (H^2/8\pi w_{cr})$ .

Thus, from radio astronomy observations (and also knowing the distance to the source ( $R$ ), we can determine the quantities  $w_{cr}$ ,  $w_e$ , and  $H$  only by fixing the values of  $\kappa_r$  and  $\kappa_H$ . Near the earth,  $\kappa_r \sim 100$ , and in quasi-equilibrium

---

\*Presented in absentia.

conditions, probably  $\kappa_H \sim 1$ . These values are usually assumed, but in doing this two far-reaching assumptions are made. In nonstationary sources of cosmic rays, it is entirely possible that  $\kappa_H < 1$  or even  $\ll 1$ . Close to strong sources of infrared and optical radiation it may turn out that  $\kappa_r \gg 100$  because electrons undergo rapid energy loss. It is possible that in some cases, if mainly electrons are accelerated,  $\kappa_r \ll 100$ .

It is, in principle, possible to use radio and X-ray data together to determine the magnetic field strength (H), itself (or the quantity  $\kappa_r \kappa_H$ ), if the radio emission mechanism is synchrotron radiation and the X-radiation is produced by inverse Compton scattering of the same relativistic electrons in a known radiation field. But, here too, we cannot find the energy of the cosmic rays  $w_{cr}$  directly without assuming the values of  $\kappa_r$  or  $\kappa_H$ .

A vital question has not yet been answered concerning the energy density of cosmic rays  $w_{cr, Mg} = w_{Mg}$  in the metagalaxy (or the metagalactic region close to the galaxy). Metagalactic models for the origin of cosmic rays are still being discussed (Setti and Woltjer, 1971; Burbidge and Brecher, 1971; Shklovskii, 1971) and are sometimes even considered preferable to galactic models for the origin of cosmic rays. In the metagalactic models,  $w_{Mg} \approx w_G$  and  $w_G \equiv w_{cr, G} \sim 10^{-12}$  erg/cm<sup>3</sup>, is the energy density of cosmic rays at the earth and, we may also assume, in a considerable part of the galaxy. I have previously given my views on the origin of cosmic rays on many occasions (Ginzburg, 1970, 1971; Ginzburg and Syrovatskii, 1964, 1967, 1971). I feel that the metagalactic models are much less likely than the galactic models of the origin of cosmic rays. The main arguments rely on energy considerations and are also connected with  $\gamma$ -ray observations. However, these and other arguments are not yet conclusive, especially in regard to local metagalactic models in which  $w_{Mg} \approx w_G$  only in a restricted region in the vicinity of the galaxy.

Since we assume fewer relativistic electrons in the metagalaxy than at the earth (Ginzburg, 1970), in the metagalactic models far from the galaxy,  $\kappa_r \gg 100$ . It is also hard to doubt that in intergalactic space  $\kappa_H \ll 1$  since for  $\kappa_H \sim 1$ ,  $H_{Mg} \sim 5 \times 10^{-6}$  oe. Therefore, we cannot rely on radio and X-ray data to determine the cosmic-ray intensity in remote regions of the galaxy and in radiogalaxies and determine the validity of the metagalactic models; it is necessary to find a new, independent method. Such a method is provided by  $\gamma$ -ray astronomy (see for instance Ginzburg and Syrovatskii, 1964, 1965; Clark, Garmire, and Kraushaar, 1968, 1970; Fazio, 1968; Stecker, 1971; Cavallo and Gould, 1971; Fichtel et al., 1972).

Protons and nuclei in cosmic rays collide with protons and nuclei of intergalactic and interstellar gas. As the result of these collisions, various particles are produced. Of particular importance here are the secondary  $\pi^0$ -mesons and  $\Sigma^0$ -hyperons which quickly decay to produce  $\gamma$ -rays. The probabilities and

kinematics of all the essential reactions are fairly well known (Stecker, 1971; Cavallo and Gould, 1971) and enable us to calculate the spectrum of  $\gamma$ -rays with an accuracy which is entirely sufficient from the point of view of cosmic-ray-origin theory (see Stecker, Chapter IX.A). The integral flux of  $\gamma$ -rays from a discrete source is given by the expression

$$F_{\gamma}(>E_{\gamma}) = \int_{\Omega} I_{\gamma}(>E_{\gamma}) d\Omega \approx \frac{5 \times 10^{23} (\sigma I_{cr}) M \text{ photons/cm}^2\text{s}}{R^2} \quad (\text{X.A-2})$$

where  $\Omega$  is the solid angle subtended by the source,  $R$  is the distance to the source (cm) and  $M$  is the mass of gas in the source in grams. The chemical abundances in the source are assumed to be the same as the common abundances of the elements (especially in the case of He) and thus the average mass of a gas nucleus is taken to be  $2 \times 10^{-24}$  g. The value for  $(\sigma I_G)_{E_{\gamma}=100 \text{ MeV}}$  is taken from Figure X.A-1 to be  $10^{-26} \text{ s}^{-1} \text{ Sr}^{-1}$  as given by Stecker (1971). Therefore

$$F_{\gamma}(>E_{\gamma}) = \frac{5 \times 10^{-3} M (w_{cr}/w_G)}{R^2} \text{ photons/cm}^2\text{s} \quad (\text{X.A-3})$$

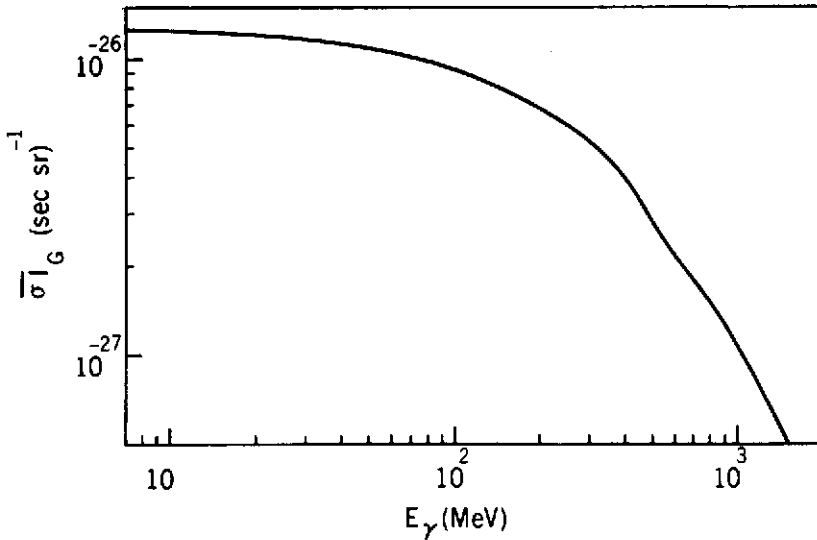


Figure X.A-1. Integral  $\gamma$ -ray production rate (from Stecker, 1971).

where  $w_{cr}$  is the cosmic-ray energy density in the source, assuming that the form of their spectrum is the same as that observed near the earth. Within the limits of this approximation, for sources like the galaxy where nonionized atomic hydrogen predominates,  $M = 1.2 M_{HI}$ , where  $M_{HI}$  is the mass of neutral atomic hydrogen.

The spectrum of  $\gamma$ -rays from  $\pi^0$ -decay is concentrated mainly in the energy range above 50 to 100 MeV (where the  $\gamma$ -rays do not originate in highly redshifted sources). (See Figure X.A-1 and Stecker, Chapter IX.A.) For  $\gamma$ -rays from pion decay, we find

$$\xi = \frac{F_{\gamma}(E_{\gamma} > 50 \text{ MeV}) - F_{\gamma}(E_{\gamma} > 100 \text{ MeV})}{F_{\gamma}(E_{\gamma} > 100 \text{ MeV})} = 0.12 \quad (\text{X.A-4})$$

In the case of bremsstrahlung radiation from relativistic electrons with the spectrum  $I_e(E) = KE^{2.6}$ ,  $\xi = 2.03$ , and for the case of synchrotron radiation or inverse Compton scattering from relativistic electrons  $\xi = 0.74$ . Thus, spectral measurements of the  $\gamma$ -ray flux allow us, in principle, to distinguish between the various production processes and establish the "nuclear" nature of the  $\gamma$ -radiation. Once this is done, measurements of the flux allow us to determine the quantity  $w_{cr}/w_G$  in the source. Here we have assumed that the cosmic-ray spectrum in the source is similar to the spectrum observed near the earth. This determination, even by the method given above, would represent an important step forward and, I feel, would be a very important achievement for high-energy astrophysics.

I wish to illustrate my remarks with two examples of the potential for  $\gamma$ -ray observations of specific astronomical objects, viz., the Magellanic clouds and the galactic center. Observations of the Magellanic clouds provide a potential test for the local metagalactic origin model as well as other metagalactic models of the origin of cosmic rays. If  $w_{Mg} \ll w_G \sim 10^{-12} \text{ erg/cm}^3$  the metagalactic models can be discarded (Ginzburg, 1972). The Large Magellanic Cloud (LMC) and the Small Magellanic Cloud (SMC) distances and neutral-hydrogen masses are approximately equal and are given by (Bok, 1966).

$$R(\text{LMC}) = 55 \text{ kpc}, R(\text{SMC}) = 63 \text{ kpc},$$

$$M_{HI}(\text{LMC}) = 1.1 \times 10^{42} \text{ g}, M_{HI}(\text{SMC}) = 0.8 \times 10^{42} \text{ g}.$$

Therefore, if  $w_{cr} = w_G$ ,

$$F_{\gamma, \text{LMC}}(> 100 \text{ MeV}) \cong 2 \times 10^{-7},$$

$$F_{\gamma, \text{SMC}}(> 100 \text{ MeV}) \cong 1 \times 10^{-7} \text{ photons/cm}^2 \text{ s} \quad (\text{X.A-5})$$

It is important here to note that the fluxes given above follow immediately for any metagalactic model because for these models, by definition, for the Magellanic clouds as well as for the galaxy, the role played by their internal cosmic-ray sources is unimportant and therefore  $w_{Mg} \approx w_G \approx w_{LMC} \approx w_{SMC}$ .

For the galactic models, on the contrary, there is no reason to expect the above quality to hold. Even assuming similar activity of cosmic-ray sources in our galaxy and the Magellanic clouds, it is probable that  $w_G > w_{LMC} > w_{SMC}$  because of the smaller sizes of the clouds and the correspondingly more rapid escape of cosmic rays from them. Besides, in our galaxy there is apparently a strong central source of cosmic rays (which will be presently discussed), but in the clouds there is probably no such source.

Thus, if the metagalactic models are valid, the flux from both Magellanic clouds should be  $\geq 3 \times 10^7$  photons/cm<sup>2</sup>s. (Any additional nonnuclear sources of  $\gamma$ -radiation in the clouds would only serve to increase the flux.)

I now turn to the important question of  $\gamma$ -radiation from the region of the galactic center. Such radiation has already been observed (see elsewhere in these proceedings). Using the values given by Clark, Garmire, and Kraushaar, (1970), and Fichtel et al. (1972), we find

$$F_\gamma(E_\gamma > 100 \text{ MeV}) = (3 - 10) \times 10^{-5} \text{ photons/cm}^2\text{s} \quad (\text{X.A-6})$$

On the basis of spectral measurements (Fichtel et al., 1972) and from several indirect observations, it seems likely that we are observing  $\gamma$ -rays from the galactic center region which were produced by cosmic rays and are the products of the decay of  $\pi^0$ -mesons. Accepting this interpretation, we shall draw several conclusions (Ginzburg and Khazan, 1972). By inserting the result (Equation X.A-6) into Equation (X.A-3), we conclude that the galactic-center region contains a cosmic-ray component of total energy

$$W_c = w_c V_c \approx (3 - 10) \times 10^{66} (w_G/n_c) \sim (3 - 10) \times 10^{54}/n_c \text{ erg} \quad (\text{X.A-7})$$

taking  $R = 10$  kpc. If we assume that the central source is larger than 300 pc, we cannot assume that the gas density is much greater than  $\sim 1 \text{ cm}^{-3}$ . (If  $L_c \sim 10^{21} \text{ cm}$ ,  $V_c \sim 10^{63} \text{ cm}^3$  and  $M_c \sim 2 \times 10^{39} n_c \sim 10^6 n_c M_\odot$  where  $M_\odot$  is the mass of the sun. If  $n_c \sim 10 \text{ cm}^{-3}$ ,  $M_c \sim 10^7 M_\odot$ , which is probably an upper limit for an area of this size.) For  $n_c \sim 1 \text{ cm}^{-3}$ , it follows from Equation (X.A-7) that  $W_c \sim (3 - 10) \times 10^{54} \text{ erg}$ , which is only an order of magnitude smaller than the total energy of cosmic rays in the galaxy (Ginzburg, 1970; Ginzburg and Syrovatskii, 1971).

On the other hand, a result of the order of  $10^{55} \text{ erg}$  is obtained from an analysis of astronomical data indicating that there was an explosion in the

region of the galactic nucleus approximately  $10^7$  years ago (Oort, 1971; Van der Kruit, 1971). A similar number for the energy of cosmic rays produced in an explosion of the galactic nucleus was used in Ginzburg and Syrovatskii (1964).

If the size of the central  $\gamma$ -ray source is less than 200 to 300 pc, then  $n_c$  can be greater than  $10 \text{ cm}^{-3}$ . We then obtain a smaller estimate for  $W_c$  from Equation (X.A-7), but the intensity of cosmic rays  $I_{\text{cr},c} \equiv I_c$  is not diminished. For example, if  $n_c = 10 \text{ cm}^{-3}$  and  $V_c = 10^{63} \text{ cm}^3$ ,  $W_c \sim (3 - 10) \times 10^{53}$  and  $I_c/I_G = W_c/W_G \sim (3 - 10) \times 10^2$ . It seems that it would be rather difficult to confine cosmic rays within a smaller volume for  $10^7$  years. Therefore the value of  $W_c \sim 3 \times 10^{53}$  erg would seem to represent a lower limit and it is more likely that  $W_c \geq 3 \times 10^{54}$  erg. If this is the case, the central cosmic-ray source would be essential from the point of view of the total energy balance of cosmic rays in the galaxy. The average power of injection would be  $U_c \sim W_c/T_c \geq 10^{40}$  erg/s with  $T_c = 10^7$  yr. The number is of the same order of magnitude as the total power of injection used in the galactic-origin models (Ginzburg and Syrovatskii, 1964; 1970).

If future measurements confirm the existence of a central galactic  $\gamma$ -ray source of  $\pi^0$ -decay origin, then we will have one more important argument against the metagalactic models for the origin of cosmic rays, since our own galaxy will then prove sufficient to supply a considerable part of the observed cosmic rays as opposed to other galaxies and quasars which would be the predominant source of cosmic rays in the metagalactic models. This would be true without even taking into account the production of cosmic rays in supernovae and pulsars. (In fact, I feel that the role of supernovae is essential.) The assumption of metagalactic sources for cosmic rays will thus become superfluous.

## REFERENCES

- Bok, B. J., 1966, *Ann. Rev. Astron. and Astrophys.*, **4**, p. 95.
- Burbidge, G., and K. Brecher, 1971, *Comm. Astrophys. and Space Sci.*, **3**, p. 140.
- Cavallo, G., and R. J. Gould, 1971, *Nuovo Cimento*, **B2**, p. 77.
- Clark, G. W., G. P. Garmire, and W. L. Kraushaar, 1968, *Astrophys. J. Letters*, **153**, p. L 1203.
- , 1970, *Bull. American Phys. Soc.*, **15**, p. 564.
- Fazio, G. G., 1968, *Ann. Rev. Astron. and Astrophys.*, **5**, p. 481.
- Fichtel, C., R. Hartman, D. Kniffen, and N. Sommer, 1972, *Astrophys. J.*, **171**, p. 31.
- Ginzburg, V. L., 1970, *Comm. Astrophys. and Space Phys.*, **2**, p. 1.

- \_\_\_\_\_, 1971, *Proc. 12th Intl. Conf. on Cosmic Rays*, Hobart, Tasmania.
- \_\_\_\_\_, 1972, *Nature Phys. Sci.*, **239**, p. 8.
- Ginzburg, V. L., and Ya. M. Khazan, 1972, *Astrophys. Letters*, **12**, p. L155.
- Ginzburg, V. L., and S. I. Syrovatskii, 1964, *The Origin of Cosmic Rays*, New York, Pergamon Press.
- \_\_\_\_\_, 1965, *Uspekhi. Fiz. Nank*, **87**, p. 65.
- \_\_\_\_\_, 1967, *Radio Astron. and the Galactic System, Proc. IAU Symp. No. 31*, H. van Woerden, Academic Press, New York.
- \_\_\_\_\_, 1971, *Proc. 12th Intl. Conf. on Cosmic Rays*, p. 53.
- Oort, J. H., 1971, *Les Noyau des Galaxies*, Pontifical Academia Scientiarum, p. 321.
- Setti, G., and L. Woltjer, 1971, *Nature Phys. Sci.*, **231**, p. 57.
- Shklovskii, I. S., 1971, *Astron. Tsirkulyar SSSR*, **661**, p. 1.
- Stecker, F. W., 1971, *Cosmic Gamma Rays*, NASA SP-249, U. S. Government Printing Office, Washington, D. C.
- Van der Kruit, P. C., 1971, *Astron. and Astrophys.*, **B**, p. 405.

## DISCUSSION

### *Ramaty:*

As far as the galactic center is concerned, what Prof. Ginzburg said is quite clear, but the cosmic rays at the earth are probably not coming from the galactic center. I suppose that what Prof. Ginzburg was trying to do here was take up the argument for galactic origin of cosmic rays. But that question is not necessarily going to be solved by understanding the origin of the  $\gamma$ -rays from the galactic center.

### *Steigman:*

I fully agree with what Reuven Ramaty has just said and the point is, you really do not know what is causing the galactic center source. It could be an enhancement of the density in the galactic center, which is likely to be the case. We do know that the nonthermal radiation background is rather uniformly distributed throughout the galaxies, so some cosmic rays are not produced predominantly in the galactic center.

I would also like to ask a question of Stecker that is related to all of this: The Copernicus results seem to indicate a large amount of molecular hydrogen in interstellar space, perhaps as much as the atomic hydrogen which is indicated by the 21-centimeter observations. A factor of 2 or so increase in the gas density would seem to bring the results for the  $\gamma$ -ray production rate per hydrogen atom below what Cavallo and Gould have suggested and even below the rate Stecker suggested. Does Stecker have any comments about that?

*Stecker:*

Yes. I'm glad you asked that. A factor of 2 was exactly what Ted Stecher and I said was needed in order to explain the OSO-3 measurements, and therefore we did postulate a significant amount of molecular hydrogen and gave arguments for it a couple of years ago (*Nature*, 226, p. 1234, 1970; see also *Nature*, 222, p. 865, 1969).

With regard to the number of cosmic rays at the galactic center and the gas at the galactic center, let me add that in the same paper we estimated that we could only explain about half of the flux seen in the direction of the galactic center on the basis of an increased gas density. On this basis I would agree with Prof. Ginzburg and also Dr. Ulmer, who is here and did some thesis work on this. It would seem that there may well be an enhancement in the cosmic-ray flux toward the galactic center.

*Cowsik:*

Concerning the source from near the galactic center, one point seems to be interesting to note. The number density of stars as we approach the galactic center increases rather quickly; locally it increases as  $R^{-3}$  and below a distance of about half a kiloparsec to a kiloparsec from the galactic center, it seems to level off. If one considers the distribution of stars and if one considers the nonthermal background and some reasonable value, in fact an upper limit on the magnetic flux that can be there, then one knows exactly what the electron density is. It's not substantially higher or lower than what is evident at the earth. In fact, it is about the same. And you know the photon density because you know the starlight density.

If you take these electrons and scatter them, you can calculate the flux of  $\gamma$ -rays that you will get. They are of the right order of magnitude and do have the right distribution of  $\gamma$ -rays towards the galactic center as seen by Clark. Of course, above this center source one needs the uniform source, which can only come by cosmic-ray prior production.

*Stecker:*

Here we should point out that there are strong observational reasons now that the galactic center does have a hard spectrum above 100 MeV and has to be primarily of  $\pi^0$ -decay origin above this energy. This is deduced from the work of Fichtel, et al. (*Astrophys. J.*, **171**, p. 31, 1972) that Prof. Ginzburg referred to, so I think this is fortunately one of the things we do not have to argue about from a theoretical point of view anymore. The flux is primarily of pion decay origin, and I think we'll hear more about it later. (See papers of Share and Kniffen, Chapters IV.A and IV.C.)

*Cowsik:*

I'm just commenting that the flux from the galactic center goes up approximately as the star density increases.

*Stecker:*

But by the same argument, we know the gas density and the dust density go up toward the galactic center.

*Cowsik:*

It goes as  $1/R$ .

*Vette (Session Chairman):*

Let's carry on this one in the coffee break.

## B. GALACTIC GAMMA RAYS: MODELS INVOLVING VARIABLE COSMIC-RAY DENSITY

A. W. Strong, J. Wdowczyk† and A. W. Wolfendale\*  
*University of Durham*

### MODELS INVOLVING VARIABLE COSMIC-RAY DENSITY

It is well known that the variation of the  $\gamma$ -ray flux around the whole galactic plane (Kraushaar et al., 1972) cannot be explained on the simple model of  $\pi^0$ -production in cosmic-ray interactions with the interstellar gas, if the cosmic-ray distribution is assumed uniform and the observed distribution of neutral hydrogen is taken as the only significant gas component (See for example, Clark et al., 1970). This model gives roughly the correct intensities away from the galactic center, but does not reproduce the observed increase by a factor of about three toward the center.

It is possible that point sources are responsible, but models involving supernova remnants as sources appear to be inadequate (de Freitas Pacheco, 1973). If the mechanism is predominantly  $\pi^0$ -decay, as indicated by the results of Fichtel et al., (1972), then other ways of producing the central increase include the presence of large amounts of molecular hydrogen or an increase in the cosmic-ray density toward the center.

### DETAILS OF THE MODELS USED AND RESULTS

We have investigated the last possibility for two particular models of the variation of cosmic-ray density with position in the galaxy. It seems likely that there will be a correlation between mean magnetic field strength ( $H$ ) and the cosmic-ray density, if the cosmic rays are generated within the galaxy. If they arise in sources of high field strength  $H_0 \gg H$ , then we might expect

---

† On leave from the Institute of Nuclear Research, Lodz, Poland.

\* Speaker.

(Woltjer, 1965), from Liouville's theorem, that the cosmic-ray density will be proportional to  $H$ . Alternatively, if there is equipartition of energy between cosmic rays and magnetic fields, then cosmic-ray density will be proportional to  $H^2$ .

Thielheim et al., (1971) have used their model of the galactic magnetic field (Thielheim and Langhoff, 1968) to predict the distribution of synchrotron radiation in the galaxy, assuming the cosmic-ray electron flux is proportional to  $H$ , and they find that it is consistent with the observations at 400 MHz.

For the variation of  $H$  with distance ( $R$ ) (kpc) from the galactic center, we have taken the radial part of their model, that is,

$$H \propto \exp\left(\frac{-R^2}{100}\right) \left\{ 1 - \exp\left(\frac{-R^2}{4}\right) \right\} \quad (\text{X.B-1})$$

The data on line-of-sight distribution of neutral hydrogen from 21-cm surveys was used to calculate the weighted column density

$$N_H(\ell, b) = \int w(\rho, \ell) n_H(\rho, \ell, b) d\rho \quad (\text{X.B-2})$$

where  $\rho$  = distance from the sun, and  $w$  is a weighting factor given by (1)  $w = 1$ , that is, constant cosmic-ray density (equivalent to metagalactic origin); (2)  $w = H/H_\odot$ , where  $H_\odot$  is the field at the sun given by Equation (X.B-1); and (3)  $w = (H/H_\odot)^2$ .

The resulting line fluxes were calculated assuming a rectangular response and adopting the yield function given by Cavallo and Gould (1971):

$$j(\ell, > 100 \text{ MeV}) = \frac{1.8 \times 10^{-25}}{4\pi} k \int_{-\theta_0}^{+\theta_0} N_H(\ell, b) db \text{ cm}^{-2} \cdot \text{s}^{-1} \cdot \text{rad}^{-1} \quad (\text{X.B-3})$$

where  $\theta_0 = 15^\circ$  and  $k$  is a constant to allow for unseen components of the interstellar gas (such as  $H_2$ ), and the possibility that the observed cosmic-ray flux at the earth may not be representative of the local mean flux. The results of these weightings are shown in Figure X.B-1, for  $k=1$ . For  $w=1$  and  $w = H/H_\odot$ , there is insufficient increase towards the center to fit the observations. For  $w = (H/H_\odot)^2$  the fit is quite good for  $k = 1.5$ , as shown in Figure X.B-2. The value  $k > 1$  is indicated by recent observations of significant amounts of  $H_2$  in dense clouds in the interstellar medium.

The advent of detectors with better angular resolution (such as that aboard SAS-2) should allow an improved assessment to be made.

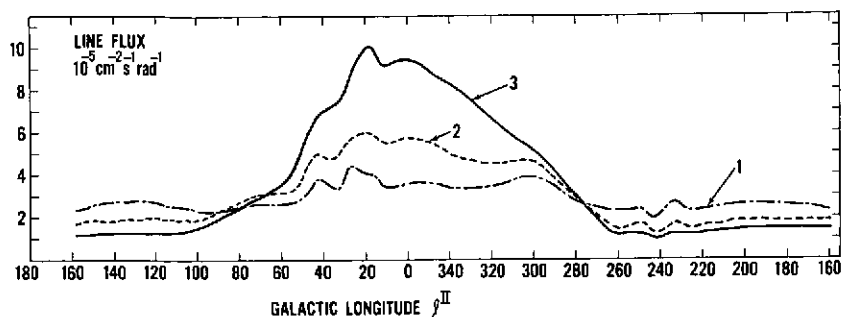


Figure X.B-1. Gamma-ray line fluxes calculated from Equation (X.B-3), with  $\theta_0 = 15^\circ$  and  $k = 1$ . The curves are for weightings (1)  $w = 1$ , (2)  $w = H/H_\odot$ , and (3)  $w = (H/H_\odot)^2$ .

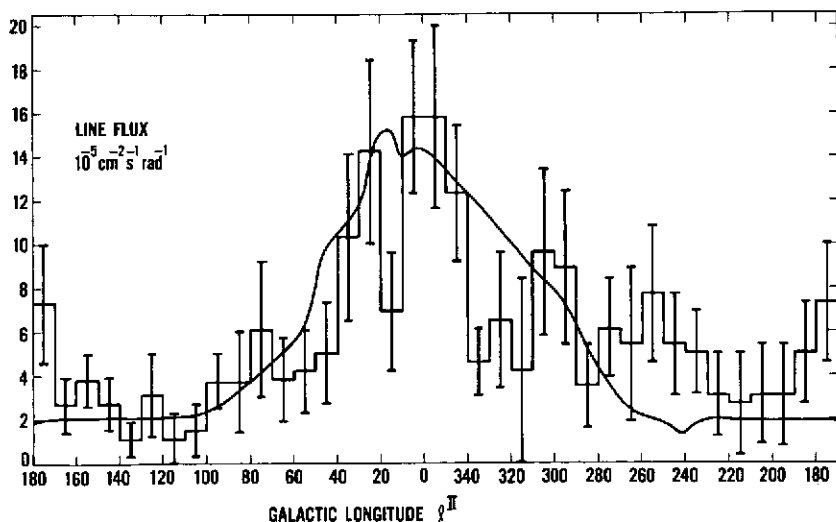


Figure X.B-2. Line fluxes observed by Kraushaar et al. (1972), after subtraction of diffuse background, and prediction of model with  $w = (H/H_\odot)^2$  and  $k = 1.5$ .

Note: This account differs in several respects from that presented at the Symposium and is to be taken as superseding that account. Stecker (Chapter IX.A) has used the most recent accelerator data to obtain a value for the yield above 100 MeV of  $1.3 \times 10^{-25} \text{ s}^{-1}$  per H atom. This implies  $k=2.1$  for Figure X.B-2. This value is still plausible for the reasons stated above.

## REFERENCES

- Cavallo, G., and R. J. Gould, 1971, *Nuovo Cimento*, **2B**, p. 77.
- Clark, G. W., G. P. Garmire, and W. L. Kraushaar, 1970, *IAU Symposium No. 37*, p. 269.
- Fichtel C. E., R. C. Hartmann, D. A. Kniffen, and M. Sommer, 1972, *Astrophys. J.*, **171**, p. 31.
- de Freitas Pacheco, J. A., 1973, *Astrophys. J. Letters*, **13**, p. L97.
- Kraushaar, W. L., G. W. Clark, G. P. Gamire, R. Borken, P. Higbie, C. Leong, and T. Thorsos, 1972, *Astrophys. J.*, **177**, p. 341.
- Thielheim, K. O., and W. Langhoff, 1968, *J. Phys. A: Gen Phys.*, **1**, p. 694.
- Thielheim, K. O., H. J. Kuchoff, W. H. Steib, and G. Wenner, 1971, *Proc. 12th Int. Conf. Cosmic Rays*, Hobart, Tasmania, **7**, p. 2612.
- Woltjer, L., 1965, *Stars and Stellar Systems, Galactic Structure*, **V**, Chicago, p. 531.

## A. PROSPECTS FOR NUCLEAR-GAMMA-RAY ASTRONOMY

Donald D. Clayton\*  
*Rice University*

### INTRODUCTION

Each new astronomy has provided us with new types of information. Radiations of vastly differing wavelengths tend naturally to have their origins in differing physical processes of emission, so that the different astronomical record, by and large, differing types of events. The enrichment of astronomical knowledge is obvious. If history is any reliable guide, we can expect to detect  $\gamma$ -ray lines emitted during the electromagnetic deexcitation of nuclei. Their observation will confirm that excited states of nuclei are being produced, and the fluxes and spectra will identify the specific nuclei and their rate of excitation. Because extreme physical circumstances are required for the production of excited nuclei at low densities where they can be seen, unique information about the source regions will be obtainable.

In this paper prospects for two sources of  $\gamma$ -rays from outside the solar system are considered. Both radioactive decay and inelastic collisions produce nuclei in excited states. As Rutherford emphasized from the beginning, the radioactivity would have all passed away were it not being continually replenished. Therefore, radioactive  $\gamma$ -ray sources in space will be associated with events of nucleosynthesis—probably supernova explosions of some type. The fluxes and spectra will depend on the yield of radioactive nuclei, their  $\gamma$ -ray emission lines, and their half-lives. Inelastic collisions with high-energy cosmic rays are probably not important sources as far as nuclear-deexcitation  $\gamma$ -rays are concerned. The average high-energy fluxes are known to be too small. The best prospect here is for much larger fluxes of MeV particles, especially near the source regions. My attention will fall outside the solar system, thereby intentionally passing over the sun, moon, and planets as interesting special sources.

---

\*Speaker.

## EXPLOSIVE NUCLEOSYNTHESIS

The idea that the common intermediate-mass nuclei are synthesized during their explosive ejection (Arnett and Clayton, 1970) from stars, rather than before it, has one extremely important observational consequence. Several abundant nuclei are ejected in the form of radioactive progenitors, and their decay outside the star can clarify many unproven hypotheses concerning nucleosynthesis. Specifically, if the  $\gamma$ -ray lines from radioactivity in supernova ejecta and in the accumulated background of the universe can be detected (and the anticipated fluxes are promising), it will be possible to:

- Prove supernovae eject new nuclei and measure the supernova yield,
- Prove nucleosynthesis occurs during the explosion rather than prior to it,
- Measure the supernova structure by the profiles of the lines and their Compton tails,
- Discover Galactic supernova remnants,
- Demonstrate that nucleosynthesis is occurring today in the universe and measure its average rate today in the isotropic background,
- Determine whether the average rate of nucleosynthesis has been relatively constant or peaks in the distant past,
- Gain additional information about the average density in the universe, and
- Evaluate evolving versus steady-state cosmologies.

That is a lot to promise; if it is correct, these observations will be as entertaining and profound as other great experiments in astronomy, such as the solar neutrino experiment and the microwave background experiment, for example. My object will be to outline these possibilities as a guide to the chances of successful detection.

### The Radioactive Species

The most abundant species having a radioactive progenitor is  $^{56}\text{Fe}$ . Bodansky, Clayton, and Fowler (1968) showed that ejecta in the process of silicon burning resemble the solar abundances between  $A = 28$  and  $A = 57$  if they contain roughly equal amounts of  $^{28}\text{Si}$  and  $^{56}\text{Ni}$ . This result suggested that several prominent nuclei, primarily  $^{44}\text{Ca}$ ,  $^{48}\text{Ti}$ , and  $^{56}\text{Fe}$  were rejected as radioactive  $^{44}\text{Ti}$ ,  $^{48}\text{Cr}$ , and  $^{56}\text{Ni}$  respectively. Clayton and Woosley (1969) strengthened that result by showing that if the silicon burning had occurred slowly enough for  $\beta$  decays to raise the neutron excess to a value for which  $^{56}\text{Fe}$  itself could be ejected during silicon burning, implausible overabundances of key species would result. They further

strengthened the case for  $^{56}\text{Ni}$  by showing that something similar to an  $e$ -process centered on  $^{56}\text{Ni}$  would also synthesize otherwise troublesome  $^{58}\text{Ni}$ , especially if the free-particle densities were somewhat in excess of their equilibrium values. Clayton, Colgate, and Fishman (1969) used these discoveries to make the first estimates of the importance of  $^{44}\text{Ti}$ ,  $^{48}\text{Cr}$ , and  $^{56}\text{Ni}$  to the  $\gamma$ -ray astronomy of young supernova remnants. Because of the centrality of the  $^{56}\text{Ni}$  versus  $^{56}\text{Fe}$  argument, Hainebach, Arnett, Woosley, and Clayton (1973 preprint) have pursued the evidence favoring  $^{56}\text{Ni}$  even further. They show that two- or three-component  $e$ -processes with differing neutron enrichments (and with freezeout corrections) overwhelmingly select  $^{56}\text{Ni}$  production when asked to produce the solar abundances by superposition. I think the evidence now makes it virtually certain that  $^{56}\text{Fe}$  was ejected dynamically from the synthesizing events as  $^{56}\text{Ni}$ . The preference for low- $\eta$  solutions [Arnett and Clayton (1970); Arnett (1971); Hainebach, Arnett, Woosley, and Clayton (1973 preprint)] in explosive burning of carbon, oxygen, and silicon and continuity arguments strongly suggest that  $^{44}\text{Ca}$  and  $^{48}\text{Ti}$  were also ejected as  $^{44}\text{Ti}$  and  $^{48}\text{Cr}$ . The solar mass fractions of these species, their half-lives, and the prominent  $\gamma$ -ray lines emitted during their decay are included in Table XI.A-1. The  $^{56}\text{Co} \rightarrow ^{56}\text{Fe}$  decay should be, because of its rich spectrum, high abundance, and 77-day half-life, the single most important radioactive decay for  $\gamma$ -ray astronomy. It remains possible, however, that a less abundant product may prove to be easier to detect if the exploding remnants remain opaque too long.

Clayton (1971) discovered that a significant fraction of  $^{60}\text{Ni}$  was probably synthesized as radioactive  $^{60}\text{Fe}$ , with  $\tau_{1/2} = 3 \times 10^5$  yr, or perhaps as  $^{60}\text{Co}$ , with  $\tau_{1/2} = 5.26$  yr. In either case,  $\gamma$ -rays of 1.17 MeV and 1.33 MeV are subsequently emitted. The arguments for and against  $^{60}\text{Fe}$  synthesis are complex and by no means certain. About 1 percent of  $^{60}\text{Ni}$  could be synthesized by arresting about half of the Cr seed at  $^{60}\text{Cr}$  (which decays to  $^{60}\text{Fe}$ ) in the rapid neutron-induced reactions on seed nuclei during explosive carbon burning (Howard, Arnett, Clayton, and Woosley 1971; 1972). Several to fifty percent of  $^{60}\text{Ni}$  may have been synthesized as  $^{60}\text{Fe}$  directly from  $^{56}\text{Fe}$ -seed nuclei in the same event. Clayton (1971) has made the intriguing observation in this regard that only  $^{60}\text{Ni}$  is abundant enough to have absorbed the  $^{56}\text{Fe}$  seed in explosive carbon burning, thereby suggesting that much of the iron seed has been arrested at  $^{60}\text{Fe}$ . Because of the strong (p,n) flows during high-temperature carbon burning, it also seems plausible that a percent or so of the  $^{60}\text{Ni}$  is due to  $^{60}\text{Co}$  nuclei ejected in the explosion. Although  $^{60}\text{Co}$  synthesis should be less efficient than  $^{60}\text{Fe}$  synthesis, it may nonetheless be more important in young remnants because of its favorable half-life, which is long enough to assure transparency yet short enough to have a detectably high decay rate. Without going into the matter further here, I

let  $p_{60}$  be the percentage (fraction  $\times 100$ ) of  $^{60}\text{Ni}$  nuclei synthesized as  $^{60}\text{Fe}$  nuclei and  $p'_{60}$  be the percentage synthesized as  $^{60}\text{Co}$ , and I expect

$$1 > p_{60}(\%) < 50$$

$$0.1 < p'_{60}(\%) < 5$$

I note here that Clayton (1971) did not explicitly include  $^{60}\text{Co}$  in his considerations. However, there do appear to be circumstances in which the  $\gamma$ -rays due to  $^{60}\text{Co}$  synthesis could, for many years, exceed those due to synthesis of all other nuclei.

The  $r$ -process synthesizes many heavy radioactive nuclei, which are expected to have unfortunately small yields. Clayton and Craddock (1965) considered the flux expected from supernova remnants if the  $r$ -process yield were great enough for the "californium hypothesis" of Type I light curves to be correct. In particular, they calculated the expectations of the Crab Nebula in that regard. There is a large range of half-lives present in initial transbismuth debris, however, so their conclusions on the 920 year-old Crab (that the strongest line should be no greater than  $10^{-4} \text{ cm}^{-2} \cdot \text{s}^{-1}$ ) would require recalculation for remnants having different ages and distances. The main problems with this idea would seem to be that it requires the  $r$ -process to be concentrated in relatively rare events in order that these nuclei not be greatly overproduced, and that there seems to be no compelling reason to associate the Type I light curves with radioactivity. I therefore currently hold little hope for this  $\gamma$ -ray source, although additional clarifying remarks will be made later.

### Typical Supernova Yield

In the absence of more certain knowledge, I will assume a simple model of galactic nucleosynthesis in supernovae. Arnett and Clayton (1970) and, more specifically, Arnett (1971) have described the conceptual framework more accurately; however, my aim is only to extract typical numbers for the typical supernova event. Let the explosively synthesized nuclei be coproduced in the same abundance ratios that we find in the solar system in identical supernova events occurring at the galactic rate

$$\dot{N}_{\text{SN}} = R e^{-t/T_R} \quad (\text{XI.A-1})$$

Fowler (1972) finds that  $T_R \approx 4 \times 10^9 \text{ yr}$  and galactic age  $A_G = 12 \times 10^9 \text{ yr}$  are not unreasonable caricatures of  $r$ -process nucleosynthesis (which I take here to characterize all explosive nucleosynthesis). Taking a current supernova

Table XI.A-1  
Average Supernova Yield ( $1.7 \times 10^9$  SN)

Nucleus	$X_{\odot}$	Progenitor	$\tau_{1/2}$	$Y_{SN}$	$E_{\gamma}$ (%) MeV
$^{56}\text{Fe}$	$1.3 \times 10^{-3}$	$^{56}\text{Co}$	77 days	$3.0 \times 10^{54}$	0.84(100), 1.24(67), 2.60(17), 1.03(16) 1.76(14), 3.26(13), 2.02(11), $e^+$ (20)
$^{56}\text{Co}$	$1.3 \times 10^{-3}$	$^{56}\text{Ni}$	6.1 days	$3.0 \times 10^{54}$	0.812(85), 0.748(51), 0.472(34), 1.56(15)
$^{48}\text{Ti}$	$2.3 \times 10^{-6}$	$^{48}\text{Cr} \rightarrow ^{48}\text{V}$	16 days	$6.2 \times 10^{51}$	0.983(100), 1.31(97), $e^+$ (50)
$^{44}\text{Ca}$	$1.9 \times 10^{-6}$	$^{44}\text{Ti} \rightarrow ^{44}\text{Sc}$	48 yr	$5.6 \times 10^{51}$	1.156(100), $e^+$ (94)
$^{60}\text{Ni}$	$2.0 \times 10^{-5}$	$^{60}\text{Fe}(\%p_{60})$ $^{60}\text{Co}(\%p_{60})$	$3 \times 10^5$ yr 5.26 yr	$4.4 \times 10^{52}$	1.17(100), 1.33(100)
$^{238}\text{U}$ (example)	$1.3 \times 10^{-10}$	<i>r</i> -process (example)	$4.5 \times 10^9$ yr	$1.3 \times 10^{47}$	Transuranic plus daughters (many weak possibilities)
$^{57}\text{Fe}$	$3.3 \times 10^{-5}$	$^{57}\text{Ni} \rightarrow ^{57}\text{Co}$	270 days	$7.5 \times 10^{52}$	0.122(98), 0.136(98)

rate  $N_{\text{SN}}^0(\text{today}) = 0.25 \text{ yr}^{-1}$  then gives  $R = 0.5 \text{ yr}^{-1}$ . The initial supernova rate would, with these particular parametric values, have been twenty times greater.

Let the average yield of the typical event be such that its product with the total number of events prior to the birth of the sun shall have produced a galactic mass having solar composition. The total number of such events is

$$N_{\text{SN}} = \int_0^{t_{\odot}} \dot{N}_{\text{SN}} dt = \dot{N}_{\text{SN}}^0 T_{\text{R}} \left[ 1 - e^{-t_{\odot}/T_{\text{R}}} \right] e^{A_{\text{G}}/T_{\text{R}}} \quad (\text{XI.A-2})$$

where  $t_{\odot}$  is the time of solar formation (approximately  $7 \times 10^9 \text{ yr}$ ). The number of events is nearly exponential in  $A_{\text{G}}/T_{\text{R}}$  and multiplied by  $T_{\text{R}}$  if  $T_{\text{R}} < t_{\odot}$ , as seems likely. With the specific choice of parameter values taken above,  $A_{\text{G}}/T_{\text{R}} = 3$  and the number of events would have been  $N_{\text{SN}} = 1.7 \times 10^9$ .

If the mass of the galaxy is  $1.8 \times 10^{11} M_{\odot}$  (Schmidt, 1965) and the mass fraction of iron in the sun is  $X_{\odot} = 1.3 \times 10^{-3}$  (Cameron, 1968), and if the average composition of the galaxy at that time was solar, the galaxy would have contained  $2.3 \times 10^8 M_{\odot}$  of  $^{56}\text{Fe}$ . The average yield for each of the  $1.7 \times 10^9$  contributing events would have been

$$M_{\text{SN}}(^{56}\text{Fe}) = \frac{2.3 \times 10^8 M_{\odot} \text{ of } ^{56}\text{Fe}}{1.7 \times 10^9 \text{ SN events}} = 0.14 M_{\odot}/\text{SN} \quad (\text{XI.A-3})$$

The corresponding number of  $^{56}\text{Fe}$  atoms per event is

$$Y_{\text{SN}}(^{56}\text{Fe}) = \frac{0.14(2.0 \times 10^{33})(6.0 \times 10^{23})}{56} = 3.0 \times 10^{54} \quad (\text{XI.A-4})$$

which would have been ejected initially as  $^{56}\text{Ni}$  atoms. These numbers for several interesting abundances formed explosively as radioactive progenitors are shown in Table XI.A-1.

It is not difficult to question the appropriateness of many of the assumptions leading to this estimate. However, my point of view is that the simplest reasonable argument is the most appropriate one for gearing our expectations.

Table XI.A-1 shows the total yield of  $^{60}\text{Ni}$  to be  $Y_{\text{SN}}(^{60}\text{Ni}) = 4.4 \times 10^{52}$  atoms/supernova. According to the earlier discussion, the yields of  $^{60}\text{Fe}$  and  $^{60}\text{Co}$  are evaluated as

$$Y_{\text{SN}}(^{60}\text{Fe}) = 4.4 \times 10^{50} p_{60} \tag{XI.A-5}$$

$$Y_{\text{SN}}(^{60}\text{Co}) = 4.4 \times 10^{50} p'_{60}$$

The yield of  $^{238}\text{U}$  under these assumptions is listed in Table XI.A-1 only as an example of transbismuth  $r$ -process yield rather than as a nucleus of particular importance for  $\gamma$ -ray astronomy. Indeed, Clayton and Craddock (1965) found that the most important nuclei for the Crab were likely to be  $^{249}\text{Cf}$  and  $^{214}\text{Bi}$ . Nonetheless it is instructive to note that this "typical  $^{238}\text{U}$  yield" is about four orders of magnitude too small for that required for the californium hypothesis of the light curve. If the latter hypothesis is correct, the  $r$ -process will have to have occurred in events about  $10^4$  times less numerous than the typical supernovae we are considering in this section. Whereas this is possible, it suggests that all Type I events are not  $r$ -process events, in which case the original hypothesis loses its "raison d'etre."

**Typical Line Fluxes**

If species  $z$  decays with mean lifetime  $\tau(z) = 1/\lambda_z$ , and if each decay is accompanied by  $g_i$  photons of type  $i$ , then the flux of those  $\gamma$ -rays at the earth due to a nearby supernova is

$$F_i = g_i \frac{\lambda_z Y_{\text{SN}}(z)}{4\pi R^2} e^{-\lambda_z t} \tag{XI.A-6}$$

where  $R$  is the distance to the supernova and  $t$  is the time since its detonation. This formula neglects attenuation due to absorption or scattering in the source and therefore, will be correct only for times which are long enough so that the expanding remnant has become transparent to  $\gamma$ -rays.

Using information from Table XI.A-1 one obtains

$$F_i(^{56}\text{Ni}) = g_i \frac{3.3 \times 10^4}{R^2 \text{ (kpc)}} e^{-(t/8.8\text{d})} \text{ cm}^{-2} \cdot \text{s}^{-1} \tag{XI.A-7}$$

$$F_i(^{56}\text{Co}) = g_i \frac{2.6 \times 10^3}{R^2 \text{ (kpc)}} e^{-(t/111\text{d})} \text{ cm}^{-2} \cdot \text{s}^{-1} \tag{XI.A-8}$$

$$F_i(^{48}\text{V}) = g_i \frac{26}{R^2 \text{ (kpc)}} e^{-(t/23\text{d})} \text{ cm}^{-2} \cdot \text{s}^{-1} \tag{XI.A-9}$$

$$F_i(^{44}\text{Ti}) = g_i \frac{2.1 \times 10^{-2}}{R^2 \text{ (kpc)}} e^{-(t/69\text{yr})} \text{ cm}^{-2} \cdot \text{s}^{-1} \quad (\text{XI.A-10})$$

$$F_i(^{60}\text{Fe}) = g_i \frac{2.7 \times 10^{-7} p_{60}}{R^2 \text{ (kpc)}} e^{-(t/4.3 \times 10^5 \text{ yr})} \text{ cm}^{-2} \cdot \text{s}^{-1} \quad (\text{XI.A-11})$$

$$F_i(^{60}\text{Co}) = q_i \frac{1.6 \times 10^{-2} p'_{60}}{R^2 \text{ (kpc)}} e^{-(t/7.6 \text{ yr})} \text{ cm}^{-2} \cdot \text{s}^{-1} \quad (\text{XI.A-12})$$

Several of these fluxes are shown in Figure XI.A-1 as a function of time. The supernova itself has been placed at  $R = 10^3$  kpc to emphasize that the  $A = 56$  lines may even be observable from supernovae in other galaxies. A supernova in M31, for example, would present a  $^{60}\text{Co}$  line flux above the detectable level of about  $10^{-4} \text{ cm}^{-2} \cdot \text{s}^{-1}$  for more than a year. These lines show a rise time rather than a pure exponential decay, because a specific model was adopted by Clayton et al. (1969), for the transparency of the expanding supernova. They took a rather optimistic (in light of recent nucleosynthesis theory) model — a  $0.5\text{-}M_{\odot}$  ball of iron expanding at  $1.7 \times 10^9 \text{ cm/s}$  so that the product of mean density times radius is

$$\bar{\rho}(t) R(t) \approx 8 \times 10^{13} t^2 \cdot \text{gm} \cdot \text{cm}^{-2} \quad (\text{XI.A-13})$$

which falls below  $10 \text{ gm} \cdot \text{cm}^{-2}$  (a rough estimate of the optical depth for  $\gamma$ -rays) for  $t > 3 \times 10^6 \text{ s}$ . Thus, at best, the lines will be poorly visible for the first month. Even then it is clear that Compton scattering will have a serious effect on the  $\gamma$ -ray spectrum near those times when they begin to emerge. Brown (1973) has calculated this effect for some special cases similar to those considered by Clayton et al. (1969). Figure XI.A-2 shows one of his results when 3.5-MeV and 1.25-MeV lines are emitted isotropically from a depth of  $18.6 \text{ gm} \cdot \text{cm}^{-2}$  within an iron sphere of radius  $37.2 \text{ gm} \cdot \text{cm}^{-2}$ . The total mass of such a sphere depends upon its metric radius, of course, so with  $R(t) = 1.7 \times 10^9 t$  we find that the mass whose line spectrum corresponds to Figure XI.A-2 is

$$M(\text{Fig. XI.A-2}) = \left( \frac{t}{2 \times 10^6 \text{ s}} \right)^2 M_{\odot} \quad (\text{XI.A-14})$$

Therefore the total mass of that example could be any reasonable multiple of a solar mass at time of order a few months. The question of the mass of layers over-lying the CO core at the time of detonation is even more uncertain, but it will clearly be worthwhile to evaluate dynamic models of  $\gamma$ -ray opacity for exploding massive evolved stars. For the time being I wish only to emphasize that whether the  $^{56}\text{Ni}$  lines emerge at all (they did in Figure XI.A-1) depends on the structure and dynamics of the exploding object. Ideally we

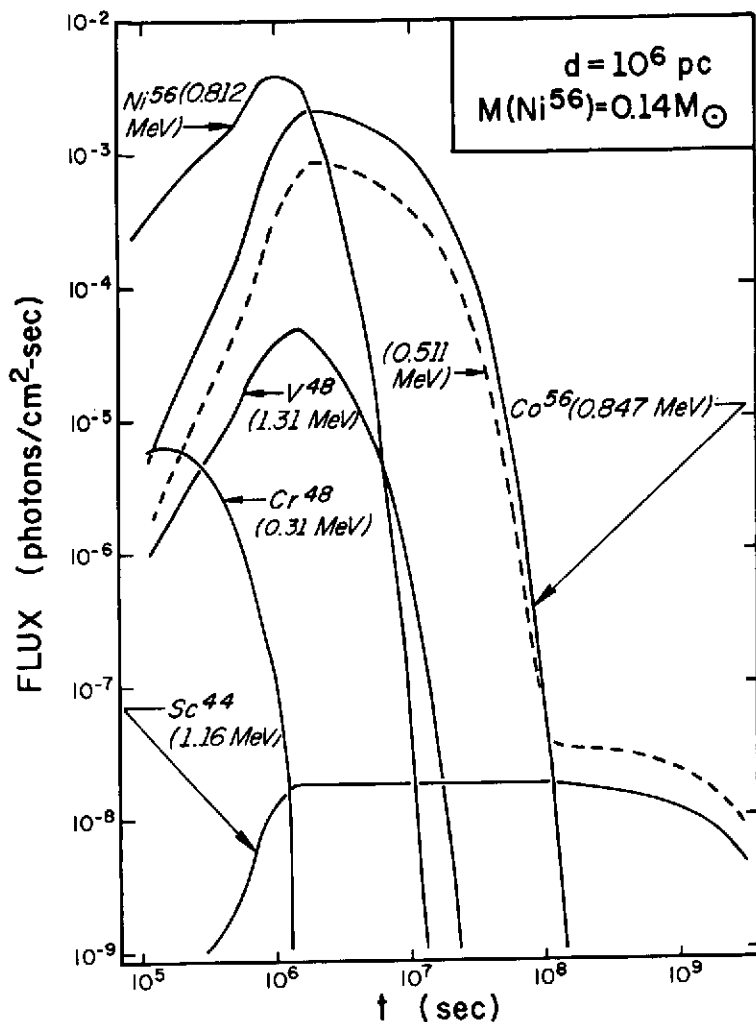


Figure XI.A-1. Prominent medium-lifetime  $\gamma$ -ray line fluxes as a function of time from a distant ( $d=10^6$  pc) supernova ejecting  $0.14M_{\odot}$  of  $^{56}\text{Ni}$  and  $2.0 M_{\odot}$  of  $^{44}\text{Ti}$ . The early growth reflects the increasing transparency of an expanding model (Clayton et al., 1969)

may one day watch these and the  $^{56}\text{Co}$  lines rise to peak intensity before beginning their decay, and the rise time of these fluxes will be a crucial measure of the structure of the exploding object. The 270-day  $^{57}\text{Co}$  lines from  $^{57}\text{Ni}$  progenitors may also play an important role in this problem (Clayton, 1973), although I have not included them here due to their relatively

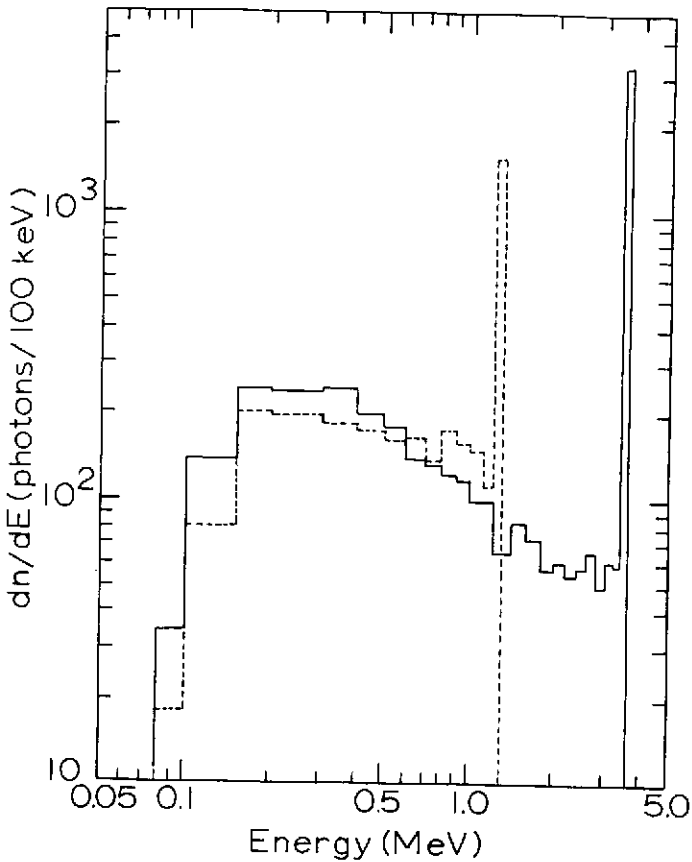


Figure XI.A-2. Effect of Compton scattering on 3.5-MeV lines (solid histogram) and 1.25-MeV lines (dashed histogram) emitted isotropically from a point at a depth of  $18.6 \text{ gm}\cdot\text{cm}^{-2}$  from the surface of an Fe sphere of radius  $37.2 \text{ gm}\cdot\text{cm}^{-2}$  (Brown, 1973).

low energies (136 keV and 122 keV). This astronomy will allow us to measure that structure somewhat analogously to the way neutrino astronomy has allowed us to measure the interior of the sun—and probably with similar surprises.

The 1.16-MeV line emitted subsequent to the decay of the  $^{44}\text{Ti}$  could be quite strong in several present galactic remnants, and will surely emerge even if the  $A = 56$  lines should happen not to get out. In this sense the  $^{44}\text{Ti}$  synthesis may prove to be extremely important. The real need, of course, is for the galaxy to arrange a visible supernova, preferably after (if ever) instruments like HEAO-B are operational. The  $A = 48$  lines, on the other hand, seem likely to be of no special importance, because they are both weaker and shorter lived than the  $^{56}\text{Co}$  lines.

The  $^{60}\text{Co}$  lines have not been entered on Figure XI.A-1, but a comparison of Equations (XI.A-12) and (XI.A-10) show that they are comparable to those of  $^{44}\text{Ti}$  for about 10 years if  $p_{60}$  is around unity (that is, about 1 percent of  $^{60}\text{Ni}$  is due to synthesis of  $^{60}\text{Co}$ , which requires about 2 percent of  $^{56}\text{Fe}$  seed to reside at  $^{60}\text{Co}$  at completion of explosive carbon burning). Remnants throughout the galaxy ( $R < 20$  kpc) should ultimately prove detectable for a decade.

The  $^{60}\text{Fe}$  lines (actually the same as the  $^{60}\text{Co}$  lines but with a much longer half-life) are also not shown in Figure XI.A-1. They are a special case due to the long  $3 \times 10^5$  yr half-life, which ensures that many radiating remnants exist but they may have large angular size due to the long time available for dispersal. For the flux to exceed a detectable  $10^{-4} \text{ cm}^{-2} \cdot \text{s}^{-1}$  requires  $R \leq 160$  pc if 10 percent of  $^{60}\text{Ni}$  is due to synthesis of  $^{60}\text{Fe}$ . A circle of 160 pc radius constitutes about  $10^{-4}$  of the area of the galactic disk and should thus contain one of the approximately  $10^4$  supernovae that should have occurred during the lifetime of  $^{60}\text{Fe}$ . However, the size of a remnant  $10^5$  years old might cover a significant fraction (even half!) of the sky for an event about 100 pc away; therefore, simple on-source-off-source differences will have to be measured with this in mind. The radiation from such sources seems more likely to appear as a general galactic background. The general flux from a wide angle containing the galactic center would be

$$F_{60}(\text{galactic}) \approx 3 \times 10^{-4} \text{ cm}^{-2} \text{ s}^{-1} \quad (\text{XI.A-15})$$

if  $p_{60}$  is about 10 percent. This is also about the same as the average flux from the galaxy due to the  $^{44}\text{Ti}$  lines (Clayton, 1971), but in this case the actual flux depends on the details of the positions and times of the last few galactic supernovae.

As a very crude estimate of transbismuth fluxes, I will assume that every transbismuth species is synthesized with a yield  $Y_{\text{SN}}$  equal to that listed for  $^{238}\text{U}$  in Table XI.A-1. There are so many different half-lives in the  $r$ -process ejecta, moreover, that one may roughly assume that, whatever the age of the remnant, there exists one  $\gamma$ -producing nucleus with a half-life approximately equal to the age of the remnant. This species produces the largest flux. In this case Equation XI.A-6 becomes

$$F_i(\lambda_i=t^{-1}) = q_i \frac{Y_{\text{SN}}(r) e^{-1}}{4\pi R^2 t} \quad (\text{XI.A-16})$$

which has the approximate value

$$\bar{F}_r = \frac{1.25 \times 10^{-5}}{R^2 (\text{kpc}) t (\text{yrs})} \text{ cm}^{-2} \cdot \text{s}^{-1} \quad (\text{XI.A-17})$$

It is obvious that these fluxes will not commonly be observable unless the  $r$ -process is restricted to much rarer events, thereby raising the yield of each

event. This conclusion, stated earlier, renders this particular prospect unlikely. Clayton and Craddock (1965) took a yield four orders of magnitude greater to provide radioactive power for the Crab light curve and were thereby able to calculate marginally detectable lines from the Crab. Equation (XI.A-17) yields only  $\bar{F}_r \approx 10^{-8} \text{ cm}^{-2} \cdot \text{s}^{-1}$  from the Crab, and is probably a more realistic estimate. The site of the *r*-process is so poorly understood, however, that a great surprise would come as no shock.

### The Universal Background

One need only appreciate that the average galactic luminosity due to radioactive  $\gamma$ -rays has been  $3 \times 10^{40} \text{ erg} \cdot \text{s}^{-1}$  to realize that their contribution to the isotropic background radiation may be significant. The cosmological principle allows us to estimate their flux very easily. Taking  $H_0 = 55 \text{ km s}^{-1} \text{ Mpc}^{-1}$  (Sandage, 1972), the observed universal density of matter is  $\rho = 1.7 \times 10^{-31} \text{ gm} \cdot \text{cm}^{-3}$  (Oort, 1958). If the average mass fraction of  $^{56}\text{Fe}$  is  $X_{\odot} (^{56}\text{Fe}) = 1.3 \times 10^{-3}$ , this corresponds to  $2.2 \times 10^{-34} \text{ gm} \cdot \text{cm}^{-3}$  of  $^{56}\text{Fe}$ . Consequently, the average iron number density in the observed universe is

$$n(^{56}\text{Fe}) = 2.3 \times 10^{-12} \text{ cm}^{-3} \quad (\text{XI.A-18})$$

The flux of these  $\gamma$ -rays/sr is (Clayton and Silk, 1969)

$$\frac{\partial F}{\partial \Omega} = \frac{c}{4\pi} g_{\gamma} n(^{56}\text{Fe}) \quad (\text{XI.A-19})$$

where  $g_{\gamma}$  is the number of  $\gamma$ -rays emitted per  $^{56}\text{Fe}$  nucleus synthesized. The value of  $g_{\gamma}$  is 2.8 for only  $^{56}\text{Co}$  decays and  $g_{\gamma} = 4.9$  if both  $^{56}\text{Ni}$  and  $^{56}\text{Co}$  decays are used. Taking the latter value yields

$$\frac{\partial F}{\partial \Omega} = 2.7 \times 10^{-2} \text{ cm}^{-2} \cdot \text{sr}^{-1} \cdot \text{s}^{-1} \quad (\text{XI.A-20})$$

To emphasize the size of this flux, Clayton and Silk (1969) pointed out that it is as large as the total integrated universal background at photon energies in excess of 300 keV. Clearly it must be an important component of that background unless the  $A = 56$  lines do not escape from their sources. Because this estimate is based on the observed mass density, it will be proportionately greater if the universe contains "hidden matter" that has also synthesized  $^{56}\text{Fe}$ .

The simple density argument does not determine the frequency distribution of the photons comprising the flux in Equation XI.A-19. For those  $^{56}\text{Fe}$  nuclei synthesized early in the universe, the associated  $\gamma$ -rays will now have been considerably red shifted. It is just this feature that allows the spectrum to carry a wholly new astrophysical datum; that is the red shift distribution in the  $\gamma$ -ray spectrum measures the distribution of the ages of  $^{56}\text{Fe}$  nuclei. Hidden in it is the chronological account of the rate of nucleosynthesis.

Let  $f(t)$  be the rate per unit of cosmic time at which  $^{56}\text{Fe}$  nuclei were (and are being) synthesized. Let it be normalized such that

$$\int_0^{t_0} f(t) dt = 1 \tag{XI.A-21}$$

so that  $f(t)dt$  is the fraction of all  $^{56}\text{Fe}$  nuclei that were synthesized at cosmic time ( $t$ ) in the interval  $dt$  ( $t_0 =$  cosmic time today). It follows that  $f(t)dt$  is also the fraction of  $A = 56$   $\gamma$ -rays whose travel times are  $t_0 - t$  in the interval  $dt$ . In any standard cosmological model the travel time  $t_0 - t$  is some function of the red shift ( $z$ ). Thus  $f(t) = f(z)$  and  $f(t) (dt/dz)dz$  becomes the fraction of the photons having the red shift  $z$  in the interval  $dz$ . The  $\gamma$ -ray source function per unit time per unit  $^{56}\text{Fe}$  nucleus per unit energy interval in the rest frame is just

$$P(E,t) = \sum_i P_i(E,t) = \sum_i g_i \delta(E - E_i) f(t) \tag{XI.A-22}$$

where the sum is over the lines of type  $i$  emitted with rest energy  $E_i$  emitted with rest energy  $E_i$  at the rate of  $g_i$   $\gamma/^{56}\text{Fe}$  nucleus synthesized. The differential flux today due to  $\gamma$ -rays of type  $i$  is

$$\begin{aligned} \frac{\partial^2 F_i}{\partial E \partial \Omega} &= \frac{c}{4\pi} n(^{56}\text{Fe}) \int_0^{t_0} \frac{R(t_0)}{R(t)} P_i \left[ \frac{R(t_0)}{R(t)} E, t \right] dt \\ &= \frac{c}{4\pi} n(^{56}\text{Fe}) \int_0^\infty (1+z) P_i \left[ (1+z) E, t \right] \frac{dt}{dz} dz \end{aligned} \tag{XI.A-23}$$

where  $E$  is the energy today of the photon and  $R(t)$  is the scale factor of the universe. (See for example McVittie, 1965). Because

$$\frac{E}{E_i} = \frac{R(t)}{R(t_0)} = \frac{1}{1+z} \tag{XI.A-24}$$

the integral over cosmic emission time can also be expressed as an integral over received energies:

$$dt = \frac{R(t_0)}{R(t)} \frac{dE}{E_i} \tag{XI.A-25}$$

This integral is easily done due to the  $\delta$ -function nature of  $P_i$  to give

$$\frac{\partial^2 F_i}{\partial E \partial \Omega} = \frac{c}{4\pi} \frac{g_i n(^{56}\text{Fe})}{E_i} \frac{R(t_0)}{\dot{R}(t_E)} f(t_E) \tag{XI.A-26}$$

where the time  $t_E$  is the solution of Equation (XI.A-24). In the Friedman dust models one has (Weinberg, 1972)

$$\frac{\dot{R}(t_E)}{R(t_E)} = \frac{E_i}{E} H_0 \left[ 1 - 2q_0 + 2q_0 \frac{E_i}{E} \right]^{1/2} \tag{XI.A-27}$$

so that Equation (XI.A-26) reads

$$\frac{\partial^2 F_i}{\partial E \partial \Omega} = \frac{c}{4\pi} \frac{g_i n(^{56}\text{Fe})}{E_i H_o} f(t_E) \left[ 1 - 2q_o + 2q_o \frac{E_i}{E} \right]^{-1/2} \quad (\text{XI.A-28})$$

Clayton and Silk (1969) evaluated the flux in a simpler form for the two cases where

$$R(t) \propto t^{1/\lambda} \quad (\text{XI.A-29})$$

They are the low-density universe ( $q_o \cong 0$ ,  $\gamma \cong 1$ ) and the Einstein-de Sitter universe ( $q_o = 1/2$ ,  $\gamma = 3/2$ ). In those cases Equation (XI.A-24) can be explicitly solved for  $t_E$  and, furthermore, the factor involving  $q_o$  simplifies:

$$\frac{\partial^2 F_i}{\partial E \partial \Omega} = \frac{c}{4\pi} \frac{g_i n(^{56}\text{Fe})}{E_i H_o} f \left[ t_o \left( \frac{E}{E_i} \right)^\gamma \right] \left( \frac{E}{E_i} \right)^{\gamma-1} \quad (\text{XI.A-30})$$

It is straightforward to confirm with Equation (XI.A-28) or Equation (XI.A-30) that

$$\int_0^{E_i} \frac{\partial^2 F_i}{\partial E \partial \Omega} dE = \frac{c}{4\pi} g_i n(^{56}\text{Fe}) \quad (\text{XI.A-31})$$

as required by photon conservation.

The spectrum due to each line is characterized by a step at the rest energy

$$\Delta \left( \frac{\partial^2 F_i}{\partial E \partial \Omega} \right)_{E=E_i} = \frac{c}{4\pi} \frac{g_i n(^{56}\text{Fe})}{E_i H_o} f(t_o) \quad (\text{XI.A-32})$$

that is directly proportional to the average rate of nucleosynthesis today in the universe. Detection of the series of correlated rest edges will confirm that nucleosynthesis is still occurring and measure its present rate  $f(t_o)$ . Each rest edge is followed at immediately lower energies by identical red shifted continua, whose shape and extent depend upon the cosmological model and the history  $f(t)$  of galactic nucleosynthesis. It is interesting to note that the ratio  $f(t_o)/H_o$  is a ratio of characteristic times:  $1/H_o$  is approximately the age of the universe and  $1/f(t_o)$  would be the time required to synthesize  $X_o$  ( $^{56}\text{Fe}$ ) at a constant rate  $f(t_o)$ .

Some simple profiles for the  $^{56}\text{Co}$  line of 1.24 MeV are shown in Figure XI.A-3. If nucleosynthesis has occurred within galaxies at a constant rate up to the present time ( $t_o$ ), and since it began at some time ( $t_*$ ), then  $f(t) = (t_o - t_*)^{-1}$

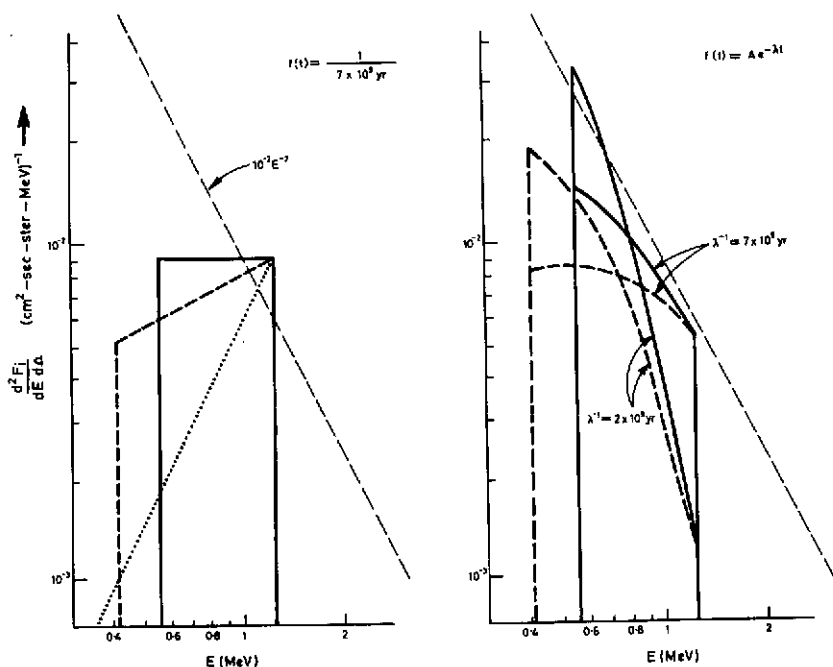


Figure XI.A-3. Differential flux due to a single line ( $^{56}\text{Co}$  at 1.24 MeV). Models of constant galactic synthesis of  $^{56}\text{Fe}$  over a period of  $7 \times 10^9$  yr are shown on the left, and models of exponentially decreasing nucleosynthesis are shown on the right. This rather short duration of galactic nucleosynthesis was chosen only for ease of comparison, so that it could fit in the age of the Einstein-de Sitter universe with  $H_0 = 75$  km/s/Mpc. The low-density universe is shown as a solid line and the Einstein-de Sitter as a dashed line. The steady-state-universe line profile is dotted on the left figure. The line  $10^{-2} E^{-2}$  is also shown to indicate the approximate level of the observed diffuse background. (Clayton and Silk, 1969).

between  $t_*$  and  $t_0$  and is zero elsewhere. The left half of Figure XI.A-3 shows that case from Clayton and Silk (1969), who took  $t_0 - t_* = 7 \times 10^9$  yrs so that it could fit easily within the Einstein-de Sitter universe based on  $H_0 = 75$  km/s/Mpc. The right half of Figure XI.A-3 shows this line profile for exponential nucleosynthesis  $f(t) = A \exp[-\lambda(t-t_*)]$ , where  $A$  is a normalization constant and  $\lambda = 1/T_R$  from Equation (XI.A-1). The two choices of  $\lambda$  shown there give different relative strengths to present-day nucleosynthesis in comparison with the initial galactic rates. The rest edges are still detectable here, but smaller than for the case of constant nucleosynthesis.

It is worth noting here that these figures are applicable to Sandage's (1972) value  $H_0 = 55$  km/s/Mpc if one only increases  $t_0 - t_*$  by the factor  $75/55$ , giving the more reasonable  $t_0 - t_* = 9.6 \times 10^9$  yr, and if the value of the flux is reduced by the factor  $(55/75)^2$ . The latter comes about because  $n(^{56}\text{Fe}) \propto H_0^2$  and  $f(t) \propto H_0$  if we require  $t_0 - t_* \propto H_0^{-1}$ . It is clear that the flux at this rest edge may well be comparable to the isotropic background, whose approximate value is shown for comparison. The model  $T_R = 4 \times 10^9$  yr and  $A_G = 12 \times 10^9$  yr used in estimating the typical supernova yield resembles the curve labeled  $\lambda = (2 \times 10^9 \text{ yr})^{-1}$  in Figure XI.A-3. Its rest edge is the smallest shown—about 15 percent of the observed background. Such small edges would go undetected unless observers design detectors and use data reduction methods designed to extract the steps from the continuous background.

The steady-state universe, shown as a dotted line in Figure XI.A-3, affords a somewhat different problem. To maintain a constant iron density requires a creation rate

$$C = 3Hn(^{56}\text{Fe}) = \text{constant} \quad (\text{XI.A-33})$$

so the  $\gamma$ -rays are created at the rate  $g_i C$ . The age distribution of  $^{56}\text{Fe}$  nuclei is no longer given by the galactic production function  $f(t)$ , because galaxies of all differing ages coexist. The density of nuclei having age  $t_0 - t$  in the interval  $dt$  is simply

$$dN(t_0 - t) = 3Hn(^{56}\text{Fe}) e^{-3H(t_0 - t)} dt \quad (\text{XI.A-34})$$

Both results follow directly from the fact that the scale factor for the proper distance between comoving-coordinate points is

$$\frac{R(t_0)}{R(t)} = e^{H(t_0 - t)} = 1+z \quad (\text{XI.A-35})$$

where  $z$  is the red shift of a photon whose travel time is  $t_0 - t$ . Since Equation (XI.A-35) is also the ratio of the rest energy  $E_i$  to the received energy  $E$ , Equation (XI.A-34) is easily rewritten as a distribution in energy of photons of type  $i$ :

$$dN_i(E) = 3g_i n(^{56}\text{Fe}) \left( \frac{E}{E_i} \right)^2 \frac{dE}{E_i} \quad (\text{XI.A-36})$$

and the differential flux is, as before,

$$\frac{\partial^2 F_i}{\partial E \partial \Omega} = \frac{c}{4\pi} \frac{dN_i(E)}{dE} \quad (\text{XI.A-37})$$

The flux is independent of both the Hubble constant and the details  $f(t)$  of galactic production, and the spectrum is proportional to  $E^2$  up to the rest edge  $E_i$ . This spectrum is the dotted one in Figure XI.A-3. It is of interest to note that Equation (XI.A-32) also gives the correct answer in this case, for the size of the rest edge, if the present production rate  $f(t_0)$  is replaced by  $3H$  according to Equation (XI.A-33):

$$\Delta \left( \frac{\partial^2 F_i}{\partial E \partial \Omega} \right)_{E=E_i} = \frac{c}{4\pi} \frac{3g_i n(^{56}\text{Fe})}{E_i} \quad (\text{XI.A-38})$$

In setting this rest edge equal to those of the evolving universe in Figure XI.A-3 we have been somewhat arbitrary, because  $f(t_0)/H_0 \approx 2$  for the evolving models in the left side of the figure, whereas the steady state gives the slightly larger value 3. However, the average proper density  $n(^{56}\text{Fe})$  could also differ slightly from the value inferred from the solar composition, but not much, because the average galactic age  $(3H_0)^{-1} \approx 6 \times 10^9$  yr was also approximately the age of our galaxy when the solar system formed.

The main point of the steady-state cosmology is that the strong rest edge and the  $(E/E_i)^2$  spectrum remain even if the galactic production function  $f(t)$  were strongly peaked in the past, as in the evolving cosmologies in the right. If the lines emerge unscattered from the sources, a strict steady-state universe will have very strong rest edges, similar to saw teeth.

Figure XI.A-4 illustrates the entire  $A=56$  spectrum for the Einstein-de Sitter case. Two points need be made: (1) the rest edges are clearly more prominent in the case of constant galactic nucleosynthesis than they are in the  $e^2$  - exponential case; but (2) the general shape of the continuum feature produced is quite similar for the two cases. The Einstein-de Sitter universe requires 30 times more mass than has been observed in galaxies, but Figure XI.A-4 assumes that only the observed galaxies contain  $^{56}\text{Fe}$ . If nonvisible matter has undergone nucleosynthesis, the spectrum normalization would have to be increased. One already sees that it cannot be increased very much, and I tentatively conclude that the density of  $^{56}\text{Fe}$  does not exceed the observed density by more than a factor of two unless the  $A=56$  lines are trapped in their sources. The fascinating thing about the Apollo-15 points of Trombka, Metzger, Arnold, Matteson, Reedy, and Peterson (1973) is the way they show positive curvatures near 400 keV. This suggests a multisource spectrum, and it is quite conceivable that the radioactivity spectrum may be significant in the overall shape. Certainly the changes of second derivative will, if they remain after further experimental scrutiny, be important keys to the origins of this spectrum. The radioactivity spectrum may be less visible if the exploding source remains opaque for several months. Compton scattering as extensive as that in Figure XI.A-2 would remove at least half of the photons from the

rest frequency at the source and redistribute them at energies of 0.5 MeV or so. If this source function were employed in Figure XI.A-4, the rest edges would be smaller by a factor of two or so, and the whole high-energy slope would be diminished in importance. At present no firm conclusion can be made because the NaI(Tl) scintillator aboard Apollo-15 had not the energy resolution to detect structure like that in Figure XI.A-4. Nonetheless, such structure should be detectable. In Figure XI.A-4, the age of this universe is  $11.8 \times 10^9$  years, and nucleosynthesis in galaxies began at  $t=2 \times 10^9$  years, corresponding to  $z=2.5$ . The spectrum has series of rest-frequency edges and red shifted continua. The rest edges, which are calculated without Compton scattering in the source, are smallest for nucleosynthesis peaked in the early galactic history. Photons in the radioactivity background are significant, but higher-energy-resolution observations will be needed to extract the presence of detailed structure. Although the density required for  $q_0 = \frac{1}{2}$  with  $H_0 = 55$  km/s-Mpc is  $\rho_c = 5.9 \times 10^{-30}$  gm-cm<sup>-3</sup>, this figure assumes that only the galaxies, with density  $\rho_G = 0.028 \rho_c$ , contain <sup>56</sup>Fe. This calculation (Clayton and Ward unpublished) is thus a lower limit to the anticipated  $\gamma$ -ray density.

### Discussion

It is within scientific grasp to learn the answers to many or all of the questions about nucleosynthesis enumerated in the Introduction. What is needed is a  $\gamma$ -ray telescope with high-energy resolution, moderately good angular resolution, and long operation times outside the earth's atmosphere while responsive to ground command. Of primary importance is energy resolution of a few percent or better to extract lines from continua and to detect rest edges in the universal continuum. Because the rest energies of the  $\gamma$ -rays and their relative production rates are known from laboratory studies, relatively sophisticated data analyses can be performed; one could sum the counting rates just before and just after each rest edge, for example, and compare the decrement with that at arbitrary energies in the spectrum. The angular resolution is needed to identify specific radiating objects (supernovae). As far as I know, the best type of instrument for accomplishing these two needs would be similar to the one I described at the NASA X- and  $\gamma$ -Ray Committee Study of November 1965—a honeycomb of parallel holes drilled through actively collimating CsI or NaI with solid-state (for example, Li-drifted Ge)  $\gamma$ -ray detectors at the bottom of each hole.

Operation outside the earth's atmosphere is necessary in order to reduce the emission background of the earth's atmosphere and its opacity. Ground command will be necessary for viewing different objects and for extracting the isotropic component. Last, but by no means least, we need nature's cooperation in presenting us with a new galactic supernova and preferably a visible one, although an invisible one could be immediately recognized by a large increase of the A=56 lines (see Equations (XI.A-7) and (XI.A-8)).

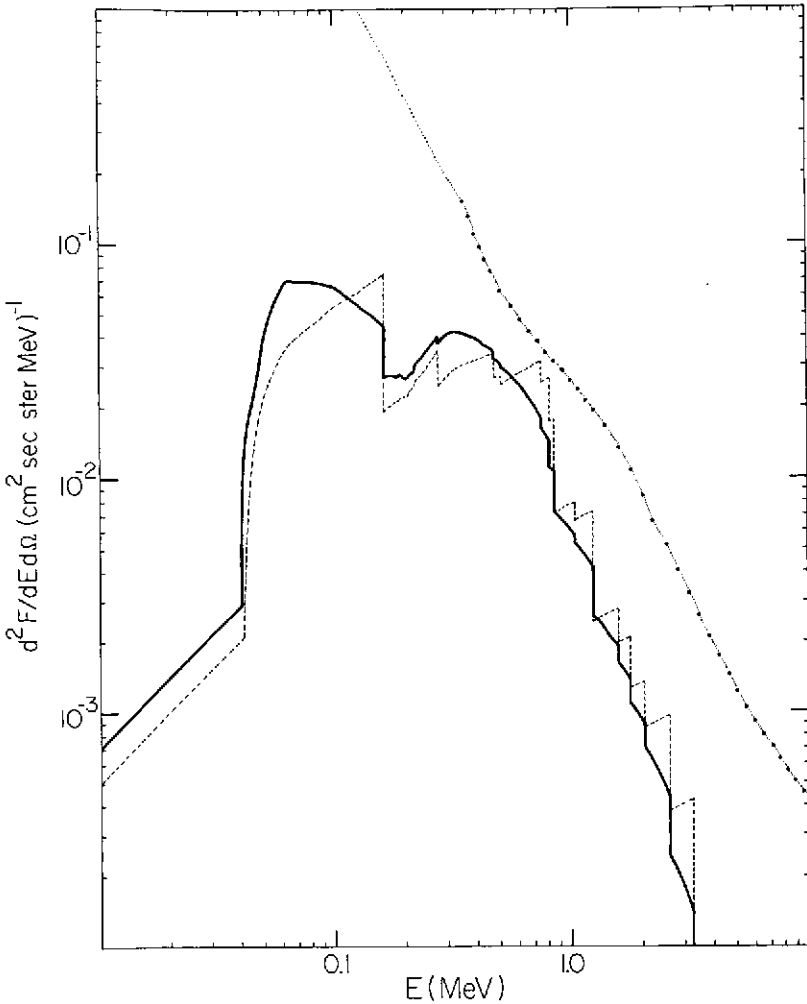


Figure XI.A-4. The composite  $^{56}\text{Ni} \rightarrow ^{56}\text{Co} \rightarrow ^{56}\text{Fe}$   $\gamma$ -ray spectrum in a specific Einstein-de Sitter universe. The solid line is an exponentially decreasing rate of nucleosynthesis/galaxy  $=e^{-2}$  of the initial rate today. The dashed line is a constant rate of nucleosynthesis/galaxy. For comparison, the dotted line is the background spectrum observed on the Apollo-15 spacecraft by Trombka et al., (1973), (heavy solid dots are data points).

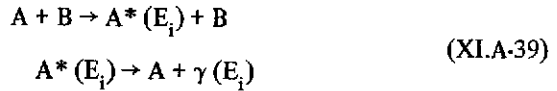
Good observation of at least one supernova is needed to measure what fraction of a  $\gamma$ -line emerges unscattered from their source, for without this calibration, the interpretation of the universal background will remain insecure; with a little bit of luck, the entire science of explosive nucleosynthesis will gain a firm

observational footing from these very special photons. Like all photons, they tell us that an electromagnetic deexcitation occurred; unlike any other photons, they alone tell us that a new nucleus was just born.

### INELASTIC SCATTERING

When particles collide with energies in excess of those of their nuclear excited states, nuclear excitation is possible by the process of inelastic scattering. Let us not consider here the interesting problems of fast particles impinging on special dense objects like the earth's atmosphere, the moon, or the sun's outer atmosphere. Gamma rays from all three sources have been observed, but I will be concerned with radiation from outside the solar system. I also wish to set aside  $\gamma$ -rays from the surfaces of stars and collapsed objects, although both may present some observable sources. By design I will restrict myself to some remarks concerning the interstellar medium and its interaction with fast particles—either a general cosmic-ray flux or special regions of high flux near sources of fast particles. The point to be made at once is that “fast particles” rather than “cosmic rays” may be a more appropriate nomenclature, because the largest cross sections and the largest fluxes may be found in the region of several MeV.

Let  $F_i$  be the  $\gamma$ -ray flux at the earth within a solid angle  $\Omega$  due to collisions



The center-of-mass kinetic energy before the collision is  $E$ , and after the collision is  $E - E_i$ . Let the cross section for this process be designated by  $\sigma_{AB}^j(E)$ . In practice, one of these particles will be a nearly stationary constituent of interstellar or circumstellar plasma, and its number density  $N_A(\underline{x}, t)$  is a function of time and place; the other particle will be regarded as the fast one with flux  $\phi_B(\underline{x}, t)$  that is also a function of time and place. Then

$$F_i = \frac{1}{4\pi} \int_{E_i}^{\infty} \int_{V(\Omega)} r^{-2} N_A \phi_B(E) \sigma_{AB}^j(E) dE dV \quad (\text{XI.A-40})$$

where the integral is over center-of-mass energies  $E > E_i$  and  $V(\Omega)$  is the volume of interstellar gas viewed by the solid angle  $\Omega$ . I will suppress the time dependence, although the arguments are evaluated at  $t - r/c$  if the flux is measured at  $t$ . Euclidean geometry is consistent with the assumption that the only  $\gamma$ -ray lines of this type we are likely to see come from the galaxy. For

an infinitesimal pencil of directions  $d\Omega$ ,  $N_A(\underline{x})$  will be constant over the volume element  $dV = r^2 d\Omega dr$  so that the differential flux is

$$dF_i = \frac{d\Omega}{4\pi} \int_{E_i}^{\infty} \int_0^{\infty} N_A(\underline{x}) \phi_B(\underline{x}, E) \sigma_{AB}^i(E) dE dr \quad (XI.A-41)$$

and if the position dependence of the fast-particle flux is ignored, this integral becomes a product of the integrated number of particles per unit area along the line of sight times the integral over the energy of the cross section times the flux.

One thing to notice immediately is that there should be another term involving the product  $N_B \phi_A(E)$  in the integrand, and, if the chemical composition of the gas were identical to that of the fast particles at fixed velocity, both integrals would give the same number of  $\gamma$ -rays. In the second case, however, the energy of the received  $\gamma$ -rays may be significantly Doppler-shifted if the particles A were moving at significant fractions of  $c$ . (I will not concern myself at all with truly relativistic velocities where pion production dominates  $\gamma$ -ray considerations and where, in any case, the fluxes are too small to produce detectable low-energy  $\gamma$ -rays.) The Doppler broadening in the second case might make the lines harder to resolve.

Let us make an order-of-magnitude estimate in order to define the ballpark. Imagine a telescope viewing the galactic disk. Let the solid angle  $\Omega$  contain interstellar gas equal to  $p_g$  percent of the galactic mass (the total interstellar gas being about  $p_g = 10$  percent) in the galactic disk. Let  $p_A$  and  $p'_B$  be the percentages of interstellar particles and of fast particles having identities A and B respectively, so that  $N_A = (p_A/100)N$  and  $\phi_B = (p'_B/100)\phi$ . (Throughout, I have chosen to express unknown parameters in percentages in order that they have expected values nearer unity in resulting expressions.) Assuming the emissivity of the disk to be nearly uniform means that the flux is comparable to the value it would have if the emission within  $V(\Omega)$  were all from the galactic center, about 10 kpc away. For that case

$$F_i(\text{galaxy}) \approx p_g (p_A p'_B + p_B p'_A) 1.8 \times 10^{-11} \bar{\phi} \bar{\sigma}_{AB}^i (\text{mb}) \text{cm}^{-2} \cdot \text{s}^{-1} \quad (XI.A-42)$$

where  $\bar{\phi} (>E_i)$ , the total flux above threshold, and  $\bar{\sigma}$  (mb) is the average cross section in units of millibarns. For example, if we consider that the 6.1-MeV radiation from  $^{16}\text{O}$  has a proton cross section of about 100 mb above its threshold (effectively about 8 MeV), and if the flux above 8 MeV is  $\bar{\phi}(>8) \approx 50 \text{ cm}^{-2} \text{ s}^{-1}$ , a not unreasonable extrapolation from observations above 30 MeV, then with  $p_{16} = 0.07$ ,  $p'_H = 90$ ,  $p_H = 90$ ,  $p'_{16} = 0.3$  (Cameron, 1968); Shapiro and Silberberg (1970) give

$$F_{16}(\text{galaxy}) \approx 3 \times 10^{-6} \text{ cm}^{-2} \cdot \text{s}^{-1}$$

if the gas in  $V(\Omega)$  is  $p_g = 1$  percent of the galactic mass. This corresponds to a total production of about  $10^{41}$   $\gamma$ -rays $\cdot$ s $^{-1}$  from the entire galactic gas, in rough agreement with the estimate of Fowler, Reeves, and Silk (1970), and a flux of about  $3 \times 10^{-5}$   $\text{cm}^{-2} \cdot \text{s}^{-1}$  with an omnidirectional counter. I do not want to argue this as the best calculation of the emissivity of the galactic disk. My point is that line fluxes of order  $10^{-5}$   $\text{cm}^{-2} \cdot \text{s}^{-1}$  will be expected from  $^{16}\text{O}^*$ , and that this detection will be only marginally possible. That is, this prospect lies near an uncertain edge of detectability.

What basic features of the estimate could be plausibly altered to obtain a larger  $\gamma$ -ray flux at the earth? One idea would be a discrete source nearby. However, one readily calculates that if a mass  $mM_\odot$  of gas concentrated at a distance  $d(\text{pc})$  is irradiated, the  $\gamma$ -ray flux at earth is

$$F_i(\text{source}) = \frac{0.8 \times 10^{-12}}{d(\text{pc})^2} m \bar{\sigma}(\text{mb}) \bar{\phi} (p_A p'_B + p_B p'_A) \quad (\text{XI.A-43})$$

so that for  $d = m = 1$ , the  $^{16}\text{O}^*$   $\gamma$ -ray flux, for example, would be  $F_{16}(\text{discrete}) = 3 \times 10^{-9} \bar{\phi} (>8 \text{ MeV})$ . Thus the flux from a discrete source can hardly be much greater than that of the disk as a whole, unless the fast particle flux  $\phi$  is very much greater (for example  $\phi > 10^5 \text{ cm}^{-2} \cdot \text{s}^{-1}$ ) than in the general cosmic radiation. This might occur for a short period following a supernova explosion, or it might occur for a long period around a rapidly rotating collapsed object.

Another attractive idea is that fast-particle flux  $\phi(E)$  could be a very steep function of energy. The solar modulation is thought to be (Goldstein, Fisk, and Ramaty, 1970) so severe for  $E < 30 \text{ MeV/nucleon}$  that measurements at earth give little insight into the general interstellar flux. If we should be so fortunate that  $\phi(E) \propto E^{-n}$  with  $n > 2$ , a great deal of special information could be extracted from sources. The high fluxes will give observable counting rates, and the steep energy dependence will produce informative threshold-dependent features. We may perhaps even expect this near the sources, because Braddy, Chan, and Price (1973) have found that big solar flares produce a very steep spectrum having  $n \approx 3.7$  with preferential acceleration of heavy ions. Of course solar flares are not the origins of cosmic rays, but let us make do with what we have and suppose that, like flares, the acceleration mechanisms for cosmic rays also produce a steep low-energy spectrum. If it is as steep as  $n=2$ , the nuclei having low excitation thresholds can be excited more strongly than more abundant nuclei having higher excitation thresholds. This point is illustrated in Figure XI.A-5, which shows the relative abundances of cosmic-ray nuclei (assuming terrestrial isotope ratios) as a function of the excitation energy

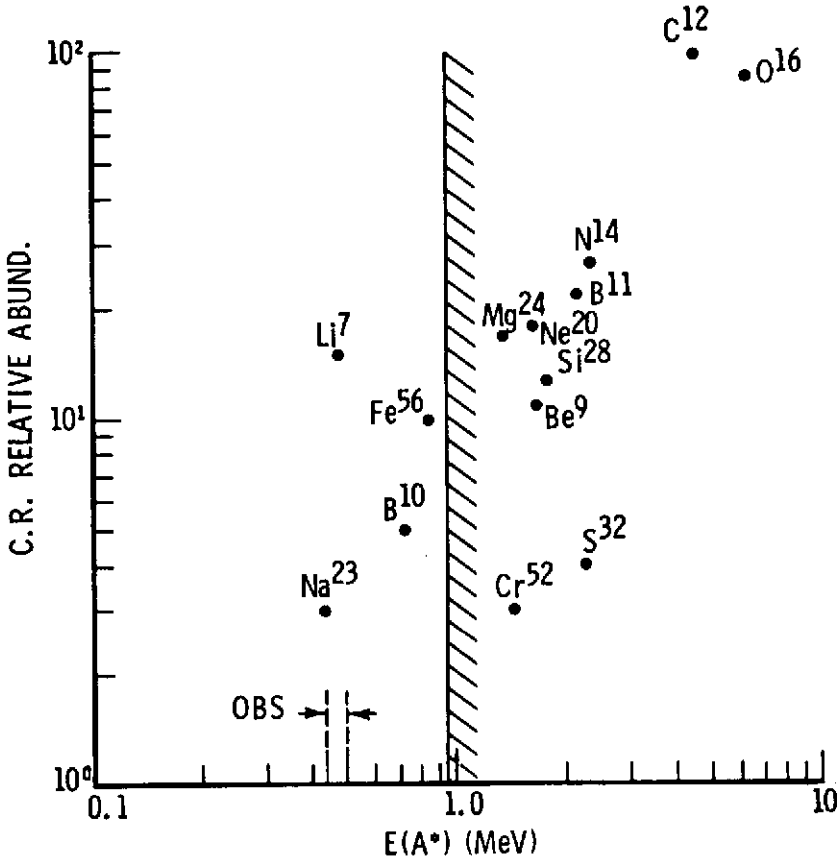


Figure XI.A-5. Relative abundances of cosmic-ray nuclei (Shapiro and Silberberg, 1970) plotted as a function of the energy of their first excitation level. Terrestrial isotope ratios have been assumed. The energy range of the line feature observed from the galactic-center region (Johnson et al., 1972) is indicated. No observations have been made above 0.93 MeV. (Fishman and Clayton, 1972).

$E_i = E(A^*)$  of their first excited states. There is a general positive slope of approximately  $E_i^{+1}$  in these abundances, which reflects only the fact that the most abundant nuclei tend to be the most stable, and those in turn tend to have the largest excitation energies.

First consider an example of how  $\gamma$ -ray astronomy could measure the exponent  $n$  in the fast-particle spectrum. The  $^{14}\text{N}$  nucleus has excited states at 2.31 and 3.94 MeV with "effective thresholds" of about 3.3 and 4.9 MeV (to allow the outgoing proton at least 1 MeV to beat the Coulomb barrier). The

excitation of the 3.95-MeV level results (96 percent) in a cascade of 1.6- and 2.3-MeV  $\gamma$ -rays, whereas the excitation of the 2.31 MeV level results only in the 2.3-MeV  $\gamma$ -rays. Thus the relative  $\gamma$ -ray fluxes should be

$$\frac{F_{2.3}}{F_{1.6}} \approx \frac{\int_{3.3}^{\infty} E^{-n} \sigma_{\text{pN}}^{2.31}(E) dE}{\int_{4.9}^{\infty} E^{-n} \sigma_{\text{pN}}^{3.95}(E) dE} + 1 \quad (\text{XI.A-44})$$

I can foresee a need for tabulations of nuclear cross sections of this type; however, if we only assume for simplicity that the ratio of these two averaged cross sections is near unity, then the  $n$  dependence is proportional to the ratio of fast particle fluxes:

$$\frac{F_{2.3}}{F_{1.6}} \propto \left(\frac{4.9}{3.3}\right)^{n-1} + 1 = 3.8 \text{ for } n = 3.5$$

whereas the corresponding ratio would be near two if there were a deficiency rather than an excess of MeV particles. One could also compare the first excited-state lines of  $^{12}\text{C}$  and  $^{16}\text{O}$ , but then the abundance ratio in the source would be an unknown. If many different lines of many different species can be observed, an interesting picture of the abundances and energy spectrum could be assembled. A related type of problem was extensively discussed by Lingenfelter and Ramaty (1967) for the case of solar flares, and many of their conclusions pass directly to extra-solar  $\gamma$ -ray astronomy. Now that some of these solar-flare  $\gamma$ -rays have been seen by OSO-7, we may expect further clarifications on prospects for the future of galactic astronomy. For fast particles more energetic than 10 MeV, the most prominent astronomical lines should be the pair-annihilation line, the 2.23-MeV radiative neutron capture by hydrogen, and the excited states of C, N, O, and Ne nuclei. Fowler, Reeves, and Silk (1970) emphasized for these particles, however, that the  $\gamma$ -ray flux is limited by the requirement that the accompanying spallation reactions not overproduce Li, Be, and B abundances. They find that the rate of production of  $^{12}\text{C}$  and  $^{16}\text{O}$   $\gamma$ -rays is less than  $10^{-26} \text{ s}^{-1}$  per interstellar H-atom. However, this limit is an average over time and place and could be greatly exceeded in limited regions for limited times.

Figure XI.A-5 shows those nuclei that will be most excitable by low-energy fast particles, so let us turn our attention to the possibility that large fluxes of particles with  $E < 5$  MeV may be common. In addition to the solar-flare observations to motivate this hypothesis, we have the fact that if the HI regions are heated by fast particles, they must surely lie in the MeV region. If the fast-particle spectrum is steeper than  $E^{-2}$ , the nuclei with low excited states are excited more frequently than the more abundant nuclei. Of all these,  $^7\text{Li}$  is anomalous in that its cosmic-ray abundance is very much

greater than the general line through Figure XI.A-5. In a steep fast-particle spectrum, the 478-keV line of  ${}^7\text{Li}^*$  should be the most prominent if the fast particles have the relative abundances of the cosmic rays. The peculiar fact was used by Fishman and Clayton (1972) in their attempt to account for the spectral feature observed toward the galactic center by Johnson, Hamden, and Haymes (1972). They point out that a 432-keV  $\gamma$ -ray due to  ${}^7\text{Li}(p,n){}^7\text{Be}^*$  (432) should accompany the main  ${}^7\text{Li}$  radiation with about one-third its intensity. Their fit to the data of Johnson et al. (1972), is shown in Figure XI.A-6. The computed solid curve is a simple power-law continuum plus the  ${}^7\text{Li}$  doublet feature at an intensity comparable to the observed counting rate. The fit is basically quite good, so the explanation could be correct. Fishman and Clayton (1972)  $p_g = 2$  percent and  $p'_{\text{Li}} = 0.08$  percent

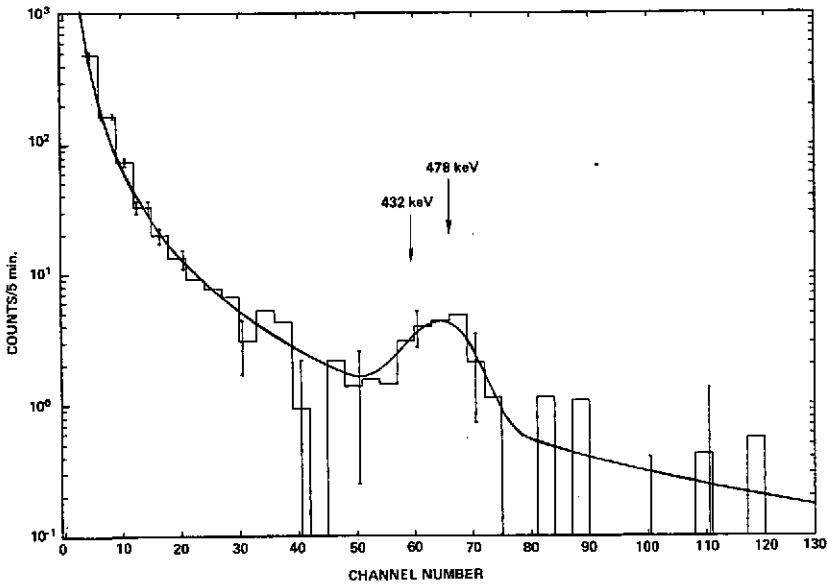


Figure XI.A-6. The curve shows the shape of the  ${}^7\text{Li}$ -inelastic-scattering feature superimposed on a smooth power-law continuum (Fishman and Clayton, 1972). The profile was computed for an energy resolution equal to that of the detector used by Johnson et al. (1972). Because of the limited resolution, the line at 432 keV due to  ${}^7\text{Li}(p,n){}^7\text{Be}^*$  is not physically separated from the line at 478 keV due to  ${}^7\text{Li}(p,p'){}^7\text{Li}^*$ , which is three times stronger. The histograms are the data of Johnson et al. (1972), with their energy channels summed in groups of three adjacent channels to reduce statistical fluctuations. The consistency of their feature with the one proposed by Fishman and Clayton (1972) is evident.

in Equation (XI.A-42), to conclude that if the radiation was from this much gas toward the galactic center, one gets  $\phi \approx 5 \times 10^4 \text{ cm}^{-2} \cdot \text{s}^{-1}$  between about 2 and 10 MeV/nucleon. This is a much larger flux than one is accustomed to think of in cosmic rays, but it is not out of line with  $E^{-3.5}$  spectra like those of a solar flare; with  $n = 3.5$  one has  $\phi(>2) \approx 900 \phi(>30)$ . The large-energy density of over  $100 \text{ eV cm}^{-3}$  would create dynamic instabilities were it a galactic-wide phenomenon, however, so it must exist instead in bottles of high-flux regions. Nonetheless, our calculation requires the amount of irradiated gas to be large enough to obtain the observed flux, so there are strong astrophysical problems here. Another problem is that the high  ${}^7\text{Li}$  abundance is usually assumed to be spallogenic from high-energy cosmic rays, so that large low-energy fluxes of this nucleus might not be expected from that point of view. My philosophy is that observational  $\gamma$ -ray astronomy is quite capable of teaching us the truth in these matters, so elaborate models for or against this particular explanation may not be appropriate at present. We also need much better evidence of the cosmic-ray flux at the solar system, because the Goldstein, Fisk, and Ramaty (1970) calculations show that the particles at earth's orbit having 30 MeV/nucleon are three to four orders of magnitude less abundant than their 50 to 100-MeV progenitors at the boundaries of the solar system. Perhaps Pioneer-10 will give us badly needed facts on this modulation problem.

(Partially supported by the National Science Foundation GP-18335)

## REFERENCES

- Arnett, W. D., and D. D. Clayton, 1970, *Nature*, 227, p. 780.
- Arnett, W. D., 1971, *Astrophys. J.*, 166, p. 153.
- Bodansky, D., D. D. Clayton, and W. A. Fowler, 1968, *Astrophys. J. Suppl.*, 16, p. 299.
- Braddy, D., J. Chan, and P. B. Price, 1973, *Phys. Rev. Letters* 30, p. L669
- Brown, R. T., 1973, *Astrophys. J.*, 179, p. 607.
- Cameron, A. G. W., 1968, *Origin and Distribution of the Elements*, L. H. Ahrens, ed., New York, Pergamon Press, p. 125.
- Clayton, D. D., 1971, *Nature*, 234, p. 291.
- , 1973, *Science*, in press.
- Clayton, D. D., and W. Craddock, 1965, *Astrophys. J.*, 142, p. 189.
- Clayton, D. D., S. Colgate, and G. J. Fishman, 1969, *Astrophys. J.*, 155, p. 75.
- Clayton, D. D., and J. Silk, 1969, *Astrophys. J.*, 158, p. L43.

- Clayton, D. D., and S. E. Woosley, 1969, *Astrophys. J.*, **157**, 1381.
- Fishman, G. J., and D. D. Clayton, 1972, *Astrophys. J.*, **178**, p. 337.
- Fowler, W. A. 1972, *Cosmology, Fusion, and Other Matters*, F. Reines, ed., Univ. of Colorado Press, Boulder, p. 67.
- Fowler, W. A., H. Reeves, and J. Silk, 1970, *Astrophys. J.*, **162**, p. 49.
- Goldstein, M. L., L. A. Fisk, and R. Ramaty, 1970, *Phys. Rev. Letters*, **25**, p. L832.
- Howard, W. M., W. D. Arnett, D. D. Clayton, and S. E. Woosley, 1971, *Phys. Rev. Letters*, **27**, p. L1607.
- , 1972, *Astrophys. J.*, **175**, p. 201.
- Johnson, III, W. N., F. R. Harnden, and R. C. Haymes, 1972, *Astrophys. J., Letters*, **172**, p. L1.
- Lingenfelter, R. E., and R. Ramaty, 1967, *High Energy Nuclear Reactions in Astrophysics*, B. Shen, ed., New York, W. A. Benjamin, Inc.
- McVittie, G. C., 1965, *General Relativity and Cosmology*, Urbana, Univ. Illinois Press.
- Oort, J. H., 1958, *Solvay Conference on Structure and Evolution of the Universe*, Brussels, R. Stoops.
- Sandage, A., 1972, *Astrophys. J.*, **178**, p. 1.
- Schmidt, M., 1965, *Galactic Structure*, A. Blaauw and M. Schmidt, eds. Chicago, University of Chicago Press, p. 528.
- Shapiro, M. M., and R. Silberberg, 1970, *Ann. Rev. of Nuclear Science*, **20**, p. 323.
- Trombka, J. I., A. E. Metzger, J. R. Arnold, J. L. Matteson, R. C. Reedy, and L. E. Peterson, 1973, *Astrophys. J.*, **181**, p. 737-746.
- Weinberg, S. 1972, *Gravitation and Cosmology*, New York, John Wiley, p. 495.

## B. POSITRONIUM FORMATION RED SHIFT OF THE 511-keV ANNIHILATION LINE

M. Leventhal\*  
*Bell Laboratories*

Energetic positrons stopping in a gas, in principle, can annihilate from either the free state with an electron bound in a gas atom or first capture an electron and form the hydrogen-like positronium atom before annihilating. Stecker (1969) and Ramaty, Stecker, and Misra (1970) have made the point that positronium formation may be of importance in astrophysics. The cross sections for positron energy loss and annihilation processes in gases are such that annihilation does not take place until the positron has slowed down to eV-type energies (Deutsch, 1953). The cross section  $\sigma_F$  for free annihilation with the emission of two antiparallel 511-keV  $\gamma$ -rays (Dirac, 1930) is many orders of magnitude smaller than the positronium formation cross section  $\sigma_P$  (Massey and Mohr, 1954) and one might think at first that it can be neglected. For 20-eV positrons incident on atomic hydrogen  $\sigma_F \approx 10^{-23} \text{ cm}^2$  and  $\sigma_P \approx 10^{-16} \text{ cm}^2$ . However, in dense gases, this is not the case because positronium formed with kinetic energy greater than its binding energy of 6.8 eV can ionize in a collision with a gas atom before annihilating. Thus the positron may eventually be slowed down to energies below the threshold  $E_T = (I-6.8)\text{eV}$  for positronium formation, where  $I$  is the first ionization potential of the stopping gas. For positron energies below  $E_T$ , only free annihilation can occur. The relative cross sections for the various elastic, inelastic, and annihilation processes involved are such that, for typical gases at atmospheric pressure, the fraction of positrons annihilating from the positronium state ( $f$ ) is in the range 20 to 50 percent. Numerous laboratory experiments have demonstrated this large positronium formation fraction (Green and Lee, 1964). As the pressure is reduced to the extremely dilute situation found in many astrophysical situations,  $f$  may approach 100 percent. An estimate of the atomic density ( $N$ ) below which  $f$  would approach 100 percent can be obtained

---

\*Speaker.

from the expression

$$N = \frac{1}{\tau \sigma_I v}$$

where  $\tau$  is the time required for a positronium ionizing collision,  $\sigma_I$  is the cross section for positronium ionization in a gas collision, and  $v$  is the positronium velocity. If  $\tau > 1.4 \times 10^{-7}$  s, the ortho-positronium annihilation lifetime (see below), free annihilation should be suppressed. Using the characteristic values of  $\sigma_I = 7 \times 10^{-17}$  cm<sup>2</sup> and  $v = 2 \times 10^8$  cm · s calculated for positronium incident upon atomic hydrogen (Massey and Mohr, 1954)  $N$  is found to be of order  $10^{15}$  atoms · cm<sup>-3</sup>. Since densities as large as  $10^{15}$  atoms · cm<sup>-3</sup> are found only in the vicinity of condensed objects, a predominantly positronium annihilation spectrum is expected in many astrophysical situations. (The possible presence of intense UV fields, which might photoionize the positronium within its annihilation lifetime, has been ignored in the above discussion. Also, it has been assumed that the temperature  $T \lesssim 10^5$  K<sup>0</sup>, that is, the hydrogen plasma, is predominantly neutral atoms.)

Positronium may be formed with its spins aligned antiparallel, the singlet-para state with spin = 0, or with the spins parallel in the triplet-ortho state with spin = 1. On a purely statistical basis, the ortho state is expected to be formed three times as often as the singlet state because of the threefold degeneracy in the azimuthal spin quantum number  $M_s = 1, 0, -1$ . Singlet positronium annihilates in  $1.3 \times 10^{-10}$  s yielding two antiparallel 511-keV  $\gamma$ -rays. Triplet positronium annihilates in  $1.4 \times 10^{-7}$  s yielding three  $\gamma$ -rays in a plane. The probability per unit energy range  $P_T(E)$  of finding a triplet  $\gamma$ -ray with a particular energy in the interval from 0 to 511 keV is given by (Ore and Powell, 1949)

$$P_T(E) = \frac{2}{(\pi^2 - 9)} \left\{ \frac{E(m-E)}{(2m-E)^2} + \frac{2m(m-E)}{E^2} \ln \left( \frac{m-E}{m} \right) - \frac{2m(m-E)^2}{(2m-E)^3} \ln \left( \frac{m-E}{m} \right) + \left( \frac{2m-E}{E} \right) \right\}$$

where  $m$  is the electron rest mass energy of 511 keV, and the distribution has been normalized to unity. A plot of  $P_T(E)$  is given in Figure XI.B-1. The positronium annihilation spectrum  $P_p(E)$  can then be constructed by adding the singlet and triplet spectra,  $P_p(E) = 0.75 \times 3 \times P_T(E) + 0.25 \times 2 \times P_S(E)$  where the weightings reflect the relative amounts of triplet and singlet formed and the number of  $\gamma$ -rays each gives. In principle, the singlet spectrum  $P_S(E)$

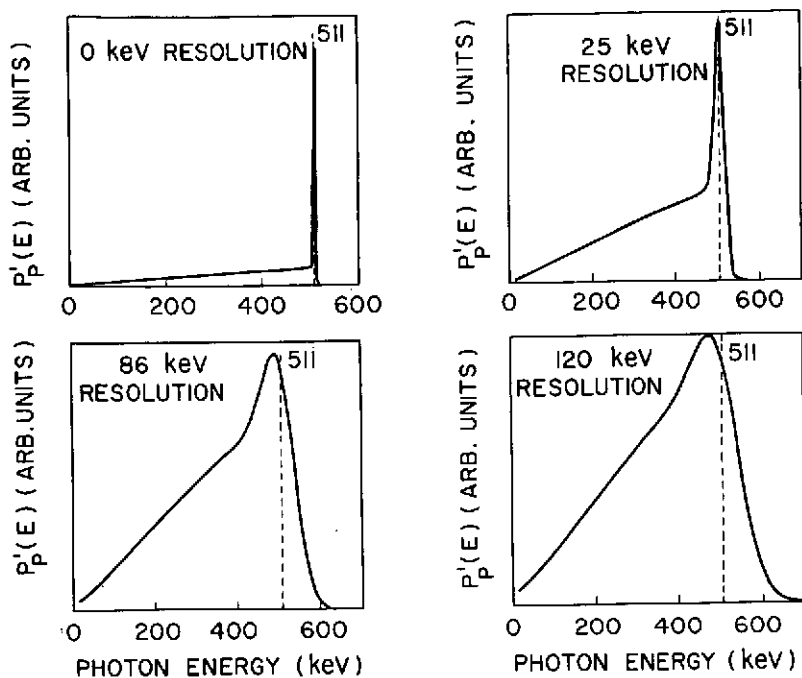


Figure XI.B-1. Plots of the detected positronium annihilation function  $P'_p(E)$  for various energy resolutions (FWHM) of the  $\gamma$ -ray detector. A Gaussian width of 3.2 keV has been assumed for the singlet annihilations. The broken curve in the upper left-hand box is a plot of the pure, triplet annihilation function  $P_T(E)$ .

should be a normalized delta function centered at 511 keV. However, the finite motion of the positronium atom will give a Doppler broadening in all real cases.  $P_p(E)$  can in principle be modified by charge exchange collisions with gas atoms, converting triplet to singlet positronium before annihilation. The cross section for this process (Massey and Mohr, 1954) is of the same order of magnitude as  $\sigma_I$ . Hence again, for densities of order  $10^{15}$  atoms  $\cdot$  cm $^{-3}$  or smaller, an unmodified  $P_p(E)$  is expected.

Finally, to obtain the observed positronium spectrum  $P'_p(E)$ , an instrumental rounding of  $P_p(E)$  must be performed because most  $\gamma$ -ray detectors in the energy range of interest have poor energy resolution. Assuming a Gaussian resolution function one obtains

$$P'_p(E) = \int_0^{\infty} \frac{1}{\sigma\sqrt{2\pi}} e^{-\frac{(E-E')^2}{2\sigma^2}} P_p(E') dE'$$

where the full width at half maximum of the convoluted function is  $2.35\sigma$ . The function  $P'_p(E)$  has been numerically evaluated on a computer. Plots of  $P'_p(E)$  for various width resolution functions are given in Figure XI.B-1.  $P_s(E')$  has been taken as a normalized Gaussian of width 3.2 keV corresponding to the Doppler broadening for 20-eV positronium. However, it is important to point out that the spectra are insensitive to the Doppler width of  $P_s(E)$  because the resolution functions are in general much broader. Clearly, positronium annihilation yields a spectrum red-shifted from 511 keV and of asymmetric shape. The apparent red shift of the peak versus resolution is plotted in Figure XI.B-2.

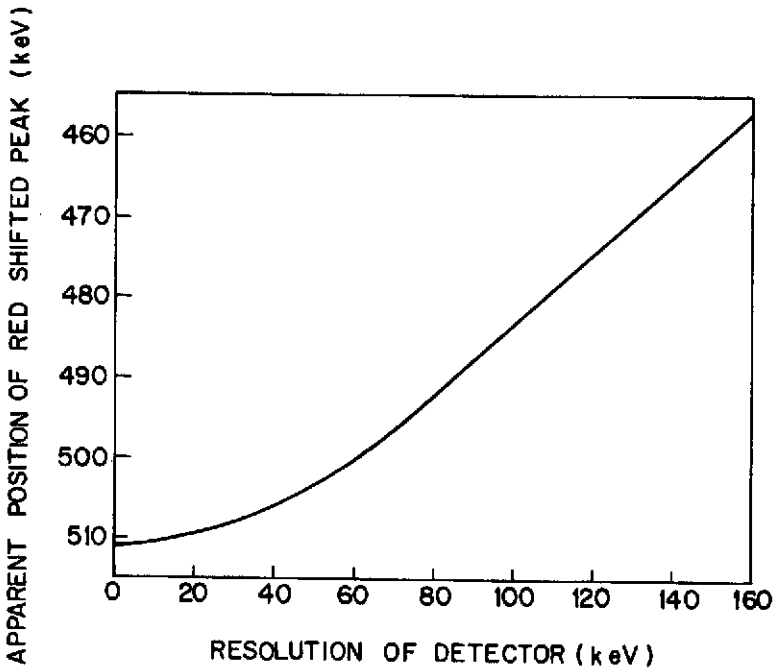


Figure XI.B-2. A plot of the apparent peak position of the detected positronium annihilation function  $P'_p(E)$  as a function of detector resolution (FWHM).

A feeble  $476 \pm 24$ -keV feature, now 5.3 standard deviations above the  $\gamma$ -ray continuum from the galactic center region, has recently been detected (Johnson, Harnden, and Haymes, 1972; Johnson and Haymes, 1973). Two interpretations of the feature have been presented: the first, that it is the 511-keV positron annihilation line red-shifted by the gravitational potential

at the surface of a neutron star (Borner, Cohen, and Ramaty, 1972; Guthrie and Tadamaru, 1973); and the second interpretation is that the feature is a nuclear  $\gamma$ -ray emitted when the  ${}^7\text{Li}$  nuclei in the cosmic rays scatter inelastically from the interstellar gas (Fishman and Clayton, 1972). Since both proposals are far from conclusive, we think it worthwhile to consider the possibility that positronium annihilation is being detected.

The feature from the galactic center region was detected with a fitted energy resolution of 86 keV (Johnson and Haymes, 1973). According to Figure XI.B-2, a positronium annihilation spectrum would have appeared peaked at 490 keV, which is consistent with the observation. Further support for the positronium hypothesis would be provided by detecting the characteristic asymmetric shape of the feature. Unfortunately because of (1) the poor statistical quality of the available data, (2) the fact that the feature sits on a large, sloping background continuum, and (3) the large energy resolution of the detectors employed, conclusions about the shape of the feature would at present be dubious. Additional data acquisition with  $\gamma$ -ray detectors of higher resolution should eventually answer this question.

Additional support for the hypothesis might come from the detection of positronium line radiation (Leventhal, 1970). Implicit in the above discussion was that annihilation took place from the ground atomic state of positronium. Some fraction of the positronium should be formed in excited states (Massey and Mohr, 1954) which optically decay before annihilating. The expected spectrum is identical to that of atomic hydrogen with all wavelengths multiplied by two because of the reduced mass factor. However, interstellar extinction in the plane of the galaxy will greatly hinder such measurements (Becklin and Neugebauer, 1968).

If positronium annihilation is indeed being observed, it is interesting to speculate on the origin of the positrons. Since the  $\gamma$ -ray telescope employed by Johnson et al. (1972) had an acceptance cone of  $24^\circ$ , a large fraction of the galactic disk was observed. Positrons produced as secondaries in the cosmic rays should be stopping and forming positronium in the galactic gas. An order of magnitude calculation of the flux at earth due to cosmic-ray positronium has been made. Assuming (1) the cosmic-ray positron flux as measured at earth (Fanselow, Hartman, Hildebrand, and Meyer, 1969) is uniform throughout the galaxy, (2) that these positrons are contained within the galactic gas until they stop, and (3) the galactic gas consists of a disk 20 kpc in diameter by 0.25 kpc wide containing one hydrogen atom  $\cdot \text{cm}^{-3}$ , a flux at earth is found which is several orders of magnitudes smaller than the observed flux of  $1.8 \pm 0.5 \times 10^3$  photons  $\text{cm}^{-2} \cdot \text{s}^{-1}$ . Hence we conclude that the positrons must be generated by some other mechanism. If the source were at the galactic center,  $D = 10$  kpc,  $7.3 \times 10^{42}$  positronium annihilations per second would be required, yielding a source luminosity of  $\sim 10^{37}$  ergs  $\cdot \text{s}^{-1}$  in the annihilation radiation alone.

**ACKNOWLEDGMENTS**

I wish to thank my Bell Labs colleagues, K. Jefferts, L. Lanzerotti, S. McCall, P. M. Platzman, J. Tyson, and R. Slusher for their enthusiastic and constructive comments, R. Fulton for computer assistance, W. Johnson and F. Harnden for helpful discussions of their experiment, M. Ruderman for bringing the problem to my attention, and G. Steigman for helpful comments.

**REFERENCES**

- Becklin, E. E., and G. Neugebauer, 1968, *Astrophys. J.*, **151**, p. 145.
- Borner, G., J. M. Cohen, and R. Ramaty, 1972, *Bull. American Asst. Soc.*, **4**, p. 410.
- Deutsch, M., 1953, *Prog. Nucl. Phys.*, **3**, p. 131.
- Dirac, P. A. M., 1930, *Proc. Camb. Phil. Soc.*, **26**, p. 361.
- Fanselow, J. L., R. C. Hartman, R. H. Hildebrand, and P. Meyer, 1969, *Astrophys. J.*, **158**, p. 771.
- Fishman, G. J., and D. D. Clayton, 1972, *Astrophys. J.*, **178**, p. 337.
- Green, J., and J. Lee, 1964, *Positronium Chemistry*, Academic Press, New York and London.
- Guthrie, P., and E. Tadamaru, 1973, *Nature Phys. Sci.*, **241**, p. 77.
- Johnson, W. N., F. R. Harnden, and R. C. Haymes, 1972, *Astrophys. J.*, **172**, p. L1.
- Johnson, W. N., and R. C. Haymes, 1973, *Astrophys. J.*, in press.
- Leventhal, M., 1970, *Proc. Nat. Acad. Sci.*, **66**, p. 6.
- Massey, H. S. W., and C. B. O. Mohr, 1954, *Proc. Phil. Soc. London*, **A67**, p. 695.
- Ore, A., and J. L. Powell, 1949, *Phys. Rev.*, **75**, p. 1696.
- Ramaty, R., F. W. Stecker, and D. Misra, 1970, *J. Geophys. Res.*, **75**, p. 1141.
- Stecker, F. W., 1969, *Astrophys. Space Sci.*, **3**, p. 579.

## C. NUCLEAR GAMMA RAYS FROM SOLAR FLARES

R. Ramaty\*  
*Goddard Space Flight Center*

### INTRODUCTION

Solar  $\gamma$ -ray line emissions at 0.5, 2.2, 4.4, and 6.1 MeV were detected during the flare of August 4, 1972, by a  $\gamma$ -ray monitor flown on OSO-7 (Chupp et al., 1973). Line emissions at 0.5 and 2.2 MeV were also detected on August 7, 1972, but only upper limits could be set on the 4.4- and 6.1-MeV lines from this flare. In previous papers (Lingenfelter and Ramaty, 1967; Cheng, 1972), the theory of nuclear reactions in solar flares was treated in detail and predictions were made as to the expected fluxes of  $\gamma$ -rays and high-energy neutrons at earth from such reactions at the sun. Following the discovery of Chupp et al. (1973) we have reviewed and updated these calculations including more recent nuclear cross sections. The results of these calculations were also presented by Ramaty and Lingenfelter (1973a).

By comparing the predicted emissions with the observations, we can show that the observed lines at 0.5, 2.2, 4.4, and 6.1 MeV are produced, respectively, by positron annihilation, deuterium deexcitation following neutron capture on hydrogen, and the deexcitation of the first nuclear levels of  $C^{12}$  and  $O^{16}$ . Furthermore, from the comparison of the calculated and observed line intensities we can deduce the spectrum of the accelerated particles at the sun independent of the assumed interaction model. The total number of accelerated particles required to produce the observed line emission, however, does depend on this model. In the subsequent treatment we shall use two limiting models: a thick-target model in which the accelerated particles move from the flare region downward into the sun, undergoing nuclear interactions as they slow down in the solar atmosphere; and a thin-target model in which the spectrum of accelerated particles is not modified during the time in which the nuclear interactions take place. The latter model assumes that either the total path length traversed by the particles at the sun is small in comparison with their

---

\*Speaker.

interaction length, or that the particle energy loss from ionization and nuclear interactions is just balanced by energy gains from acceleration.

We have recalculated the fluxes of various  $\gamma$ -ray lines expected from accelerated particle interactions in solar flares: at 0.511 MeV from positron annihilation, at 2.23 MeV from neutron capture on hydrogen, and at 1.63, 1.99, 2.31, 4.43, 5.5, and 6.14 MeV from deexcitation of nuclear levels in C, O, N, and Ne.

These calculations are based on an ambient solar composition given by H:He:C:N:O =  $1:10^{-1}:5.3 \times 10^{-4}:10^{-4}:9.2 \times 10^{-4}$  (Cameron, 1967) and an accelerated particle population consisting of protons with spectrum

$$N(P) = P_0^{-1} \exp(-P/P_0). \quad (\text{XI.C-1})$$

Here  $P$  is rigidity,  $P_0$  is a characteristic rigidity which we treat as a free parameter, and  $N(P)$  is the total number of protons per unit rigidity. In the calculations,  $N(P)$  is normalized at the sun to one particle of rigidity greater than zero.

For the thick-target model, the yield of secondaries from a particular type of interaction is given by

$$Q_s = \eta \int_0^\infty dP N(P) \int_0^x dx' \sigma(P') \exp(-(x-x')/L), \quad (\text{XI.C-2})$$

where  $\eta$  is the number of target atoms per gram of solar material,  $\sigma$  is the cross section as a function of rigidity, and  $x$  and  $L$  are the stopping range and nuclear interaction length of protons of rigidity  $P$  (both measured in  $\text{g} \cdot \text{cm}^{-2}$ ). This yield has the units of secondaries per incident proton of rigidity greater than zero.

For the thin-target model, the instantaneous production rate of secondaries from the same type of interaction is

$$q_s = n c \int_0^\infty dP N(P) \beta \sigma(P) \quad (\text{XI.C-3})$$

where  $n$  is the number density of the ambient solar material in  $\text{cm}^{-3}$ , and  $c \beta$  is the velocity of a proton of rigidity ( $P$ ). The units of  $q_s$  are secondaries per second per proton of rigidity greater than zero.

PHOTON PRODUCTION

Line emission at 0.511 MeV is produced from the annihilation of positrons. The principal source of positrons in solar flares are nuclear reactions of accelerated particles with the ambient solar atmosphere. These reactions produce  $\pi^+$ -mesons and a variety of radioactive isotopes which decay by positron emission. The main positron emitters, their formation reactions, threshold energies, half-lives and maximum positron energies are given in Table XI.C-1. Except for the reactions  $N^{14} (p, n) O^{14}$  (for example, Andouze et al., 1967) and  $N^{14} (p, d) C^{11}$  (Jacobs et al., 1972), the cross sections for these reactions were given in Lingenfelter and Ramaty (1967). The resultant positron yields are given in Figures XI.C-1 and XI.C-2 for the thick- and thin-target models, respectively.

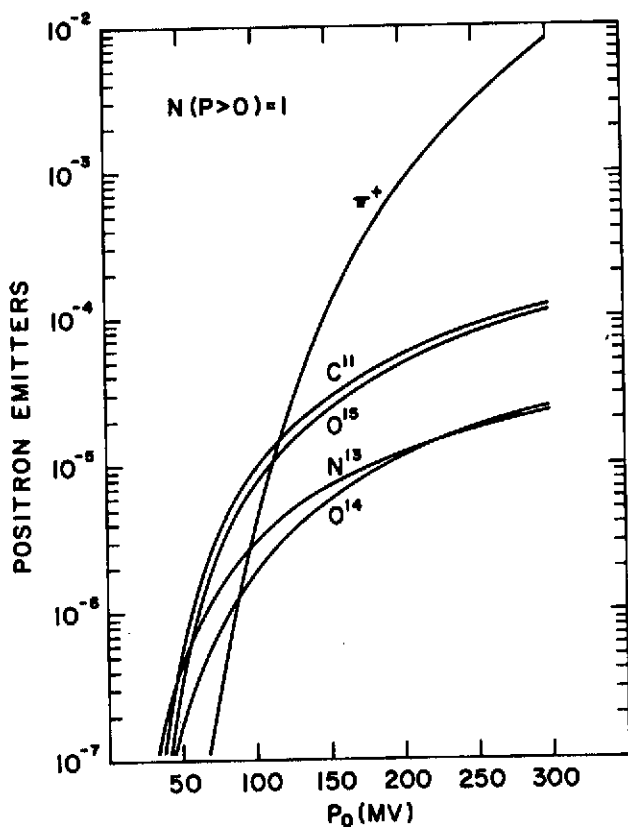


Figure XI.C-1. Yield of positron emitters at the sun for the thick-target model.

Table XI.C-1  
Positron Emitters

$\beta^+$ Emitter and Decay Mode	Maximum Positron Energy (MeV)	Half-life (min)	Production Mode	Threshold Energy (MeV)
$C^{11} \rightarrow B^{11} + \beta^{11} + \nu$	0.97	20.5	$C^{12} (p, pn) C^{11}$	20.2
			$N^{14} (p, 2p2n) C^{11}$	13.1
			$N^{14} (p, \alpha) C^{11}$	2.9
			$O^{16} (p, 3p3n) C^{11}$	28.6
$N^{13} \rightarrow C^{13} + \beta^+ + \nu$	1.19	9.96	$N^{14} (p, pn) N^{13}$	11.3
			$O^{16} (p, 2p2n) N^{13}$	5.54
$O^{14} \rightarrow N^{14} + \beta^+ + \nu$	1.86	1.18	$N^{14} (p, n) O^{14}$	6.4
$O^{15} \rightarrow N^{15} + \beta^+ + \nu$	1.73	2.07	$O^{16} (p, pn) O^{15}$	16.54

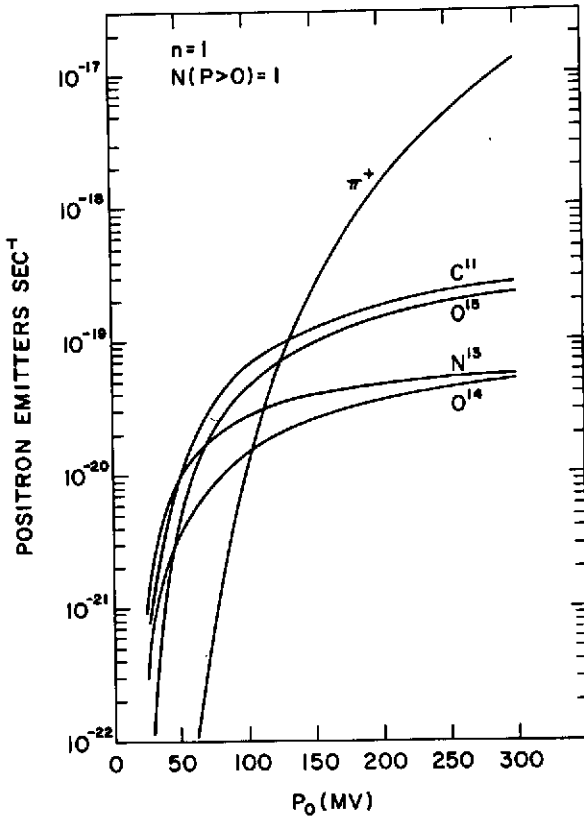


Figure XI.C-2. Production rate of positron emitters at the sun for the thin-target model.

The intensity of the 0.511-MeV line depends on the number of positrons that annihilate at the sun. For the thick-target model it is reasonable to assume that all the flare-produced positrons will ultimately annihilate at the sun. But, for the thin-target model, it is possible that a significant fraction of the positrons will escape from the sun before they annihilate. The determination of this fraction, however, is beyond the scope of the present paper and we defer the discussion on this for future research. For simplicity, in the subsequent calculations we assume that all flare-produced positrons annihilate at the sun, but keep in mind that this assumption may lead to too many 0.511 photons in the case of the thin-target model.

The annihilation radiation yield at 0.511 MeV also depends on the mode of positron annihilation. Positrons annihilate either directly with a free electron or in a bound state of positronium. In the latter case, the annihilations

proceed from a  $^1S$  state leading to two 0.511-MeV photons, or from a  $^3S$  state leading to a 3-photon continuum. Because the 3-photon continuum does not contribute to line emission at 0.511 keV, and because the probability of forming the  $^3S$  state is three times that of forming the  $^1S$  state, positronium formation and its annihilation produces on the average only one-half of a 0.511 photon per positron as compared to two photons for free annihilation. This point was discussed in detail by Stecker (1969) for positron annihilation in interstellar space. However, in the much higher density of the solar atmosphere we expect that only a small fraction of the positrons will annihilate from the  $^3S$  state of positronium. This is expected because the collision frequency of positronium with ambient electrons can be sufficiently high to either dissociate the positronium or to cause a transition to the  $^1S$  state before the annihilation of the  $^3S$  state. Also, the rate of positronium formation in a plasma is greatly reduced in comparison with positronium formation in a neutral medium. Thus, if the flare region is highly ionized, free annihilation will dominate over positronium annihilation (Ramaty and Lingenfelter, 1973b).

By allowing two photons per positron at the sun, the time-integrated 0.511-MeV line intensity at earth for the thick-target model is

$$F(0.511) = \frac{1}{2\pi R^2} [Q_s(\pi^+) + Q_s(C^{II}) + Q_s(N^{13}) + Q_s(O^{14}) + Q_s(O^{15})] \quad (XI.C-4)$$

where the various  $Q_s$ 's are given in Figure XI.C-1. The units of  $F$  are photons  $\text{cm}^{-2}$  per proton of rigidity greater than zero. For the thin-target model we obtain an equation similar to Equation (XI.C-4), with  $F$  and  $Q_s$  replaced by the instantaneous rates  $\phi$  and  $q_s$ . The units of  $\phi$  are photons  $\text{cm}^{-2} \cdot \text{s}^{-1}$  per proton of rigidity greater than zero. The resultant 0.511-MeV photon fluxes are given in Figures XI.C-3 and XI.C-4, for the thick- and thin-target models, respectively.

Next we consider the 2.23-MeV line resulting from the deexcitation of deuterium following neutron capture on hydrogen. The principal neutron-producing reactions and their cross sections were discussed by Lingenfelter and Ramaty (1967, and references therein). To these reactions we have added the reaction  $N^{14}(p, n)O^{14}$  mentioned previously which is important for low-energy protons ( $< 15$  MeV). The neutron-producing reactions are summarized in Table XI.C-2. The total neutron yields for the thick- and thin-target models are then obtained by using the appropriate cross sections in

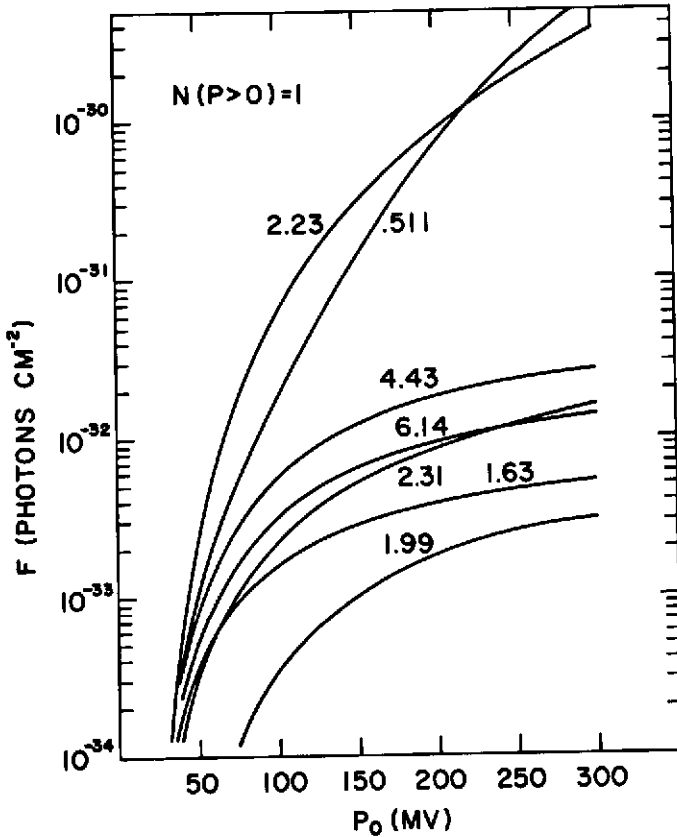


Figure XI.C-3. Time-integrated photon fluxes at earth in the thick-target model.

Equations (XI.C-2) and (XI.C-3). Having obtained the neutron yields, we have to consider the propagation of neutrons in the solar atmosphere because 2.23-MeV photons are not produced if the neutrons escape from the sun or decay in the solar atmosphere.

Neutron propagation in the solar atmosphere is determined predominantly by scattering (elastic and inelastic) and capture by protons. The total neutron-proton scattering cross section  $\sigma_s$  is essentially constant at 20 barns for neutron energies from 1 eV to 10<sup>5</sup> eV and then drops to about 0.1 barn at 100 MeV (Hughes and Schwartz, 1958). The capture cross section is inversely proportional to velocity and is given by  $\sigma_c \cong 2.2 \times 10^{-6} \beta^{-1}$ , where  $\sigma_c$  is measured in barns and  $c\beta$  is the velocity of the neutron. Since for all energies of interest  $\sigma_s \gg \sigma_c$ , the neutron mean-free path in the solar

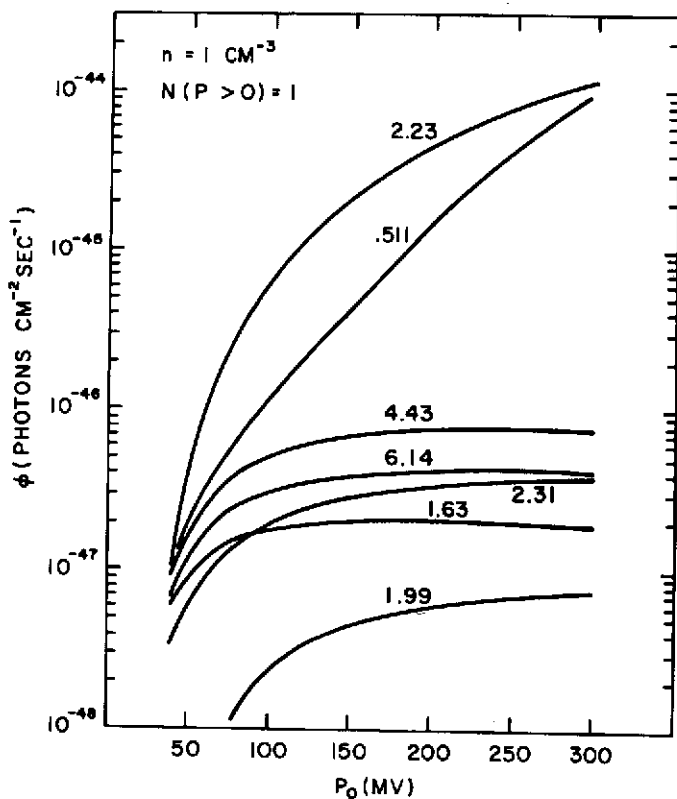


Figure XI.C-4. Instantaneous photon fluxes at earth in the thin-target model.

atmosphere is determined principally by neutron-proton scattering. Using the columnar density of the solar atmosphere as given by Allen (1963), we find that a 10-MeV neutron moving radially outward from the sun will probably escape from the solar atmosphere before making even one collision if it is produced in a region of density less than  $10^{17} \text{ cm}^{-3}$ . This density corresponds to a depth of about 300 km below the base of the chromosphere. Because solar flares occur in the chromosphere or corona, it is reasonable to assume that for both interaction models all upward-moving neutrons are going to escape from the sun. The downward-moving neutrons on the other hand decay or are captured, depending on whether the capture time is greater or smaller than the half-life of the neutrons. From the capture cross section ( $\sigma_c$ ), the capture time ( $t_c$ ) is given by

$$t_c = (c\beta n\sigma_c)^{-1} \cong \frac{1.5 \times 10^{19}}{n(\text{cm}^{-3})} \text{ s} \quad (\text{XI.C-5})$$

Table XI.C-2  
Neutron-Producing Reactions

Reaction	Threshold Energy MeV/Nucleon
$H^1 (p, n\pi^+) H^1$	292.3
$He^4 (p, pn) He^3$	25.9
$He^4 (p, 2pn) H^2$	32.8
$He^4 (p, 2p2n) H^1$	35.6
$C^{12} (p, n \dots)$	19.8
$N^{14} (p, n \dots)$	6.3
$O^{16} (p, pn \dots)$	16.5
$Ne^{20} (p, pn \dots)$	17.7

As can be seen,  $t_c$  is independent of energy and is inversely proportional to the density ( $n$ ) of the region where the neutrons interact with the ambient medium. From the previous discussion it follows that downward-directed neutrons probably will not collide with the ambient gas until they reach the photosphere where  $n$  is of the order  $10^{17} \text{ cm}^{-3}$ . Thus  $t_c \cong 150 \text{ s}$ , and since the half-life of the neutron is 720 s, it follows that most of the neutrons will be captured before they decay. Furthermore, since the neutron capture occurs at a columnar depth of about  $10^{24} \text{ cm}^{-2}$  or  $1.6 \text{ g} \cdot \text{cm}^{-2}$  while the stopping range of a 2.2-MeV photon is about  $25 \text{ g} \cdot \text{cm}^{-2}$ , all the upward-moving photons resulting from deuterium deexcitation will escape from the sun. Assuming isotropic production of neutrons in the interaction region, the 2.23-MeV line intensity at earth for the thick- and thin-target models, respectively, are

$$F(2.23) = \frac{1}{4\pi R^2} \frac{1}{2} Q_s(n) \tag{XI.C-6}$$

$$\phi(2.23) = \frac{1}{4\pi R^2} \frac{1}{2} q_s(n) \tag{XI.C-7}$$

where  $Q_s(n)$  and  $q_s(n)$  are the total neutron yields as calculated from Equations (XI.C-2) and (XI.C-3).

The calculations of the other intensities at 1.63, 1.99, 2.31, 4.43, 5.5, and 6.14 MeV in Figures XI.C-3 and XI.C-4 are straightforward. Unlike the 0.511- and 2.23-MeV lines, these emissions are prompt, that is, the excited states or secondary products decay by photon emission in a time scale much shorter than any characteristic time of the flare process.

Line emission at 4.43 and 6.14 MeV results from the deexcitation of the first nuclear levels of  $C^{12}$  and  $O^{16}$ , respectively. The intensity of the 6.14-MeV line is the same as calculated by Lingenfelter and Ramaty (1967). The intensity of the 4.43-MeV line is about 50 percent greater than in Lingenfelter and Ramaty (1967), because it is possible to produce  $C^{12(4.43)}$  by the spallation of  $O^{16}$ , a process which was neglected in that paper. The calculations for this process, given in Figures XI.C-3 and XI.C-4, are based on cross sections measured by Zobel et al. (1968).

Radiation at 2.31 MeV corresponds to the first nuclear level of  $N^{14}$ . The 2.31-MeV line is produced by the direct excitation of the first and second levels of  $N^{14}$ . The latter is at 3.94 MeV and it deexcites 96 percent of the time through the first level, thereby producing a 1.63-MeV photon in addition to the 2.31-MeV photon. In addition to direct excitation, the first level of  $N^{14}$  can also be populated by the decay of  $O^{14}$ , which is produced by the reaction  $N^{14}(p,n)O^{14}$ .  $O^{14}$   $\beta$  decays 99.4 percent of the time to  $N^{14(2.31)}$ , and hence each  $\beta$ -decay is accompanied by a 2.31-MeV photon. As mentioned previously, the 1.63-MeV line is formed by the deexcitation of  $N^{14(3.94)}$ . In addition, this line is also produced by the deexcitation of the first level of  $Ne^{20}$ . Finally the 1.99-MeV line results from the deexcitation of  $C^{11}$  which is formed from the spallation of  $C^{12}$ . The cross section for this process is given by Zobel et al. (1968).

The principal reason for showing the 1.99- and 2.31-MeV lines is that in studies with detectors of poor energy resolution, these lines could, in principle, be confused with the deuterium deexcitation line. As can be seen from Figures XI.C-3 and XI.C-4, however, the  $C^{11(1.99)}$ -MeV line is negligible in comparison with the deuterium line. On the other hand, the 2.31-MeV line from  $N^{14}$  could compete with the 2.23-MeV line at low  $P_0$ 's. If all the emission at  $\sim 2.2$  MeV is from  $N^{14}$ , however, the intensities of the 4.43-MeV and 6.14-MeV lines should be about the same as that of the 2.2-MeV line. As will be discussed below, this was not the case for the August 4, 1972 event. Therefore, for this flare at least, we conclude that the 2.2-MeV line is produced almost entirely by neutron capture.

We have summarized in Table XI.C-3 the principal mechanism leading to line emission in the solar atmosphere. In addition to the lines given in Figures XI.C-3 and XI.C-4, we have listed in Table XI.C-3 lines at 5.2 MeV from  $O^{15}$  and  $N^{15}$  and at 7.12 MeV from  $O^{16}$ . From the cross sections of Zobel et al.

Table XI.C-3  
Gamma-Ray Line Emission Mechanisms

Photon Energy (MeV)	Origin	Production Mode
0.511	Positron annihilation	Table 1
2.23	Deuterium deexcitation following neutron capture	Table 2
1.63	Ne <sup>20(1.63)</sup> deexcitation	Ne <sup>20</sup> (p, p') Ne <sup>20(1.63)</sup>
	N <sup>14(3.94)</sup> ⇒ N <sup>14(2.31)</sup> deexcitation	N <sup>14</sup> (p, p') N <sup>14(3.94)</sup>
2.31	N <sup>14(2.31)</sup> deexcitation	N <sup>14</sup> (p, p') N <sup>14(2.31)</sup> N <sup>14</sup> (p, p') N <sup>14(3.94)</sup> ⇒ N <sup>14(2.31)</sup> N <sup>14</sup> (p, n) O <sup>14</sup> ⇒ N <sup>14(2.31)</sup>
4.43	C <sup>12(4.43)</sup> deexcitation	C <sup>12</sup> (p, p') C <sup>12(4.43)</sup> O <sup>16</sup> (p, ) C <sup>12(4.43)</sup>
5.2	O <sup>15(5.20)</sup> deexcitation	O <sup>16</sup> (p, ) O <sup>15(5.20)</sup>
	N <sup>15(5.28)</sup> deexcitation	O <sup>16</sup> (p, ) N <sup>15(5.28)</sup>
6.14	O <sup>16(6.14)</sup> deexcitation	O <sup>16</sup> (p, p') O <sup>16(6.14)</sup>
7.12	O <sup>16(7.12)</sup> deexcitation	O <sup>16</sup> (p, p') O <sup>16(7.12)</sup>

(1968), the intensities of both these lines should be approximately 50 percent of the 6.14-MeV line intensity.

### DISCUSSION

Let us now compare the results of our calculations with the observations of Chupp et al. (1973) for the August 4, 1972, flare. We defer the discussion on the August 7, 1972, observations, since the  $\gamma$ -rays from this flare were observed only after the flare maximum and hence they require a more detailed treatment of the time dependence of the  $\gamma$ -ray intensities.

In Figures XI.C-5 and XI.C-6, the shaded areas represent the time-averaged ratios of the measured 0.5-, 4.4-, and 6.1-MeV line intensities to the measured 2.2-MeV line. The curves represent the calculated ratios as functions of the characteristic rigidity ( $P_0$ ), for the thick-target model in Figure XI.C-5 and the thin-target model in Figure XI.C-6. As can be seen, the calculated 4.43 and 6.14 curves are strong functions of  $P_0$ .

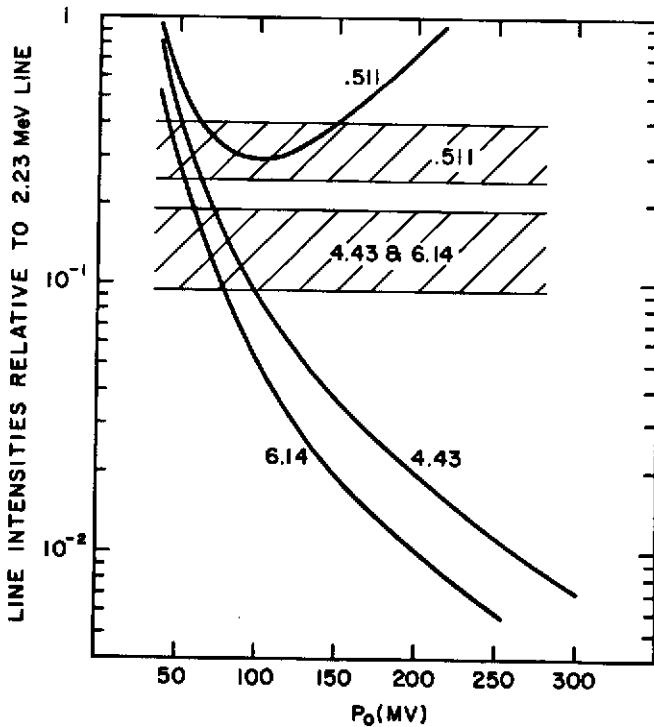


Figure XI.C-5. Relative line intensities for the thick-target model.

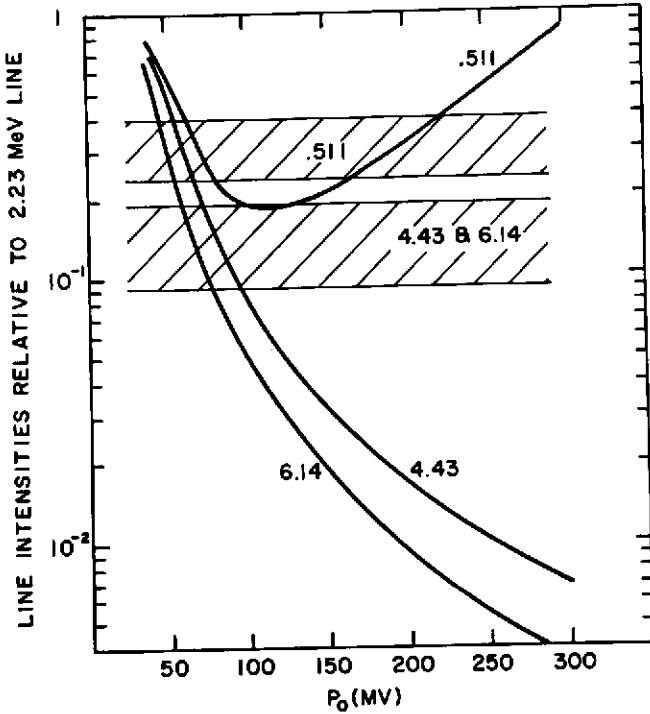


Figure XI.C-6. Relative line intensities for the thin-target model.

Therefore, the comparison of these ratios with the measurements allows us to deduce the value of the characteristic rigidity ( $P_0$ ). We find that for both models  $P_0$  has to be in the range 70 to 80 MV. This range of  $P_0$ 's should be compared with values of  $P_0$  as obtained from charged-particle observations near earth.

According to Bostrom et al. (1972), the peak proton intensities after the flare of August 4, 1972, were:  $j(> 10 \text{ MeV}) = 10^6 \text{ cm}^{-2} \text{ s}^{-1}$ ,  $j(> 30 \text{ MeV}) = 2.6 \times 10^5 \text{ cm}^{-2} \text{ s}^{-1}$ , and  $j(> 60 \text{ MeV}) = 8 \times 10^4 \text{ cm}^{-2} \text{ s}^{-1}$ . From these intensities we can deduce the local proton density ( $u$ ) in the interplanetary medium. If  $u(P) \propto \exp(-P/P_0)$ , and if the protons are nonrelativistic

$$u(> P) = j(> P) (mc/e) (P + P_0)^{-1} \quad \text{(XI.C-8)}$$

From Equation (XI.C-8) and the integral intensities  $j(> P)$  given above, we can calculate values of  $u(> P)$  for various  $P_0$ 's. For  $P_0 = 6.5 \text{ MV}$  we obtain

proton densities as follows:

$$u(> 10 \text{ MeV}) = 1.53 \times 10^{-4}, \quad u(> 30 \text{ MeV}) = 2.67 \times 10^{-5}, \quad \text{and} \\ u(> 60 \text{ MeV}) = 6.13 \times 10^{-6}.$$

These numbers are plotted in Figure XI.C-7 as functions of  $P$ . The straight lines are exponentials in rigidity with  $P_0 = 60 \text{ MV}$  and  $P_0 = 70 \text{ MV}$ , and they bracket the observed proton densities. The charged-particle observations at the peak of the proton event are therefore consistent with a characteristic rigidity of about 60 to 70 MV. Furthermore, this characteristic rigidity remains essentially the same for the remainder of the particle event (J. King, private communication).

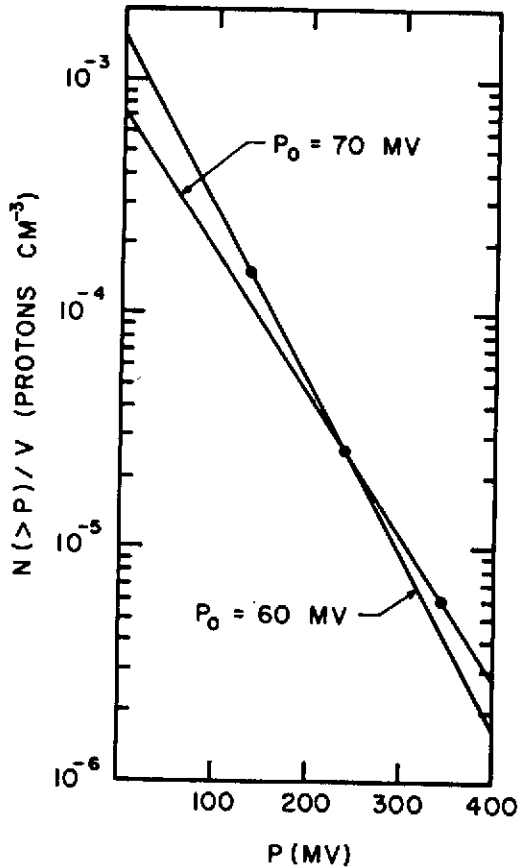


Figure XI.C-7. Proton densities in the interplanetary medium from local particle measurements.

The similarity between the proton spectrum as observed near earth and the proton spectrum at the sun as deduced from the  $\gamma$ -ray observations, seems to imply that, at least for the August 4, 1972, flare, both the escape of particles from the flare region and their propagation in the interplanetary medium are essentially independent of energy.

Let us now calculate the total number of protons at the sun. In the case of the thick-target model this calculation is independent of the ambient density ( $n$ ) but requires the knowledge of the time-integrated photon flux from the flare. According to Chupp et al. (1973), the average intensity of the 2.2-MeV line from 0616 UT to 0632 UT on August 4, 1972, was  $0.22 \text{ photons cm}^{-2} \text{ s}^{-1}$ , and thus the total photon flux in the 6-min time interval was  $80 \text{ photons cm}^{-2}$ . This is only a lower limit because OSO-7 went into earth eclipse at 0632 UT before the termination of the  $\gamma$ -ray event. The total  $\gamma$ -ray flux, however, was probably not much larger, since as indicated by the microwave data (Toyokawa Observatory, private communication), the acceleration of the charged particles probably ceased at 0635 UT, 3 min after the eclipse of OSO-7.

For a flux of  $80 \text{ photons cm}^{-2}$  and  $P_0$  ranging from 60 MV to 70 MV, we find from Figure XI.C-3 that  $N(>P)$  is between  $1.4$  and  $6 \times 10^{33}$ . These numbers should be compared with the number of protons released from the flare based on measurements of the proton flux near earth. This number can be obtained from the local densities shown in Figure XI.C-7 if we assume that the particles fill some volume ( $V$ ) in the interplanetary medium to that density. A conservative estimate of this volume would be to assume that it is that of a cone of opening angle  $30^\circ$  with vertex at the sun and height 1.5 AU. This is consistent with the fact that the August 4 flare was located at  $15^\circ$  N latitude on the sun and that some charged particles were observed on the Pioneer-10 space probe at 2 AU from the sun (B. J. Teegarden, private communication). The volume ( $V$ ) is therefore  $\sim 10^{39} \text{ cm}^3$ , and from Figure XI.C-7,  $N(>P)$  is  $7 \times 10^{35}$  and  $1.5 \times 10^{36}$  for  $P_0$  equal to 70 MV and 60 MV, respectively. When compared with the values of  $N(P > 0)$  deduced above from the  $\gamma$ -ray observations for the thick-target model, we see that possibly not more than about 1 percent of the flare-accelerated protons could have escaped downward into the sun. However, we should note that this conclusion is strongly dependent on our estimate of the total number of protons at the sun, based on the local proton observations. Clearly a more detailed understanding of the source function of flare protons in the interplanetary medium is required.

In the case of the thin-target model, the instantaneous photon flux at earth directly determines the emission measure at the sun, that is, the product  $nN(P > 0)$ . From Figure XI.C-4 we find that the observed flux of  $0.22 \text{ photons cm}^{-2} \cdot \text{s}^{-1}$  implies that  $nN$  is  $1$  to  $2 \times 10^{45} \text{ cm}^{-3}$  for  $P_0$  ranging from 70 MV to 60 MV. Then, using the values of  $N(P > 0)$  as deduced from the proton flux near earth, we get ( $n$ ) is  $1.5$  to  $3 \times 10^9 \text{ cm}^{-3}$ . As before, note

that this density is subject to the uncertainty in the total number of protons at the sun obtained from the local observations.

Let us finally evaluate the total energy in the flare-accelerated protons that produce  $\gamma$ -rays at the sun. For the spectrum given in Equation (XI.C-1) and for nonrelativistic protons, the average proton energy is  $P_0^2/Mc^2$ . Therefore, for the thick-target model, the energy in the  $1.4$  to  $6 \times 10^{33}$  protons as deduced above is  $1.2$  to  $3.7 \times 10^{28}$  ergs.

For the thin-target model, both the instantaneous  $\gamma$ -ray production rate and the instantaneous proton energy loss rate depend on the product of the ambient density ( $n$ ) and the total number of protons at the sun. The ratio of these two rates, therefore, is independent of both  $n$  and  $N$  and depends only on the spectrum of the accelerated particles, that is,  $P_0$  in our calculations. This point was first made by Lingenfelter (1969). For the proton distribution in Equation (XI.C-1), normalized to one proton of rigidity greater than zero, the instantaneous energy loss rate ( $W$ ) to ionization, excitation and nuclear interactions in ambient hydrogen of unit density is given in Table XI.C-4. As can be seen, for  $P_0$ 's between 60 to 70 MV,  $W$  is very closely equal to  $1.7 \times 10^{-18}$  ergs  $\cdot$  s $^{-1}$ . Using the values of  $Nn$  given above, we see that  $\gamma$ -ray production by flare-accelerated protons is accompanied by the dissipation of  $1.7$  to  $3.4 \times 10^{27}$  ergs  $\cdot$  s $^{-1}$ . For the time interval of 6 min during which  $\gamma$ -rays were observed, the total dissipated energy is  $0.6$  to  $1.2 \times 10^{30}$  ergs.

This energy is comparable to the total of  $\sim 2 \times 10^{30}$  ergs emitted in H $\alpha$  by the flare of August 4, 1972, (H. Zirin, private communication) and is consistent with the suggestion of Gordon (1954) that the optical energy from flares results from ionization losses of accelerated particles. On the other hand, in the thick-target model the ionization losses of the  $\gamma$ -ray producing protons is only a few percent of the observed optical energy; in this case additional energy loss may be expected from electrons.

Table XI.C-4

Energy Loss Rate of the Proton Distribution in Equation (XI.C-1) in Solar Material of  $n = 1 \text{ cm}^{-3}$

$P_0$ (MV)	$W$ (erg s $^{-1}$ )
20	$2 \times 10^{-18}$
30	$2 \times 10^{-18}$
40	$1.9 \times 10^{-18}$
60	$1.8 \times 10^{-18}$
80	$1.6 \times 10^{-18}$
100	$1.5 \times 10^{-18}$
120	$1.4 \times 10^{-18}$
200	$1.2 \times 10^{-18}$
300	$1.1 \times 10^{-18}$

## REFERENCES

- Allen, C. W., 1963, *Astrophysical Quantities*, London.
- Audouze, J., M. Ephere, and H. Reeves, 1967, *High-Energy Nuclear Reactions in Astrophysics*, B. S. P. Shen, W. A. Benjamin, eds., New York, p. 255.
- Bostrom, C. O., J. W. Kohl, and R. W. McEntire, 1972, *The Solar Proton Flux - August 2-12, 1972*, The Johns Hopkins University, Applied Physics Laboratory, Silver Spring, Maryland.
- Cameron, A. G. W., 1967, *Origin and Distribution of Elements*, L. H. Ahrens, ed., Pergamon Press, London.
- Cheng, C. C., 1972, *Space Sci. Rev.*, 13, p. 3.
- Chupp, E. L., D. J. Forrest, P. R. Higbie, A. N. Suri, C. Tsai, and P. P. Dunphy, 1973, *Nature*, 241, p. 333.
- Gordon, I. M., 1954, *Dokl. Akad. Nauk SSSR*, 96, p. 813.
- Hughes, D. J., and R. B. Schwartz, 1958, *Neutron Cross Sections*, Brookhaven National Laboratory, Upton, New York.
- Jacobs, W. W., D. Bodansky, J. M. Cameron, D. Oberg, and P. Russo, 1972, *Bull. American Phys. Soc.*, 17, p. 479.
- Lingenfelter, R. E., and R. Ramaty, 1967, *High-Energy Nuclear Reactions in Astrophysics*, B. S. P. Shen, and W. A. Benjamin, eds., New York, p. 99.
- Lingenfelter, R. E., 1969, *Solar Phys.*, 8, p. 341.
- Ramaty, R., and R. E. Lingenfelter, 1973a, *High Energy Phenomena on the Sun, Conference Proceedings*, R. Ramaty and R. G. Stone, eds., GSFC X-693-73-193, p. 301.
- , 1973b, *Conference Papers, Thirteenth International Conference on Cosmic Rays*, Denver, Colorado, paper 134.
- Stecker, F. W., 1969, *Astrophys. Space Sci.*, 3, p. 479.
- Zobel, W., F. C. Maienschein, J. H. Todd, and G. T. Chapman, 1968, *Nucl. Sci. and Eng.*, 32, p. 392.

## DISCUSSION

*White:*

Could you elaborate a little bit more on the difference between the experimental observation and the theoretical calculations?

*Ramaty:*

In my first calculation with Richard Lingenfelter, we took certain numbers published by Bill Webber who calculated the total number of protons at the sun using a three-dimensional isotropic diffusion model in the interplanetary medium. Just by doing that, but propagating the particles in a reasonably small solid angle, something like  $30^\circ$ , we get a reduction of a factor of 50 in the total number of protons at the sun.

For this particular flare of August 4, we get reasonable agreement if I assume that only about 10 percent of the protons seen at the earth are coming from the sun. In this case, according to Frank McDonald, the observed particles at earth were in great part accelerated by flare-produced shock waves.

*White:*

Can you definitely ascribe it to the number of protons observed, rather than the number of  $\text{g}/\text{cm}^2$  traversed by the charged particles at the sun?

*Ramaty:*

I think I can, but of course there are two models: the thick-target model, which is completely independent of the number of  $\text{g}/\text{cm}^2$ , and the thin target, for which the relevant parameter is the ambient density in the flare.

What you get from the  $\gamma$ -rays is a product, a total number of particles from the sun times the ambient density: the so-called emission measure.

## A. ULTRA-HIGH ENERGY GAMMA RAYS

A. W. Strong, J. Wdowczyk,\* and A. W. Wolfendale  
*University of Durham*

### INTRODUCTION

The problem of the origin of the cosmic radiation is well known. Although there are many potential sources in the galaxy such as novae, supernovae, pulsars, and the galactic nucleus, there is great difficulty in explaining the observed isotropy of the radiation above  $10^{17}$  eV where the galactic magnetic field is not strong enough to randomize the particle directions and considerable anisotropies should result. The suggestion of an extragalactic origin for all the radiation demands a rather high-energy density of this component throughout the universe ( $\sim 1 \text{ eV} \cdot \text{cm}^{-3}$ ), but if only particles above  $10^{15}$  eV or so come predominantly from outside the galaxy this difficulty disappears.

If these very energetic primaries are indeed of extragalactic origin, their interaction with the radiations in space, principally the relict radiation (Penzias and Wilson, 1965, and later papers), becomes a process of importance. The protons will lose energy by way of interaction with this radiation and produce, successively as the energy is increased,  $e^+e^-$  pairs and pions. In turn, the energy loss would be expected to show up as an increase in slope of the energy spectrum of protons recorded at the earth.

There is the well known increase of slope at  $\sim 3 \times 10^{15}$  eV and it is conceivable that this arises from just such interactions, principally  $e^+e^-$  production, at early stages of the evolution of the universe when the relict radiation was at a higher temperature than its present value of 2.7 K (Hillas, 1968; Strong et al., 1973a,b). The latter authors have calculated the flux of  $\gamma$ -rays expected to result from such interactions and, although they are hardly of 'ultra-high' energy, they will be considered briefly later because their origin is similar to that of the much higher  $\gamma$ -rays which are the main subject of this work.

---

\*Speaker.

If cosmic-ray protons did not start to be produced until comparatively late stages in the evolution of the universe when the temperature of the relict radiation was close to its present value,  $e^+e^-$  production would cause a reduction of primary proton intensity by a factor  $\sim 3$  above  $\sim 3 \cdot 10^{18}$  eV and pion production would cause a reduction starting at  $\sim 5 \cdot 10^{19}$  eV and reaching a factor  $\sim 100$  above  $\sim 2 \cdot 10^{20}$  eV. Such a reduction does not appear to have been detected experimentally (although at the energies in question, the number of events detected, that is, extensive air showers, is small and errors of energy determination are not negligible). A possible way out of the problem is to assume that the production spectrum of primary protons above  $10^{19}$  eV is flatter than that at lower energies so that after attenuation the spectrum at the earth has roughly the same slope as that below  $10^{19}$  eV. Although this idea is perhaps improbable, it is by no means impossible. Clearly in this case, there will be significant energy going into pions and electrons and eventually  $\gamma$ -rays, and these will be, in principle, detectable. The details to be described in the following sections are taken largely from the work of Wdowczyk et al. (1972).

## INTERACTION OF PROTONS WITH THE RELICT RADIATION

### The Attenuation Length for Photomeson Production

The interaction process has been considered by a number of authors starting with Greisen (1966) and Zatsepin and Kuzmin (1966), and an accurate analysis has been given by Stecker (1968). Stecker (1968) has summarized experimental data on the total photomeson production cross section and inelasticity for high-energy protons in the relict radiation as a function of  $\gamma$ -ray energy in the proton rest system and used the data in the derivation of  $\lambda_a$  ( $\lambda_a = (K_p n_\gamma \sigma)^{-1}$  where  $K_p$  is the inelasticity of the interaction,  $n_\gamma$  is the photon density, and  $\sigma$  is the meson production cross section). The values of  $\lambda_a$  derived in this way are given in Figure XII.A-1. Kuzmin and Zatsepin (1968) and Adcock (1970, private communication) have derived values of the interaction length ( $\lambda_1$ ) as a function of  $E_p$ , and these values are close to what would be expected from Stecker's results.

### Energy Spectrum of Protons

Wdowczyk et al. (1972), considered two limiting forms for the energy spectrum of protons at the earth, as shown in Figure XII.A-2. The higher intensities (A) come from the work of Linsley (1963) and the lower spectrum (B) is that due to Andrews et al. (1971). Although the latter seems more probable, results for both will be given so that interpolation (or extrapolation) may be made if results are needed for some other spectrum.

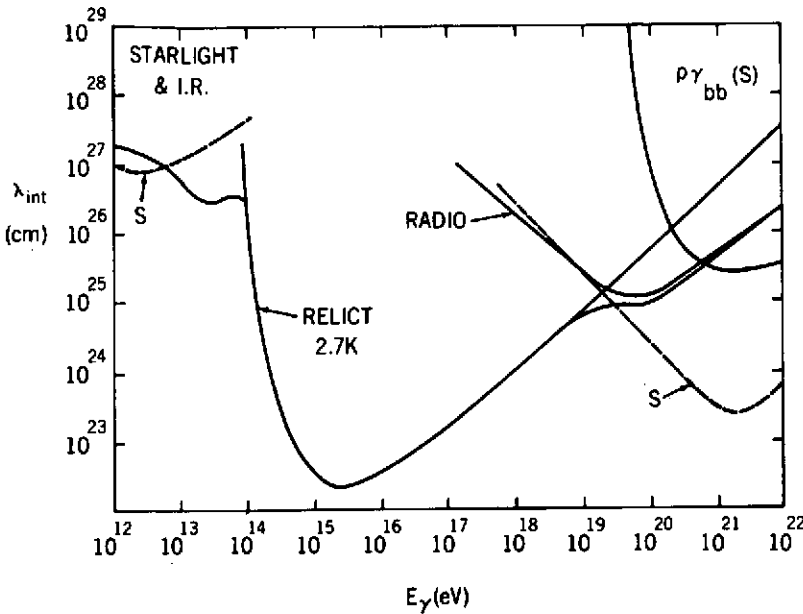


Figure XII.A-1. Interaction length against photon energy for collisions of energetic photons with photons of the various photon fields ( $e^+e^-$  production only). The full lines represent the calculations of Wdowczyk et al. (1972), and the dotted lines those of Stecker (1971). Also shown (top right-hand corner) is the attenuation length for protons in the relict radiation from the work of Stecker (1968).

**Energy Spectrum of  $\gamma$ -Rays on Production**

In Wdowczyk et al. (1972), use was made of Stecker's data to calculate the production spectra of  $\pi^0$ -mesons, and in turn that of  $\gamma$ -rays, with the results shown in Figure XII.A-2. An important datum is the total energy going into  $\gamma$ -rays: for A this is

$$7 \times 10^{-25} \text{ eV} \cdot \text{cm}^{-3} \cdot \text{s}^{-1} \text{ from } \pi^0\text{-mesons, together with}$$

$$4 \times 10^{-25} \text{ eV} \cdot \text{cm}^{-3} \cdot \text{s}^{-1} \text{ from } e^+e^- \text{ pairs.}$$

For spectrum B the corresponding figures are

$$6 \times 10^{-26} \text{ eV} \cdot \text{cm}^{-3} \cdot \text{s}^{-1} \text{ from } \pi^0\text{-mesons and}$$

$$\approx 4 \times 10^{-25} \text{ eV} \cdot \text{cm}^{-3} \cdot \text{s}^{-1} \text{ from } e^+e^- \text{ pairs.}$$

(The spectra A and B are very similar in the energy region where pair production is important.)

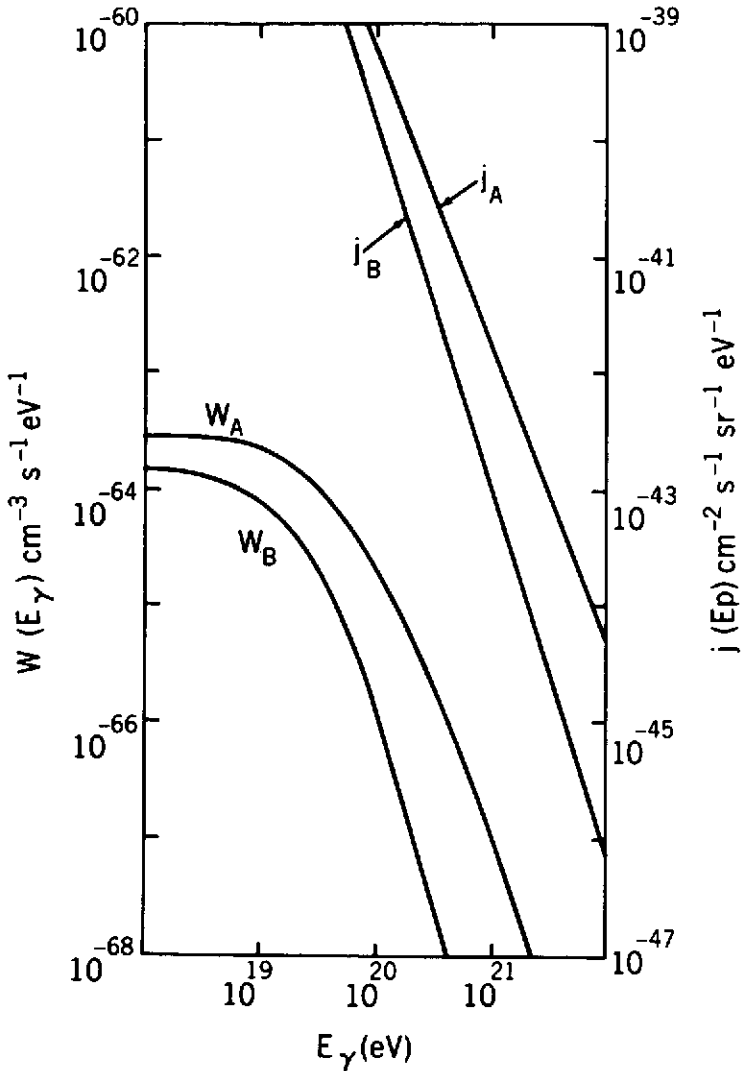


Figure XII.A-2. Alternative primary proton spectra  $j_A$  and  $j_B$  and the corresponding  $\gamma$ -production spectra,  $W(E_\gamma)$ , from Wdowczyk et al. (1972).

With spectrum A and assuming a residence time for photons in the universe of  $T = 13 \times 10^9 \text{y} = 4 \times 10^{17} \text{s}$ , the integrated  $\gamma$ -ray intensity is  $7 \times 10^2 \text{eV} \cdot \text{cm}^{-2} \cdot \text{s}^{-1} \cdot \text{sr}^{-1}$ , and the energy density is  $3 \times 10^{-7} \text{eV} \cdot \text{cm}^{-3}$ .

This energy density can be compared with that in the proton spectrum at the earth above  $5 \times 10^{19} \text{eV}$  of  $\sim 3 \times 10^{-10} \text{eV} \cdot \text{cm}^{-3}$ . The large disparity is

because of the fact mentioned in the first section of this paper: that the proton spectrum on production must be much flatter than that observed. Essentially, the detected protons come from within one attenuation length ( $\sim 3 \times 10^{25}$  cm at a mean energy of  $3 \times 10^{20}$  eV) whereas  $\gamma$ -rays come from the whole of the universe ( $\sim 10^{28}$  cm).

The production spectra in Figure XII.A-2 are close to those given by Stecker (1973, and private communication) for the same alternative proton spectra.

## PROPAGATION OF $\gamma$ -RAYS THROUGH THE UNIVERSE

### Extragalactic Radiation Fields

Summaries of the radiation fields and the corresponding interaction mean-free paths for  $\gamma$ - $\gamma$  collisions have been given by a number of authors, notably Gould and Schreder (1967a, b), Stecker (1971), and Wdowczyk et al. (1972). There is, understandably, agreement for the relict radiation, but a small disparity for starlight and IR, and a large disparity for the radio background. A comparison is made in Figure XII.A-1 between the results of Wdowczyk et al. (1972) — full line—and that of Stecker (1971)—an updating of Gould and Schreder, 1967a, b)—dotted line. Of importance for the propagation of  $\gamma$ -rays above  $10^{20}$  eV is the difference in the radio background, and this needs to be considered. The problem of measuring the isotropic component of the radio background at the earth is severe and experimental differences are rather great. Wdowczyk et al. (1972), used the measurements of Clark et al. (1970), which show a fall off in intensity at photon energies below  $10^{-8}$  eV, and insofar as these measurements are later than those used by the other authors, their analysis will be used here. It is interesting to note that if the shorter interaction lengths are valid for  $E > 10^{20}$  eV, then the result will be a reduction in the intensity of such  $\gamma$ -rays at the earth but an increase in intensity at energies just below this value.

### The Interaction Process

The generated high-energy photons will interact with the photons of the various radiation fields to produce electron pairs,  $\gamma + \gamma \rightarrow e^+ + e^-$ . Muon pairs can also be produced if the energy is high enough ( $E_\gamma > 10^{19}$  eV for relict radiation) and the mean-free paths for muon-pair and electron-pair production eventually become equal; however, in the energy region where a significant effect would occur, the radio background takes over.

The interaction process has been examined in some detail by Bonometto and Lucchin (1971), Allcock and Wdowczyk (1972), and by Wdowczyk et al. (1972). The authors have pointed out the important fact that at high-photon energies the angular distribution of the electrons peaks in the forward and

backward directions so that in the laboratory system one of the electrons takes an increasingly large fraction of the energetic photon energy. In the absence of an extragalactic magnetic field of magnitude above  $\sim 10^{11}$  G (see Wdowczyk et al., 1972), the electrons produced will collide with the relict photons and produce further energetic photons by the inverse Compton effect; in this way a  $\gamma$ -ray cascade will be built up.

### First Generation $\gamma$ -Spectrum

Whether or not magnetic fields are present, the  $\gamma$ -ray spectrum of Figure XII.A-2 will be generated and a first generation spectrum  $I_1(E_\gamma) = 1/4\pi W(E_\gamma) \lambda(E_\gamma)$  will be formed. This spectrum has been calculated in Wdowczyk et al. (1972), for proton spectra A and B with the result shown in Figure XII.A-3.

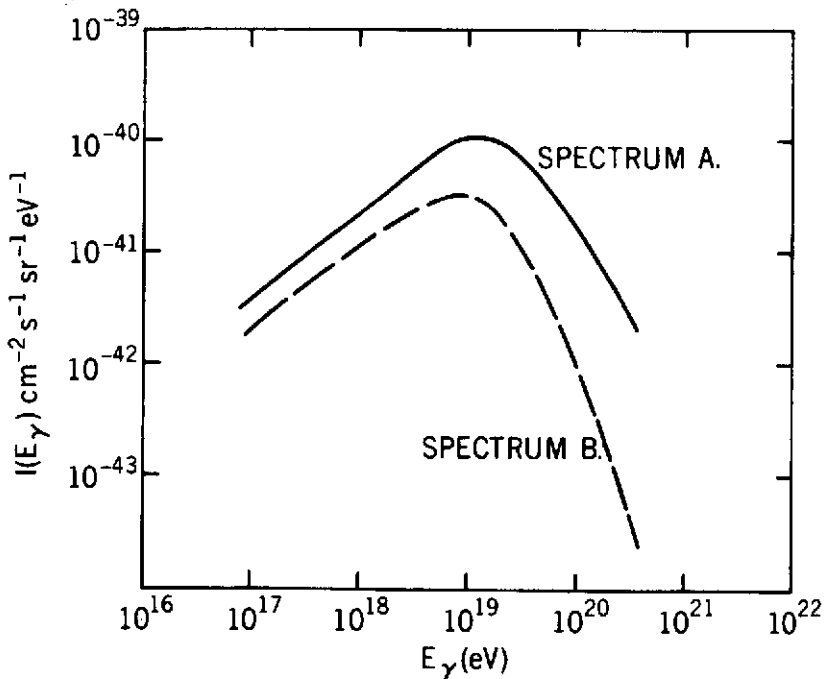


Figure XII.A-3. First generation production spectra from Wdowczyk et al. (1972). If the mean extragalactic magnetic field exceeds  $10^{10}$  G or so, cascading will be inhibited and these will be the spectra of  $\gamma$ -rays above  $\sim 10^{18}$  eV.

### Cascading in the Absence of Galactic Magnetic Fields

The cascading problem is one of some complexity, and the only calculations reported to date appear to be those in Wdowczyk et al. (1972). An order of magnitude estimate of the upper limit to the intensity at low energies (where most of the energy will eventually lie) can be obtained from energy conservation. For example, if starlight were to be disregarded (that is,  $\lambda_1$  for starlight  $> 10^{28}$  cm) then, very roughly, the intensity would have an average value below  $10^{14}$  eV (Figure XII.A-1) of  $I_c (< 10^{14}$  eV) given by

$$\int_{E_0}^{10^{14} \text{ eV}} E_\gamma I_c(E_\gamma) dE_\gamma \approx 7 \times 10^2 \text{ eV} \cdot \text{cm}^{-2} \cdot \text{s}^{-1} \cdot \text{sr}^{-1}$$

for proton spectrum A; (where  $E_0 \ll 10^{14}$  eV); that is

$$I_c(E_\gamma < 10^{14} \text{ eV}) \approx 10^{-25} \text{ cm}^{-2} \cdot \text{s}^{-1} \cdot \text{sr}^{-1} \cdot \text{eV}^{-1}$$

Similarly, in the presence of considerable starlight but no radiation causing attenuation below  $10^{11}$  eV, we would expect

$$I_c(E_\gamma < 10^{11} \text{ eV}) \approx 10^{-19} \text{ cm}^{-2} \cdot \text{s}^{-1} \cdot \text{sr}^{-1} \cdot \text{eV}^{-1}$$

again for proton spectrum A.

The diffusion equations were solved in Wdowczyk et al. (1972) giving the energy spectra shown in Figures XII.A-4 and XII.A-5. It can be seen that the intensities at low energies are not inconsistent with what would be expected from the remarks in the previous paragraph.

### Cascading in the Presence of Galactic Magnetic Fields

The presence of significant fields causes the electrons produced in  $\gamma$ - $\gamma$  collisions to lose energy by synchrotron radiation and thus give rise to 'low' energy  $\gamma$ 's rather than to transfer most of their energy to a single photon by Compton interactions. The problem was considered in Wdowczyk et al. (1972), and results were given for what might be a reasonable field:  $\langle B \rangle = 10^{-9}$  gauss. Not surprisingly, perhaps, the synchrotron spectrum so derived is rather similar to that from cascading, below  $10^{15}$  eV. However, a note of caution is necessary because of the effect of the field on the proton spectrum. It is possible to envisage a situation where the proton spectrum is higher elsewhere and the  $\gamma/p$  ratio at the earth would be correspondingly higher.

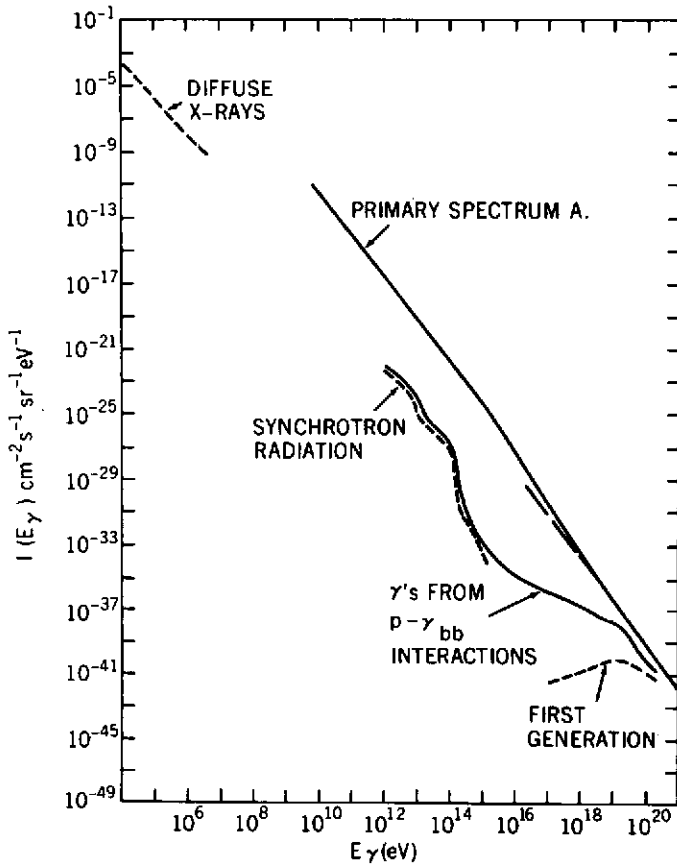


Figure XII.A-4. Gamma-ray spectra over the whole energy range, from Wdowczyk et al. (1972). The diffuse X-ray spectra summarized by Ipavich and Lenchek (1970) are also shown, as is primary proton spectrum A.

### SUMMARY OF PREDICTIONS CONCERNING $\gamma$ -RAYS ABOVE $10^{12}$ eV

The intensities of  $\gamma$ -rays shown in Figures XII.A-4 and XII.A-5 (for the case of  $\langle B \rangle \gtrsim 10^{11}$  G) have been used to give the  $\gamma/p$  ratios shown in Figure XII.A-6.

It will be noticed that the ratios are approaching measurable fractions at energies above  $10^{19}$  eV. Of particular interest is the peak in the region of  $2 \times 10^{19}$  eV which comes from the effect of the transition from domination by relict radiation to that by the radio background at this energy (Figure XII.A-1). An approximate analysis was made in Wdowczyk et al. (1972) of

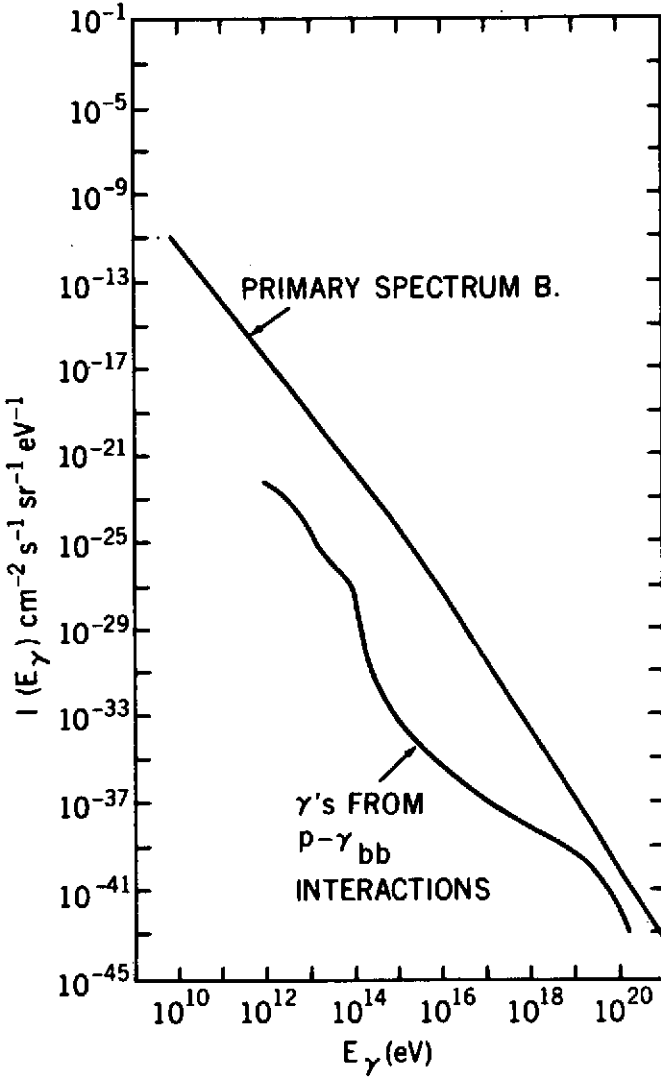


Figure XII.A-5. Gamma-ray spectrum for primary proton spectrum B, from Wdowczyk et al. (1972). (approximate - relaxed from Figure XII.A-4).

the upper limit that can be set on this ratio from studies of extensive air showers ( $\gamma$ -initiated showers would be poor in muons compared with proton-initiated showers). It can be seen that so far the experimental limit is significantly higher than the maximum predicted ratio. However, there are sufficient uncertainties in our knowledge of extragalactic parameters to make it

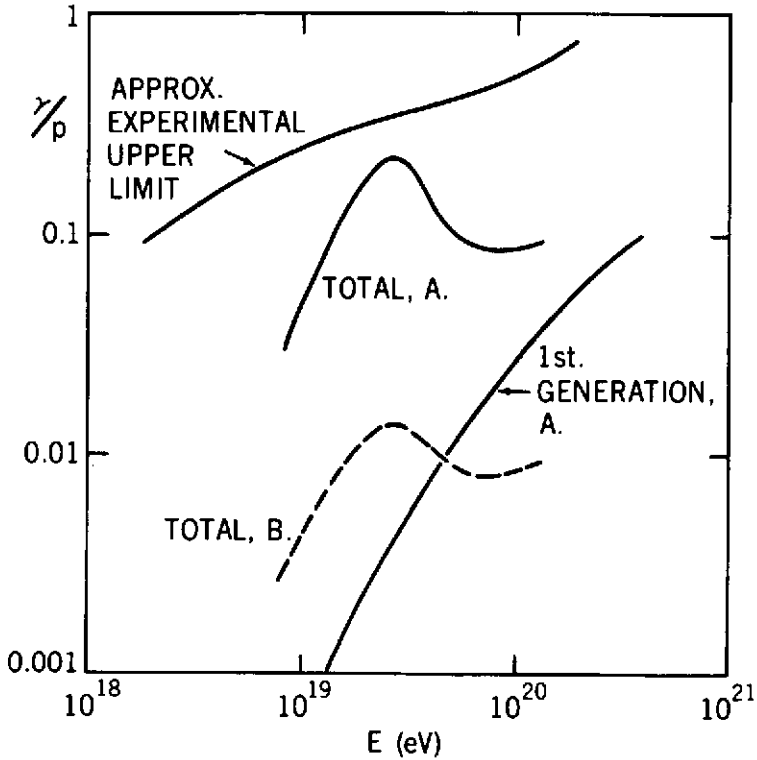


Figure XII.A-6.  $\gamma/p$  ratio from Wdowczyk et al. (1972).

possible that detectable fluxes of very energetic  $\gamma$ 's do exist, and it is urged that systematic searches be made. One point that should be stressed in this connection is the possibility of a nonuniform radio background; this could produce a transition effect which would concentrate  $\gamma$ -ray energy in a particular region to an even greater extent than in the present case and give rise to a much higher ratio.

### GAMMA-RAYS IN AN EVOLVING UNIVERSE

As remarked in the Introduction, there is the possibility that the kink in the proton spectrum at  $3 \times 10^{15}$  eV is connected with electron-pair production on the relict radiation at early epochs. The  $\gamma$ -rays expected from these interactions may allow constraints to be put on models in which the primary spectrum above  $10^{14}$  eV is of extragalactic origin; this topic therefore has relevance to the ultra high-energy  $\gamma$ -region.

Strong et al. (1973a, b), have examined the problem in detail and their derived  $\gamma$ -spectrum at the earth is given in Figure XII.A-7. As will be appreciated, although the total energy in the spectrum will be constant (it is  $\sim 1.7 \times 10^5 \text{ eV} \cdot \text{cm}^{-2} \cdot \text{s}^{-1} \cdot \text{sr}^{-1}$ ), the spectral shape will depend on the energy

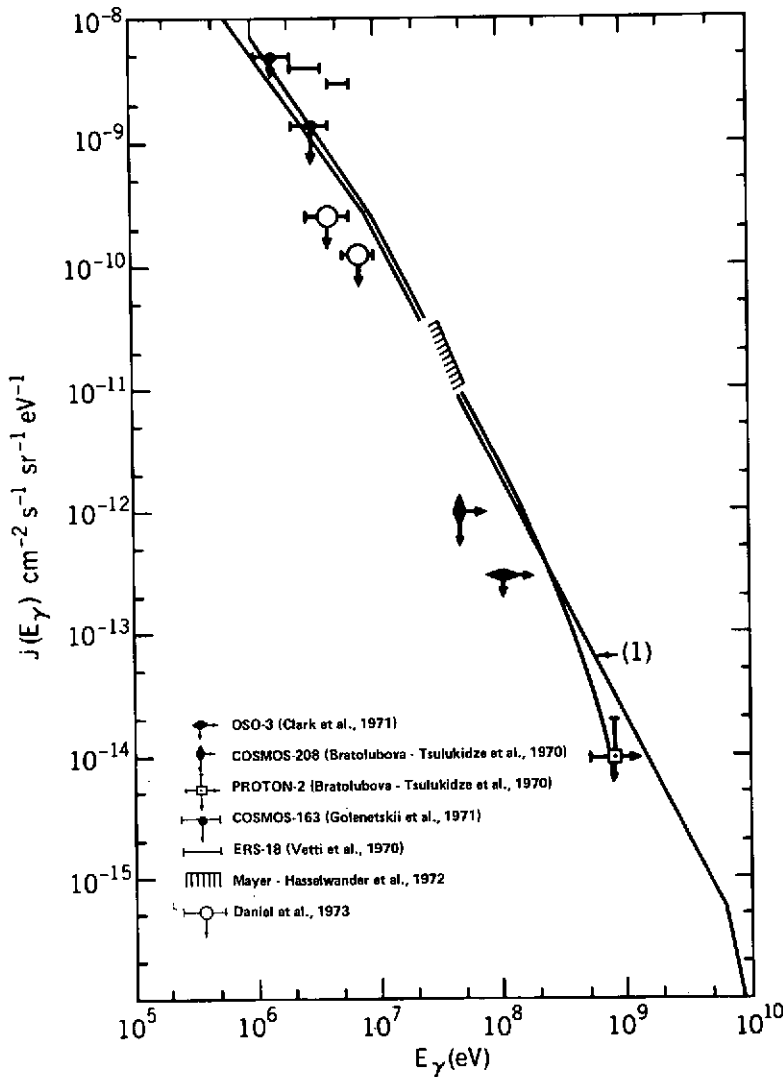


Figure XII.A-7. Comparison of observed and predicted isotropic flux of  $\gamma$ -rays. The predicted intensities are from the work of Strong et al. (1973), with (1) representing the more probable situation.

density of extragalactic starlight. The  $\gamma$ -ray spectra in Figure XII.A-7 correspond to different assumptions about the variation of starlight density with epoch.

The experimental situation is not clear. There appear to be a number of intensities below the expected spectra and if these are correct then the suggested origin of the proton spectrum kink is not correct (although this does not preclude the very energetic protons of this energy being of extragalactic origin). However, the recent measurements of Mayer-Hasselwander et al. (1972), are in good agreement with the prediction.

A firm conclusion cannot be made at this stage; therefore, although with new measurements being made at the present time, this problem, at least, should be solved rather soon.

#### ACKNOWLEDGMENTS

The authors wish to thank the Science Research Council of the U.K. for the provision of research grants to support this work.

#### REFERENCES

- Allcock, M. C., and J. Wdowczyk, 1972, *Il Nuovo Cimento*, **9**, p. 315.
- Andrews, D., D. M. Edge, A. C. Evans, R. J. Reid, R. M. Tennent, A. A. Watson, J. G. Wilson, and A. M. Wrey, 1971, *Proc. 12th Int. Conf. on Cosmic Rays*, Hobart, Australia, **3**, p. 995.
- Bonometto, S. A., and F. Lucchin, 1971, *Letters Nuovo Cimento*, **2**, p. 1299.
- Bratolubova-Tsulukidze, L. I., N. L. Grigorov, L. F. Kalinkin, A. S. Melioransky, E. A. Pryakhin, I. A. Savenko, and V. Ya. Yufarkin, 1970, *Acta Phys. Hung.*, **29**, Suppl. 1, p. 123.
- Clark, G. W., G. P. Garmire, and W. L. Kraushaar, 1971, *Proc. 12th Int. Conf. on Cosmic Rays*, Hobart, Australia, **1**, p. 91.
- Clark, T. A., L. W. Brown, and J. K. Alexander, 1970, *Nature*, **228**, p. 847.
- Daniel, R. R., G. Joseph, and P. J. Lavakare, 1973, *X-Ray and Gamma-Ray Astrophysics, IAU Symposium No. 55*, (Madrid), H. Bradt and R. Giacconi, eds., D. Reidel, Dordrecht, Holland.
- Goetskii, S. V., 1971, *Astrophys. J. Letters*, **9**, p. L69.

- Gould, R. J., and G. P. Schreder, 1967a, *Phys. Rev.*, **155**, p. 1404.  
———, 1967b, *Phys. Rev.*, **155**, p. 1408.
- Greisen, K., 1966, *Phys. Rev. Letters*, **16**, p. L748.
- Hillas, A. M., 1968, *Canadian J. Phys.*, **46**, p. S623.
- Ipavich, F. M., and A. M. Lenchek, 1970, *Phys. Rev.*, **D2**, p. 266.
- Kuzmin, V. A., and G. T. Zatsepin, 1968, *Canadian J. Phys.*, **46**, p. S617.
- Linsley, J., 1963, *Proc. Int. Conf. on Cosmic Rays*, Jaipur, **4**, p. 77.
- Mayer-Hasselwander, H. A., K. Pfeffermann, H. Pinkau, H. Rothermel and M. Sommer, 1972, *Astrophys. J. Letters*, **175**, p. L23.
- Penzias, A. A., and R. W. Wilson, 1965, *Astrophys. J.*, **142**, p. 19.
- Stecker, F. W., 1968, *Phys. Rev. Letters*, **21**, p. L1016.  
———, 1971, *Cosmic Gamma Rays*, Mono Book Corp., Baltimore.  
———, 1973, *Astrophys. and Space Sci.*, **20**, p. 47.
- Strong, A. W., J. Wdowczyk, and A. W. Wolfendale, 1973a, *Nature*, **241**, p. 109.  
———, 1973b, *J. Phys. A.*, in press.
- Vette, J. I., D. Gruber, J. Matteson, and L. E. Peterson, 1970, *Astrophys. J. Letters*, **160**, p. L161.
- Wdowczyk, J., W. Tkaczyk, and A. W. Wolfendale, 1972, *J. Phys. A.*, **5**, p. 1419.
- Zatsepin, G. T., and V. A. Kuzmin, 1966, *Zh. Eksperim. Teor. Fiz. Letters*, **4**, p. L114.

## A. A COMPARISON OF THE RECENTLY OBSERVED SOFT GAMMA-RAY BURSTS WITH SOLAR BURSTS AND THE STELLAR SUPER- FLARE HYPOTHESIS\*†

F. W. Stecker and K. J. Frost  
*Goddard Space Flight Center*

Recently, Klebesadel, Strong, and Olsen (1973) reported the exciting discovery of  $\gamma$ -ray bursts having a typical duration of the order of seconds and typical photon energies of the order of hundreds of keV. This observation has now been confirmed by Cline, Desai, Klebesadel, and Strong (1973) using the detector aboard the satellite IMP-6 (Chapter VII.A).

Predictions of  $\gamma$ -ray bursts from supernovae have been made by Colgate (1968), but there are several difficulties in interpreting the observed bursts as originating in supernovae. In particular, the observed bursts have typical durations of the order of seconds with multiple bursts being common. They also appear to have soft exponential spectra with photon energies in the range of 150 to 250 keV. They have been observed to occur frequently with no apparent correlation with observed supernova events.

In contrast to the observed events, Colgate (1968) has predicted that  $\gamma$ -ray bursts from supernovae would have durations of the order of  $10^{-5}$  s and hard power-law energy spectra with a characteristic energy of about 2 GeV. It thus appears to us possible that the observed bursts do not originate in supernovae, and that alternative possibilities for the origin of these bursts should be explored. We suggest here the alternative possibility that these outbursts are simply giant versions of the X-ray bursts typically seen in solar flares.

The observed  $\gamma$ -ray bursts bear a strong resemblance in many respects to the solar X-ray bursts observed recently with a 2-s time resolution (Frost, 1969; Kane, 1969). Figure XIII.A-1 shows a representative nonthermal solar X-ray burst. This burst is dominated by two impulsive spikes, each about 10 s in duration. If a burst such as this were emitted by a star other than the sun,

---

\*Post-Symposium theoretical paper, see Introduction.

†Published in *Nature Physical Science*, October 1, 1973.

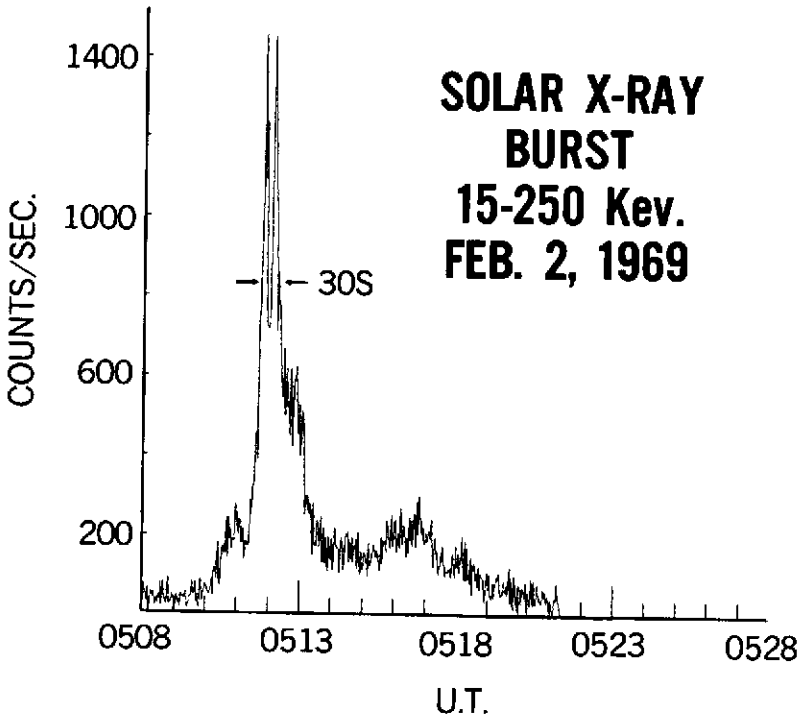


Figure XIII.A-1. A solar X-ray burst observed on OSO-5 with a time structure similar to that observed for the nonsolar bursts.

then only the narrowest parts of the burst might be detected above the background noise. Such bursts would appear to be shorter than solar bursts as is the case with the recently observed nonsolar bursts. Thus there may be little intrinsic difference between the time-scales of solar bursts and the suggested stellar bursts at the source. In both cases, the time scale is much longer than that predicted for supernovae.

The spectral characteristics of the nonsolar bursts have been measured by Cline et al. (1973; see also Chapter VII.A). These spectral data from IMP-6 are found to be well described by an exponential spectrum of the form  $I \propto e^{-E/E_0}$  with  $E_0$  being between 150 and 250 keV for a typical initial burst. Subsequent bursts in multiple-burst events appear to be softer with  $E_0 \sim 100$  keV. The spike component of solar X-ray bursts could also fit an exponential energy spectrum with  $E_0 \sim 100$  keV (Frost, 1969). The multiple spike characteristics seen in the nonsolar bursts are commonly seen in solar X-ray bursts as well.

We therefore consider it generally plausible that these bursts are caused by the bremsstrahlung of electrons accelerated to high energies in a stellar flare event. Assuming the acceleration to depend only on the strength of the effective field seen by the electrons, and not on electron energy, the final energy of the electron will be determined by the time the electron spends in the field. If we assume this acceleration time to be collisionally determined, the average time being  $T$ , the probability ( $P$ ) of an electron being accelerated for time ( $t$ ) is given by the distribution

$$dP/dt = T^{-1} e^{-t/T} \quad (\text{XIII.A-1})$$

The spectrum of accelerated electrons would then be of the form

$$I(E)dE \propto (dE/E_0) e^{-E/E_0} \quad (\text{XIII.A-2})$$

where the mean acceleration rate is given by the constant  $E_0/T$  and  $E_0$  is the average electron energy. The resulting photon spectrum should then also approximate an exponential form. The above considerations are fairly general and it appears that they may be applicable to both solar and nonsolar bursts.

We conclude that the time scale, mean photon energy, and energy spectrum shape (therefore possibly the acceleration mechanism) for both the solar and nonsolar bursts are strikingly similar. There is so much similarity that it is a bit surprising considering that there is such a wide variation of surface conditions among the various stars in the galaxy. There does however appear to be one important difference. The nonsolar bursts that have been observed, which presumably must be both the closest and strongest of the nonsolar bursts, have a much greater intrinsic intensity than their solar counterparts. The strongest solar flares could have a total energy of  $\sim 10^{32}$  erg (Bruzek, 1967). The bursts seen by Klebesadel et al. (1973) involve an energy flux of  $\sim 10^{-5} - 10^{-4}$  erg/cm<sup>2</sup>. Denoting this flux by  $\epsilon$ , the X-ray energy at the source is given by

$$\mathcal{E} \cong 2\pi R^2 \epsilon \quad (\text{XIII.A-3})$$

assuming the source flare radiates into  $2\pi$  sr. Assuming  $\epsilon \cong 3 \times 10^{-5}$  erg/cm<sup>2</sup>, a source at a distance  $R = 10$  pc would have a typical total X-ray energy  $\mathcal{E} \cong 2 \times 10^{35}$  erg and a corresponding total energy of  $10^{38}$  to  $10^{39}$  erg. A stellar burst of the type hypothesized here would then involve the acceleration of  $\sim 10^6$  to  $10^7$  times more electrons than a strong solar flare. We may speculate that such an event might involve a star with a magnetic field strength  $\sim 10^3$  times larger than the sun. Such fields may not be uncommon, particularly in stars earlier than FO, although the observational establishment of these fields is difficult and often impossible (Babcock, 1960). In addition, common

white dwarf stars may have surface fields up to  $3 \times 10^7$  G (Ostriker, 1970) so that they may be likely sources for these bursts. It seems reasonable to assume that such stars as are likely to produce the observed bursts should be near enough so that no concentration toward the galactic plane should be expected.

The stellar flare hypothesis immediately lends itself to various observational tests. Possible observational consequences are: (1) repetitions of the bursts at the same position; (2) simultaneous radio bursts at the same position; and (3)  $\gamma$ -ray lines at 0.51 MeV (positron annihilation), 2.23 MeV ( $n+p \rightarrow d+\gamma$ ), 4.4 MeV ( $C^{12*}$ ) and 6.1 MeV ( $O^{16*}$ ) as have been seen in strong solar flares (Chupp et al., 1973, see also Chapter VI.A). These lines may be present because the flare can accelerate protons as well as electrons so that various nuclear reactions may occur in the flare.

If the stellar flare hypothesis is verified, it may imply a significant source of low-energy cosmic-rays in the solar neighborhood (and throughout the galaxy), depending on the frequency and intensity of the flares.

The authors wish to thank Drs. T. Cline and R. Ramaty for valuable discussions and T. Cline for communicating his data to us prior to publication.

#### REFERENCES

- Babcock, H. W., 1960, *Stars and Stellar Systems*, IV, Univ. of Chicago Press, Chicago.
- Bruzek, A., 1967, *Solar Physics*, J. Xanthakis, ed., Interscience Pub. Co., London.
- Chupp, E. L., D. J. Forrest, P. R. Higbie, A. N. Suri, C. Tsai, and P. P. Dunphy, 1973, *Nature*, **241**, p. 33.
- Cline, T. L., V. D. Desai, R. W. Klebesadel, and I. B. Strong, 1973, *Astrophys. J. Letters*, in press.
- Colgate, S. A., 1968, *Can. J. Phys.*, **46**, p. S476.
- Frost, K. J., 1969, *Astrophys. J. Letters*, **158**, p. L159.
- Kane, S. R., 1969, *Astrophys. J. Letters*, **157**, p. L139.
- Klebesadel, R. W., I. B. Strong, and R. A. Olsen, 1973, *Astrophys. J. Letters*, **182**, p. L85.
- Ostriker, J. P., 1970, *Acta Phys.*, **29**, Suppl. 1, p. 69.

**SECTION 3**  
**COSMOLOGY**

## A. MATTER-ANTIMATTER COSMOLOGY

R. Omnès\*

*Université de Paris*

### INTRODUCTION

Antimatter is quite a relevant subject for a meeting dealing with cosmic  $\gamma$ -rays because annihilation is an important potential source of hard photons. Therefore I am glad to have this occasion to report upon some recent work concerning the possible existence of antimatter on a large scale.

The starting point of these investigations was an attempt to understand the origin of matter as being essentially analogous to the origin of the background thermal radiation. This background radiation is probably a remnant of a prior situation where the universe was hot and space was much more compact than it is now. It was noticed long ago (Gamow, 1948; Alpher, 1948; Alpher, Bethe, and Gamow, 1948; Alpher and Herman, 1948a, 1948b, 1949, 1950, 1951, 1953; Alpher, Herman, and Gamow, 1948, 1949; Alpher, Follin, and Herman, 1953; and Alpher, Gamow, and Herman, 1967) that, according to general relativity, an isotropic universe had to pass through conditions where the temperature at early times was very high (this is the hot, big-bang cosmology). When the temperature was somewhat higher than 100 MeV, thermal radiation contained all kinds of elementary particles including, among others, nucleons and antinucleons. It is therefore tempting to wonder whether matter is a remnant of these particles. Preliminary investigations of this question showed however that a sufficiently efficient separation could not come from statistical fluctuations (Goldhaber, 1956; Zel'dovitch, 1965). More precisely, if we introduce the basic parameter  $\eta = N/N_\gamma$  which is invariant under expansion (where  $N$  is the present particle density of matter and  $N_\gamma$  the density of thermal photons), one finds that statistical fluctuations give (Zel'dovitch, 1965)

$$\eta \leq 10^{-18}$$

whereas the observed value is

$$\eta = 10^{-8} \text{ to } 10^{-10} \quad (\text{XIV.A-1})$$

---

\*Speaker.

Therefore, some mechanism of separation between matter and antimatter, more efficient than mere fluctuations, had to be found.

A few years ago it was noticed that nucleon-antinucleon interactions at intermediate energy (less than 1 GeV) could produce such a separation (Omnès, 1969). The basic idea is the following: According to the mesonic theory of nuclear forces (Ball, Scotti, and Wong, 1969; Aldrovandi and Caser, 1972), it turns out that the S-wave scattering of nucleons and antinucleons is repulsive, that is, the scattering lengths are positive. The same result is also found from a phenomenological analysis of nucleon-antinucleon interactions (Bryan and Phillips, 1968). This important feature can in principle be checked experimentally by measuring the energy of X-rays emitted by the protonium ( $p\bar{p}$ ) atom (Caser and Omnès, 1972) with enough precision. This experiment is now under way at CERN (Backenstoss, private communication). If this effective low-energy repulsion between nucleons and antinucleons turns out to be correct, it could in principle induce a separation between nucleons and antinucleons among the particles constituting thermal radiation at high temperatures.

This hypothesis has been analyzed theoretically, by using a variety of different models (Omnès, 1969, 1970, 1972a, 1972b; Aldrovandi and Caser, 1972; and Cisneros, 1973), with the following conclusion: Separation could indeed be the result of a phase separation occurring above a critical temperature which is of the order of 300 MeV. Some approximations had to be made in all of these models so that this conclusion can only be considered as tentative. I shall not deal in detail with this question here.

A detailed study of the universe evolution when the temperature drops from 300 MeV to 30 keV has been performed recently (Aldrovandi et al., unpublished) with the following results:

- The parameter  $\eta$  is essentially stabilized after a period of intense annihilation at  $T = 1$  MeV at the value

$$\eta \geq 10^{-9} \quad (\text{XIV.A.2})$$

(only a lower limit could be obtained).

- The system of matter and antimatter constitutes an emulsion (that is, a three-dimensional maze). The size of such an emulsion can be characterized by the ratio  $L$  between a large volume  $V$  and the area of the matter-antimatter boundary  $S$  enclosed in this volume

$$L = \left\langle \frac{V}{S} \right\rangle \quad (\text{XIV.A.3})$$

L is equal to  $10^{4.5}$  cm when  $T = 1$  MeV and a volume  $L^3$  contains at that time a mass of matter of the order of  $10^{13}$  g.

- Neutrons are lost by annihilation around 1 MeV so that there is no helium formation at this stage.

Here again, I shall not deal with the details of this analysis.

**COALESCENCE**

I come now to the first subject of this talk which is to show how annihilation along the matter-antimatter boundary can induce important fluid motions by the effect of which the emulsion size L will grow tremendously during the radiative period. This effect has been called coalescence (Omnès, 1971a, b, c; Aldrovandi et al., 1973).

First, let me stress that this effect is relevant for any antimatter model of the universe. Even if the separation effect described above were but a theoretician's dream, coalescence would still be the essential feature of a model where matter and antimatter would be given in separate regions in the initial conditions at time zero (Harrison, 1968, 1970) or any other conceivable model. This investigation has been carried out by Aldrovandi, Caser, Puget, and Omnès (to be published).

The basic idea of the model is the following. Along the matter-antimatter boundary, annihilation produces high-energy particles: photons, electrons, and positrons. These particles, together with secondary particles which they put into motion by collisions, carry their momentum to the fluid which is made of matter (or antimatter) and radiation over some distance  $\lambda$ . Let us consider the case where the boundary has a curvature radius R and  $\lambda \ll R$ . Because as many particles generated by annihilation are going towards matter as are going towards antimatter, the pressure they exert on both sides of the boundary is inversely proportional to the area of the effective surface where they are stopped. These areas are proportional to  $(R + \lambda)^2$  and  $(R - \lambda)^2$  so that a discontinuity pressure [p] appears along the boundary:

$$[p] = 2 p_a \frac{\lambda}{R} \tag{XIV.A-4}$$

where  $p_a$  is the annihilation pressure carried by the high-energy particles.

Equation (XIV.A-4) is of a well-known type: it is essentially the Laplace-Kelvin formula which gives the discontinuity pressure associated with a surface tension with coefficient

$$\alpha = 2 p_a \lambda \tag{XIV.A-5}$$

so that we expect it to reduce the boundary area, that is, according to Equation (XIV.A-3), to increase  $L$ . This is coalescence.

Perhaps it should be mentioned at this stage that the amount of matter or antimatter connected within the emulsion is infinite despite the finite value of  $L$  (that is, you can go to infinity by staying within the maze) (de Gennes et al., 1959; Broadbent and Hammersley, 1957). As a result, coalescence is but an unfolding of the boundary.

### THE THEORY OF COALESCENCE

The details of the analysis look a bit different when the temperature is respectively larger or smaller than 100 eV, because (in the first case), high-energy photons have a small mean-free path (because of the reaction  $\gamma + \text{thermal photon} \rightarrow e^+ e^-$ ). Below  $T = 100$  eV, this mean-free path becomes larger than  $L$  so that primary photons (due to annihilation of  $\pi^0$ -mesons) do not contribute to coalescence. I shall restrict myself to this last case.

In order to quantitatively treat the coalescence effect, one performs an analysis of the transfer and thermalization of particles. High-energy particles as well as thermal photons and matter electrons are described by a set of Boltzmann equations.

Primary high-energy electrons (generated by  $\pi^- \rightarrow \mu^- \rightarrow e^-$ ) first give their momentum to thermal photons by Compton scattering. Thereby they give rise to X-rays which carry the momentum. These X-rays travel along a distance  $\lambda_0 = (N \sigma_T)^{-1}$  and give all their momentum to some electrons by Compton scattering. After this first collision they travel a distance much longer than  $L$  before being thermalized so that their energy is homogeneously distributed over the emulsion and does not affect the motion of the fluid. The second-generation electrons transfer their momentum, partly to thermal photons through Compton collisions (say a fraction  $\xi$  of this momentum) and partly to the matter plasma by Coulomb collisions (that is, a fraction  $1 - \xi$ ).

It is a somewhat trivial but tedious exercise to compute the spectra of the particles and to write the Boltzmann equations that describe these processes. Once we have these Boltzmann equations, we can write hydrodynamical equations by taking, as usual, the first few moments of the particles' distributions. For the plasma we get an equation of motion which is

$$\rho_m \frac{d\vec{v}}{dt} = (1 - \xi) \frac{\vec{J}}{\lambda_0} - \frac{\rho_m \vec{v}}{\tau_D} + \frac{\vec{P}}{\tau_0} - \vec{\nabla} \cdot \vec{P}_m \quad (\text{XIV.A-6})$$

where  $\rho_m$  is the plasma mass density.  $\vec{J}$  is the momentum density of X-rays.  $\vec{P}$  is the density of momentum of thermal photons so that the third term in

the right-hand side represents the momentum given by radiation to the plasma. The second-term represents the inverse effect: The plasma transfers its momentum to photons within a time of drag  $\tau_D$ . One has

$$\tau_0 = \lambda_0/c \qquad \tau_D = \frac{3}{4} \frac{\rho_m}{\rho_\gamma} \tau_0 \qquad \text{(XIV.A-7)}$$

The last term in Equation (XIV.A-6) represents the effect of the plasma pressure that is negligible in general except near the boundary where annihilation creates a loss in particles.

The equations for thermal photons need not be written here because, even when they are written in a form involving hydrodynamical motion plus diffusion, they are still ugly. Let us note only that for distances larger than  $\lambda_0$  (the thermal photons mean-free path), the system plasma + radiation behaves like a unique fluid obeying the equation of motion:

$$\rho \frac{d\vec{V}}{dt} = - \vec{\nabla} \frac{E}{3} + \frac{\vec{J}}{\lambda_0} + \eta_v \left[ \nabla^2 \vec{V} + \frac{1}{3} \vec{\nabla} (\vec{\nabla} \cdot \vec{V}) \right] \qquad \text{(XIV.A-8)}$$

Here E is the energy density of thermal radiation (E/3 is the pressure) and  $\eta_v$  is the viscosity coefficient

$$\eta_v = \frac{8}{27} \frac{\lambda_0 E}{c} \qquad \text{(XIV.A-9)}$$

Equation (XIV.A-8) must be supplemented by an equation for the energy transfer which is

$$\frac{\partial E}{\partial t} + \vec{\nabla} \cdot \left( \vec{J}_c - D \vec{\nabla} E + \frac{4}{3} E \vec{V} \right) = 0 \qquad \text{(XIV.A-10)}$$

These equations of motion must be completed by a boundary condition that gives the pressure discontinuity across the boundary. The basic idea has already been given and the passage from kinetic equations to discontinuity follows the lines provided by the kinetic theory of surface tension. One gets

$$\left[ \frac{E}{3} \right] = \frac{4}{3} \frac{J(0) \lambda_0}{R} = \frac{\alpha}{R} \qquad \text{(XIV.A-11)}$$

### THE ANNIHILATION RATE

The annihilation pressure  $p_a$  or the momentum density  $c J(0)$  are determined by the rate of annihilation at the boundary. To compute it, one can use Equation (XIV.A-6). Essentially what happens is that annihilation creates a dip in the plasma density which tends to be filled under the effect of the plasma pressure gradient  $\vec{\nabla} p_m$  while the corresponding flow of matter is slowed down by the drag of plasma against radiation. Thus,

$$J(0) \cong N \left[ \frac{kT}{4\pi m_p} \frac{\tau_0}{t} \right]^{\frac{1}{2}} m_p c \quad (\text{XIV.A-12})$$

As a result, it is found that only a small fraction of matter ( $\lesssim 10^{-2}$ ) is annihilated during the coalescence period so that  $\eta$  does not decrease appreciably.

### THE RATE OF COALESCENCE

Given the hydrodynamical equations together with the boundary condition (Aldrovandi and Caser, 1972), one can compute the rate of change of  $L$  with time. In fact, the extreme geometrical complexity of the emulsion can be turned into advantage by averaging the equations over a large volume  $V$ . This leads to a simple equation for the variation of  $L$ :

$$\ddot{L} = \frac{\alpha(t)}{\rho(t)} L^{-2} \quad (\text{XIV.A-13})$$

which can be explicitly solved, taking into account the rate of change of  $\alpha$  and  $\rho$  with time which is due to expansion. The result is again quite simple, namely

$$L^3 = \frac{16}{5} \frac{\alpha}{\rho} t^2 \quad (\text{XIV.A-14})$$

It is found therefore that  $L$  increases with time, which is coalescence.

For numerical purposes, one can compute the mass ( $M$ ) contained within a typical volume ( $V$ ) of the emulsion. We have chosen for  $V$  the average volume which is seen from an interior point, which turns out to be given by

$$V = 8 \pi L^3 \quad (\text{XIV.A-15})$$

so that

$$M = \rho_m V \quad (\text{XIV.A-16})$$

For  $T = 3000 \text{ K}$ ,  $t = 10^{13} \text{ s}$  (the conventional end of the radiative period), one gets

$$M \cong 10^{43} \text{ g} \quad (\text{XIV.A-17})$$

that is, a galactic mass.

### THE SIZE OF INHOMOGENEITIES: GALAXY FORMATION

We have found that coalescence quite naturally generates inhomogeneities of matter and antimatter that can be the origin of galaxies.

In fact, things are not that simple; because of annihilation, matter is kept ionized in the symmetric universe a much longer time than in the conventional hot big-bang model, so that coalescence can still go on during this long recombination period and generate much higher masses. Moreover, drag becomes less effective, which tends to increase the rate of coalescence. Furthermore, the viscosity becomes much smaller so that turbulence can be generated.

The study of this long recombination period is still incomplete. I believe Puget and Stecker will say more about it in this Symposium (Stecker and Puget, 1972; Chapter XV.A). The masses of matter will be larger than before, that is, in the range of mass of clusters and matter will have a turbulent motion (that is, the kind of situation first envisioned by Ozernoy and Chibisov (1970)). The main difficulty ordinarily found with turbulence (that is, its dissipation at the end of the radiative period (Peebles, 1972; Dallaporta, 1972)) is much reduced here since turbulence would be generated by the coalescence motion itself.

### ANTIMATTER AND $\gamma$ -RAYS

Coming back to the subject of this meeting, it is interesting to consider the consequences of this model as far as  $\gamma$ -ray detection is concerned. For the sake of the argument, we shall consider the Stecker-Puget model where whole clusters are made of only one type of matter. These clusters are born from the largest eddies generated by coalescence.

In such a case (Stecker and Puget, 1972; Steigman, 1971, 1972) annihilation on the boundaries of clusters is too weak to be detectable at the present level. Apparently, the only detectable  $\gamma$ -rays come from early annihilation and could be seen in the isotropic background around 1 MeV after being red-shifted (Stecker et al., 1971). This effect will be described in a communication by Stecker (see Chapter IX.A).

### WHAT IS THE EVIDENCE FOR ANTIMATTER?

Except for the 1-MeV bump in the X-ray background, the present model has behaved somewhat like a hat from which a rabbit was drawn: the correct amount of matter in the universe has been computed; Stecker and Puget claim that the model gives the right kind of turbulence (that is, the right size for the largest eddies and the right velocities) to agree with the parameters of clusters and galaxies (namely, their mass and angular momentum), so that it gives exactly those cosmological parameters which up to now had been hidden in the initial conditions. Furthermore, the model has also shown a remarkable knack for embodying past objections (Stecker et al., 1971) and using them for progress: the hat is still being brushed but the rabbit is alive and well (Aldrovandi et al., unpublished; Omnès, 1971a, 1971b, 1971c; Aldrovandi et al., 1973).

However, one feels quite frustrated to find how difficult it is to show experimentally the existence of antimatter.

I am now going to describe briefly one conceivable type of consequence. It concerns a possible mechanism for the activity of quasars and Seyfert galaxies which is yet far from being properly analyzed. In fact, I only mention it here because of its possible relevance to  $\gamma$ -ray astronomy, and my excuse for releasing it too early will be the occasion provided by this meeting.

### AN ECUMENIC MODEL OF QUASARS

Many models of quasars have already been proposed. Some are as follows: (Zel'dovitch and Novikov, 1971; Burbidge and Burbidge, 1967; Schmidt, 1969; Robinson, Schild, and Schucking, 1963)

- Quasars have been tentatively identified with supermassive stars (Hoyle and Fowler, 1963; Fowler, 1964). The main difficulty for this theory comes from the star temperature which is too low for nuclear energy to be produced efficiently. One must therefore appeal to rotational energy, but this raises difficult problems of conversion (Fowler, 1966; Rosburgh, 1965; Bisnovatyi-Kogan et al., 1967; Bardeen, 1966; Wagoner, 1969).
- A nonrelativistically rotating supermassive star tends to collapse rapidly. This has led to a variety of models for quasars where some stabilization is provided by rotation (Fowler, 1966; Rosburgh, 1965; Bisnovatyi-Kogan et al., 1967; Bardeen, 1966; Wagoner, 1969), turbulence, or magnetic fields (Layzer, 1965; Ozernoy, 1966). These last two agents are good stabilizers, but turbulence should be continuously generated by a process which, to my knowledge, has not yet been found.

- Several models of quasars identify them with star clusters (Gold et al., 1965; Ulam and Walden, 1964; Woltjer, 1964; Miller and Parker, 1964; Spitzer and Saslaw, 1966). For our purpose, the basic aspect of this class of models is the importance attributed to collisions.
- One has suggested antimatter as an efficient source of energy for quasars (Teller, 1966; Burbidge and Hoyle, 1956; Ekspong et al., 1966). Here the difficulty is to propose a specific structure for the matter-antimatter system (Aldrovandi et al., unpublished; Schatzman, 1970). One must also be aware of the limitations imposed to annihilation by the observation of high-energy  $\gamma$ -rays (Clark et al., 1968; Steigman, 1969).

I shall briefly describe another model for quasars that has been suggested by the matter-antimatter symmetric cosmology. Because it reconciles many features of already existing proposals, it might be called an ecumenic model. A convenient consequence of this model is that most relevant calculations have already been published in the literature.

Let us now state the model. A supermassive star  $\Sigma$  made of antimatter is located within the nucleus of a matter galaxy. Energy is generated by the annihilation of accreting matter and impinging stars. Heat being thus produced in a stochastic manner, large temperature differences are produced between the regions where annihilation is taking place and the average temperature. Turbulent convection is therefore continuously generated. On the other hand, high magnetic fields are expected.

There are reasons derived from our cosmological model to expect the occurrence of such a peculiar object. It is conceivable (even though, not yet quite clear or necessary) that, by effect of the coalescence motions, some amount of antimatter may be trapped within matter. The general characteristics of coalescence as described above show that the mass of this inclusion cannot be too small as compared to a galactic mass, say  $M \gtrsim 10^8 M_{\odot}$ . The contraction of such a mass of antimatter will take place after recombination as a consequence of annihilation pressure (that is, the high-energy electrons and positrons produced by annihilation communicate their momentum to matter and antimatter if there is a magnetic field. Such a strong boundary pressure can induce contraction (Sunyaev and Zel'dovitch, 1972). In this way we expect that a supermassive star such as  $\Sigma$  could be produced.

It may be that  $\Sigma$  has a hard early life and there are a few unsolved problems concerning this period. It is necessary that stabilization by turbulence or magnetic fields occur very soon after the birth of  $\Sigma$  to avoid collapse and this point has not been clarified (although, in this model, we expect galaxies to contract at the same epoch as  $\Sigma$  because of the same mechanism). Also, one does not know why  $\Sigma$  should stand in the galactic nucleus; perhaps its large

mass could serve to start the initial condensation of the galaxy, or its motion in the galaxy could lead it to the center either by gravitational effects (Spitzer, 1971) or because of a specific viscosity generated by annihilation (Lequeux, private communication).

Assuming the existence of such an object, we will now show that it behaves in many ways like a quasar. For the sake of definiteness, we shall consider an object  $\Sigma$  with mass  $10^8 M_{\odot}$  with a radius  $R = 1$  pc. situated at the center of a galactic nucleus. We shall use data concerning our galaxy for the environment density so that most of the accreting matter is probably in the form of stars (Rougoor and Oort, 1960). One finds that 2.2 stars (with a solar mass) are entering into  $\Sigma$  every year with a velocity 1000 km/s. The average particle density  $\langle N \rangle$  in  $\Sigma$  is  $10^9$  antiprotons per  $\text{cm}^3$ , and the average mass density  $\langle \rho \rangle$  is  $10^{-15}$  g/cm<sup>3</sup>.

The characteristics of  $\Sigma$  are well known (Zel'dovitch and Novikov, 1971). Its density profile is that of a polytrope with index  $n = 3$ . The temperature  $T$  is related to the density  $\rho$  by

$$T = 1.97 \times 10^7 \text{ K} \left( \frac{M}{M_{\odot}} \right)^{1/6} \rho_{\text{c.g.s.}}^{1/3} \quad (\text{XIV.A-18})$$

The thermal luminosity is given by

$$L_{\text{th}} = 1.3 \times 10^{38} \left( \frac{M}{M_{\odot}} \right) \text{ erg/s} \quad (\text{XIV.A-19})$$

However, it should be pointed out that this value for  $L_{\text{th}}$  can be overestimated if large magnetic fields contribute to the pressure near the surface. If it were left to itself,  $\Sigma$  would start gravitational collapse when it reaches a critical state corresponding to a central density and a radius

$$\rho_c \cong 2 \times 10^{18} \left( \frac{M}{M_{\odot}} \right)^{-7/2} \text{ g/cm}^3 \quad (\text{XIV.A-20})$$

$$R_c (M/M_{\odot} = 10^8) = 3 \times 10^{-2} \text{ pc.} \quad (\text{XIV.A-21})$$

(if one assumes  $\Sigma$  to be made of pure hydrogen).

The energy of  $\Sigma$  is then independent of its mass

$$E_c = -4 \times 10^{54} \text{ ergs} \tag{XIV.A-22}$$

An important quantity is the evolution time of  $\Sigma$ , which can be quite small if  $\Sigma$  is not stabilized otherwise, namely

$$t_c = - \frac{E_c}{L_{th}} \geq 10^9 \left( \frac{M}{M_\odot} \right)^{-1} \text{ yr} \tag{XIV.A-23}$$

$\Sigma$  is heated by infalling stars which begin to annihilate when they penetrate antimatter. Their initial velocity is  $(GM/R)^{1/2} = V$ . The star surface is heated by annihilation. An energy flux is produced which is essentially given by  $\Phi = VN mc^2$  where  $m$  is the proton mass. (When  $V$  is reduced, this flux becomes of the order of  $V_s N mc^2$  where  $V_s$  is the local sound velocity.) The cascade of thermalizing particles has been analyzed in another context (Aldrovandi et al., 1973). First, X-rays are produced by the products of annihilation ( $\gamma, e^\pm$ ) via pair production, Compton effect, and the reactions  $\gamma + \text{thermal photon} \rightarrow X$  and  $e + \text{thermal photon} \rightarrow X$ . These X-rays are thermalized by Compton effect later. Large quantities of energy are accumulated near the surface of the star where the particle density is much larger than  $N$ . Two cases are possible which have only been analyzed grossly, and both lead to the same result: either strong convective motions take place which blow off the star envelope, or energy is transported by diffusion over a distance of the order of the star radius. In that case, the local temperature becomes larger than  $10^7$  K. Once again, this leads to a blowing off of the envelope by evaporation.

The long-distance transport of energy in  $\Sigma$ , in which the main pressure is radiative, will take place through shock waves. These shock waves will leave a complicated pressure distribution resulting into turbulence. Altogether, the annihilation process appears to be rather complicated and violent and it is very difficult to analyze it in detail. The only simple relation which can be derived comes from energy balance:

$$2 \pi R^2 n V M_\odot c^2 = \langle L \rangle \tag{XIV.A-24}$$

Here  $n$  is the star density around  $\Sigma$  and  $\langle L \rangle$  the average luminosity, in general higher than  $L_{th}$ . Many parameters are free here, so that it is no surprise that the highest known quasar luminosities are easily obtained.

One will not detect the original products of annihilation. Gamma-rays produced by  $\pi^0$  mesons will be stopped in a short distance by several processes

(pair production interactions with protons and electrons, Compton effect, pair production by collision with thermal photons) so that this model does not contradict the limit set upon annihilation by  $\gamma$ -ray astronomy (Clark et al., 1968).

The most difficult question that is raised by this model is to describe the kind of average equilibrium which will take place in  $\Sigma$ . It is only locally heated by annihilation in a random way and the energy is carried mostly by turbulence and shock waves. It would obviously be essential to analyze this kind of process and see what limitations can be imposed on the radius (by star penetration) and on the encounter frequency (by the evolution time of  $\Sigma$ ). We have not yet done this work because we were not able to master the problems of transfer which are involved. Let us note only a favorable circumstance: strong fluid motions should be continuously generated, which would tend to stabilize  $\Sigma$  (Layzer, 1965; Ozernoy, 1966).

Another unsolved problem concerns magnetic fields. It is a general consensus that annihilation can produce large magnetic fields, although only preliminary studies of this effect have been made (Schatzman, 1970; Peyraud, 1971; Aly, to be published). Large-scale magnetic fields can also be present in  $\Sigma$  since its origin or they can be produced by relative motions (including differential rotation).

Things are complicated by the violent events which the model predicts. Too much local energy generation can result in instabilities, ejection of antimatter, rejection of matter, even disruption of  $\Sigma$  (considering the small value of  $E_c$ ). However,  $\Sigma$  will not suffer fragmentation (Montmerle, 1971). Despite the nightmarish character such a system may have for a theoretician, it does not look incompatible with what is observed.

An important new feature of this kind of model concerns the lifetime of quasars. Typical values of  $M = 10^8 M_\odot$  and  $\langle L \rangle = 10^{46}$  ergs/s give a lifetime  $\tau \cong 10^9$  years. Values of  $M/M_\odot$  up to  $10^2$  times higher are still compatible with the model. This shows that quasars have been active since the origin of galaxies. Therefore, the highest red shifts of quasars provide important cosmological information. Furthermore a strong evolution towards decay is predicted with the right order of lifetime (Schmidt, 1970).

To conclude, let us now list what relations can be made between the model and observations.

- Evolution (Schmidt, 1970)
- The validity of the "Christmas tree" behavior for compact radio sources (Kellerman, 1972; Dend, 1972). The individual flashes corresponding here to a new star or a new cloud annihilating.

- The analogy between Seyfert galaxies and quasars. In this model, the difference is only quantitative. All quasars should be in a galaxy (Kristian, 1972), even if it is only a dwarf one, as one would expect if the ratio between the masses of matter and antimatter is not far from one.
- The ejected matter, in the form of dust and gas, has a stellar composition. Such ejected matter constitutes the atmosphere of  $\Sigma$ , which agrees with the characteristics of the emission lines (Burbidge and Burbidge, 1967).
- Multiple absorption red shifts are probably due to gas ejected by radiation pressure and quenched by line-locking (Wampler, 1972).
- Infrared emission might be due to synchrotron emission by annihilation electrons in a high magnetic field (Low, 1970), but most probably it is due to external dust. Indeed, such dust should be abundant near a region where stars explode.
- The origin of extended radio sources frequently associated with quasars and of the cosmic electrons radiating in these sources would be explained in this model as previously suggested by Layzer (1965) and Ozernoy (1966).

Important observations to test the model might come from X-ray and  $\gamma$ -ray observations of quasars with a low-density central star, if it turns out that enough lower-energy  $\gamma$ -rays from annihilation can escape. A cutoff in the energy of these  $\gamma$ -rays could be seen at a value related to the temperature existing in the annihilation region.

## REFERENCES

- Aldrovandi, R., and S. Caser, 1972, *Nucl. Phys.*, **B38**, p. 593.
- , 1972, *Nucl. Phys.*, **B39**, p. 306.
- Alpher, R. A., 1948, *Phys. Rev.*, **74**, p. 1577.
- Alpher, R. A., H. A. Bethe, and G. Gamow, 1948, *Phys. Rev.*, **73**, p. 803.
- Alpher, R. A., J. W. Follin, and R. C. Herman, 1953, *Phys. Rev.*, **92**, p. 1347.
- Alpher, R. A., G. Gamow, and R. Herman, 1967, *Proc. Nat. Acad. Sci.*, **58**, p. 2179.
- Alpher, R. A., and R. Herman, 1948a, *Phys. Rev.*, **74**, p. 1737.
- , 1948b, *Nature*, **162**, p. 774.
- , 1949, *Phys. Rev.*, **75**, p. 1089.

- , 1950, *Rev. Mod. Phys.*, **22**, p. 153.
- , 1951, *Phys. Rev.*, **84**, p. 60.
- , 1953, *Ann. Rev. of Nucl. Sci.*, **2**, p. 1.
- Alpher, R. A., R. Herman, and G. Gamow, 1948, *Phys. Rev.*, **74**, p. 1198.
- , 1949, *Phys. Rev.*, **75**, p. 3321.
- Ball, J. S., A. Scotti, and D. Y. Wong, 1969, *Phys. Rev.*, **142**, p. 1000.
- Bardeen, J. M., and S. P. S. Hnand, 1969, *Astrophys. J.*, **144**, p. 953.
- Bisnovatyi-Kogan, G. S., Ya. B. Zel'dovitch, and I. D. Novikov, 1967, *Ast. Zh.*, **44**, p. 525.
- Broadbent, S. R., and J. M. Hammersley, 1957, *Proc. Camb. Phil. Soc.*, **53**, p. 629.
- Bryan, R. A., and R. J. N. Phillips, 1968, *Nucl. Phys.*, **B5**, p. 201.
- Burbidge, G. R., and E. M. Burbidge, 1967, *Quasistellar Objects*, Freeman, San Francisco.
- Burbidge, G. R., and F. Hoyle, 1956, *Nuovo Cimento*, **4**, p. 558.
- Caser, S., and R. Omnès, 1972, *Phys. Letters*, **39B**, p. L369.
- Cisneros, A., 1973, *Phys. Rev.*, **D7**, p. 362.
- Clark, G. W., G. P. Garmire, and W. L. Kraushaar, 1968, *Astrophys. J.*, **153**, p. 203.
- Dallaporta, N., and F. Lucchin, 1972, *Astron. and Astrophys.*, **19**, p. 123.
- de Gennes, P. G., P. Lafore, and J. P. Millot, 1959, *J. de Physique et le Radium*, **20**, p. 624.
- Dend, W., 1972, Communication at the 6th Texas Symp., New York, in press.
- Ekspong, A. G., N. R. Yamdagni, and B. Bonnevier, 1966, *Phys. Rev. Letters*, **16**, p. L564.
- Fowler, W. A., 1964, *Rev. Mod. Phys.*, **36**, pp. 545, 1104.
- , 1966, *Astrophys. J.*, **144**, p. 180.
- Gamow, G., 1948, *Phys. Rev.*, **74**, p. 505.
- , 1948, *Nature*, **162**, p. 680.
- Gold, T., W. I. Axford, and E. C. Ray, 1965, *Advances in Astron. and Astrophys.*, **3**, Z. Kopal, ed.
- Goldhaber, M., 1956, *Science*, **124**, p. 218.

- Harrison, E. R., 1968, *Mon. Nat. Roy. Astro. Soc.*, **142**, p. 129.
- , 1970, *Commun. Math. Phys.*, **18**, p. 301.
- Hoyle, F., and W. A. Fowler, 1963, *Nature*, **197**, p. 533. (also in *M. N. R. A. S.*, 1963, **125**, p. 169.)
- Kellerman, K., 1972, Comm. at the 6th Texas Symp., New York.
- Kristian, J., 1972, Comm. at the 6th Texas Symp., New York.
- Layzer, D., 1965, *Astrophys. J.*, **141**, p. 837.
- Low, F. J., 1970, *Astrophys. J. Letters*, **159**, p. L173.
- Miller, R. H., and E. N. Parker, 1964, *Astrophys. J.*, **140**, p. 150.
- Montmerle, T., 1971, Thesis, Paris.
- Omnès, R., 1969, *Phys. Rev. Letters*, **23**, p. L38.
- , 1970, Comments and Addenda, *Phys. Rev.*, **1**, p. L723.
- , 1971a, *Astron. and Astrophys.*, **11**, p. 450.
- , 1971b, *Astron. and Astrophys.*, **10**, p. 228.
- , 1971c, *Astron. and Astrophys.*, **15**, p. 275.
- , 1972a, *Phys. Rep.*, **3C**, p. 1.
- , 1972b, Proceedings of the IAU Meeting on Dense Matter, Boulder.
- Ozernoy, L. M., 1966, *Astr. Zh.*, **43**, p. 300.
- Ozernoy, L. M., and G. V. Chibisov, 1970, *Soviet Ast. A. J.*, **14**, p. 915.
- Peebles, R., 1972, *Comments Astrophys. Space Phys.*
- Peyraud, N., 1971, *Astron. and Astrophys.*
- Robinson, I., A. Schild, and E. E. Schucking, ed., 1963, *Quasistellar Sources and Gravitational Collapse*, Univ. of Chicago Press.
- Rosburgh, I. W., 1965, *Nature*, **207**, p. 363.
- Rougeor, G. W., and J. H. Oort, 1960, *Proc. Nat. Acad. Sci. U. S.*, **46**, p. 1.
- Schatzman, E., 1970, *Phys. and Astrophys.*, CERN, Geneva.
- , 1970, CERN Lectures.
- Schmidt, M. 1969, *Ann. Rev. of Astron. and Astrophys.*, p. 527.
- , 1970, *Astrophys. J.*, **162**, p. 371.

- Spitzer, L. J., 1971, *Nuclei of Galaxies*, O'Connell, ed., North-Holland.
- Spitzer, L. J., and W. C. Saslaw, 1966, *Astrophys. J.*, **143**, p. 400.
- Stecker, F. W., D. L. Morgan, Jr., and J. Bredekamp, 1971, *Phys. Rev. Letters*, **27**, p. L1469.
- Stecker, F., and J. L. Puget, 1972, *Astrophys. J.*, **178**, p. 57.
- Steigman, G., 1969, *Nature*, **224**, p. 477.
- Sunyaev, R. A., and Ya. B. Zel'dovitch, 1972, *Astron. and Astrophys.*, **20**, p. 189.
- Teller, E., 1966, *Perspectives in Modern Physics*, R. E. Marshak, ed., Interscience, New York.
- Ulam, S. M., and W. E. Walden, 1964, *Nature*, **201**, p. 1202.
- Wagoner, R. V., 1969, *Ann. Rev. Astr. Astrophys.*, **7**, p. 553.
- Wampler, D., 1972; Comm. at the 6th Texas Symp., New York.
- Woltjer, L., 1964, *Nature*, **201**, p. 803.
- Zel'dovitch, Ya. B., 1965, *Advances Astron. Astrophys.*, Z. Kopal, ed., **3**, p. 241.
- Zel'dovitch, Ya. B., and I. D. Novikov, 1971, *Relativistic Astrophysics*, University of Chicago Press.

## B. THE DEUTERIUM PUZZLE IN THE SYMMETRIC UNIVERSE

B. Leroy, J. P. Nicolle, and E. Schatzman\*  
*Observatoire de Meudon*

In our present understanding of the model of the symmetric universe, we are led to the following picture proposed by Omnès (1972)†:

- Separation era, during which a partial separation between baryons and antibaryons takes place, at  $t < 10^{-5}$  s or  $kT > 350$  MeV (critical temperature of the phase transition);
- Annihilation era ( $t < 1600$  s,  $350 \text{ MeV} > kT > 25$  keV). At the end of the annihilation era, the annihilation pressure becomes efficient to produce the coalescence;
- Coalescence era ( $1400 \text{ s} < t < 10^6$  years;  $25 \text{ keV} > kT > 1/3$  eV). At the end of the coalescence era, the mean-free path of the products of the annihilation become comparable to the size of the emulsion.

During the annihilation era, the size of the emulsion is governed by the diffusion of nucleons. If we look more closely at the situation, we can see, as shown by Steigman (preprint) that the main process is the diffusion of neutrons (at least, as long as there are neutrons). The only way in which neutrons can be kept in the emulsion is by neutron electron scattering. However, this can last only as long as there are blackbody electrons. As soon as the temperature drops below 0.5 MeV, the number of free electrons, which goes like  $10^{32.3} T_{\text{MeV}}^{-3} 10^{-(0.25/T \text{ MeV})}$ , decreases very quickly. If the size of the emulsion is large enough the neutrons are kept until nucleogenesis takes place around  $T \sim 0.1$  MeV. If the size of the emulsion is too small, the neutrons are lost (they annihilate at the boundary of the emulsion), and no nucleosynthesis can take place. From the analysis of the diffusion process, this seems to be the case.

---

\*Speaker.

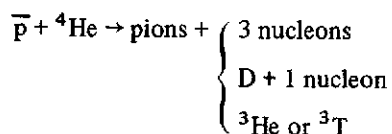
†Further references can be found in the paper quoted.

In the following we shall consider how the present abundance of deuterium can be used as an independent proof that no nucleosynthesis has taken place and therefore that neutrons were lost before nucleosynthesis. The argument is the following:

1. we consider the nucleosynthesis during the radiative era;
2. we estimate the relevant cross sections;
3. we estimate the maximum abundance of  ${}^4\text{He}$  at the end of the nucleosynthesis era; and
4. we solve the diffusion problem in order to get an estimate of the rate of loss of the neutrons. This leads to a correction factor to the rate of formation of  ${}^4\text{He}$ . An estimate of this correction factor, to match the maximum abundance of  ${}^4\text{He}$ , leads to an estimate of the maximum size of the emulsion.

### NUCLEOSYNTHESIS DURING THE RADIATIVE ERA

Let us consider the reactions taking place between nuclei and antinuclei at the boundaries of the emulsion. Let us assume that we have only protons and alpha particles. The reaction



leads mainly to the production of nucleons and the destruction of  $\alpha$ -particles. Half of the nucleons produced are destroyed in flight in the regions of antimatter, either in  $\bar{N}N$  reactions or in  $N\bar{\alpha}$  reactions (Figure XIV.B-1). Let us call  $R$  the probability of the reaction  $\bar{N}N$  in flight and  $(1-R)$  the probability of the reaction  $N\bar{\alpha}$  in flight. Neglecting provisionally the production of deuterium and tritium, we have the following expressions for the rate of reaction.

$$\begin{aligned} \frac{dp}{dt} = & -\langle\sigma v\rangle_{p\bar{p}} p\bar{p} + \langle\sigma v\rangle_{p\bar{\alpha}} \left[ -1 - \frac{3}{2}R + \frac{9}{2}(1-R) \right] p\bar{\alpha} \\ & + \frac{3}{2}\langle\sigma v\rangle_{p\bar{\alpha}} p\bar{\alpha} + \langle\sigma v\rangle_{\alpha\bar{\alpha}} \left[ \frac{3}{2} - \frac{3}{2}R + \frac{9}{2}(1-R) \right] \alpha\bar{\alpha} \end{aligned}$$

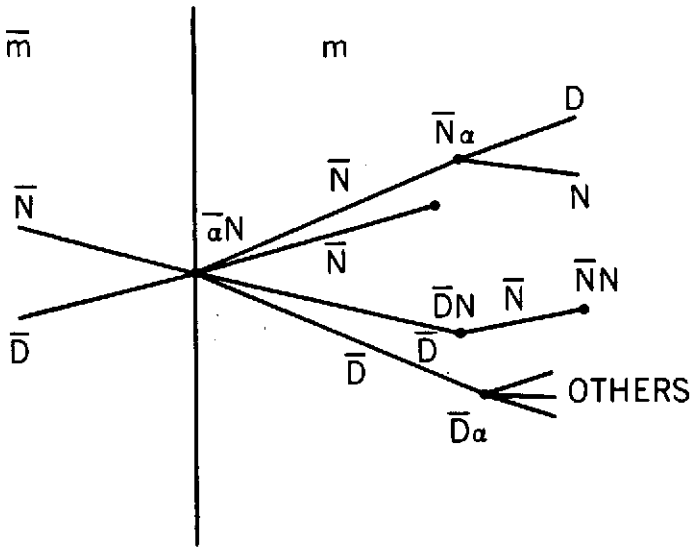


Figure XIV.B-1. Schematic representation of the annihilation at the interface and the secondary reactions taking place in flight. Only the main reactions have been plotted following the  $\bar{\alpha}N$  reaction at the interface. A symmetric figure would have to be drawn for the  $\bar{\alpha}N$  reaction.

$$\frac{d\alpha}{dt} = - \langle \sigma v \rangle_{\bar{p}\alpha} \bar{p}\alpha + \langle \sigma v \rangle_{\bar{p}\bar{\alpha}} \left[ -\frac{3}{2}(1-R) \right] \bar{p}\bar{\alpha} + \langle \sigma v \rangle_{\alpha\bar{\alpha}} \left[ -1 - \frac{3}{2}(1-R) \right] \alpha\bar{\alpha}$$

By taking a proper average over space, and assuming  $\langle p \rangle = \langle \bar{p} \rangle$ ,  $\langle \alpha \rangle = \langle \bar{\alpha} \rangle$ , calling  $\lambda$  and  $\mu$  the ratios

$$\lambda = \frac{\langle \sigma v \rangle_{\bar{p}\alpha}}{\langle \sigma v \rangle_{\bar{p}\bar{p}}} ; \quad \mu = \frac{\langle \sigma v \rangle_{\alpha\bar{\alpha}}}{\langle \sigma v \rangle_{\bar{p}\bar{p}}}$$

we obtain

$$\frac{dp}{d\alpha} = \frac{p^3 + 2\lambda p^2\alpha + p\alpha^2(-5\lambda^2 + \frac{3}{4}\mu) - \frac{33}{4}\lambda\mu\alpha^3}{\lambda p^2\alpha + p\alpha^2(\mu + \lambda^2) + \frac{5}{2}\alpha^3\lambda\mu}$$

In a similar way, we can consider the rate of production of deuterium. Estimating that the most important part in the balance equation for the deuterium arises from the deuterium production, we obtain, B being the branching ratio in the  $\bar{p}\alpha$  reaction

$$\frac{dD}{dp} \cong \frac{\frac{\lambda p \alpha}{2} B \left( p + \frac{5}{2} \alpha \lambda \right)}{p^3 + 2\lambda p^2 \alpha + p \alpha^2 \left( -5\lambda^2 + \frac{3}{4} \mu \right) - \frac{33}{4} \lambda \mu \alpha^3}$$

It results from the experiments of Barkas et al. (1957), that in the reaction  $\bar{p}$ -nucleus, 1.3 pion on the average is absorbed in the nucleus, out of the average 5 pions produced in the annihilation.

After annihilation, we are left with an  ${}^3\text{He}$  or a  ${}^3\text{T}$  in excited states. We shall assume that the final nuclei left are in the same ratio as observed by Zaimidoroga (1965, 1967) for the pion capture by  ${}^3\text{He}$ . According to the summary given by Koltun (1969), we have the following ratios:

$\pi^- + \text{He}^3 \rightarrow \text{H}^3 + \pi^0$	15.8 ± 0.8 %
$\pi^- + \text{He}^3 \rightarrow \text{H}^3 + \gamma$	6.9 ± 0.5 %
$\pi^- + \text{He}^3 \rightarrow p + 2n$	57.8 ± 5.4 %
$\pi^- + \text{He}^3 \rightarrow \text{D} + n$	15.9 ± 2.5 %
$\pi^- + \text{He}^3 \rightarrow \text{D} + n + \gamma$	3.6 ± 1.2 %
$\pi^- + \text{He}^3 \rightarrow p + 2n + \gamma$	?

To summarize briefly these data, assuming that the  $\pi^-$  can do the same to  ${}^3\text{H}$  as to  ${}^3\text{He}$ , we shall accept the following branching ratios:

$\bar{p} + \alpha \rightarrow {}^3\text{X} + \pi \rightarrow 3\text{N} + \pi$	60 %
$\bar{p} + \alpha \rightarrow {}^3\text{X} + \pi \rightarrow \text{N} + {}^2\text{D} + \pi$	20 %
$\bar{p} + \alpha \rightarrow {}^3\text{X} + \pi \rightarrow {}^3\text{Y} + \pi$	20 %

From these data, we conclude immediately that very little  ${}^4\text{He}$  must have been left at the beginning of the radiative era, otherwise a too large abundance of  ${}^2\text{D}$  would have been produced.

#### ESTIMATE OF THE CROSS SECTION AND RATES OF FORMATION

The  $\langle \sigma v \rangle$  includes both the nuclear part and the effect of the convergence of the wave function for capture at low energy. We have

$$\sigma v = \sigma_{\text{nucl}} v \frac{2\pi n}{1 - e^{-2\pi n}}$$

with  $n = Z_1 Z_2 e^2 / \hbar v$ . If we compare the two cross sections, and calculate the ratio

$$\lambda = \frac{\langle \sigma v \rangle_{\bar{p}\alpha}}{\langle \sigma v \rangle_{p\bar{p}}}$$

we have to include the effect of the charge of the  $\alpha$ , the effect of the relative mass and of the relative velocity in the collision.

Assuming, as already suggested by Schatzman (1970),

$$\frac{\sigma_{\text{nucl}} \bar{p}\alpha}{\sigma_{\text{nucl}} p\bar{p}} \cong 3.5$$

we obtain

$$\lambda = \frac{\langle \sigma v \rangle_{\bar{p}\alpha}}{\langle \sigma v \rangle_{p\bar{p}}} \cong 7$$

In the same way, we obtain, as an estimate,

$$\mu = \frac{\langle \sigma v \rangle_{\alpha\bar{\alpha}}}{\langle \sigma v \rangle_{p\bar{p}}} \cong 56$$

With these values, we get the main contribution to the rate of change of the abundances (for small values of  $\alpha$  and D),

$$\frac{dp}{d\alpha} = \frac{1}{\lambda} \frac{p}{\alpha}$$

which gives

$$\alpha = \alpha_0 (p/p_0)^\lambda$$

and

$$\frac{dD}{dp} = -\frac{\lambda B}{2} \left( \frac{\alpha_0}{p_0^\lambda} \right) p^{\lambda-1}$$

which gives

$$D = D_0 - \frac{B}{2} \alpha_0 \left( \frac{p}{p_0} \right)^\lambda$$

We see that deuterium is built up, whereas  $\alpha$ -particles are destroyed. Assuming that we start with zero deuterium, we have

$$D_0 = \frac{B}{2} \alpha_0$$

where the origin is taken at the end of the nucleosynthesis. The final concentration (observed at the present time) gives

$$\frac{D_0}{p} = \frac{D_0}{p_0} \frac{p_0}{p} \equiv \delta \quad \text{or} \quad \frac{D_0}{p_0} = \delta \frac{p}{p_0}$$

from which we derive:

$$\frac{\alpha_0}{p_0} = \frac{2}{B} \delta \frac{p}{p_0}$$

If we take the value of  $\delta$  at the surface of the earth, as given by Urey et al. (1932), and Craig (1961),  $\delta \cong 2.10^{-4}$  and with  $(2/B) \cong 10$ , we obtain

$$\frac{\alpha_0}{p_0} \cong 2.10^{-3} \frac{p}{p_0}$$

If we take the protosolar gas value of Geiss and Reeves (1972),  $\delta = 3.10^{-5}$ , we obtain

$$\frac{\alpha_0}{p_0} = 3.10^{-4} \frac{p}{p_0}$$

The ratio  $(p/p_0)$  is the annihilation ratio between 0.1 MeV, and 1/3 eV. From the recent work of Aldrovandi, Caser, Omnès, and Puget (1973), it is quite clear that most of the annihilation has taken place already by  $T = 25$  keV, and we cannot expect  $(p/p_0)$  to be very small. For further calculations, we shall take  $(p/p_0) \cong 0.1$ , or  $(\alpha_0/p_0) \cong 2.10^{-4}$ , which represents a depletion factor  $\Delta$

at the end of the nucleosynthesis, compared to the results of Wagoner, Fowler, and Hoyle (1967), of the order of  $10^{-3}$ .

This confirms entirely what has been announced earlier, that is to say that there is very little  $^4\text{He}$  left at the end of the epoch of nucleosynthesis.

**RATE OF LOSS OF THE NEUTRONS AND  $^4\text{He}$  FORMATION**

In order to get an idea of the rate of loss of the neutrons, we shall consider the diffusion with a time dependent diffusion coefficient to the surface of a sphere with a radius growing with time.

The equation of diffusion,

$$D \frac{1}{r^2} \frac{\partial}{\partial r} r^2 \frac{\partial \phi}{\partial r} = \frac{\partial \phi}{\partial t}$$

with  $\phi = 0$  at  $r = a(t)$ , can be solved in the following way:

Introducing  $r = x a(t)$ ,  $0 \leq x \leq 1$ ,  $d\tau = D dt/a^2$ , we have

$$\frac{1}{x^2} \frac{\partial}{\partial x} x^2 \frac{\partial \phi}{\partial x} = \frac{\partial \phi}{\partial \tau}$$

A solution is  $\phi = \sin \pi x/x \exp(-\pi^2 \tau)$ , from which we derive the time scale of depletion by diffusion towards the boundary

$$\left( \frac{dn}{dt} \right)_{\text{Diff}} = - \frac{\pi^2 D}{a^2} n$$

The equation of conservation of the neutrons becomes

$$\frac{dn}{dt} = - n \frac{\pi^2 D}{a^2} - \frac{n}{\tau_n} + \frac{p}{\tau_p}$$

We are concerned with the last phase of nucleosynthesis, for  $kT < 1 \text{ MeV}$ , for which  $\tau_p$  increases very quickly to infinity. If we simplify the equation of formation of the  $\alpha$ 's to a pure neutron capture process we obtain

$$\frac{d\alpha}{dt} = \langle \sigma v \rangle_{pn} pn$$

and the number of  $\alpha$ 's at the end of the nucleogenetic period is

$$\alpha = \int \langle \sigma v \rangle_{pn} p n_0 \exp \left( - \int \frac{1}{\tau_n} + \frac{\pi^2 D}{a^2} dt' \right) dt$$

We shall simplify the whole problem by assuming that the depletion factor  $\Delta$  can be estimated by the quantity

$$\Delta = \left\langle \exp \left( - \int \frac{\pi^2 D}{a^2} dt' \right) \right\rangle$$

The average  $\Delta$  is obtained in the following way. We calculate the amount of helium formed from the temperature  $T_1$  where the rate of destruction  ${}^4\text{He}$  ( $\gamma, n$ )  ${}^3\text{He}$  becomes negligible ( $T_1 \cong 0.8$  MeV). The concentrations  $p$  and  $n_0$  are proportional to the expansion factor to the minus cube, and we can write

$$\Delta \cong \frac{\int_0^{T_1} T^3 dT \exp \left[ - \int \frac{\pi^2 D}{a^2} dt' \right]}{\int_0^{T_1} T^3 dT}$$

From the estimate of the integral, and writing  $a = a_0 T^{-n}_{\text{MeV}}$ , it is possible to get an estimate of  $a_0$ . The result is not very sensitive to the value of  $n$ . With  $n = 17/6$  (corresponding to the rate of growth during the coalescence period), a diffusion coefficient

$$D = 10^{8.15} T_{\text{MeV}}^{-5/2} 10^{(0.25/T)}$$

we obtain for  $\Delta = 10^{-3}$  a maximum value

$$a_0 < 10^{4.69} \text{ for } \delta = 2.10^{-4} \qquad a_0 < 10^{4.64} \text{ for } \delta = 3.10^{-5}$$

If we consider the formation of  ${}^3\text{He}$  and if we take the abundance ratio  ${}^3\text{He}/\text{H}$  as  $10^{-5}$ , we obtain  $a_0 < 10^{4.60}$ . This is quite compatible with the diffusion length. For a sphere

$$L_D = \pi \left( \int D dt \right)^{1/2} \cong 10^{4.25} T_{\text{MeV}}^{-9/4}$$

## CONCLUSION

From this short discussion, we see that the low abundance of deuterium is some sort of proof that the neutron loss has actually taken place before the beginning of the nucleogenesis.

We can then assume either that the diffusion length actually determines the size of the emulsion, and it seems quite possible that the abundance of the  $\alpha$ 's was vanishingly small at the end of the nucleogenesis, or that the abundance of deuterium and other light elements results from the nucleogenesis. It then leads to a determination of the size of the emulsion during the nucleogenesis. In fact, a small amount of coalescence before the end of the annihilation period would be enough to increase the size of the emulsion beyond the diffusion length and put the two determinations in complete agreement.

A final comment is interesting to make: Since the beginning of the theory of the symmetric universe, a number of criticisms have been made, which have been met with success, one after the other. Just like a puzzle, the pieces have been found to adjust to each other. In the present case, one has the feeling that the new piece has just matched a hole between two pieces. This gives great confidence for the future of the model.

## REFERENCES

- Aldrovandi, R., S. Caser, R. Omnès, and J. L. Puget, 1973, *Astron. and Astrophys.*, in press.
- Barkas, W. H. et al., 1957, *Phys. Rev.*, **105**, p. 1037.
- Craig, H., 1961, *Science*, **133**, p. 1833.
- Geiss, J., H. Reeves, 1972, *Astron. and Astrophys.*, **18**, p. 126.
- Koltun, D. S., 1969, *Adv. in Nucl. Phys.*, **3**, p. 149.
- Omnès, R., 1972, *Phys. Reports*, **3 C**, p. 1.
- Schatzman, E., 1970, *Phys. and Astrophys.*, CERN lectures.
- Urey, H. C. et al., 1932, *Phys. Rev.*, **40**, p. 1.
- Wagoner, R. V., W. A. Fowler, and F. Hoyle, 1967, *Astrophys. J.*, **148**, p. 3.
- Zaimidoroga, O. A. et al., 1965, *Sov. Phys.-JETP*, **21**, p. 848.
- Zaimidoroga, O. A. et al., 1967, *Sov. Phys.-JETP*, **24**, p. 1111.

## C. ANTIMATTER IN THE UNIVERSE?

Gary Steigman\*  
*Yale University*

### INTRODUCTION

In several previous papers you have heard of the development of a cosmological model that is symmetric in the sense that exactly half the particles in the universe are, in fact, antiparticles. You have also heard of some of the observational consequences of such a model, particularly as they relate to  $\gamma$ -ray astronomy. The conclusion the previous speakers have reached is that it is possible to build such a model without violating the many constraints set by observation. I am much less convinced than they are of this conclusion and have in the past addressed myself to some of the problems posed by a "symmetric" cosmology. Although I think we are all agreed that this subject is in a rather early stage of development and that there are many as yet unsolved problems, the subject is sufficiently important to justify our continuing interest in it.

In these remarks, I wish to adopt an approach that is different from that of the previous speakers. Rather than asking if a symmetric cosmological model can be constructed that is consistent with observations, I wish to ask the question, "If the universe does indeed contain equal amounts of matter and antimatter, how would we know about it?" There are several straightforward ways in which antimatter could signal its presence to us, and I shall discuss them shortly. As we shall see, there is no evidence whatever for large amounts of antimatter in the universe. From that we may reach one of two conclusions. Either the universe is not symmetric, or, if it is, the ubiquitous antimatter prefers to remain clandestine (see Puget, Chapter XV.A for relevant discussion). If indeed we adopt the latter conclusion, then the limits set by observations

---

\*Speaker.

set severe restraints on the possible cosmological models. The conclusion that appears to emerge is that matter and antimatter must be separated on the scale of clusters of galaxies if the universe really is symmetric. Much of what I am going to present has already appeared in print so I shall limit myself to a general discussion, omitting the details which may be found in the original papers. (Steigman, 1969; Steigman, 1971; Steigman and Strittmatter, 1971; Steigman, 1972).

### DIRECT EVIDENCE

In principle it is easy to detect the presence of antimatter. You travel to where you suspect a concentration of antimatter, put your detector down (the most rudimentary device will do), and watch. If your detector disappears then you better get out of there fast; you have detected antimatter. Seriously though, just such experiments have in fact been performed within the solar system via the manned flights to the moon and the unmanned probes to Venus. Now we know, as we suspected with very good reason, that the moon and Venus are made of ordinary matter. Even before the days of space flights we had pretty good reason to believe the solar system was all made of ordinary matter; the solar wind which sweeps out from the sun past the planets acts as a probe just as our detector would.

Unfortunately, we are not likely to learn very much about a sizable part of our galaxy by this method. However, we are fortunate that rather than having to travel around ourselves there are obliging particles which come to us: the cosmic rays. Now, unfortunately, the cosmic rays give us no information about their sources because (except for the very highest energy cosmic rays) they are tied to the magnetic field and do not travel in straight lines. Therefore, we cannot be sure of what region of space we are sampling when we examine the cosmic rays. However, we can be certain that, despite extensive searches, no antinucleus has ever been found in the cosmic rays. Now, at some level ( $\sim 1$  part in  $\geq 10^4$ ) we would expect to detect secondary antiprotons in the cosmic rays. The secondary production of antihelium or heavier antinuclei in collisions between the cosmic rays and the interstellar gas will be down by many orders of magnitude. These antinuclei would provide, if detected, clear evidence that somewhere in the galaxy (universe?) there were large amounts of antimatter. Evenson (1972) has set limits to the fraction of helium nuclei which are antihelium. No antihelium nucleus has been found and at the 95-percent confidence level he finds a fractional limit for the rigidity range 1 to 10 GV, of  $1 \times 10^{-3}$  and for the range 10 to 25 GV, of  $8 \times 10^{-2}$ . For heavier antinuclei, a limit at the 95-percent confidence level has been set by Golden et al. (1973, private communication), for rigidities 4 to 125 GV, of  $5 \times 10^{-3}$ , by Buffington et al. (1972), for rigidities  $< 33$  GV of  $2 \times 10^{-4}$ . In the range 33 to 100 GV their limit is  $2 \times 10^{-2}$ .

As I emphasized, we cannot be sure where the observed cosmic rays come from. From the ratio of light (Li, Be, B) nuclei to medium (C, N, O) nuclei we know that the cosmic rays must be able to travel several hundred parsecs in a few million years. So the cosmic rays we sample probably come from a volume whose typical dimension is roughly a few hundred parsecs. They may in fact come from a much larger volume. The isotropy of the cosmic rays, the smoothness of the distribution of galactic, nonthermal, radio emission, and the relative constancy of the cosmic ray flux at earth over periods as long as 4.5 billion years all indicate the cosmic rays we observe fill a volume comparable in size to and perhaps even greater than our galaxy. The lack of antimatter in the cosmic rays gives us good evidence that every second star in our galaxy is not made of antimatter. Indeed, the limits on antinuclei in the cosmic rays are already so low that even if a small fraction (perhaps one percent or so) of them were extragalactic in origin, they would be telling us that very few, if any, extragalactic systems could be made of antimatter.

In summary, the cosmic rays provide us with the only practical means of sampling the universe outside our solar system. The evidence is straightforward: no antinuclei have ever been found in the cosmic rays. Therefore, some region of space contains very little, if any, antimatter. Unfortunately, we cannot be certain which region of space it is.

### INDIRECT EVIDENCE

When matter and antimatter meet, they annihilate. The annihilation products are typically pions; there are roughly 5 to 6 charged and neutral pions in a typical annihilation. The charged pions decay into muons with the emission of a muon neutrino; the neutral pions decay most often into two  $\gamma$ -rays. The muons themselves decay into electrons (and positrons) with the emission of both an electron neutrino and a muon neutrino. The end products of a typical annihilation are high-energy electron-positron pairs,  $\gamma$ -rays, and two kinds of neutrinos. We can therefore hope to learn of the presence of antimatter indirectly by detecting the products of its annihilation with ordinary matter. The electron-positron pairs will probably not travel very far from where they are created either because they will be tied to magnetic fields or because they will scatter on any photons present (starlight, infrared, blackbody, and so forth) and lose energy rapidly. Furthermore, we know there exist mechanisms for accelerating electrons and positrons to high energy in any case (pulsars). Hence the electron-positron component of annihilation is not likely to provide us with any unambiguous information about the presence of antimatter.

Neutrinos, of course, are very difficult to detect. As a result, large fluxes are required; hence, the limits one might set are not very interesting. A major

fraction of the matter in the universe would have to be annihilating before a detectable flux of neutrinos would be produced. If that were the case there would be other, more immediate consequences. Of course, a strong, nearby source (for example, the galactic center) might produce a detectable flux of neutrinos, but there too we would expect other, more obvious effects (for example,  $\gamma$ -ray emission). For a discussion of these questions see Steigman and Strittmatter, 1971.

Finally, we come to the  $\gamma$ -rays produced in annihilation. It is of course most appropriate that they be discussed at this conference. A typical annihilation produces a spectrum of  $\gamma$ -rays extending from several tens of MeV to several hundred MeV. On the average, 3 to 4  $\gamma$ -rays are produced per annihilation. Observations of  $\sim 100$  MeV  $\gamma$ -rays then enable us to place limits on the amount of contemporaneous annihilation.

The OSO-3 observations (Kraushaar, et al., 1972) of  $\sim 100$ -MeV  $\gamma$ -rays indicates a galactic component superimposed upon an isotropic, presumably extragalactic component. From their results, we can draw the following conclusions (Steigman, 1969; Steigman, 1971; Steigman, 1972). If there is a cool, neutral, intergalactic gas that is symmetric, its density could be no larger than  $n \sim 10^{-11} \text{ cm}^{-3}$ . I remind you that the average density of matter in galaxies is  $\gtrsim 10^{-7} \text{ cm}^{-3}$ ; hence such a cool, intergalactic gas would constitute a minor component of our universe. For a hot, ionized, intergalactic gas we find that if it is symmetric, then its density must be low ( $\lesssim 10^{-9} \text{ cm}^{-3}$ ). If, in fact, there is a hot, intergalactic gas whose density is close to the critical density, the fraction of it which could be mixed matter and antimatter would be less than one part in  $10^8$ . Thus, either such a gas is not symmetric, or it maintains very well separated regions of matter and antimatter. While on the subject of intergalactic gas, it is worth pointing out that the Coma cluster of galaxies has been detected as an X-ray source (Gursky et al., 1971) whose spectrum is interpreted as thermal bremsstrahlung radiation from a hot intracluster gas. If this interpretation is correct, then from the lack of  $\gamma$ -rays from Coma, we can say that less than one part in  $10^4$  of that gas is antimatter.

The observations of the galactic,  $\gamma$ -ray component indicates an annihilation rate per interstellar hydrogen atom of less than  $10^{-25} \text{ s}^{-1}$ . If, in fact, these  $\gamma$ -rays are interpreted as annihilation products, we can set the following limits on the antimatter component in the galaxy: If the annihilation occurs in interstellar clouds, less than one particle in  $10^{16}$  is an antiparticle; the annihilation occurs in the intercloud medium, the limits are less than one in  $10^{12}$ . Indeed, it is worth pointing out that an antiparticle will only survive  $\sim 30$  years in an interstellar cloud and  $\sim 300,000$  years in the intercloud medium; both times are very short compared to the age of the galaxy ( $\sim 10^{10}$  years). Hence, it is clear that any model that requires the galaxy to be symmetric must find

an extremely efficient mechanism which keeps large amounts of matter and antimatter very well separated over long periods of time. The most straightforward interpretation is of course that the galaxy probably contains no macroscopic amounts of antimatter.

Finally, a word about  $\gamma$ -ray sources. There have been no detections of extragalactic  $\gamma$ -ray sources at about the level of  $\sim 10^{-5}$  photons/cm<sup>2</sup>/s. If we wish to use annihilation as an energy source for some of the more spectacular extragalactic objects (for example, QSOs, Seyfert galaxies, radio galaxies, and so forth) then we predict that they would be  $\gamma$ -ray sources. The lack of detections of any of them as sources sets severe restraints on such models. Either annihilation has nothing to do with these sources or, somehow, the  $\gamma$ -rays are absorbed at the source. This latter suggestion is not unreasonable. However, it should be remembered that twice as much energy is released in  $\gamma$ -rays as in electron-positron pairs in a typical annihilation. Then we must inquire into the effect on the source if these  $\gamma$ -rays are to be absorbed. Will the absorption result in reradiation in another part of the spectrum? Can such a model be made consistent with all observations?

## CONCLUSIONS

We have been discussing the means of detecting the presence of antimatter in the universe. We have seen there are several, straightforward, observational tests and all have, thus far, proved negative. The most straightforward interpretation of these results is that the universe is, in fact, not symmetric. Of course, it is possible the universe is symmetric, but the matter and antimatter are well separated from each other. Choosing between these two possibilities must, of course, be a personal decision. Perhaps, in making this decision, we should all bear in mind a quotation which sits, framed, on the desk of William A. Fowler at Caltech. He attributes it to, "Proverbs for Graduate Students, 1933." It reminds us that, "The terrible tragedies of science are the horrible murders of beautiful theories by ugly facts."\*

---

\*In the discussion following my talk, D. Clayton of Rice suggested that we search for the evidence of annihilation by looking for the 1-GeV  $\gamma$ -ray line formed when nucleons and antinucleons annihilate directly into two  $\gamma$ -rays. This purely electromagnetic channel should occur but only very infrequently when compared to the strong interaction channels via mesons. A rough estimate indicates only one in  $\sim 10^4$  to  $10^6$  annihilations will be of the two  $\gamma$ -type. The two  $\gamma$ -annihilation has been searched for, unsuccessfully, in several experiments (Gursky et al., 1971; P. Nemethy, 1973, private communication). As a result I do not expect a detectable  $\sim 1$ -GeV annihilation line even if all the observed  $\sim 100$ -MeV  $\gamma$ -rays are from annihilation.

## REFERENCES

- Buffington, A., L. H. Smith, G. F. Smoot, L. W. Alvarez, and M. A. Wahlig, *Nature*, **236**, p. 335.
- Evenson, P., 1972, *Astrophys. J.*, **176**, p. 797.
- Gursky, H., E. Kellogg, S. Murray, C. Leong, H. Tananbaum, and R. Giacconi, 1971, *Astrophys. J. Letters*, **167**, p. L81.
- Kraushaar, W. L., G. W. Clark, G. P. Garmire, R. Borke, P. Higbie, V. Leong, and T. Thorsos, 1972, *Astrophys. J.*, **177**, p. 341.
- Steigman, G., 1969, *Nature*, **224**, p. 477.
- , 1971, *Proc. Int. Sch. Phys. Enrico Fermi*, R. K. Sachs, ed., Academic Press, Course XLVII, p. 373.
- , 1972, *Cargese Lectures in Physics*, **6**, E. Schatzman, ed., Gordon and Breach.
- Steigman, G., and P. A. Strittmatter, 1971, *Astron. and Astrophys.*, **11**, p. 279.

# A. GAMMA-RAY BACKGROUND SPECTRUM AND ANNIHILATION RATE IN THE BARYON-SYMMETRIC BIG- BANG COSMOLOGY

J. L. Puget\*  
*Observatoire de Meudon*

## INTRODUCTION

The negative results of the search for antimatter nuclei in cosmic rays imply that if there is symmetry between matter and antimatter in the universe, each kind must be gathered in separated regions of galaxy or galaxy-cluster size. In such a case, in order to try to get experimental information on the problem of baryon symmetry on a cosmological scale we have to rely mostly on the observation of annihilation products. Among the annihilation products are  $\gamma$ -rays and neutrinos that have very long mean-free paths. Neutrinos especially can reach us from dense regions; Steigman and Strittmatter (1971) used upper limits on the neutrino flux from space to put upper limits on the annihilation in Seyfert galaxies. Nevertheless, for the diffuse background due to annihilation on a cosmological scale,  $\gamma$ -rays are the best test available because they are easier to detect than neutrinos.

Two kinds of  $\gamma$ -rays are produced in matter-antimatter annihilation; 0.511-MeV  $\gamma$ -rays from positron annihilations (4.81 per annihilation); 70-MeV  $\gamma$ -rays from  $\pi^0$  decay (3.4 per annihilation). The number of  $\gamma$ -rays of each kind is roughly the same, and to compare them as a possible source of information on the annihilation rate we must look at their absorption cross section and also at the background due to other sources.

The absorption cross sections are respectively  $10^{-25}$  and  $1.8 \times 10^{-26}$  cm<sup>2</sup> for 0.5 and 70-MeV  $\gamma$ -rays. In a dense universe there is a "window" between 1 MeV and 10 GeV in which  $\gamma$ -rays observed might come from a red shift of about 100 (see Stecker, Chapter IX.A). The X-ray background between

---

\*Speaker.

40 keV and 1 MeV can be represented by a power law with a spectral index 2.1, so it is more likely to detect the 70-MeV annihilation  $\gamma$ -rays than the 0.5 MeV  $\gamma$ -rays.

These considerations prove that the best direct experimental test for presence of antimatter on a cosmological scale lies in observations of the  $\gamma$ -ray background spectrum between 1 and 70 MeV.

### EXPERIMENTAL DATA AND RED-SHIFTED GAMMA-RAYS FROM ANNIHILATION

It has been shown by Stecker, Morgan, and Bredekamp (1971) that the excess of  $\gamma$ -rays observed above 1 MeV could be explained by annihilation of  $\gamma$ -rays coming from high red shift. They computed the spectrum (see Stecker, Chapter IX.A) using a simple theoretical model for the annihilation rate dependence on the red shift

$$\Psi_v = \Psi_{v,0} (1+z)^{6.36}$$

(where  $\Psi_v$  is the annihilation rate per unit volume and  $z$  is the red shift) and they chose the constant  $\Psi_{v,0}$  to fit the data. That led them to the conclusion, already found by Steigman (1969), that matter and antimatter cannot be mixed up in equal quantities in intergalactic space with a density larger than  $10^{-12} \text{ cm}^{-3}$ .

The most recent data (see Chapters III.A and IV.C) show very good agreement with the spectrum computed by Stecker et al. (1971), and leads us to a detailed discussion of the annihilation rate for red shifts lower than 100. The theoretical spectrum below 70 MeV but above  $\sim 5$  MeV (where absorption is negligible) is a power law with an index ( $m - 3.5$ ) if the annihilation rate is written in the form

$$\Psi_v = \Psi_{v,0} (1+z)^m$$

for

$$\Omega = \frac{n_0}{n_{\text{crit}}} = 1$$

( $n_{\text{crit}}$  is the so-called critical density of the Einstein-de Sitter model) and ( $m - 3$ ) for  $\Omega = 0$ .

To get a good fit of the data one needs a spectral index of the order of 3 which means that  $m$  must be such that

$$6 \lesssim m \lesssim 6.5$$

so one can consider that the annihilation rate will fit the data if it falls in the range

$$\Psi_{\nu} = 10^{-34 \pm 0.5} (1+z)^{6.25 \pm 0.25} \text{ s}^{-1} \text{ cm}^{-3} \quad (\text{XV.A-1})$$

### MATTER-ANTIMATTER COSMOLOGY: THEORY

In the recent years, a baryon-symmetric cosmology has been developed in the framework of the big bang theory of the universe and is summarized in these proceedings by Omnès and Schatzman (Chapters XIV.A and B). In this model, matter and antimatter separate at an early stage and at the end of the coalescence period (which coincides with the recombination time) forming an emulsion of characteristic size given by

$$L = 5 \times 10^{29} (1+z)^{-\frac{17}{6}} \text{ cm} \quad (1+z > 600)$$

The fluid motions induced by the coalescence process on a scale of the order of  $L$  reach a velocity

$$v \sim \frac{L}{t} = 8.3 \times 10^{11} (1+z)^{1.34} \text{ cm} \cdot \text{s}^{-1} \quad (1+z < 600)$$

I want to discuss now what could happen in such a model after recombination (which takes place around  $1+z \sim 600$ ) in order to discuss the problem of the annihilation rate. The following theory has been worked out by Stecker and Puget (1972). The evolution of the characteristic dimension  $L$  of the emulsion as a function of red shift is plotted in Figure XV.A-1. At the time we wrote our original paper (Stecker and Puget, 1972), the theory of coalescence in the radiative period had not yet been completely worked out, and we developed a simple model in terms of cloud collisions to put upper and lower limits on  $L$ . Recent work (Aldrovandi et al., preprint) allows us to plot the value of  $L$  up to the recombination red shift, and the corresponding fluid velocities induced by coalescence (Figure XV.A-2). One can compute the Reynolds number corresponding to those coalescence motions and see that large-scale turbulence is generated near recombination.

In a matter-antimatter symmetric big bang, the annihilation electrons and positrons produce a large flux of X-rays by interaction with the cosmic blackbody

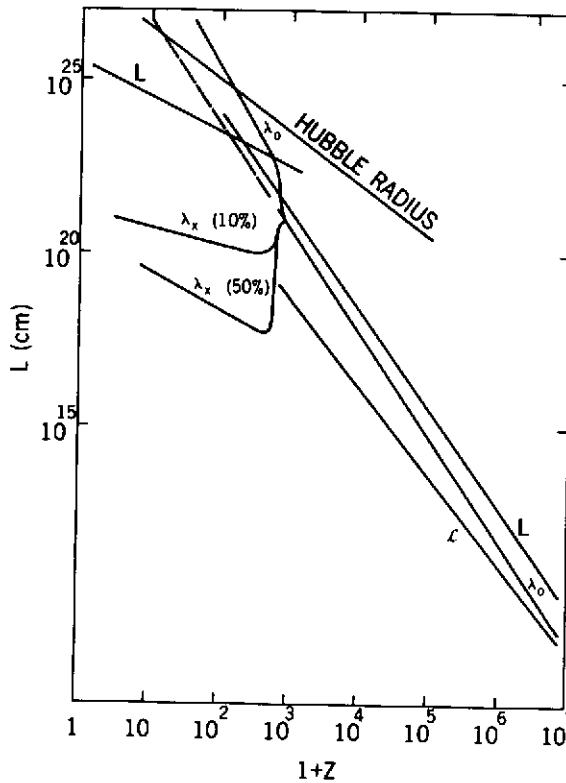


Figure XV.A-1. The different lengths relevant to the problem plotted as a function of red shift.  $\lambda_0$  is the mean free path of thermal photons;  $\lambda_x$  (10%) the mean free path of X-rays corresponding to 10 percent ionization rate; and  $\lambda_x$  (50%) the mean free path of X-rays corresponding to 50 percent ionization rate.

photons, and these X-rays tend to keep the matter ionized longer than in a nonsymmetric big bang. Furthermore, the recombination occurs very gradually and ionization remains high near the boundary regions, as shown on Figure XV.A-3. The viscosity which was determined by the radiation field drops to the kinematic viscosity which is 10 orders of magnitude lower when matter (or antimatter) becomes neutral and decouples from the radiation field. The large-scale fluid motions then become supersonic. In order to compare the parameters of the annihilation-generated turbulence with the parameters of primordial turbulence used by Ozernoy et al. (1970) and Ozernoy (1971), in their theory of galaxy formation, we have neglected the remaining ionization after a red shift of  $\sim 600$  in a first step. We find a good

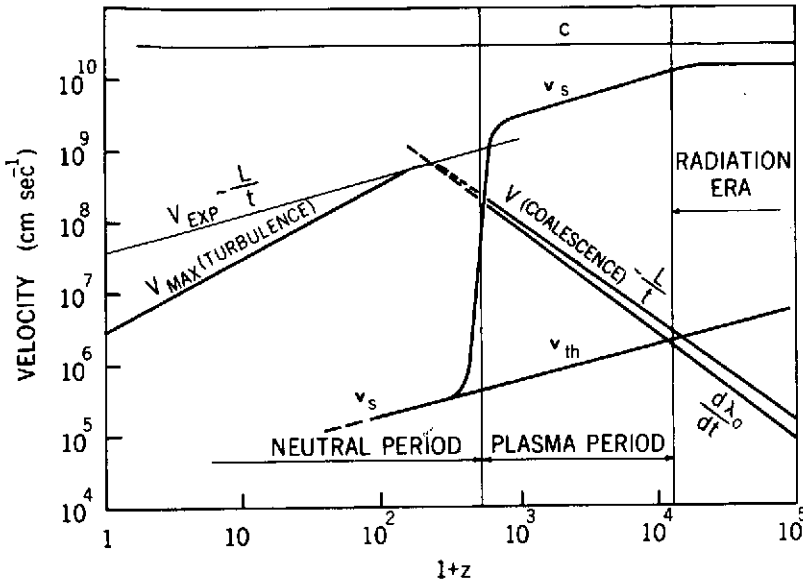


Figure XV.A-2. The velocities relevant to the problem plotted as a function of red shift.

agreement taking account of the uncertainties in the theory of generation of turbulence.

I want to underline here the differences between the symmetric model and the nonsymmetric one. Dallaporta and Lucchin (1972, preprint) have shown that it is likely that a primordial turbulence will be dissipated before recombination. In our model, turbulence is generated near or even during recombination, so this problem disappears. The question of dissipation during the phase of supersonic turbulence (before galaxy formation) and after galaxy formation might also be a very serious one as shown by Silk (1972, preprint). In the original model we just assumed for simplicity that no coalescence at all takes place after  $z \sim 600$ . In fact, a source of motion exists. The ionization near the boundary shown on Figure XV.A-3 which is due to photoionization collisions implies that the momentum carried away by these X-rays is transmitted to the matter with a mean-free path which is of the order of the width of the ionized region. We are in a case where the annihilation pressure generates a surface tension of the type discussed by Omnès and coworkers (see Omnès, Chapter XIV.A). This surface tension, which induces coalescence during the radiative period, will also take place here and even if the corresponding increase of size is negligible (which is certainly true for low  $z$  as we shall see later), the fluid motions induced will compensate the dissipation of kinetic energy, at least partially.

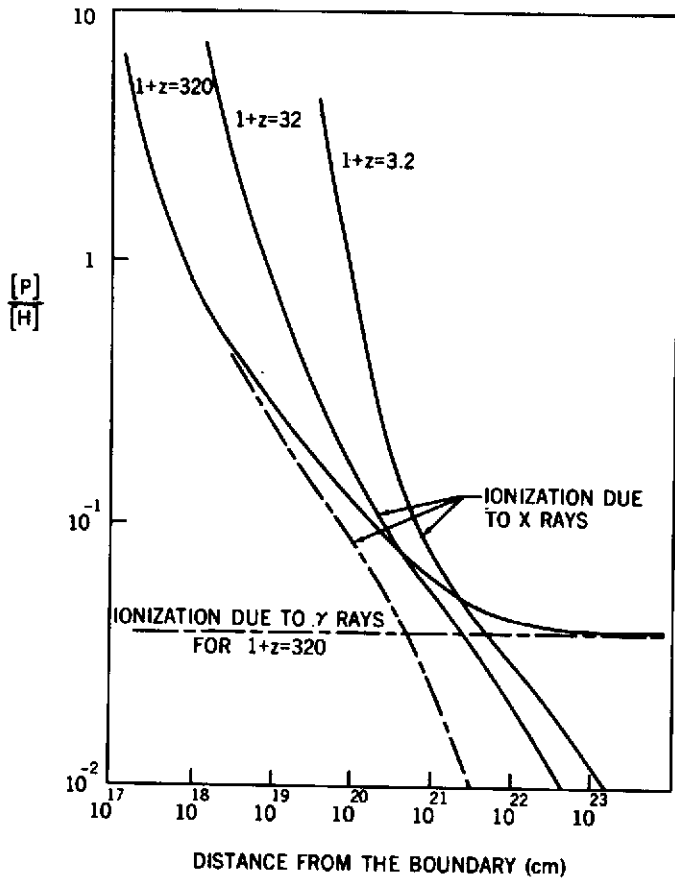


Figure XV.A-3. The ratio of the proton density to the neutral hydrogen density given for three values of the red shift as a function of the distance from the annihilation layer.

The theory of the galaxy formation period, which includes such phenomena as galaxy formation from the density fluctuations induced by shocks in the supersonic turbulence generated at recombination time, formation of clusters by the breaking up of the emulsion into separate clouds, and production of magnetic fields on the boundaries between matter and antimatter, is obviously a very complicated problem and it is not possible at this point to rely on a complete theory of this period to discuss the annihilation rate.

I shall now change my point of view and, keeping in mind the general picture, give a detailed discussion of the annihilation rate based on the consistency of our arguments with the observations on one hand, and on the

elements of our theory which have been worked out so far on the other hand.

### ANNIHILATION RATE AT $Z \ll 1$

As we have seen, the theory does not tell us if the regions of matter and antimatter are of a galaxy cell size or of a galaxy-cluster cell size, so I shall consider both hypotheses. If dense clusters contain as much matter as antimatter there will be several sources of annihilation. I shall consider these sources without going into the details, considering only the conclusion we shall be lead to.

#### Intergalactic Gas

Observations of diffuse sources of X-rays in 20 rich clusters show that a hot intergalactic gas, containing about as much mass as the galaxies themselves, must exist in clusters. This intergalactic medium must form an emulsion of matter and antimatter and, considering the magnetic fields produced on the boundaries, the diffusion can be slowed down to a level such that the annihilation rate does not exceed the value given by Equation (XV.A-1).

#### Galaxies (or antigalaxies) and Intergalactic-Gas

The velocities of galaxies (or antigalaxies) in a rich cluster are large (up to  $10^3$  km/s), and the crossing time for a galaxy is smaller than the age of the universe, so a galaxy could be surrounded by matter or antimatter with equal probability. Accretion of intergalactic gas on large galaxies will produce an annihilation rate

$$\Psi_{v, g/IG} \sim 1.2 \times 10^{-30} \frac{M}{M_{\odot}} \text{ s}^{-1} \text{ cm}^{-3}$$

where  $M$  is the mass accreted by all the galaxies in one cluster per year. Therefore,  $M$  must be smaller than  $10^4 M_{\odot}$  so as not to conflict with the annihilation rate given by Equation (XV.A-1). This value seems too small.

#### GALAXY-ANTIGALAXY COLLISIONS

Detailed study of galaxy-antigalaxy collisions have shown that the annihilated mass is probably of the order of magnitude of  $M_A$  with

$$M_A = M_T \frac{v}{c}$$

$$\Psi_{v, g\bar{g}} = \frac{1.25 \times 10^{-16}}{\tau}$$

where  $\tau$  is the average collision time for one cluster,  $V$  is the relative velocity,  $M_T$  the total interstellar gas mass of the galaxy; any evaluation of the collision time gives  $\tau \ll 10^{18}$  which means again that the annihilation rate from such a process would produce more  $\gamma$ -rays than observed.

If we consider cluster size regions, the annihilation takes place only on boundary regions and, even for a dense intergalactic gas, magnetic fields slow down the diffusion enough to bring the annihilation rate below the rate given by Equation (XV.A-1) (Puget, 1971).

In conclusion, we shall make the hypothesis that clusters and groups of galaxies are of matter only or antimatter only; this gives us the present value of  $L$ :

$$L_0 = 2.5 \times 10^{25} \text{ cm}$$

Considering that for low  $z$ ,  $L$  is changing only with the expansion of the universe because, for coalescence to take place, the fluid motions must be such that

$$V_f > V_{\text{exp}} = \frac{L}{t} = 4 \times 10^7 (1+z)^{3/2}$$

$V_{\text{exp}}$  is shown in Figure XV.A-2 from which it is clear that no significant coalescence can take place for  $z < 200$  because the expansion velocity is then much larger than the maximum fluid velocity which we can expect.

We shall use  $L = L_0 (1+z)^{-1}$  up to  $(1+z) \sim 200$  and  $L = 5 \times 10^{29} (1+z)^{-17/6}$  for  $1+z > 200$ . (We must nevertheless keep in mind that this last relation has not been fully justified for  $200 < (1+z) < 600$  when the regions far from any boundary are neutral.)

### ANNIHILATION RATE FOR $(1+z) < 100$

There is some observational evidence that cluster formation occurs at rather low red shifts. In our picture, the depression of density on boundary regions becomes deeper and larger and eventually gravity overcomes expansion and bound clusters are formed. We shall neglect this process here because other processes like ionizing radiation from quasars or young galaxies for  $z < 3$  also modify the picture.

Let us study the motion of the plasma. For that purpose we need to find how the anisotropy and the temperature gradient affect the motion of the plasma. Physically, due to the importance of Thomson collisions of the electrons of the plasma with blackbody photons and with the X-rays and  $\gamma$ -rays produced in annihilation, we examine the motion of the plasma on

each side of the annihilation layer at distances much smaller than the mean-free path of thermal photons. Technically, we write the Boltzman equation for the photons and integrate it to get the equations of momentum conservation and energy conservation, to which we add the equations of motion of the plasma. These three equations have four unknown quantities: the temperature gradient, the anisotropy of the photon distribution, the velocity, and the density of the plasma. We can eliminate the first two in order to get an equation of motion of the plasma which has to be combined with the continuity equation,

$$\frac{d}{dt}nv + NV(1 - \xi) \frac{c}{\lambda_0} e^{-u} - v_s^2 \frac{\partial n}{\partial x} - \frac{nv}{\tau_D} - \int_x^L \frac{NV}{L\tau_0} \frac{n - n_0}{n_0} dx = 0 \quad (\text{XV.A-2})$$

where  $v$  is the plasma velocity,  $n$  the plasma density,

$$n_0 = \langle n \rangle, N = n(x=0), V = v(x=0), u = \int_0^x \frac{n}{\lambda} dx, \tau_D = \tau_0 k^{-1} = \frac{\lambda_0}{c} k^{-1},$$

$\xi$  is the fraction of the momentum of the X-rays which is transmitted to the blackbody photons,  $v_s$  is the thermal velocity of the plasma, and

$$k = \frac{\rho_{\text{radiation}}}{\rho_{\text{matter}}}$$

During the radiative period, the second, third, and fifth terms of this equation of motion of the plasma are negligible for distances smaller than, or of the order of

$$\mathcal{L} = \sqrt{2\tau_D v_s^2 t}$$

which is the distance over which the density gradient extends. ( $\tau_D$  is the characteristic time for slowing down of charged particles by the radiation field.) The equation is then a simple diffusion equation and the solution for  $n$  is:

$$n(x, t) = \frac{n_0}{\sqrt{4\pi\tau_D v_s^2 t}} \int_0^\infty e^{-\frac{(x-y)^2}{4\tau_D v_s^2 t}} dy$$

and

$$NV = (n v)_{z=0} = \frac{n_0 v_s (\tau_D)}{2\sqrt{\pi} t}^{1/2}$$

$n(x)$  and  $v(x)$  are plotted on Figure XV.A-4.

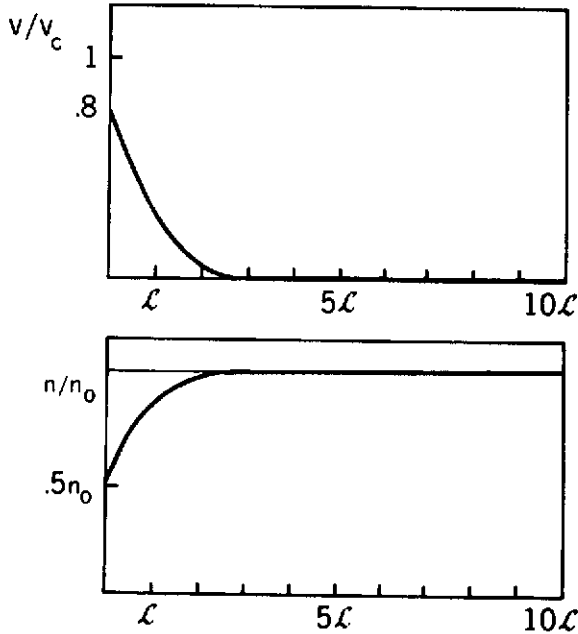


Figure XV.A-4. The density and velocity of the plasma given as a function of the distance from the boundary. The unit for the  $v$  scale is  $v_c = v_s (\tau_D/\pi t)^{1/2}$

The annihilation rate is then given by

$$\Psi_v = \frac{3 (n v)_{x=0}}{L} = 7.3 \times 10^{-29} (1+z)^{61/12}$$

The fifth term of Equation (XV.A-2) corresponds to the anisotropy of the photon field inducing a heat flow which dissipates the excess energy left by X-rays and  $\gamma$ -rays in the regions where  $n$  is larger than the average density ( $n_0$ ). For  $x \gg L$ , it is the dominant term for the motion of the plasma, but it does not affect the annihilation rate in a noticeable way.

When  $(1+z)$  becomes lower than  $1.4 \times 10^3$ , the third term in Equation (XV.A-2) which is the flux of momentum from X-rays to the plasma, becomes as large as the fourth term which is the pressure gradient of the plasma. The annihilation rate then is given by

$$\Psi_v = \frac{3}{L} n_0 v_s \left( \frac{\tau_D}{t} \right)^{1/2} \frac{e^{-A^2}}{2\sqrt{\pi}} \left[ \frac{3}{8k} (1 - \text{Erf } A) + 1 \right]^{-1}$$

with

$$A = \left[ \int_0^t \tau_D \frac{NV}{n_0} \frac{1}{\lambda_0} (1 - \xi) dt' \right] (4 \tau_D v_s^2 t)^{-1/2}$$

where

$$\text{Erf}(x) = \frac{2}{\sqrt{\pi}} \int_0^x e^{-u^2} du.$$

(Aldrovandi et al., 1973 preprint)

For  $\xi$  small enough to be negligible compared to 1,  $A$  is in fact almost a constant  $\cong 4.2$

and

$$\frac{NV}{n_0 v_s} = \frac{4k}{3\sqrt{\pi}} \left( \frac{\tau_D}{t} \right)^{1/2} e^{-A^2}$$

Thus,

$$\Psi_v = 1.7 \times 10^{-32} (1+z)^{73/12}$$

This solution is valid down to  $(1+z) \sim 600$ . Below that value it breaks down for two reasons having opposite effects:

- $L$  might increase more slowly than  $(1+z)^{-17/6}$  due to recombination;
- The mean-free path of the X-rays produced by the annihilation-generated electrons and positrons, which was equal to  $\lambda$ , becomes much shorter due to the large photoionization cross-section as shown on Figure XV.A-1.

The equation of motion of the plasma in the vicinity of the boundary remains the same because of the ionization due to X-rays (see Figure XV.A-3)\* but the momentum left in the plasma per unit time and unit volume is now proportional to  $\lambda_x^{-1}$  instead of  $\lambda_0^{-1}$ . ( $\lambda_x$  is taken equal to the distance from the boundary for which  $n_p/n_H = 1$ .) Figure XV.A-4 shows the density and velocity of the plasma as a function of distance from the boundary in units of  $v_c = v_s (\tau_D/\pi t)^{1/2}$ .

The equation giving the annihilation rate has to be solved numerically. The result is shown in Figure XV.A-5\*, which gives the annihilation rate as a function of red shift compared with the rate given by Equation (XV.A-1).

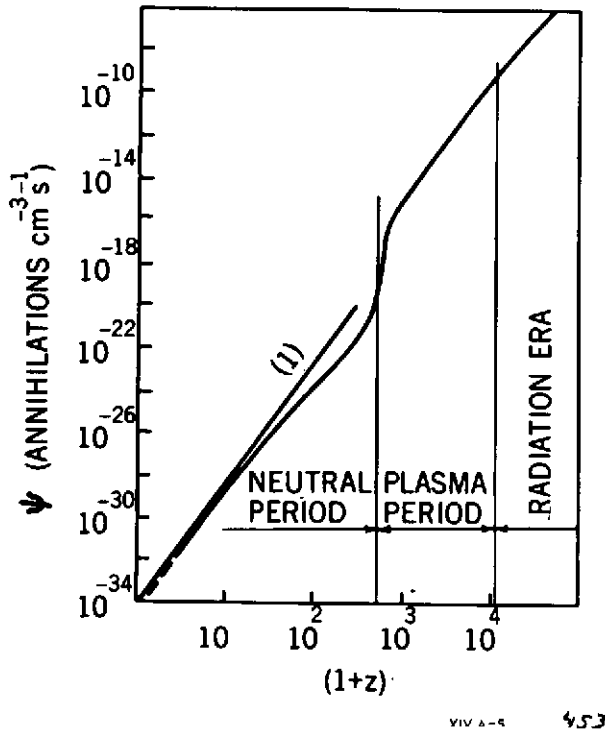


Figure XV.A-5. The annihilation rate is given as function of red shift.

Considering the uncertainties in these calculations, the agreement is as good as can be expected. The major uncertainties affect the rate for the range  $(1+z) \leq 5$  and cannot affect the  $\gamma$ -ray spectrum between 1 and 15 MeV

\*The results given on Figures XV.A-3 and XV.A-5 are from preliminary numerical evaluations; exact numerical computations will be published later.

very much. Furthermore, the  $\gamma$ -ray flux must fall off for energies above 70 MeV and below 1 MeV, so the theoretical spectrum is quite well defined. If the good agreement of this spectrum with the data is confirmed by future measurements, a way of checking this model will be to look at angular fluctuation of the background as a function of energy. The  $\gamma$ -rays observed at the energy  $E_\gamma$  come mostly from a red shift  $(1+z) \sim 70/E_{\gamma(\text{MeV})}$  and the angular fluctuations will be related to  $L(1+z)$ .

## REFERENCES

- Ozernoy, L. M., G. V. Chibisov, 1970, *Astr. Zh.*, **47**, p. 749 (English translation in *Soviet Astro. A. J.*, **14**, p. 915.
- Ozernoy, L. M., 1971, *Astrophys. J. Letters*, **7**, p. L201.
- Puget, J. L., 1971, *Nature*, **230**, p. 173.
- Stecker, F. W., D. Morgan, and J. Bredekamp, 1971, *Phys. Rev. Letters*, **27**, p. L1469.
- Stecker, F. W., and J. L. Puget, 1972, *Astrophys. J.*, **178**, p. 57.
- Steigman, G., 1969, *Nature*, **224**, p. 477.
- Steigman, G., and P. A. Strittmatter, 1971, *Astron. and Astrophys.*, **11**, p. 279.

**B. DISTORTION OF THE MICROWAVE BLACK-  
BODY BACKGROUND RADIATION IMPLIED  
BY THE BARYON-SYMMETRIC COSMOL-  
OGY OF OMNES AND THE GALAXY  
FORMATION THEORY OF  
STECKER AND PUGET**

F. W. Stecker\*

*Goddard Space Flight Center*

J. L. Puget

*Observatoire de Paris*

One consequence of the baryon-symmetric cosmological model of Omnès is the continuing annihilation of matter and antimatter throughout all stages in the evolution of the universe. This annihilation can cause a distortion in the microwave blackbody spectrum from a purely thermal spectrum because of deposition of annihilation energy at red shifts less than  $10^4$  and particularly at red shifts less than  $10^3$ . The theory of this distortion was first discussed by Zel'dovich and Sunyaev (1969; see also Sunyaev and Zel'dovich 1970a, 1970b). They show that because of the varying evolution of the optical depth of the universe to radiation at various wavelengths and because the Compton process conserves photon number and does not lead to pure thermalization, two different distortions arise in the blackbody spectrum. Distortions in the Rayleigh-Jeans ( $\propto \nu^2$ ) portion of the spectrum are due to energy deposition at red shifts between  $10^4$  and  $10^3$  (Zel'dovich, Illarionov, and Sunyaev, 1972). Distortions in the Wien portion of the spectrum ( $\propto e^{-\nu}$ ) are due to energy deposition at lower red shifts after the cosmic gas cools to its atomic state and thermalization does not take place as efficiently.

In order to quantitatively estimate the expected distortions, we define the parameter

---

\*Speaker.

$$q \equiv \int \frac{\Delta \epsilon(t)}{\epsilon(t)} dt \quad (\text{XV.B-1})$$

which is a measure of the maximum fraction of the energy density in the radiation that contributes to the nonthermal part of the microwave background.

In Equation (XV.B-1),  $\epsilon(t)$  is the energy density in the blackbody radiation as a function of time (or red shift  $z$ , where  $t = t(z)$ ).

It then follows that

$$q \cong \int dz \frac{\Psi_v(z) M_p c^2}{\epsilon(z)} \frac{dt}{dz} \quad (\text{XV.B-2})$$

where  $\Psi_v(z)$  is the annihilation rate function discussed in the main paper by Puget (Chapter XV.A).

For the red shift range  $600 < z < 10^4$ , the annihilation rate is given by

$$\Psi_v(z) = 1.7 \times 10^{-32} (1+z)^{6+1/12} \text{ cm}^{-3} \text{ s}^{-1} \quad (\text{XV.B-3})$$

(see Puget, Chapter XV.A). The resulting value of  $q_{\text{R-J}}$  affecting the Rayleigh-Jeans part of the spectrum is then

$$q_{\text{R-J}} \cong 1.2 \times 10^{-2} \quad (\text{XV.B-4})$$

which is, in fact, an upper limit because part of the energy goes into large-scale fluid motions. The corresponding distortion in the Rayleigh-Jeans part of the blackbody spectrum is of the order of 2 percent, well below the observational uncertainties of about 20 percent in the wavelength region greater than 1 cm.

For the red shift range  $z < 600$ , we will adopt the annihilation rate fitting the  $\gamma$ -ray observations (that is, the largest value consistent with the present observations (see Puget, Chapter XV.A)).

$$\Psi_v(z) \cong 10^{-34} (1+z)^{6.25} \text{ cm}^{-3} \text{ s}^{-1} \quad (\text{XV.B-5})$$

The resulting value of  $q$  affecting the Wien part of the blackbody spectrum is

$$q_w \cong 6 \times 10^{-5} \quad (\text{XV.B-6})$$

This may be related to the parameter  $y$  used in the calculations of Zel'dovich and Sunyaev, since

$$y = q/4 \cong 1.5 \times 10^{-5} \quad (\text{XV.B-7})$$

This is well below the observational upper limit on  $y$  set by Zel'dovich and Sunyaev of 0.15.

In fact, we expect more distortion than indicated by Equation (XV.B-7) because of dissipation of turbulence created at higher red shifts which feeds energy into the microwave background below  $z = 600$ . To estimate this effect, we have made a more detailed numerical calculation of the mean gas temperature as a function of red shift (Stecker, Puget, and Bredekamp, in preparation) and used the relation given by Zel'dovich and Sunyaev

$$y_T \cong n_o \sigma_o c H_o^{-1} \int dz \frac{kT_{e2}}{m_e c} (1+z)^{1/2} \quad (\text{XV.B-8})$$

where  $n_o$  is the present mean gas density in the universe, taken to be  $3 \times 10^{-6} \text{ cm}^{-3}$ ,  $\sigma_o$  is the Thomson cross section, and  $H_o$  is the Hubble constant where  $H_o^{-1} \cong 6 \times 10^{17} \text{ s}$ . We then obtain from Equation (XV.B-8) a value of

$$y_T \cong 2 \times 10^{-4} \ll 0.15 \quad (\text{XV.B-9})$$

Sunyaev and Zel'dovich discussed the problem of blackbody distortion due to antimatter annihilation, but they estimated the annihilation rate without taking account of limitations due to annihilation pressure on the boundary regions between matter and antimatter. They therefore overestimated the annihilation rate by a large factor (see Stecker and Puget, 1972).

Our conclusion is that the annihilation rate for our model of galaxy formation (Stecker and Puget, 1972), while large enough to provide the turbulence needed to explain galaxy formation (Stecker and Puget, 1972; Aldrovandi, Caser, Omnès, and Puget, preprint), does not produce a distortion in conflict with present observations of the microwave blackbody radiation.

## REFERENCES

- Aldrovandi, R., S. Caser, R. Omnès, and J. L. Puget, (Preprint LPTHE 73/5, to be published).  
 Stecker, F. W., and J. L. Puget, 1972, *Astrophys. J.*, **178**, p. 57.

Sunyaev, R. A., and Ya. B. Zel'dovich, 1970a, *Astrophys. and Space Sci.*, **7**, p. 3.

—————, 1970b, *Astrophys. and Space Sci.*, **9**, p. 368.

Zel'dovich, Ya. B., A. F. Illarioniv, and R. A. Sunyaev, 1972, *Zh. Eksp. Teor. Fiz.*, **62**, p. 1217.

Zel'dovich, Ya. B., and R. A. Sunyaev, 1969, *Astrophys. and Space Sci.*, **4**, p. 301.

**SECTION 4**  
**FUTURE DIRECTIONS**  
**IN GAMMA-RAY ASTRONOMY**

**A. A PANEL DISCUSSION ON  
THE FUTURE DIRECTION OF  
GAMMA-RAY ASTRONOMY \***

**Giovanni Fazio**

*Harvard and Smithsonian Astrophysical Observatories*

**Carl Fichtel**

*Goddard Space Flight Center*

**Glenn Frye**

*Case Western Reserve*

**Kenneth Greisen**

*Cornell*

**Albert Metzger**

*Jet Propulsion Laboratory*

**Evry Schatzman**

*Paris Observatory*

**Floyd Stecker**

*Goddard Space Flight Center*

**Jacob Trombka**

*Goddard Space Flight Center*

*The following discussion was convened at the final session of the NASA International Symposium and Workshop on Gamma-Ray Astrophysics to sum up the present status of the field and discuss its future. The remarks below are based on a transcript of this discussion. They are free and informal. Because extensive editorial work was necessary, the editors apologize for any misinterpretation of remarks that may be present.*

---

\*The panel consisted of the following members.

*FICHTEL:*

One thing that has impressed me is that, indeed, we do now have an observational science. I think we were in an awkward position a few years ago when there was really very little to talk about. I think we now not only have actual results that are coming forward from many different areas, but also see that there is a tremendous wealth of data that should be forthcoming in the near future. I am not going to give a speech, so I am going to stop in just a moment, but I will say I do think there can be a tremendous interaction between experimenters. I know Klaus Pinkau's group and ours always talk in terms of trying to exchange information very quickly so we can use this to feedback and look at things. And I certainly am willing to try to work with the people doing balloon experiments.

I know, for example, there is tremendous interest in very high energy region of about a GeV, and we will work with Ken Greisen on research in this region. We have a very great stimulus now, we will see the field expand, although perhaps not quite so rapidly as X-ray astronomy, but certainly very rapidly. And now I think the theoreticians deserve a chance.

*FAZIO:*

I would like to say a few words about the importance of getting the SAS (Small Astronomy Satellite) results. I think a good part of the future of  $\gamma$ -ray astronomy depends on what comes out of this satellite. That is, whether it becomes a growing, ever more fruitful area or whether it just dies greatly depends on what is produced. So I would like to make a call to get out the data as quickly as possible since many of the balloon groups are very dependent on it for their future planning.

*FICHTEL:*

Needless to say, we are working very—extremely—hard (with the SAS data). I am certainly willing to cooperate on an informal basis to let people know our tentative results, if they want to take their chances on tentative results.

*FAZIO:*

I realize, just as anybody in this field does, the complications of trying to add up data over several weeks. Indeed most of the time it is very, very difficult.

*FICHTEL:*

That kind of thing is possible; however, it is difficult to run the sensitivity programs. They take a while. So for example, we may know something is there but be reluctant for a while to say what it is.

FAZIO:

Yes, I fully agree.

SCHATZMAN:

I think that generally speaking, the theoreticians are very eager to see the improvements in  $\gamma$ -ray astronomy, and by this I mean an extension of the range of energies which are covered by the observations, particularly toward higher energies. Also important is increasing the resolving power and precision and maybe increasing the energy resolutions.

A couple of years ago I became interested in  $\gamma$ -rays produced in supernova explosions (a subject discussed by Clayton).<sup>\*</sup> If there were the production of elements, spallation products of these atoms would be  $\gamma$ -radioactive and quite a few of them would decay with a short radioactive period of the order of seconds or days. Thus we have to consider the possibility of detecting a  $\gamma$ -ray flash at the time of an explosion. This can be considered as feasible if the next supernova does not explode too far away from us. If I remember the numbers properly, if an explosion takes place at a distance of less than 10 megaparsecs, we should have the sensitivity to detect the flash, assuming that the proper instrumentation is in space at the time of the outburst and that it looks in the proper direction. But the trouble is that at the time the explosion becomes visible, it is likely that most of the radioactive elements will have already decayed because the time between the beginning of the bursts and the observation of maximum light can be several days. So at least in the case of a supernova of Type I, which is one with a slow maximum, it is likely that by the time it is optically visible, the  $\gamma$ -ray flash has disappeared.

But on the other hand, as far as nucleosynthesis is concerned, the issue can be extremely important because presently the amount of nucleosynthesis which takes place in supernovae is a matter of speculation. If we look for the  $\gamma$ -rays coming from radioactive products produced by nucleosynthesis, they could be observable.

TROMBKA:

Along these lines, maybe I am going to put some people on the spot. I think one of the major developments that have to come about is the development of solid-state detectors of high enough detection efficiencies in order to see the line fluxes. We heard some reports on what is going on. Could we ask for a little further information? What seems to be the direction of the Lockheed group? What is going on in terms of the development of larger detectors and

---

<sup>\*</sup>See Chapter XI.A.

the development of intrinsic detectors so that the mechanical problems involved in flying these detectors will be easier?

*NAKANO:*

Intrinsic germanium is the way to go, as far as not having to maintain solid-state detectors at cryogenic temperatures. But right now the intrinsic-germanium detectors are not nearly as large as the drifted detectors. What is needed is more detector sensitivity and some way to gang these detectors together, something very similar to what Bud Jacobson of Jet Propulsion Laboratory is doing. I would say, if one really wants the biggest sensitive area one can get, that would mean using drifted detectors, at least for now. But they are making strides on the intrinsic detectors. The biggest one that I know of is a cylindrical detector of about  $30 \text{ cm}^3$ , but perhaps in a year or two they will catch up in development to the other detectors.

*FAZIO:*

Is there a supernova burst mode in SAS-2?

*FICHTEL:*

Yes. The problem is a little different. I assume when you (Schatzman) spoke of a flash of  $\gamma$ -rays, you meant nuclear lines. There is an interesting concept suggested by Colgate that if the hydromagnetic shock-wave model is indeed correct, there will be a photon pulse of very high energy  $\gamma$ -rays that will come out which is very, very short—a tiny fraction of a second. We looked at some of the experimental ways you might detect such an event. It turns out with the atmospheric fluorescence experiments and the mode we suggested for SAS originally, there is not much chance for detection of this flash. But if you go to somewhat lower energies, I think there is a real chance to detect these flashes, because you can possibly see at least ten times as far as the Virgo cluster. You then have a reasonable chance to see such an event.

Bob Hartman and Mike Sommer came up with an interesting concept where you have very large scintillators which can detect several pulses in a very short time with very fast time resolution. This will in fact be on a balloon flight that will be launched from Palestine, Texas, in the near future. This would be another very interesting phenomenon for someone to look for in the flash phase because this kind of flash is uniquely associated, as Colgate has shown, with the cosmic-ray hydromagnetic origin theory. If you don't see one of these flashes, then Colgate can't be right.

*GREISEN:*

The thing that I have been impressed with at this meeting is that despite fears in the past that the cosmic  $\gamma$ -rays, like the cosmic rays themselves, might be almost a featureless waste (a continuum) that one could not extract precise knowledge from because of the lack of detailed features, it seems not to be so. There seems to be an abundance of features and any single mechanism for production of the  $\gamma$ -rays does not seem to be able to account for the whole energy range. There seem to be a number of bumps that add up to produce what in the first approximation is only a smooth spectrum, but on closer examination has structure. That has also reinforced the dictum of the Astronomical Society, which they have been insisting on over the years, that it really is important to investigate the full range of the electromagnetic spectrum. The results observed, even in opposite extremes of the spectrum, tend to be coupled through theoretical models very tightly with each other and impose constraints on each other.

I think that in spite of the fact that each of us experimenters has a special interest, and has to have one (one has an obligation to push for development of opportunities for his particular little area), we should all remember the importance of uniting as a group to support this multispectral concept. While the great value of this has been shown, in particular in close looks at the low-energy  $\gamma$ -rays, particular questions were also raised and fascinating hints were shown in the data at lower energies that suggest it is also important to look at the higher energy  $\gamma$ -rays, not only at the discrete sources, but also at the continuum.

If, for instance, a substantial part of the radiation around 100 MeV comes from annihilation processes, we know that that spectrum peaks at around 100 MeV and cuts off sharply beyond that, as mentioned by Floyd Stecker earlier (see Chapter IX.A). If cosmological origin is important, it was made clear that one can predict other features that should show up as distortions of this spectrum.

Well, I have a feeling that we are almost marking sort of a birthday of  $\gamma$ -ray astronomy. It is true it is not exactly the birthday today. There was a satellite launched a little while ago, the SAS-2. There have been some forward steps by means of balloons, but really the planned shuttle program should open up a new era. I don't think this can be over-emphasized because one has to put the emphasis on the word "should." It is by no means obvious that it will open a new area, because the whole program might be spent in nonscientific enterprises, but there is a possibility that we really could have many scientific opportunities as long as money is provided for performing experiments.

The whole shuttle program will only be justified if there are many missions and each mission should carry something worthwhile. And the worthwhile things

to get out in space are the things that will see parts of the universe that can't be seen from the ground or to do experiments that you couldn't do down here.

I think that high-energy astrophysics, ultra-violet, X-ray or  $\gamma$ -ray astronomy, is not the only important thing to do on the shuttle, but it's one of the most important. So I hope we gain opportunities in the near future to make this whole subject achieve a real stature and not remain forever in an infant stage, where it is now.

*STECKER:*

As a theoretical type, I would like to second your remarks about the bumps and distortions in the continuum spectrum. It is the bumps and wiggles that keep us in business. In this regard, I think one of the theoretical emphases would be on getting better energy resolution at all energy ranges so we can see and study the bumps and wiggles, particularly in regard to what they say about the cosmological origin of the diffuse background.

This wasn't brought out, but if those  $\gamma$ -rays are cosmological, then there may be another absorption effect at around 10-GeV energy.\* We haven't done too much with that energy range yet, but I hope we will keep extending ourselves up into that energy range, and also I hope that some of these theoretical points that are brought out from time to time by people like us will be noticed by experimentalists, to the extent that it might help direct the investigations. As an example of this, I can cite the Apollo-15, -16 and -17 results that were reported on.

In that detector experiment the primary purpose was to gather information about lunar  $\gamma$ -rays and the detector did an excellent job, but the detector was also kept on in transearth orbit to look at the cosmic background in a theoretically critical energy range and we found some very surprising features which may have exciting implications, which we heard about from Professors Omnès, Schatzman, and Puget.

*FRYE:*

I would like to address my remarks a little more particularly to the time-gap between SAS-2 and the shuttle program. And this naturally is when balloon observations must be done from the top of the atmosphere. With many of us interested in this energy region and this type of observation, I think it is a worry to all of us that there is going to be an observational hiatus when the SAS-2 experiment is over. I am assuming that it will operate for one or two years.

---

\*See Fazio and Stecker, *Nature*, **226**, 135 (1970).

I would like to make a couple of comments about the balloon technique—what one might be able to do in this period until the shuttle is operational.

One point is that in the very interesting region from 10 to 30 or 40 MeV, with regard to the diffuse measurements, the flux that is reported for these measurements is as large as the atmospheric background if you are at the order of  $1 \text{ g/cm}^2$ . So there is not as strong an argument for being on a satellite in this energy region as one has for other energy intervals. One still has the very long observation time from the satellite, but any experiment that looks at the Crab in this region at the very minimum is going to have to contend with this background.

Therefore, one avenue that I think people should look at, and really take a long look at, is trying to build larger-area detectors. With a large collecting area you have better statistics per unit time. To take advantage of the advances in balloon technology, either higher altitude or super-pressure balloons have potentiality for many days of observation. Also, with respect to the Crab in particular, one does need the very accurate sub-millisecond timing, so that until again something of either the HEAO (High Energy Astronomy Observatory) or shuttle capability comes along, these observations are going to have to be made from balloons.

#### GREISEN:

I would like to ask a question. It is obvious down in the energy range related to the HEAO  $\gamma$ -ray apparatus experiment utilizing solid-state detectors where one is looking for particular energy transitions, that one really needs very fine energy resolution. But in your (Stecker) statement calling for better energy resolutions at higher energies, I know we need better ones because there is essentially none there now. But I have the feeling that all the models that were proposed failed to produce any very sharp features. The bumps were broad bumps and so on. And I think it would be somewhat misleading if it got to be stated as a requirement for these experiments that there be fine energy resolution. Do you see any real need for energy resolution better than something like a factor of two, or say 50 percent at energies above 30 MeV?

#### STECKER:

It is true that above 30 MeV you probably expect broad features, but we have seen several sets of theoretical curves, and the curves have different curvatures. And one would like, from the theoretical point of view and this is of course somewhat academic, to determine as exactly as possible a good spectral shape because, as was brought out in this conference, log-log spectra aren't always straight lines. The shape of the spectrum can then become very important in distinguishing one theoretical model as opposed to another, even when you don't have a sharp feature.

*GREISEN:*

Yes, but you don't need to have very good determination of the energy for each event in order to derive the shape if you study and understand your instrumental response.

*FRYE:*

Certainly, if I could interject, within the  $\pi^0$ -region of 100 MeV or so, one would like at least 20-percent resolution to see if there is any feature that one can ascribe to that.

*FICHTEL:*

I would like to completely support Floyd (Stecker), because I think we are finding even now that if you are going to really measure a spectral fall-off, for example, you really need something more like 10- or 20-percent energy resolution rather than a factor of two if you are going to see a sharp fall-off and see at what energy it occurs. So I think that argument is certainly true. You are really going to have to do what Floyd (Stecker) wants.

*STEIGMAN:*

Another way to get the shape of the spectrum is not necessarily to have very good resolution in any particular energy, but to extend the energy range over which you can observe. Is it harder to extend the energy range or to build better resolution detectors?

*FICHTEL:*

One of the problems in extending the energy range is a problem of sensitivity. In other words, if you can measure the energy better, you don't need so many photons, and ultimately we run out of photons at some energy.

*GREISEN:*

I think the question from the audience (Steigman) can't be answered in general. It is different with each different apparatus and every different part of the energy range. But ordinarily, the methods available for measuring energy are very difficult to make precise. If one observes the scattering of electrons in 30 plates of a spark chamber, one has a very limited sample of a random distribution, and the mean is not very accurately determined.

I think it is well enough determined for these purposes, because that dip that you are looking for is not so extremely sharp. At very, very high energies other methods start to become available for measuring energy, either based on scattering or something like transition radiation. But always it comes down to

detecting a small number of samples of a random variable. And if one really felt pushed to make a 10-percent energy resolution throughout the energy range, you might close down the whole business, Floyd, all the way.

*STECKER:*

I don't think 10 percent here is necessary.

*GREISEN:*

On the other hand, when you can use an intrinsic detector and stop a low-energy particle, then it is possible to get 2-percent resolution, or something like that.

*METZGER:*

If I could comment on the same subject, in the energy region that I was discussing in terms of the two HEAO  $\gamma$ -ray instruments, there is distinct contrast, and one doesn't get something for nothing. With solid-state detectors one gets the resolution and identifies the feature, hopefully, but at the same time, at least in terms of present technology, the efficiency of the detection is much less. So the discovery of the feature is not as well done with a solid-state detector as with the more efficient sodium-iodide system.

Of course, this means that there is a logic in flying a HEAO mapping experiment of the Peterson type utilizing NaI(Tl) detectors, first, to determine where the promising areas to look might be. Later, one can study these areas by making use of solid-state detectors with the high-resolution experiment proposed by Bud Jacobson of JPL.

*STECKER:*

I want to throw out another related question to the experimenters. On Monday we had a long discussion about problems with the intrinsic detector-produced radiation in sodium-iodide crystal detectors, particularly in the region around 1 MeV, which is important theoretically for cosmological reasons for such models as the matter-antimatter cosmology. Therefore, it would be nice from the theoretical point of view to minimize as much as possible these detector background problems. Although there were quite a few comments about past and present experiments, I would like to hear some comments about minimizing this problem in the future.

*METZGER:*

You couldn't have picked a tougher energy range.

*TROMBKA:*

Part of the minimization will be achieved after an understanding of the intrinsic radiation. You run into other problems also. What you usually want is high Z-type materials in order to stop the  $\gamma$ -radiation, to get good efficiency, and so forth. In doing so, you are hurting yourself immediately in terms of the spallation problem. I think the problem will have to be overcome by obtaining a real understanding of the cosmic-ray-induced spectrum and then seeing whether one can see keys within the spectrum itself, in order to interpret the magnitude of this effect.

*PIEPER:*

Jack, it seems to me absolutely remarkable that the four experiments that have been done in that region, the ERS, Ranger, and the two experiments on Apollo, all agree in terms of the spectra of counts/cm<sup>2</sup>·s<sup>-1</sup> in pulse-height space. All fall on top of each other with the exception of one single point, and the problem really is to translate that spectrum from pulse-height space into photon space and that is where the experiment doesn't need to be done again. What needs to be done is to learn how to interpret it.

*TROMBKA:*

I think one of the major efforts for Al (Metzger) and myself will be the study of the spallation problem in detail. To this end, we did the Apollo-17 experiment and hope to continue on Skylab with some other materials to get a better understanding of it.

Another area I think that we have to work on, partially on HEAO, is determining the isotropy of the  $\gamma$ -ray flux. Along these lines, we at Goddard are looking at the use of small satellites. It turns out, even with the spallation products building up, one can look at isotropy with rather simple techniques. I know Dr. Pieper and I are interested in this and some people from France are also interested in this. There are a number of experiments that can be done relatively simply. One can do rather meaningful experiments rather simply and hopefully inexpensively. Our idea, and hopefully some of the others will express theirs, is to use a pancake-shaped detector. If you remember from my talk, the counting efficiency of a detector is strongly dependent on angular distribution of the incident flux. By rotating a properly shaped detector in an anisotropic field, one gets a significant variation in the count rate which reflects the isotropy or anisotropy of the flux. Our calculations indicate that a crystal of about 5 cm in height by 20 cm in diameter can detect anisotropies of a little less than one percent. In order to minimize problems due to spallation and induced activity, the spacecraft can be surrounded so that the total spacecraft mass is inside of an anticoincidence mantle.

*SCHATZMAN:*

In connection with the anisotropies there is the question of the angular fluctuations in intensity. What seems critical for the antimatter cosmology is the angle of  $1/10$  of a degree, and this is a fairly small angle. I understand that presently you can expect to detect deviations over one or two degrees, but this doesn't seem to bring any important information if the cosmological model is correct. Further information could be obtained with better angular resolution.

*METZGER:*

At what minimum energy would that angular resolution be required to be useful?

*SCHATZMAN:*

It turns out, due to the fact that the angle for a given length depends on the distance due to relativity effect, that the angular fluctuation you can expect at high red shifts is constant. So from  $z \geq 2$ , let's say for example, to  $z = 100$ , it is  $1/10$  of a degree.

*MEMBER OF THE AUDIENCE:*

I just wanted to make a comment on that point. For, let's say, 50 to 70 MeV annihilation  $\gamma$ -radiation in the type of cosmological model we have discussed, the type of fluctuation we can expect is a one percent fluctuation.

*WHITE:*

May I emphasize that in the region from 1 to 10 MeV, to detect  $\gamma$ -rays one should make use of the process with the highest cross section that one has, and that of course is the Compton process. And one should make use of the material which is best for taking advantage of that cross section; therefore, one would want to go to a low  $Z$ -material rather than a high  $Z$ -material.

Secondly, in order to get rid of the background, one can do a number of things. One can, of course, make the angular resolution as good as possible. This gets rid of background problems. One can also surround the detector completely with anticoincident scintillators in order to get rid of charged-particle background. One can get rid of the backward-going  $\gamma$ -rays by being sure of the anticoincidence in backward direction. One can get rid of neutrons by using time-of-flight techniques.

So there are a number of things one can do to get rid of background. In addition, if one wants to get the total  $\gamma$ -ray energy, one can go farther than people have gone today. One can use a two-Compton scatterer, and one can

make the second scatterer so big that the total  $\gamma$ -ray energy is deposited in it and thus measure the total energy of the  $\gamma$ -ray. One then has the scattered electron in the scatterer, so one obtains the total energy of the  $\gamma$ -ray. Then one doesn't have the uncertainties that we discussed in the double-scatter experiment. One can also get very high efficiencies by making the detector very large. Therefore, in the region that you are talking about, near an MeV, I recommend two-Compton-scatter telescopes very highly.

*FRYE:*

I might add to this that if one does make the first scatter in a visual detector where you see the recoil, then you completely determine the kinematics and this produces better angular resolution than one has in a system where you just get the energy deposition. And we have such a system. I don't have any data on it yet.

*RAMATY:*

I would like to make two comments. There is another astrophysical process which leads to  $\gamma$ -ray lines which, even though not as efficient as nucleosynthesis, has an advantage that we are almost sure it is going to occur. This process is induced by accelerated charged particles on ambient nuclei.

The other thing I would like to say concerns solar flares for which Floyd Stecker said that everything is understood. It is true that the mechanism for  $\gamma$ -ray production in flares is understood, but what is important in solar flares is to get an understanding of the magnitude of the solar flare. Only for one of the flares, a big flare, were  $\gamma$ -ray lines seen. And I remind you that the flux that was seen was about  $0.1 \text{ photons cm}^{-2} \text{ s}^{-1}$ , which is much higher than the fluxes of  $10^{-5} \text{ cm}^{-2} \text{ s}^{-1}$  to be studied in future experiments. If the threshold or sensitivity for detection of  $\gamma$ -rays is going to be lower, I think one can in principle learn quite a lot about the mechanism of flares. Although in this conference the main emphasis was on galactic and extragalactic phenomena, I think that this point is worth mentioning.

*STECKER:*

I didn't mean to imply that everything was understood. I just meant the basic physical processes were understood as opposed, for example, to some of the other production processes discussed.

*RAMATY:*

I think in the case of the flares, we can take off from there and start understanding flares, because we don't really have to argue too much about the radiation process.

*STEIGMAN:*

In other parts of the electromagnetic spectrum, theoreticians are somewhat constrained by another piece of information that we have and that is polarization measurement. Is there any hope whatever to get polarization measurements in the several MeV energy range?

*FRYE:*

Well, it is possible in principle from the spark chamber where you observe the pair and measure the polarization of the pair. So, in principle, the information is there. It depends on the detector and the fluxes that you have. This is one of the things that all of us must keep in the back of our minds, but I think we are one order of magnitude away from this now, when fluxes are just being confirmed.

*FAZIO:*

You need an awful lot of photons from a known source to get enough statistics to do the polarization. Really that is what it comes down to.

*GREISEN:*

Could I comment that the angle that everyone sees so far on the pairs isn't the initial opening angle, but the angle created by the multiple Coulomb scattering, which has nothing to do with the polarization. So that one is forced to observe the pair very close to the vertex and that means really extremely close. The problem is partly one of maintaining even emulsion. It turns out, depending on what energy you are interested in, you have to invoke some length of track if you want to measure an angle of some precision, such as 100  $\mu\text{m}$  and in that length of track, already the scattering exceeds the original opening angle in some cases.

The problem is difficult and almost certainly drives one to an instrument that has low detection efficiency. That is because you have to observe the pair before it crosses much matter and so it is hard to have a high conversion efficiency. So it is a problem of counting rate. I can't overstress the importance of being able to do experiments that have enough observation time and a large enough detection area of the instrument to make possible these finer details. It seems to me something like the time I remember on top of Mount Evans, with clouds all around, and it looked as though the whole Rocky Mountains had only two peaks. There is that whole mountain range down below, but one needs have a little more vision to see it.

I think the sights should be set not on just barely being able to tell the source is there, but getting enough information about it to try to approach a kind of

question like polarization, which is one of the hardest. There are some that are easier, but still seem hard enough. But it is true that currently, in the MeV range, one of the hardest problems isn't just the counting statistics, but background problems.

However, I want to emphasize that above 50 or 100 MeV and on up, there is a lot of promise. But the action is in attaining a better sensitivity. That is of the order of  $10^{-7} \text{ cm}^{-2} \text{ s}^{-1}$ . There are a few sources which may give  $10^{-5}$ , as possibly the closest source at the best time, but to pursue this subject, we have to be able to measure down in that range and you have to do very little calculating to see what that amounts to. If you have a  $10^3 \text{ cm}^2$  detector with an efficiency of 10 percent, so it is effectively 100 cm, you will get one count in a day with that sort of source. The sort of number of counts that is needed to extract detailed information is thousands. So clearly, that is not a very promising instrument. One needs a larger instrument and long observing times.

*FAZIO:*

Again, worrying about the future of the balloon-borne aspects of the field, Glenn (Frye) commented that there would be a gap between SAS-2 and the time when the shuttle program begins. Now, at one time there was a HEAO experiment planned with a larger area spark chamber. Could I ask what is the situation on that now, Carl?

*FICHTEL:*

Yes. Very succinctly, we are essentially in the same position as the low-energy experiment of Bud Jacobson of JPL. The high-energy  $\gamma$ -ray experiment which has 10 or 20 times the sensitivity of SAS and good energy resolution is, as is Jacobson's experiment, one of the candidate experiments for HEAO-C, and a selection has not yet been made on the new mini-HEAO.

It could indeed provide, of course, a very important next step because as everyone has said in this conference, what we need to do next is get more sensitivity and energy resolution in this range and to determine really what the shuttle experiment should be—whether the shuttle experiment should, for example, concentrate on angular resolution, details of energy, or indeed, continue to an even higher-sensitivity survey. So, as with the low-energy  $\gamma$ -ray experiment, it's in limbo right now.

*FAZIO:*

To get down into the sensitivity region where you are talking about thousands of counts on a source, really requires one or two orders of magnitude better sensitivity over what we are doing right now.

*GREISEN:*

Let me describe the situation a little bit. In our recent flight where we did see the pulse from the Crab, we looked at it for a few hours and we got something like 30 events from each of the peaks. That's not very much for telling pulse structure. But if we were in a satellite environment, our background that we have to contend with would be down by two orders of magnitude and a reasonable time of observation, instead of being 3 hours, could be 300 hours; it could be increased by two orders of magnitude. There are then four orders of magnitude gained in the combination of time and background, which is two orders of magnitude anyway in signal-to-noise ratio. One could have not only good photon statistics, but the noise could be smoothed out in that time, so that one would really be able to see fine details of pulse structure, even at high energies.

I received a letter from John Bachall at Princeton, as soon as they got a preprint of our paper saying that 'that's fine for a starter, but can you measure the polarization—because for these high-energy  $\gamma$ -rays from the pulsar, the polarization would tell the mechanism of production?' It turns out that it is not unfeasible. Instead of looking for orientation of the polarization plane, there is a very nice method that is in use at Stanford and Cornell at high energies with electrons. This involves the use of graphite. At very high energies, because the recoil momentum of the nucleus when the pair production occurs is so low when the nucleus is in a crystal, pair production is strongly inhibited for some planes of polarization.

They can use that method to produce a beam that has a polarization as high as 20 or 30 percent by selective absorption, and so one could use that device too. It's very efficient, actually, for measuring polarization. It would be possible to measure the background spectrum very, very quickly around 1 GeV or 100 MeV, but it would also be possible to measure it all the way to  $10^{11}$  eV, which means well beyond the type of cutoff that Floyd Stecker was discussing. This could be done if one could have an instrument of the type that has several square meters of sensitive area and if one could be free to take data, not just for a couple of hours after a balloon launch once a year, but steadily.

*MEMBER OF THE AUDIENCE:*

I think there's one area that we may have slighted in this discussion, and it's probably been the one area in which the strongest evidence has existed for  $\gamma$ -radiation at energies above 50 MeV, namely the  $\gamma$ -radiation from the galactic plane. Now, we all know it's there, or at least we think it's there. The question is, let's say it's there and SAS has a look at it. Where is it? What fine resolution do we obtain? What do we learn about cosmic-ray densities and matter densities there? I think that is a very important subject which we are forgetting

about, so maybe we should consider questions about the angular resolution we can obtain in the future in studying the galactic plane.

*FICHTEL:*

Clearly, there should be a significant structure to the flux from the galactic plane. We already know that there is a broad distribution—I think the word “diffuse” should be avoided, because there is no implication at this point that it is only diffuse. There is clearly a hard component, as well as a soft, and it will be extremely important to find out exactly what this is. And I am fairly certain that one is going to want to have a finer angular resolution than we presently have.

In fact, I suspect that indeed SAS, as far as the plane is concerned will answer many questions. It is also going to only whet one’s appetite for a very fine angular resolution experiment of the future. Sometimes there is the conflict between sensitivity and fine angular resolution. For something as intense as the galactic plane as we now know it to be, we could indeed back off on sensitivity in order to pick up the finer angular resolution. I think indeed, this would be one of the next steps for the future.

*FRYE:*

If one is really trying to look forward to payloads that might be put on the Space Shuttle, I think it is quite obvious from the series of discussions here that there is a strong indication that in another decade there isn’t going to be any one  $\gamma$ -ray detector that will have the energy range, time resolution, capability for polarization, and so forth. It’s going to take a divergence, really, in the design of the various instruments to cover these measurements. I wish I could hope that there were going to be many shuttles and that we could design instruments that would have these capabilities. I would hope that the scientific community would be able to generate some scientific pressure and make our case with the people who will eventually decide what goes on board the shuttle.

*SHAPIRO:*

I would remind you that according to present ideas, if there are to be any shuttles, there will be many shuttles. And that means, of course, that this is not so much the question as the other one that’s already been raised: How well physicists and astrophysicists will be prepared? How well they can be prepared, as a result of adequate support in the intervening years, to take proper advantage of at least some of those many shuttle flights that are projected.

*FAZIO:*

Maury (Shapiro), you said "many." We are going to have to hope they are going to fund many.

*MEMBER OF THE AUDIENCE:*

The whole basis of having a shuttle is that you can make it "cheap" per pound if you had many. Some of us, of course, have reservations as to how many can be used scientifically, since we don't know in detail about it, or even broadly perhaps, about any of the other projected uses. We have no way of knowing whether there may be ample justification on other grounds for having many (shuttles). I should think that scientists could easily be embarrassed by the frequency of opportunities.

*GREISEN:*

It's something like the possibility of building a glorious new art museum to house art treasures and then not having any money left to buy any of the art treasures.

*METZGER:*

The shuttle has, among its capabilities, the ability to take things into orbit and then leave them there for extended periods of time. And it seems to me, that of the various modes that the shuttle offers, this is the one with the most attraction in our part of the spectrum, because, as you pointed out, time is of the essence.

*GREISEN:*

Shouldn't we propose a resolution to that effect?

*METZGER:*

But one other reason why that is a very useful way to go is that it allows several experiments to be up for a long period of time together. One has many promising experiments over this wide energy range, but simply flying them in sequence is not going to tell as much as the ability to combine them simultaneously.

*GREISEN:*

In that connection, I would like to point out that even if the shuttle experiments are semi-independent, they can work together better than some present experiments can. For instance, if the analysis of data from the SAS-2 should indicate something very interesting, and if they propose to those of us who

do, to look at it with balloon experiments, it will take us an awful long while (at least for our group—I don't know about Glenn Frye's)—to get ourselves together and be able to fly a balloon. I presume it would take a lot less time than that to reorient—that is, to point—some satellite which had instruments we were observing with all the time. Presumably within minutes the satellite could be ready to look at another object.

*FICHTEL:*

That's correct, except for the time scale. The SAS-2 magnetic tracking is rather slow and usually takes a few orbits (to reorient). Of course, if it's close by, maybe  $60^\circ$  or so, we could do it in one orbit and you are talking about hours rather than minutes. So, if anybody sees something that you think is interesting, we would be most happy to hear about it or look at it. We certainly would let you know, as we said, if we think we see something.

*MEMBER OF THE AUDIENCE:*

The panel expressed a concern about the gap between SAS-2 and HEAO. I think this point cannot be stressed enough. In particular, I am sure that some of you are very familiar with the tragic road that HEAO has gone. HEAO is by now almost a four-letter word and nothing else. The priority that the  $\gamma$ -ray experiments have on HEAO is extremely low. On the third mission, they are considered, but that's about it. And they are competing directly with cosmic-ray experiments. So, as far as HEAO is concerned, I wouldn't give one penny in that basket. I am very pessimistic.

If I can get to the shuttle for just a second. The shuttle has the capability of putting one million pounds per year in orbit, but there is no research and development money available to conduct some of these experiments. So by the time (1985 or so) you put a million pounds per year in orbit, you don't know what to put up, because you don't have any money left to do anything.

Now what surprises me is that nobody mentioned that the Europeans are working very hard on  $\gamma$ -ray experiments, which should be the logical thing in between SAS and HEAO. In fact, they are very fortunate that HEAO isn't going, or at least not going as fast as we think it should. Is there anybody here in the audience who can tell us about COS-B?

*SOMMER:*

I could tell you just about what the COS-B would be. That is why I wanted to speak, because nobody mentioned it. Well, you may have seen some things about COS-B in the literature. As you may know, it is a European collaboration between France, Germany, and Italy—

LEWIN:

And Holland.

SOMMER:

And Holland. And it is supposed to have quite a high sensitivity for sources. For example, it should be able to detect fluxes like  $10^{-7} \text{ cm}^{-2} \cdot \text{s}^{-1}$ . I am not involved with it, but I know a little bit about it. They are making some calibrations in Hamburg and up to now everything seems to be going along quite well. It's supposed to be launched in 1975, I think. So this is quite soon and it should be a good link between the SAS-2 experiment and the presumed shuttle experiment.

MEMBER OF THE AUDIENCE:

We took the COS-B payload to CERN and we investigated the background properties. The data at the moment are just being evaluated. We plan to make a balloon flight with this COS-B payload late this year. The program is to launch COS-B in February 1974.

TROMBKA:

Do we have some COS-B sensitivity data?

FAZIO:

I just happened to look up the Madrid (IAU Symposium) discussion that we had on it. You might correct me if it has been updated. I notice here that the threshold is around 30 MeV. It is a wire spark chamber with an energy calorimeter. The sensitive area is about  $576 \text{ cm}^2$ . I think it may have been about 600. The area-solid angle factor is about  $70 \text{ cm}^2 \cdot \text{sr}$ . The energy resolution will be about 50 percent at 100 MeV. The satellite will be spin-stabilized and placed in a highly eccentric orbit. This was an important thing, I thought, that was different. The main advantages of this eccentric orbit are the reduction of earth albedo and the reduction of radiation-belt effects, minimum occultation by the earth, longer observing times, and adequate ground station coverage.

MEMBER OF THE AUDIENCE:

Does it have very good time resolution for the Crab?

MEMBER OF THE AUDIENCE:

Time resolution criteria were set up at a time when one did not know that the Crab Pulsar existed, so one could not include the time resolution which enables periods to be seen of this order.

*FAZIO:*

Another experiment that we really didn't hear very much about was the TD-1, which is up now. I have some more figures on the sensitivity of the TD-1. It has a sensitive area of  $130 \text{ cm}^2$ , an area-solid angle factor of  $28 \text{ cm}^2 \cdot \text{sr}$ , and an angular resolution of about  $3^\circ$ . What is it for SAS-2?

*FICHTEL:*

SAS is about  $512 \text{ cm}^2$ .

*FAZIO:*

And COS-B is about 600, so you can see how the area is increasing.

*GREISEN:*

I wonder, Carl (Fichtel), whether you could show some rough diagram of the angular resolution for SAS-2?

*FICHTEL:*

It is roughly around  $1.7^\circ$  at 100 MeV, and it gets better at higher energies and poorer at lower energies. There are some calibration points that are not complete.

*GREISEN:*

Another question: At about what energy does it cease to be possible to get an energy measurement by observing the scatter?

*FICHTEL:*

It just doesn't fade away. It is about 25 percent at the heart of the energy range from 50 to 70 MeV. By the time you get up to 150 MeV, you are down to possibly the factor of two energy resolution you mentioned.

*TROMBKA:*

Time does not permit us to continue the discussion. I would like to thank all the panel members, the participating panelists, and all of the speakers this week. To me it has been an extremely exhilarating symposium.

We thank you.

**LIST OF AUTHORS**

- Adcock, C., 316  
Adler, I., 42, 43, 50  
Albats, P., 116, 118, 121, 135, 136  
Aldrovandi, R., 336, 337, 340, 342,  
343, 345, 356, 369, 383  
Allcock, M. C., 319  
Allen, C. W., 304  
Alpher, R. A., 335  
Aly, J. J., 346  
Anand, K. C., 200  
Andouze, J., 299  
Andrews, D., 316  
Arnett, W. D., 264-266  
Arnold, J. R., 41, 279  
Arons, J. R., 55, 237, 240, 242
- Babcock, H. W., 331  
Bachall, J., 401  
Backenstoss, G., 336  
Badhwar, G., 123  
Ball, J. S., 336  
Bardeen, J. M., 342  
Barkas, W. H., 354  
Becklin, E. E., 295  
Berger, M. J., 47, 78  
Bethe, H. A., 335  
Beuermann, K. P., 128  
Bisnovatyi-Kogan, G. S., 342  
Bleeker, J. A. M., 24, 28  
Blumenthal, G. R., 189  
Bodansky, D., 264  
Bok, B. J., 252  
Boldt, E. A., 21  
Bonometto, S. A., 319  
Borner, G., 295
- Bosia, G., 153  
Bostrom, C. O., 309  
Bowyer, C. S., 191  
Braddy, D., 284  
Bratolyubova-Tsulukidze, L. I., 123  
Brecher, K., 55, 188, 190, 240, 241,  
250  
Bredekamp, J., 151, 196, 368, 383  
Brini, D., 37  
Broadbent, S. R., 338  
Brown, R. H., 157  
Brown, R. T., 10, 11, 270, 272  
Browning, R., 109, 112, 113  
Bruzek, A., 331  
Bryan, R. A., 336  
Buffington, A., 362  
Bunner, A., 3-9  
Burbidge, E. M., 342, 343, 347  
Burbidge, G. R., 194, 250, 342, 347
- Cameron, A. G. W., 268, 283, 298  
Caser, S., 336, 337, 340, 356, 383  
Cavallo, G., 213, 214, 216-218,  
250, 251, 256, 260  
Chan, J., 284  
Cheng, C. C., 297  
Chibisov, G. V., 341  
Chudakov, A. E., 153  
Chupp, E. L., 57, 165, 297, 308,  
311, 332  
Cisneros, A., 336  
Clark, G. W., 40, 103, 123, 147, 197,  
202, 213, 250, 253, 256, 259,  
343, 346  
Clark, T. A., 319

- Clayton, D. D., 55, 71, 102, 139, 140, 211, 263-266, 269-271, 273, 274, 276, 277, 280, 285, 287, 295, 365, 389
- Cline, T. L., 57, 175, 329, 330
- Cohen, J. M., 295
- Colgate, S. A., 140, 265, 329, 390
- Comstock, G. M., 218, 219
- Cowsik, R., 29, 185, 188, 190, 192, 194, 197, 202, 203, 207-210, 212, 233, 240, 241, 246, 256, 257
- Craddock, W., 266, 269, 274
- Craig, H., 356
- Cunningham, C., 21
- Cusimano, F. J., 155
- Dahlbacka, G. H., 107, 108, 112, 113
- Dallaporta, N., 341, 371
- Damle, S. V., 55, 192, 232
- Daniel, R. R., 128, 207
- Davidson, A., 3, 4, 5, 6, 8, 9
- Deerenberg, A. J. M., 24, 28
- de Freitas Pacheco, J. A., 259
- de Gennes, P. G., 338
- Dend, W., 346
- Derdeyn, S. M., 142
- Desai, V. D., 175, 329
- Deutsch, M., 291
- Dilworth, C., 213, 216, 217
- Dirac, P. A. M., 291
- Ducros, G., 21
- Duggal, S. P., 170
- Dumas, A., 28
- Dunphy, P., 173
- Dyer, C. S., 26, 27, 48, 49, 53, 61, 83, 90, 91-93, 123
- Ekspong, A. G., 343
- Eldridge, J. S., 50
- Engel, A. R., 26
- Evenson, P., 362
- Fanselow, J. L., 295
- Fazio, G. G., 103, 133, 153, 159, 212, 213, 216, 217, 237, 240, 250, 387-389, 390, 392, 399, 400, 403, 405, 406
- Felten, J. E., 3, 185, 212, 240
- Fichtel, C. E., 105-108, 111, 128, 139, 146, 147, 213, 250, 253, 257, 259, 387-390, 394, 400, 402, 404, 406
- Field, G. B., 3, 9, 11, 12, 31, 34, 194
- Fishman, G. J., 48, 49, 53, 61, 62, 64, 68, 83, 90, 91, 94, 97, 123, 265, 285, 287, 295
- Fisk, L. A., 284, 288
- Follin, J. W., 335
- Fomin, V. P., 158
- Forrest, D. J., 71, 92, 165
- Fowler, W. A., 264, 266, 284, 286, 342, 357, 365
- Frost, K. J., 180, 329
- Frye, G. M., Jr., 105, 107, 111, 113, 116, 122, 123, 159, 162, 231, 387, 392, 394, 398-400, 402, 404
- Fuligni, F., 37
- Gal'per, A. M., 103
- Gamow, G., 151, 335
- Garmire, G. P., 4, 8, 103, 114, 123, 197, 250, 253
- Geiss, J., 356
- Giacconi, R., 31, 191, 193
- Ginzburg, V. L., 139, 212, 213, 249, 250, 252-257
- Gold, T., 194, 343
- Golden, 362
- Goldhaber, M., 335
- Goldman, D. T., 64
- Goldsmith, D. W., 213, 217-221
- Goldstein, H., 64
- Goldstein, M. L., 284, 288
- Golenetskii, S. V., 55, 61, 128, 135, 150, 192, 234, 235
- Gordon, I. M., 312

- Gorenstein, P., 8, 21, 28, 29  
Gould, R. J., 10, 11, 159, 189, 194,  
212-214, 216-218, 240, 250, 251,  
256, 260, 319  
Grader, R., 5  
Green, J., 291  
Greisen, K., 316, 387-388, 391, 393-  
395, 399, 401, 403, 406  
Grindlay, J. E., 155-157, 159-162  
Gursky, H., 15, 191, 364, 365  
Guthrie, P., 295
- Hainebach, K., 265  
Hammersley, J. M., 338  
Harnden, F. R., 57, 287, 294  
Harrison, E. R., 151, 337  
Hartman, R. C., 139, 295, 390  
Hayakawa, S., 6, 8, 187, 189, 213  
Haymes, R. C., 57, 287, 294, 295  
Hearn, D., 116  
Heitler, W., 212  
Helmken, H. F., 109, 111, 120, 160  
Henry, R. C., 9, 11, 12, 21  
Herman, R. C., 335  
Higbie, P. R., 165  
Hildebrand, R. H., 295  
Hill, F. W., 17  
Hillas, A. M., 315  
Hoffman, J. A., 109, 111, 120, 159,  
161  
Hones, E. W., 57  
Horine, E., 162  
Horstman, H., 23, 28, 37, 40  
Horstman-Moretti, E., 22, 23, 37  
Howard, W. M., 265  
Hoyle, F., 194, 240, 342, 343, 357  
Hudson, H. S., 123  
Hughes, D. J., 303  
Hutcheon, I. D., 202  
Hutchinson, G. W., 105
- Illarionov, F., 381  
Imhof, W. L., 71, 73, 77, 80  
Ipavich, F. M., 322
- Jacobs, W. W., 299  
Jacobson, A. S., 71, 99, 390, 395, 400  
Jansky, K. G., 103  
Jenkins, E. B., 6  
Johnson, R. G., 71, 77  
Johnson, W. N., III, 57, 285, 287,  
294, 295  
Jones, F. C., 212  
Joseph, G., 128
- Kane, S. R., 329  
Kaplon, F., 123  
Kasturirangan, K., 123, 127  
Kato, T., 3, 8  
Kellerman, K., 346  
Khazan, Ya. M., 253  
King, J., 310  
Kinzer, R. L., 109, 116-118, 121-  
123, 125, 128  
Klebesadel, R. W., 175, 179, 181,  
329, 331  
Kniffen, D. A., 105, 128, 139, 209,  
210, 232, 234, 246, 257  
Kobetich, E. J., 29, 188, 190, 194,  
240  
Koltun, D. S., 354  
Kraushaar, W. L., 3, 55, 103-105,  
108, 111, 114, 123, 129, 135,  
139, 140, 147, 197, 204, 216,  
217, 219, 232, 246, 250, 253,  
259, 261, 364  
Kristian, J., 347  
Kurfess, J. D., 117, 119, 135  
Kuzmin, V. A., 316
- Lang, R. R., 191  
Langhoff, W., 260  
Lavakare, P. J., 128  
Layzer, D., 342, 346, 347  
Lee, J., 291  
Leighton, H. I., 166  
Lenchek, A. M., 322  
Lequeue, J., 344  
Leray, J. P., 121

- Leroy, B., 351  
 Leventhal, M., 291, 295  
 Levy, D. J., 213, 217-221  
 Lewin, W., 97, 405  
 Lincoln, J. V., 166  
 Ling, J. C., 24  
 Lingfelter, R. E., 167, 170, 286,  
 297, 299, 302, 306, 312, 314  
 Linsley, J., 316  
 Long, C. D., 153  
 Low, F. J., 347  
 Lucchin, F., 319, 371  
  
 Manchanda, R. K., 20, 24  
 Maringelli, M., 153  
 Massey, H. S. W., 291-293, 295  
 Matteson, J. L., 28, 41, 279  
 Mayer, Hasselwander, H. A., 55, 123,  
 128, 129, 135, 150, 232, 234, 235,  
 326  
 McBreen, B., 118, 120, 121  
 McCammon, D., 10, 30  
 McCray, R., 237, 240  
 McDonald, F. B., 173, 314  
 McVittie, G. C., 275  
 Metzger, A. E., 30, 41, 43, 57, 93, 94,  
 97, 209, 210, 279, 387, 395-397,  
 403  
 Meyer, P., 295  
 Miller, R. H., 343  
 Misra, D., 291  
 Mohr, C. B. O., 291-293, 295  
 Montmerle, T., 346  
 Morfill, G. E., 26, 27, 49, 53, 61, 123  
 Morgan, D. L., Jr., 55, 151, 196, 240,  
 242, 368  
 Morrison, P., 55, 139, 188, 190, 208,  
 211-213, 239, 241  
  
 Nakano, G. H., 71, 72, 77, 390  
 Navarra, G., 153  
 Nemethy, P., 365  
 Neugebauer, G., 295  
 Nicolle, J. P., 351  
  
 Noonan, T. W., 11  
 Novikov, I. D., 342, 344  
  
 Ögelmann, H., 105, 128  
 Olsen, R. A., 329  
 Omnes, R., 151, 239, 243, 335-337,  
 342, 351, 356, 369, 371, 381,  
 383, 392  
 O'Mongain, E. P., 116, 155  
 Oort, J. H., 254, 274, 344  
 Ore, A., 292  
 Ostricker, J. P., 332  
 Overbeck, J. W., 71, 73  
 Ozernoy, L. M., 341, 342, 346,  
 347, 370  
  
 Pal, Ya. A., 55, 103, 123, 133, 135,  
 241  
 Palmieri, T. M., 5, 21, 28  
 Parker, E. N., 343  
 Parlier, B., 121, 122, 135, 136  
 Peebles, R., 341  
 Penzias, A. A., 315  
 Perek, L., 201  
 Peterson, L. E., 24-27, 41, 61, 94,  
 95, 97, 123, 127, 135, 246, 279  
 Petrosian, V., 194  
 Peyraud, N., 346  
 Phillips, R. J. N., 336  
 Pieper, G. F., 93, 396  
 Pinkau, K., 133, 388  
 Pollack, J. B., 213, 216, 217  
 Pomerantz, P., 170  
 Porter, N., 161, 162  
 Powell, J. L., 292  
 Prakasarao, A. S., 21  
 Price, P. B., 284  
 Prilutskii, O. F., 241-243  
 Puget, J. L., 236, 239, 240, 243,  
 337, 341, 342, 356, 361, 367,  
 369, 374, 381-383, 392  
  
 Quenby, J. J., 26

- Ramaty, R., 71, 167, 170, 173, 194,  
 255, 284, 286, 288, 291, 295, 297,  
 299, 302, 306, 314, 398  
 Ramsden, D., 109  
 Rangan, K. K., 24  
 Rao, U. R., 123, 127  
 Reagan, J. B., 71, 77  
 Reedy, R. C., 41, 47, 279  
 Rees, M. J., 237, 241  
 Reeves, H., 284, 286, 356  
 Reppin, C., 165, 173  
 Riegler, G., 4, 8  
 Rieke, G. H., 153, 159  
 Robinson, I., 342  
 Roll, P. G., 17, 19  
 Rosburgh, I. W., 342  
 Rothenflug, R., 24  
 Rougoor, G. W., 344  
 Rozental, I. L., 241  
 Rudstam, G., 62, 83, 85  
  
 Sandage, A., 274, 278  
 Sanders, W., 4, 6, 7  
 Saslaw, W. C., 343  
 Savage, B. D., 6  
 Schatzman, E., 239, 243, 343, 346,  
 351, 355, 369, 387, 389, 390,  
 392, 397  
 Schild, A., 342  
 Schmidt, M., 268, 342, 346  
 Schreder, G. P., 319  
 Schucking, E. E., 342  
 Schwartz, D. A., 15, 17, 24-28, 38-40,  
 123, 195, 232  
 Schwartz, R. B., 303  
 Scotti, A., 336  
 Seeman, N., 109, 125, 128  
 Seltzer, S. M., 47, 78  
 Setti, G., 241, 250  
 Seward, F. D., 5, 193  
 Shapiro, M. M., 62, 90, 91, 283, 285,  
 402, 403  
 Share, G. H., 55, 94, 103, 117, 125,  
 128, 140, 232, 246, 257  
  
 Shklovskii, I. S., 250  
 Silberberg, R., 62, 63, 283, 285  
 Silk, J., 3, 55, 129, 185, 191, 192,  
 195, 200, 240, 274, 276, 277,  
 284, 286, 371  
 Slattery, P., 219  
 Smith, L. H., 231  
 Sobel, H. W., 64  
 Sommer, M., 390, 405  
 Spitzer, L. J., 343, 344  
 Sreekantan, B. V., 219  
 Stecher, T. P., 213, 246, 256  
 Stecker, F. W., 55, 57, 129, 135,  
 139, 150, 151, 180, 187, 188,  
 196, 201-203, 207-218, 221,  
 222, 224, 229-231, 233, 236-  
 240, 242, 243, 246, 250-252,  
 256, 257, 261, 291, 302, 316,  
 317, 319, 329, 341, 342, 367-  
 369, 381, 383, 387, 391-395,  
 398, 401  
 Steigman, G., 210, 243, 255, 341,  
 343, 351, 361, 362, 364, 367,  
 368, 394, 399  
 Stepanian, A. A., 158  
 Stephens, S. W., 57  
 Strittmatter, P. A., 362, 364, 367  
 Strong, A. W., 129, 259, 315, 325  
 Strong, I. B., 175, 181, 329  
 Sullivan, J. D., 203  
 Sunyaev, R. A., 241, 243, 343,  
 381, 383  
 Suri, A. N., 165  
 Syrovatskii, S. I., 212, 213, 250,  
 253, 254  
  
 Tadamaru, E., 295  
 Teegarden, B. J., 311  
 Teller, E., 343  
 Terzian, Y., 191  
 Thielheim, K. O., 260  
 Toor, A., 22  
 Tornabene, H. S., 155

- Trombka, J. I., 30, 41-43, 47, 50, 53, 67, 69, 90, 93-95, 123, 127, 129, 133-135, 150, 181, 232, 234, 235, 246, 279, 281, 387, 389, 396, 406  
 Tsao, C. H., 62, 63  
 Tucker, W., 8, 29  
  
 Ulam, S. M., 343  
 Ulmer, M. P., 256  
 Urey, H. C., 356  
  
 Valdez, J. V., 105  
 Valentine, D., 123  
 Van der Kruit, P. C., 254  
 Vedrenne, G., 55, 135, 150, 234, 235  
 Vette, J. I., 43, 54, 55, 92, 94, 95, 127, 208-210, 257  
 Vladimirsky, B. M., 158  
  
 Waddington, C. J., 105  
 Wagoner, R. V., 342, 357  
 Walden, W. E., 343  
 Wampler, D., 347  
 Wang, C. P., 105, 116, 122, 123  
 Ward, R. A., 280  
 Wdowczyk, J., 259, 315-324  
 Weekes, T. C., 158, 159, 162  
 Weinberg, S., 275  
 Wheaton, W. A., 180  
 White, S., 210, 313, 314, 397  
 Wilkinson, D. T., 17, 19  
 Williamson, F. W., 4, 7  
 Wilson, R. W., 315  
 Wolfendale, A. W., 259, 315  
 Woltjer, L., 250, 260, 343  
 Womack, E. A., 71, 73  
 Wong, D. Y., 336  
 Woosley, S. E., 264, 265  
 Wright, P. J., 109, 212, 240  
  
 Zaimidoroga, O. A., 354  
 Zatsepin, G. T., 153, 316  
 Zel'dovich, Ya. B., 335, 342-344, 381, 383  
 Zirin, H., 312  
 Zobel, W., 306